

# Lecture notes on Dynamical Systems in Economics and Finance

Gian Italo Bischi\*, Fabio Lamantia<sup>†</sup> and Davide Radi<sup>‡</sup>

April 2018

## Abstract

This is the collection of classroom notes that summarize the lessons on Dynamical systems delivered during the course on "Theory of games and Dynamical Systems" given at Università di Urbino "Carlo Bo" during the Fall semester of academic year 2014/2015 and Spring semester of 2015/2016. These classroom notes also include some snapshots about mathematical background, as well as some examples and related mathematical tools, that generally are not included in the undergraduate course on "General Maths". The content of these classroom notes is just a summary of the main topics and examples given during the course, and is not intended to be a substitute of standard books on dynamical systems or economic dynamics, that students are invited to use for a more general and exhaustive exposition of the topics.

## Contents

<b>1</b>	<b>Introduction</b>	<b>4</b>
1.1	The art of mathematical modelling . . . . .	4
1.2	Dynamical systems in economics . . . . .	4
<b>2</b>	<b>Dynamical systems, some general definitions.</b>	<b>7</b>
<b>3</b>	<b>Continuous-time dynamical systems</b>	<b>15</b>
3.1	The simplest one: 1-dimensional linear dynamical system . . . . .	16
3.2	Qualitative analysis and linearization procedure for the logistic model. . . . .	20
3.3	Qualitative analysis of 1-dimensional nonlinear models in continuous time . . . . .	22
3.4	Local bifurcations in 1-dimensional nonlinear models in continuous time . . . . .	25
3.4.1	Fold bifurcation. . . . .	26
3.4.2	Transcritical (or stability exchange) bifurcation. . . . .	27
3.4.3	Pitchfork bifurcation . . . . .	28
<b>4</b>	<b>Two-dimensional Dynamical Systems in continuous time</b>	<b>30</b>
4.1	Linear systems . . . . .	34
4.1.1	Some example of computations of explicit solutions for linear models . . . . .	39
4.2	Nonlinear dynamic models in two dimensions. . . . .	44
4.3	Periodic solutions and limit cycles . . . . .	50
4.4	Bifurcations of 2-dimensional dynamical systems . . . . .	52

---

\*gian.bischi@uniurb.it

<sup>†</sup>fabio.lamantia@unical.it

<sup>‡</sup>radidavide85@gmail.com

<b>5</b>	<b>n-dimensional dynamical systems in continuous time</b>	<b>70</b>
5.1	Linear systems . . . . .	71
5.2	Nonlinear systems . . . . .	73
<b>6</b>	<b>Discrete-time dynamical systems</b>	<b>84</b>
6.1	The simplest one: 1-dimensional linear homogeneous . . . . .	86
6.2	Qualitative analysis of 1-dimensional nonlinear models in discrete time . . . . .	89
6.3	Local bifurcations of one-dimensional discrete dynamical systems . . . . .	93
6.4	The logistic map . . . . .	96
6.5	Basins of attraction in one-dimensional discrete dynamical systems . . . . .	104
6.6	Some economic examples . . . . .	109
6.6.1	Nonlinear Cobweb with adaptive expectations . . . . .	109
6.6.2	Financial market with heterogeneous agents . . . . .	111
<b>7</b>	<b>Two dimensional discrete dynamical systems</b>	<b>115</b>
7.1	Linear systems . . . . .	116
7.2	Nonlinear discrete dynamical systems in 2 dimensions . . . . .	119
7.3	Some economic examples . . . . .	124
7.3.1	A model of financial markets with heterogeneous traders . . . . .	124
7.3.2	A duopoly game with linear demand and gradient dynamics . . . . .	127
7.3.3	A duopoly game with isoelastic demand and gradient dynamics . . . . .	131
7.4	Discrete dynamical system represented by noninvertible maps . . . . .	134
7.4.1	Critical sets. Definitions and simple examples . . . . .	135
7.4.2	Trajectories, attractors and basins . . . . .	142
7.4.3	Critical sets and the delimitation of trapping regions. . . . .	143
7.4.4	Critical sets and the creation of non connected basins . . . . .	145
7.5	Some economic examples . . . . .	145
7.5.1	Global properties of the Cournot duopoly model with linear demand and gradient dynamics . . . . .	146
7.5.2	Global analysis of a marketing Model . . . . .	153
<b>8</b>	<b>Repeated and evolutionary games as dynamical systems</b>	<b>162</b>
8.1	Cournot games with rational players . . . . .	164
8.2	Bounded rationality and incomplete information . . . . .	165
8.2.1	Adaptive expectations . . . . .	178
8.3	Evolutionary games . . . . .	178
8.3.1	Replicator dynamics with one population of players . . . . .	179
8.3.2	Replicator dynamics with two populations of players . . . . .	185
8.3.3	Replicator dynamics in discrete time . . . . .	190
<b>9</b>	<b>An introduction to optimal control in continuous time</b>	<b>193</b>
9.1	Bellman's optimality principle: the Hamilton-Jacobi-Bellman equation . . . . .	196
9.2	From HJB to Pontryagin's Maximum Principle . . . . .	198
9.3	Some basic examples . . . . .	200
9.4	Current value formulations . . . . .	204
9.4.1	Economic Examples . . . . .	206

<b>10 Appendix</b>	<b>224</b>
10.1 Complex Numbers . . . . .	224
10.1.1 Properties of sum and product of complex numbers. . . . .	225
10.1.2 Polar form of a complex number . . . . .	226
10.1.3 Exponential form of a complex number . . . . .	227
10.1.4 Complex numbers and polynomial equations . . . . .	228
10.2 Some examples of solutions of first order ODE . . . . .	228
10.2.1 Integrals as ODE . . . . .	228
10.2.2 First order linear ODE . . . . .	229
10.2.3 Separation of variables	
231	

# 1 Introduction

These lecture notes should provide an introduction to the study of dynamic models in economics and social sciences, both in discrete and continuous time, by the methods of the qualitative theory of dynamical systems. At the same time, the students should also practice (and hopefully appreciate) the "art" of mathematical modelling real systems and time evolving processes.

## 1.1 The art of mathematical modelling

The mathematical representation of a real system (physical, biological, social, economic etc.) starts from a rigorous and critical analysis of the systems to be described, their main features and basic principles. Measurable quantities (i.e. quantities that can be expressed by numbers) that characterize its state and its behaviour must be identified in order to describe the system mathematically. This leads to a schematic description of the system, generally a simplified representation, expressed by words, diagrams and symbols. This stage is represented by the lower side of the rectangle in fig. 1. This task is generally carried out by specialists of the real system, such as economists, social scientists etc. The second stage is described by the right vertical side of the rectangle, and consists in the translation of the schematic model into a mathematical model, expressed by mathematical symbols and operators. This leads us to the upper side, dedicated to the mathematical study of the model, by using mathematical tools, proofs, and/or numerical methods. The output of this process is expressed in mathematical terms, such as propositions (i.e. Theorems) with proofs or mathematical expressions. Then these mathematical results must be translated into the natural language and terms typical of the system described, that is economic or biologic or physical terms, in order to obtain laws or statements useful for the application considered. This closes the path around the rectangle, but often it is not the end of the modellization process. In fact, if the results obtained are not satisfactory, in the sense that they do not agree with the observations or experimental data, then one needs to re-examine the model, by adding some details or by changing some basic assumptions, and start again the whole procedure.

Our course in Dynamical Systems in Economics is a Math course, so we should be mainly concerned with the upper portion of the rectangle: from a dynamic model to the results through a mathematical analysis by using analytic, geometric and numerical methods. However, during the course we will often move down to the level of model building as well, because it is the most creative stage, leading from reality to its formalization in the form of a mathematical model. This requires competence and fantasy, the reason why we call it "the art of math modelling".

## 1.2 Dynamical systems in economics

Dynamical systems are systems that change over time, and the mathematical theory of dynamical systems describes them by using dynamic variables, i.e. functions of time that define their state as time goes on, in other words their time evolution. Emblematic is the title of a book on the theory of dynamical systems published in 1980 by Steve Smale, a famous American mathematician that also obtained important results in economics: the title is "The Mathematics of Time". This branch of mathematics has been first introduced in Physics, where differential equations have been used to describe the motion of objects, from particles to planets, including oscillatory systems, fluid dynamics etc. Similar equations of motion have then be applied to the description of ecological systems (e.g. in population dynamics and interactions among species) or biological problems (such as blood circulation) or the time development of chemical reactions, as well as in economic problems (such as

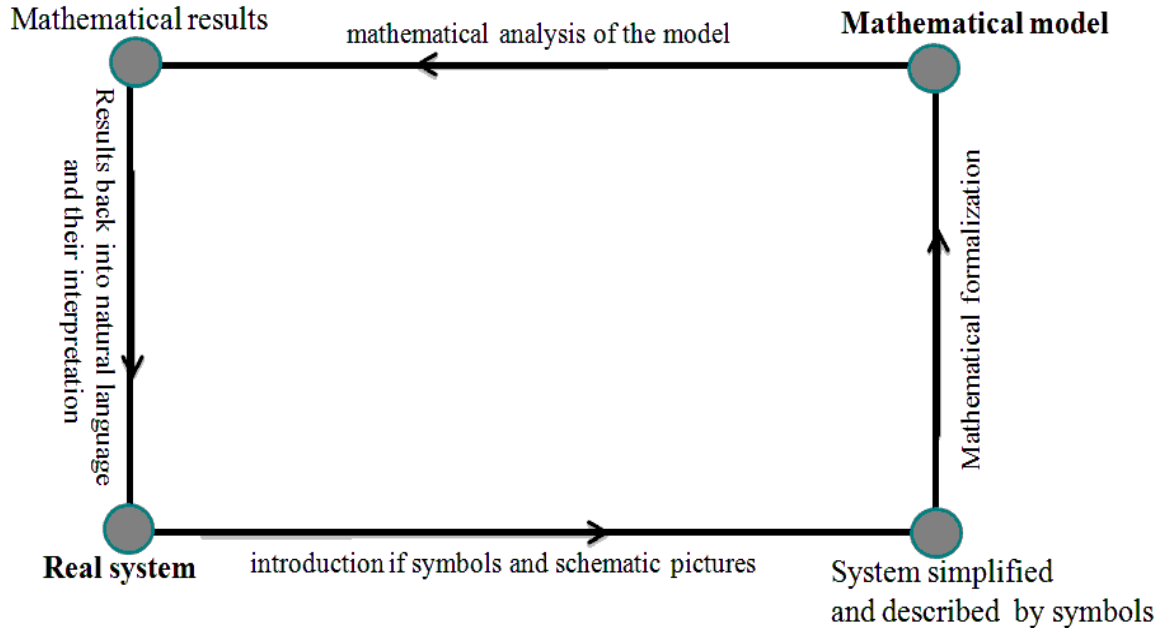


Figure 1: The process of mathematical modelling.

the time changes of prices in a market, or quantities of goods produced in industrial or agricultural systems). All these systems and phenomena can be described by suitable (generally simplified) models where given functions of time are used to characterize their state at a given time, and by equations that state how such state variables evolve in time, so that one may try to forecast their future states on the basis of the knowledge of their state at a given time. These are the equations of motion (i.e. the model) used to characterize the rate of change of the dynamic variables. Of course, in the presence of complex systems and phenomena it is not easy to calculate the state of the modelled systems at each time in the future, and often only qualitative and generic properties can be inferred.

Moreover, often the simplified mathematical models used to mimic the time evolution of real systems are only caricatures, artificial schematic representations expressed by mathematical objects (functions, parameters, derivatives) that can be improved when the results obtained are not confirmed by experiments and observations.

The simulation of the time evolution of economic systems by using the language and the formalism of dynamical systems (i.e. differential or difference equations according to the assumption of continuous or discrete time) dates back to the early days of the mathematical formalization of models in economics and social sciences.

However, in the last decades the importance of dynamic modelling in economics and finance increased because of the parallel trends in mathematics on one side and economics and social sciences on the other side, and the two developments are not independent, in the sense that the new issues in mathematics favoured the enhancement of understanding of economic systems and policies, and the needs of more and more complex mathematical models in economic and social studies stimulated the creation of new branches in mathematics and the development of existing ones.

Indeed, in recent mathematical research a flourishing literature in the field of qualitative theory of

nonlinear dynamical systems, with the related concepts of attractors, bifurcations, dynamic complexity, deterministic chaos, has attracted the attention of many scholars of different fields, from Physics to Biology, from Chemistry to Economics and Sociology, etc. These mathematical topics became more and more popular even outside the restricted set of academic specialists. Concepts like bifurcations (also called catastrophes in the eighties), fractals, chaos, entered and deeply modifies several research fields, not only in the scientific research but even in the literature, cinema etc.

On the other side, during the last decades, also economic modelling has been witnessing a paradigm shift in methodology, and the recent economic and financial crisis has strengthened this trend. Indeed, despite its notable achievements, the standard approach based on the paradigm of the rational and representative agent (endowed with unlimited computational ability and perfect information) as well as the underlying assumption of efficient markets, fails to explain many important features of economic systems, and has been criticized on a number of grounds. At the same time, a growing interest has emerged in alternative approaches to economic agents' decision making, which allow for factors such as bounded rationality and heterogeneity of agents, social interaction, and learning, where agents' behaviour is governed by simpler "rules of thumb" (or "heuristics") or "trial and error" or even "imitation" mechanisms. Of course, starting from these assumptions of bounded rationality, the modelled agents are generally not able to choose what is "optimal", but they can at most obtain, using a famous expression of Simon (Nobel laureate in 1978) what is "good enough" for them, thus replacing the concept of optimal behavior with the (apparently lower) concept of "satisficing behaviour".

The result of this approach may seem, at a first sight, a quite unsatisfactory and dismissive (in the sense of understating, reductive) representation of economic agents facing a decision. However, the significance of this approach is much more interesting and meaningful if it is used at each step of a repeated decision process, i.e. iterated over time. In fact, under some circumstances, the repetition of boundedly rational decisions based on trial and error, or imitation of the better, or comparison between expected and realized results, that we will denote by the general term "adaptive" in the following, may be a much more realistic (and even more rational) behaviour with respect to a rigid optimizing attitude, based on fixed rules assumed as fundamental axioms of rational behavior. Indeed, the latter attitude (typical of mainstream economic modelling where economic agents are assumed to behave as if they already know the laws that govern the evolution of the system where they operate, like a physicist who knows the law of motion of simple physical devices) may be quite misleading (even dangerous) when applied in the presence of incomplete information about the system where the economic agents operate, or about other agents' degree of rationality, or if the system evolution is characterized by intrinsic uncertainty, as it occurs when the time evolution is governed by nonlinear laws allowing for chaotic behavior, with the associated phenomenon of sensitivity to arbitrarily small perturbations (a quite common situation in economics and social sciences). In fact, the adaptive agents are allowed, by definition, to adjust their repeated actions according to the information collected as the system evolves, and a repeated (step-by-step) comparison of the expected results of their decisions with the observed ones allows them to adapt to circumstances.

Moreover, an adaptive system, even if it is governed by local (or myopic) decision rules of boundedly rational and heterogeneous agents, may converge in the long run to a rational equilibrium, i.e. the same equilibrium forecasted (and instantaneously reached) under the assumption of full rationality and full information of all economic agents. This may be seen as an evolutionary interpretation of a rational equilibrium, and some authors say that in this case the boundedly rational agents are able to learn, in the long run, what rational agents already know under very pretentious rationality assumptions. However, it may happen that under different starting conditions or as a consequence of exogenous perturbations, the same adaptive process leads to non-rational equilibria as well, i.e. equilibrium

situations which are different from the ones forecasted under the assumption of full rationality, as well as to dynamic attractors characterized by endless asymptotic fluctuations that never settle to a steady state. The coexistence of several attracting sets, each with its own basin of attraction, gives rise to path dependence, irreversibility, hysteresis and other nonlinear and complex phenomena commonly observed in real systems in economics, finance and social sciences, as well as in laboratory experiments.

From the description given above, it is evident that the analysis of adaptive systems can be formulated in the framework of the theory of dynamical systems. i.e. systems of ordinary differential equations (continuous time) or difference equations (discrete time); the qualitative theory of nonlinear dynamical systems, with the related concepts of stability, bifurcations, attractors and basins of attraction, is a major tool for the analysis of their long run (or asymptotic) properties. Not only in economics and social sciences, but also in physics, biology and chemical sciences, such models are a privileged instrument for the description of systems that change over time, often described as "nonlinear evolving systems", and their long-run aggregate outcomes can be interpreted as "emerging properties", sometimes difficult to be forecasted on the basis of the local (or step-by-step) laws of motion.

Of course, the use of Nonlinear Dynamics in Economics is well-established since the early contributions of N. Kaldor and R. Goodwin in the 40s-50s. Even in more recent neoclassical models, the theory of nonlinear systems has yielded important results on the 'indeterminacy' and bifurcations of stationary competitive equilibria. However, its use is often restricted to the analysis of the 'local' behavior of the system. As a consequence, this approach is unsuitable to investigate the 'global' effects of nonlinearity ('emergent phenomena'). Such effects are often remarkable, although they cannot be detected from the behavior of the system in the vicinity of the stationary equilibria. So a global qualitative analysis of the economic models, both in continuous and in discrete time, is necessary. Such a global analysis can be rarely obtained by analytical methods, and a combination of analytical, geometric and numerical methods is necessary to grasp the main qualitative features of a nonlinear dynamic system in order to understand, at least qualitatively, its asymptotic (or long-run) behaviour. For this reason the usage of some computer software for the numerical simulation of dynamical system is necessary in order to understand and appreciate the methods introduced in this course.

## 2 Dynamical systems, some general definitions.

In this section we introduce some general concepts, notations and a minimal vocabulary about the mathematical theory of dynamical systems.

A *dynamical system* is a mathematical model, i.e. a formal, mathematical description, of an evolving system, that is a real system whose state changes as time goes on. This includes, as a particular case, systems whose state remains constant, that will be denoted as systems at equilibrium.

The first step to describe such systems in mathematical terms is the characterization of their "state" by a finite number, say  $n$ , of measurable quantities, denoted as "state variables", expressed by real numbers

$$x_1, \dots, x_n$$

where  $x_i \in \mathbb{R}$ ,  $i = 1, \dots, n$ . For example in an economic system these numbers may be the prices of  $n$  commodities in a market, or the respective quantities, or they can represent other measurable indicators, like level of occupation, or salaries, or inflation. In an ecologic system these  $n$  number used to characterize its state may be the numbers (or densities) of individuals of each species, or

concentration of inorganic nutrients or chemicals in the environment. In a physical system<sup>1</sup> the state variables may be the positions and velocities of the particles, or generalized coordinates or related momentums of a mechanical system, or temperature, pressure etc. in a thermodynamic system.

This ordered set of real numbers can be seen as a vector  $\mathbf{x} = (x_1, \dots, x_n) \in \mathbb{R}^n$ , i.e. a "point" in an  $n$ -dimensional space, and this allows us to introduce a "geometric language", in the sense that a 1-dimensional dynamical system is represented by point along a line, a 2-dimensional one by a point in a Cartesian plane and so on.

Sometimes only the values of the state variables included in a subset of  $\mathbb{R}^n$  are suitable to represent the real system. For example only non-negative values of  $x_i$  are meaningful if  $x_i$  represents a price in an economic system or the density of a species in an ecologic one, or it can be that in the equations that define the system a state variable  $x_i$  is the argument of a mathematical function that is defined in a given domain, like a logarithm, a square root or a rational function. As a consequence, only the points in a subset of  $\mathbb{R}^n$  are admissible states for the dynamical system considered, and this leads to the following definition

**Definition.** *The state space (or phase space)  $M \subseteq \mathbb{R}^n$  is the set of admissible values of the state variables.*

As a dynamical system is assumed to evolve with time, these numbers are not fixed but are functions of time  $x_i = x_i(t)$ ,  $i = 1, \dots, n$ , where  $t$  may be a real number (*continuous time*) or a natural number (*discrete time*). The latter assumption may sound quite strange, whereas it represents a common assumption in systems where changes of the state variables are only observed as a consequence of events occurring at given time steps (*event-driven time*). For example, it is quite common in economic and social sciences where in many systems the state variables can change as a consequence of human decisions that cannot be continuously revised, e.g. after production periods (the typical example is output of agricultural products) or after the meetings of an administration council or after the conclusions of contracts etc. (*decision-driven time*).

So, in the following we will distinguish these two cases, according to the domain of the state functions:  $x_i : \mathbb{R} \rightarrow \mathbb{R}$  or  $x_i : \mathbb{N} \rightarrow \mathbb{R}$ , i.e. the continuous or discrete nature of time. In any case, the purpose of dynamical systems is the following: given the state of the system at a certain time  $t_0$ , compute the state of the system at time  $t \neq t_0$ . This is equivalent to the knowledge of an operator

$$\mathbf{x}(t) = \mathbf{G}(t, \mathbf{x}(t_0)) \tag{1}$$

where boldface symbols represent vectors, i.e.  $\mathbf{x}(t) = (x_1(t), \dots, x_n(t)) \in M \subseteq \mathbb{R}^n$  and  $\mathbf{G}(\cdot) = (G_1(\cdot), \dots, G_n(\cdot)) : M \rightarrow M$ . If one knows the *evolution operator*  $\mathbf{G}$  then from the knowledge of the *initial condition* (or *initial state*)  $\mathbf{x}(t_0)$  the state of the system at any future time  $t > t_0$  can be computed, as well as at any time of the past  $t < t_0$ . Generally we are interested in the forecasting of future states, especially in the asymptotic (or long-run) evolution of the system as  $t \rightarrow +\infty$ , i.e. the fate, or the destiny of the system. However, even the flashback may be useful in some cases, like in detective stories when the investigators from the knowledge of the present state want to know what happened in the past.

The vector function  $\mathbf{x}(t)$ , i.e. the set of  $n$  functions  $x_i(t)$ ,  $i = 1, \dots, n$  obtained by (1), represents the parametric equations of a *trajectory*, as  $t$  varies. In the case of continuous time  $t \in \mathbb{R}$  the trajectory is a curve in the space  $\mathbb{R}^n$ , that can be represented in the  $n + 1$ -dimensional space  $(\mathbb{R}^n, t)$ , and denoted

---

<sup>1</sup>Physics is the discipline where the formalism of dynamical system has been first introduced, since 17<sup>th</sup> century, even if the modern approach, often denoted as qualitative theory of dynamics systems, has been introduced in the early years of the 20<sup>th</sup> century.



as *integral curve*, or in the state space (also denoted as "phase space")  $\mathbb{R}^n$ , see fig. 2. In the latter case the direction of increasing time is represented by arrows, and the curve is denoted as *phase curve*.

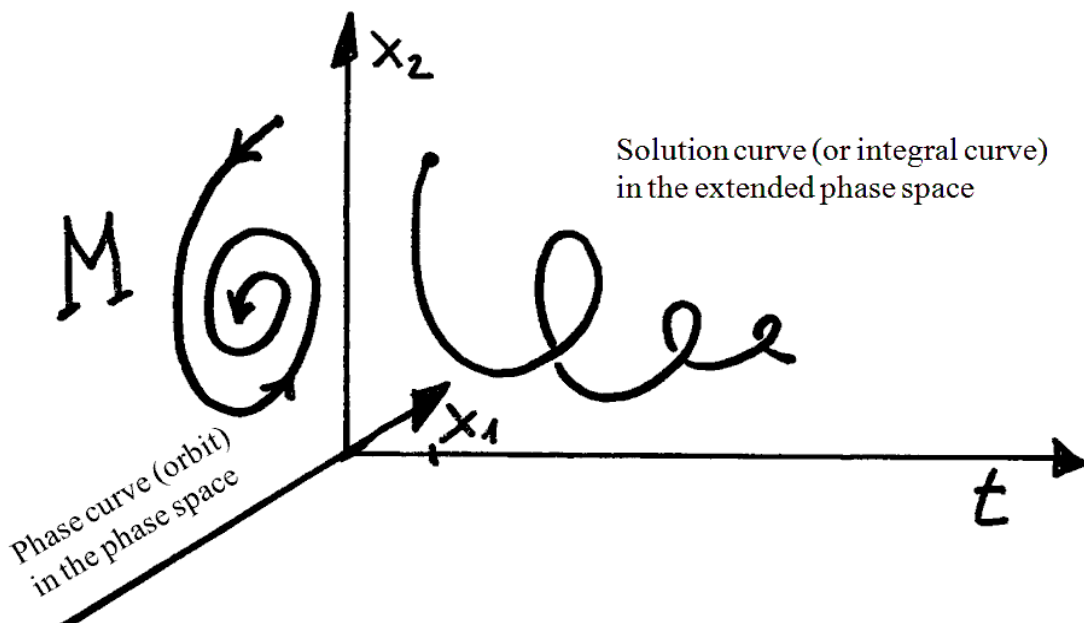


Figure 2: Integral curve and its projection (phase curve).

In the case of discrete time a trajectory is a sequence (i.e. a countable set) of points, and the time evolution of the system jumps from one point to the successive one in the sequence. Sometimes line segments can be used to join graphically the points, moving in the direction of increasing time, thus getting an ideal piecewise smooth curve by which the time evolution of the system is graphically represented (see fig. 3)

An *equilibrium (stationary state or fixed point)*  $\mathbf{x}^* = (x_1^*, \dots, x_n^*)$  is a particular trajectory such that all the state variables are constant

$$\mathbf{x}(t) = \mathbf{G}(t, \mathbf{x}^*) = \mathbf{x}^* \quad \text{for each } t > t_0$$

An equilibrium is a trapping point, i.e. any trajectory through it remains in it for each successive time:  $\mathbf{x}(t_0) = \mathbf{x}^*$  implies  $\mathbf{x}(t) = \mathbf{x}^*$  for  $t \geq t_0$ . This definition can be extended to any subset of the phase space:

**Definition** A set  $A \subseteq M$  is trapping if  $\mathbf{x}(t_0) \in A$  implies  $\mathbf{x}(t) = \mathbf{G}(t, \mathbf{x}(t_0)) \in A$  for each  $t > t_0$ .

This can also be expressed by the notation  $\mathbf{G}(t, A) \subseteq A$ , where

$$\mathbf{G}(t, A) = \{\mathbf{x} \in M : \exists t \geq t_0 \text{ and } \mathbf{x}(t_0) \in A \text{ so that } \mathbf{x} = \mathbf{G}(t, \mathbf{x}(t_0))\}$$

So, any trajectory starting inside a trapping set cannot escape from it. We now define a stronger property, in the sense that it concerns particular kinds of trapping sets.

**Definition** A closed set  $A \subseteq M$  is invariant if  $\mathbf{G}(t, A) = A$ , i.e. each subset  $A' \subset A$  is not trapping.

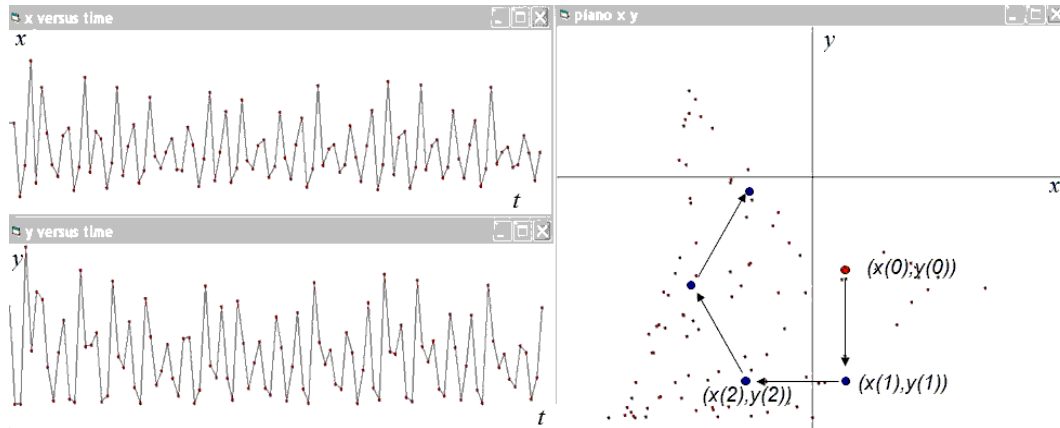


Figure 3: Discrete time dynamical system in two dimensions.

In other words, any trajectory starting inside an invariant set remains there, and all the points of the invariant set are reached by a trajectory starting inside it. Notice that an equilibrium point is a particular kind of invariant set (let's say the simplest). However, we will see many other kinds of invariant sets, where interesting cases of non constant trajectories are included.

We now wonder what happens if we start a trajectory from an initial condition close to an invariant set, i.e. in a neighborhood of it.

The trajectory may enter the invariant set (and then it never escape from it) or it may remain around it or it may go elsewhere, far from it. This leads us to the concept of stability of an invariant set (a well known concept for motions in the gravitational field, see fig.4).

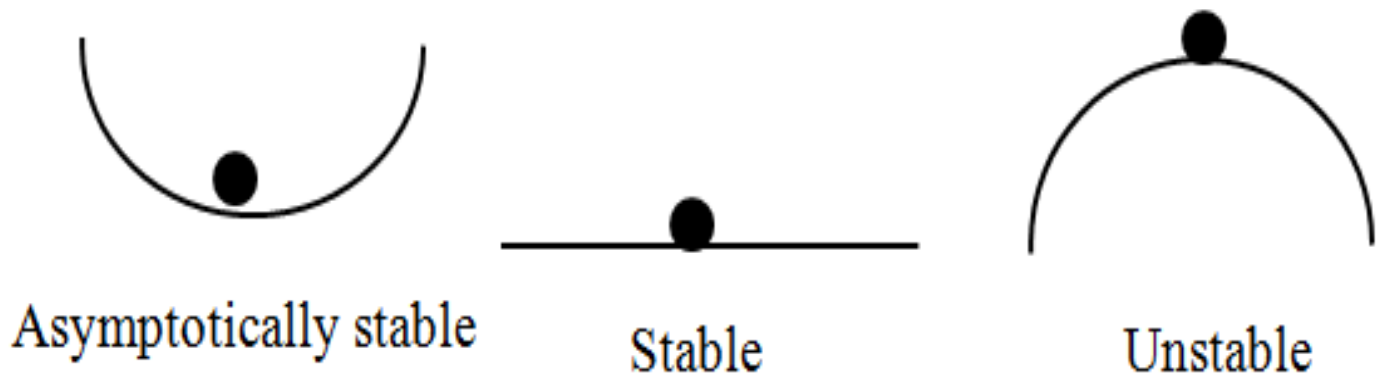


Figure 4: Analogy with gravitational field.

**Definition (Lyapunov stability)** *An invariant set  $A$  is stable if for each neighborhood  $U$  of  $A$  there exists another neighborhood  $V$  of  $A$ , with  $V \subseteq U$ , such that any trajectory starting from  $V$  remains inside  $U$ .*

In other words, Lyapunov stability means that all the trajectories starting from initial conditions outside  $A$  and sufficiently close to it remain around it (see the schematic picture in fig. 5). Instability

is the negation of stability, i.e. an invariant set  $A$  is unstable if a neighborhood  $U \supset A$  exists such that initial conditions taken arbitrarily close to  $A$  exist that generate trajectories that exit  $U$ .

The following definition is stronger

**Definition (Asymptotic stability)** An invariant set  $A$  is asymptotically stable (and it is often called *attractor*) if:

- (i)  $A$  is stable (according to the definition given above)
- (ii)  $\lim_{t \rightarrow +\infty} \mathbf{G}(t, \mathbf{x}) \in A$  for each initial condition  $\mathbf{x} \in V$ .

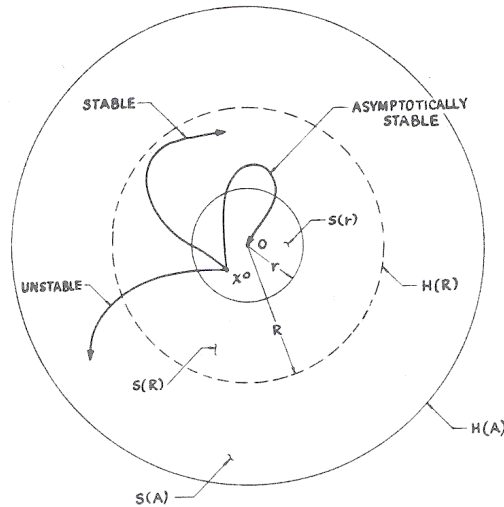


Figure 5: Stability, asymptotic stability, instability.

In other words, asymptotic stability means that the trajectories starting from initial conditions outside  $A$  and sufficiently close to it not only remain around it, but tend to it in the long run (i.e. asymptotically), see the schematic pictures in fig.6. At a first sight, the condition (ii) in the definition of asymptotic stability seems to be stronger than (i), hence (i) seems to be superfluous. However it may happen that a neighborhood  $U \supset A$  exists such that initial conditions taken arbitrarily close to  $A$  generate trajectories that exit  $U$  and then go back to  $A$  in the long run (see the last picture in fig.6)

Of course, all these definitions expressed in terms of neighborhoods can be restated by using a norm (and consequently a distance) in  $\mathbb{R}^n$ , for example the euclidean norm  $\|\mathbf{x}\| = \sqrt{\sum_{i=1}^n x_i^2}$  from which the distance between two points  $\mathbf{x} = (x_1, \dots, x_n)$  and  $\mathbf{y} = (y_1, \dots, y_n)$  can be defined as  $\|\mathbf{x} - \mathbf{y}\| = \sqrt{\sum_{i=1}^n (x_i - y_i)^2}$ . As an example we can restate the definitions given above for the particular case of an equilibrium point.

Let  $\mathbf{x}(t) = \mathbf{G}(t, \mathbf{x}(t_0))$ ,  $t \geq 0$ , a trajectory starting from the initial condition  $\mathbf{x}(t_0) = \mathbf{G}(t_0, \mathbf{x}(t_0))$  and  $\mathbf{x}^*$  an equilibrium point  $\mathbf{x}^* = \mathbf{G}(t, \mathbf{x}^*)$  for  $t \geq 0$ . The equilibrium  $\mathbf{x}^*$  is stable if for each  $\varepsilon > 0$  there exists  $\delta_\varepsilon > 0$  such that  $\|\mathbf{x}(t_0) - \mathbf{x}^*\| < \delta_\varepsilon \implies \|\mathbf{x}(t) - \mathbf{x}^*\| < \varepsilon$  for  $t \geq 0$ . If in addition  $\lim_{t \rightarrow \infty} \|\mathbf{x}(t) - \mathbf{x}^*\| = 0$  then  $\mathbf{x}^*$  is asymptotically stable. Instead, if an  $\varepsilon > 0$  exists such that for each  $\delta > 0$  we have  $\|\mathbf{x}(t) - \mathbf{x}^*\| > \varepsilon$  for some  $t > 0$  even if  $\|\mathbf{x}(t_0) - \mathbf{x}^*\| < \delta$ , then  $\mathbf{x}^*$  is unstable.

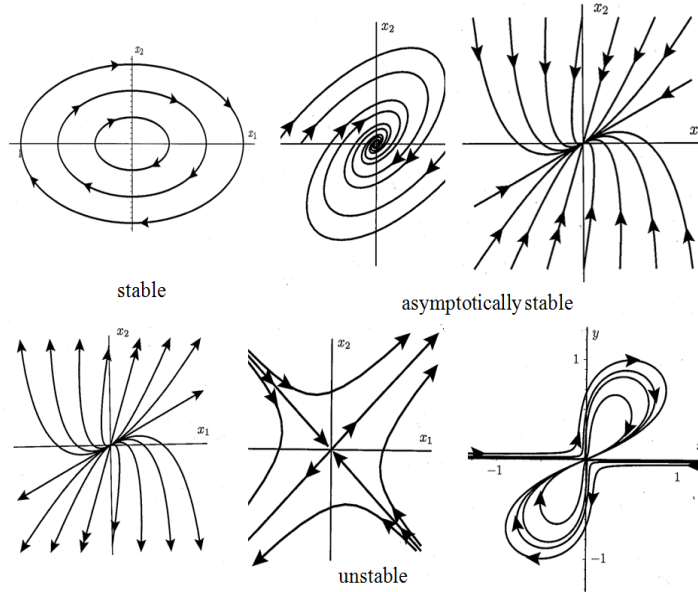


Figure 6: Phase portraits.

These definitions are local, i.e. concern the future behaviour of a dynamical system when its initial state is in an arbitrarily small neighborhood of an invariant set. So, they can be used to characterize the behaviour of the system under the influence of small perturbation from an equilibrium or another invariant set. In other words, they give an answer to the question: given a system at equilibrium, what happens when small exogenous perturbation move its state slightly outside the equilibrium state? However, in the study of real systems we are also interested in their global behaviour, i.e. far from equilibria (or more generally from invariant sets) in order to consider finite (and not always small) perturbations and to answer questions like: how far can an exogenous perturbation shift the state of a system from an equilibrium remaining sure that it will spontaneously go back to the originary equilibrium? This kind of questions leads to the concept of basin of attraction of an attractor

**Definition (Basin of attraction)** *The basin of attraction of an attractor  $A$  is the set of all points  $\mathbf{x} \in M$  such that  $\lim_{t \rightarrow +\infty} \mathbf{G}(t, \mathbf{x}) \in A$ , i.e.  $B(A) = \{\mathbf{x} \in M \text{ such that } \lim_{t \rightarrow +\infty} \mathbf{G}(t, \mathbf{x}) \in A\}$ .*

If  $B(A) = M$  then  $A$  is called *global attractor*. Generally the extension of the basin of a given attractor gives a measure of its robustness with respect to the action of exogenous perturbations. However this is a quite rough argument, as shown in the qualitative sketches of fig.7 on the left, where basins are represented such that greater measure does not imply greater robustness due to their peculiar shapes. Moreover, when basins are considered, one realizes that in some cases stable equilibria may be even more vulnerable than unstable ones (see fig. 7 on the right).

Other important indicators should be critically considered. For example, how fast is the convergence towards an attractor? Even if an invariant set is asymptotically stable and it has a large basin, an important question concerns the speed of convergence, i.e. the amount of time which is necessary to reduce the extent of a perturbation. In fact, in some cases this time interval may be too much for any practical purpose. For example, if a group of economists use a dynamical system to model the behaviour of an economic system after a crisis, and they conclude that on the basis of their studies the

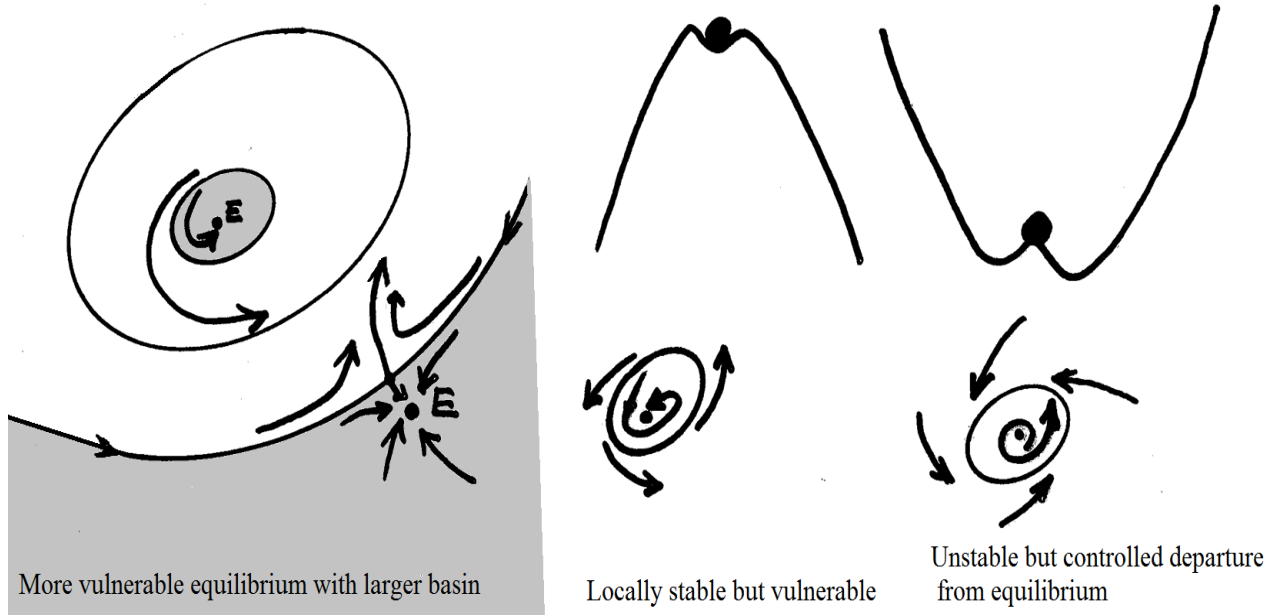


Figure 7: Local stability extent.

system will go back to the ordinary pre-crisis equilibrium, we are quite happy. But if they complete this statement by saying that this may require 500 years, then their stability statement may be not so encouraging.

These arguments (as well as many others that we will give in the following) lead us to the necessity of a deep understanding of the global behaviour of a dynamical system in order to give useful indications about the performance of the real system modelled.

The main problem is that, generally, the operator  $\mathbf{G}$  that allows to get an explicit representation of the trajectories of the dynamical system for any initial condition in the phase space, is not known, or cannot be expressed in terms of elementary functions or its expression is so complicated that it cannot be used for any practical purpose. In general a dynamical system is expressed in terms of *local evolution equations*, also denoted as *dynamic equations* or *laws of motion*, that state how the dynamical system changes as a consequence of small time steps. In the case of continuous time the evolution equations are expressed by the following set of *ordinary differential equations* (ODE) involving the time derivative, i.e. the speeds of change, of each state variable

$$\begin{aligned} \frac{dx_i(t)}{dt} &= f_i(x_1(t), \dots, x_n(t); \boldsymbol{\alpha}), \quad i = 1, \dots, n \\ x_i(t_0) &= \bar{x}_i \end{aligned} \quad (2)$$

where the time derivative at the left hand side represents, as usual, the speed of change of the state variable  $x_i(t)$  with respect to time variations, the functional relations give information about the influence of the same state variable  $x_i$  (self-control) and of the other state variables  $x_j$ ,  $j \neq i$  (cross-control) on such rate of change, and  $\boldsymbol{\alpha} = (\alpha_1, \dots, \alpha_m)$ ,  $\alpha_i \in \mathbb{R}$ , represents  $m$  real parameters, fixed along a trajectory, which can assume different numerical values in order to represent exogenous influences on the dynamical systems, e.g. different policies or effects of the outside environment. The modifications induced in the model after a variation of some parameters  $\alpha_i$  are called *structural modifications*, as

such changes modify the shape of the functions  $f_i$ , and consequently the properties of the trajectory.

The set of equations (2) are "differential equations" because their "unknowns" are functions  $x_i(t)$  and they involve not only  $x_i(t)$  but also their derivatives. We refer the reader to standard textbooks and the huge literature about differential equations in order to study their general properties and methods of solutions. In these lecture notes we will just use them in the formulation and the qualitative understanding of the models.

In the theory of dynamical systems it is usual to replace the Leibniz notation  $\frac{dx}{dt}$  of the derivative with the more compact "dot" notation  $\dot{x}$  introduced by Newton. With this notation, the dynamical system (2) is indicated as

$$\dot{x}_i = f_i(x_1, \dots, x_n; \boldsymbol{\alpha}), \quad i = 1, \dots, n \quad (3)$$

Differential equations of order greater than one, i.e. involving derivatives of higher order, can be easily reduced to systems of differential equations of order one in the form (2) by introducing auxiliary variables. For example the second order differential equation

$$\ddot{x}(t) + a\dot{x}(t) + bx(t) = 0 \quad (4)$$

with initial conditions  $x(0) = x_0$  and  $\dot{x}(0) = v_0$  can be reduced to the form (3) by defining  $x_1(t) = x(t)$  and  $x_2(t) = \dot{x}(t)$ , so that the equivalent system of two first order differential equations becomes

$$\begin{aligned} \dot{x}_1 &= x_2 \\ \dot{x}_2 &= -bx_1 - ax_2 \end{aligned}$$

with  $x_1(0) = x_0, x_2(0) = v_0$ .

If along a trajectory the parameters explicitly vary with respect to time, i.e. some  $\alpha_i = \alpha_i(t)$  are functions of time, then the model is called *nonautonomous*. Also a nonautonomous model can be reduced to an equivalent autonomous one in the normal form (2) of dimension  $n + 1$  by introducing the dynamic variable  $x_{n+1} = t$  whose time evolution is governed by the added first order differential equation  $\dot{x}_{n+1} = 1$ .

In the case of discrete time, the evolution equations are expressed by the following set of *difference equations* that inductively define the time evolution as a sequence of discrete points starting from a given initial condition

$$\begin{aligned} x_i(t+1) &= f_i(x_1(t), \dots, x_n(t); \boldsymbol{\alpha}), \quad i = 1, \dots, n \\ x_i(0) &= \bar{x}_i \end{aligned} \quad (5)$$

Also in this case a higher order difference equation, as well as a nonautonomous difference equation, can be reduced to an expanded system of first order difference equations of order one. For example the second order difference equations

$$x(t+1) + ax(t) + bx(t-1) = 0$$

starting from the initial conditions  $x(-1) = x_0, x(0) = x_1$  can be equivalently rewritten as

$$\begin{aligned} x(t+1) &= -ax(t) - by(t) \\ y(t+1) &= x(t) \end{aligned}$$

where  $y(t) = x(t-1)$ , with initial conditions are  $x(0) = x_1$ ,  $y(0) = x_0$ . Analogously, a nonautonomous difference equation

$$x_{t+1} = f(x_t, t)$$

becomes

$$\begin{aligned} x_{t+1} &= f(x_t, y_t) \\ y_{t+1} &= y_t + 1 \end{aligned}$$

where  $y_t = t$ .

So, the study of (2) and (5) constitutes a quite general approach to dynamical systems in continuous and discrete time respectively. They are local representations of the evolution of systems that change with time. Their qualitative study, i.e. how one can (at least qualitatively) deduce from them the existence and the properties of attracting sets, their basins, and their qualitative changes as the control parameters are let to vary, is the aim of the next chapters.

We will first consider the case of continuous time, then the case of discrete time by stressing the analogies and differences between these two time scales.

### 3 Continuous-time dynamical systems

In this chapter we will consider dynamic equations in the form (2), starting from problems with  $n = 1$ , i.e. 1-dimensional models where the state of the system is identified by a single dynamical variable, and then we move to  $n = 2$ . In both cases we will first consider linear models, for which an explicit expression of the solution  $\mathbf{G}$  can be obtained, and then we move to nonlinear models for which we will only give a qualitative description of the equilibrium points, their stability properties and the long-run (or asymptotic) properties of the solutions without giving their explicit expression. We will see that such qualitative study (also denoted qualitative or topological theory of dynamical system, a modern point of view developed in the 20<sup>th</sup> century) essentially reduces to the solution of equations and inequalities, without the necessity to use advanced methods and tools from calculus (essentially no integrals, only derivatives and basic algebra). As we will see, a very important role in this theory is played by graphical analysis, and a fruitful trade-off between analytic, geometric and numerical methods.

However, these methods built up a solid mathematical theory based on general theorems that can be found in the textbooks indicated in the references. Here we just give a sufficiently general (for the goals of these lecture notes) theorem of existence and uniqueness of solutions of ordinary differential equations

**Theorem (existence and uniqueness)** *If the functions  $f_i$  have continuous partial derivatives  $\frac{\partial f_i}{\partial x_k}$  in  $M$  and  $x(t_0) \in M$ , then there exists a unique solution  $x_i(t)$ ,  $i = 1, \dots, n$ , of the system (2) such that  $x(t_0) = \bar{x}$ , and each  $x_i(t)$  is a continuous function.*

Indeed, the assumptions of this theorem may be weakened, by asking for bounded variations of the functions  $f_i$  in the equations of motion (2), such as the so called Lipschitz conditions. However the assumptions of the previous Theorem are suitable for our purposes. Moreover, other general theorems are usually stated to define the conditions under which the solutions of the differential equations have a regular behavior. We refer the interested reader to more rigorous books, see the bibliography for details.

### 3.1 The simplest one: 1-dimensional linear dynamical system

Let us consider the following dynamic equation

$$\dot{x} = \alpha x, \quad \text{with initial condition } x(t_0) = x_0 \quad (6)$$

It states that the rate of growth of the dynamic variable  $x(t)$  is proportional to itself, with proportionality constant  $\alpha$  (a parameter). If  $\alpha > 0$  then whenever  $x$  is positive it will increase (positive derivative means increasing). Moreover, as  $x$  increases also the derivative increases, so it increases faster and so on. This is what, even in the common language, is called "exponential growth", i.e. "the more we are, the more we increase". Instead, whenever  $x$  is negative it will decrease (negative derivative) so it will become even more negative and so on... This is a typical unstable behaviour.

On the contrary, if  $\alpha < 0$  then whenever  $x$  is positive it will decrease (and will tend to become negative) whereas when  $x$  is negative the derivative is positive, so that  $x$  will increase and tend to become positive. A stabilizing behaviour.

In this case an explicit solution can be easily obtained to confirm these arguments. In fact, it is well known, from elementary calculus, that the only function whose derivative is proportional to the function itself is the exponential, so  $x(t)$  will be in the general form  $x(t) = ke^{\alpha t}$ , where  $k$  is an arbitrary constant that can be determined by imposing the initial condition  $x(t_0) = x_0$ , hence  $ke^{\alpha t_0} = x_0$ , from which  $k = x_0 e^{-\alpha t_0}$ . After replacing  $k$  in the general form we finally get the (unique) solution

$$x(t) = x_0 e^{\alpha(t-t_0)} \quad (7)$$

The same solution can be obtained by a more standard integration method, denoted as separation of the variables, shown in fig. 8. In this course we are not interested in the several (and interesting per se) tricks to find analytic solutions of particular classes of differential equations, however we will give a couple of them just to show how they work in the Appendix. Instead, we are mainly interested in the qualitative approach, that consists in the identification of the equilibrium points and their stability.

Some graphical representations of (7), with different values of the parameter  $\alpha$  and different initial conditions, are shown in fig. 9 in the form of integral curves, with time  $t$  represented along the horizontal axis and the state variable along the vertical one. Among all the possible solutions there is also an equilibrium solution, corresponding to the case of vanishing time derivative  $\dot{x} = 0$  (equilibrium condition). In fact, from (6) we can see that the equilibrium condition corresponds to the equation  $\alpha x = 0$  which, for  $\alpha \neq 0$ , gives the unique solution  $x^* = 0$ . Indeed, the trajectory starting from the initial condition  $x_0 = 0$  is given by  $x(t) = 0$  for each  $t$ , i.e. starting from  $x_0 = 0$  the system remains there forever. However, as shown in fig. 9, different behaviours of the system can be observed if the initial condition is slightly shifted from the equilibrium point, according to the sign of the parameter  $\alpha$ . In fact if  $\alpha > 0$  (left panel) then the system amplifies this slight perturbation and exponentially departs from the equilibrium (unstable, or repelling, equilibrium) whereas if  $\alpha < 0$  (right panel) then the system recovers from the perturbation going back to the equilibrium after a given return time (asymptotically stable, or attracting, equilibrium).

This qualitative analysis of existence and stability of the equilibrium can be obtained even without any computation of the explicit analytic solution (7), by solving the equilibrium equation  $\alpha x = 0$  and by a simple algebraic study of the sign of the right hand side of the dynamic equation (6) around the equilibrium, as shown in fig. 10. This method simply states that if the right hand side of the dynamic equation (hence  $\dot{x}$ ) is positive then the state variable increases (arrow towards positive direction of the axis), if  $\dot{x} < 0$  then  $x$  decreases (arrow towards negative direction).



$$\frac{dx}{dt} = rx \quad \text{con} \quad x(t_0) = x_0$$

$$\int_{x_0}^{x(t)} \frac{dx}{x} = \int_{t_0}^t r dt \quad \Longrightarrow \quad [\ln(x)]_{x_0}^{x(t)} = r[t]_{t_0}^t$$

$$\ln x(t) - \ln x_0 = r(t - t_0)$$

$$\ln \frac{x(t)}{x_0} = r(t - t_0) \quad \Longrightarrow \quad \frac{x(t)}{x_0} = e^{r(t-t_0)}$$

Figure 8:

This 1-dimensional representation (i.e. along the line) is the so called phase diagram of the dynamical system, where the invariant sets are represented (the equilibrium in this case) together with the arrows that denote tendencies associated with any point of the phase space (and consequently stability properties)

Of course, the knowledge of the explicit analytic solution gives more information, for example the time required to move from one point to another. For example, in the case  $\alpha < 0$ , corresponding to stability of the equilibrium  $x^* = 0$ , we can state that after a displacement of the initial condition at distance  $d = \|x_0 - x^*\|$  from the equilibrium, the time required to reduce such a perturbation at the fraction  $\frac{d}{e}$  (where  $e$  is the Neper constant  $e \simeq 2.7$ ) is  $T_r = -\frac{1}{\alpha}$ , an important stability indicator known as *return time*. As it can be seen, as the parameter  $\alpha$  goes to 0 the return time tends to infinity. In fact, if  $\alpha = 0$  all the points are equilibrium points, i.e. any initial condition generates a constant trajectory that remains in the same position forever.

As an example, let us consider the dynamic equation that describes the growth of a natural population. If  $x(t)$  represents the number of individuals in a population (of insects, or bacteria, or fishes or humans),  $n > 0$  represents the natality (or birth) rate and  $m > 0$  represents the mortality (or death) rate then a basic balance equation used in any population model states that

$$\dot{x} = nx - mx = (n - m)x$$

which is of the form (6) with  $\alpha = n - m$ . Of course in this case, due to the meaning of the model, only non-negative values of the state variable  $x$  are admissible. This equation is also known as the Malthusian model, from the work of T.R. Malthus "An essay of the principle of the population" (1798). The qualitative analysis of this model states that if natality is greater than mortality then the population exponentially increases, if the two rates are identical the population remains constant and if mortality exceeds natality the population exponentially goes to extinction. A quite reasonable

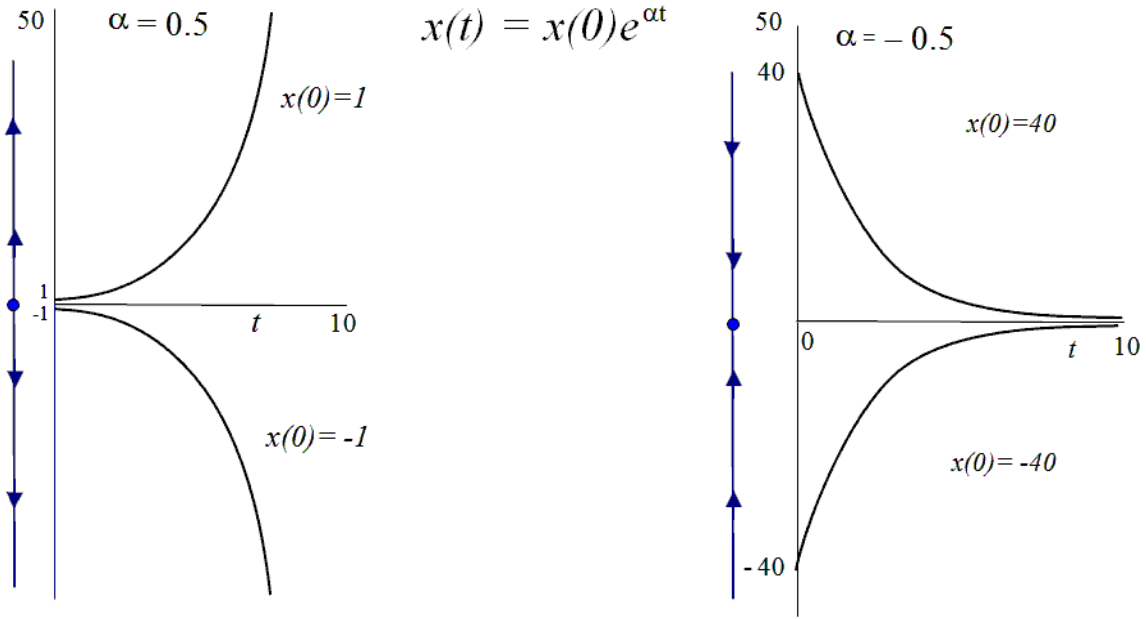


Figure 9:

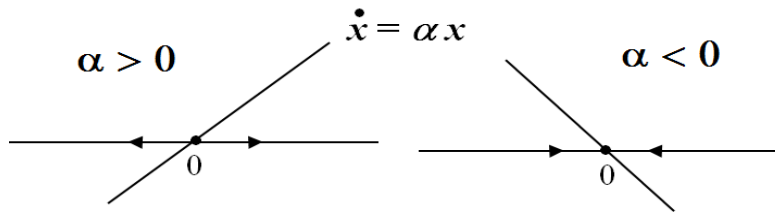


Figure 10: .

result.

We now introduce a modification in the simple population growth model by introducing a constant immigration (emigration) term  $b > 0$  ( $< 0$ )

$$\dot{x} = \alpha x + b \tag{8}$$

Now the equilibrium condition  $\dot{x} = 0$  becomes  $\alpha x + b = 0$  from which the equilibrium is  $x^* = -\frac{b}{\alpha}$ . If  $\alpha < 0$  and  $b > 0$  (endogenously decreasing population with constant immigration) then the equilibrium is positive and stable (as  $\dot{x} < 0$  for  $x > x^*$  and  $\dot{x} > 0$  for  $x < x^*$ , see fig. 11). Instead, for  $\alpha > 0$  and  $b < 0$  (endogenously increasing population with constant emigration) the equilibrium is positive and unstable.

We conclude by noticing that the dynamic model (8) is called linear non homogeneous (or affine) and can be reduced into the form (6) by a change of variable (a translation). In fact, let us define the new dynamic variable  $X = x - x^* = x + \frac{b}{\alpha}$ . This change of variable corresponds to a translation

that brings the new zero coordinate into the equilibrium point. If we replace  $x = X - \frac{b}{\alpha}$  into (8) we get  $\dot{X} = \alpha X$ . Then we have the linear model (6) in the dynamic variable  $X(t)$ , with initial condition  $X(t_0) = x_0 + \frac{b}{\alpha}$ , whose solution is  $X(t) = X(t_0)e^{\alpha(t-t_0)}$ . Going back to the original variable, by using the transformation  $X = x + \frac{b}{\alpha}$ , we obtain

$$x(t) = \left(x_0 + \frac{b}{\alpha}\right) e^{\alpha(t-t_0)} - \frac{b}{\alpha}.$$

This is a first example of conjugate dynamical systems, as the models (6) and (8) can be transformed one into the other by an invertible change of coordinates. We will give a more formal definition of conjugate (or qualitative equivalent) dynamic models in the following chapters.

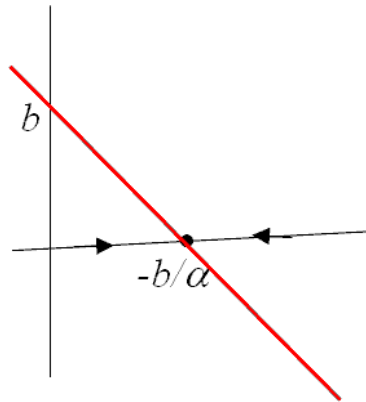


Figure 11:

Let us now consider a dynamic formalization of a partial market of a single commodity, under the Walrasian assumption that the price of the good increases (decreases) if the demand is higher (lower) than supply. The simplest dynamic equation to represent this assumption is given by

$$\dot{p} = f(p) = k [D(p) - S(p)] \quad (9)$$

where  $q = D(p)$  represents the demand function, i.e. the quantity demanded by consumers when the price of the good considered is  $p$ ,  $q = S(p)$  represents the supply function, i.e. the quantity of the good that producers send to the market when the price is  $p$ ,  $k > 0$  is a constant that gives the speed by which the price reacts to disequilibria between supply and demand. The standard occurrence is that supply function  $S(p)$  is increasing and demand function is decreasing, as shown in fig. 12. The equilibrium point  $p^*$  is located at the intersection of demand and supply curves, and it is stable because the derivative of  $p$  is positive on the left and negative on the right of  $p^*$ , so that  $p^*$  is always reached in the long run even if the initial price  $p(0)$  is not an equilibrium one (or equivalently if the price has been displaced from the equilibrium price). An analytic solution of the dynamic equations can be obtained under the assumption that demand and supply functions are linear

$$D(p) = a - bp ; S(p) = a_1 + b_1p$$

where all the parameters  $a, b, a_1, b_1$  are positive. In fact, in this case the dynamic equation is a linear differential equation with constant coefficients

$$\dot{p} = -k(b + b_1)p + k(a - a_1)$$

which is in the form (8) and has equilibrium point  $p^* = \frac{a-a_1}{b+b_1}$ . As we will see in the next sections, a similar analysis, based on the linearization of the model around the equilibrium point, is possible by computing the slopes of the functions (i.e. their derivatives) at the equilibrium point.

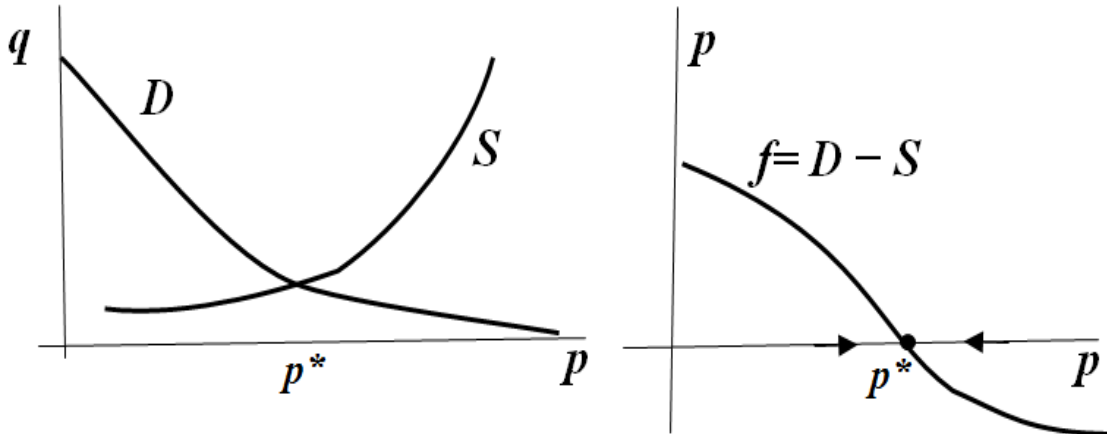


Figure 12: Price dynamics in the standard case.

Let us now consider a different demand curve, obtained by assuming that consumers exhibit a non-standard behaviour for intermediate prices. In the situation shown in fig. 13, even if demanded quantity is high for low prices and low for high prices, like in the standard case, we assume that for intermediate prices consumers prefer to buy the good at higher price because they use price as a quality indicator. Such assumption leads to a "bimodal" shape of the demand function (i.e. with two inversion points, a relative minimum and relative maximum) that may intersect the supply curve in three points, like in fig. 13, and consequently three coexisting equilibrium prices, say  $p_1^* < p_2^* < p_3^*$ . By using the qualitative analysis, we can see that the time derivative of the price  $p(t)$  is positive whenever  $p < p_1^*$  or  $p_2^* < p < p_3^*$ , i.e. where  $D(p) > S(p)$ . This leads to a situation of *bistability* as both the lowest equilibrium price  $p_1^*$  and the highest one  $p_3^*$  are asymptotically stable, each with its own basin of attraction, whereas the intermediate unstable equilibrium price  $p_2^*$  separates the basins, i.e. it acts as a watershed located on the boundary between the two basins.

### 3.2 Qualitative analysis and linearization procedure for the logistic model.

The population model described in the previous section is quite unrealistic as it admits unbounded population growth, which is impossible in a finite world. As already noticed by Malthus (1798), when the population density becomes too high, scarcity of food or space (overcrowding effect) causes mortality, proportional to the population density. So an extra mortality term, say  $sx$ , should be added to the natural mortality  $m$ , and thus the model becomes

$$\dot{x} = f(x) = nx - (m + sx)x = \alpha x - sx^2 \quad (10)$$

which is a nonlinear dynamic model. Also in this case, after separation of the variables, an analytic solution can be found by integrating a rational function. In fact, from  $\int_{x_0}^{x(t)} \frac{dx}{x(\alpha - sx)} = \int_0^t dt$  (notice that

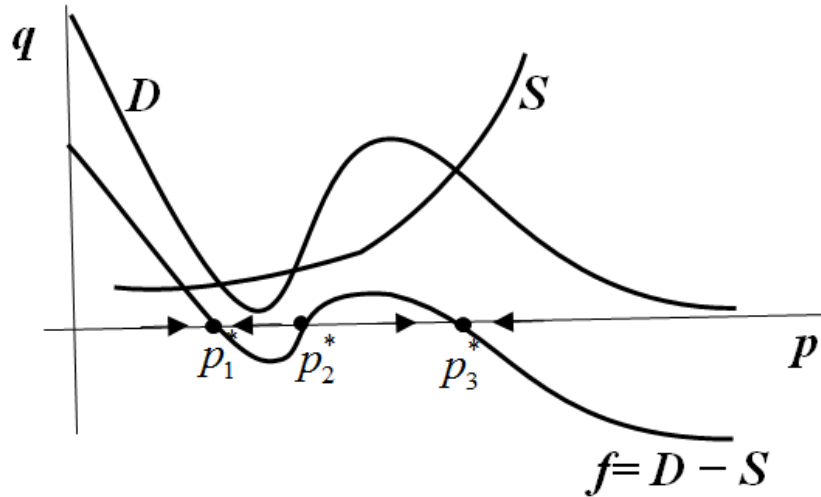


Figure 13: Price dynamics in the case with "snob" inversion in the demand function.

the initial condition  $x(0) = x_0$  has been imposed) after some algebraic transformations of the rational function the following solution is obtained

$$x(t) = \frac{\alpha x_0 e^{\alpha t}}{\alpha + s x_0 (e^{\alpha t} - 1)} \quad (11)$$

whose graph (for different initial conditions) is shown in fig. 14.

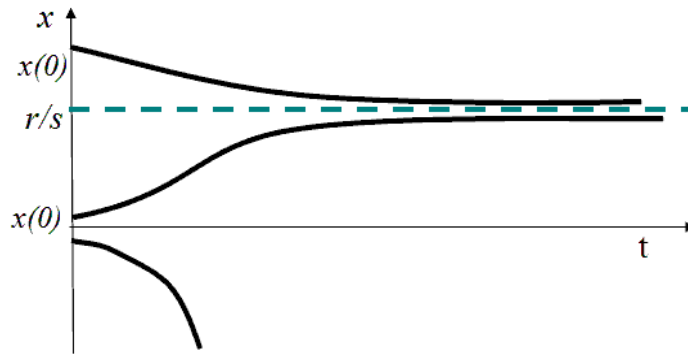


Figure 14: Integral curves for the logistic equation.

As it can be seen from the graph of  $x(t)$  in (11), all solutions starting from a positive initial condition asymptotically converge to the attracting equilibrium  $K = \frac{\alpha}{s}$  (usually called carrying capacity in the language of ecology) represented by the horizontal asymptote. Another equilibrium point exists, given by the extinction equilibrium  $Q = 0$ , which is repelling.

However, the possibility to find an analytic solution by integrating a nonlinear differential equation is a rare event, so we now try to infer the same conclusions without finding the explicit solution, i.e. by using qualitative methods. As usual, the first step is the localization of the equilibrium points,

solutions of the equilibrium condition  $\dot{x} = 0$ , i.e.  $f(x) = x(\alpha - sx) = 0$ , from which the two solutions  $x_0^* = 0$  and  $x_1^* = \frac{\alpha}{s}$  are easily computed. In order to determine their local stability properties, it is sufficient to notice that the graph of the right hand side of (10), see fig.15, has negative slope around the equilibrium  $x_1^*$ , so that  $\dot{x}$  is positive on the left and negative on the right, and vice-versa at the equilibrium  $x_0^*$ , as indicated by the arrows along the  $x$  axis (the 1-dimensional state space of the system). This can be analytically determined even without the knowledge of the whole graph of the function, as it is sufficient to compute the sign of the  $x$ -derivative of the right hand side at each equilibrium point. In fact, it is well known that the derivative computed in a given point of the graph represents the slope of the graph (i.e. of the line tangent to the graph) at that point. So, the local behaviour of the dynamical system in a neighborhood of an equilibrium point, hence its local stability as well, is generally the same as the one of the linear approximation (i.e. the tangent). This rough argument will be explained more formally in the next section. In the particular case of the logistic model (10) the derivative is  $\frac{df}{dx} = f'(x) = \alpha - 2sx$ , and computed at the two equilibrium points becomes  $f'(0) = \alpha > 0$ ,  $f'(\frac{\alpha}{s}) = -\alpha < 0$ , hence  $Q = 0$  is unstable,  $K = \frac{\alpha}{s}$  is stable. Moreover the parameter  $\alpha$  can be seen as an indicator of how fast the system will go back to the stable equilibrium after a small displacement, as the *return time* for the linear approximation is  $T_r = 1/\alpha$ .

Before ending this part, we notice that the equilibrium points  $x_0^* = 0$  and  $x_1^* = \frac{\alpha}{s}$  are two (constant) solutions of (10), whose graphs in the plane  $(t, x)$  are horizontal lines. Thus, by the theorem of existence and uniqueness of a solution stated above, any other (nonconstant) solution  $x(t)$  of (10) cannot cross these two horizontal lines. From (10) by a simple second-degree inequality, it is easy to see that  $\dot{x} > 0$  occurs whenever  $x \in (0, \frac{\alpha}{s})$ . Moreover, being  $\frac{d^2x}{dt^2} = \frac{d\dot{x}}{dt} = \alpha\dot{x} - 2s\dot{x}x = \dot{x}(\alpha - 2sx)$ , we deduce that  $x(t)$  is strictly decreasing and concave whenever  $x(0) \in (-\infty, 0)$  and that  $x(t)$  is strictly decreasing and convex whenever  $x(0) \in (\frac{\alpha}{s}, +\infty)$ . Finally, when  $x(0) \in (0, \frac{\alpha}{s})$ ,  $x(t)$  is strictly increasing and from convex becomes concave when  $x(t) = \frac{\alpha}{2s}$ , see again fig. 14.

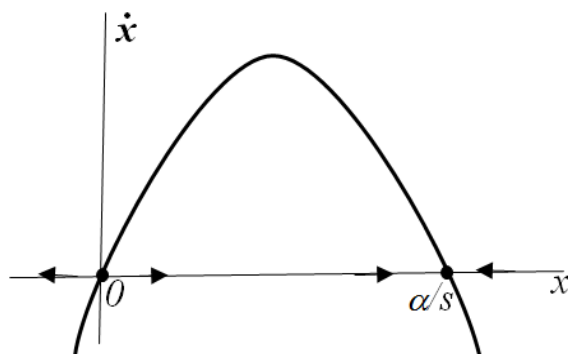


Figure 15: Right hand side of logistic equation (10).

### 3.3 Qualitative analysis of 1-dimensional nonlinear models in continuous time

The qualitative method used to understand the dynamic properties of the logistic equation can be generalized to any one-dimensional dynamic equation in continuous time

$$\dot{x} = f(x) \tag{12}$$

It consists, first of all, in the localization of the equilibrium points according to the equilibrium condition  $\dot{x} = 0$ , i.e. the solutions of the equation  $f(x) = 0$ .

As a consequence of the Theorem of uniqueness, oscillations are not possible for a 1-dimensional dynamical system in continuous time, hence for a system starting from any initial condition which is not an equilibrium, only increasing or decreasing solutions can be obtained. Hence just four different phase portraits characterize the dynamic behaviour of the 1-dimensional system around an equilibrium, as shown in fig.16

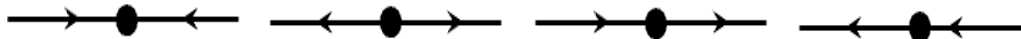


Figure 16: The four different kinds of local phase portraits around an isolated equilibrium point.

Of course, if an initial condition coincides with an equilibrium point, i.e.  $x(0) = x^*$  and  $f(x^*) = 0$ , then the unique solution is  $x(t) = x^*$  for  $t \geq 0$ . In other words, starting from an equilibrium point, the system remains there forever. The natural question arising is what happens if the initial condition is taken close to an equilibrium point, i.e. if the system is slightly perturbed from the equilibrium considered. Will the distance from the equilibrium increase or will the perturbation be reduced so that the system spontaneously goes back to the ordinary equilibrium? An answer to this question is easy in the case of hyperbolic equilibria, defined as equilibrium points with nonvanishing derivative, i.e.  $f'(x^*) \neq 0$ . In fact, if  $x^*$  is one of such solutions and  $f'(x^*) \neq 0$ , then the right hand side of (12) can be approximated by the first order Taylor expansion (linear approximation)

$$f(x) = f(x^*) + f'(x^*)(x - x^*) + o(x - x^*) = f'(x^*)(x - x^*) + o(x - x^*)$$

being  $f(x^*) = 0$ . So, if  $f'(x^*) \neq 0$  and we neglect the higher order terms then we obtain a *linear approximation* of the dynamical system (12). In fact, if we translate the origin of the  $x$  coordinate into the equilibrium point by the change of variable  $X = x - x^*$ , that represents the displacement between  $x(t)$  and the equilibrium points  $x^*$ , then (12) becomes

$$\dot{X} = \alpha X$$

with  $\alpha = f'(x^*)$ , i.e. a linear differential equation in the form (6), that governs the time evolution of the system in a neighborhood of the equilibrium point  $x^*$ . Of course, this linear differential equation constitutes only a local approximation, i.e. for initial conditions taken in a sufficiently small neighborhood of the equilibrium point considered. This leads to the following result:

**Proposition (1-dim. local asymptotic stability in continuous time).** *Let  $x^*$  be an equilibrium point of (12), i.e.  $f(x^*) = 0$ . If  $f'(x^*) < 0$  then  $x^*$  is a locally asymptotically stable equilibrium; if  $f'(x^*) > 0$  then  $x^*$  is unstable.*

This gives a simple method to classify the stability of an hyperbolic equilibrium. Instead, for a non-hyperbolic equilibrium, i.e. a point  $x^*$  such that  $f(x^*) = 0$  and  $f'(x^*) = 0$ , nothing can be said about the stability of  $x^*$ , and further investigations are necessary, involving higher order derivatives or, equivalently, the knowledge of the shape of the function  $f(x)$  around  $x^*$ . In fig.17 we can see, through four simple examples, that all possible phase portraits can be obtained around a non-hyperbolic equilibrium.

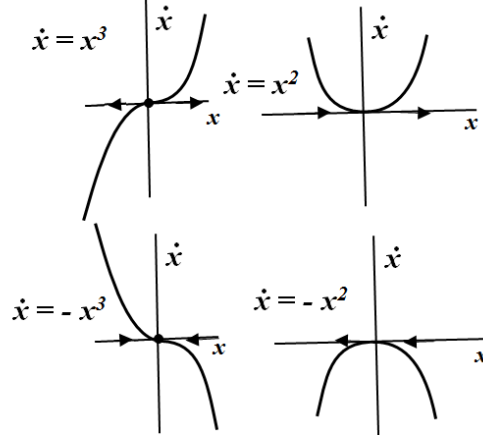


Figure 17: Four examples of different phase portraits around the non-hyperbolic equilibrium  $x^* = 0$  such that  $f(x^*) = 0$  and  $f'(x^*) = 0$ .

These situations characterized by a non-hyperbolic equilibrium point have been denoted as *structurally unstable*, in the sense that a slight (i.e. arbitrarily small) modification of the shape of the function  $f(x)$  generally leads to a modification in the stability property as well as in the number of equilibrium points. Such a modification may be caused by the presence of parameters that may be used as devices (or policies) to modify the shape of the function  $f$ . Such slight modifications leading to qualitatively different dynamic scenarios are denoted as *bifurcations*, and are described in the next section. To end this section we stress that the notion of structural stability should not be confused with that of dynamic stability: The latter deals with the effect on the trajectories of a small displacement of the initial condition (i.e. of the phase point), whereas the former deals with the effect, on the phase portrait (i.e. the dynamic scenario) of a slight modification of the function  $f$  due to a slight change of the value of a parameter.

Before giving a complete classifications of the bifurcations, we give some examples. Let us consider the case of a fishery with constant harvesting, i.e. a fish population  $x(t)$  characterized by a logistic growth equation, which is exploited for commercial purposes. Let us assume that in each time period a constant quota  $h$  is harvested. This leads to the following dynamic model

$$\dot{x} = x(\alpha - sx) - h \quad (13)$$

where the quota  $h$  is a parameter that indicates the policy imposed by an authority to regulate the fishing activity. The right hand side of the dynamic equation is a vertically translated parabola, as shown in fig. 18 with increasing values of  $h$ . The equilibrium points, determined by imposing the equilibrium condition  $x(\alpha - sx) - h = 0$ , are given by  $x_0^* = \frac{\alpha - \sqrt{\alpha^2 - 4hs}}{2s}$  and  $x_1^* = \frac{\alpha + \sqrt{\alpha^2 - 4hs}}{2s}$  provided that  $h < \frac{\alpha^2}{4s}$ . The qualitative analysis shows that the higher equilibrium  $x_1^*$  is stable, and gives the equilibrium value at which the harvested population settles, whereas the lower is unstable, and constitutes the boundary that separates the basin of attraction of  $x_1^*$  and the set of initial conditions leading to extinction. A sort of "survival threshold": If, due to some accident, the initial condition falls below  $x_0^*$  then the dynamics of the system will lead it to extinction. Moreover, if the harvesting



quota exceeds the value  $\frac{\alpha^2}{4s}$ , then the two equilibrium points merge and then disappear. This occurs when the graph of the right hand side of (13) is tangent to the horizontal axis: the two equilibria merge into a unique (non-hyperbolic) equilibrium. This is a bifurcation, after which no equilibrium exists and the only possible evolution is a decrease of population towards extinction.

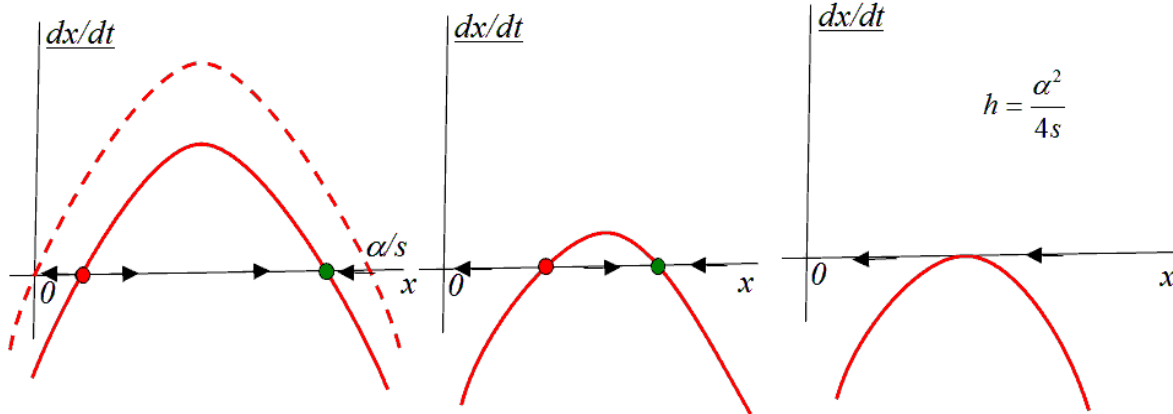


Figure 18: Example of fold bifurcation (or catastrophe) in the fishery with constant harvesting model.

This sequence of these dynamic situations, shown in fig. 18, are summarized in the diagram of fig. 19, called *bifurcation diagram*, where in the horizontal axis is represented the bifurcation parameter  $h$  and in the vertical axis are reported the equilibrium values, represented by a continuous line when stable and by a dashed line when unstable. As it can be seen, as far as  $h < \frac{\alpha^2}{4s}$  we observe only quantitative modifications, i.e. the stable equilibrium decreases and the unstable one increases (thus causing the shrinking of the basin of attraction), whereas at the bifurcation value an important qualitative change occurs, leading to the disappearance of the two equilibrium points and consequently to a completely different dynamic scenario. This is the essence of the concept of bifurcation, related to slight modifications of a parameter leading to a qualitatively different phase diagram. It is worth to notice that in this case the bifurcation occurring for increasing values of the "policy parameter"  $h$  is characterized by irreversibility (or hysteresis effect). In fact, if the harvesting quota  $h$  is gradually increased until it crosses the bifurcation point, then the fish population will decrease, see point  $A$  in fig. 19. At this stage, even if the parameter  $h$  is decreased to reach a pre-bifurcation value  $h < \frac{\alpha^2}{4s}$ , it may be not sufficient to bring the system back to the stable equilibrium, because the phase point is trapped below the survival threshold  $x_0^*$ .

### 3.4 Local bifurcations in 1-dimensional nonlinear models in continuous time

Two one-dimensional dynamical systems  $\dot{x} = f(x)$  and  $\dot{x} = g(x)$  are qualitatively equivalent if they have the same number of equilibrium points that orderly have, along the phase line, the same stability properties. This equivalence relation define classes of equivalent dynamical systems on the line, see e.g. the sketch represented in fig. 20. One of these dynamical systems is structurally stable if after a slight modification of the graph of the function at the right hand side, for example a small variation of a parameter, it remains in the same equivalence class. In other words, such small variation only causes quantitative modifications of the equilibrium points. Instead if an arbitrarily small modification causes a qualitative change in the number and/or in the stability properties of the equilibria, so that

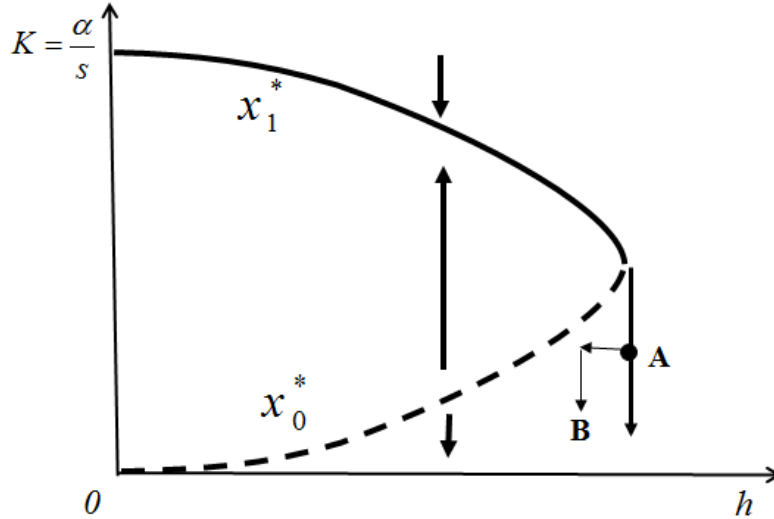


Figure 19: Bifurcation diagram with harvesting quota  $h$  as a bifurcation parameter. Hysteresis effect.

the system enters a different equivalence class, then a bifurcation occurs at the boundary between two equivalence classes, and the system is said structurally unstable when it is along the boundary. These bifurcation situations, i.e. these situations of structural instability, are characterized by the presence of one or more non-hyperbolic equilibrium points.

The kinds of bifurcations through which such qualitative changes occur can be classified into a quite limited number of categories.

### 3.4.1 Fold bifurcation.

This bifurcation is characterized by the creation of two equilibrium points, one stable and one unstable, as a parameter varies. Of course, if the same parameter varies in the opposite direction, at the bifurcation point two equilibrium points, one stable and one unstable, merge and then disappear. A canonical example is given by the dynamical system  $\dot{x} = f(x) = \mu - x^2$  as the parameter  $\mu$  varies through the bifurcation value  $\mu_0 = 0$  (see fig. 21, where the bifurcation diagram is shown as well). Notice that two equilibrium points  $x_{1,2}^* = \pm\sqrt{\mu}$  only exist for  $\mu \geq 0$ , and they are coincident  $x_{1,2}^* = 0$  for  $\mu = 0$  and non-hyperbolic, as  $f'(x) = -2x$  vanishes for  $x = 0$ . Instead, for  $\mu > 0$  the two equilibrium points are one stable and one unstable being  $f'(x_1^*) = f'(-\sqrt{\mu}) = 2\sqrt{\mu} > 0$  and  $f'(x_2^*) = f'(\sqrt{\mu}) = -2\sqrt{\mu} < 0$ . Of course, if we start our analysis from a positive value of the parameter  $\mu$  and decrease it until it reaches and crosses the bifurcation value  $\mu = 0$ , we observe two equilibrium points, one stable and one unstable that join at  $\mu = 0$  and then disappear. It is worth to notice that the unstable equilibrium represents the boundary of the basin of attraction of the stable one, so we may describe this bifurcation by saying that a stable equilibrium collides with the boundary of its basin and then disappears.

A model where this kind of bifurcation occurs is given in the previous section by the dynamical system (13) which describes a population with logistic growth and harvesting with fixed quotas.

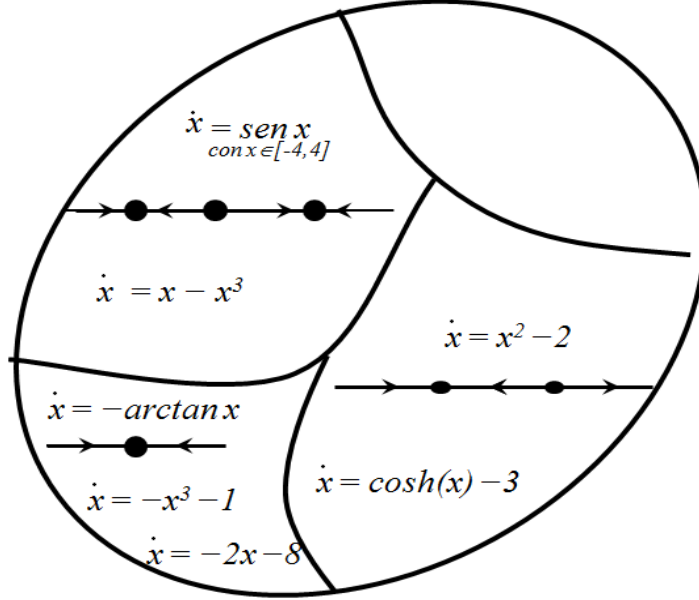


Figure 20:

### 3.4.2 Transcritical (or stability exchange) bifurcation.

This bifurcation is characterized by the existence of two equilibrium points, one stable and one unstable, that merge at the bifurcation point and after the bifurcation they still exist but both with opposite stability property, i.e. the once stable becomes unstable whereas the once unstable becomes stable. A canonical example is given by the dynamical system  $\dot{x} = f(x) = \mu x - x^2$  as the parameter  $\mu$  varies through the bifurcation value  $\mu_0 = 0$  (see fig. 22, where the bifurcation diagram is shown as well). Notice that two equilibrium points  $x_1^* = 0$  and  $x_2^* = \mu$  always exist: they are coincident  $x_{1,2}^* = 0$  for  $\mu = 0$  and non-hyperbolic, as  $f'(x) = \mu - 2x$  vanishes for  $\mu = 0$  and  $x = 0$ . As  $f'(x_1^*) = f'(0) = \mu$  and  $f'(x_2^*) = f'(\mu) = -\mu$ ,  $x_1^* = 0$  is stable for  $\mu < 0$  and unstable for  $\mu > 0$  whereas  $x_2^* = \mu$  is unstable for  $\mu < 0$  and stable for  $\mu > 0$ . So we can say that they merge at the bifurcation point and exchange their stability.

As an economic example let us consider a simplified version of the neoclassical model of Solow (1956)

$$\dot{k} = sy(k) - nk \quad (14)$$

where  $k = \frac{K}{L}$  represents the capital per unit of labour,  $y = \frac{Y}{L}$  is the production per labour unit,  $y(k)$  is the production function,  $s$  is the saving rate (or propensity to save) and  $n$  is the labour growth rate. The production function is increasing and concave:

$$y(0) = 0; \quad y'(k) > 0, \quad y''(k) < 0.$$

For suitable values of the parameters  $n$  and  $s$  two equilibrium points exist, such that  $sy(k) = nk$ , i.e. located at the intersections between the curve  $y(k)$  and the line of slope  $n$ , say  $k_0^* = 0$  and  $k^* > 0$ . If a critical value  $s_0$  exists such that  $sy'(0) = n$ , then it represents a transcritical bifurcation value, as schematically shown in fig. 23.

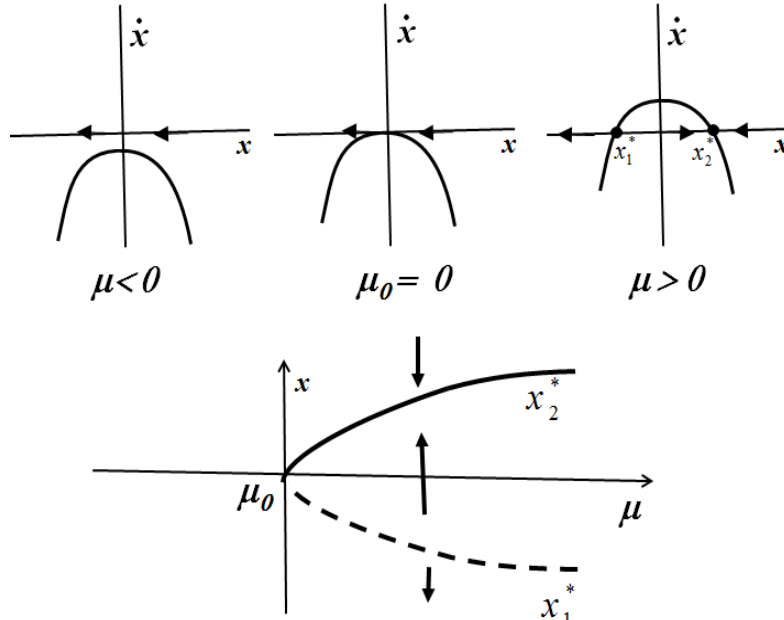


Figure 21: Fold bifurcation

### 3.4.3 Pitchfork bifurcation

This bifurcation is characterized by a transition from a single equilibrium point to three equilibria: the one already existing changes its stability property as the bifurcation parameter crosses the bifurcation point, and this leads to the simultaneous creation of two further equilibria. Of course, if the same parameter varies in the opposite direction, at the bifurcation point two equilibrium points merge and disappear and only the central one survives, even if it changes its stability property. A canonical example is given by the dynamical system  $\dot{x} = f(x) = \mu x - x^3$  as the parameter  $\mu$  varies through the bifurcation value  $\mu_0 = 0$  (see fig. 24, where the bifurcation diagram is shown on the left). Notice that the equilibrium points  $x_0^* = 0$  always exists, and two further ones,  $x_{1,2}^* = \pm\sqrt{\mu}$  for  $\mu \geq 0$ . All three are coincident  $x_0^* = x_{1,2}^* = 0$  for  $\mu = 0$ , thus giving a unique non-hyperbolic equilibrium at the bifurcation point. In fact, from  $f'(x) = \mu - 3x^2$  follows that  $f'(0) = \mu$ , hence  $x_0^*$  is stable for  $\mu < 0$  and unstable for  $\mu > 0$ . Instead, for  $\mu > 0$  the two newly born equilibrium points  $x_{1,2}^*$  are both stable being  $f'(\pm\sqrt{\mu}) = -\mu < 0$ . Of course, if we start our analysis from a positive value of the parameter  $\mu$  and decrease it until it reaches and cross the bifurcation value  $\mu = 0$ , we observe three equilibrium points, the one in the middle unstable and two stable at opposite sides, that join at  $\mu = 0$  and then disappear while the central one becomes stable. It is worth to notice that for  $\mu > 0$ , when three equilibrium points exist, a situation of two coexisting stable equilibria, each with its own basin of attraction, occurs. Moreover, the central (unstable) equilibrium represents the boundary that separates the two basins of attraction in this situation of bistability.

This kind of bifurcation is called *supercritical pitchfork bifurcation* in order to distinguish it from the *subcritical*, represented in the right portion of fig.24, where a unique unstable equilibrium becomes stable at the bifurcation value with the simultaneous creation of two unstable equilibrium points located at opposite sides, and constitutes the upper and lower boundary of the basin of attraction

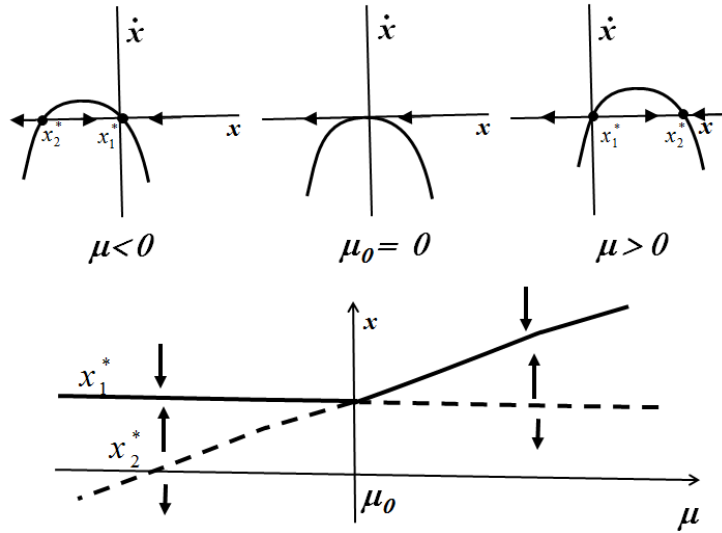


Figure 22: Transcritical bifurcation

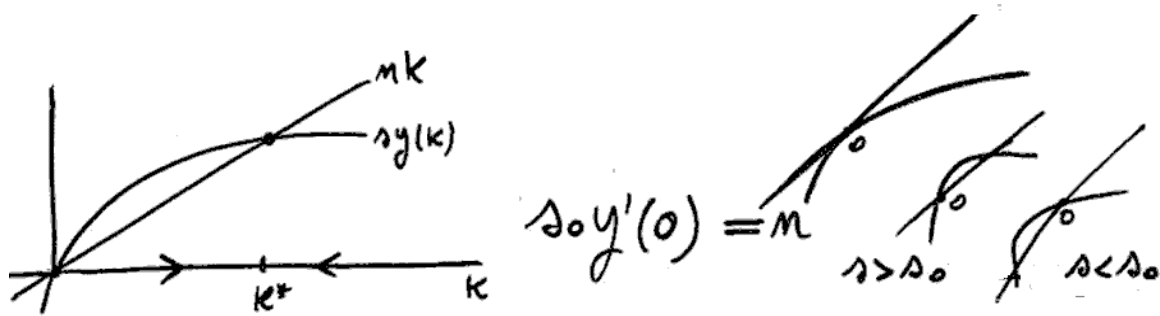


Figure 23:

of the central stable one. The canonical dynamical system that gives rise to a subcritical pitchfork bifurcation is  $\dot{x} = f(x) = x^3 - \mu x$ , as the parameter  $\mu$  is increased through the bifurcation value  $\mu_0 = 0$ .

As an economic example let us consider a simplified version of the Kaldor Model:<sup>2</sup>

$$\dot{Y} = \alpha [I(Y) - S(Y)] \quad (15)$$

where  $Y$  is the national income,  $I(Y)$  is the investment function and  $S(Y)$  represents the saving function. Kaldor's basic idea is that the marginal propensity  $I'(Y)$  is positive but varying so that it has an S-shaped graph as shown in fig. 25. This captures the fact that the propensity to invest has a given "normal" slope for intermediate values of income  $Y$  whereas its slope is lower for small values as well as high values of  $Y$ , due to missing opportunities to invest for low  $Y$  and because of decreasing economies of scale for too high income. This shape, associated to a linear saving function  $S = sY$ ,

<sup>2</sup>An extended version of this model is presented below.

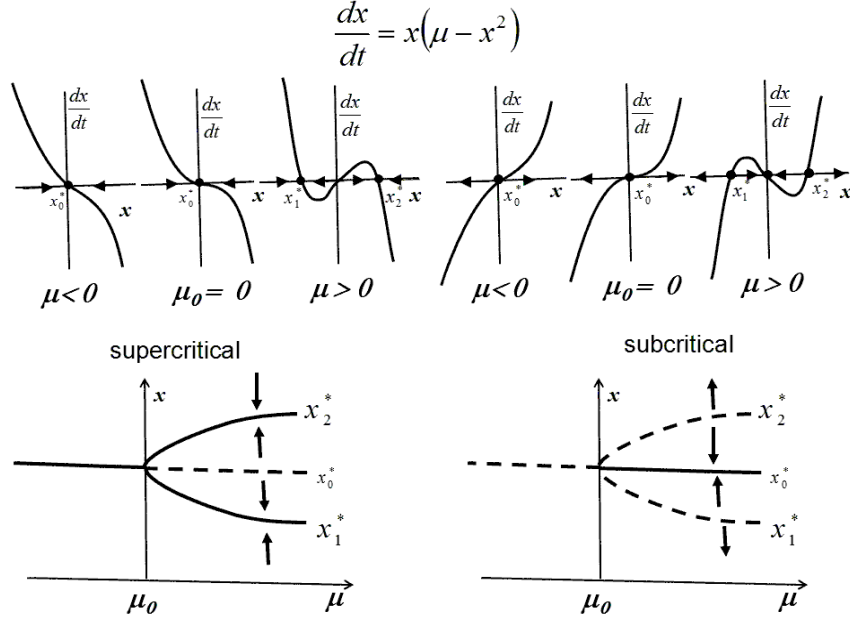


Figure 24: Supercritical (left) and subcritical (right) pitchfork bifurcation.

gives rise to one or three equilibrium points according to the slope  $s$ . If we fix the central (or normal) equilibrium and the investment function is symmetric with respect to this "central" equilibrium point, then a supercritical pitchfork bifurcation occurs for decreasing values of the slope  $s$ . For example, we can use the "sigmoidal" function  $\arctan()$  in order to imitate the shape of the "kaldorian" investment function

$$I(Y) = sY_c + \arctan(\beta(Y - Y_c)) \quad (16)$$

so that the two curves  $I(Y)$  and  $S(Y)$  intersect at the "normal" central equilibrium  $Y_c$ , and two further intersections appear for decreasing values of  $s$  through the pitchfork bifurcation value  $s_0 = \beta$ , where  $\beta$  represents a sensitivity parameter that measures how much investments increase as a consequence of increased income in a neighborhood of the central equilibrium  $Y_c$ .

## 4 Two-dimensional Dynamical Systems in continuous time

In this section we consider dynamic models of systems whose state is described by two variables, say  $x_1(t)$  and  $x_2(t)$ , which are interdependent, i.e. the time evolution of  $x_1(t)$ , expressed by its time derivative  $\dot{x}_1$ , can be influenced by itself and by  $x_2(t)$ , and the same holds for  $\dot{x}_2$ :

$$\begin{aligned} \dot{x}_1 &= f_1(x_1(t), x_2(t)) \\ \dot{x}_2 &= f_2(x_1(t), x_2(t)) \end{aligned} \quad (17)$$

A general method to get a qualitative global view of the phase portrait of a model in the form (17) is obtained by a representation, in the phase space  $(x_1, x_2)$ , of the two curves of equation  $f_1(x_1, x_2) = 0$  and  $f_2(x_1, x_2) = 0$ , usually called *nullclines* (see fig. 26). The points of intersection of these curves

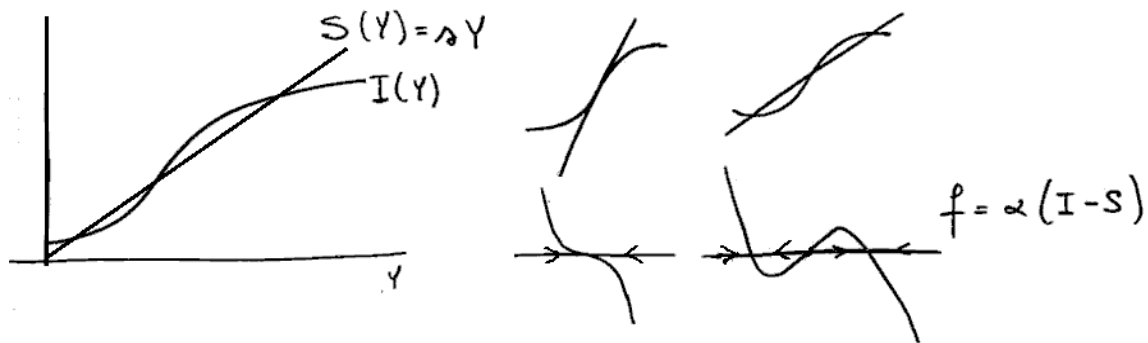


Figure 25:

are the equilibrium points, solutions of the following system of two equations with two unknowns

$$\begin{aligned} f_1(x_1, x_2) &= 0 \\ f_2(x_1, x_2) &= 0 \end{aligned} \tag{18}$$

Moreover, the two curves subdivide the phase plane into zones characterized by different signs of the time derivatives  $(\dot{x}_1, \dot{x}_2)$  as shown by the red arrows in fig. 26. The resulting directions (obtained by the usual graphical rule of vector sum) give a qualitative idea of the dynamics of the model in each region of the phase plane.

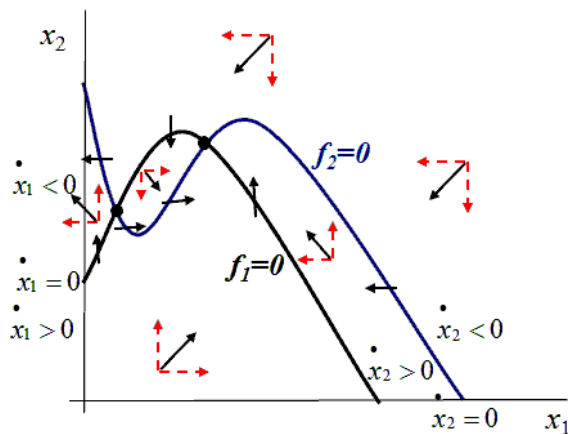


Figure 26: Nullclines and phasors in a qualitative sketch of a two-dimensional dynamical system in continuous time.

As an example of this method, let us consider the prey-predator model, also known as Lotka-

Volterra model<sup>3</sup>

$$\begin{aligned}\dot{x}_1 &= \alpha x_1 - s x_1^2 - b x_1 x_2 = x_1(\alpha - s x_1 - b x_2) \\ \dot{x}_2 &= -d x_2 + c x_1 x_2 = x_2(c x_1 - d)\end{aligned}\tag{19}$$

where  $x_1 = x_1(t)$  represents the numerosity (or the density) in a given region of a species (the prey) that feeds from the environment, and  $x_2 = x_2(t)$  represents the numerosity (or density) of predators that can only take nourishment from the prey population  $x_1$ . In the absence of predators ( $x_2 = 0$ ) the prey population evolves according to the usual logistic growth function, whereas in the absence of preys ( $x_1 = 0$ ) predators exhibit an exponential decay at rate  $d$  (mortality for starvation). The interaction term, proportional to the product  $xy$  under the assumption of random motion of prey and predators in the region considered (like in gas kinetics) has a negative effect on preys and positive on predators. This simple ecological model was proposed by the Italian mathematician Vito Volterra to explain the endogenous mechanism leading to oscillations in the fish harvesting observed in the Adriatic Sea.

Let us first consider the simpler case obtained by assuming  $s = 0$  (like in the first model proposed by Volterra). In this case, the nullcline  $\dot{x}_1 = 0$  is given by  $x_1 = 0$ , i.e. the vertical axis, or the horizontal line  $x_2 = \frac{\alpha}{b}$ , and the nullcline  $\dot{x}_2 = 0$  is given by  $x_2 = 0$ , i.e. the horizontal axis, or the vertical line  $x_1 = \frac{d}{c}$  (see fig. 27). The coordinate axes are trapping sets, i.e. any trajectory starting from an initial condition taken on the vertical axis  $x_1 = 0$  remains there (as the rate of change of  $x_1$  is  $\dot{x}_1 = 0$  on it) and the corresponding trajectory goes to 0, the exponential decline of predators in the absence of preys. Instead along the trapping horizontal axis  $x_2 = 0$  the prey population increases without any bound, as the term of overcrowding is neglected being in this case  $s = 0$ . In order to understand what happens starting from initial conditions interior to the positive orthant, i.e. from initial situations of coexistence of preys and predators, we represent the horizontal and vertical arrows with orientations according to the signs of  $\dot{x}_1$  and  $\dot{x}_2$  (see fig. 27). The directions of the phase vectors (also called *phasors*) clearly indicate a counterclockwise cyclic motion. This represents an oscillatory motion of both  $x_1(t)$  and  $x_2(t)$ , hence endogenous or self-sustained oscillations. This is an important result, because it states that a dynamic system can exhibit autonomous oscillations, without any oscillatory forcing term. In other words a system with interacting components can oscillate even if nobody shakes it from outside.

An intuitive explanation of this dynamic behaviour can be easily provided in the case of the prey-predator system modelled by Volterra. In fact, let us assume that at the initial time a few preys and a lot of predators are present, i.e. a small  $x_1$  value and a large  $x_2$  value, an initial state located in the upper-left quadrant of the phase space. In this case predators suffer for scarcity of food, and their number will decline. After this decline a few predators remain and preys will increase because of low predatory pressure. After this preys' population increase predators will have plenty of available food and consequently their population will increase, and this will lead to severe predatory pressure and thus a decay in preys' population. So, we again find the system in a situation with a few preys and a lot of predators, and the same process will be repeated, thus giving the cyclic time evolution.

Some trajectories starting from different initial conditions are shown in the left panel of fig. 28, whereas the versus time representation of a typical trajectory can be seen in the right panel. Of course, the trajectory starting from the positive equilibrium point  $E = \left(\frac{d}{c}, \frac{\alpha}{b}\right)$ , located at the intersection of

<sup>3</sup>Lotka, A.J., "Analytical Note on Certain Rhythmic Relations in Organic Systems", Proc. Natl. Acad. Sci. U.S., 6, 410–415, (1920).

Volterra, V., "Variazioni e fluttuazioni del numero d'individui in specie animali conviventi", Mem. Acad. Lincei Roma, 2, 31–113, (1926)



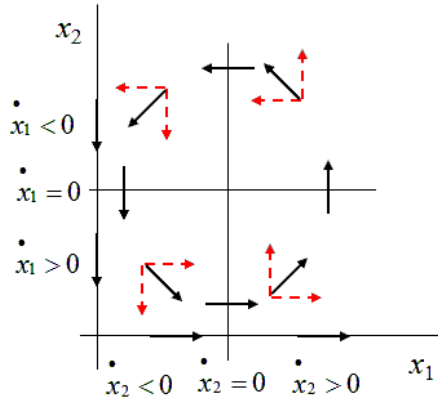


Figure 27: Phasors for the classical prey-predator Volterra model.

two nullclines, will remain there forever. However, if a perturbation causes a shift of the phase point from  $E$  then endless oscillations will start, with greater amplitude according to the distance of the initial condition (i.e. the entity of the shift) from the equilibrium point. Of course also  $O = (0, 0)$  is an equilibrium point, located at the intersections of the nullclines that coincide with the coordinate axes. A classification of these equilibrium points will be proposed in the next section.

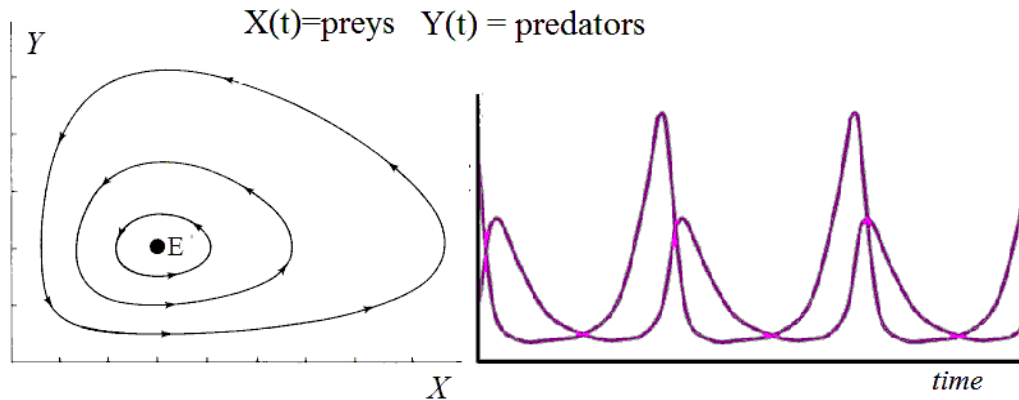


Figure 28: Trajectory represented as a phase curve (left) and versus time (right) in the prey-predator Volterra classical model.

One may wonder what happens if the overcrowding parameter  $s > 0$ , i.e. the prey population alone follows a logistic growth. In this case the prey nullcline has equation  $\alpha - sx_1 - bx_2 = 0$ , i.e. it is a tilted line with negative slope (see fig.29). It is not easy to understand how the trajectories change by the qualitative method of nullclines and phasors. A numerical representation of a typical trajectory in the phase plane as well as the corresponding time paths  $x_1(t)$  and  $x_2(t)$  are shown in fig.29; however a more detailed analysis will be possible with the methods described in the next sections.

We end this section by stressing the fact that endogenous oscillations are a well known phenomenon in a capitalistic economy, where up and down patterns have been (and currently are) observed in the main macroeconomic indicators. As we will see in more details later in these lecture notes, the

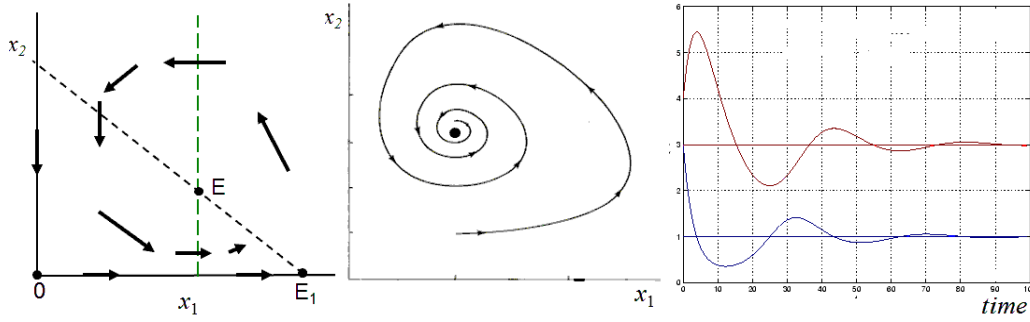


Figure 29: Prey-predator model with logistic growth of the preys.

same dynamic equations proposed by Volterra to describe the time evolution of preys' and predators' populations have been used (with founded motivations) by the economist Richard Goodwin in 1967 to represent endogenous business cycles, by using salaries and occupation as dynamic variables. This is an example of how dynamic models can be usefully applied in different fields.

#### 4.1 Linear systems

Following the same path as for the one-dimensional case, let us first of all consider a linear homogeneous system of two differential equations of first order (i.e. involving only the first derivative of the dynamic variables) with constant coefficients in the (normal) form:

$$\begin{cases} \dot{x}_1 = a_{11}x_1(t) + a_{12}x_2(t) \\ \dot{x}_2 = a_{21}x_1(t) + a_{22}x_2(t) \end{cases} \quad (20)$$

This linear system can be written in matrix form

$$\dot{\mathbf{x}} = \mathbf{A}\mathbf{x} \quad (21)$$

where

$$\mathbf{A} = \begin{pmatrix} a_{11} & a_{12} \\ a_{21} & a_{22} \end{pmatrix}; \quad \mathbf{x}(t) = \begin{pmatrix} x_1(t) \\ x_2(t) \end{pmatrix}; \quad \dot{\mathbf{x}}(t) = \begin{pmatrix} \dot{x}_1(t) \\ \dot{x}_2(t) \end{pmatrix}$$

The aim of this section is to show a procedure to find the solutions of this system that reduces to a very simple algebraic method that essentially consists in the solution of a second degree algebraic equation (in the field of complex numbers).

However, before stating this result, we outline the arguments at the basis of the proof.

An important general property of a linear system of ordinary differential equations is that given two solutions, say

$$\boldsymbol{\varphi}(t) = \begin{pmatrix} \varphi_1(t) \\ \varphi_2(t) \end{pmatrix} \quad \text{and} \quad \boldsymbol{\psi}(t) = \begin{pmatrix} \psi_1(t) \\ \psi_2(t) \end{pmatrix}$$

any linear combination of them

$$\mathbf{y}(t) = \alpha\boldsymbol{\varphi}(t) + \beta\boldsymbol{\psi}(t), \quad \text{with } \alpha, \beta \in \mathbb{R} \quad (22)$$

is a solution of (20) as well. In fact, assuming that both  $\varphi(t)$  and  $\psi(t)$  satisfy (21) being them solutions, we obtain

$$\dot{\mathbf{y}} = \alpha \dot{\varphi} + \beta \dot{\psi} = \alpha \mathbf{A}\varphi + \beta \mathbf{A}\psi = \mathbf{A}(\alpha\varphi + \beta\psi) = \mathbf{A}\mathbf{y}$$

so that also  $\mathbf{y}(t)$  is a solution. This means that the set of all the solutions, obtained with different "weights"  $\alpha$  and  $\beta$  in the linear combination, is a vector space. Moreover, it is possible to prove that it has dimension 2, i.e. all the solutions can be generated as linear combinations of just two independent solutions, that form a base of the vector space. The definition of independent solutions is the usual one: given two solutions, say again  $\varphi(t)$  and  $\psi(t)$ , they are independent if  $\alpha\varphi(t) + \beta\psi(t) = \mathbf{0} \forall t$  implies  $\alpha = \beta = 0$ . In order to check such independence it is possible to use the Wronskian determinant

$$W(t) = \det \begin{pmatrix} \varphi_1(t) & \psi_1(t) \\ \varphi_2(t) & \psi_2(t) \end{pmatrix} = \varphi_1(t)\psi_2(t) - \psi_1(t)\varphi_2(t)$$

If  $W(t) \neq 0$  for at least a  $t$  value, then the two solutions  $\varphi(t)$  and  $\psi(t)$  are independent. In fact, it is possible to prove that only one of the following is true:  $W(t) = 0 \forall t$  or  $W(t) \neq 0 \forall t$ . Hence it is sufficient to check it for just one value of  $t$ , for example  $W(0) \neq 0$ .

So, in order to find the general solution (i.e. all the possible solutions) of (20) it is sufficient to find just two of them which are independent. Then the general solution will be in the form (22) and, by imposing an initial conditions  $x_1(0), x_2(0)$  the two constants  $\alpha$  and  $\beta$  can be uniquely determined by solving the following linear algebraic system

$$\alpha \begin{pmatrix} \varphi_1(0) \\ \varphi_2(0) \end{pmatrix} + \beta \begin{pmatrix} \psi_1(0) \\ \psi_2(0) \end{pmatrix} = \begin{pmatrix} \varphi_1(0) & \psi_1(0) \\ \varphi_2(0) & \psi_2(0) \end{pmatrix} \begin{pmatrix} \alpha \\ \beta \end{pmatrix} = \begin{pmatrix} x_1(0) \\ x_2(0) \end{pmatrix}$$

which is a linear system whose coefficient matrix is nonsingular, being  $W(0) \neq 0$  its determinant.

In the following we show a direct method to find two independent solutions. Following again the same arguments as in the one-dimensional case, let us propose a "trial solution" in exponential form, i.e.

$$x_i(t) = v_i e^{\lambda t}, \quad i = 1, 2 \quad (23)$$

As  $\dot{x}_1(t) = \lambda v_1 e^{\lambda t}$  and  $\dot{x}_2(t) = \lambda v_2 e^{\lambda t}$ , after replacing this trial solution into (20) we get

$$\begin{cases} \lambda v_1 e^{\lambda t} = a_{11} v_1 e^{\lambda t} + a_{12} v_2 e^{\lambda t} \\ \lambda v_2 e^{\lambda t} = a_{21} v_1 e^{\lambda t} + a_{22} v_2 e^{\lambda t} \end{cases}$$

and after simplification of all the identical exponential it becomes

$$\begin{cases} (a_{11} - \lambda)v_1 + a_{12}v_2 = 0 \\ a_{21}v_1 + (a_{22} - \lambda)v_2 = 0 \end{cases} \quad \text{or} \quad (\mathbf{A} - \lambda\mathbf{I}) \mathbf{v} = \mathbf{0} \quad (24)$$

an algebraic linear homogeneous system with unknowns  $v_1$  and  $v_2$  and parameter  $\lambda$ . This homogeneous systems has non-trivial solutions (i.e. solutions different from  $(0, 0)$ ). provided that

$$\det \left( \begin{bmatrix} a_{11} - \lambda & a_{12} \\ a_{21} & a_{22} - \lambda \end{bmatrix} \right) = 0. \quad \text{or} \quad \det(\mathbf{A} - \lambda\mathbf{I}) = 0$$

This condition can be expressed in the form of the "characteristic equation"

$$\lambda^2 - Tr(A)\lambda + Det(A) = 0 \quad (25)$$

where  $Tr(A) = a_{11} + a_{22}$  (the sum of diagonal elements of the matrix  $\mathbf{A}$ ) and  $Det(A) = a_{11}a_{22} - a_{12}a_{21}$  (the determinant of the matrix  $\mathbf{A}$ ).

This is a standard problem of linear algebra, known as eigenvalue problem. In fact, in matrix form it can be expressed as

$$\mathbf{A}\mathbf{v} = \lambda\mathbf{v} \quad \text{with } \mathbf{v} \neq \mathbf{0} \quad \text{and } \lambda \in \mathbb{C}$$

i.e. the linear operator  $\mathbf{A}$ , applied to the vector  $\mathbf{v}$ , gives a vector  $\lambda\mathbf{v}$  proportional to it, let's say in the same direction. The real number  $\lambda$  is called *eigenvalue* and the solution vector  $\mathbf{v}$  *eigenvector*.

To sum up,  $\mathbf{v}e^{\lambda t}$  is a solution of (20) if and only if  $[\mathbf{A} - \lambda\mathbf{I}]\mathbf{v} = 0$ , i.e.  $\lambda$  is an eigenvalue of  $\mathbf{A}$  with corresponding eigenvector  $\mathbf{v} \neq \mathbf{0}$ , i.e.  $\det[\mathbf{A} - \lambda\mathbf{I}] = 0$  or, equivalently, if  $\lambda$  satisfies the characteristic equation (25). This reduces the problem of finding two independent solutions of (20) to the computation of two solutions of the second degree algebraic equation (25). According to the sign of the discriminant of the characteristic equation,  $Tr(A)^2 - 4Det(A)$ , we can have two real distinct, two real coincident or two complex conjugate eigenvalues. This will give rise to different kinds of phase portraits, as explained below (see also fig. 30 and 31).

1. If we have two real, distinct and negative eigenvalues  $\lambda_2 < \lambda_1 < 0$ , i.e.  $Tr(A)^2 - 4\det(A) > 0$  with  $Tr(A) < 0$  and  $Det(A) > 0$ , then the two independent solutions are  $\mathbf{v}_1e^{\lambda_1 t}$  and  $\mathbf{v}_2e^{\lambda_2 t}$ , both decreasing to 0 as  $t \rightarrow \infty$ . The general solution is

$$\mathbf{x}(t) = c_1\mathbf{v}_1e^{\lambda_1 t} + c_2\mathbf{v}_2e^{\lambda_2 t} \quad (26)$$

where the two constants  $c_1$  and  $c_2$  are uniquely determined according to the initial condition  $x(0) = (x_1(0), x_2(0))$ . The corresponding phase diagram is represented in fig. 30 and the asymptotically stable equilibrium is called *stable node* (or *sink*)

2. If we have two real, distinct and positive eigenvalues  $\lambda_1 > \lambda_2 > 0$ , i.e.  $Tr(A)^2 - 4\det(A) > 0$  with  $Tr(A) > 0$  and  $Det > 0$ , then the two independent solutions are  $\mathbf{v}_1e^{\lambda_1 t}$  and  $\mathbf{v}_2e^{\lambda_2 t}$ , both increasing to  $\infty$  as  $t \rightarrow \infty$ . The general solution is again of the form (26), the corresponding phase diagram is represented in fig. 30 and the unstable equilibrium  $(0, 0)$  is called *unstable node* (or *source*).
3. If we have two real distinct eigenvalues of opposite sign,  $\lambda_2 < 0 < \lambda_1$ , i.e.  $Tr(A)^2 - 4\det(A) > 0$  with  $Det < 0$ , then the two independent solutions  $\mathbf{v}_1e^{\lambda_1 t}$  and  $\mathbf{v}_2e^{\lambda_2 t}$  are one increasing to  $\infty$  and one decreasing to 0 as  $t \rightarrow \infty$ . The corresponding phase diagram is represented in fig. 30 and the unstable equilibrium  $(0, 0)$  is called *saddle*. Notice that an invariant line exists, called *stable manifold* (along the direction indicated by the eigenvector  $\mathbf{v}_2$  associated with the negative eigenvalue, whereas the line along the eigenvector  $\mathbf{v}_1$ , associated to the positive eigenvalue, is referred to as the *unstable manifold*), on which the dynamics is asymptotically convergent to the equilibrium  $(0, 0)$ . Nevertheless the equilibrium is unstable, and the kind of notion around it may even be misleading, as the generic trajectory first moves towards it (so that it may look as a convergent trajectory) whereas it then turns away from the equilibrium.
4. If we have two coincident and negative eigenvalues  $\lambda_1 = \lambda_2 = \lambda < 0$  (and consequently  $\mathbf{v}_1 = \mathbf{v}_2 = \mathbf{v}$ ), i.e.  $Tr(A)^2 - 4\det(A) = 0$  with  $Tr < 0$ , then two independent solutions are  $\mathbf{v}e^{\lambda t}$  and  $t\mathbf{v}e^{\lambda t}$ , both converging to 0 as  $t \rightarrow \infty$ , and the general solution becomes

$$\mathbf{x}(t) = c_1\mathbf{v}e^{\lambda t} + c_2t\mathbf{v}e^{\lambda t} \quad (27)$$

The corresponding phase diagram is represented in fig. 30 and the stable equilibrium  $(0, 0)$  is called *stable improper node* (or *stable star node* in particular symmetric situations).

5. If we have two coincident and positive eigenvalues  $\lambda_1 = \lambda_2 = \lambda > 0$  (and consequently  $\mathbf{v}_1 = \mathbf{v}_2 = \mathbf{v}$ ), i.e.  $Tr(A)^2 - 4\det(A) = 0$  with  $Tr > 0$ , then we have the same general solution and the corresponding phase diagram is obtained from the previous one just reversing the arrows and is called *unstable improper node* (or *unstable star node* in particular symmetric situations).

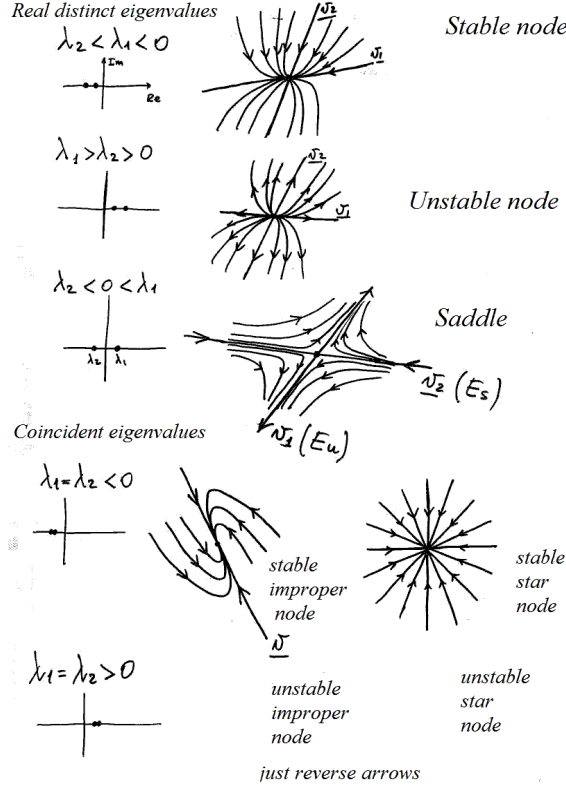


Figure 30: Local phase portraits with real eigenvalues.

6. If  $Tr(A)^2 - 4\det(A) < 0$  we have two complex conjugate eigenvalues  $\lambda_1 = a + ib$  and  $\lambda_2 = a - ib$ , where  $a = \text{Re}(\lambda) = \frac{Tr(A)}{2}$  is the real part and  $b = \text{Im}(\lambda) = \frac{\sqrt{4\text{Det}(A) - Tr(A)^2}}{2}$  is the imaginary part. Again two independent solutions are  $\varphi(t) = \mathbf{v}_1 e^{\lambda_1 t}$  and  $\bar{\varphi}(t) = \mathbf{v}_2 e^{\lambda_2 t}$ , with both the eigenvalues as well as the corresponding eigenvectors complex. However,  $\bar{\varphi}(t)$  is the complex conjugate of  $\varphi(t)$ , and we can write them in trigonometric form

$$\varphi(t) = \mathbf{v}_1 e^{at} (\cos(bt) + i \sin(bt)) \quad \text{and} \quad \bar{\varphi}(t) = \bar{\mathbf{v}}_1 e^{at} (\cos(bt) - i \sin(bt)).$$

As any linear combination of two solutions is again a solution of (20) we can obtain two independent real solutions in the form

$$\begin{aligned} \frac{1}{2} (\varphi(t) + \bar{\varphi}(t)) &= \text{Re } \varphi(t) = (\text{Re } \mathbf{v}_1) e^{at} \cos(bt) \\ \frac{1}{2i} (\varphi(t) - \bar{\varphi}(t)) &= \text{Im } \varphi(t) = (\text{Im } \mathbf{v}_1) e^{at} \sin(bt) \end{aligned}$$

So, the general solution can be written in the form

$$\mathbf{x}(t) = e^{at} [c_1 (\text{Re } \mathbf{v}_1) \cos(bt) + c_2 (\text{Im } \mathbf{v}_1) \sin(bt)] \quad (28)$$

from which we can see that the part inside square brackets causes oscillations around the equilibrium  $(0,0)$  whereas the exponential term outside the square brackets determines the expanding or contracting nature of the oscillations: if  $a < 0$ , i.e.  $Tr(A) < 0$ , then the oscillations exhibit decreasing amplitude and converge to the equilibrium  $(0,0)$ , if  $a > 0$ , i.e.  $Tr(A) > 0$ , then the oscillations increase in amplitude and diverge. Finally, if  $a = 0$ , i.e.  $Tr(A) = 0$ , then the oscillations are of constant amplitude. The corresponding phase diagrams are represented in fig. 31, and the corresponding phase diagrams are denoted as *stable focus* (or *stable spiral*), *unstable focus* (or *unstable spiral*) and *centre* respectively. Notice that the case of complex eigenvalues is the first one giving oscillations, and the imaginary part of the eigenvalues  $b = \frac{\sqrt{4Det(A)-Tr(A)^2}}{2}$  determines the time required to complete a whole oscillation, given by  $T = \frac{2\pi}{b}$ .

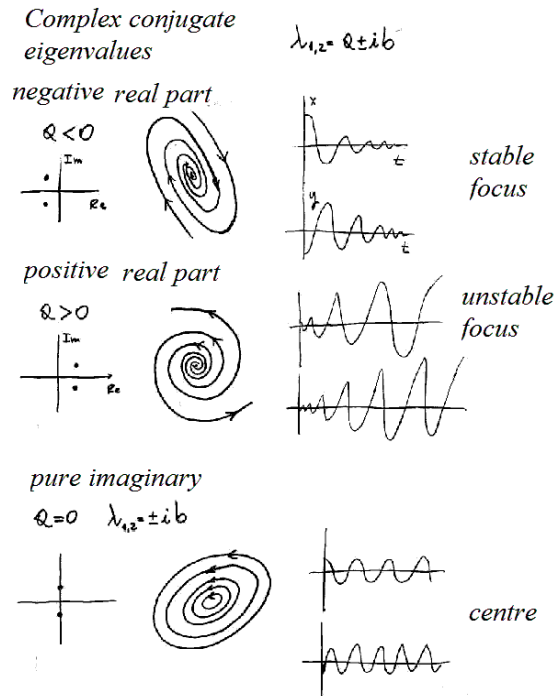


Figure 31: Local phase portraits with complex eigenvalues.

To summarize all these cases it is useful to represent the trace  $Tr(A)$  and the determinant  $Det(A)$  on the coordinate axes of a cartesian plane (see fig. 32), together with the curve of equation  $Tr(A)^2 - 4Det(A) = 0$  (a parabola with vertex in the origin of the axes). Above the parabola we have  $Tr(A)^2 - 4Det(A) < 0$ , hence oscillatory behaviour, below it we have  $Tr(A)^2 - 4Det(A) > 0$ , so we have nodes and saddles according to the sign of  $Det(A)$ .

**Remark (important)** *It is worth to notice that asymptotic stability of the unique equilibrium occurs only in the quadrant with  $Tr(A) < 0$  and  $Det(A) > 0$ . Moreover, in this case of linear dynamic models the local asymptotic stability is equivalent to global asymptotic stability, i.e. if the equilibrium is stable it attracts all the initial conditions  $(x_1(0), x_2(0)) \in R^2$ . Instead, when the equilibrium is unstable, then all the initial conditions starting outside the equilibrium generate diverging trajectories.*

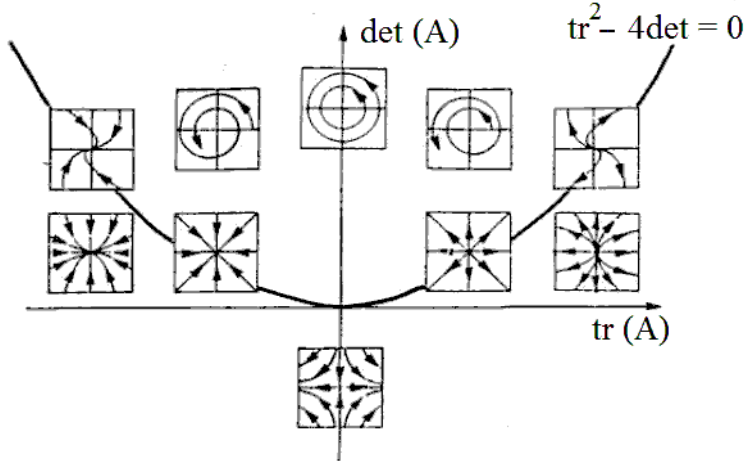


Figure 32: Different phase portraits in the Trace-Determinant diagram.

Some other particular cases can be noticed. For example, if  $Det(A) \neq 0$  then the linear homogeneous algebraic system to obtain the equilibrium points  $\mathbf{Ax} = \mathbf{0}$  has the unique solution  $(0, 0)$ , whereas if  $Det(A) = 0$  then infinitely many equilibrium points exist, located along a line through the origin. These equilibria are non-hyperbolic being one of the eigenvalues equal to zero. Even in the case of  $Tr(A) = 0$  and  $Det(A) > 0$  the equilibrium point is denoted as non-hyperbolic as the real part of the eigenvalues vanishes. These will identify the bifurcation cases when dealing with 2-dimensional nonlinear dynamic models (in continuous time) that depend on a bifurcation parameter.

#### 4.1.1 Some example of computations of explicit solutions for linear models

Let us consider, as an example

$$\begin{cases} \dot{y}(t) = 2y(t) - 2z(t) \\ \dot{z}(t) = -3y(t) + z(t) \end{cases}$$

that can be interpreted as a positive influence of self-interactions, i.e. each state variable increases its rate of growth, and a negative influence of cross-interactions, i.e. each state variable inhibits the rate of growth of the other one. In matrix form it becomes:

$$\begin{bmatrix} \dot{y}(t) \\ \dot{z}(t) \end{bmatrix} = \begin{bmatrix} 2 & -2 \\ -3 & 1 \end{bmatrix} \begin{bmatrix} y(t) \\ z(t) \end{bmatrix}$$

As the trace of the matrix is  $Tr = 3$  and the determinant is  $Det = -4$ , on the basis of the analysis given above we deduce that the eigenvalues are both real and with opposite sign. In fact, the characteristic equation  $\lambda^2 - 3\lambda - 4 = 0$  has solutions  $\lambda_1 = -1$ ,  $\lambda_2 = 4$ . So, we can immediately conclude the qualitative analysis by saying that the equilibrium  $O = (0, 0)$  is a saddle.

In order to get the explicit expression of the solutions, we need to compute the corresponding eigenvectors:

$$\lambda_1 = -1 : \begin{bmatrix} 2 - \lambda_1 & -2 \\ -3 & 1 - \lambda_1 \end{bmatrix} \begin{bmatrix} v_1^1 \\ v_1^2 \end{bmatrix} = \begin{bmatrix} 0 \\ 0 \end{bmatrix} \Rightarrow \begin{bmatrix} 3 & -2 \\ -3 & 2 \end{bmatrix} \begin{bmatrix} v_1^1 \\ v_1^2 \end{bmatrix} = \begin{bmatrix} 0 \\ 0 \end{bmatrix}$$

As expected, this is a linear homogeneous algebraic system with two unknowns and rank=1, so  $\infty^1$  solutions exist such that  $3v_1^1 - 2v_2^1 = 0$ , i.e. in the form  $\mathbf{v}_1 = \begin{bmatrix} v_1^1 \\ v_2^1 \end{bmatrix} = \begin{bmatrix} 1 \\ 3/2 \end{bmatrix}$  obtained by choosing  $v_1^1 = 1$ . Analogously, for the other eigenvalue we have

$$\lambda_2 = 4 : \begin{bmatrix} 2 - \lambda_2 & -2 \\ -3 & 1 - \lambda_2 \end{bmatrix} \begin{bmatrix} v_2^1 \\ v_2^2 \end{bmatrix} = \begin{bmatrix} 0 \\ 0 \end{bmatrix} \Rightarrow \begin{bmatrix} -2 & -2 \\ -3 & -3 \end{bmatrix} \begin{bmatrix} v_2^1 \\ v_2^2 \end{bmatrix} = \begin{bmatrix} 0 \\ 0 \end{bmatrix}$$

hence  $v_2^1 + v_2^2 = 0$  from which  $\mathbf{v}_2 = \begin{bmatrix} v_2^1 \\ v_2^2 \end{bmatrix} = \begin{bmatrix} 1 \\ -1 \end{bmatrix}$ .

All the solutions can be written in the form of linear combinations of these two independent solutions:

$$\begin{bmatrix} y(t) \\ z(t) \end{bmatrix} = c_1 \mathbf{v}_1 e^{\lambda_1 t} + c_2 \mathbf{v}_2 e^{\lambda_2 t} = c_1 \begin{bmatrix} 1 \\ 3/2 \end{bmatrix} e^{-t} + c_2 \begin{bmatrix} 1 \\ -1 \end{bmatrix} e^{4t}$$

Given an initial solution, e.g.  $\begin{bmatrix} y(0) \\ z(0) \end{bmatrix} = \begin{bmatrix} 4 \\ 3 \end{bmatrix}$ , the two constants  $c_1$  and  $c_2$  can be determined as the unique solution of the following algebraic system

$$\begin{bmatrix} 1 & 1 \\ \frac{3}{2} & -1 \end{bmatrix} \begin{bmatrix} c_1 \\ c_2 \end{bmatrix} = \begin{bmatrix} 4 \\ 3 \end{bmatrix}$$

that give  $c_1 = 3$  and  $c_2 = 1$ .

A numerical simulation is shown in fig.33, where the red trajectory is obtained by taking an initial condition along the direction indicated by the eigenvector  $\mathbf{v}_1$  associated with the negative eigenvalue  $\lambda_1$  (*stable invariant manifold*) e.g.  $\begin{bmatrix} y(0) \\ z(0) \end{bmatrix} = \mathbf{v}_1 q$ ,  $q > 0$ . The other trajectories initially move towards  $(0,0)$  and then turn away from it, asymptotically to the line along the direction of the eigenvalue  $\mathbf{v}_2$  associated with the positive eigenvalue  $\lambda_2$  (*unstable invariant manifold*). Another example:

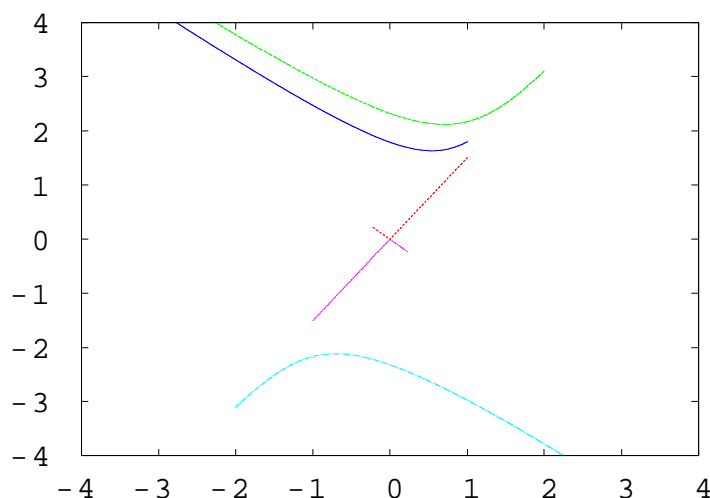


Figure 33: Numerical computed trajectory with real eigenvalues.



$$\begin{cases} \dot{y}(t) = -5y(t) + 8z(t) \\ \dot{z}(t) = -y(t) + z(t) \end{cases}$$

From the matrix form:

$$\begin{bmatrix} \dot{y}(t) \\ \dot{z}(t) \end{bmatrix} = \begin{bmatrix} -5 & 8 \\ -1 & 1 \end{bmatrix} \begin{bmatrix} y(t) \\ z(t) \end{bmatrix}$$

we have  $Tr = -4$ ,  $Det = 3$  hence two real and negative eigenvalues (stable node). Indeed, the characteristic equation  $\lambda^2 + 4\lambda + 3$  has solutions  $\lambda_1 = -3$ ,  $\lambda_2 = -1$ . The eigenvectors are obtained as:

$$\begin{bmatrix} -5 - \lambda_1 & 8 \\ -1 & 1 - \lambda_1 \end{bmatrix} \begin{bmatrix} v_1^1 \\ v_1^2 \end{bmatrix} = \begin{bmatrix} 0 \\ 0 \end{bmatrix} \text{ with } \lambda_1 = -3 \Rightarrow \begin{bmatrix} -2 & 8 \\ -1 & 4 \end{bmatrix} \begin{bmatrix} v_1^1 \\ v_1^2 \end{bmatrix} = \begin{bmatrix} 0 \\ 0 \end{bmatrix}$$

hence  $-v_1^1 + 4v_1^2 = 0$  and with  $v_1^1 = 1$  we get  $\mathbf{v}_1 = \begin{bmatrix} 1 \\ 1/4 \end{bmatrix}$ ;

$$\text{with } \lambda_2 = -1 \Rightarrow \begin{bmatrix} -4 & 8 \\ -1 & 2 \end{bmatrix} \begin{bmatrix} v_2^1 \\ v_2^2 \end{bmatrix} = \begin{bmatrix} 0 \\ 0 \end{bmatrix}$$

we get  $\mathbf{v}_2 = \begin{bmatrix} 1 \\ 1/2 \end{bmatrix}$  and the general solution

$$\begin{bmatrix} y(t) \\ z(t) \end{bmatrix} = c_1 \begin{bmatrix} 1 \\ 1/4 \end{bmatrix} e^{-3t} + c_2 \begin{bmatrix} 1 \\ 1/2 \end{bmatrix} e^{-t}$$

from which a particular solution is obtained by imposing an initial condition  $\begin{bmatrix} y(0) \\ z(0) \end{bmatrix}$ .

For the following example

$$\begin{cases} \dot{y}(t) = y(t) - 5z(t) \\ \dot{z}(t) = y(t) + z(t) \end{cases}$$

we have  $Tr^2 - 4Det = 2^2 - 4 \cdot 6 = -20 < 0$ , hence complex conjugate eigenvalues with positive real part (being  $Tr > 0$ ). This means that the equilibrium  $(0, 0)$  is an unstable focus. Indeed, the characteristic equation  $\lambda^2 - 2\lambda + 6 = 0$  has solutions  $\lambda_1 = \frac{2+2i\sqrt{5}}{2} = 1 + i\sqrt{5}$ ,  $\lambda_2 = \frac{2-2i\sqrt{5}}{2} = 1 - i\sqrt{5}$ . The complex eigenvectors are obtained from:

$$\begin{bmatrix} 1 - \lambda_1 & -5 \\ 1 & 1 - \lambda_1 \end{bmatrix} \begin{bmatrix} v_1^1 \\ v_1^2 \end{bmatrix} = \begin{bmatrix} 0 \\ 0 \end{bmatrix} \text{ with } \lambda_1 = 1 + i\sqrt{5} \Rightarrow \begin{bmatrix} -i\sqrt{5} & -5 \\ 1 & -i\sqrt{5} \end{bmatrix} \begin{bmatrix} v_1^1 \\ v_1^2 \end{bmatrix} = \begin{bmatrix} 0 \\ 0 \end{bmatrix}$$

hence  $v_1^1 - i\sqrt{5}v_1^2 = 0$  and with  $v_1^2 = 1$  we get  $\mathbf{v}_1 = \begin{bmatrix} i\sqrt{5} \\ 1 \end{bmatrix}$ ; Analogously,

$$\text{with } \lambda_2 = 1 - i\sqrt{5} \Rightarrow \begin{bmatrix} i\sqrt{5} & -5 \\ 1 & i\sqrt{5} \end{bmatrix} \begin{bmatrix} v_2^1 \\ v_2^2 \end{bmatrix} = \begin{bmatrix} 0 \\ 0 \end{bmatrix}$$

gives  $\mathbf{v}_2 = \bar{\mathbf{v}}_1 = \begin{bmatrix} -i\sqrt{5} \\ 1 \end{bmatrix}$ . The general complex solution is

$$\begin{bmatrix} y(t) \\ z(t) \end{bmatrix} = c_1 \begin{bmatrix} i\sqrt{5} \\ 1 \end{bmatrix} e^{(1+i\sqrt{5})t} + c_2 \begin{bmatrix} -i\sqrt{5} \\ 1 \end{bmatrix} e^{(1-i\sqrt{5})t}$$

where  $c_1$  and  $c_2$  are arbitrary complex numbers. However, remembering that

$$e^{(1 \pm i\sqrt{5})t} = e^t e^{\pm i\sqrt{5}t} = e^t \left[ \cos(\sqrt{5}t) \pm i \sin(\sqrt{5}t) \right]$$

we have

$$\begin{aligned} \phi_1(t) &= \begin{bmatrix} i\sqrt{5} \\ 1 \end{bmatrix} e^t e^{i\sqrt{5}t} = e^t \begin{bmatrix} i\sqrt{5} \cos(\sqrt{5}t) - \sqrt{5} \sin(\sqrt{5}t) \\ \cos(\sqrt{5}t) + i \sin(\sqrt{5}t) \end{bmatrix} = \\ &= e^t \left[ \begin{pmatrix} -\sqrt{5} \sin(t\sqrt{5}) \\ \cos(t\sqrt{5}) \end{pmatrix} + i \begin{pmatrix} \sqrt{5} \cos(t\sqrt{5}) \\ \sin(t\sqrt{5}) \end{pmatrix} \right] = \end{aligned}$$

and

$$\phi_2(t) = e^t \left[ \begin{pmatrix} -\sqrt{5} \sin(t\sqrt{5}) \\ \cos(t\sqrt{5}) \end{pmatrix} - i \begin{pmatrix} \sqrt{5} \cos(t\sqrt{5}) \\ \sin(t\sqrt{5}) \end{pmatrix} \right]$$

we can obtain two independent real solutions:

$$\psi_1 = \frac{\phi_1(t) + \phi_2(t)}{2} = e^t \begin{pmatrix} -\sqrt{5} \sin(t\sqrt{5}) \\ \cos(t\sqrt{5}) \end{pmatrix} ; \psi_2 = \frac{\phi_1(t) - \phi_2(t)}{2i} = e^t \begin{pmatrix} \sqrt{5} \cos(t\sqrt{5}) \\ \sin(t\sqrt{5}) \end{pmatrix}$$

as a base to get the general real solution

$$\begin{aligned} \begin{bmatrix} y(t) \\ z(t) \end{bmatrix} &= c_1 e^t \begin{pmatrix} -\sqrt{5} \sin(t\sqrt{5}) \\ \cos(t\sqrt{5}) \end{pmatrix} + c_2 e^t \begin{pmatrix} \sqrt{5} \cos(t\sqrt{5}) \\ \sin(t\sqrt{5}) \end{pmatrix} \\ &= e^t \left[ c_1 \begin{pmatrix} -\sqrt{5} \sin(t\sqrt{5}) \\ \cos(t\sqrt{5}) \end{pmatrix} + c_2 \begin{pmatrix} \sqrt{5} \cos(t\sqrt{5}) \\ \sin(t\sqrt{5}) \end{pmatrix} \right] \end{aligned}$$

Again, a particular solution is obtained by imposing a given initial condition. Fig.34 shows some trajectories numerically, each obtained by taking an initial condition close to the unstable focus  $(0,0)$ . To end this set of examples, let us consider what happens in the case of coincident eigenvalues  $\lambda_1 = \lambda_2 = \lambda$ , a solution of the characteristic equation with algebraic multiplicity 2 occurring when  $Tr(A) - 4 \det(A) = 0$ . We can distinguish two cases, according to the number of independent eigenvectors (*geometric multiplicity*  $mg(\lambda)$ ) associated with the eigenvalue of algebraic multiplicity 2. In fact,  $mg(\lambda) \leq 2$  according to the following relation

$$mg(\lambda) = \dim(V) - rank(A - \lambda I)$$

where  $\dim(V)$  represents the dimension of the phase space, hence  $\dim(V) = 2$  in our case, and  $rank(A - \lambda I)$  is the rank of the homogeneous algebraic system whose solutions are the eigenvectors. The two cases are:

(a)  $mg(\lambda) = 2$ , i.e. two independent eigenvectors exist because  $rank(A - \lambda I) = 0$ .

(b)  $mg(\lambda) = 1$ , i.e. only one independent eigenvector exists being  $rank(A - \lambda I) = 1$ .

In case (a) two independent solutions exist, given by  $\mathbf{v}_1 e^{\lambda t}$  and  $\mathbf{v}_2 e^{\lambda t}$ , where  $\mathbf{v}_1$  and  $\mathbf{v}_2$  are two independent eigenvectors associated to  $\lambda$ , and then one can proceed by considering all the linear combinations of these two independent solutions as general solution, as usual.

Otherwise, in case (b) it can be proved that two independent solutions are given by  $\mathbf{v} e^{\lambda t}$  and  $\mathbf{v} t e^{\lambda t}$ , where  $\mathbf{v}$  is the only independent eigenvector.

As an example, let us consider the following linear model:

$$\begin{cases} \dot{y}(t) = 3y(t) - z(t) \\ \dot{z}(t) = y(t) + z(t) \end{cases}$$

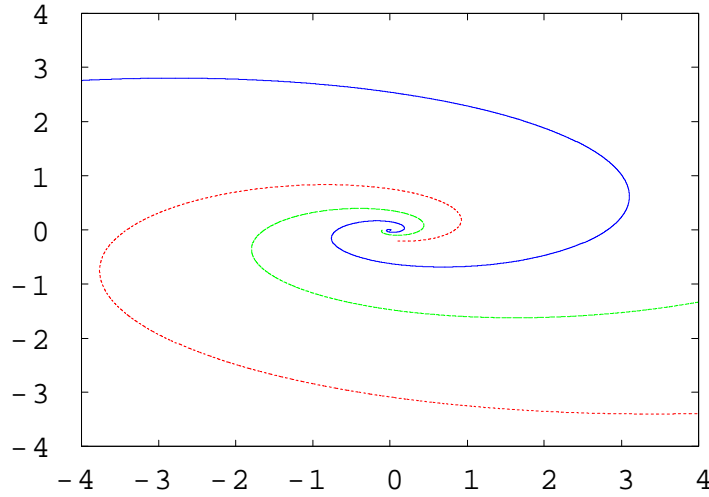


Figure 34: Numerically computed trajectory with complex eigenvalues.

that, as usual, can be written in the matrix form:

$$\begin{bmatrix} \dot{y}(t) \\ \dot{z}(t) \end{bmatrix} = \begin{bmatrix} 3 & -1 \\ 1 & 1 \end{bmatrix} \begin{bmatrix} y(t) \\ z(t) \end{bmatrix}$$

As  $Tr = 4$  and  $Det = 4$  we have  $Tr^2 - 4Det = 16 - 16 = 0$ , and the unique eigenvalue  $\lambda = 2$  of algebraic multiplicity 2 is obtained. From

$$\begin{bmatrix} 3 - \lambda_1 & -1 \\ 1 & 1 - \lambda_1 \end{bmatrix} \text{ with } \lambda = 2 \Rightarrow \begin{bmatrix} 1 & -1 \\ 1 & -1 \end{bmatrix} \begin{bmatrix} v_1^1 \\ v_1^2 \end{bmatrix} = \begin{bmatrix} 0 \\ 0 \end{bmatrix}$$

we can see that  $rank(A - \lambda I) = 1$ , hence the geometric dimension of the eigenspace is  $2 - 1 = 1$ , and  $\mathbf{v} = \begin{bmatrix} 1 \\ 1 \end{bmatrix}$ . Besides the solution  $\phi_1(t) = c_1 \begin{bmatrix} 1 \\ 1 \end{bmatrix} e^{2t}$  a second solution is proposed in the form  $\phi_2(t) = \begin{bmatrix} a_1 \\ a_2 \end{bmatrix} te^{2t} + \begin{bmatrix} b_1 \\ b_2 \end{bmatrix} e^{2t}$ , where the two vectors must be determined so that  $\dot{\phi}_2(t) = A\phi_2(t)$ , i.e.

$$\begin{bmatrix} a_1 \\ a_2 \end{bmatrix} e^{2t} + \begin{bmatrix} a_1 \\ a_2 \end{bmatrix} 2te^{2t} + \begin{bmatrix} b_1 \\ b_2 \end{bmatrix} 2e^{2t} = A \begin{bmatrix} a_1 \\ a_2 \end{bmatrix} te^{2t} + A \begin{bmatrix} b_1 \\ b_2 \end{bmatrix} e^{2t}$$

equivalent to

$$e^{2t} \left( \begin{bmatrix} a_1 \\ a_2 \end{bmatrix} + \begin{bmatrix} b_1 \\ b_2 \end{bmatrix} 2 - A \begin{bmatrix} b_1 \\ b_2 \end{bmatrix} \right) + te^{2t} \left( \begin{bmatrix} a_1 \\ a_2 \end{bmatrix} 2 - A \begin{bmatrix} a_1 \\ a_2 \end{bmatrix} \right) = 0$$

which is true provided that both the expressions inside brackets vanish, i.e.

$$A \begin{bmatrix} a_1 \\ a_2 \end{bmatrix} = 2 \begin{bmatrix} a_1 \\ a_2 \end{bmatrix}$$

that is  $\begin{bmatrix} a_1 \\ a_2 \end{bmatrix}$  is an eigenvector of  $\lambda = 2$ , i.e.  $\begin{bmatrix} a_1 \\ a_2 \end{bmatrix} = \mathbf{v} = \begin{bmatrix} 1 \\ 1 \end{bmatrix}$ , and

$$[A - 2I] \begin{bmatrix} b_1 \\ b_2 \end{bmatrix} = \begin{bmatrix} a_1 \\ a_2 \end{bmatrix}$$

where  $\begin{bmatrix} b_1 \\ b_2 \end{bmatrix}$  is called "generalized eigenvector". From

$$\begin{bmatrix} 1 & -1 \\ 1 & -1 \end{bmatrix} \begin{bmatrix} b_1 \\ b_2 \end{bmatrix} = \begin{bmatrix} 1 \\ 1 \end{bmatrix}$$

we get  $\begin{bmatrix} b_1 \\ b_2 \end{bmatrix} = \begin{bmatrix} 1 \\ 0 \end{bmatrix}$ .

All in all, the general solution becomes

$$\begin{bmatrix} y(t) \\ z(t) \end{bmatrix} = c_1 \begin{bmatrix} 1 \\ 1 \end{bmatrix} e^{2t} + c_2 \left( \begin{bmatrix} 1 \\ 1 \end{bmatrix} t + \begin{bmatrix} 1 \\ 0 \end{bmatrix} \right) e^{2t}$$

The equilibrium in an *unstable improper node*, and some trajectories obtained starting from initial conditions close to  $(0, 0)$  are shown in fig.35.

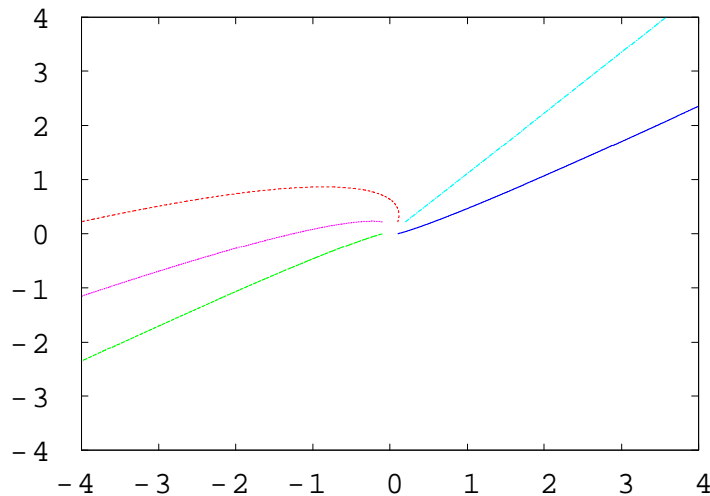


Figure 35: Unstable improper node.

## 4.2 Nonlinear dynamic models in two dimensions.

Let us consider a nonlinear model in the form (17) and let  $E = (x_1^*, x_2^*)$  be an equilibrium point, solution of the system (18). Differently from the linear models, in the nonlinear case several equilibrium points can coexist. However, what we have seen for a linear system can be used to understand the local

behaviour of a nonlinear system around a single equilibrium, i.e. *locally*, in a neighborhood of the equilibrium point. We recall that a neighborhood of a point of  $\mathbf{x}^* \in \mathbb{R}^n$  is a set  $N_r(\mathbf{x}^*)$  defined as

$$N_r(\mathbf{x}^*) = \{\mathbf{x} \in \mathbb{R}^n \mid \|\mathbf{x} - \mathbf{x}^*\| < r\} \text{ for some } r > 0$$

where  $\|\cdot\|$  is a norm, such as the Euclidean norm  $\|\mathbf{x}\| = \sqrt{\sum_{i=1}^n x_i^2}$ . Hence in  $\mathbb{R}^n$  a neighborhood is an open disk of radius  $r$  and centre  $\mathbf{x}^*$ . In the following we will characterize the local phase portrait in a neighborhood of an equilibrium point  $E = (x_1^*, x_2^*)$  by using the linear approximation of the nonlinear system obtained by the first order Taylor expansion

$$\begin{aligned} f_1(x_1, x_2) &= f_1(x_1^*, x_2^*) + \left. \frac{\partial f_1}{\partial x_1} \right|_E (x_1 - x_1^*) + \left. \frac{\partial f_1}{\partial x_2} \right|_E (x_2 - x_2^*) + o(\|\mathbf{x} - \mathbf{x}^*\|) \\ f_2(x_1, x_2) &= f_2(x_1^*, x_2^*) + \left. \frac{\partial f_2}{\partial x_1} \right|_E (x_1 - x_1^*) + \left. \frac{\partial f_2}{\partial x_2} \right|_E (x_2 - x_2^*) + o(\|\mathbf{x} - \mathbf{x}^*\|) \end{aligned}$$

where the symbol  $o(\cdot)$  represents higher order infinitesimal terms as  $\mathbf{x} \rightarrow \mathbf{x}^*$ . Being  $E$  an equilibrium,  $f_i(x_1^*, x_2^*) = 0$ ,  $i = 1, 2$ , so if we define the *Jacobian matrix* as the matrix that collects the four partial derivatives

$$\mathbf{J}(x_1, x_2) = \begin{bmatrix} \left. \frac{\partial f_1}{\partial x_1} \right|_E (x_1, x_2) & \left. \frac{\partial f_1}{\partial x_2} \right|_E (x_1, x_2) \\ \left. \frac{\partial f_2}{\partial x_1} \right|_E (x_1, x_2) & \left. \frac{\partial f_2}{\partial x_2} \right|_E (x_1, x_2) \end{bmatrix}$$

and we substitute the Taylor expansion, then (17) can be written as

$$\begin{bmatrix} \dot{X}_1 \\ \dot{X}_2 \end{bmatrix} = \mathbf{J}(x_1^*, x_2^*) \begin{bmatrix} X_1 \\ X_2 \end{bmatrix} + o(\|\mathbf{X}\|)$$

where  $X_1 = x_1 - x_1^*$ ,  $X_2 = x_2 - x_2^*$  are coordinated centered in  $E$ , i.e. that measure the displacement from the equilibrium. Under suitable conditions we can use the linear approximation around  $\mathbf{x}^*$  to classify the local phase portrait according to the following result

**Linearization Theorem** *Let the nonlinear system (17) have an equilibrium  $\mathbf{x}^*$  such that all the eigenvalues of  $J(\mathbf{x}^*)$  have nonvanishing real part. Then in a neighborhood of  $\mathbf{x}^*$  the local phase portrait of (17) is qualitatively equivalent to that of the linear approximation.*

This is a quite informal and intuitive version of a more general theorem known as Hartman-Grobman Theorem. Here below we give a more rigorous version of it, extended to  $n$  dimensions, where the definition of qualitative (or topological) equivalence is included as well.

**Theorem (Hartman-Grobman, 1964)** *Given a nonlinear system of differential equations  $\dot{\mathbf{x}} = f(\mathbf{x})$ ,  $\mathbf{x} \in \mathbb{R}^n$ , let  $\mathbf{x}^* \in \mathbb{R}^n$  be an equilibrium point, i.e.  $f(\mathbf{x}^*) = 0$ . If  $\mathbf{x}^*$  is hyperbolic, i.e. all the eigenvalues of the Jacobian matrix  $J(\mathbf{x}^*)$  have nonvanishing real part, then the general solution  $\mathbf{y}(t) \in \mathbb{R}^n$  of the linear system  $\dot{\mathbf{y}} = J(\mathbf{x}^*)\mathbf{y}$  is such that a neighborhood  $U$  of  $x^*$  exists and an homeomorphism  $\mathbf{y} = \mathbf{h}(\mathbf{x})$  exists, with  $h$  defined in  $U$  and with values in a neighborhood of the equilibrium  $\mathbf{0}$  of the linear system, such that  $\mathbf{y}(t) = \mathbf{h}(\mathbf{x}(t)) \forall t \in \mathbb{R}$  with  $\mathbf{x}(t) \in U$  solution of  $\dot{\mathbf{x}} = f(\mathbf{x})$ .*

We recall that a homeomorphism is a continuous and invertible function.

The Hartman-Grobman theorem essentially states that the trajectories of a nonlinear dynamic model in a neighborhood of an hyperbolic equilibrium are similar to the ones of its linear approximation

whose matrix of coefficients is given by the Jacobian matrix computed at the equilibrium. This implies that any hyperbolic equilibrium point of a nonlinear dynamical system can be classified as a stable (unstable) node, or a saddle, or a stable (unstable) focus as for the corresponding linear approximation. The corresponding phase portraits may be in some way distorted (stretched, rotated etc.) however they are topologically equivalent. In particular the stable and unstable invariant manifold of saddles still exist, even if they are no longer lines but smooth curves tangent to the eigenvectors of the corresponding linear approximation.

A corollary of the Hartman-Grobman Theorem and the knowledge of the general solutions of linear systems, is given by the following proposition about local asymptotic stability of an equilibrium, that will be easily extended to continuous-time dynamical systems of dimension  $n$ .

**Theorem on local asymptotic stability.** *Let  $\mathbf{x}^*$  be an equilibrium point of  $\dot{\mathbf{x}} = f(\mathbf{x})$ ,  $\mathbf{x} \in \mathbb{R}^n$ . If all the eigenvalues of  $J(\mathbf{x}^*)$  have negative real part then  $\mathbf{x}^*$  is a locally asymptotically stable equilibrium. If at least one eigenvalue of the Jacobian matrix  $J(\mathbf{x}^*)$  has positive real part then  $\mathbf{x}^*$  is unstable.*

To sum up, given an equilibrium point we can analyze the local qualitative behaviour in a neighborhood of an hyperbolic equilibrium (i.e. the qualitative structure of the phase portrait around it) just studying the eigenvalues of the Jacobian matrix computed in it, that follows immediately from the computation of the trace and the determinant according to the classification listed for linear systems. However this procedure only gives information about the local behaviour around the equilibrium points, and nothing about the global behaviour, even if this is usually a good starting point to have a global view as well.

We also stress that the Hartman-Grobman Theorem provides no information about the behaviour of the dynamical system around non-hyperbolic equilibria, i.e. when the determinant or the trace of the Jacobian matrix vanish. Such non generic situations are often characterized by structural instability, and in the presence of a parameter they may give rise to bifurcations, as will be discussed in the next Section.

As an example. Let us consider the system of nonlinear differential equations

$$\begin{cases} \dot{x}_1 &= 2x_1 - x_1^2 - 2x_1x_2 \\ \dot{x}_2 &= 2x_2 - x_2^2 - 2x_1x_2 \end{cases} \quad (29)$$

with a generic initial condition  $(x_1(0), x_2(0)) \in \mathbb{R}^2$ .

The equilibrium points are the solutions of

$$\begin{aligned} x_1(2 - x_1 - 2x_2) &= 0 \\ x_2(2 - x_2 - 2x_1) &= 0 \end{aligned}$$

given by  $O = (0, 0)$ ,  $A = (2, 0)$ ,  $C = (0, 2)$ ,  $E = (\frac{2}{3}, \frac{2}{3})$ . Given the Jacobian matrix

$$\mathbf{J}(x_1, x_2) = \begin{bmatrix} 2 - 2x_1 - 2x_2 & -2x_1 \\ -2x_2 & 2 - 2x_1 - 2x_2 \end{bmatrix}$$

a classification of the equilibrium points is easily obtained by the method of linear approximation based on the computation of the Jacobian in each of them.

$$\mathbf{J}(O) = \begin{bmatrix} 2 & 0 \\ 0 & 2 \end{bmatrix}$$

is a diagonal matrix, hence the eigenvalues are readily computed being them the diagonal entries<sup>4</sup>:  $\lambda_1 = \lambda_2 = 2 > 0$ . Hence the equilibrium is a repelling node, and due to the particular symmetric structure of the model, the equilibrium point of the corresponding linear approximation is a star node.

$$\mathbf{J}(A) = \begin{bmatrix} -2 & 0 \\ -4 & -2 \end{bmatrix}$$

is a triangular matrix, so even in this case the eigenvalues are given by the diagonal entries:  $\lambda_1 = \lambda_2 = -2$ , and we have a stable improper node. Analogously for the equilibrium  $B$ . Finally,

$$\mathbf{J}(E) = \begin{bmatrix} -\frac{2}{3} & -\frac{4}{3} \\ -\frac{4}{3} & -\frac{2}{3} \end{bmatrix}$$

from which we can see that  $Tr(E) = -\frac{4}{3} < 0$  and  $Det(E) = -\frac{4}{3} < 0$ . Hence,  $E$  is a saddle. It is easy to verify that the eigenvalues are  $\lambda_1 = -2$  with corresponding eigenvector  $\mathbf{v}_1 = (1, 1)$  (tangent to the stable manifold) and are  $\lambda_2 = \frac{2}{3}$  with corresponding eigenvector  $\mathbf{v}_2 = (1, -1)$  (tangent to the unstable manifold), see fig. 36. Notice that, due to the symmetric form of (29), in this case the line along the direction indicated by  $\mathbf{v}_1 = (1, 1)$  is the invariant stable manifold. Moreover, as usual, such stable manifold constitutes the boundary that separates the basins of the two stable equilibrium points  $A$  and  $B$ .

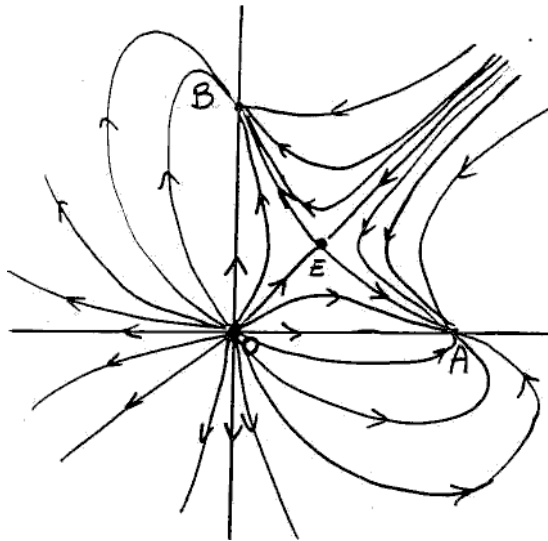


Figure 36: Phase portrait for a Volterra competition model.

The restriction of the system (29) to the positive orthant  $\mathbb{R}_+^2 = \{(x_1, x_2) \in \mathbb{R}^2 | x_1 \geq 0; x_2 \geq 0\}$ , is an example of Volterra model of competition between two species

$$\begin{cases} \dot{x}_1 = \alpha_1 x_1 - s_1 x_1^2 - b_1 x_1 x_2 \\ \dot{x}_2 = \alpha_2 x_2 - s_2 x_2^2 - b_2 x_1 x_2 \end{cases} \quad (30)$$

<sup>4</sup>The property that the diagonal entries coincide with the eigenvalues of the matrix holds for all triangular matrices.

where each species alone grows according to a logistic law of motion, and the interaction has a negative effect on both, as each of them is assumed to subtract food to the other one. The study of this model led to the mathematical formulation of the principle of competitive exclusion: if two species need the same vital resources, then only one will survive. Which species will survive depends on the parameters that characterize each species behaviour as well as on the initial advantage (i.e. the initial condition). This principle can be extended to the case of  $n$  species, and may have several applications even in social and economic systems. A good exercise is to generalize the results obtained in the particular case considered above to the more general model (30) in order to understand the role of each parameter on existence and stability of equilibria.

**Another ecological example: the prey-predator Lotka-Volterra model.**

The prey-predator Lotka Volterra model has been already described at the beginning of this section. Let us consider again the model (19) and compute its equilibrium points, solutions of the algebraic system

$$\begin{aligned} x_1(\alpha - sx_1 - bx_2) &= 0 \\ x_2(cx_1 - d) &= 0 \end{aligned} \tag{31}$$

given by

$$O = (0, 0); \quad A = \left(\frac{\alpha}{s}, 0\right); \quad E = \left(\frac{d}{c}, \frac{\alpha c - sd}{bc}\right); \tag{32}$$

The equilibrium  $O$  represents the extinction of both species, so its stability indicates that there are no viability conditions for both species, at least for initial conditions in its basin of attraction; if the equilibrium  $A$  is stable, then the ecological conditions are not suitable to allow predators' survival. Only the stability of the equilibrium  $E$  can ensure the coexistence of the two species, provided it is positive, i.e.  $\alpha c > sd$ , and for initial conditions in its basin. In order to study the local stability of the three equilibrium points, let us consider, as usual, the Jacobian matrix

$$\mathbf{J}(x_1, x_2) = \begin{bmatrix} \alpha - 2sx_1 - bx_2 & -bx_1 \\ cx_2 & cx_1 - d \end{bmatrix}$$

and compute it in each equilibrium point. At the equilibrium

$$\mathbf{J}(0, 0) = \begin{bmatrix} \alpha & 0 \\ 0 & -d \end{bmatrix}$$

we have a diagonal matrix with eigenvalues  $\lambda_1 = \alpha > 0$  and  $\lambda_2 = -d < 0$ , so that the equilibrium  $O$  is a saddle. It is easy to check that, as usual with a diagonal matrix, the eigenvector associated with the first eigenvalue (the positive one in this case) is  $\mathbf{v}_1 = \begin{bmatrix} 1 \\ 0 \end{bmatrix}$ , hence the unstable manifold is along the horizontal axis. Instead, the eigenvector associated with the second eigenvalue (the negative one in this case) is  $\mathbf{v}_2 = \begin{bmatrix} 0 \\ 1 \end{bmatrix}$ , so the stable manifold of the saddle is along the vertical axis. Notice that

both the coordinate axes are invariant lines. In fact,  $x_1 = 0$  implies  $\dot{x}_1 = 0$ , so a trajectory starting from an initial condition on the vertical axis, i.e.  $(0, x_2(0))$  with  $x_2(0) > 0$ , is trapped inside it and is governed by the one dimensional restriction  $\dot{x}_2 = -dx_2$ , hence exhibits an exponential decay (the decay of predator population in the absence of preys). The same holds for the horizontal axis  $x_2 = 0$ , and the dynamics on that trapping line is given by the logistic growth of preys' population in the



absence of predators. As shown in section 3.2, such dynamics converge to the equilibrium  $A$ . This is confirmed by the analysis of

$$\mathbf{J}(A) = \begin{bmatrix} -\alpha & -b\frac{\alpha}{s} \\ 0 & c\frac{\alpha}{s} - d \end{bmatrix}$$

which is a triangular matrix, hence the eigenvalues are given, again, by the diagonal entries,  $\lambda_1 = -\alpha < 0$  and  $\lambda_2 = c\frac{\alpha}{s} - d < 0$ , negative for  $\alpha c < sd$  and positive otherwise. Hence the equilibrium  $A$  is a stable node if  $\alpha c < sd$ , whereas it is a saddle if  $\alpha c > sd$ . Notice that the latter is also the condition for the positivity of the equilibrium  $E$ , thus confirming that stability of  $A$  is equivalent to the extinction of predators' population. When  $\alpha c = sd$ , equilibrium  $A$  is non-hyperbolic and merges with  $E$ , being in this case also  $\frac{d}{c} = \frac{\alpha}{s}$  which implies  $E = A$ . This is typical example of a transcritical bifurcation. Notice that  $\mathbf{v}_1 = \begin{bmatrix} 1 \\ 0 \end{bmatrix}$ , hence the equilibrium  $A$  is always stable in the horizontal direction,

whereas the eigenvector associated to  $\lambda_2$ , given by  $\mathbf{v}_2 = \begin{bmatrix} 1 \\ \frac{sd - \alpha c - \alpha s}{\alpha b} \end{bmatrix}$ , is transverse to the horizontal axis, and is tangent to the unstable manifold when  $A$  is a saddle (see fig.37).

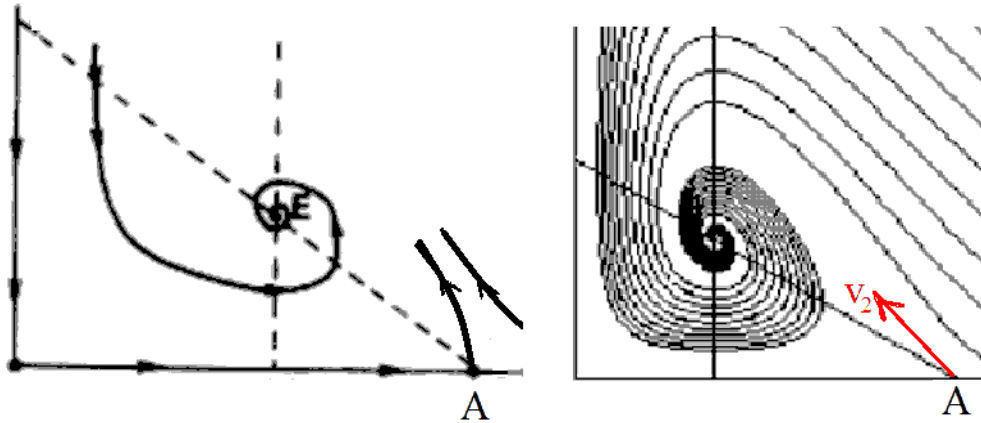


Figure 37: Phase portraits for a prey-predator model with logistic growth of preys.

The stability of the equilibrium of coexistence  $E$  is obtained through

$$\mathbf{J}(E) = \begin{bmatrix} -\frac{sd}{c} & -\frac{bd}{c} \\ \frac{\alpha c - sd}{b} & 0 \end{bmatrix}$$

from which  $Tr(\mathbf{J}) = -\frac{sd}{c} \leq 0$  and  $Det(\mathbf{J}) = \frac{d(\alpha c - sd)}{c} > 0$  whenever the equilibrium  $E$  has positive coordinates. If  $s > 0$  then the equilibrium  $E$  is locally asymptotically stable whenever it is positive. Moreover, being  $Tr(\mathbf{J})^2 - 4Det(\mathbf{J}) = \frac{d^2 s}{c^2} (s + 4) - 4d\alpha < 0$ , if  $\alpha > \frac{ds}{4c^2} (s + 4)$  then  $E$  is a stable focus (see fig.37). A particular case occurs if  $s = 0$ , as  $Tr(\mathbf{J}) = 0$  and consequently we have pure imaginary eigenvalues (i.e. eigenvalues with real part equal to zero). This implies that  $E$  is non-hyperbolic, hence the Hartman-Grobman Theorem cannot be applied. However, it can be shown that in this very particular case the trajectories are given by closed curves around  $E$ , which is marginally stable. This has been proved by Volterra in 1926 and can be confirmed numerically as shown in fig.28. Some other numerical simulations are shown here below.

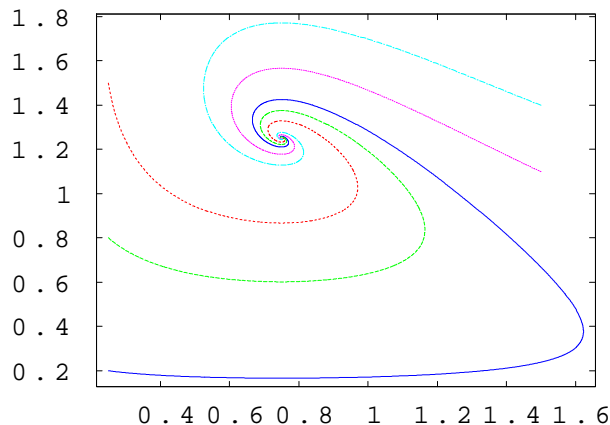


Figure 38: Parameters:  $\alpha = 1, s = b = 0.5, c = 0.4, d = 0.3$ . Initial conditions: blue (0.25, 0.2); pale blue (1.5, 1.4); red (0.25, 1.5); green (0.25, 0.8); magenta (1.5, 1.2).

We now propose another modification of the prey-predator model by introducing an effect of satiation of predators' appetite, i.e. we assume that predators cannot eat more than a given upper limit. This is expressed by the following model proposed by Rosenzweig and McArthur in 1963<sup>5</sup>

$$\begin{aligned} \dot{x}_1 &= \alpha x_1 - s x_1^2 - b \frac{x_1 x_2}{h + x_1} \\ \dot{x}_2 &= -d x_2 + c \frac{x_1 x_2}{h + x_1} \end{aligned} \quad (33)$$

where the function  $g(x_1) = \frac{x_1}{h+x_1}$  is a typical "saturation function" (see fig.42) with the following properties:  $g(0) = 0$  (no eating without preys),  $g'(x_1) > 0$ , i.e. it increases with  $x_1$  (more preys implies more food to eat) but saturates, i.e.  $g(x_1) \rightarrow 1$  as  $x_1 \rightarrow \infty$  (too many preys lead to appetite saturation). The constant  $h$ , called "half saturation constant", gives a measure of how fast is appetite satiation, as  $g(h) = \frac{1}{2}$ .

The dynamic behaviour of this model is characterized by the presence of an invariant closed orbit on which trajectories move periodically, like in the classical Lotka-Volterra model. However, in this case the closed orbit is unique and attracts the trajectories around it. Such orbit will be called limit cycle.

### 4.3 Periodic solutions and limit cycles

From the examples shown in the previous sections we have seen that with 2-dimensional dynamical systems in continuous time, differently from what happens for 1-dimensional systems, the invariant sets are not only given by equilibrium points. In fact, we can also have invariant closed orbits on which periodic trajectories exist, defined as solutions  $\mathbf{x}(t) = \varphi(t)$  for which there is a  $T > 0$  such that  $\varphi(t+T) = \varphi(t)$  and for each  $|t_1 - t_2| < T$  we have  $\varphi(t_1) \neq \varphi(t_2)$ .  $T$  is called *period* of the periodic trajectory. As usual for an invariant set, the question of stability arises (see section 2): if a trajectory

<sup>5</sup>M. Rosenzweig and R. MacArthur (1963) "Graphical representation and stability conditions of predator-prey interaction", *American Naturalist* vol. 97, pp. 209-223.

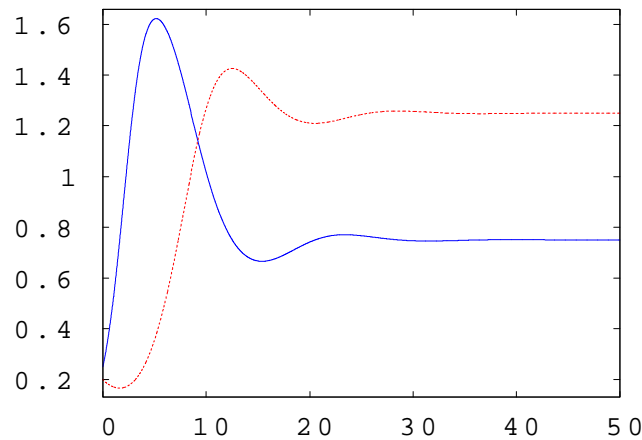


Figure 39: Versus time (temporal series) representation. Prey (red) and predator (blue) populations. Parameters as in the previous picture, initial condition  $(0.2, 0.25)$ .

starts from an initial condition belonging to the invariant closed orbit  $\Gamma$ , then it remains trapped inside  $\Gamma$  by definition, but what about trajectories starting *around* it, i.e. from a neighborhood of  $\Gamma$ ? Do they approach  $\Gamma$  asymptotically for  $t \rightarrow \infty$ ? or, do they move away from it? or, do they remain distinct from  $\Gamma$  and close to it? These are the cases shown in fig. 44, where a new kind of attractor or repeller existing in 2-dimensional dynamical systems is shown: the *limit cycle*. These kinds of solutions are very interesting in economic modelling, as they represent self-sustained cyclic behaviours, that every time go back to an already "visited" state, repeating the same path periodically.

Some general theorems and methods exist, for continuous time 2-dimensional dynamical systems, to detect the presence of limit cycles, as well as some results on bifurcations that create them, as we will see in the following.

First of all, in  $\mathbb{R}^2$  the *Jordan curve lemma* states that any closed orbit  $\Gamma$  divides the plane into two connected and disjoint regions, one inside and one outside the closed curve, such that two points taken one in the inside region and one outside, can only be connected by a trajectory crossing  $\Gamma$ . This implies that if a smooth<sup>6</sup> dynamical system of the plane has a closed invariant curve, then any trajectory starting from an initial condition inside it remains inside forever, and the same must hold for a trajectory starting outside. In other words, both regions are trapping. This is due to the fact that two trajectory cannot cross in an ordinary point due to the Theorem of uniqueness, hence a trajectory starting inside  $\Gamma$  cannot exit it because this cannot occur without crossing the orbit  $\Gamma$ .

This lemma, which is quite intuitive for a system of the plane, is no longer true in more than two dimensions, as it is possible to move from A to B in fig. 45 without crossing the closed curve  $\Gamma$  if the third dimension is available. And the same holds with discrete time even in two dimensions as the trajectories in discrete time can jump from a point to another. So, the following Theorem, which is a consequence of the *Jordan curve lemma*, only holds for two-dimensional dynamical systems.

<sup>6</sup>By the term *smooth* we mean a  $C^{(1)}$  dynamical system, i.e. expressed by equations of motion with continuous derivatives, so that the Theorem of existence and uniqueness apply.

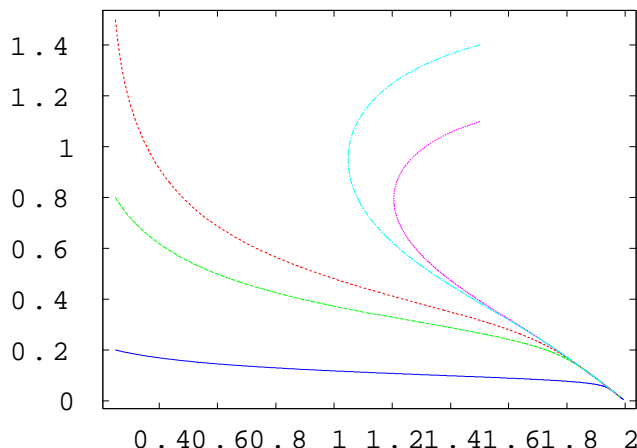


Figure 40: Parameters' values:  $\alpha = 1, s = b = 0.5, c = 0.1, d = 0.3$ . Initial conditions: blue (0.25, 0.2); pale blue (1.5, 1.4); red (0.25, 1.5); green (0.25, 0.8); magenta (1.5, 1.2).

**Poincaré-Bendixson Theorem:** Let  $\dot{\mathbf{x}} = \mathbf{f}(\mathbf{x})$  be a set of two ordinary differential equations defined in an open set  $G \subseteq \mathbb{R}^2$ , and let  $D \subset G$  be a compact (i.e. closed and bounded) trapping set that does not contain any equilibrium point. Then  $D$  must contain at least one closed invariant orbit of the dynamical system.

Figure 46 illustrates the meaning of the theorem.

A corollary of this theorem states that if  $K \subseteq G$  is a non empty compact and trapping set then it must contain an equilibrium point or a closed invariant orbit. Moreover, if  $\Gamma$  is a closed orbit such that its interior region is entirely included into  $G$  (the set where the dynamical system is defined) then  $\Gamma$  must include at least one equilibrium point.

The Poincaré-Bendixson gives an existence result, that is it can be used to detect the presence of limit cycles, but gives no information about their stability or creation/destruction as a consequence of bifurcations as some parameters are varied.

We will see in the next section an application of the Poincaré-Bendixson theorem to the Rosenzweig-MacArthur model (33).

#### 4.4 Bifurcations of 2-dimensional dynamical systems

In section 4.1 we have seen that a topological classification of the unique equilibrium point of a 2-dimensional linear dynamical system is reduced to a simple inspection of the sign of the trace and the determinant of the matrix of coefficients. In particular, the equilibrium is asymptotically stable whenever the trace is negative and the determinant is positive. If the coefficients depend on some parameters it may happen that, starting from a configuration with a stable equilibrium, a continuous variation of a parameter leads to a change in sign of the trace or of the determinant, so that the equilibrium loses stability. In a linear system this implies that a dynamic scenario of global asymptotic convergence to the equilibrium is transformed into a situation of global divergence, i.e. any initial condition outside the equilibrium leads to an explosive trajectory going infinitely far from the equilibrium point. In other words, in a linear system the local behaviour and the global behaviour

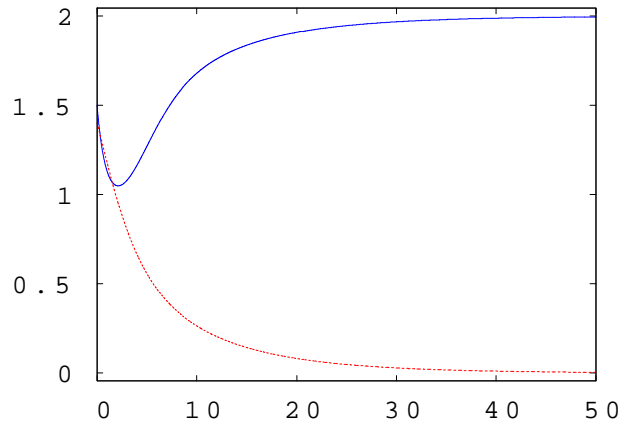


Figure 41: With the same parameters as in the previous picture,  $x_1(t)$  (blue),  $x_2(t)$  are represented versus time, starting from the initial condition  $(1.5, 1.4)$ .

coincide.

According to the Hartman-Grobman Theorem, the topological classification of an (hyperbolic) equilibrium point of a nonlinear system can be obtained by the same procedure, provided that the matrix of coefficient of the linear approximation is obtained from the Jacobian matrix computed at the equilibrium considered. However, this equivalence is only local, i.e. it holds in a neighborhood (no info on the size) of the equilibrium point considered. So, in general nothing guarantees that such local classification can be extended globally, to the whole phase space. Moreover, a nonlinear system may have several equilibrium points (and even other invariant sets, such as the closed invariant orbits discussed in the previous section) so the global phase portrait may be quite complicated and cannot be, in general, deduced by a simple union of local phase portraits obtained around the hyperbolic equilibria. But the differences between linear and nonlinear models are not limited to these local/global considerations, as remarkable differences are related to the study of structural stability, i.e. what happens when, due to slight variations of some parameters, one or more equilibrium points change their stability properties, i.e. the trace and/or the determinant of a Jacobian matrix computed at an equilibrium point show a sign change. Indeed, in general such transitions of an equilibrium point from stable to unstable do not just imply a transition from stability to instability, but are associated with the creation/destruction of other equilibrium points around them or even to the creation/destruction of invariant closed orbits. The former occurrence will be described in terms of *fold*, *transcritical* or *pitchfork* bifurcations, as already seen in the case of one-dimensional dynamical systems, whereas the latter case will be described by a new kind of bifurcation, that has no one-dimensional analogue, denoted as *Andronov-Hopf bifurcation*. It will be characterized by the presence of complex conjugate eigenvalues crossing the imaginary axis, i.e. changing the sign of their real part, or equivalently situations with positive determinant and vanishing trace in the Jacobian matrix. All phenomena related to the presence of oscillatory behaviour (due to focus, or spiral, equilibrium points) hence only occurring in dimension greater than one.

Therefore, while for linear systems a loss of stability leads to uninteresting dynamic scenarios, as loss of stability implies global divergence, in the case of nonlinear models the bifurcations leading to the loss of stability of an equilibrium may open new interesting dynamic scenarios, characterized by

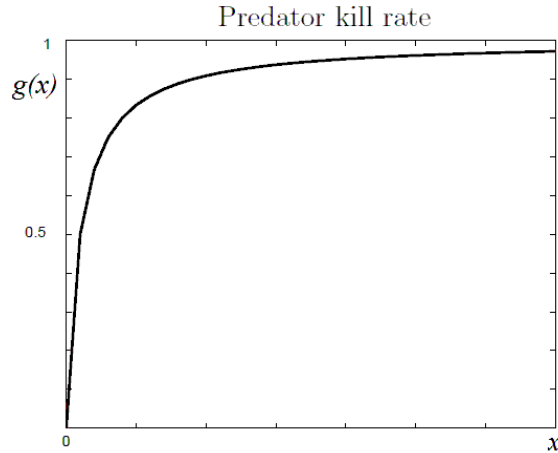


Figure 42: Predators' saturation of appetite: Holling uptake function.

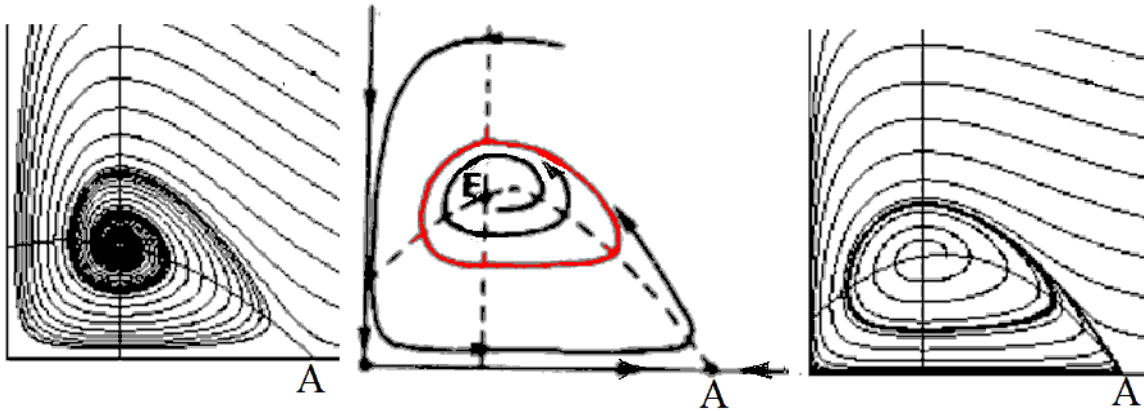


Figure 43: Creation of a stable limit cycle in the Rosenzweig-McArthur prey-predator model.

new equilibria and even new kinds of attracting sets. This means that the regions of the space of parameters characterized by instability of one or more equilibrium points may indicate the outcome of more interesting and even intriguing global phase portraits, characterized by coexistence of several attracting sets each with its own basin of attraction separated by basin boundaries on which unstable equilibria are located.

In the following part of this section we recall in a more formal way some definitions and local bifurcations already described in an intuitive (mainly graphical) way in section 3.4, and then we will introduce the Andronov-Hopf bifurcation.

As already intuitively stated, the notion of structural stability is strictly related to the definition of topological equivalence between two dynamical systems.

**Definition** A dynamical system  $\dot{\mathbf{x}} = \mathbf{f}(\mathbf{x})$ ,  $\mathbf{x} \in \mathbb{R}^n$ , is topologically equivalent (or conjugate) to the dynamical system  $\dot{\mathbf{y}} = \mathbf{g}(\mathbf{y})$ ,  $\mathbf{y} \in \mathbb{R}^n$ , if a homeomorphism  $h : \mathbb{R}^n \rightarrow \mathbb{R}^n$ ,  $\mathbf{y} = \mathbf{h}(\mathbf{x})$ , exists that transforms the phase portrait (i.e. all the orbits) of the  $\mathbf{x}$  of the former into the phase portrait in the

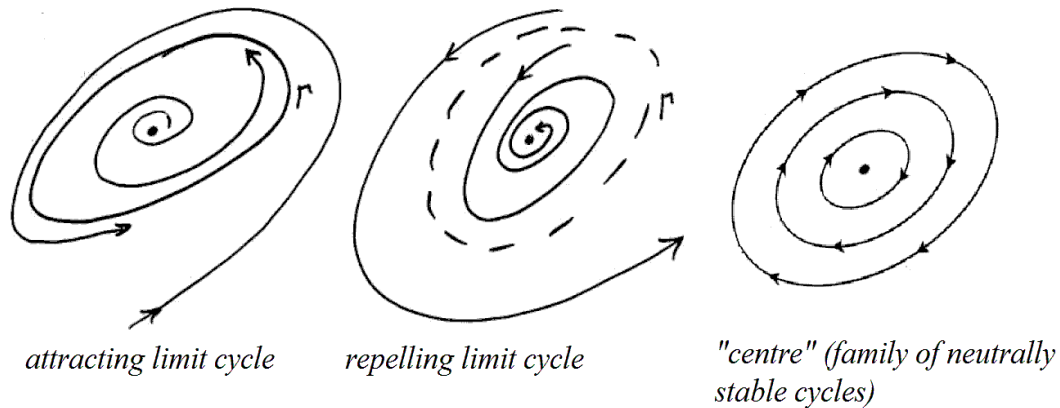


Figure 44: Lomit cycles.

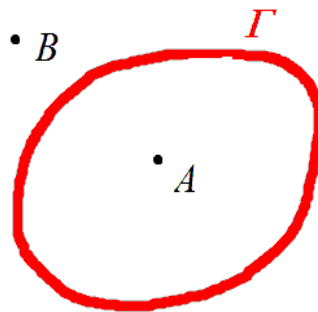


Figure 45: Jordan curve.

$\mathbf{y}$  space of the latter, preserving the direction of time.

We recall that an homeomorphism is an invertible function  $\mathbf{h}$  such that both  $\mathbf{h}$  and  $\mathbf{h}^{-1}$  are continuous.

Given a dynamical system that depends on a parameter

$$\dot{\mathbf{x}}(t) = \mathbf{f}(\mathbf{x}(t), \mu), \quad \mathbf{x}(t) \in \mathbb{R}^n, \quad \mu \in \mathbb{R}$$

let us consider its phase diagram. Of course it will depend on  $\mu$ , in the sense that different values of the parameter  $\mu$  will cause modifications (let's say deformations, distortions etc.) of the phase lines. Such variations of the global phase portrait may be only quantitative (displacements or continuous deformations that are topologically equivalent) or qualitative (an arbitrarily small variation of  $\mu$  leads to a phase portrait which is not equivalent, due to a local stability change and/or to the creation/destruction of invariant sets, such as equilibrium points or closed orbits). This leads to the following definition

**Definition** The transition between two non equivalent phase diagrams due to the variation of a parameter is called *bifurcation*.

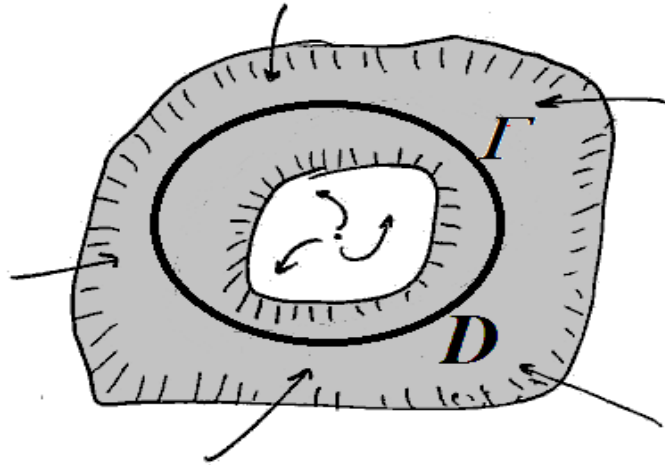


Figure 46: Qualitative illustration of Poincaré-Bendixson theorem.

In other words, a bifurcation is a qualitative modification of the phase diagram of a dynamical system when a parameter crosses a critical (or threshold) value, called *bifurcation value*. It is worth to notice that the kinds of bifurcations can be classified according to a quite limited number of cases. Without entering the details of a more general topological view of this phenomenon, we just mention that the existence of a limited set of possible bifurcations is related to a general theory on structural stability of vector fields depending on parameters, known as singularity theory or theory of catastrophes.<sup>7</sup>

If a real eigenvalue, say  $\lambda_1(\mu)$ , changes its sign at the bifurcation value  $\mu_0$ , i.e. it crosses through the origin of the complex plane moving along the real axis as the parameter  $\mu$  is varied through  $\mu_0$ , then along the invariant manifold associated to  $\lambda_1$  we have one of the one-dimensional bifurcations already described for one-dimensional system, namely a fold (or tangent) bifurcation, also denoted as saddle-node bifurcation in dimension greater than 1, or a transcritical bifurcation or a pitchfork bifurcation. This bifurcation only affects the qualitative dynamic behaviour along the one-dimensional invariant manifold associated to  $\lambda_1$ , as shown in the qualitative pictures 47.

In this case at each value of the parameter  $\mu$  is associated a planar phase portrait around the bifurcating equilibrium, hence a three-dimensional bifurcation diagram is required to represent the bifurcation, with a coordinate axis on which the parameter  $\mu$  is measured and the 2-dimensional phase plane where the corresponding invariant sets are graphically represented, see e.g. fig.48 where the case of a supercritical pitchfork bifurcation is qualitatively shown. In other words, these bifurcations are caused by a single real eigenvalue that changes the sign, associated to an eigenvalue that vanishes, i.e. a change of sign of the determinant of the Jacobian matrix, can be described in terms of the corresponding bifurcations of the one-dimensional restriction of the 2-dimensional dynamical system along the invariant manifold associated with the eigenvalue vanishing at the bifurcation value of the parameter.

In order to give a classification, in the following we generalize and make more precise the classifi-

<sup>7</sup>See e.g. René Thom, *Stabilité Structurale et Morphogénèse, Essai d'une Théorie Générale des Modèles*, Benjamin, New York, 1971, or V.I. Arnold "Catastrophe Theory", Springer-Verlag, 1992.



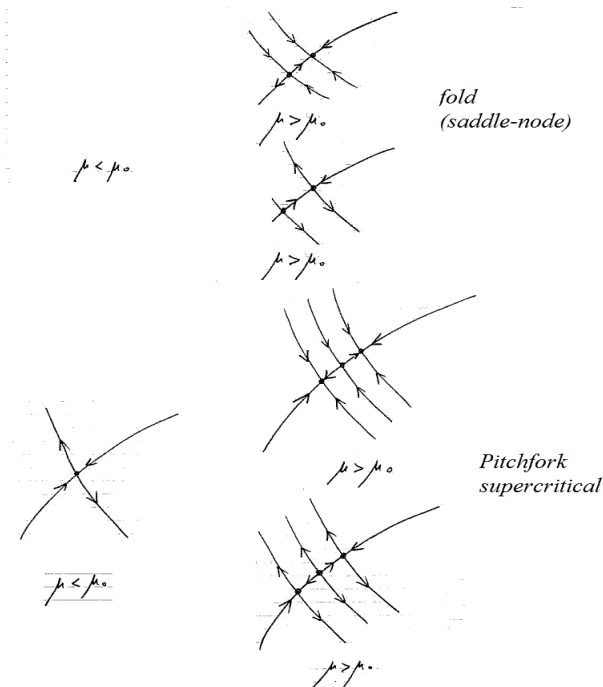


Figure 47: saddle-node and pitchfork in a 2-dim. dynamical system

cation of such bifurcations. If we denote by

$$\dot{x} = f(x, \mu), \quad x \in \mathbb{R}, \quad \mu \in \mathbb{R}$$

the one-dimensional restriction of the 2-dimensional dynamical system along the invariant manifold along which the bifurcation occurs, such that  $f$  is smooth and  $x^*(\mu)$  is the equilibrium such that for  $\mu = 0$  we have  $x^*(0) = 0$  with associated eigenvalue  $\lambda(0) = f_x(0, 0) = 0$ , we have the following classification:

- If  $f_{xx}(0, 0) \neq 0$  and  $f_\mu(0, 0) \neq 0$  then the restriction is topologically equivalent to the normal forms:

$$\dot{y} = \mu \pm y^2$$

i.e. the normal forms of the fold bifurcation.

- If  $\frac{\partial f(x, \mu)}{\partial x} = 0$  (vanishing eigenvalue);  $\frac{\partial^3 f(x, \mu)}{\partial x^3} \neq 0$  and  $\frac{\partial^2 f(x, \mu)}{\partial \mu \partial x} \neq 0$ , then the restriction is topologically equivalent to the normal form

$$\dot{y} = \mu y - y^3$$

and according to the sign of  $\frac{\partial^3 f(x, \mu)}{\partial x^3}$  and  $\frac{\partial^2 f(x, \mu)}{\partial \mu \partial x}$  we have a supercritical or a subcritical pitchfork bifurcation.

- If  $\frac{\partial f(x, \mu)}{\partial x} = 0$  (vanishing eigenvalue);  $\frac{\partial^2 f(x, \mu)}{\partial x^2} \neq 0$ ;  $\frac{\partial^2 f(x, \mu)}{\partial \mu \partial x} \neq 0$ . then the restriction is topologically equivalent to the normal form

$$\dot{y} = \mu y - y^2$$

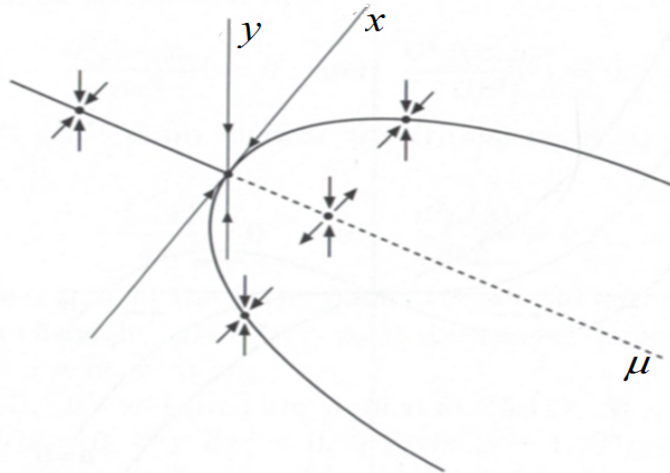


Figure 48: Pitchfork in a bifurcation diagram for 2-dim. dynamical system..

and we have a transcritical (or stability exchange) bifurcation.

It is worth to stress that in all these cases the equilibrium points involved are nodes and saddles, that become non-hyperbolic at the bifurcation. Instead, in the case of spiral (or focus) equilibriums that change stability due to a couple of complex conjugate eigenvalues that cross the imaginary axis, i.e.  $\lambda_{1,2} = \pm i\omega_0$ , hence due to a positive determinant of the Jacobian matrix and a trace that changes its sign. The corresponding bifurcation is known as Hopf (or Andronov-Hopf) bifurcation.

**Theorem (Andronov, 1933, Hopf, 1942).** Let us consider the 2-dimensional dynamical system

$$\dot{\mathbf{x}} = \mathbf{f}(\mathbf{x}, \mu), \quad \mathbf{x} \in \mathbb{R}^2, \quad \mu \in \mathbb{R}$$

with  $\mathbf{f}$  formed by two smooth functions, and let  $\mathbf{x}^*(\mu)$  be an isolated equilibrium point, i.e.  $\mathbf{f}(\mathbf{x}^*, \mu) = 0$ . Let us assume that the eigenvalues  $\lambda_{1,2}(\mu) = \alpha(\mu) \pm i\omega(\mu)$  are complex for  $\mu$  in a neighborhood of  $\mu_0$  and that for  $\mu = \mu_0$  they are purely imaginary, i.e. the real part vanishes:  $\alpha(\mu_0) = 0$ ,  $\omega(\mu_0) = \omega_0 > 0$ . If  $\left. \frac{\partial \text{Re} \lambda_{1,2}}{\partial \mu} \right|_{\mu=\mu_0} > 0$  (transversality condition) holds then  $\mathbf{x}^*$  is a stable focus for  $\mu < \mu_0$  and an unstable focus for  $\mu > \mu_0$ , and at  $\mu = \mu_0$  a closed invariant orbit  $\Gamma$  is created around  $\mathbf{x}^*$  such that one of the following holds:

- (i)  $\Gamma$  exists for  $\mu > \mu_0$  and is a stable limit cycle (supercritical case)
- (ii)  $\Gamma$  exists for  $\mu < \mu_0$  and is an unstable limit cycle (subcritical case)
- (iii) infinitely many closed invariant curves exist for  $\mu = \mu_0$  which are neutrally stable (centre case).

The period of the trajectories moving around is  $T(\mu) = \frac{2\pi}{\omega_0} + o(|\mu - \mu_0|)$  and in cases (i) and (ii) the amplitude of  $\Gamma$  increases as the bifurcation parameter moves away from the bifurcation value proportionally to  $\sqrt{|\mu - \mu_0|}$ .

To sum up, this bifurcation is a device to create limit cycles (see fig. 49).

In the supercritical case, when the equilibrium from stable focus is transformed into an unstable focus, a small stable limit cycle is created around it, and attracts the trajectories starting inside

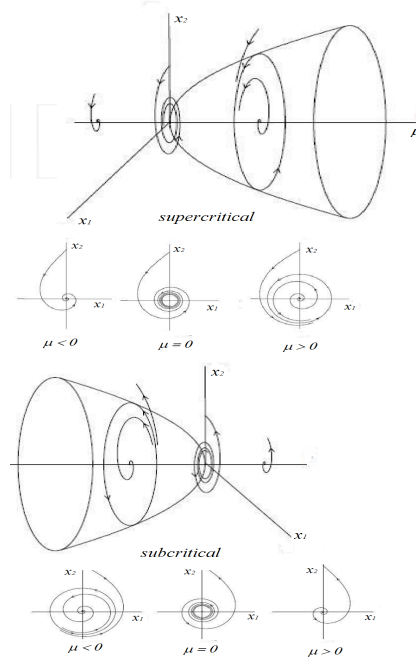


Figure 49: Hopf bifurcation.

the cycle, close to (but different from) the equilibrium, as well as those starting outside it. So, the loss of stability is denoted as "*soft*" in the sense that trajectories issuing from a neighborhood of the equilibrium remain close to it even if they oscillate around it without converging. Instead, in the subcritical case an unstable closed orbit surrounds the stable equilibrium and constitutes the boundary that delimitates its basin of attraction. As the bifurcation parameter approaches its bifurcation value, the basin shrinks because the unstable orbit collapses to the equilibrium point, and then disappears. Hence after the bifurcation the orbits issuing from the unstable equilibrium are not confined and move towards another attracting set, that may be a different equilibrium or some other closed orbit of large amplitude already existing towards infinity (i.e. diverging trajectories). This situation is also denoted as "*hard stability loss*".

It is worth to notice that in the case of a supercritical Hopf bifurcation, at the bifurcation value the non hyperbolic equilibrium is stable, whereas in the case of subcritical bifurcation at the bifurcation value the non hyperbolic equilibrium is unstable.

Let us also notice that the case (iii) is similar to what happens in a linear system when the trace of the matrix of coefficient changes its sign while the determinant is positive so that a pair of complex conjugate eigenvalues cross the imaginary axis, see the bifurcation diagram shown in fig. 50.

As an example, let us consider the following "normal form"

$$\begin{cases} \dot{x}_1 = \mu x_1 - x_2 - x_1(x_1^2 + x_2^2) \\ \dot{x}_2 = x_1 + \mu x_2 - x_2(x_1^2 + x_2^2) \end{cases} \quad (34)$$

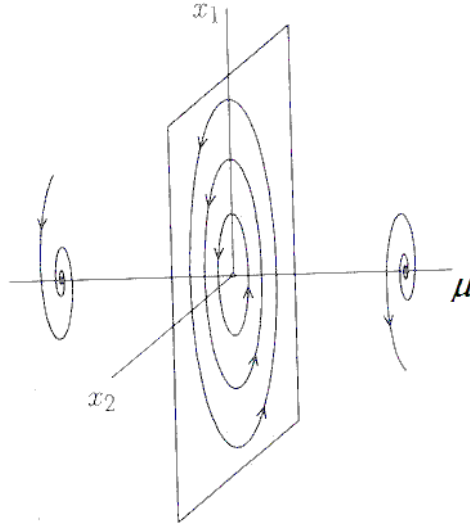


Figure 50: Hopf in the linear case.

The unique equilibrium is  $\mathbf{x}^* = (0, 0)$  where the Jacobian matrix is

$$\mathbf{J}(x^*) = \begin{bmatrix} \mu & -1 \\ 1 & \mu \end{bmatrix}$$

whose eigenvalues are  $\lambda_{1,2} = \mu \pm i$ , hence it is immediate to see that for  $\mu = 0$  a Andronov-Hopf bifurcation occurs as the two complex conjugate eigenvalues cross the imaginary axis at  $\mu = 0$  going from left to right for increasing  $\mu$ . Analytical methods to distinguish super/subcritical cases exist, based on higher order derivatives, however we can try to see numerically if a stable limit cycle exists for  $\mu > 0$  or an unstable one (bounding the basin of  $\mathbf{x}^*$ ) exists for  $\mu < 0$ .

However in this case, due to the particular structure of the dynamical system, the model can be written in a simpler form by using polar coordinates  $r$  (distance from the equilibrium) and  $\theta$  (angle of rotation):

$$\begin{aligned} x_1(t) &= r(t) \cos \theta(t) \\ x_2(t) &= r(t) \sin \theta(t) \end{aligned}$$

from which

$$\begin{aligned} \dot{x}_1 &= \dot{r} \cos(\theta) - r \sin(\theta) \dot{\theta} \\ \dot{x}_2 &= \dot{r} \sin(\theta) + r \cos(\theta) \dot{\theta} \end{aligned}$$

Replacing  $x_1, x_2, \dot{x}_1, \dot{x}_2$  in (34) the model becomes

$$\begin{cases} \dot{r} = r(\mu - r^2) \\ \dot{\theta} = 1 \end{cases}$$

The second equation indicates a constant rotation speed, the first the presence of an equilibrium  $r = 0$  which is stable for  $\mu \leq 0$  (even if it is not hyperbolic at  $\mu = 0$ ) and a further equilibrium  $r = \sqrt{\mu}$  ( $r$  can only assume positive values) that coincides with  $r = 0$  for  $\mu = 0$  and departs from it for  $\mu > 0$ . This newborn equilibrium is stable, and represents a limit cycle of radius  $r(\mu) = \sqrt{\mu}$  around the unstable equilibrium  $r = 0$  for  $\mu > 0$ . So, the bifurcation occurring at  $\mu = 0$  represents a supercritical Andronov-Hopf bifurcation.

As an exercise it can be proved that the following model exhibits a subcritical Andronov-Hopf bifurcation at  $\mu = 0$

$$\begin{cases} \dot{x}_1 = \mu x_1 - x_2 + x_1(x_1^2 + x_2^2) \\ \dot{x}_2 = x_1 + \mu x_2 + x_2(x_1^2 + x_2^2) \end{cases}$$

It can be noticed that at the bifurcation value  $\mu = 0$  the equilibrium  $(0, 0)$ , corresponding with  $r = 0$  in polar coordinates, is stable in the supercritical case and unstable in the subcritical case. If we consider only the linear part (identical in both the systems proposed) given by

$$\begin{cases} \dot{r} = \mu r \\ \dot{\theta} = 1 \end{cases}$$

we can notice that the equilibrium  $r = 0$  is asymptotically stable for  $\mu < 0$  and unstable for  $\mu > 0$ , but differently from the nonlinear case, at  $\mu = 0$  it is a centre, with infinitely many limit cycles around it. In fact, for  $\mu = 0$  we have  $\dot{r} = 0$ , hence any  $r > 0$  is an equilibrium. However all these closed invariant circles disappear for  $\mu > 0$ .

#### **An economic example: The Kaldor business cycle model (1940).**

This is a two-dimensional nonlinear dynamical system to model the endogenous generation of oscillations in an economic system.<sup>8</sup> Let  $Y(t)$  be the national income (or output) and  $K(t)$  the capital stock at time  $t$ . The model can be expressed as

$$\begin{cases} \dot{Y} = \alpha (I(Y, K) - S(Y, K)) \\ \dot{K} = I(Y, K) - \delta K \end{cases} \quad (35)$$

where the rate of change  $\dot{Y}$  of the output is proportional to the difference between investment  $I(Y, K)$  and savings  $S(Y, K)$ , the positive proportionality constant  $\alpha$  being the a measure of the speed of reaction of the national income to such difference.

Kaldor assumes that investments  $I(Y, K)$  are positively influenced by income  $Y$ , i.e.  $\frac{\partial I}{\partial Y} := I_Y > 0$ , and investments decrease if the capital stock increases, i.e.  $\frac{\partial I}{\partial K} := I_K < 0$ . The latter assumption is related to the fact that if the capital level is very high entrepreneurs are not motivated to invest to increase production. For sake of simplicity Kaldor assumes that saving  $S$  is an increasing function of  $Y$  with<sup>9</sup>  $0 < S_Y < 1$ , and also an increasing function of the capital stock, i.e.  $S_K \geq 0$ . The fact that the level of economic activities, measured by  $Y$ , increases proportionally to the demand excess  $I(Y, K) - S(Y, K)$  is in agreement with the short-period dynamics assumed in Keynesian models.

Also the second dynamic equation is quite standard, as it states that the rate of growth of the capital stock  $K$  is given by the level of investments  $I(Y, K)$  and reduced by a depreciation (or capital decay) rate  $\delta$ .

<sup>8</sup>Kaldor, N., A Model of the Trade Cycle, The Economic Journal, Vol. 50, No. 197, (Mar., 1940), pp. 78-92.

<sup>9</sup>The condition  $S_Y < 1$  states the principle of Keynesian multiplier, being  $S_Y$  the reciprocal of the Keynesian multiplier  $\frac{1}{1-C_Y}$  where  $C_Y$  is the consumption propensity given by  $C_Y = 1 - S_Y$ .

Following these general assumptions, let us consider for sake of simplicity a linear saving function depending on  $Y$  only, and a nonlinear investment function with "saturation effects" for small and high values of  $Y$  as well:

$$\begin{aligned} S(Y) &= \sigma Y, \text{ with } 0 \leq \sigma \leq 1 \\ I(Y, K) &= \sigma\mu + \gamma \left( \frac{\sigma\mu}{\delta} - K \right) + \arctan(Y - \mu) \end{aligned}$$

so the following "Kaldorian" model is obtained:

$$\begin{cases} \dot{Y} = \alpha (\sigma\mu + \gamma \left( \frac{\sigma\mu}{\delta} - K \right) + \arctan(Y - \mu) - \sigma Y) \\ \dot{K} = \sigma\mu + \gamma \left( \frac{\sigma\mu}{\delta} - K \right) + \arctan(Y - \mu) - \delta K \end{cases}$$

From the equilibrium conditions  $\dot{Y} = 0$  and  $\dot{K} = 0$  we get

$$\begin{aligned} \sigma\mu + \gamma \left( \frac{\sigma\mu}{\delta} - K \right) + \arctan(Y - \mu) - \sigma Y &= 0 \\ \sigma\mu + \gamma \left( \frac{\sigma\mu}{\delta} - K \right) - \delta K &= -\arctan(Y - \mu) \end{aligned}$$

hence

$$\begin{aligned} K &= \frac{\sigma}{\delta} Y \\ \sigma \left( 1 + \frac{\gamma}{\delta} \right) (Y - \mu) &= \arctan(Y - \mu) \end{aligned}$$

The point  $P = \left( \mu, \frac{\sigma\mu}{\delta} \right)$  is always an equilibrium of the model (35), however two further equilibrium points may be created as further intersections, symmetric with respect to  $Y = \mu$ , between the line  $z = \sigma \left( 1 + \frac{\gamma}{\delta} \right) (Y - \mu)$  and the sigmoid curve  $z = \arctan(Y - \mu)$ , as the slope of the line is varied. The Jacobian matrix

$$\mathbf{J}(Y, K) = \begin{bmatrix} \alpha \left( \frac{1}{1+(Y-\mu)^2} - \sigma \right) & -\alpha\gamma \\ \frac{1}{1+(Y-\mu)^2} & -\gamma - \delta \end{bmatrix}$$

at the equilibrium  $P$  becomes

$$\mathbf{J}(P) = \begin{bmatrix} \alpha(1 - \sigma) & -\alpha\gamma \\ 1 & -\gamma - \delta \end{bmatrix}$$

hence

$$\begin{aligned} Tr(\mathbf{J}(P)) &= \alpha(1 - \sigma) - \gamma - \delta \\ Det(\mathbf{J}(P)) &= -\alpha(1 - \sigma)(\gamma + \delta) + \alpha\gamma \end{aligned}$$

and from the stability conditions  $Tr(\mathbf{J}(P)) < 0$ ,  $Det(\mathbf{J}(P)) > 0$  we obtain

$$\begin{aligned} Tr(\mathbf{J}(P)) < 0 &\Rightarrow \alpha < \frac{\gamma + \delta}{(1 - \sigma)} \text{ or } \sigma > \frac{\alpha - \gamma - \delta}{\alpha} \\ det(\mathbf{J}(P)) > 0 &\Rightarrow \sigma > \frac{\delta}{\gamma + \delta} \end{aligned}$$

These two stability conditions define a region of stability in the space of the parameters. For example, if we consider the parameters' plane  $(\alpha, \sigma)$  the stability region is bounded by the curve (branch of an equilateral hyperbola)  $\sigma = \sigma_h = \frac{\alpha - (\gamma + \delta)}{\alpha}$  that represents a Hopf bifurcation curve, and the horizontal line  $\sigma = \sigma_p = \frac{\delta}{\gamma + \delta}$  that represents a pitchfork bifurcation curve. In fig. 51 the stability

region in the parameters' plane  $(\alpha, \sigma)$  is represented by the grey-shaded region. If, starting from the stability region with  $\alpha > \delta + \gamma$ , the propensity to save is decreased below the Hopf bifurcation value  $\sigma_h = \frac{\delta}{\gamma + \delta}$  then a supercritical Hopf bifurcation occurs after which a stable limit cycle is created on which periodic oscillations occur. The same occurs for  $\sigma > \frac{\delta}{\delta + \gamma}$  and speed of adjustment  $\alpha$  increasing beyond the bifurcation value  $\alpha_h = \frac{\delta + \gamma}{1 - \sigma}$ . In these cases the model is suitable to describe endogenously generated oscillations. However, if starting from a set of parameters inside the stability region the propensity to save  $\sigma$  is decreased below  $\sigma_p$ , then a pitchfork bifurcation occurs at which two stable nodes are created, one below and one above the central equilibrium, which becomes a saddle at the bifurcation. After the bifurcation, bistability is observed, with two equilibrium points characterized by a lower and an higher value of national income  $Y$ , each with its own basin of attraction separated by the stable set of the saddle: a poverty trap and a richness trap. These two different situations may be both present in the lower-right region of the plane, i.e. with sufficiently high values of  $\alpha$  and low values of  $\sigma$ , with dynamic scenarios given by three equilibria (two stable spirals with a saddle in the middle whose spiralling stable set separates the basins) surrounded by a large stable limit cycle.

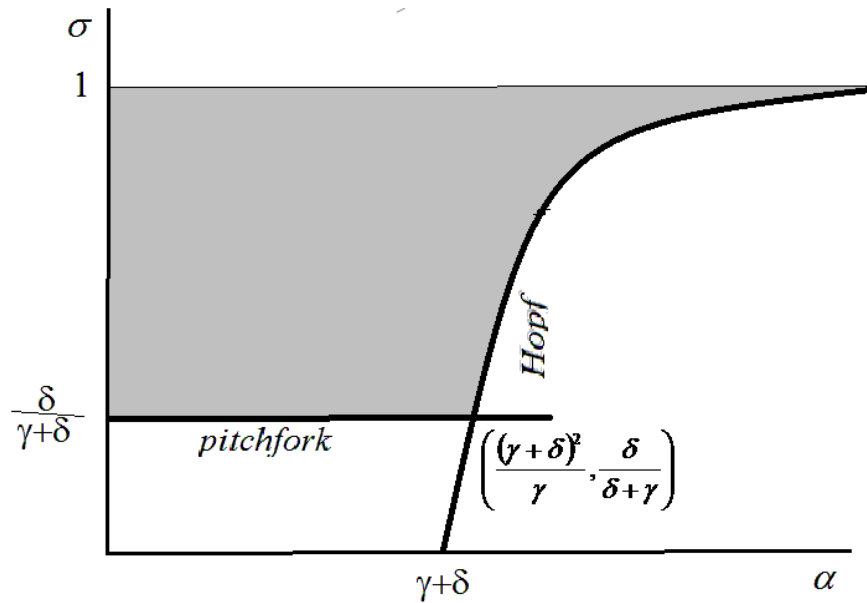


Figure 51: Stability region of the central equilibrium and bifurcation curves for the Kaldor model.

So, this version of the Kaldor model exhibits many different dynamic scenarios, some expected on the basis of the local stability analysis, but other situations can only be revealed through a global numerical explorations with different sets of parameters.

As an example, let us consider the model with the following parameters:  $\gamma = 0.4; \delta = 0.1; \mu = 1$ , so that the bifurcation curves become  $\sigma = \sigma_h = 0.2$  and  $\sigma = \sigma_p = 1 - \frac{0.5}{\alpha}$ . The following numerical experiments can be performed:

- $\alpha = 1, \sigma = 0.6$ ;  $P$  is the unique equilibrium, a stable focus.
- $\alpha = 2, \sigma = 0.6$ ,  $P$  is the unique equilibrium, an unstable focus, surrounded by a stable limit cycle.

- $\alpha = 1, \sigma = 0.1$  three equilibrium points exist, a saddle point and two stable nodes.
- If  $\alpha = 0.65$  and  $\sigma$  is decreased from 0.3 to 0.1, first a Hopf bifurcation occurs and then a Pitchfork.
- For  $\alpha = 1$  and  $\sigma = 0.19$  a large stable limit cycle surrounding three unstable equilibria.
- $\alpha = 0.9, \sigma = 0.18$  a stable limit cycle surrounding three equilibria: a central saddle point and two stable focuses each surrounded by an unstable limit cycle that bounds the corresponding basin, see fig.52.

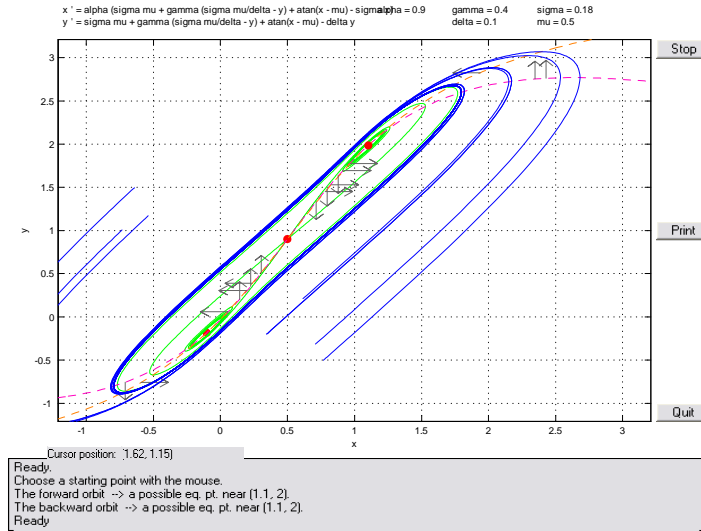


Figure 52: Coexisting equilibria and limit cycles in the Kaldor model.

### Goodwin's endogenous business cycle model (1967).

In 1967, Goodwin proposed a business cycle model where the dynamic variables are occupation and salaries.<sup>10</sup> On the basis of macroeconomic assumptions, Goodwin obtained a two-dimensional dynamic model formally identical to a Lotka-Volterra model, so that trajectories are characterized by endogenous oscillations. We briefly describe the economic assumptions on which the dynamic model is built. Given the measurable quantities:  $Y$  = National income,  $L$  = Number of occupied workers,  $N$  = Total number of available workers (active population),  $K$  = Capital stock,  $\omega$  = Per capita salary,  $a = \frac{Y}{L}$  = Labour productivity, the dynamic variables are defined as

$$v(t) = \frac{L}{N}, \text{ fraction of occupied workers (occupation)}$$

$$u(t) = \frac{\omega L}{Y} = \frac{\omega}{a} \text{ fraction of national income for salaries (salaries quota)}$$

The model is based on the following assumptions:

- 1- All the salaries  $\omega L$  received by the workers are used for consumption;

<sup>10</sup>R. M. Goodwin (1967) "A Growth Cycle", in C.H. Feinstein, editor, Socialism, Capitalism and Economic Growth. Cambridge: Cambridge University Press



2- The profit of capitalists  $Y - \omega L$  is totally invested:

$$\dot{K} = I = Y - \omega L$$

hence

$$\dot{K} = Y - \omega L = Y \left(1 - \frac{\omega L}{Y}\right) = Y \left(1 - \frac{\omega}{a}\right)$$

The rate of change of the dynamic variables is obtained as follows:

$$\frac{\dot{v}}{v} = \frac{d}{\mathbf{J}} \ln \left(\frac{L}{N}\right) = \frac{\dot{L}}{L} - \frac{\dot{N}}{N}$$

We also assume that the population grows at a constant rate  $\beta$ , i.e.  $\frac{\dot{N}}{N} = \beta$ , the rate of change of occupation determined as

$$L = \frac{Y}{Y} L = \frac{Y}{a} \Rightarrow \frac{\dot{L}}{L} = \frac{d}{\mathbf{J}} \ln(L) \underset{a = \frac{Y}{L}}{=} \frac{d}{\mathbf{J}} \ln\left(\frac{Y}{a}\right) = \frac{\dot{Y}}{Y} - \frac{\dot{a}}{a}$$

the technological progress grows at a constant rate  $\alpha$ , i.e.  $\frac{\dot{a}}{a} = \alpha$ , and the ratio between capital and income is constant, i.e.  $\frac{K}{Y} = \gamma$ , then we get

$$\frac{K}{Y} = \gamma \Rightarrow \frac{d}{\mathbf{J}} \left(\frac{K}{Y}\right) = 0 \Leftrightarrow \frac{\dot{K}Y - \dot{Y}K}{Y^2} = 0 \Leftrightarrow \frac{\dot{K}}{K} = \frac{\dot{Y}}{Y}$$

Replacing  $\frac{\dot{Y}}{Y}$  with  $\frac{\dot{K}}{K}$  in the expression of  $L$  we get

$$L = \frac{\dot{K}}{K} - \alpha$$

and from the model's assumption  $\dot{K} = Y \left(1 - \frac{\omega}{a}\right)$  follows that

$$\frac{\dot{K}}{K} = \frac{Y}{K} \left(1 - \frac{\omega}{a}\right) = \frac{1}{\gamma} (1 - u)$$

where  $u = u(t)$  is the dynamic variable. From

$$\frac{\dot{L}}{L} = \frac{1}{\gamma} (1 - u) - \alpha$$

we get the first dynamic equation about occupation:

$$\dot{v} = v \left[ -\alpha - \beta + \frac{1}{\gamma} (1 - u) \right] = v \left[ r - \frac{1}{\gamma} u \right]$$

The dynamic equation of salaries is obtained according to

$$\frac{\dot{u}}{u} = \frac{d}{J} \ln \left( \frac{\omega L}{Y} \right) = \frac{d}{J} \ln \left( \frac{\omega}{a} \right) = \frac{\dot{\omega}}{\omega} - \frac{\dot{a}}{a} = \frac{\dot{\omega}}{\omega} - \alpha$$

The rate of change of real salaries is positively influenced by occupation  $v$  according to a given a function  $f(v)$

$$\frac{\dot{\omega}}{\omega} = f(v)$$

see fig. 53 taken from Goodwin (1967):

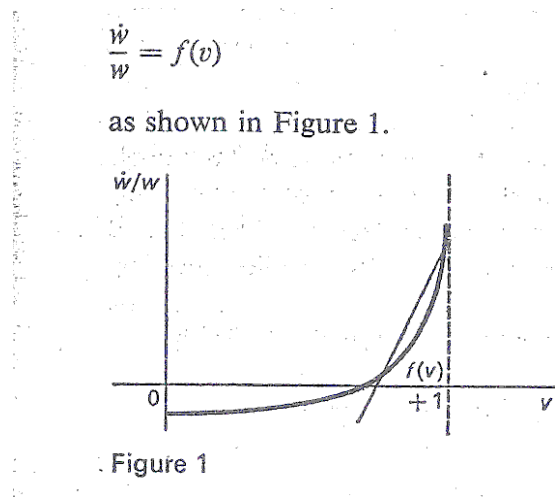


Figure 53: From Goodwin (1967)

For sake of simplicity (but this is a quite strong assumption) the function  $f$  (that expresses the Phillips curve) is assumed to be linear

$$f(v) = \rho v - \delta$$

from which we get the dynamic equation for salaries

$$\dot{u} = u [\rho v - \delta - \alpha]$$

All in all, the Goodwin model is obtained in the form:

$$\begin{cases} \dot{v} = v \left[ r - \frac{1}{\gamma} u \right] \\ \dot{u} = u [\rho v - (\alpha + \delta)] \end{cases}$$

which is a classical Volterra model with neutral stability, where  $v$  represents the prey population and  $u$  predators' one. Like in the classical Volterra model of 1926, any trajectory moves along a different closed invariant curve according to the initial condition, and these orbits are not confined inside the square  $(v, u) \in [0, 1] \times [0, 1]$  as they should be according to the definition of the dynamic variables. This is a consequence of the fact that the function  $f(v)$ , that should be characterized by a vertical asymptote in  $v = 1$  as in fig. 53, has been approximated by a linear function.

A good exercise should be to replace the linear  $f(v) = \rho v - \delta$  with a more realistic nonlinear one, such as  $f(v) = \frac{v-\delta}{1-v}$  with  $0 < \delta < 1$ .

**Goodwin model with inflation** Following Flaschel (1984)<sup>11</sup> the rate of change of real salaries is assumed to be not only positively influenced by occupation  $v$  but also negatively influenced by inflation rate  $i(u)$ , which is assumed to be a function of salary level

$$\frac{\dot{\omega}}{\omega} = f(v) - \mu i(u)$$

where  $\mu$  is a proportionality parameter that reflects how much real salaries are influenced by inflation.

The function  $i(u)$  is assumed to be expressed by

$$i(u) = (1 + \tau)u - 1$$

So, the dynamics of the occupation rate becomes

$$\dot{u} = u[\rho v - \delta - \mu((1 + \tau)u - 1) - \alpha]$$

and the modified Goodwin model is:

$$\begin{cases} \dot{v} = v \left[ r - \frac{1}{\gamma}u \right] \\ \dot{u} = u [\rho v - \alpha - \delta - \mu((1 + \tau)u - 1)] \end{cases}$$

The equilibrium points are

$$E_1 = (0, 0); E_2 = \left( 0, \frac{\mu - \alpha - \delta}{\mu(1 + \tau)} \right); E_3 = \left( \frac{\alpha + \delta + \mu((1 + \tau)r\gamma - 1)}{\rho}, r\gamma \right)$$

In order to study the stability of the equilibrium points let us compute the Jacobian matrix:

$$\mathbf{J}(v, u) = \begin{bmatrix} r - \frac{1}{\gamma}u & -\frac{1}{\gamma}v \\ u\rho & \rho v - \alpha - \delta - \mu(2(1 + \tau)u - 1) \end{bmatrix}$$

at the equilibrium points.

$$\mathbf{J}(E_1) = \begin{bmatrix} r & 0 \\ 0 & -\alpha - \delta + \mu \end{bmatrix}$$

hence  $\lambda_1 = r$ ,  $\lambda_2 = -\alpha - \delta + \mu_2$ .

$$\mathbf{J}(E_2) = \begin{bmatrix} r - \frac{1}{\gamma}u & 0 \\ u\rho & -\mu(1 + \tau)u \end{bmatrix} = \begin{bmatrix} \frac{r\gamma\mu(1+\tau) - \mu + \alpha + \delta}{\gamma\mu(1+\tau)} & 0 \\ \frac{\mu - \alpha - \delta}{\mu(1+\tau)}\rho & -\mu + \alpha + \delta \end{bmatrix}$$

where the equilibrium condition  $\rho v - \alpha - \delta - \mu((1 + \tau)u - 1) = 0$  has been used to simplify  $J_{2,2}$ . The eigenvalues are  $\lambda_1 = \frac{r\gamma\mu(1+\tau) - \mu + \alpha + \delta}{\gamma\mu(1+\tau)}$ ,  $\lambda_2 = -\mu + \alpha + \delta$ . Finally:

$$\mathbf{J}(E_3) = \begin{bmatrix} 0 & -\frac{1}{\gamma}v \\ u\rho & -\mu(1 + \tau)u \end{bmatrix} = \begin{bmatrix} 0 & -\frac{\alpha + \delta + \mu((1 + \tau)r\gamma - 1)}{\gamma\rho} \\ r\gamma\rho & -\mu(1 + \tau)r\gamma \end{bmatrix}$$

<sup>11</sup>Flaschel, P. (1984) Some stability properties of Goodwin's growth cycles. Zeitschrift fuer Nationaloekonomie 44, 281-285.

where the equilibrium conditions  $r - \frac{1}{\gamma}u = 0$  and  $\rho v - \alpha - \delta - \mu((1 + \tau)u - 1) = 0$  have been used to simplify  $J_{1,1}$  and  $J_{2,2}$ . The stability conditions become

$$\begin{aligned} Tr\mathbf{J}(E_3) &= -\mu(1 + \tau)r\gamma < 0 \text{ if and only if } \mu > 0 \\ \det\mathbf{J}(E_3) &= \frac{\rho}{\gamma}v^*u^* > 0 \text{ provided that } v^* > 0 \text{ and } u^* > 0 \end{aligned}$$

For sufficiently small values of  $\mu$  (both positive and negative) the eigenvalues are complex conjugate as  $\Delta = Tr\mathbf{J}(E_3)^2 - 4\det\mathbf{J}(E_3) < 0$  because this is true when  $\mu = 0$  (for which  $\Delta = -4\det\mathbf{J}(E_3) < 0$ ) hence by continuity it must be true for  $\mu$  values in a neighborhood of 0. So, the necessary conditions for an Hopf bifurcation hold. However, for  $\mu = 0$  we have infinitely many orbits around  $E_3$  (a "centre" situation) and no closed orbits exist for  $\mu \neq 0$ , like in a linear case.

**Again the Rosenzweig MacArthur model.** From the equilibrium conditions of the model (33)

$$\begin{aligned} x_1 \left( \alpha - sx_1 - b\frac{x_2}{h+x_1} \right) &= 0 \\ x_2 \left( -d + c\frac{x_1}{h+x_1} \right) &= 0 \end{aligned}$$

we obtain the nullclines  $\dot{x}_1 = 0$  for  $x_1 = 0$  or  $x_2 = \frac{1}{b}(-sx_1^2 + \alpha x_1 + (\alpha - s)h)$  (the vertical axis and a concave parabola);  $\dot{x}_2 = 0$  for  $x_2 = 0$  or  $x_1 = \frac{dh}{c-d}$  (the horizontal axis and a vertical line). At the three intersections of the nullclines are located three equilibrium points

$$O = (0, 0); \quad A = \left( \frac{\alpha}{s}, 0 \right); \quad E = \left( \frac{dh}{c-d}, \frac{h(\alpha(c-d) - sdh)}{b(c-d)^2} \right)$$

The Jacobian matrix

$$\mathbf{J}(x_1, x_2) = \begin{bmatrix} \alpha - 2sx_1 - \frac{bhx_2}{(h+x_1)^2} & -\frac{bx_1}{h+x_1} \\ \frac{chx_2}{(h+x_1)^2} & \frac{cx_1}{h+x_1} - d \end{bmatrix}$$

at the interior equilibrium becomes

$$\mathbf{J}(E) = \begin{bmatrix} \alpha - \frac{2shd}{c-d} - \frac{\alpha(c-d) - shd}{c} & -\frac{bd}{c} \\ \frac{c(\alpha(c-d) - shd)}{bc} & 0 \end{bmatrix}$$

and the stability conditions

$$\begin{aligned} Tr(\mathbf{J}(E)) &< 0 \iff \alpha < \frac{sh(c+d)}{c-d} \\ Det(\mathbf{J}(E)) &> 0 \iff \alpha > \frac{shd}{c-d} \end{aligned}$$

So, if  $\frac{shd}{c-d} < \alpha < \frac{sh(c+d)}{c-d}$  then the equilibrium  $E$  is stable; if  $\alpha$  decreases below  $\frac{shd}{c-d}$  then a transcritical bifurcation occurs at which  $E = A$  and then  $E$  exits the positive orthant (i.e. exits the phase space of the model); if  $\alpha$  increases beyond  $\frac{sh(c+d)}{c-d}$  an Andronov-Hopf bifurcation occurs at which a stable limit cycle is created around the unstable focus  $E$  (see fig.43).

The existence of a limit cycle can also be determined by the Poincaré-Bendixson Theorem, as shown in fig. 54: the grey-shaded region, which is bounded from outside by the unstable set of the saddle  $A$ , the upper dashed line and the coordinate axes and from inside by the dashed circle around

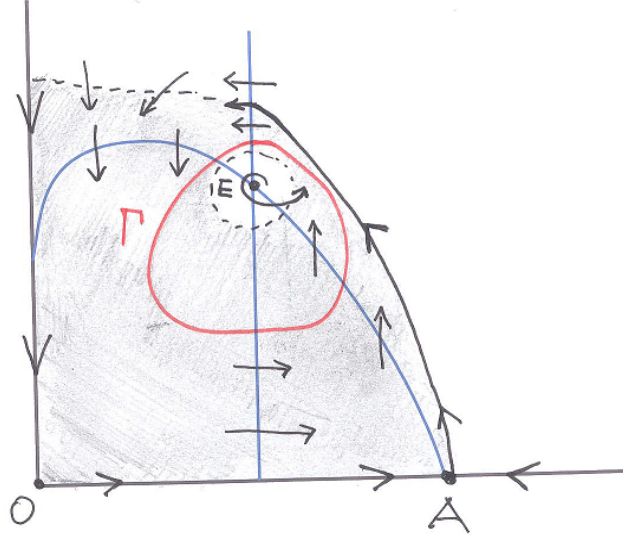


Figure 54: Poincaré-Bendixson theorem in a modified Goodwin model.

$E$ , is a compact trapping annular region that contains no equilibrium points. Hence it must include at least one limit cycle, indicated by the red closed invariant curve  $\Gamma$ . Now we know that the limit cycle is generated through the Andronov-Hopf bifurcation.

**Exercise: An advertising diffusion model.** The following model, proposed as exercise, has been published by G. Feichtinger (1995) to show how some widely accepted rules to publicize products in marketing practice lead to persistent fluctuations of selling. Let us assume that the population in a marketing system is subdivided into two groups:  $x_1(t)$  is the number of potential buyers of a given product and  $x_2(t)$  is the number of actual buyers at time  $t$ . Potential consumers are not yet buyers because they do not know the existence of that product, however they can become aware of the product after they meet actual buyers (word-of-mouth information). So, the diffusion of information about the product considered is proportional to the number of encounters, i.e. the product between respective densities (like in the ecological models with random encounters). However in this case the diffusion of information is also positively influenced by advertising activities  $a(t) = \alpha x_2(t)$ , proportional to the number of buyers with  $\alpha > 0$  proportionality constant that reflects advertising efficacy. The model also includes the possibility that actual buyers decide to change the brand, i.e. they buy a similar product from another (concurrent) firm producing it, at a rate  $\beta > 0$  (so they are no longer actual buyers even if they remain potential buyers), whereas a fraction  $\varepsilon > 0$  of consumers leave the market forever. Finally, denoting by  $k > 0$  the rate of new potential customers entering the system, the model becomes

$$\begin{cases} \dot{x}_1 = k - \alpha x_1 x_2^2 + \beta x_2 \\ \dot{x}_2 = \alpha x_1 x_2^2 - (\beta + \varepsilon) x_2 \end{cases}$$

It can be proved that the model undergoes a supercritical Andronov-Hopf bifurcation (see fig. 55).

**Van der Pol equation.** This is a famous example, a differential equation of the second order (i.e. involving the second order derivative) used to describe oscillations in physical devices, also used

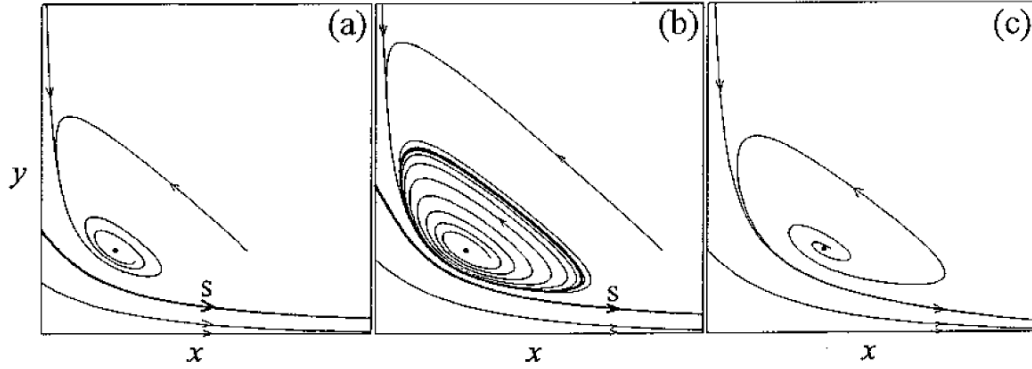


Figure 55: From Feichtinger, Ghezzi and Piccardi "Chaotic behaviour in an advertising diffusion model", International Journal of Bifurcation and Chaos (1995)

by Goodwin (1951) to represent oscillations in an economic system

$$\ddot{x} - \mu(1 - x^2)\dot{x} + x = 0 \quad (36)$$

As usual for second order differential equations, it can be re-written in the standard form of a system of first order differential equations by defining a new dynamic variable  $y(t) = \dot{x}$ , so that (36) can be equivalently written as

$$\begin{aligned} \dot{x} &= y \\ \dot{y} &= \mu(1 - x^2)y - x \end{aligned} \quad (37)$$

as  $\dot{y} = \ddot{x}$ . The study of (37) follows the usual steps. It is easy to see that the unique equilibrium is  $O = (0, 0)$  and the Jacobian matrix

$$\mathbf{J}(x, y) = \begin{bmatrix} 0 & 1 \\ -2\mu xy - 1 & \mu(1 - x^2) \end{bmatrix}$$

computed at the equilibrium becomes

$$\mathbf{J}(O) = \begin{bmatrix} 0 & 1 \\ -1 & \mu \end{bmatrix}$$

Hence  $Tr(\mathbf{J}(O)) = \mu < 0$  for  $\mu < 0$ , and  $Det(\mathbf{J}(O)) = 1 > 0 \forall \mu$ , from which the equilibrium is a stable focus for  $\mu < 0$  and becomes an unstable focus as  $\mu$  increases beyond the bifurcation value  $\mu = 0$ , at which a supercritical Hopf bifurcation occurs.

## 5 n-dimensional dynamical systems in continuous time

Many of the results about linear systems, linearization of nonlinear ones around equilibrium points, their stability and related bifurcations, can be extended to  $n$ -dimensional dynamical systems with  $n > 2$ , i.e. with more than two dynamic variables. However, as we will see, some important differences are worth to be emphasized, first of all the possibility of chaotic trajectories and chaotic attractors for  $n \geq 3$ .

## 5.1 Linear systems

For a linear system  $\dot{\mathbf{x}} = \mathbf{A}\mathbf{x}$ ,  $\mathbf{x} \in \mathbb{R}^n$ , with  $\mathbf{A}$   $n \times n$  matrix of constant coefficients, we again have solutions given by linear combinations of functions like:

$$\mathbf{v}e^{\lambda t}, \mathbf{v}te^{\lambda t}, \mathbf{v}t^2e^{\lambda t}, \dots, \mathbf{v}e^{\operatorname{Re}(\lambda)t} \cos(\operatorname{Im}(\lambda)t), \mathbf{v}e^{\operatorname{Re}(\lambda)t} \sin(\operatorname{Im}(\lambda)t), \mathbf{v}te^{\operatorname{Re}(\lambda)t} \cos(\operatorname{Im}(\lambda)t), \mathbf{v}te^{\operatorname{Re}(\lambda)t} \sin(\operatorname{Im}(\lambda)t), \dots$$

where  $\lambda$  is a (real or complex) solution of the characteristic equation  $\det(\mathbf{A} - \lambda\mathbf{I}) = 0$ , expressed by an algebraic equation of degree  $n$

$$P(\lambda) = \lambda^n + a_1\lambda^{n-1} + a_2\lambda^{n-2} + \dots + a_{n-1}\lambda + a_n = 0 \quad (38)$$

where again  $a_1 = \operatorname{Tr}(\mathbf{A}) = a_{11} + a_{22} + \dots + a_{nn}$ ,  $a_k$ ,  $k = 2, \dots, n-1$ , given by a sum of  $n$  minors of order  $k$ ,  $a_n = \det(\mathbf{A})$ . Let  $\mathbf{v} \in \mathbb{R}^n$  be a corresponding eigenvector, solution of the homogenous linear system, of order  $n$ ,  $(\mathbf{A} - \lambda\mathbf{I})\mathbf{v} = \mathbf{0}$ . The condition for the asymptotic stability of the unique equilibrium  $\mathbf{0}$  is that all the eigenvalues<sup>12</sup> have negative real part, i.e.  $\operatorname{Re}(\lambda) < 0$  for each eigenvalue. This can be equivalently stated as  $\operatorname{Re}(\lambda_1) < 0$  where  $\lambda_1$  is the dominant eigenvalue, defined as the one with maximum real part in the set of all eigenvalues (i.e. the rightmost one in the complex plane). Of course, we can have a single real dominant eigenvalue or a couple of complex conjugate dominant eigenvalues.

If the dominant eigenvalue  $\lambda_1$  is real and negative, then the long run dynamics towards the equilibrium is monotonic as all the possible oscillatory modes associated with complex eigenvalues vanish in the long run more fastly than the solution associated to  $\lambda_1$ . The return time is estimated as  $T_r = -\frac{1}{\lambda_1}$ .

If the dominant eigenvalue is a couple of complex conjugate ones, hence with the same real part  $\operatorname{Re}(\lambda_1)$ , then an oscillatory convergence is observed in the long run with *characteristic return time*  $T_r = -\frac{1}{\operatorname{Re}(\lambda_1)}$  and *rotation period*  $T_{rot} = \frac{2\pi}{\operatorname{Im}(\lambda_1)}$ .

A necessary condition for all the eigenvalues (i.e. the solutions of the characteristic equation 38) to have negative real parts is  $a_k > 0$  for  $k = 1, \dots, n$ .

A necessary and sufficient condition for the same property is formulated through the *Routh-Hurwitz* criterion, which is expressed in terms of the coefficients  $a_k$ ,  $k = 1, \dots, n$ , of (38) as follows.

**Routh-Hurwitz criterion.** *Let us consider the matrix formed by coefficient of (38) arranged in the following matrix*

$$\begin{bmatrix} a_1 & 1 & 0 & 0 & 0 & \dots & 0 \\ a_3 & a_2 & a_1 & 1 & 0 & \dots & 0 \\ a_5 & a_4 & a_3 & a_2 & a_1 & \dots & 0 \\ \dots & \dots & & & & & \\ 0 & 0 & 0 & 0 & 0 & \dots & a_n \end{bmatrix} \quad (39)$$

*Then all the solutions of (38) have negative real parts if and only if the leading principal minors of the matrix (39) are positive.*

For example, for  $n = 2$  we have  $a_1 > 0$  and  $\det \begin{bmatrix} a_1 & 1 \\ 0 & a_2 \end{bmatrix} > 0$ , i.e.  $a_1 a_2 > 0$ , equivalent to the already stated stability conditions  $a_1 > 0$  and  $a_2 > 0$ , i.e.  $\operatorname{Tr}(\mathbf{A}) < 0$  and  $\det(\mathbf{A}) > 0$ .

<sup>12</sup>According to the Fundamental Theorem of Algebra a polynomial  $P(\lambda)$  of degree  $n$  always has  $n$  complex solutions (counted with proper multiplicity in the case of coincident ones). Moreover, if the coefficients  $a_k$  of the polynomial are real numbers, like in our case, for each complex root with  $\operatorname{Im}(\lambda) \neq 0$  the complex conjugate is a root as well.

For  $n = 3$  the criterion gives  $a_1 > 0$ ,  $\det \begin{bmatrix} a_1 & 1 \\ a_3 & a_2 \end{bmatrix} > 0$  and  $\det \begin{bmatrix} a_1 & 1 & 0 \\ a_3 & a_2 & a_1 \\ 0 & 0 & a_3 \end{bmatrix} > 0$ , equivalent to  $a_1 > 0$ ,  $a_3 > 0$  and  $a_1 a_2 > a_3$ .

For  $n = 4$ ,  $a_1 > 0$ ,  $\det \begin{bmatrix} a_1 & 1 \\ a_3 & a_2 \end{bmatrix} > 0$ ,  $\det \begin{bmatrix} a_1 & 1 & 0 \\ a_3 & a_2 & a_1 \\ 0 & a_4 & a_3 \end{bmatrix} > 0$  and  $\det \begin{bmatrix} a_1 & 1 & 0 & 0 \\ a_3 & a_2 & a_1 & 1 \\ 0 & a_4 & a_3 & a_2 \\ 0 & 0 & 0 & a_4 \end{bmatrix} > 0$ , equivalent to  $a_1 > 0$ ,  $a_2 > 0$ ,  $a_3 > 0$ ,  $a_4 > 0$  and  $a_1 a_2 a_3 - a_3^2 - a_4 a_1^2 > 0$ .

And so on for higher  $n$ .

As an example, let us consider the fourth degree equation  $z^4 + 5z^3 + 13z^2 + 9z + 10 = 0$ . We are not able to solve it, however as the coefficients are all positive and  $5 \cdot 13 \cdot 9 - 9^2 - 10 \cdot 5^2 = 254 > 0$  we can deduce that all its 4 roots have negative real part (they may be all real, or two real and two complex conjugate, or two pairs of complex conjugate).

So, again, the problem of stability of the equilibrium of a linear dynamical system is reduced to a set of algebraic conditions, even if these conditions are, of course, more and more complicated as the dimension of the dynamical system increases. If the coefficients of the dynamical systems, and consequently of the characteristic equation, depend on one or more parameters, the stability conditions can be used to detect changes of stability as the parameters are varied. In the case of linear systems a transition from stability to instability means a transition from global asymptotic stability to divergent trajectories.

Another interesting result about localization of eigenvalues in the complex plane is expressed by the following

**Gerschgorin Circle Theorem.** Let  $A = [a_{ij}]$  be a square matrix with complex entries  $a_{ij} \in \mathbb{C}$ . Let

$$D_k = \left\{ z \in \mathbb{C} \text{ such that } |z - a_{kk}| \leq \sum_{j=1, j \neq k}^n |a_{kj}| \right\}, k = 1, \dots, n$$

be the set of  $n$  disks with centered in the  $k^{\text{th}}$  diagonal entry and radius given by the sum of the absolute values of the non-diagonal entries of the same row. Then all the eigenvalues of  $A$  must be contained in the union of the  $n$  disks.

**Corollary.** As the eigenvalues of a matrix and its transpose are the same, the disks may be defined with reference to columns

$$D'_k = \left\{ z \in \mathbb{C} \text{ such that } |z - a_{kk}| \leq \sum_{j=1, j \neq k}^n |a_{jk}| \right\}, k = 1, \dots, n$$

hence the region of the complex plane allowed to eigenvalues is given by the intersection of the two unions, i.e.

$$\left( \bigcup_{k=1}^n D_k \right) \cap \left( \bigcup_{k=1}^n D'_k \right)$$

Figure 56 gives an example of the application of the Gerschgorin Theorem.



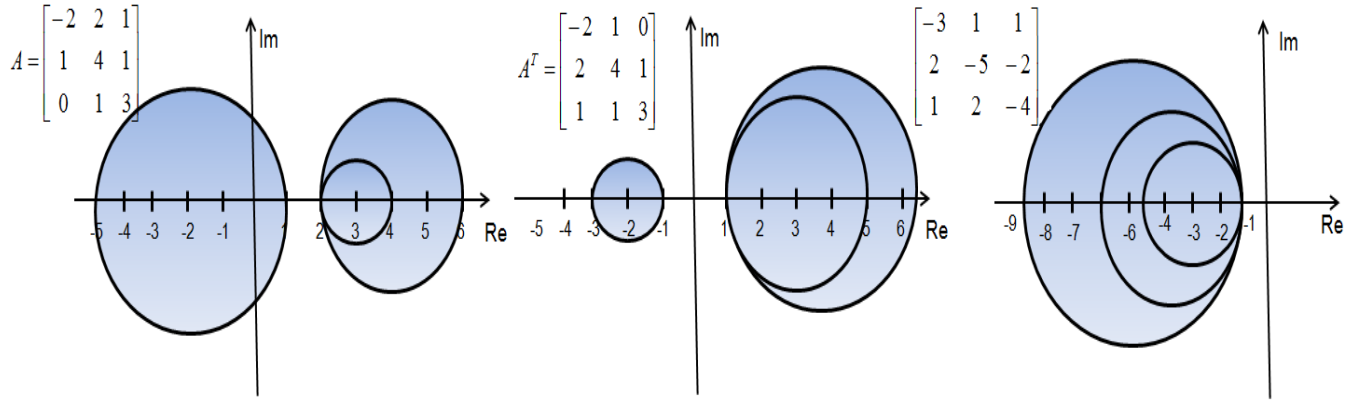


Figure 56: Application of the Gerschgorin Circle Theorem.

The Gerschgorin Theorem provides an useful application to the study of stability in the case of negative diagonal dominant matrices.

**Definition** A matrix is diagonal dominant if for each row (or each column) the following inequality holds

$$|a_{kk}| > \sum_{j=1, j \neq k}^n |a_{kj}| \quad \left( |a_{kk}| > \sum_{j=1, j \neq k}^n |a_{jk}| \right)$$

Moreover, if  $a_{kk} < 0$  for each  $k$  then the matrix is called negative diagonal dominant.

An immediate corollary of the Gerschgorin Theorem is the following

**Corollary** If a matrix is negative diagonal dominant then all its eigenvalues have negative real part.

From the point of view of dynamical systems, this stability statement can be expressed by saying that if self-control (i.e. the inhibitory effect that a dynamic variable exerts on itself) is stronger than joint influence of all other variables, then the system is stable. As an example, let us consider the following linear dynamical system

$$\begin{aligned} \dot{x}_1 &= -3x_1 + x_2 + x_3 \\ \dot{x}_2 &= 2x_1 - 5x_2 + 2x_3 \\ \dot{x}_3 &= x_1 + 2x_2 - 4x_3 \end{aligned}$$

whose Gerschgorin disks are shown in fig.57 here below.

## 5.2 Nonlinear systems

Let us consider an  $n$ -dimensional dynamical system in the form

$$\dot{\mathbf{x}} = \mathbf{f}(\mathbf{x}; \mu), \quad \mathbf{x} \in \mathbb{R}^n, \quad \mu \in \mathbb{R}. \quad (40)$$

and let  $\mathbf{x}^*(\mu)$  be an equilibrium point, implicitly defined as a solution of the nonlinear system  $\mathbf{f}(\mathbf{x}; \mu) = 0$  of  $n$  equations with  $n$  unknowns. In order to study the local stability and to have an idea of the

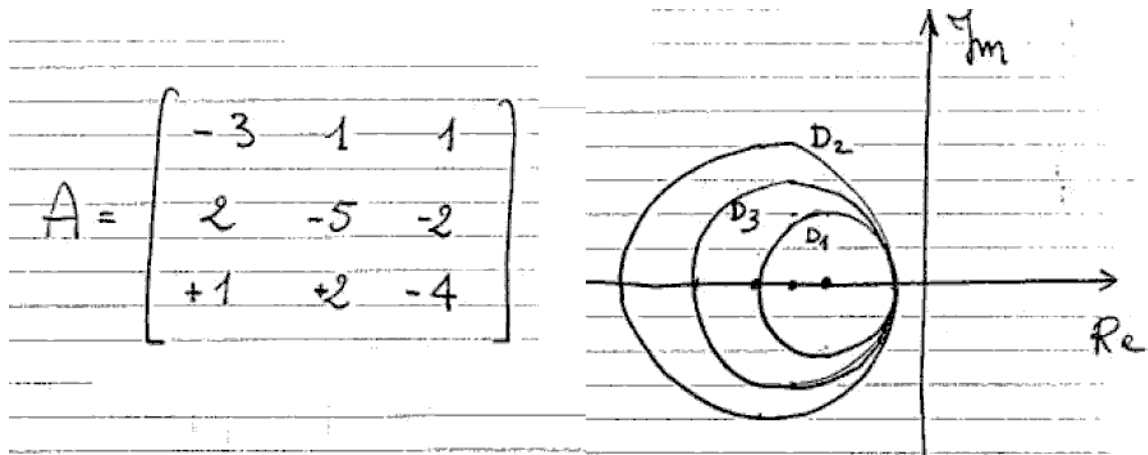


Figure 57: Another example.

kind of local phase portrait in a neighborhood of each equilibrium point, the linear approximation  $\dot{\mathbf{X}} = \mathbf{J}(\mathbf{x}^*(\mu))\mathbf{X}$  can be considered, where  $\mathbf{J}(\mathbf{x}^*(\mu)) = \left[ \frac{\partial f_i}{\partial x_j} \Big|_{\mathbf{x}^*} \right]$  is the  $n \times n$  Jacobian matrix computed at the equilibrium point considered, and  $\mathbf{X} = \mathbf{x} - \mathbf{x}^*$  is the displacement from the equilibrium. If the equilibrium point is hyperbolic, i.e. all the eigenvalues of  $\mathbf{J}(\mathbf{x}^*)$  have non vanishing real part, then the study of the local stability of the equilibrium is reduced to the study of the stability of the linear approximation, and even the local qualitative behaviour of the dynamical system can be deduced from the study of the linear approximation, according to the Hartman-Grobman Theorem. In particular, we have the result that if all the eigenvalues have negative real part then the equilibrium is locally asymptotically stable. Moreover, the dominant eigenvalue (or dominant couple, in the case of complex conjugate dominant eigenvalues) provides information about the kind of equilibrium we are dealing with and the speed of convergence to the equilibrium.

In analogy with what we have seen for the two-dimensional nonlinear dynamical systems, if the dominant eigenvalue (or couple of dominant eigenvalues) moves from negative to positive real part (i.e. cross the imaginary axis) as some parameter is varied, i.e. if some of the Routh-Hurwitz conditions change sign, then a bifurcation occurs at which the equilibrium considered becomes unstable. This is generally associated with some other change in phase portrait, such as creation/destruction of equilibrium points or closed invariant curves, or merging of equilibria with stability exchange. In particular, if the eigenvalue crossing the imaginary axis is real, then we have the usual one-dimensional bifurcations along the invariant direction tangent to the corresponding eigenvector (i.e. fold, or saddle-node, or pitchfork or transcritical), whereas if a couple of complex conjugate eigenvalues crosses the imaginary axis with imaginary part different from zero, then an Andronov-Hopf bifurcation occurs leading to the creation of a closed invariant curve in the plane of the two independent real eigenvectors associated (also called center manifold). These bifurcations lead to scenarios similar to the ones already seen for two-dimensional systems, but with a richer variety related to the presence of other dimensions, see e.g. the qualitative sketches in three dimensions shown in fig. 58).

As it can be noticed, the Jordan curve lemma no longer holds, as trajectories can jump from inside to outside a closed invariant curve in the center manifold by moving outside their plane. This allows the formation of more complicated attractors that cannot exist in two dimensions, which are sometimes called "strange attractors" along which aperiodic motions can be observed with some fea-

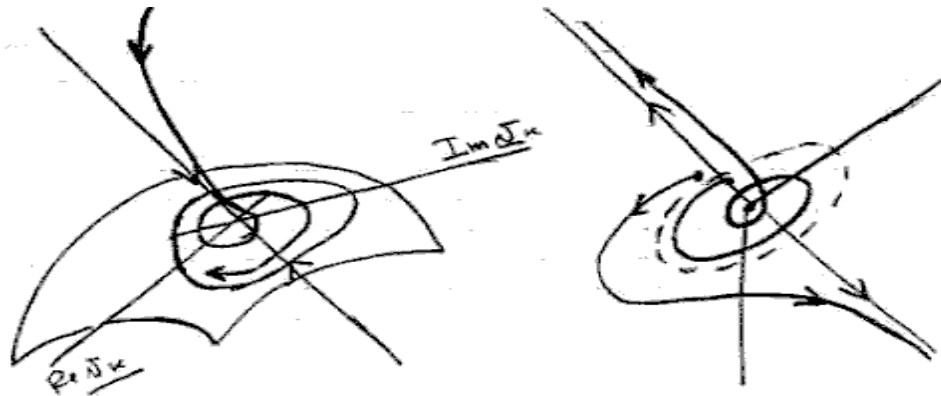


Figure 58: Saddle-focus in 3 dimensions.

tures that opened a remarkable field of studies under the name of "*deterministic chaos*", an apparent oxymoron. In fact, the two words "deterministic" and "chaos" express two quite counterpoised meanings. Deterministic means without uncertainty, predictable, regular, where any cause implies clear effects or consequences. Chaos is generally referred to confused, unpredictable, irregular systems, where consequences of a given cause are not clear. Indeed, what we are considering in this course on dynamical systems is completely and perfectly deterministic, because given an initial condition and the knowledge of the dynamic equations, a unique time evolution (i.e. a trajectory) of the dynamical system is obtained. This allows one to compute the future state of the system for any time without any uncertainty, as it was expressed by the French mathematician Pierre Simon Laplace in 1776 in the following famous statement<sup>13</sup> "*We may regard the present state of the universe as the effect of its past and the cause of its future. An intellect which at a certain moment would know all forces that set nature in motion, and all positions of all items of which nature is composed, if this intellect were also vast enough to submit these data to analysis, it would embrace in a single formula the movements of the greatest bodies of the universe and those of the tiniest atom; for such an intellect nothing would be uncertain and the future just like the past would be present before its eyes*". This statement, that was mainly motivated by the usage of dynamical systems to describe the motion of rigid bodies (included astronomical motions) is now known as the *Laplacian determinism*, and the intellect which is assumed to know the equations of motion of the Universe and the its exact state at a given time is sometimes called *Laplace's demon*.

The concept of deterministic chaos<sup>14</sup> in the theory of dynamical systems was first glimpsed by Henri Poincaré during his attempt to find the trajectories of a three-body system in the presence of the gravitational force. This problem was considered by Poincaré in order to participate to a contest sponsored in 1887 by the king of Sweden Oscar II in honour of his 60th birthday, where some mathematical questions were proposed. One of the questions in this contest was to show rigorously that the solar system as modeled by Newton's differential equations is dynamically stable. Poincaré reduced this question to the famous three-body problem, which revealed itself to be very difficult. In essence, the three body problem consists of nine simultaneous differential equations. While Poincaré

<sup>13</sup>See Pierre Simon Laplace, *Théorie analytique des probabilités*. Paris: V. Courcier, 1820.

<sup>14</sup>However the term "chaos" in this context was first introduced in the paper "Period three implies chaos" by Tien-Yien Li and James A. Yorke, *The American Mathematical Monthly*, December 1975.

did not succeed in giving a complete solution, his work was so impressive that he was awarded the prize anyway. As remarked by Weierstrass, who was one of the judges "the work of Poincaré cannot indeed be considered as furnishing the complete solution of the question proposed, but that it is nevertheless of such importance that its publication will inaugurate a new era in the history of celestial mechanics." In practice, in his work Poincaré started the study of dynamical systems by using topological methods or qualitative theory. In other words, he was the inventor of the "qualitative" methods to study dynamical systems that we also are using in this lecture notes. One striking feature of the nonlinear dynamical system studied by Poincaré was described by Poincaré himself as an extraordinary sensitivity of trajectories with respect to arbitrarily small, even negligible, variations of the initial conditions. Even without the possibility to visualize numerical computations of the trajectories, Poincaré described the extreme irregularity of time paths obtained, and the intricacy of highly intermingled trajectories ("I can imagine them in my mind but I cannot describe how complicated they are"). His description of the phenomenon of sensitive dependence on initial conditions is one of the most famous pages of mathematical literature<sup>15</sup>:

*"If we knew exactly the laws of nature and the situation of the universe at the initial moment, we could predict exactly the situation of that same universe at a succeeding moment. But even if it were the case that the natural laws had no longer any secret for us, we could still only know the initial situation approximately. If that enabled us to predict the succeeding situation with the same approximation, that is all we require, and we should say that the phenomenon had been predicted, that it is governed by laws. But it is not always so; it may happen that small differences in the initial conditions produce very great ones in the final phenomena. A small error in the former will produce an enormous error in the latter. Prediction becomes impossible, and we have an apparently fortuitous phenomenon."*

In this sense systems that are deterministic exhibit a behaviour so irregular that appear to be similar to chaotic motions, governed by stochastic influences.

The discovery of such irregularities, and related difficulties to make reliable predictions in some nonlinear dynamical systems, initially had not a strong impact. The question was stressed, and became quite popular and pervasive in the Sixties of 20<sup>th</sup> century, after the work by the American mathematician and meteorologist Edward Lorenz, who noticed this difficulties in making predictions in some dynamic models used in weather forecasting. The dynamic equations used by Lorenz are quite simple, even if they are not linear. They can be expressed by the following three-dimensional dynamical system

$$\begin{cases} \dot{x}_1 = \sigma(x_2 - x_1) \\ \dot{x}_2 = \rho x_1 - x_2 - x_1 x_3 \\ \dot{x}_3 = x_1 x_2 - \beta x_3 \end{cases} \quad (41)$$

where the dynamic variables  $x_i(t)$ ,  $i = 1, 2, 3$ , as well as the parameters, represent quantities used to describe weather conditions. For a given set of parameters, namely  $\sigma = 10$ ,  $\beta = 2.666$ ,  $\rho = 20$ , and initial conditions  $x_1(0) = 10$ ,  $x_2(0) = 10$ ,  $x_3(0) = 10$ , figure (59) shows  $x_1(t)$  obtained by a numerical simulation of (41). It is quite evident how the trajectory is irregular. However, the most striking phenomenon lies in the fact that a modification of the initial condition  $x_3(0)$  of a very negligible quantity, e.g. subtracting  $10^{-6}$  so that we start the numerical simulation from  $x_3(0) = 9.99999$  instead of  $x_3(0) = 10$ , a time series  $x_3(t)$  is obtained that, even if at the early time steps is quite similar to the previous one, becomes very different from the other as time goes on. This phenomenon of sensitivity to initial conditions, already described by Poincaré in 1903, became widely known after the paper by

---

<sup>15</sup>From the book: H. Poincaré "Science and Method", 1903.

E. Lorenz (1963) "Deterministic non-periodic flow" in the Journal of the Atmospheric Sciences, and is now popularly known as the "*butterfly effect*", so called because of the title of a paper given by Edward Lorenz in 1972 to the American Association for the Advancement of Science in Washington, D.C., entitled "*Predictability: Does the Flap of a Butterfly's Wings in Brazil set off a Tornado in Texas?*" The flapping wing represents a small change in the initial condition of the system, which causes a chain of events leading to large-scale phenomena. Had the butterfly not flapped its wings, the trajectory of the system might have been vastly different.

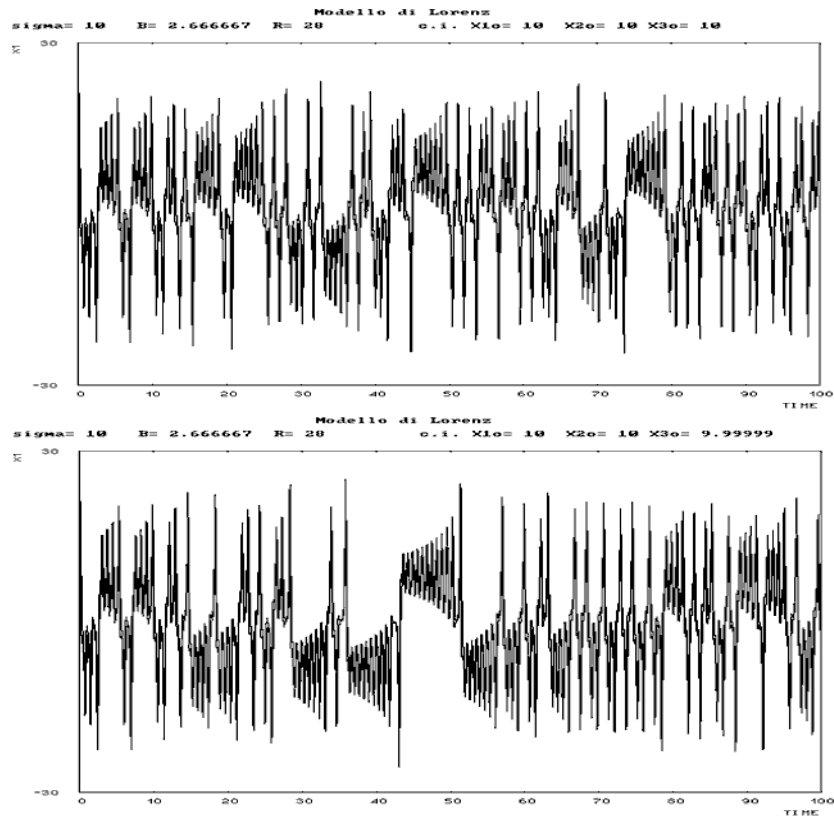


Figure 59: Versus time representation of  $x_1(t)$  along a trajectory of the Lorenz model (41) obtained with parameters  $\sigma = 10$ ,  $\beta = 2.666$ ,  $\rho = 20$  and initial conditions  $x_1(0) = 10$ ,  $x_2(0) = 10$ ,  $x_3(0) = 10$  (upper panel);  $x_1(0) = 10$ ,  $x_2(0) = 10$ ,  $x_3(0) = 9.99999$ . (lower panel)

The phenomenon of sensitive dependence on initial conditions (or butterfly effect) evidenced how difficult may be to make forecasting even if a dynamic phenomenon is represented by deterministic equations (when they are even slightly nonlinear). Small differences in initial conditions (such as those due to rounding errors in numerical computation) yield widely diverging outcomes for such dynamical systems, rendering long-term prediction impossible in general. This happens even though these systems are deterministic, meaning that their future behavior is fully determined by their initial conditions, with no random elements involved. This was summarized by Edward Lorenz by the sentence: "When the present determines the future, but the approximate present does not approximately determine the future".

So, the statement "if one knows the equations of motion then one can reliably forecast the future

states of a system starting from the knowledge of its state at a given time", is not true in general. This had a strong impact in economics as well. In fact, the paradigm of the rational agent in economics, on which is based the mainstream economic theory after the Sixties of the 20<sup>th</sup> century, is based on the assumption that economic agents have correct expectations about future states of the economy because they know the equations of motion of the economic systems. The existence of deterministic chaos in economic models based on rational expectations leads to an evident contradiction.

Of course, the same nonlinear model can behave regularly (converging to an equilibrium or to a periodic orbit) for some sets of parameters and exhibit chaotic dynamics for different parameters' values, and a goal of the qualitative study of a continuous time nonlinear dynamical system of dimension greater than two is the detection of the parameters' changes leading to such irregular behaviour.

The discovery (or, better, the re-discovery after the clear statement of Poincaré in 1903) of this kind of trajectories in deterministic models opened in the Sixties and Seventies of 20<sup>th</sup> century a huge stream of literature in the field of the theory of dynamical system, and this caused a sort of revolution in several disciplines, including physics, chemistry, sociology, engineering, economics, biology. The so called "chaos theory" even entered fiction, cinema and philosophical debates.<sup>16</sup>

However, even in the presence of chaotic behaviour some regularities can be detected. For example, if the trajectories are represented in the phase space one can see that the shape of the attracting set where the chaotic trajectories are confined may be characterized by interesting topological properties. For example, if a chaotic trajectory of the Lorenz model is represented in the phase space  $(x_1, x_2, x_3)$  a structure like the one shown in fig. 60 is obtained. If a trajectory starts from an initial condition inside that set then it remains there and covers any point of it as time goes on, i.e. it is an invariant set. Moreover, if a trajectory starts outside it (not too far) then it moves towards the set, where it exhibits irregular (i.e. non-periodic) time paths and sensitive dependence on initial conditions. For this reason such invariant set is denoted as "chaotic attractor" or "strange attractor". The shape and extension of this attracting compact set may give useful information about the long-run dynamics of the dynamical system, even if it exhibits deterministic chaos. In fact one can obtain upper and lower bounds (ceiling and floor) for the dynamics of each dynamic variable, even if its time series is quite irregular.

So, even if from one side the discovery of deterministic chaos weakens the predictive capacity of nonlinear dynamical systems, it gives some hope that apparently random phenomena may be generated by a deterministic model (even with a few dynamic variables and with a simple mathematical expression).

Another famous three-dimensional dynamical system that, for given sets of parameters, gives rise to chaotic attractors is the following

$$\begin{cases} \dot{x}_1 = -x_2 - x_3 \\ \dot{x}_2 = x_1 + ax_2 \\ \dot{x}_3 = bx_1 - cx_3 + x_1x_3 \end{cases}$$

known as Rössler model, see below a chaotic attractor obtained with parameters  $a = 0.32$ ,  $b = 0.30$ ,  $c = 4.50$ .

The only equilibrium of this model is  $O = (0, 0, 0)$ , where the Jacobian matrix becomes

$$J(0, 0, 0) = \begin{bmatrix} 0 & -1 & -1 \\ 1 & a & 0 \\ b & 0 & -c \end{bmatrix}$$

---

<sup>16</sup>See e.g. the popularization book by James Gleick "Chaos: Making a New Science", Viking Penguin, 1987 .

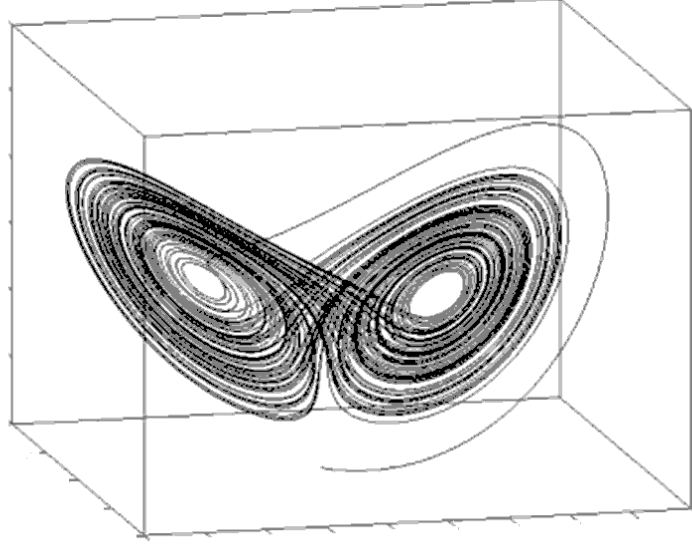


Figure 60: Lorenz attractor.

and the characteristic equation

$$\lambda^3 + (c - a)\lambda^2 + (1 + b - ac)\lambda + c - ab = 0$$

from which the Routh-Hurwitz stability conditions are obtained:

$$c > a; \quad c > ab; \quad (c - a)(1 + b - ac) > c - ab$$

For example, if we fix  $b = 1$  the stability conditions in the plane  $(c, a)$  are given by

$$a < \min \left[ c, \frac{1}{c} \right]$$

i.e.  $a < 1$  for  $c \leq 1$ ;  $a < \frac{1}{c}$  for  $c > 1$ , and correspond to the grey shaded stability region represented in fig. 62. It is easy to see that with  $b = 1$  and  $a = c$  (with  $c < 1$ ) the characteristic equation becomes  $\lambda [\lambda^2 - (a^2 - 2)] = 0$ , from which we get  $\lambda_1 = 0$  (non-hyperbolic case) and  $\lambda_{2,2} = \pm i\sqrt{a^2 - 2}$ ; instead for  $b = 1$  and  $a = 1/c$  (with  $c < 1$ ) we get  $\lambda^3 + \frac{c^2-1}{c}\lambda^2 + \lambda + \frac{c^2-1}{c} = 0$  that has the two purely imaginary roots  $\lambda_{1,2} = \pm i$  (non-hyperbolic case) and  $\lambda_3 = \frac{1-c^2}{c}$ .

An interesting dynamic scenario is obtained for  $a = 0.38$ ,  $b = 0.30$ ,  $c = 4.82$ , given by a saddle-focus with the one shown in fig. 63, where a homoclinic orbit is represented. This orbit has the particular feature that it firstly goes far from the equilibrium along its unstable manifold and then it is folded back by nonlinearities and approaches the equilibrium through converging spirals, related to two complex conjugate eigenvalues with negative real part. A similar situation, known as homoclinic Shilnikov scenario, is a typical prelude to chaotic behaviour.

We do not enter into more details about deterministic chaos, and in particular we avoid to give here a more rigorous definition of it, because we prefer to postpone such a discussion when dealing

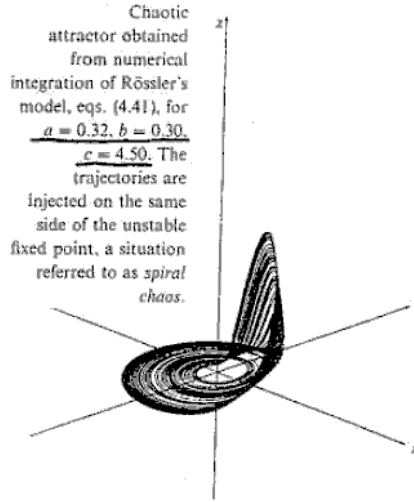


Figure 61: Rosser chaotic attractor.

with discrete-time dynamical systems, for which deterministic chaos can even be obtained with one-dimensional dynamic models and with very mild nonlinearities.

We end this section by an example leading to a three-dimensional economic model

**An economic model expressed by Lorenz equations.** We consider a dynamic model proposed by Malliaris and Stein (1995) in the paper "Financial modelling from stochastics to chaotics and back to stochastics" in *Modeling techniques for financial markets and bank management*. The model assumes the form of the Lorenz system

$$\begin{cases} \dot{x} = s(-x + y) \\ \dot{y} = x(r - z) - y \\ \dot{z} = -bz + xy \end{cases} \quad (42)$$

where  $x(t)$  represents the volatility excess of the price of a financial asset,  $y(t)$  the volatility of the average Bayesian errors by traders, where this error is measured as the difference between the subjective estimate of the price today and the objective price at the expiration of the future price. The third dynamic variable  $z(t)$  is a measure of the excess speculation. The first equation states that the rate of change of the price volatility of an asset is proportional to the difference between errors and volatility itself. The second equation describes the dynamics of the Bayesian error, which depends upon the noisiness of the system and the average cost of sampling by the market participants, influenced by the type of people attracted to the market. The second equation involves all three dynamic variables and the parameter  $r$  compared with  $z(t)$ . The Bayesian error, which is self-controlled by itself, is increased by a component due to speculation  $x(r - z)$ . The rationale of the process is the following: if there are a few speculators ( $r > z$ ), the noisiness of the system prevails. This happens for two reasons: 1) when there are few speculators even small variations in the necessity to make hedging of risks produce large variations of future prices 2) when there are a few speculators then their information set is reduced. Instead, when there are many speculators ( $r < z$ ), the information set increases, the variance around the average decreases and the market is in general more informed. The basic idea is that speculation tends to stabilize the market.



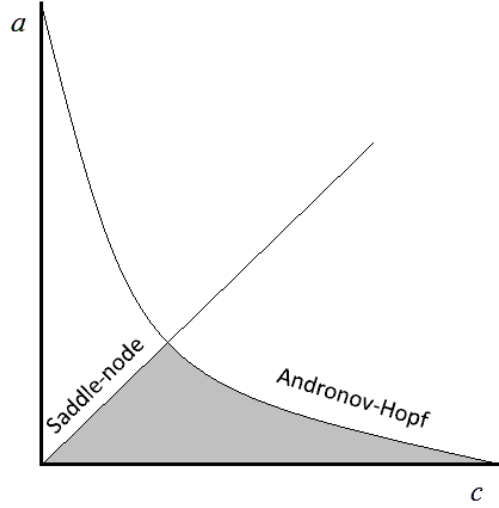


Figure 62: Bifurcation curves in the parameters' plane.

The third dynamic equation gives the rate of change of speculation excess. The motivation of it is that for higher volatility there are several ways to make profits, hence greater volatility is associated with more speculators.

The model is characterized by three parameters:  $r$  indicates the critical amount of speculation beyond which speculation have a stabilizing effect;  $b$  indicates the speed of decrease of excess of speculation;  $s$  measures the speed of convergence of volatility.

From equilibrium conditions  $\dot{x} = \dot{y} = \dot{z} = 0$  we get

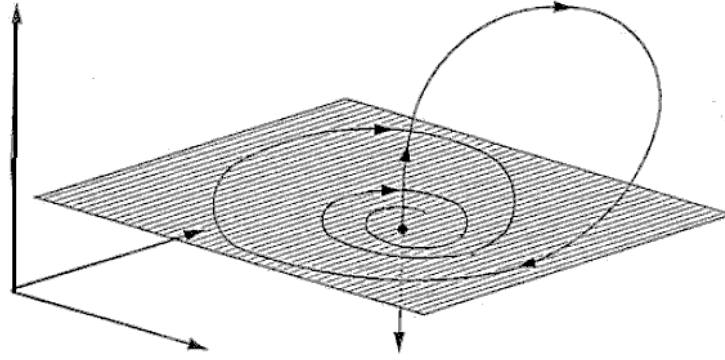
$$E_0 = (0, 0, 0); E_1 = \left( \sqrt{b(r-1)}, \sqrt{b(r-1)}, r-1 \right); E_2 = \left( -\sqrt{b(r-1)}, -\sqrt{b(r-1)}, r-1 \right)$$

The Jacobian matrix of (42)

$$\mathbf{J} = \begin{bmatrix} -s & s & 0 \\ r-z & -1 & -x \\ y & x & -b \end{bmatrix}$$

computed at each equilibrium gives:

$$\begin{aligned} \mathbf{J}(E_0) &= \begin{bmatrix} -s & s & 0 \\ r & -1 & 0 \\ 0 & 0 & -b \end{bmatrix} \\ \mathbf{J}(E_1) &= \begin{bmatrix} -s & s & 0 \\ 1 & -1 & -\sqrt{b(r-1)} \\ \sqrt{b(r-1)} & \sqrt{b(r-1)} & -b \end{bmatrix} \\ \mathbf{J}(E_2) &= \begin{bmatrix} -s & s & 0 \\ 1 & -1 & \sqrt{b(r-1)} \\ -\sqrt{b(r-1)} & -\sqrt{b(r-1)} & -b \end{bmatrix} \end{aligned}$$



Shilnikov type homoclinic orbit

Figure 63: Shilnikov scenario.

The characteristic equation for the equilibrium  $E_0$  is

$$\det \left( \begin{bmatrix} -s - \lambda & s & 0 \\ r & -1 - \lambda & 0 \\ 0 & 0 & -b - \lambda \end{bmatrix} \right) = 0$$

i.e.

$$P(\lambda) = \lambda^3 + (s + 1 + b)\lambda^2 + (b + sb + s - sr)\lambda + sb(1 - r) = 0$$

and from the Routh-Hurwitz conditions  $E_0$  is stable if

$$\begin{aligned} s + 1 + b &> 0 \\ (s + 1 + b)(b + sb + s - sr) - sb(1 - r) &> 0 \\ sb(1 - r)[(b + sb + s - sr)(s + 1 + b) - sb(1 - r)] &> 0 \end{aligned}$$

The first stability condition is always true. The second becomes

$$(s + 1 + b)(1 + s)b + (1 + s)s - (1 + s)sr > 0$$

and is satisfied if and only if

$$r < \frac{b(s + 1 + b)}{s} + 1$$

while the third condition becomes

$$r < 1.$$

As the third condition implies the second one, it follows that  $E_0$  is locally asymptotically stable if  $r < 1$ . This means that it is stable whenever it is the unique equilibrium. In fact, the other two equilibrium points only exist for  $r > 1$ , and for  $r = 1$  the three equilibria coincide. So, we expect a pitchfork bifurcation at  $r = 1$ .

The characteristic equation of  $E_{1,2}$ , given by

$$\det \left( \begin{bmatrix} -s - \lambda & s & 0 \\ 1 & -1 - \lambda & -\sqrt{b(r-1)} \\ \sqrt{b(r-1)} & \sqrt{b(r-1)} & -b - \lambda \end{bmatrix} \right) = 0$$

becomes

$$P(\lambda) = \lambda^3 + (1 + b + s)\lambda^2 + b(r + s)\lambda + 2sb(r - 1) = 0$$

and the Routh-Hurwitz stability conditions are

$$\begin{aligned} 1 + b + s &> 0 \\ (1 + b + s)b(r + s) - 2sb(r - 1) &> 0 \\ 2sb(r - 1)[(1 + b + s)b(r + s) - 2sb(r - 1)] &> 0 \end{aligned}$$

From the second condition follows

$$b(1 + b - s)r + b(3 + b + s)s > 0$$

where, assuming  $(1 + b - s) < 0$  (i.e. a high speed of convergence of volatility) we obtain that the equilibrium points  $E_{1,2}$  exist and are stable for  $1 < r < r^*$ , where  $r^* = \frac{(3+b+s)s}{(s-1-b)} > 1$ , and they become unstable for  $r > r^*$ .

This stability result has the following economic interpretation: if  $r$ , the critical amount of speculation required to reduce the volatility related to Bayesian errors in forecastings, is less than 1 then the system converges to a situation of total absence of volatility. If  $r > 1$  but less than the threshold value  $r^*$  then the system will be characterized by a constant characteristic volatility in the long run. Instead if  $r > r^*$  then we have oscillations, that may be periodic or chaotic.

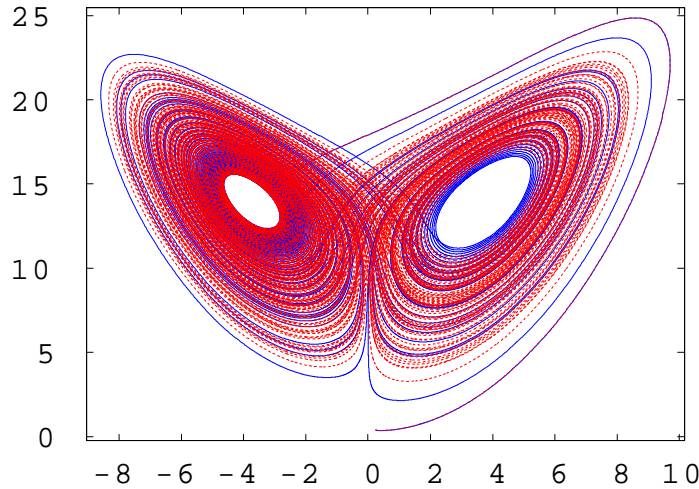


Figure 64: Lorenz attractor again.

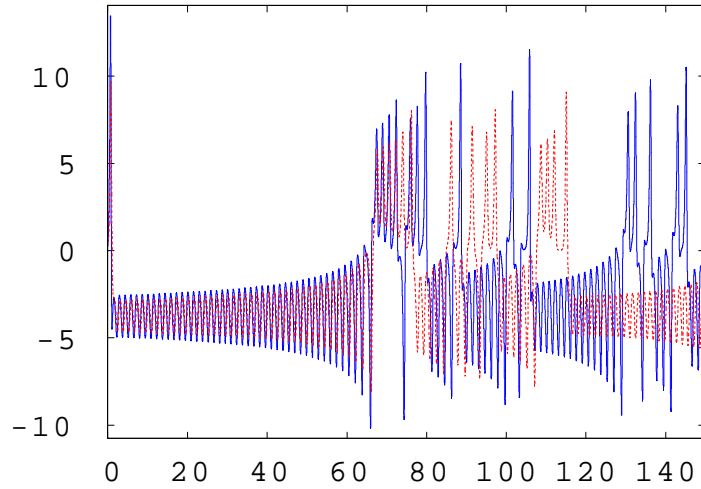


Figure 65: Time patterns along the Lorenz attractor.

In fig.64 two chaotic trajectories are represented in the phase subspace  $x, z$ , obtained with parameters  $s = 5$ ,  $r = 15$ ,  $b = 1$  with the two initial conditions  $x(0) = 0.25$ ,  $y(0) = 0.2$ ,  $z(0) = 0.4$  (blue trajectory);  $x(0) = 0.25$ ,  $y(0) = 0.2$ ,  $z(0) = 0.4$  (red trajectory).

In fig.65, with the same set of parameters, the time series (versus time representation) of  $x(t)$  is shown with two initial conditions almost identical,  $x(0) = 0.25$ ,  $y(0) = 0.2$ ,  $z(0) = 0.41$  (blue series);  $x(0) = 0.25$ ,  $y(0) = 0.2$ ,  $z(0) = 0.4$  (red series) thus showing the sensitive dependence on initial conditions (butterfly effect).

## 6 Discrete-time dynamical systems

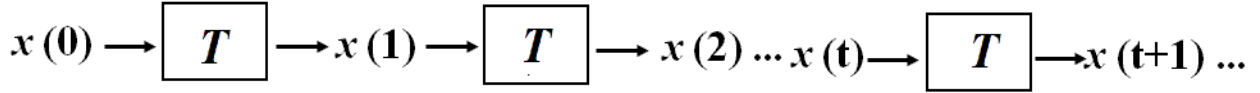
Dynamical systems (5) with discrete time  $t \in \mathbb{N}$ , naturally arise in economic and social modelling, where changes in the state of a system occur as a consequence of decisions that cannot be continuously revised (event-driven time). Given a characteristic time interval  $\Delta t$ , taken as a unit of time advancement  $\Delta t = 1$ , if  $\mathbf{x}(t) \in \mathbb{R}^n$  represents the state of the system at a given time  $t$ , then the state at the next time  $t + 1$  is obtained by the application of a map, i.e. a transformation or a function  $T : M \rightarrow M$  defined in the phase space  $M \subseteq \mathbb{R}^n$  into itself

$$\mathbf{x}(t + 1) = T(\mathbf{x}(t)) \tag{43}$$

So, a single application of the transformation  $T$  represents a "unit time advancement" of the state of the dynamical system

$$\mathbf{x}(t) \longrightarrow \boxed{T} \longrightarrow \mathbf{x}(t + 1)$$

and the repeatedly application (or *iteration*) inductively defines a trajectory



In other terms, a trajectory is obtained by the composition of a map with itself

$$\mathbf{x}(1) = \mathbf{T}(\mathbf{x}(0)); \quad \mathbf{x}(2) = \mathbf{T}(\mathbf{x}(1)) = \mathbf{T}(\mathbf{T}(\mathbf{x}(0))) = \mathbf{T}^2(\mathbf{x}(0)); \quad \dots ; \quad \mathbf{x}(n) = \mathbf{T}^n(\mathbf{x}(0))$$

or, more briefly, it can be written as the sequence

$$\tau(\mathbf{x}(0)) = \{\mathbf{x}(t) \in M: \mathbf{x}(t) = \mathbf{T}^n(\mathbf{x}(0)), \dots t \in \mathbb{N}\}.$$

Discrete-time dynamical systems can be obtained through a discretization of continuous-time dynamical system by replacing time derivative with the corresponding incremental ratio, that is,

$$\text{from } \dot{x}_i = f_i(\mathbf{x}) \text{ with } \dot{x}_i = \frac{dx_i}{\mathbf{J}} \approx \frac{x_i(t + \Delta t) - x_i(t)}{\Delta t} \quad \text{and} \quad \Delta t = 1$$

we get

$$x_i(t + 1) = x_i(t) + f_i(\mathbf{x}(t)) = T_i(\mathbf{x}(t))$$

However many economic dynamic models are directly obtained under a discrete time framework. For example let us consider the well known *Cobweb Model*.<sup>17</sup> A given good is sold in the market at a unit price  $p(t)$ . The quantity demanded by consumers is a function of the price  $Q^d(t) = D(p(t))$  denoted as demand function, usually a continuous and decreasing function (hence invertible). The supply function expresses the output decided by producers as a function of the price  $Q^s(t) = S(p^e(t))$ , where  $p^e(t)$  represents the price expected by producers at time  $t$  on the basis of the information they have when that decide the quantity to be produced. Let  $\Delta t = 1$  be the amount of time necessary to realize the production process (i.e. the production lag from production decision to product realization. e.g. maturation period for agricultural products or production time for an industrial process). Then the economic equilibrium condition  $Q^d(t) = Q^s(t)$  becomes

$$D(p(t)) = S(p^e(t)) \tag{44}$$

Under the assumption of naïve expectations  $p^e(t) = p(t - 1)$ , i.e. without reliable information the producers expects that the price at the end of production will be the same prevailing at the beginning, the model becomes

$$D(p(t)) = S(p(t - 1))$$

and by applying the inverse of demand function  $p = D^{-1}(q)$  and after a simple time translation it assumes the standard explicit form

$$p(t + 1) = D^{-1}(S(p(t))) = T(p(t)) \tag{45}$$

For example, with linear demand and linear supply functions  $D(p) = a - bp$  and  $S(p) = -c + dp$  the model becomes

$$p(t + 1) = T(p(t)) = -\frac{d}{b}p(t) + \frac{a + c}{b} \tag{46}$$

---

<sup>17</sup>Ezekiel, M. (1938), The cobweb theorem, *Quarterly Journal of Economics*, 52(2), 255-280.

This dynamic model is known as the "cobweb model".

Another example is the Cournot duopoly model, where two firms produce at time  $t$  the quantities  $q_1(t)$  and  $q_2(t)$  of the same good (or homogeneous goods) and sell it in the same market characterized by an inverse demand function  $p = D^{-1}(Q)$ , where  $Q = q_1 + q_2$  is the total quantity produced. If  $C_i(q_i)$ ,  $i = 1, 2$ , are the respective cost functions, then the profits of the two firms are given by

$$\begin{aligned}\Pi_1(q_1, q_2) &= pq_1 - C_1(q_1) = D^{-1}(q_1 + q_2)q_1 - C_1(q_1) \\ \Pi_2(q_1, q_2) &= pq_2 - C_2(q_2) = D^{-1}(q_1 + q_2)q_2 - C_2(q_2)\end{aligned}$$

hence the profit function of each firm also depends on the production of the other one, the source of interdependence being the demand function.

At each time  $t$  each firm decides its next period production  $q_i(t+1)$  (to be realized after the production lag  $\Delta t = 1$ ) in order to maximize its own profit. However, at time  $t$  each firm does not know the production decision of the other firm, so an expected value must be considered in the maximization problems

$$q_i(t+1) = \arg \max_{q_i(t+1)} \Pi_i(t+1) = \arg \max_{q_i} [D^{-1}(q_i + q_{-i}^e(t+1))q_i - C_i(q_i)] \quad (47)$$

For example, if we consider linear demand and linear cost functions,  $p = a - b(q_1 + q_2)$  and  $C_i(q_i) = c_i q_i$ , then producer 1 faces the optimization problem

$$\max_{q_1(t+1)} \Pi_1(t+1) = \max_{q_1} [(a - c_1)q_1 - bq_1q_2^e(t+1) - bq_1^2]$$

From the first order condition (necessary condition for a maximum)  $\frac{\partial \Pi_1}{\partial q_1} = 0$ , we get  $(a - c_1) - bq_2^e(t+1) - 2bq_1 = 0$  from which it is  $q_1(t+1) = -\frac{1}{2}q_2^e(t+1) + \frac{a-c_1}{2b}$ . The second order condition  $\frac{\partial^2 \Pi_1}{\partial q_1^2} = -2b < 0$  ensures that it is indeed a maximum. If we solve the same problem for the second firm and we assume naïve expectations, i.e. that  $q_j^e(t+1) = q_j(t)$ , we obtain the following two-dimensional linear discrete time dynamical system

$$\begin{cases} q_1(t+1) = B_1(q_2(t)) = -\frac{1}{2}q_2(t) + \frac{a-c_1}{2b} \\ q_2(t+1) = B_2(q_1(t)) = -\frac{1}{2}q_1(t) + \frac{a-c_2}{2b} \end{cases} \quad (48)$$

Instead, if the (inverse) demand function is assumed to be isoelastic (in particular with unitary elasticity) with the form  $p = \frac{1}{Q}$ , then the same arguments lead to the following nonlinear discrete dynamical system

$$\begin{cases} q_1(t+1) = R_1(q_2(t)) = \sqrt{q_2(t)/c_1} - q_2(t) \\ q_2(t+1) = R_2(q_1(t)) = \sqrt{q_1(t)/c_2} - q_1(t) \end{cases} \quad (49)$$

## 6.1 The simplest one: 1-dimensional linear homogeneous

The simplest discrete time recurrence is the linear homogeneous iterated map

$$x(t+1) = ax(t) \quad (50)$$

with initial condition  $x(0) = x_0$ . The general solution of (50) can be obtained inductively, being  $x(1) = ax_0$ ,  $x(2) = ax(1) = a^2x_0$ ,  $x(3) = ax(2) = a^3x_0 \dots$

$$x(t) = x_0 a^t \quad t \in \mathbb{N} \quad (51)$$

The sequence (51) converges to the unique asymptotic equilibrium  $x^* = 0$  if  $|a| < 1$ , i.e.  $-1 < a < 1$ . In this case we say that (50) is a contraction mapping, as at each iteration the distance of  $x(t)$  from  $x^* = 0$  is reduced of the factor  $|a|$ . For example, if  $a = \frac{1}{2}$  then  $x(1) = \frac{1}{2}x_0$ ,  $x(2) = \frac{1}{4}x_0$  etc. The same holds for  $a = -\frac{1}{2}$ , even if this occurs through oscillations of decreasing amplitude:  $x(1) = -\frac{1}{2}x_0$ ,  $x(2) = \frac{1}{4}x_0$ ,  $x(3) = -\frac{1}{8}x_0$  etc. So, for negative values of  $a$  the sequence (51) oscillates around  $x^* = 0$ , as it assumes the same sign of  $x_0$  at even iterations and opposite sign at odd iterations. It is worth to stress that oscillations can be obtained with a one-dimensional discrete-time dynamical system, whereas this was impossible in the case of one-dimensional smooth systems in continuous time. Of course this is due to the fact that the points generated by (50) can jump between different points without touching the intermediate points. Diverging sequences are obtained for  $|a| > 1$ , monotonically diverging if  $a > 1$ , diverging through oscillations if  $a < -1$ . For example  $a = 2$  give  $x(1) = 2x_0$ ,  $x(2) = 4x_0$  etc., whereas  $a = -2$  gives  $x(1) = -2x_0$ ,  $x(2) = 4x_0$ ,  $x(3) = -8x_0$  etc. Finally, for  $a = 1$  the identity map is obtained, whose iteration gives a constant sequence  $x(t) = x_0$  for each  $t \in \mathbb{N}$ , whereas  $a = -1$  gives the oscillating sequence  $x(t) = (-1)^t x_0$ . All these cases are summarized in fig. 66.

We can see the map  $x' = ax$  as a transformation of the real line into itself, i.e. a function that transforms each point  $x \in \mathbb{R}$  into its unique image  $x' \in \mathbb{R}$ . If we consider a segment  $AB$ , i.e. the closed interval  $AB = \{x \in \mathbb{R}, A \leq x \leq B\}$ , and we apply the transformation  $x' = ax$  to all the points of the segment, then a new segment  $A'B'$  whose length will be  $A'B' = |a|AB$ , i.e. it will be contracted of the factor  $a$  if  $|a| < 1$ , expanded if  $|a| > 1$ , and with the same length if  $|a| = 1$ . Moreover, its orientation will remain the same, i.e.  $A < B$  implies  $A' < B'$ , if  $a > 0$ , whereas its orientation will be reversed, i.e.  $A < B$  implies  $A' > B'$ , whenever  $a < 0$ .

From the general solution (51) of the linear recurrence (50), the solution of nonhomogeneous linear map can be easily obtained. In fact, given

$$x(t+1) = ax(t) + b \quad (52)$$

it can be noticed that if it converges, then it converges to the unique steady state (or fixed point)  $x^*$  characterized by the condition  $x(t+1) = x(t)$ . Thus,  $x^*$  is the solution of the equation  $x = ax + b$ , i.e. it is  $x^* = \frac{b}{1-a}$ , provided that  $a \neq 1$ . The change of coordinates  $X(t) = x(t) - x^* = x(t) - \frac{b}{1-a}$  that translates the fixed point into in origin, transforms the affine (or linear non homogeneous) recurrence into a linear homogeneous one. In fact, by replacing  $x(t) = X(t) + \frac{b}{1-a}$  into (52) we get  $X(t+1) = aX(t)$ , i.e. in the form (50), and consequently the general solution is  $X(t) = X(0)a^t$ , from which going back to the ordinary variable

$$x(t) = \left(x_0 - \frac{b}{1-a}\right) a^t + \frac{b}{1-a} \quad (53)$$

Such solution converges to  $x^* = \frac{b}{1-a}$  for  $|a| < 1$ , oscillates between  $-x_0$  and  $x_0$  for  $a = -1$ ; finally, in the particular case  $a = 1$ , (52) becomes the arithmetic sequence  $x(t+1) = x(t) + b$ , whose solution is  $x(t) = x_0 + bt$ , which is increasing or decreasing according to the sign of  $b$ .

This completely solves, for example, the linear cobweb model with naïve expectations (46) whose equilibrium is  $p^* = \frac{a+c}{b+d}$ , located at the intersection of the demand and supply curves, and the solution starting from the initial price  $p(0) = p_0$  is


$$p(t) = \left(p_0 - \frac{a+c}{b+d}\right) \left(-\frac{d}{b}\right)^t + \frac{a+c}{b+d} \quad (54)$$

•  $|a| < 1$  (contraction)

➤  $0 < a < 1$  

*Contraction and orientation preserving.*


*It monotonously converges to  $x^* = 0$*

➤  $-1 < a < 0$  

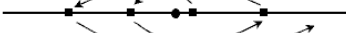
*Contraction and orientation reversing*

*The iteration converges to  $x^* = 0$  through oscillations*

•  $|a| > 1$  (expansion)

➤  $a > 1$ ,   
*expanding and orientation preserving*

*It diverges monotonically*

➤  $a < -1$  

*expanding and orientation reversing*

*It diverges through oscillations*

✓ Particular (bifurcation) values

$a = 1$   $x_t = x_0$  constant

$a = -1$   $x_t = (-1)^t x_0$  alternating values

Figure 66:

The corresponding time series exhibit oscillatory behaviour, being  $-\frac{d}{b} < 0$ : they are convergent to  $p^*$  when  $b > d$ , i.e. the decreasing demand function is steeper than the increasing supply, diverging otherwise (see figure 67)

Systems evolving in discrete time are quite common in economics and finance. A very basic example is the law for computing the time value of money if a compound interest is added at given time periods. If  $r$  is the effective interest rate per period  $\Delta t = 1$ , then the following difference equation allows one to compute the one-period interest starting from the initial capital

$$M(t+1) = M(t) + rM(t) = (1+r)M(t) \quad \text{with } M(0) = C_0 \quad (55)$$

from which the general law that directly gives the future value after  $n$  periods, given the initial value of the capital  $C_0$ , is

$$M(n) = C_0(1+r)^n \quad (56)$$

Another example is obtained by considering the equation of motion of the price  $p(t)$  of an asset with price  $p_0$  at time  $t_0$  and constant dividends  $\bar{y}$

$$Rp(t) - p(t-1) = \bar{y}$$

with  $R = 1 + r$ , where  $r > 0$  is the risk-free interest,  $0 < r < 1$ . The general solution is

$$p(t) = \bar{p} + (p_0 - \bar{p}) \frac{R^{t_0}}{R^t}$$



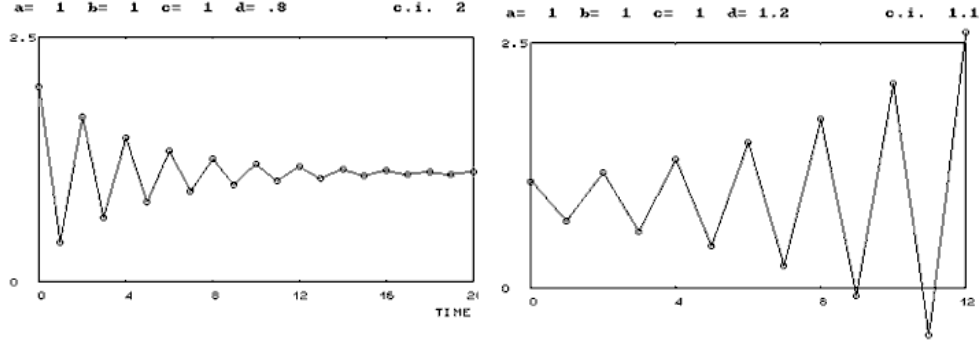


Figure 67:

where  $\bar{p} = \frac{\bar{y}}{R-1}$  is the constant fundamental price (given by the discounted sum of all future dividends starting from  $t_0$  at which  $p(t_0) = p_0$ ), and  $(p_0 - \bar{p})$  is a financial bubble. In order to avoid the explosion of the bubble as  $t \rightarrow \infty$  a "non-bubble condition" must be introduced

$$\lim_{t \rightarrow \infty} \frac{(p_0 - \bar{p})}{R^t} = 0$$

which is true provided that  $R > 1$  as stated above. This implies that a displacement from the fundamental value can only be a transitory phenomenon, and consequently the rational economic agents believe that the fundamental value will prevail in the long run.

## 6.2 Qualitative analysis of 1-dimensional nonlinear models in discrete time

Let us consider now a general discrete-time dynamical system with one dynamic variable

$$x(t+1) = f(x(t)) \tag{57}$$

with initial condition  $x(0) = x_0$ . The equilibrium points (or fixed points) are defined by the equilibrium condition  $x(t+1) = x(t)$ , i.e. are the solutions of the equation

$$f(x) = x \tag{58}$$

Let  $x^*$  be a solution of (58). Then a linear approximation of (57) in a neighborhood of  $x^*$  can be obtained as  $f(x) = f(x^*) + f'(x^*)(x - x^*) + o(x - x^*) = x^* + f'(x^*)(x - x^*) + o(x - x^*)$ , leading to the linear approximation

$$x(t+1) = x^* + f'(x^*)(x - x^*)$$

that reduces to the linear homogeneous case  $X(t+1) = aX(t)$  after the translation  $X(t) = x(t) - x^*$  that measures the displacement from the equilibrium point. From the discussion about the linear case of the previous section the following result immediately follows

**Proposition (1-dim. local asymptotic stability in discrete time).** *Let  $x^*$  be an equilibrium point of (57), i.e.  $f(x^*) = x^*$ . If  $|f'(x^*)| < 1$  then  $x^*$  is a locally asymptotically stable equilibrium; if  $|f'(x^*)| > 1$  then  $x^*$  is unstable.*

Indeed, if  $x^*$  is hyperbolic, which in the case of discrete dynamical systems means that  $|f'(x^*)| \neq 1$ , the Hartman-Grobman theorem (1959-1960) can be stated as follows: *Let  $x^*$  be a hyperbolic fixed point of (57), with  $f$  differentiable. Then there exists a neighborhood of  $x^*$  where map (57) is topologically conjugate to its linear approximation.*

Notice that in the case of discrete time the stability condition  $-1 < f'(x^*) < 1$  includes both an upper and a lower threshold for the slope of the function  $f$  at the equilibrium point, and the two limiting values  $-1$  and  $+1$  constitute two different conditions of nonhyperbolicity of the equilibrium point. The condition of nonhyperbolicity  $f'(x^*) = 1$  corresponds to the analogous condition  $f'(x^*) = 0$  for continuous time one-dimensional models. We will see in the following that if such condition is crossed as a parameter varies then the bifurcations that occur are similar to those detected in continuous-time models. Instead, the other nonhyperbolicity condition  $f'(x^*) = -1$  has no analogue in continuous time models, as it is characterized by oscillatory behaviour. Indeed, the presence of negative derivative is often related to phenomena of overshooting (or over-reaction). This means that even if we have a decreasing map around  $x^*$ , i.e.  $f(x) > x^*$  in a left neighborhood of  $x^*$  and  $f(x) < x^*$  in a right neighborhood of  $x^*$ , so that  $x(t+1) > x(t)$  if  $x(t)$  is on the left of  $x^*$  and  $x(t+1) < x(t)$  if  $x(t)$  is on the right of  $x^*$ , a trajectory starting from a neighborhood of  $x^*$  will jump from one side to another of  $x^*$ ; thus, either convergence does not occur or, if convergence is obtained, being  $-1 < f'(x^*) < 0$ , then it takes place through oscillations.

Before discussing the possible bifurcations of 1-dimensional nonlinear models, we describe a useful graphical method that is widely used to obtain the trajectories of a one-dimensional discrete dynamical system (57), even in a nonlinear case, without any analytic computation. This method is based on the knowledge of the graph of the function  $y = f(x)$ . It consists in drawing such graph on a cartesian plane together with the diagonal  $y = x$ . Starting from the initial condition  $x_0$  on the horizontal axis, the successive value of the recurrence  $x(1)$  is obtained by moving upward up to the graph and then to the left, on the vertical axis (the codomain) where the values (images) are represented. Then, in order to continue the iteration of the function, this value must be brought back to the horizontal axis, i.e. from the codomain to the domain, in order to apply the function again. This can be done by using the diagonal, locus of point such that  $y = x$ : the point  $x(1)$  is moved horizontally towards the diagonal and then vertically towards the horizontal axis (see fig. 68). Then the process is repeated again to get  $x(2)$  etc.

Notice that some portions of the horizontal and vertical movements have been travelled back and forth, so that they can be deleted and the movements reduced to the following: starting from  $x_0$  on the diagonal, *vertical to the graph, horizontal to the diagonal where  $x(1) = f(x_0)$  is placed, then vertical to the graph, horizontal to the diagonal where  $x(2) = f(x(1))$  is placed* and so on... This graphical construction, called *staircase diagram* allows us to get the whole trajectory as a set of points along the diagonal. See the other examples in fig.68, in particular the oscillatory trajectory shown in the right panel, obtained with a decreasing map.

In fig.69 this method is applied to the map  $f(x) = \sqrt{x}$ , whose iteration can be simply obtained by a pocket calculator, starting from any initial condition  $x(0) > 0$  and repeatedly pressing the square-root key. It will be easily realized that it always converges to the globally stable fixed point  $x^* = 1$ .

From these preliminary arguments it is evident that in the case of decreasing one-dimensional discrete time dynamical systems, whose trajectories are obtained by iterated maps, oscillations and even periodic cycles are obtained. Consider, for example, the map  $f(x) = \frac{1}{x}$ , i.e. the recurrence  $x(t+1) = \frac{1}{x(t)}$  that leads to a cycle of period two  $\left(x_0, \frac{1}{x_0}\right)$  for each initial condition  $x_0 \neq 0$ . Or

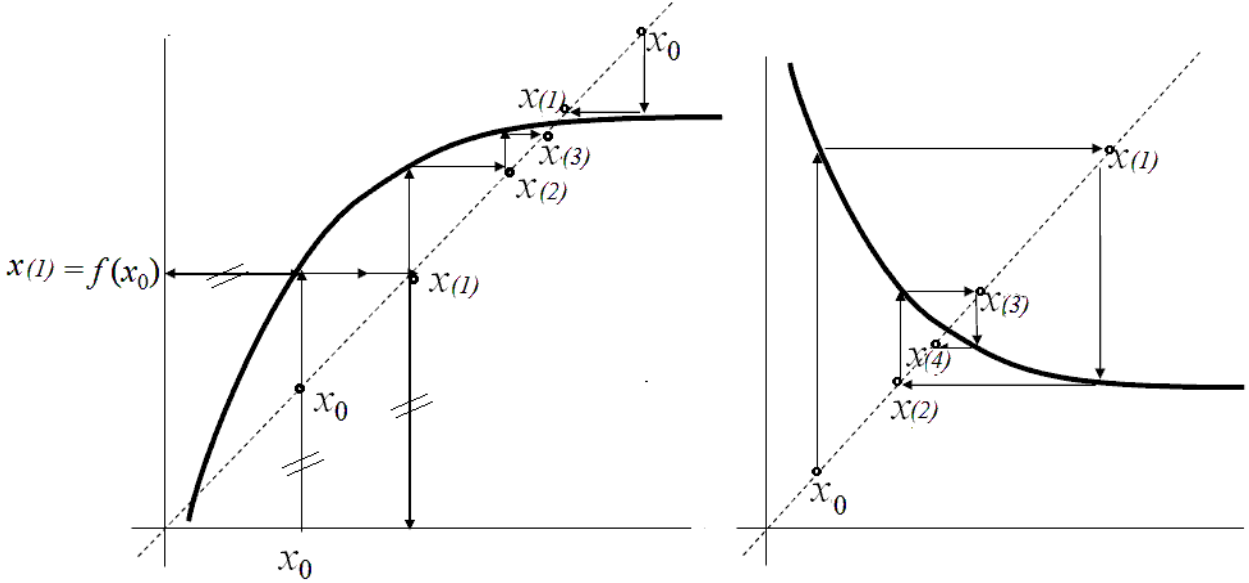


Figure 68: Staircase diagram

the map  $f(x) = x^2 - 1$  that, starting from  $x_0 = 0$  gives the cycle  $x(1) = -1$ ,  $x(2) = 0$ ,  $x(3) = -1$ . Moreover, starting from another initial condition such as  $x_0 = \frac{3}{2}$ , it generates  $x(1) = \frac{5}{4} = 1.25$ ,  $x(2) = 0.5625$ ,  $x(3) = -0.6836$ ,  $x(4) = -0.5327$ ,  $x(5) = -0.7162$ ,  $x(6) = -0.4870$ ,  $x(7) = -0.7628$ ,  $x(8) = -0.4181$ , and then slowly approaches the 2-cycle  $(-1, 0)$ .

In other words, not only periodic sequences exist where after a given number of iterations the same value is reached and then the same set of numbers repeats indefinitely, but also there are sequences that approach asymptotically such periodic sets. Several situations of this kind are obtained with the iterated quadratic<sup>18</sup> map

$$f(x) = x^2 - \alpha \quad (59)$$

with parameter's values in the range  $\alpha \in (0, 2)$ . This map can be iterated very easily even with a pocket calculator and many different situations, from convergence to a fixed point to convergence to a periodic sequence or even aperiodic and very irregular sequences are obtained. Try, for example with  $\alpha = 1.3$  and with  $\alpha = 2$ , starting e.g. from  $x(0) = 0.5$ . Some staircase diagrams of this quadratic map are shown in figures 70 and 71.

We end this section by giving a definition of periodic cycle as well as the conditions for its stability.

A periodic cycle of period  $k$  is a set of points  $C_k = \{c_1, c_2, \dots, c_k\}$  such that  $c_i \neq c_1$ ,  $i = 2, \dots, k$ ,  $f(c_i) = c_{i+1}$ ,  $i = 1, \dots, k-1$ , and  $f(c_k) = c_1$ . So, the periodic points can be obtained as  $C_k = \{c_1, f(c_1), f^2(c_1), \dots, f^{k-1}(c_1)\}$  with  $f^k(c_1) = c_1$ . This last equality states that  $c_1$  is a fixed point of the composite function  $f^k(x)$ . Indeed, as the initial periodic point of the cycle is arbitrary, any periodic point of a  $k$  cycle is a fixed point of  $f^k$ , i.e.  $f^k(c_i) = c_i$  for each  $i = 1, \dots, k$ . This is quite intuitive, because, after  $k$  iterations of  $f$ , all the points of the  $k$ -cycle are obtained and the initial point is reached again. In other words, if the map  $f$  is applied iteratively starting from a  $k$ -periodic point and we look at the result at intervals of  $k$  iterations, then we see always the same point.

<sup>18</sup>Quadratic means polynomial of degree two.

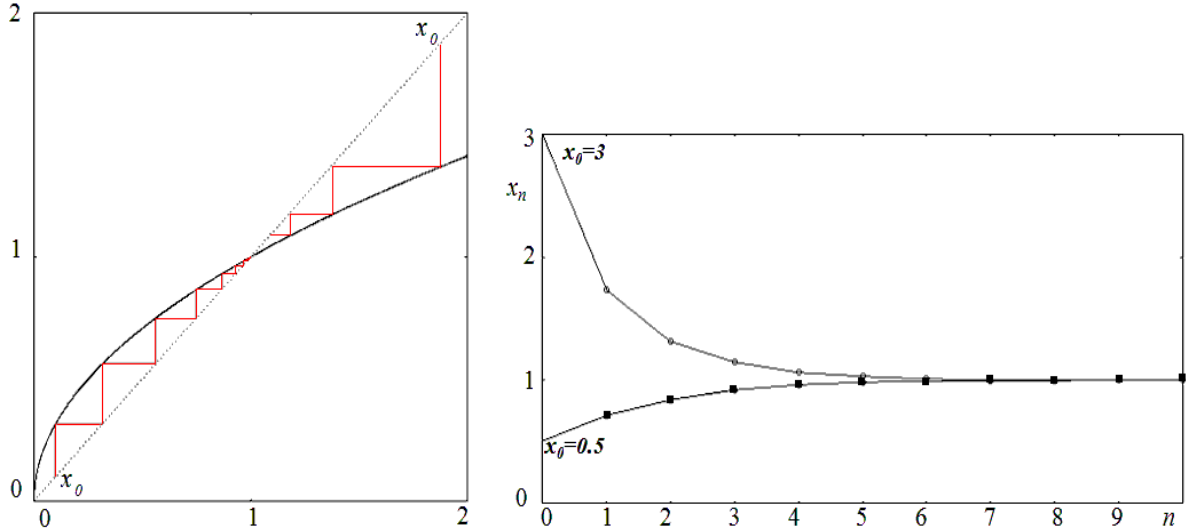


Figure 69: Square root map: staircase diagram (above) and versus time (below).

Notice that every periodic point  $c_i$  of a  $k$ -cycle  $C_k$  is a fixed point of  $f^k(x)$  but it is not a fixed point of any  $f^j(x)$  with  $j < k$ . Indeed, a fixed point  $x^*$  of  $f(x)$  is also a fixed point of any composite function  $f^j(x)$  for any  $j > 1$ , as  $f(x^*) = x^*$  implies  $f^2(x^*) = f(f(x^*)) = f(x^*) = x^*$  and so on. So, the  $k$ -periodic points are all and only the fixed points of  $f^k(x)$  which are not fixed points of  $f^j(x)$  for any  $j < k$ .

The stability of a  $k$ -cycle  $C_k$  can be determined by the study of the stability of one of its periodic points  $c_i$  as a fixed point of  $f^k(x)$ , i.e. by the condition  $\left| \frac{df^k}{dx}(c_i) \right| < 1$ . By using the chain rule for the derivation of composite functions, the derivative of the composite function  $f^k(x)$  can be reduced to the product of the derivatives of the simpler function  $f(x)$  along the  $k$ -periodic points

$$\frac{df^k}{dx}(c_i) = f'(c_1) \cdot f'(c_2) \cdot \dots \cdot f'(c_k) = \prod_{i=1}^k f'(c_i)$$

This can be easily proved inductively. In fact, for  $k = 2$  from  $f(c_1) = c_2$  and  $f(c_2) = c_1$  we obtain

$$\frac{df^2}{dx}(c_1) = f'(f(c_1))f'(c_1) = f'(c_2)f'(c_1) \text{ and analogously for } \frac{df^2}{dx}(c_2). \text{ So, if } \frac{df^{k-1}}{dx}(c_1) = \prod_{i=1}^{k-1} f'(c_i)$$

then for the derivative in  $c_1$  of  $f^k(x) = f(f^{k-1}(x))$  we get  $f'(f^{k-1}(c_1)) \frac{df^{k-1}}{dx}(c_1) = f'(c_k) \prod_{i=1}^{k-1} f'(c_i) =$

$$\prod_{i=1}^k f'(c_i).$$

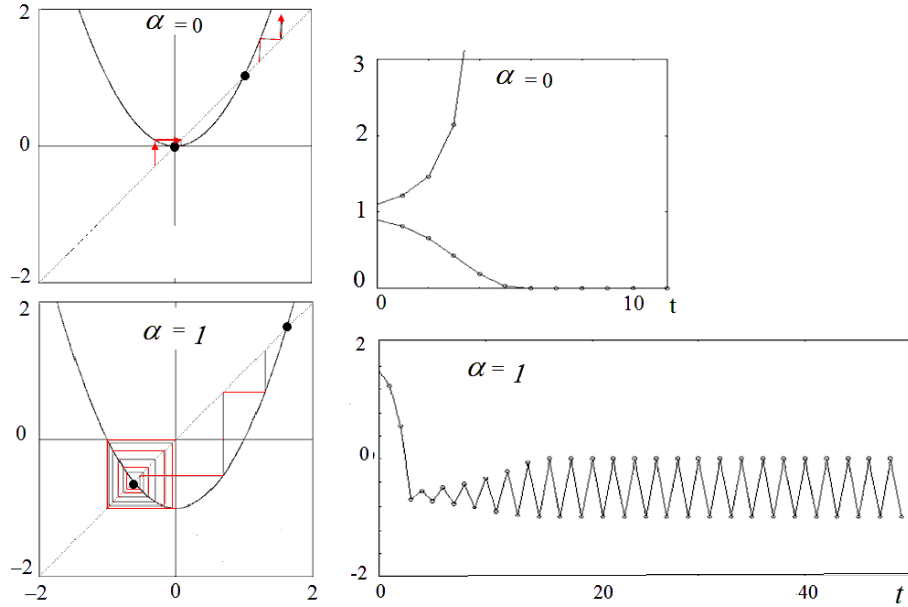


Figure 70: Myrberg map with  $\alpha = 0$  (left) and  $\alpha = 1$  (right).

### 6.3 Local bifurcations of one-dimensional discrete dynamical systems

Let us consider a one-dimensional discrete dynamical system whose structure depends on a parameter  $\alpha \in \mathbb{R}$

$$x(t+1) = f(x(t); \alpha)$$

and let  $x^*(\alpha)$  be a fixed point defined implicitly by the equilibrium equation  $f(x; \alpha) = x$ . The stability condition  $|f'(x^*(\alpha))| < 1$  indicates that as the parameter  $\alpha$  varies the fixed point can lose stability through two bifurcation conditions, at which the fixed point is non-hyperbolic,  $f'(x^*(\alpha)) = +1$  and  $f'(x^*(\alpha)) = -1$ . As one of these two bifurcation conditions is crossed a local bifurcation occurs at which the fixed point changes its stability property and something else happens, as shown in the pictures here below where some canonical maps are given, as well as their graphs and bifurcation diagrams. Notice that the three local bifurcations occurring with multiplier  $f'(x^*(\alpha)) = +1$  are essentially the same as those occurring in dynamical system in continuous time, the only difference being that in this case the tangency occurs along the diagonal, where the fixed points are located, and consequently involve slope 1.

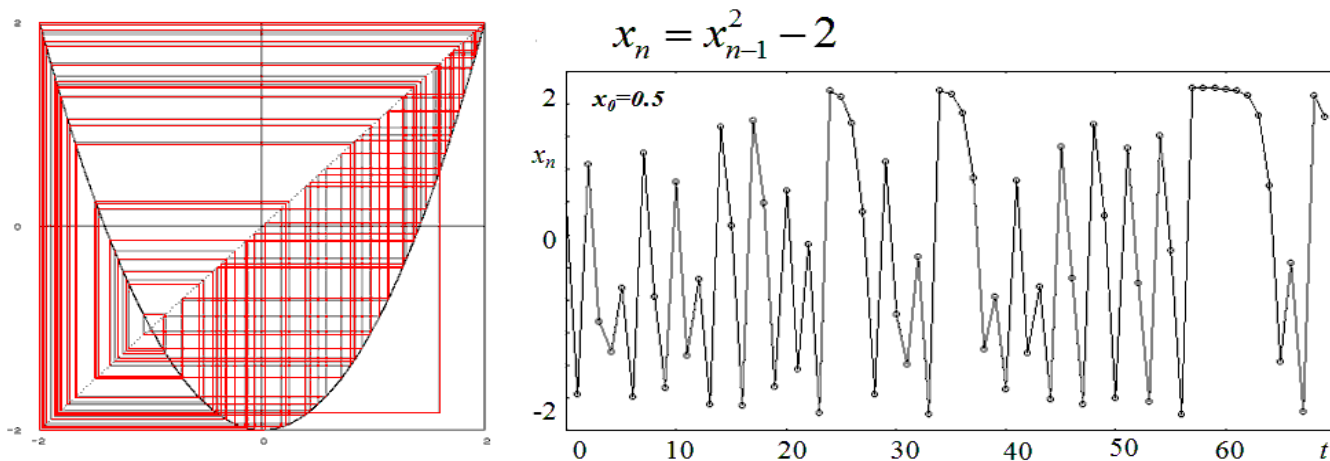
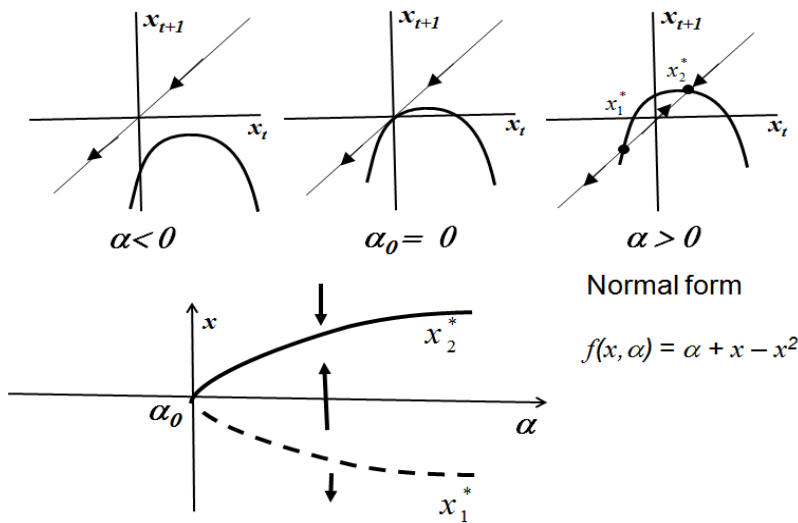


Figure 71: Myrberg map with  $\alpha = 2$

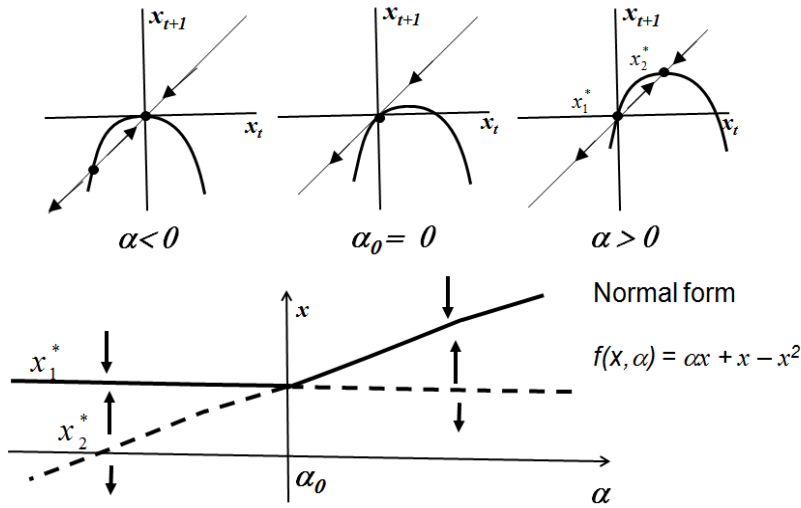
*Multiplier  $\lambda = f'(x^*)$  through value 1*

**Fold bifurcation**



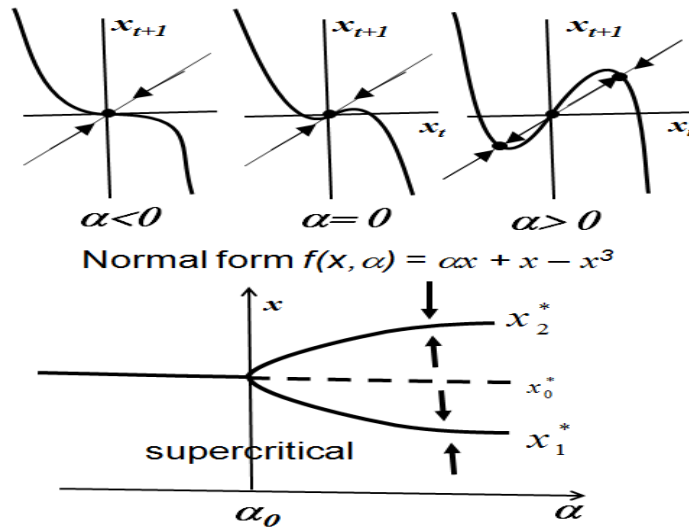
Multiplier  $\lambda = f'(x^*)$  through value 1

**Transcritical bifurcation**



Multiplier  $\lambda = f'(x^*)$  through value 1

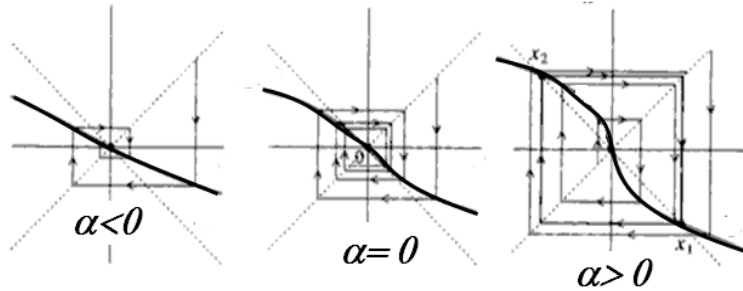
**Pitchfork bifurcation**



What is new is the bifurcation occurring with multiplier  $f'(x^*(\alpha)) = -1$ , denoted as *flip bifurcation*, at which the fixed point changes its oscillatory stability (i.e. convergence through damped oscillations) into oscillatory instability (i.e. trajectories starting very close to  $x^*$  exhibit oscillatory expansion).

Multiplier  $\lambda = f'(x^*)$  through value  $-1$

**Flip ( or period doubling) bifurcation**



Normal form  $f(x, \alpha) = -(1+\alpha)x + x^3$

However, differently from the linear case where the oscillatory expansion has no limits, leading to oscillatory divergence, in the nonlinear case a creation of a 2-periodic cycle occurs at the bifurcation value. This 2-periodic cycle may be stable if it is created around the unstable fixed point (supercritical case) thus attracting the trajectories escaping from a neighborhood of  $x^*$ , or unstable if it exists around the stable fixed point (subcritical case) thus bounding its basin of attraction.

It is worth to notice that this bifurcation, leading to the creation of two periodic points of a 2-cycle, causes the creation of two new fixed points of the map  $f^2(x) = f(f(x))$ , besides the previously existing  $x^*$  as any fixed point of  $f(x)$  is also a fixed point of  $f^2(x)$ . So, the flip bifurcation of  $f$  is associated with a pitchfork bifurcation of  $f^2(x)$ . Indeed, if  $f'(x^*) = -1$  then  $\frac{df^2}{dx}(x^*) = f'(f(x^*))f'(x^*) = f'(x^*)f'(x^*) = (-1)(-1) = +1$ , a bifurcation condition of  $f^2$  corresponding to a pitchfork bifurcation.

All the local bifurcations described above can be observed in periodic cycles as well. In fact, when a periodic cycle  $C_k = \{c_1, c_2, \dots, c_k\}$  with associated multiplier  $\lambda(C_k) = \prod_{i=1}^k f'(c_i)$  changes its stability properties due to a variation of a parameter, if the multiplier exits the stability range  $-1 < \lambda(C_k) < 1$  through the value  $+1$  then a bifurcation of the cycle is observed, that may be of fold type (a couple of  $k$ -cycle, one stable and one unstable, are created or destroyed through their merging) of transcritical type (two  $k$ -periodic cycles of opposite stability merge and exchange their stability) or of pitchfork type (two further  $k$ -periodic cycles are created at the bifurcation). Instead if the multiplier exits the stability range  $-1 < \lambda(C_k) < 1$  through the value  $-1$  then a flip bifurcation of the  $k$ -cycle is observed at which a cycle of double period  $2k$  is created.

**6.4 The logistic map**

In this section we consider the quadratic map

$$x(t + 1) = \mu x(t)(1 - x(t)), \quad \mu > 0 \tag{60}$$

whose graph is represented by a concave parabola that intersects the diagonal in the two fixed points

$$x_0^* = 0 \text{ and } x_1^* = 1 - \frac{1}{\mu} \tag{61}$$



Its expression is quite similar to the logistic model in continuous time (10), hence it has been called *logistic map*. Indeed, it can be obtained by a discretization of (10) that gives

$$x(t+1) = (1 + \alpha)x(t) - sx(t)^2 \quad (62)$$

which is topologically conjugate (hence dynamically equivalent) to (60). In fact, by the linear (hence invertible) change of variable  $y = \frac{s}{1+\alpha}x$ , i.e. by replacing  $x(t) = \frac{1+\alpha}{s}y(t)$  and  $x(t+1) = \frac{1+\alpha}{s}y(t+1)$  in (62), we get  $y(t+1) = (1 + \alpha)y(t) - (1 + \alpha)y(t)$ , identical to (60) with  $\mu = 1 + \alpha$ .

The map (62) is indeed used to model the time evolution of a population reproducing at non-overlapping breeding seasons.

The same map (62) can be obtained from (55) if we imagine to impose a tax proportional to the square of the money

$$M(t+1) = (1 + r)M(t) - sM(t)^2 \quad (63)$$

Let us notice that, in this case, if we ask, given an initial capital  $M(0) = C_0$ , what will be the accumulated future value after  $n$  years according to (63), it is quite difficult to give an answer by an analytical expression that gives  $M(n)$  as a function of  $C_0$  like in (56). In fact we have  $M(1) = (1 + r)C_0 - sC_0^2$ ,  $M(2) = (1 + r)M(1) - sM(1)^2 = (1 + r)[(1 + r)C_0 - sC_0^2] - s[(1 + r)C_0 - sC_0^2]^2$ , i.e. a 4<sup>th</sup> degree polynomial,  $M(3) = (1 + r)M(2) - sM(2)^2$  is a 8<sup>th</sup> degree polynomial in  $C_0$  and so on...  $M(10)$  is a complete polynomial in  $C_0$  of degree  $2^{10} = 1024$ , a computation impossible for any practical purpose.

This just to show that, even if the analytical computation of the solution of a difference equation is always possible in principle by composing the iterate map with itself, this is practically impossible when it is nonlinear.

Moreover, the sequences generated by the recurrence (60) may become quite complicated, as we will see in the following. We stress that the same holds for any quadratic map, as all second degree polynomials are topologically conjugate. For example, (60) is conjugate with the map (59) through the coordinate change  $y = -\frac{1}{\mu}x + \frac{1}{2}$  with  $\alpha = \frac{\mu^2}{4} - \frac{\mu}{2}$ .

What makes famous the logistic map (60) is the article "Simple mathematical models with very complicated dynamics", published in 1976 by Robert M. May in *Nature*, from which many other papers followed where the same model was used in several fields, included economics and finance. The paper of May ends with the "*evangelical plea for the introduction of these difference equations into elementary mathematics courses, so that students' intuition may be enriched by seeing the wild things that simple nonlinear equations can do. [...] The elegant body of mathematical theory pertaining to linear systems, and its successful application to many fundamentally linear problems in the physical sciences, tends to dominate even moderately advanced University courses in mathematics and theoretical physics. The mathematical intuition so developed ill equips the student to confront the bizarre behaviour exhibited by the simplest of discrete nonlinear systems, such as equation (60). Yet such nonlinear systems are surely the rule, not the exception, outside the physical sciences. Simple mathematical models with very complicated dynamics. I would therefore urge that people be introduced to, say, equation (60) early in their mathematical education. This equation can be studied phenomenologically by iterating it on a calculator, or even by hand. Its study does not involve as much conceptual sophistication as does elementary calculus. Such study would greatly enrich the student's intuition about nonlinear systems. Not only in research, but also in the everyday world of politics and economics, we would all be better off if more people realised that simple nonlinear systems do not necessarily possess simple dynamical properties*".

We now follow May's invitation and propose a qualitative study of some properties of the map (60), and this study will lead us to encounter the phenomenon of deterministic chaos in a much simpler

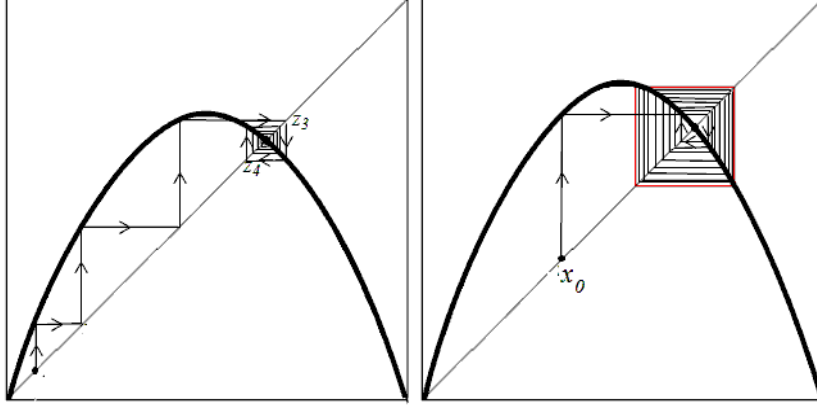


Figure 72: Left: Staircase diagram of a trajectory obtained with  $\mu = 2.7$ . Right: Trajectory obtained with  $\mu = 3.2$ .

model than the one we have seen when dealing with systems of at least three ordinary differential equations.

The stability of the two fixed points (61) is readily determined through the computation of the derivative  $f'(x) = \mu(1 - 2x)$  at the fixed points,  $f'(x_0^*) = \mu$  and  $f'(x_1^*) = 2 - \mu$ . From the stability conditions  $|f'(x_i^*)| < 1$ ,  $i = 0, 1$ , we have that  $x_0^* = 0$  is locally asymptotically stable for  $\mu < 1$  and  $x_1^*(\mu) = 1 - \frac{1}{\mu}$  is locally asymptotically stable for  $1 < \mu < 3$ . At  $\mu = 1$  a transcritical bifurcation occurs at which the two fixed points merge and exchange their stability properties: in fact  $x_1^*(\mu) < 0$  and unstable for  $0 < \mu < 1$ , whereas  $x_1^*(\mu) > 0$  and stable as  $\mu$  increase across the bifurcation value  $\mu = 1$  at which  $x_0^* = x_1^* = 0$ . Notice that at  $\mu = 2$   $f'(x_1^*) = 0$  ( $x_1^*$  is said to be superstable) and then the slope  $f'(x_1^*)$  of the tangent at  $x_1^*$  becomes negative for  $\mu > 2$  (hence we have oscillatory convergence, see fig. 72, left panel). At  $\mu = 3$  a flip bifurcation of  $x_1^*$  occurs at which a stable cycle of period two, say  $C_2 = \{\alpha, \beta\}$ , is created around the unstable fixed point see fig. 72, right panel.

The periodic points  $\alpha$  and  $\beta$  can be computed as fixed points of  $F(x) = f^2(x) = f(\mu x(1 - x))$  given by the fourth degree map  $F(x) = \mu(\mu x(1 - x)(1 - \mu x(1 - x)))$ . Its fixed points, solutions of  $F(x) = x$ , are solutions of the equation  $x[\mu^2(1 - x)(1 - \mu x(1 - x)) - 1] = 0$ . We already know that  $x_0^* = 0$  and  $x_1^* = \frac{\mu - 1}{\mu}$  are fixed points of  $F(x)$ . Hence the equation can be factorized as  $x\left(x - \frac{\mu - 1}{\mu}\right)\left[x^2 + \left(\frac{\mu + 1}{\mu}\right)x + \left(\frac{\mu + 1}{\mu^2}\right)\right] = 0$  from which the two fixed points of  $F(x)$  that are not fixed points of  $f(x)$ , i.e. the 2-periodic points  $\alpha$  and  $\beta$ , are  $\frac{\mu + 1 \pm \sqrt{(\mu - 3)(\mu + 1)}}{2\mu}$ , existing for  $\mu \geq 3$  (at  $\mu = 3$  they coincide with the bifurcating equilibrium  $x_1^*$ ). As shown in fig. 73, at  $\mu = 3$  a pitchfork bifurcation for  $F(x)$  occurs, leading to the creation of two new stable fixed points of  $F(x)$  corresponding to the periodic points of a stable cycle of period 2.

The stability of this cycle can be checked by the computation of the derivative of  $F(x)$  in one of them, given by  $F'(\alpha) = F'(\beta) = f'(\alpha)f'(\beta)$ . Just after the bifurcation this derivative is slightly less than 1, then it decreases as  $\mu$  increases beyond the bifurcation value  $\mu = 3$  until it becomes  $-1$  at  $\mu = 1 + \sqrt{6} \simeq 3.449$ . This correspond to a second flip bifurcation, this time of  $F(x)$ , at which the cycle  $C_2$  loses stability and a stable cycle of period 4 of  $f(x)$  is created. If  $\mu$  is further increased then also the cycle of period 4 becomes unstable and a stable cycle of period 8 is created, and so on. Indeed,

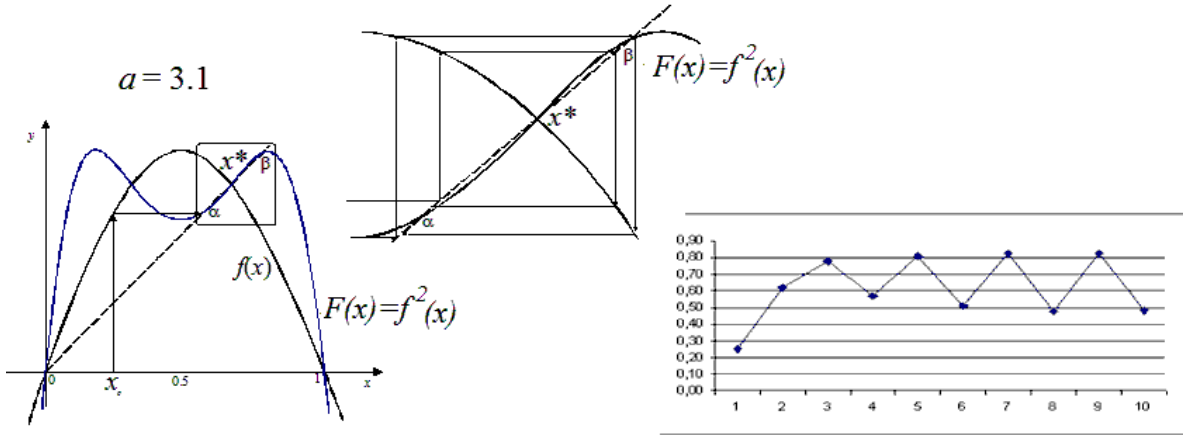


Figure 73: Flip bifurcation.

infinitely many stable cycles of period  $2^n$  are created, which become unstable as  $\mu$  is increased. All this sequence of period doubling bifurcations (also called period doubling cascade) occurs in a finite range of the parameter  $\mu$ . In fact, if we denote by  $\mu_1 = 3$  the first bifurcation value,  $\mu_2 = 1 + \sqrt{6}$  the second one and so on, the distance between two successive bifurcation points  $\Delta_n = \mu_{n+1} - \mu_n$  decreases and tends to 0, i.e. as  $\mu$  increases the bifurcations become more and more frequent and accumulate at the limit point  $\mu_\infty = 3.56994571869\dots$

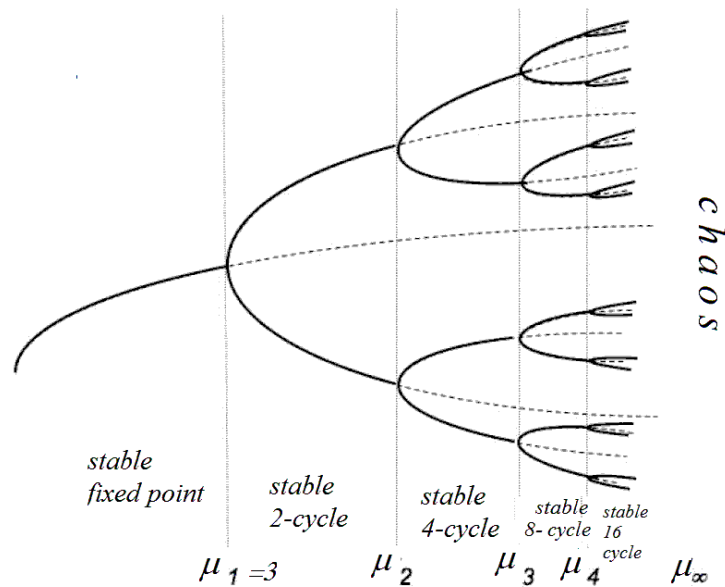


Figure 74: Schematic picture of early steps of period doubling sequence

After this limit point all cycles of period  $2^n$ ,  $n \in \mathbb{N}$  have been created and have become unstable, periodic trajectories of any period can appear as well as aperiodic trajectories, i.e. bounded trajectories generated by the infinite iteration of (60) and that never hit an already visited point. Such trajectories

are called chaotic, their points fill an invariant interval (or set of intervals) in which the following properties hold (used sometimes as a definition of existence of deterministic chaos)

- 1) *infinitely many unstable periodic points exist, which are dense in the invariant set;*
- 2) *an aperiodic trajectory exists that is dense in the set;*

*An invariant set for which these two properties hold is said to be chaotic.*

As a consequence of these two conditions we have that the sensitivity with respect to the initial conditions (or butterfly effect) also exists, that is often added as the third (and most famous) property

- 3) Sensitivity to initial conditions. *Two trajectories starting from different, although arbitrarily close, initial conditions remain bounded but their reciprocal distance exponentially increases and, in a finite time, becomes as large as the state variables.*

The first property, about the existence of dense and repelling periodic points inside the invariant set where chaotic dynamics occur, is the key to understand the "microscopic reason" for the occurrence of chaotic dynamics. In fact, it is quite intuitive that the motion inside a trapping bounded set where infinitely many and dense repellers are nested, will be quite irregular, like the motion of a bouncing ball inside a flipper where elastic repellers are present, or like a man walking inside a overcrowded place. The second property, also called "mixing" property, states that a trajectory exists that moves erratically inside the invariant set filling it completely, see fig. 75 where the initial portion of a trajectory is shown by a staircase diagram that, if continued, will cover completely the interval  $[f(c), c]$  where  $c$  is the maximum value (vertex of the parabola). Trajectories starting outside this interval will enter it and never escape (hence it is an attractor) and will cover completely all the points of it in the long run. In fact, as the dense trajectory is aperiodic, according to property 2, it will never reach an already visited point (say after  $k$  iterations) after which the countable set of  $k$  points will be repeated periodically. This means that in the long run (after infinitely many iterations) it densely fills all the space available for the motion inside the invariant set.

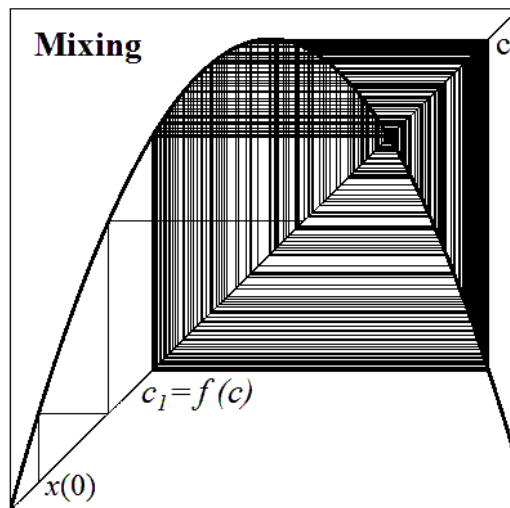


Figure 75:

Finally, the third property, which is a consequence of the other two, is given by the extreme sensitivity of trajectories with respect to small, even negligible, changes of the initial condition. This

is illustrated in fig. 76, where two trajectory, say  $x(t)$  and  $y(t)$ , are shown both generated for  $\mu = 4$  but starting from initial conditions that differ by  $10^{-6}$ , namely  $x(0) = 0.1$  and  $y(0) = 0.100001$ . As it can be seen (by a direct comparison of the two time series or by looking at versus-time representation of the distance between their points  $|x(t) - y(t)|$ ), the difference between the two time series remains negligible during the early iterations, then this difference grows up until the distance between the two trajectories becomes of the same order of magnitude as the single values, i.e. an error of 100% is obtained by this negligible difference in the initial conditions. Of course, the property of sensitive dependence on initial conditions makes any long-term prediction quite meaningless, even if based on the knowledge of the deterministic law of motion that governs the time evolution of the system. Remember the clear description of this phenomenon given by Poincaré at the beginning of 20<sup>th</sup> century.

On the other side, the discovery of the phenomenon of deterministic chaos may be used to give the hope that at the basis of time evolutions that appear to be quite irregular (erratic, random) a deterministic law of motion exists, of course nonlinear and in a condition of deterministic chaos. In other words, even at the basis of very irregular and disordered phenomena may be worth to look for (even simple) deterministic law of motion.

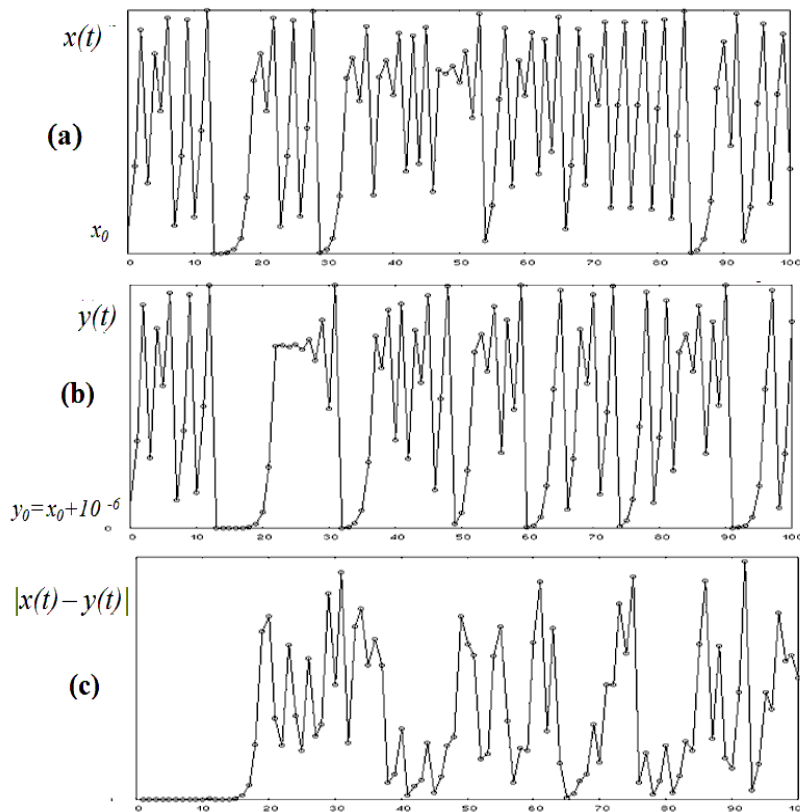


Figure 76: Two trajectories obtained from  $\mu = 4$  are represented versus time:  $x(t)$ , obtained starting from initial condition  $x_0 = 0.1$  (panel (a)) and  $y(t)$  starting from  $y_0 = 0.100001$  (panel (b)). In panel (c) the difference  $|x(t) - y(t)|$  is represented.

Another signal of regularity in the realm of chaos is worth to be noticed. In fact, let us remark that, as stressed while looking at fig. 75, the trapping interval inside which periodic or aperiodic

dynamics occur has an obvious upper bound, given by the maximum value  $c$ , and a lower bound given by its image  $c_1 = f(c)$ . So, even if the motion inside this trapping interval may be chaotic, in any case upper and lower bounds can be given. This may give useful information, for example, when a model that shows deterministic chaos is used to simulate the irregular paths of prices in a stock market. Natural upper and lower bounds may be a useful information. The same holds in the case of model for weather forecastings, as these models cannot be used to obtain daily weather forecastings in the long run, however the boundaries of the invariant attracting set inside which asymptotic dynamics are bounded can give information on the long-run evolution of climate.

Moreover, the knowledge of maximum and minimum values (i.e. the foldings of the graph of the iterated function) as well as their images, may show more complex structures of allowed and forbidden regions for asymptotic dynamics, as shown in fig.77, where the vertex of the parabola  $c$  and its images  $c_i = f^i(c)$ ,  $i = 1, \dots, 3$  bound a trapping region with a hole inside (i.e. the union of two disjoint intervals) and even if the dynamics is chaotic, no iterated points are allowed to enter the hole between the two intervals. This important property, that will be stressed even in the case of higher dimensional discrete dynamical systems, is related with the shape of chaotic attractors (see e.g. the Lorenz or Rossler attractors in continuous time) and can put some order in the topological properties of chaotic systems.

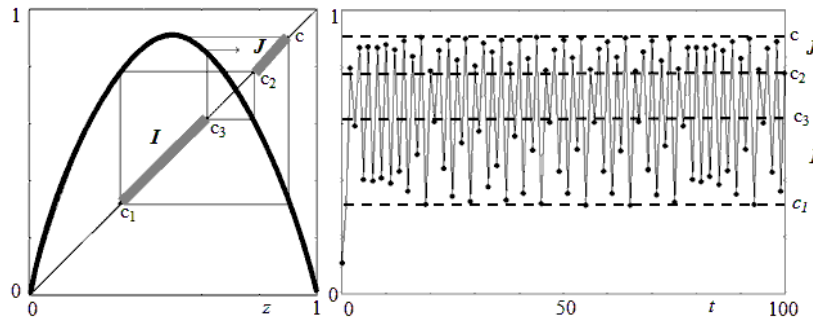


Figure 77: Attracting invariant intervals bounded by critical points (maximum and its images) for  $\mu = 3.61$

A summary of these dynamic scenarios is given in fig.78, where for different values of the parameter  $\mu$  the corresponding staircase diagrams are shown in the left column, and the same is shown in the central column after the early 50 iterations have been removed (the so called "transient portion" of the trajectory, before it reaches the asymptotic attractor) and in the column in the right the same trajectory is represented versus time, i.e. as a time series.

A different kind of "summary" of the different dynamic scenarios, obtained as the bifurcation parameter  $\mu$  is increased, is given by the bifurcation diagram (see fig.79) obtained measuring the different values of  $\mu$  in the horizontal axis while along the vertical axis the points of a trajectory are reported (after a given transient portion has been discarded). This means that, starting from a given initial condition, the attractor reached by the trajectory is represented for each value of  $\mu$ . The complete bifurcation diagram for  $\mu \in [0, 4]$  is given in fig.79, and a restricted portion of it is the fig.80, where the period doubling sequence, the transition to chaos, as well as the cyclic chaotic intervals (or chaotic bands) bounded by the critical point and its images are more visible.

Another evident feature that can be seen in the bifurcation diagram is the presence, for certain ranges of the bifurcation parameter, of white strips where chaos seems to disappear for a while and

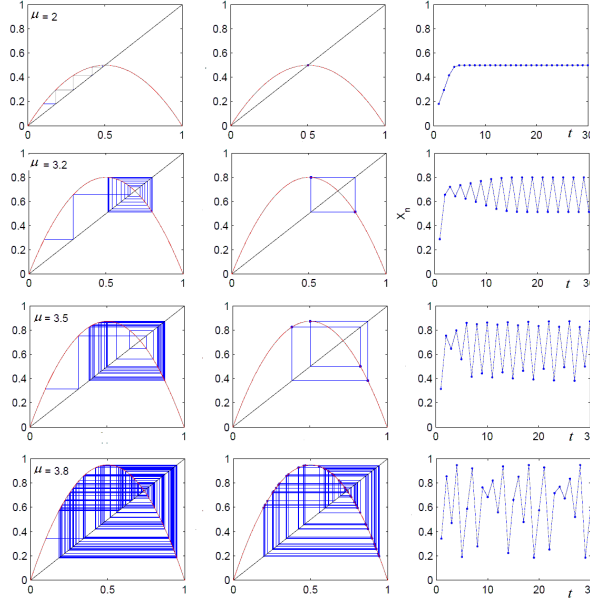


Figure 78: Summary of different dynamic scenarios of the logistic map.

the overall dynamics are captured by an attracting periodic cycle. These strips are called "periodic windows". Quite evident is the periodic window of a 3-cycle obtained for values of  $\mu$  around 3.85. Indeed, enlargements of the bifurcation diagram show that such periodic windows are infinitely many, for example a stable cycle of period 5 is visible in a narrow white strip around  $\mu = 3.74$  etc. A periodic window of period  $k$  is created through a fold bifurcation of  $f^k(x)$ , see for example in fig. 81 the graph of  $f^3(x)$  leading to the sudden creation of three couples of fixed points (each couple formed by one stable and one unstable fixed point) due to a tangency between the graph of  $f^3(x)$  and the diagonal. Notice that the number of relative maximum and minimum points of  $f^k(x)$  increases as  $k$  increases, and the simultaneous tangencies are  $k$ . Each couple of fixed points, created at the fold bifurcation, corresponds to a couple of periodic points of  $f$ , one stable and one unstable, belonging to a stable and unstable  $k$ -cycle respectively. As  $\mu$  is further increased then each fold behaves as a small quadratic map characterized by one maximum or one minimum (called a unimodal map) hence the stable cycle will loose stability via a flip bifurcation followed by the period doubling cascade. So, from each periodic point inside a periodic window a small bifurcation diagram with the same structure of the whole bifurcation diagram can be observed (see the enlargement in fig. 81), thus giving rise to an inner self-similarity structure typical of fractal structures.

We end this section by giving a geometric interpretation of the observed phenomena.

First of all, let us notice that the logistic map is a noninvertible map. In fact, the map  $x' = f(x) = \mu x(1 - x)$  is such that a unique image  $x'$  is associated at each  $x$  in the function domain, whereas given a value  $x'$  in the codomain we obtain two preimages, computed as

$$x_1 = f_1^{-1}(x') = \frac{1}{2} - \frac{\sqrt{\mu(\mu - 4x')}}{2\mu}; \quad x_2 = f_2^{-1}(x') = \frac{1}{2} + \frac{\sqrt{\mu(\mu - 4x')}}{2\mu}. \quad (64)$$

Of course, if  $x' > \frac{\mu}{4}$ , i.e. taking  $x'$  above the maximum value, no real preimages are obtained. We

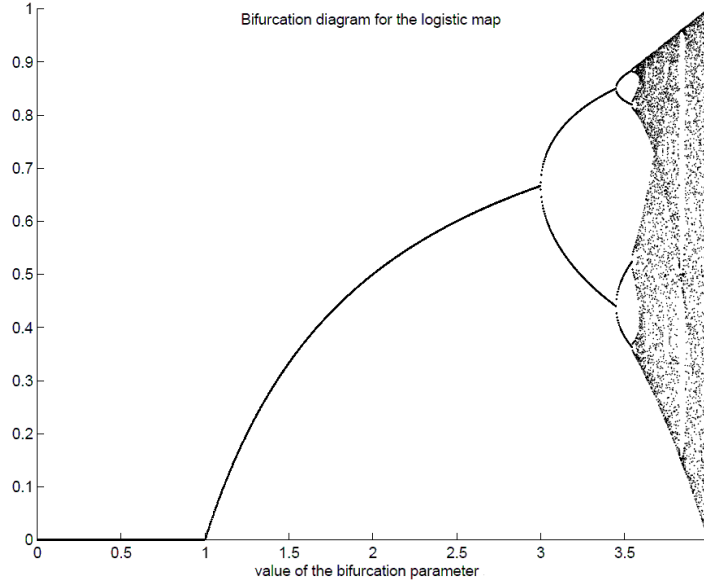


Figure 79: Complete bifurcation diagram of the logistic map.

say that the logistic map is a  $Z_0 - Z_2$  noninvertible map, and the critical point  $c = \mu/4$  separates the real line into the two subsets:  $Z_0 = (c, +\infty)$ , where no inverses are defined, and  $Z_2 = (-\infty, c)$ , whose points have two rank-1 preimages (see fig. 82). If  $x' \in Z_2$ , its two rank-1 preimages (64) are located symmetrically with respect to the point  $c_{-1} = 1/2 = f_1^{-1}(\mu/4) = f_2^{-1}(\mu/4)$ . Hence,  $c_{-1}$  is the point where the two merging preimages of  $c$  are located. As the logistic map is differentiable, at  $c_{-1}$  the first derivative vanishes. Geometrically, the action of a noninvertible map can be expressed by saying that it “folds and pleats” its domain, so that distinct points are mapped into the same point. This is equivalently stated by saying that several inverses are defined, and these inverses “unfold”  $S$  (see fig. 83).

It can be noticed that, as the map is partially increasing (for  $x < c_{-1}$  where  $f'(x) > 0$ ) and partially decreasing (for  $x > c_{-1}$  where  $f'(x) < 0$ ), it is orientation preserving for  $x < c_{-1}$  and orientation reversing for  $x > c_{-1}$ . So, a nonlinear map with a relative maximum or minimum, will “fold” any segment that includes  $c_{-1}$ . In fact, as it can be seen in fig. 82, as the point  $x$  in the domain varies from 0 to 1 the corresponding image moves up and down and the sum of the two segments is greater than 1. This can be expressed by saying that the map folds and stretches. So, the repeated application of the map consists in the repeated geometric application of stretching and folding actions (see e.g. the action of  $f^2(x) = f(f(x))$  in fig. 82). This implies that a small initial segments (i.e. a set of points initially very close) after many applications of stretching and folding actions will be quite dispersed. This is another way to state sensitivity dependence on initial conditions.

## 6.5 Basins of attraction in one-dimensional discrete dynamical systems

Given the discrete dynamical system  $x(t+1) = T(x(t))$ ,  $x \in \mathbb{R}$ , whose trajectories are generated by the iteration of the map  $x' = T(x)$ , let us consider an invariant attracting set  $A \subset \mathbb{R}$  (recall that  $A$  is trapping, i.e. if  $x \in A$  then  $T^n(x) \in A$  for any  $n > 0$ ). The *Basin of attraction of  $A$*  is the set of all



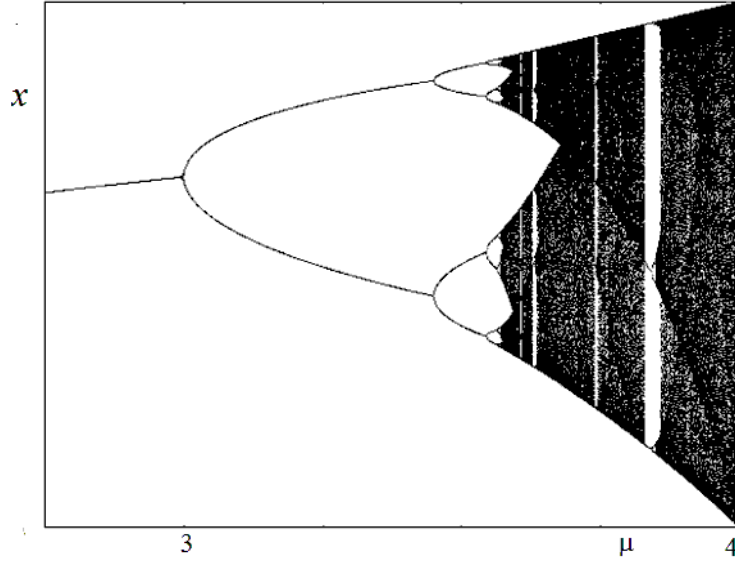


Figure 80: Bifurcation diagram of the logistic map.

the points that generate trajectories converging to  $A$

$$\mathcal{B}(A) = \{x | T^n(x) \rightarrow A \text{ as } n \rightarrow +\infty\}. \quad (65)$$

Starting from the definition of attracting set, let  $U(A)$  be a neighborhood of  $A$  whose points converge to  $A$ . Of course  $U(A) \subseteq \mathcal{B}(A)$ , but note that also the points of the phase space which are mapped inside  $U$  after a finite number of iterations belong to  $\mathcal{B}(A)$ . Hence, the *total basin of  $A$*  (or briefly the basin of  $A$ ) is given by

$$\mathcal{B}(A) = \bigcup_{n=0}^{\infty} T^{-n}(U(A)), \quad (66)$$

where  $T^{-1}(x)$  represents the preimages of  $x$  (remember that the preimages of  $x$  may not exist or may be more than one if the map  $T$  is noninvertible, i.e. if it has several distinct inverses) and  $T^{-n}(x)$  represents the set of points that are mapped into  $x$  after  $n$  iterations of the map  $T$ .

Let us first consider one-dimensional, continuous and invertible maps. If  $f : I \rightarrow I$  is a continuous and increasing function, then the only possible invariant sets are the fixed points. When many fixed points exist, say  $x_1^* < x_2^* < \dots < x_k^*$ , they are alternately stable and unstable: the unstable fixed points are the boundaries that separate the basins of the stable ones. Starting from an initial condition where the graph of  $f$  is above the diagonal, i.e.  $f(x_0) > x_0$ , the generated trajectory is an increasing sequence converging to the stable fixed point on the right, or it is diverging to  $+\infty$ . On the other hand, starting from an initial condition such that  $f(x_0) < x_0$ , the trajectory is a decreasing sequence converging to the fixed point on the left, or it is diverging to  $-\infty$  (see fig. 84, where  $p^*$  is a stable fixed point, and its basin is bounded by two unstable fixed points  $q^*$  and  $r^*$ ).

An example is shown in fig. 85 where the increasing function  $f(x) = \mu \cdot \arctan(x - 1)$  is considered for increasing values of  $\mu$ . For  $\mu < 1$  a unique fixed point exists which is globally asymptotically stable. At  $\mu = 1$  a fold bifurcation occurs at which a pair of fixed points is created, one stable and

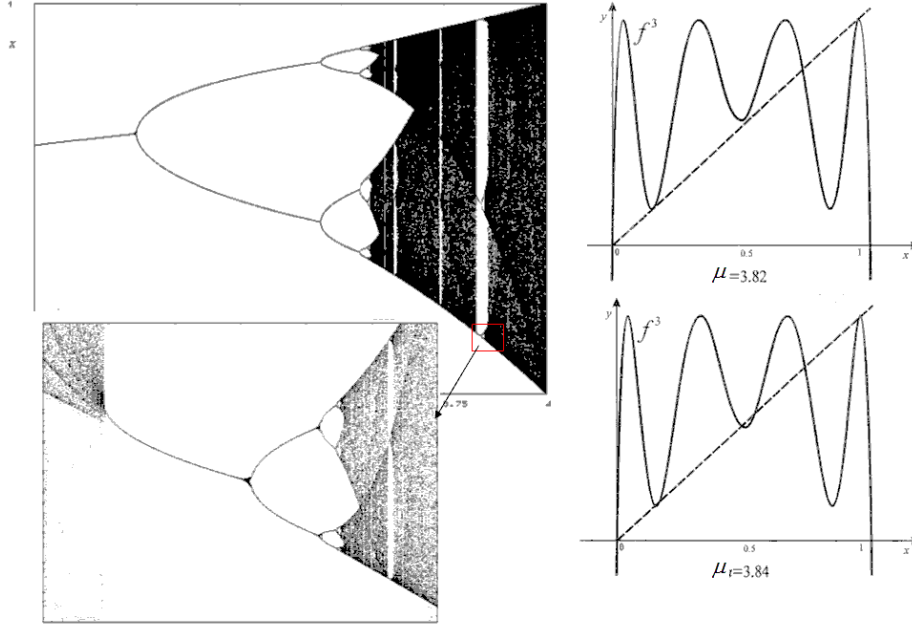


Figure 81: Periodic windows and related fold bifurcations of the logistic map.

one unstable, leading to a situation of bistability where the unstable equilibrium is the boundary that separates the two basins of attraction.

If  $f : I \rightarrow I$  is a continuous and decreasing map, the only possible invariant sets are one fixed point (unique) and cycles of period 2. In fact, if  $f(x)$  is a decreasing map then  $f^2(x)$  is increasing, hence it can only have fixed points one of which, say  $x^*$ , is the (unique) fixed point of  $f(x)$  and the other ones (if any) always appear in pairs at opposite sides with respect to  $x^*$  and represent couples of periodic points of cycles of period 2. Such periodic points of the cycles of period 2 are alternately stable and unstable, the unstable ones being boundaries of the basins of the stable ones (see Fig. 86, where the basin of the unique fixed point  $x^*$  of the map  $f(x) = 1 - ax^3$  is bounded by the periodic points  $\alpha_1, \alpha_2$  of an unstable cycle of period 2, and when  $x^*$  becomes unstable through a flip bifurcation as the parameter  $a$  increases, a stable 2-cycle  $\{\beta_1, \beta_2\}$  is created around it, whose basin is still bounded by the unstable cycle  $\{\alpha_1, \alpha_2\}$ . Initial conditions outside the interval  $(\alpha_1, \alpha_2)$  diverge, i.e. belong to the "basin of infinity".

In general, in the case of one-dimensional invertible maps the only kinds of attractors are fixed points and cycles of period two. In the first case, the basin is an open interval which includes the fixed point, and in the second case, the basin is the union of two open intervals, each one including an attracting periodic point.

If the map is invertible, then the basins of the attracting sets are always intervals that include the attractors. This may be no longer true if the map is noninvertible, as in this case non connected portions of the basins may exist that are far from the attractor to which their points converge. This is due to the "unfolding action" of the inverses that may create preimages of a neighborhood of an attractor far from the related attractor. As a first example, let us consider the logistic map (60) whose graph is represented again in Fig. 87. As far as  $\mu < 4$ , every initial condition  $x_0 \in (0, 1)$  generates

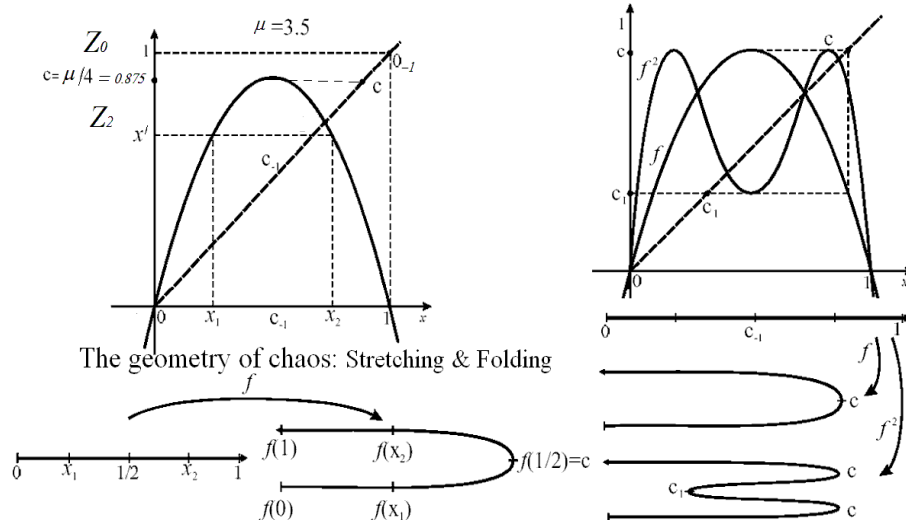


Figure 82: Stretching and folding.

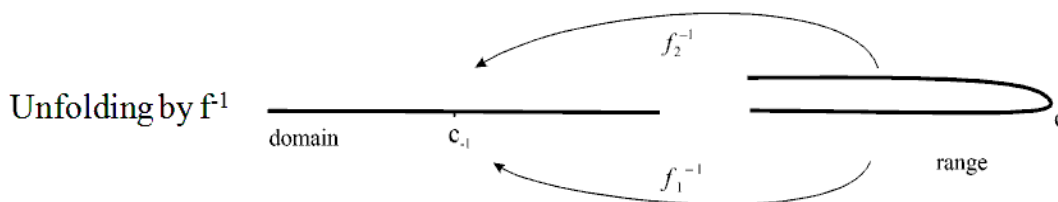


Figure 83: Unfolding

bounded sequences, converging to a unique attractor  $A$  (which may be the fixed point  $x_1^* = \frac{\mu-1}{\mu}$  or a more complex attractor, periodic or chaotic). Initial conditions out of the interval  $[0, 1]$  generate sequences diverging to  $-\infty$ .

The boundary that separates the basin of attraction  $\mathcal{B}(A)$  of the attractor  $A$ , from the basin  $\mathcal{B}(\infty)$  is formed by the unstable fixed point  $x_0^* = 0$  and its rank-1 preimage (different from itself),  $0_{-1} = 1$ . Observe that, of course, a fixed point is always preimage of itself, but in this case also another preimage exists because  $x_0^* \in Z_2$ . If  $\mu < 4$ , as in the left panel of fig. 87, then the maximum value (vertex)  $c = \mu/4 < 0_{-1} = 1$ , where  $c$  is the critical point (maximum) that separates  $Z_0$  and  $Z_2$ . Hence the basin's boundary  $0_{-1} = 1 \in Z_0$ . When we increase  $\mu$ , at  $\mu = 4$  we have  $0_{-1} = c = 1$ , i.e. a contact between the critical point and the basin boundary occurs. This is a global bifurcation, which changes the structure of the basin (really it destroys the basin). In fact, for  $\mu > 4$  (right panel of fig. 87) we have  $0_{-1} < c$ , and the portion  $(0_{-1}, c)$  of  $\mathcal{B}(\infty)$  enters  $Z_2$ . This implies that new preimages of that portion are created, which belong to  $\mathcal{B}(\infty)$  according to (66). Now almost every point belongs to the basin of divergent trajectories, the only points which are left on the interval  $I$  are the points belonging to a chaotic invariant set  $\Lambda$ , a subset of zero measure on which the restriction of the map is still chaotic, a chaotic repeller.

A similar situation occurs for a unimodal  $Z_0 - Z_2$  map where the attractor at infinity is replaced

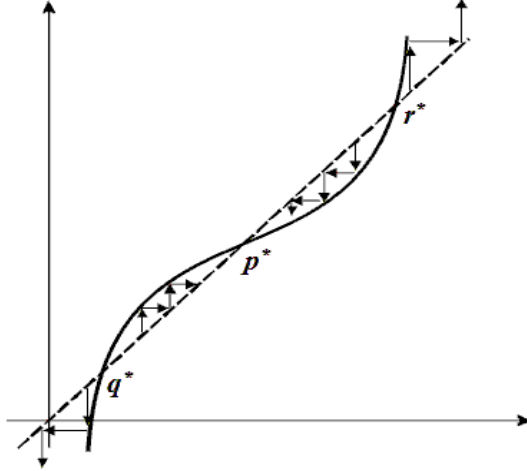


Figure 84: Basins for an increasing map.

by an attracting fixed point, as the one shown in the left panel of fig. 88. As in the previous example, we have an attractor  $A$ , which may be the fixed point  $p$  (or some other invariant set around it) with a simply connected basin bounded by the unstable fixed point  $q$  and its rank-1 preimage  $q_{-1}$ . This example differs with respect to the previous one because in this case initial conditions taken in the complementary set generate trajectories converging to the stable fixed point  $r$ . This means that the basin  $\mathcal{B}(r)$  is formed by the union of two non-connected portions:  $B_0 = (-\infty, q) \subset Z_2$ , which contains  $r$  (called *immediate basin*, the largest connected component of the basin which contains the attractor) and  $B_1 = (q_{-1}, +\infty) = f^{-1}(B_0) \subset Z_0$ . In the figure the two non-connected portions of the basin  $\mathcal{B}(r)$  are marked by green bold lines. A global basin bifurcation occurs, if a parameter variation causes an increase of the critical point  $c$  (maximum value) until it crosses the basin boundary  $q_{-1}^*$ . If this happens, the interval  $(q_{-1}, c)$ , which is part of  $B_1$ , enters  $Z_2$ , and infinitely many non-connected portions of  $\mathcal{B}(r)$  emerge, nested inside in the interval  $(q, q_{-1})$ . After this bifurcation the total basin can still be expressed as the union of all the preimages of any rank of the immediate basin  $B_0$ .

Another interesting situation is obtained if we change the right branch of the map by folding it upwards such that another critical point, a minimum, is created. Such a situation is shown in the central panel of fig. 88. This is a noninvertible  $Z_1 - Z_3 - Z_1$  map, where  $Z_3$  is the portion of the codomain bounded by the relative minimum value  $c_{\min}$  and relative maximum value  $c_{\max}$ . In the situation shown in the central panel we have three attractors: the fixed point  $r$ , with  $\mathcal{B}(r) = (-\infty, q)$  represented by green color along the diagonal, the attractor  $A$  around  $p$ , with basin  $\mathcal{B}(A) = (q, z)$ , represented by orange color, bounded by two unstable fixed points, and  $+\infty$  (i.e. positively diverging trajectories) with basin  $\mathcal{B}(+\infty) = (z, +\infty)$ . In this case all the basins are immediate basins, each being given by an open interval that includes the attractor. In the situation shown in the central panel, both basin boundaries  $q$  and  $z$  are in  $Z_1$ , so they have only themselves as unique preimages (like for an invertible map). However, the situation drastically changes if, for example, some parameter variation causes the minimum value  $c_{\min}$  to move downwards, until it goes below  $q$  (as in the right panel). After the contact  $c_{\min} = q$  that marks the occurrence of a global bifurcation, the portion  $(c_{\min}, q)$  enters  $Z_3$ , so new preimages  $f^{-k}(c_{\min}, q)$  appear. These preimages constitute non-connected portions of  $\mathcal{B}(r)$  nested inside  $\mathcal{B}(A)$ , and are represented by the thick green portions of the diagonal intermingled with orange portions that belong to  $\mathcal{B}(A)$ .

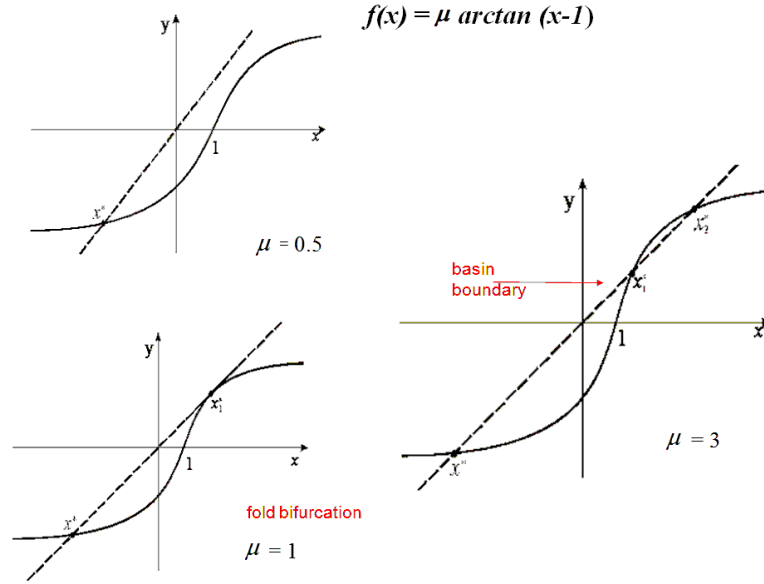


Figure 85: Fold bifurcation and creation of a new basin of attraction.

## 6.6 Some economic examples

### 6.6.1 Nonlinear Cobweb with adaptive expectations

Let us consider again the cobweb model (44),  $D(p(t)) = S(p^e(t))$ , that with naïve expectations and linear demand and supply functions gives the linear discrete-time model (46) showing oscillatory convergence to  $p^* = \frac{a+c}{b+d}$  when  $b > d$  and divergence otherwise (see fig. 89, where the shape of the staircase diagram justifies the name of the model).

We now introduce a nonlinear supply function that represents a production saturation effect

$$S(p) = \arctan(\lambda(p - 1))$$

where  $\lambda$  represents the slope of the supply at the reference price  $p = 1$ .

With the same linear demand function, the cobweb model with naïve expectations  $D(p(t)) = S(p(t - 1))$  gives rise to the following nonlinear discrete dynamic model

$$p(t) = f(p(t - 1)) = \frac{1}{b} [a - \arctan(\lambda(p(t - 1) - 1))].$$

The map  $f(x)$  is decreasing, and by using the supply slope  $\lambda$  as a bifurcation parameter the equilibrium price  $p^*$  (located at the intersection between demand and supply, see fig. 90) undergoes a flip bifurcation for increasing values of  $\lambda$  as shown in the bifurcation diagram of fig. 91, where two staircase diagrams, before and after the bifurcation, are shown. So, differently from the linear model, after the stability loss of the equilibrium price a bounded oscillatory dynamics is obtained, which converges to a cycle of period 2.

A further modification of the model consists in the introduction of adaptive expectations

$$p^e(t + 1) = p^e(t) + \alpha(p(t) - p^e(t)) \quad 0 \leq \alpha \leq 1 \quad (67)$$

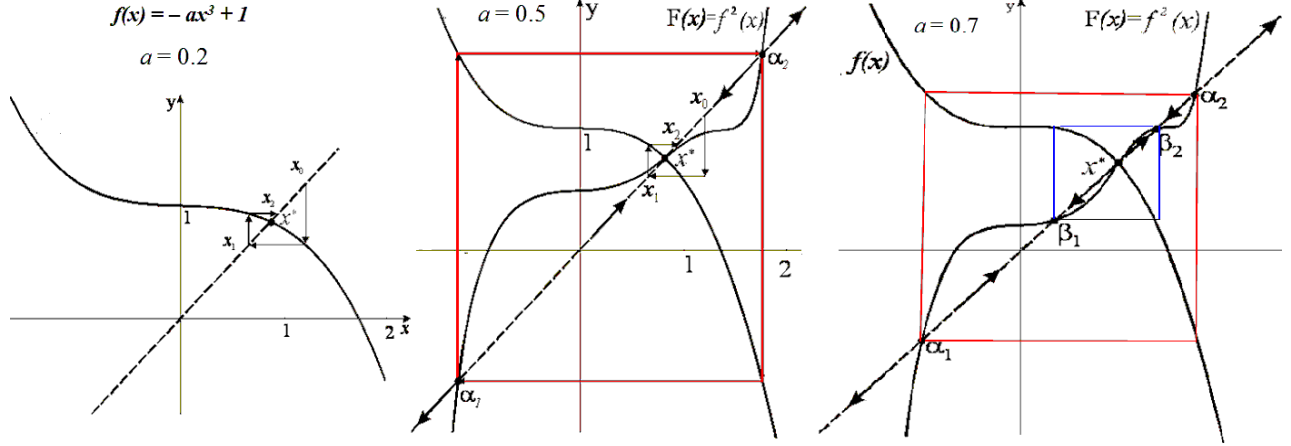


Figure 86: Basins in a decreasing map.

in the model

$$p(t) = f(p^e(t)) = \frac{1}{b} [a - \arctan(\lambda(p^e(t) - 1))] \quad (68)$$

The equation of price expectations dynamics (67) can be describes as follows. At any time  $t$  producers observe the discrepancy between the realized price  $p(t)$  and the expected price for the same period  $(p(t) - p^e(t))$  and according to such observed "estimation error" correct the previous price estimate  $p^e(t)$  in order to obtain the next one: if the expected price was underestimated, i.e.  $p^e(t)$  reveals to be less than the observed one  $p(t)$ , then they increase the current estimation in order to form the next expected price  $p^e(t+1)$ ; if the expected price  $p^e(t)$  was overestimated, i.e. it reveals to be greater than the one observed by producers, then they decrease it to form the next expected price. The value of the parameter  $\alpha$  modulates the entity of the correction: notice that for  $\alpha = 1$  adaptive expectations (67) reduce to naïve expectations  $p^e(t+1) = p(t)$ . In this sense (67) is a generalization of naïve expectations as these are included as a particular case. Instead in the other limiting case  $\alpha = 0$  we obtain a complete inertia  $p^e(t+1) = p^e(t)$ , as producers never change their initial guess  $p^e(0)$  on the basis of observed prices.

By inserting  $p(t) = f(p^e)$  inside (67) we get a law of motion in the space of expected prices

$$p^e(t+1) = F(p^e(t)) = p^e(t) + \alpha(f(p^e) - p^e(t)) = (1 - \alpha)p^e(t) + \alpha f(p^e) \quad (69)$$

From the dynamics of expected prices (69) the corresponding dynamics of realized prices (i.e. prices really observed in the market) is obtained by the transformation  $p(t) = f(p^e(t))$  in (68), a transformation from beliefs to realizations.

In order to analyze the dynamic behaviour of (69) let us notice that the function  $F(p)$  is a convex combination (i.e. a weighted average) of the identity function (whose graph is the diagonal) and the decreasing function  $f$ , so its graph is placed between the two graphs (see the left panel of fig. 92), being closer to the diagonal as  $\alpha \rightarrow 0$  and closer to the graph of  $f$  as  $\alpha \rightarrow 1$ .

From the derivative  $F'(p) = 1 - \alpha + \alpha f'(p) = 1 - \alpha - \frac{\alpha}{b} \frac{\lambda}{1 + \lambda^2(p-1)^2}$  we can see that for  $\alpha > \frac{b}{b+\lambda}$  it vanishes in two points  $p = 1 \pm \frac{1}{\lambda} \sqrt{\frac{\alpha(\lambda+b)-b}{b(1-\alpha)}}$ , relative minimum and maximum (see fig. 92). Moreover,

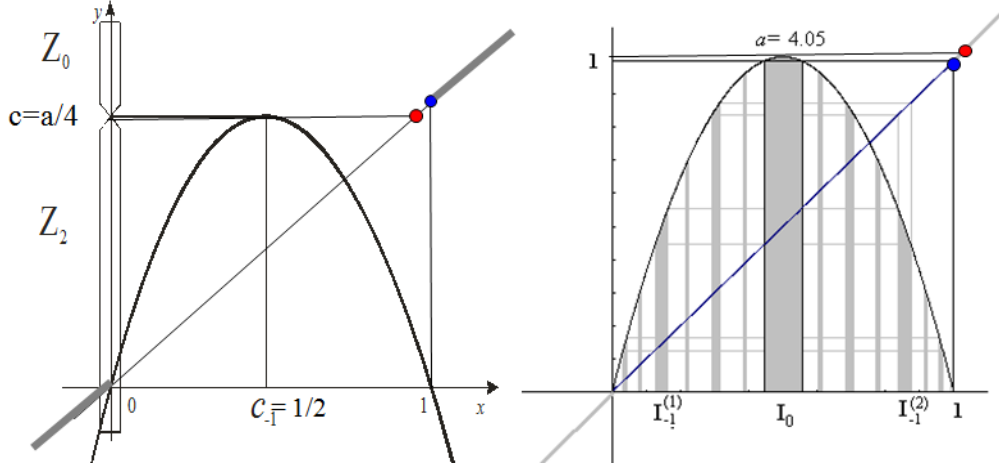


Figure 87: Logistic map at the final bifurcation.

it is always stable for sufficiently small values of  $\alpha$ , whereas for a given value of  $\alpha$  the equilibrium becomes unstable through a flip bifurcation for increasing values of  $\lambda$ . Differently from the model with naïve expectations, where the decreasing map (even if nonlinear) could not have attractors more complex than a cycle of period 2, in this case, being the map noninvertible (i.e. characterized by the presence of turning points, relative maximum and minimum in this case) the first period doubling bifurcation is followed by a sequence of successive period doublings (the period doubling route to chaos) as shown in the bifurcation diagram of fig. 92.

### 6.6.2 Financial market with heterogeneous agents

Let  $p(t)$  be the logarithm of the price of a risky asset at time  $t$  in a stock market. If we denote by  $\Delta D(t)$  the excess of demand at time  $t$  of the asset considered, the discrete time dynamics of  $p(t)$  is governed by the law

$$p(t+1) = p(t) + \gamma \Delta D(t) \quad (70)$$

expressing the fact that if  $\Delta D > 0$ , i.e. in the presence of a positive excess of demand, the asset price increases, whereas with  $\Delta D < 0$  (selling excess) the asset price decreases. The positive constant  $\gamma$  is a measure of the market reactivity (or speed of adjustment). We assume that in the market two kinds of economic agents operate, denoted as fundamentalists and chartists (or technical traders). The fundamentalists are assumed to have a reasonable estimate of the fundamental value  $F$  of the asset and they believe that, whenever the price is different from  $F$ , it will go back towards it; in other words, if  $p(t) < F$ , then fundamentalists believe that the stock is currently underestimated and its price will increase in the next period. In this case, they buy the asset; on the other hand, if  $p(t) > F$ , then fundamentalists believe that the stock is currently overestimated and its price will decrease. Consequently, they sell it in the market. This mechanism can be modelled through the following linear relation

$$\Delta D^F(t) = \alpha (F - p(t))$$

where the positive constant  $\alpha$  gives a measure of the weight of the fundamentalists in the market. In contrast, the technical traders (or chartists, as they do not believe in the fundamental price  $F$  but prefer to look at the trend observed in the charts, i.e. in the financial newspapers) believe in the

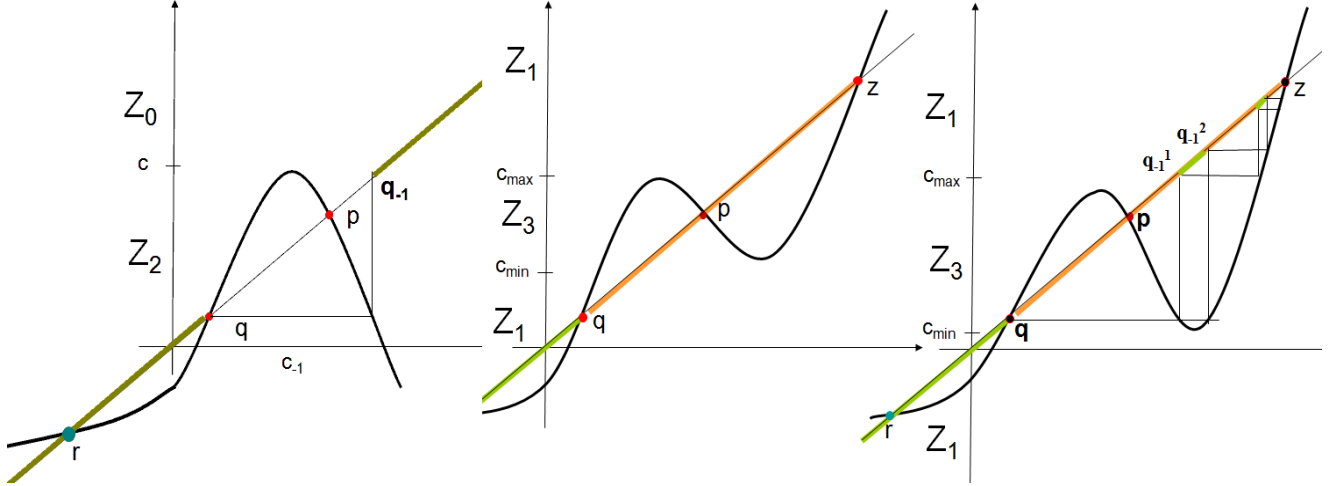


Figure 88: Contact bigurations of basins in noninvertible maps.

persistence of bull and bear markets: If  $p(t) > F$  then they believe that bull market will prevail by imitation and the price will continue to increase in the next period (hence they buy the asset), whereas if  $p(t) < F$  then they believe it is a bear phase and then it will further decrease (hence they sell it). This can be expressed as

$$\Delta D^C(t) = \beta(p(t) - F)$$

where  $\beta > 0$  gives a measure of the weight of the chartists in the market. Plugging these two expressions of the demand excess into (70) we get

$$p(t+1) = p(t) + \gamma(\Delta D^F(t) + \Delta D^C(t)) = p(t) + \gamma(\alpha(F - p(t)) + \beta(p(t) - F))$$

which can be written as the following linear one-dimensional dynamic model in discrete time

$$p(t+1) = f(p(t)) = (1 + \gamma(\beta - \alpha))p(t) - \gamma F(\beta - \alpha) \quad (71)$$

For this model, we can easily write the analytic solution. For our purposes, it is sufficient to state that from the equilibrium equation  $p(t+1) = p(t)$  we get the equilibrium price  $p^* = F$ , which is stable if  $-1 < 1 + \gamma(\beta - \alpha) < 1$ , i.e.  $0 < \alpha - \beta < \frac{2}{\gamma}$ .

The asset market positively diverges if  $1 + \gamma(\beta - \alpha) > 1$ , i.e. if  $\beta > \alpha$ , which means a prevalence of chartists with respect to fundamentalists. Moreover, the price diverges through oscillations if  $1 + \gamma(\beta - \alpha) < -1$ , which is equivalent to  $\alpha > \beta + \frac{2}{\gamma}$ . This condition can be interpreted by saying that fundamentalists are too many and too reactive as well. The first instability result is somehow expected, as the presence of chartists typically destabilized the emergence of the fundamental price. Instead, the second instability result due to the prevalence of fundamentalists may appear as a surprising result, as fundamentalists' demand function tends to bring the price back to its fundamental value. However, if this "stabilizing tendency" is too strong it causes a typical overshooting phenomenon, as a too strong return to the fundamental equilibrium in discrete time may imply to jump over it up to leading to diverging oscillations.

An evident shortcoming of the linear model described above is that whenever the equilibrium price loses stability we obtain divergence (as always occurs in linear models). So, we introduce now



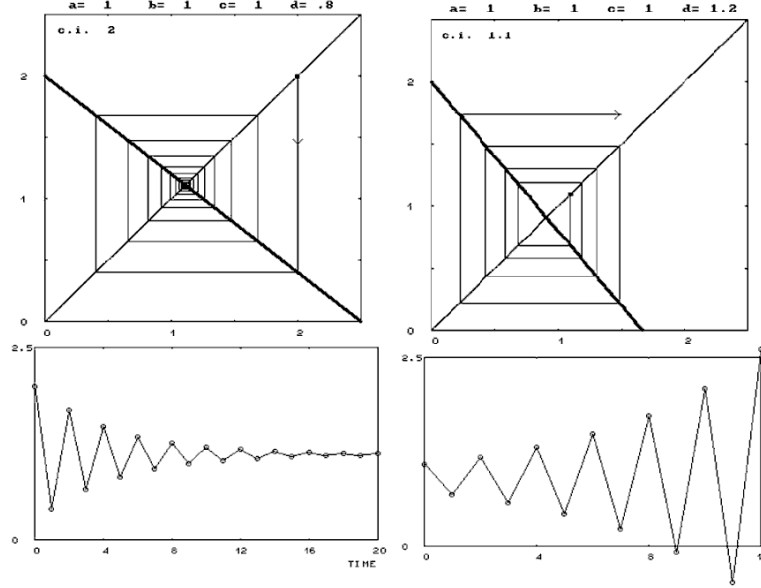


Figure 89: Oscillations of price in a Cobweb model.

a nonlinearity by assuming "prudent chartists" in the sense that if the price  $p(t)$  is too far from the fundamental price  $F$  then their extrapolative reaction of following the trend saturates. This is represented by the following modification of the chartists' demand excess

$$\Delta D^C(t) = \beta \arctan(p(t) - F)$$

As usual the  $\arctan(\cdot)$  function is a sign-preserving function, in the sense that  $\text{sign}(\cdot) = \text{sign}(\arctan(\cdot))$ , but differently from a linear function it saturates approaching horizontal asymptotes. With this modification the model becomes

$$p(t+1) = f(p(t)) = p(t) + \gamma(\alpha(F - p(t)) + \beta \arctan(p(t) - F))$$

We still have the equilibrium point  $p^* = F$  but now we can have, for sufficiently high values of  $\beta$ , two further fixed points (see fig. 93)

In fact, from the stability condition  $|f'(p)| < 1$ , that becomes  $-1 < 1 + \gamma(-\alpha + \frac{\beta}{1-(p-F)^2}) < 1$ , equivalent to

$$\alpha - \frac{2}{\gamma} = \beta_f < \beta < \beta_p = \alpha$$

we can see that a stability loss of  $p^* = F$  occurs for  $\beta$  increasing beyond  $\beta_p = \alpha$ . This is a pitchfork bifurcation for  $f(p)$ . As  $\beta$  decreases below  $\beta_f = \alpha - \frac{2}{\gamma}$ , a flip bifurcation occurs.

Some numerical computations are now shown in order to confirm and better understand the consequences of the local bifurcations detected. We will consider the set of fixed parameters  $F = 10$ ,  $\gamma = 2.5$ ,  $\alpha = 1.2$ , and use  $\beta$  (the weight of chartists in the composition of asset demand) as bifurcation parameter. For this set of parameters we have  $\beta_f = 1.2 - \frac{2}{2.5} = 0.4$  and  $\beta_p = 1.2$ .

The bifurcation diagram shown in fig. 94 illustrates what happens when the bifurcation parameter  $\beta$  increases beyond  $\beta_p$ : a supercritical pitchfork bifurcation occurs at which the stable equilibria are

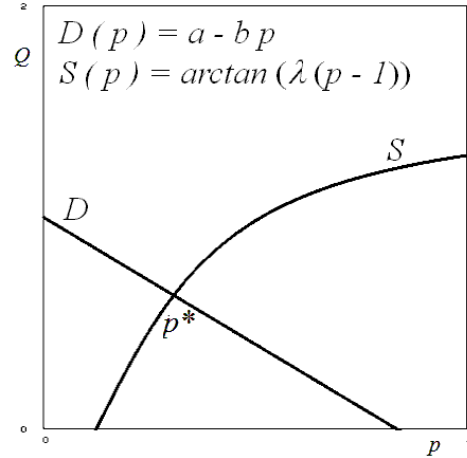


Figure 90: Nonlinear supply function and linear demand function.

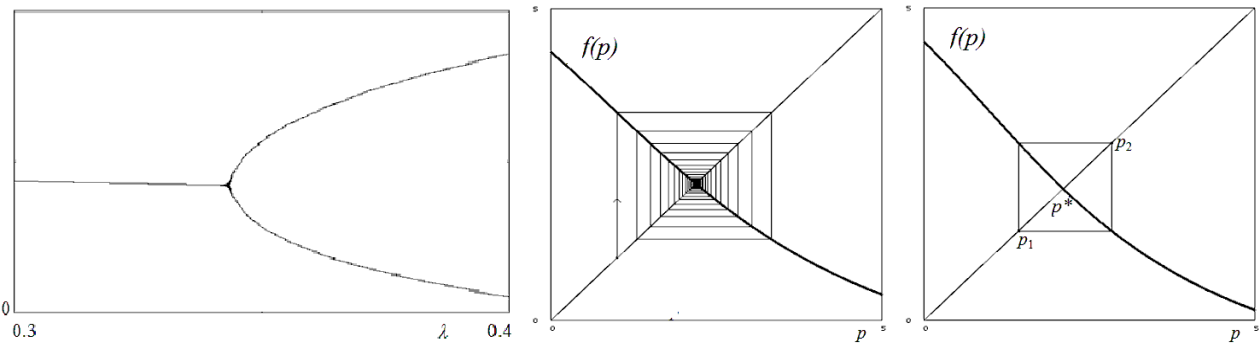


Figure 91: Flip bifurcation for the nonlinear cobweb model.

created, one above and one below the fundamental price  $F$  (represented by black and blue colors respectively). The fundamental price becomes unstable after the bifurcation and constitutes the boundary that separates the two basins of the coexisting equilibrium points. If  $\beta$  is further increased, then both the symmetric stable fixed points lose stability through a supercritical flip bifurcation, at which two coexisting stable cycles of period 2 are created, whose basins are still separated by the intermediate fundamental price  $F$ . This flip bifurcation opens the usual period doubling cascade (or period doubling route to chaos) leading to two coexisting chaotic attractors.

A remarkable global bifurcation occurs when the two separated and coexisting chaotic attractors have a contact with the common basin boundary (i.e. the fundamental price). In fact, after this contact the two separated chaotic attractors merge and form a unique chaotic set, which is a global attractor. The kind of trajectories occurring after this global bifurcation is shown in fig. 95, where a typical time series generated with  $\beta = 5$  is shown. As it can be seen the kind of motion exhibit some chaotic oscillations in the upper part, then a transition in the lower and so on, and no regularity can be detected about the transition times between upper and lower oscillations or vice-versa.

The bifurcation at which the two chaotic attractors merge is denoted as "global" because it cannot be detected by the study of the local approximation of the iterated map around the equilibrium point,

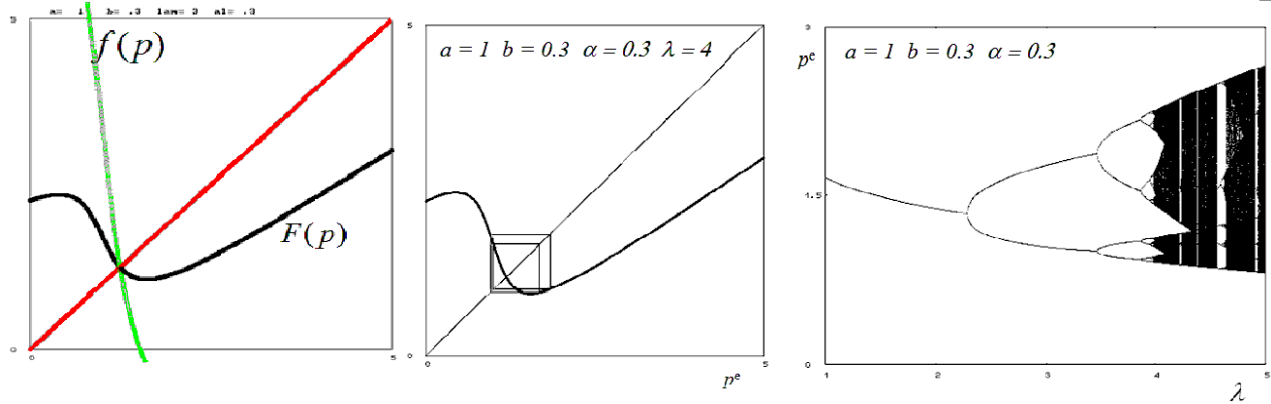


Figure 92: Nonlinear cobweb with adaptive expectations.

but it is related with contacts between critical points (i.e. maximum and minimum values or their images) and basin boundaries, i.e. unstable equilibrium points or their preimages. In fact, as shown in the previous sections, the points that bound the chaotic intervals are given by maximum or minimum values and their images, whereas the basin boundaries are separated by unstable equilibrium points or their preimages.

We now investigate what happens on the left side of the stability range of  $p^* = F$ , i.e. when  $\beta$  decreases below the flip bifurcation value  $\beta_f$ . We may expect the creation of a stable cycle of period 2, but numerical iterations show only oscillating and diverging trajectories for  $\beta$  values below  $\beta_f$ . This is due to the fact that the flip bifurcation occurring at  $\beta_f$  is of subcritical type, as it can be seen in the left panel of fig. 96, where both the graph of  $f(x)$  (bold curve) and  $f^2(x)$  (thin curve) are shown. From this picture it is evident that for  $\beta > \beta_f$ , i.e. in the range of stability of  $F$ , an unstable 2-cycle exists (indicated by the intersections of  $f^2(x)$  with the diagonal) that bounds the basin of the stable fixed point  $p^* = F$  and shrinks as  $\beta$  is decreased. When  $\beta$  reaches the bifurcation value  $\beta_f$  the unstable 2-cycle collapses into the fixed point which becomes unstable thus giving a hard stability loss. Fig.96 summarizes the local bifurcations observed in the model.

## 7 Two dimensional discrete dynamical systems

A discrete dynamical system (43) with two dynamic variables, say  $x_1(t)$  and  $x_2(t)$  with  $t \in \mathbb{N}$ , assumes the form

$$\begin{aligned} x_1(t+1) &= T_1(x_1(t), x_2(t)) \\ x_2(t+1) &= T_2(x_1(t), x_2(t)) \end{aligned} \quad (72)$$

and needs an initial condition  $(x_1(0), x_2(0))$  in order to generate a trajectory in the two-dimensional phase space. The equilibrium points of the dynamical system (72) are the fixed points of the map  $T: \mathbb{R}^2 \rightarrow \mathbb{R}^2$ , defined by the system of two equations with two unknowns

$$\begin{cases} T_1(x_1, x_2) = x_1 \\ T_2(x_1, x_2) = x_2 \end{cases} \quad (73)$$

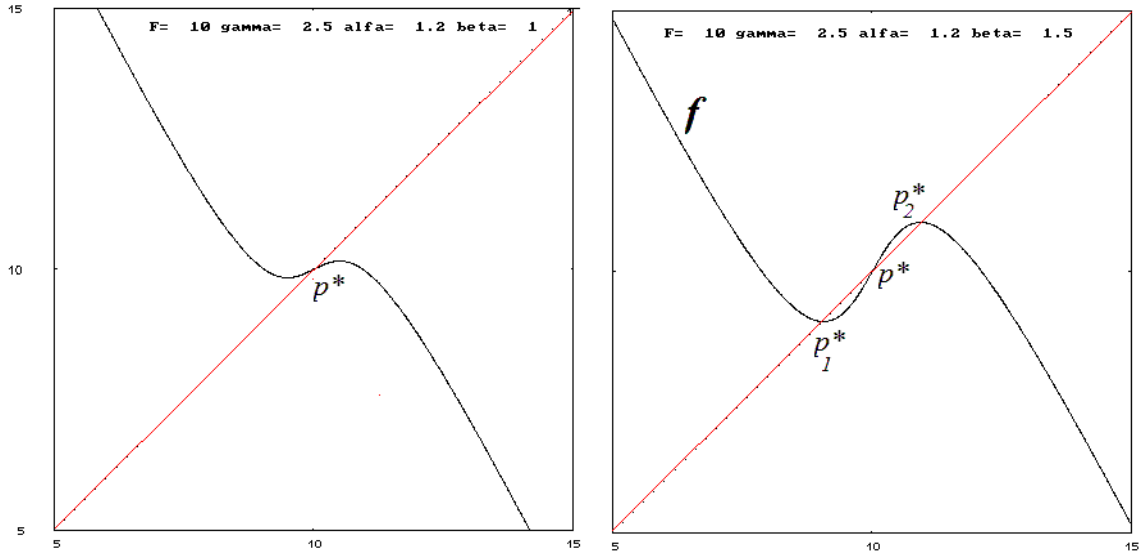


Figure 93: One-dimensional model of financial market with heterogeneous agents: fundamentalists and chartists.

Periodic cycles can be defined like in the case of one-dimensional iterated maps, just replacing  $x' = f(x)$  with  $\mathbf{x}' = \mathbf{T}(\mathbf{x})$  with  $\mathbf{x} \in \mathbb{R}^2$  and  $\mathbf{T}(\mathbf{x}) = (T_1(\mathbf{x}), T_2(\mathbf{x}))$ . The stability of fixed points as well as the stability of  $k$ -periodic cycles (each periodic point being a fixed point of  $\mathbf{T}^k$ ), as well as the kind of motion in a neighborhood of the fixed point or the periodic cycle, can be determined through the linearization of the map  $T$  in a neighborhood of the fixed point (or of any periodic point of the cycle). So, let us first analyze the dynamic properties of iterated linear maps.

## 7.1 Linear systems

Let us consider the following linear (homogeneous) system of two difference equations in the (normal) form:

$$\begin{cases} x_1(t+1) = a_{11}x_1(t) + a_{12}x_2(t) \\ x_2(t+1) = a_{21}x_1(t) + a_{22}x_2(t) \end{cases} \quad (74)$$

that can be written in the matrix form

$$\mathbf{x}(t+1) = \mathbf{A}\mathbf{x}(t) \quad (75)$$

where  $\mathbf{A} = \begin{pmatrix} a_{11} & a_{12} \\ a_{21} & a_{22} \end{pmatrix}$ ;  $\mathbf{x}(t) = \begin{pmatrix} x_1(t) \\ x_2(t) \end{pmatrix}$ .

Like in the case of linear dynamical systems in continuous time, the general solution, i.e. set of all the solutions of (74), is obtained from the linear combinations of two independent solution. Moreover, also in this case, these two solutions are searched by proposing a "trial solution" in the same form as the one obtained for the one-dimensional linear difference equation, i.e.

$$x_i(t) = v_i \lambda^t, \quad i = 1, 2 \quad (76)$$

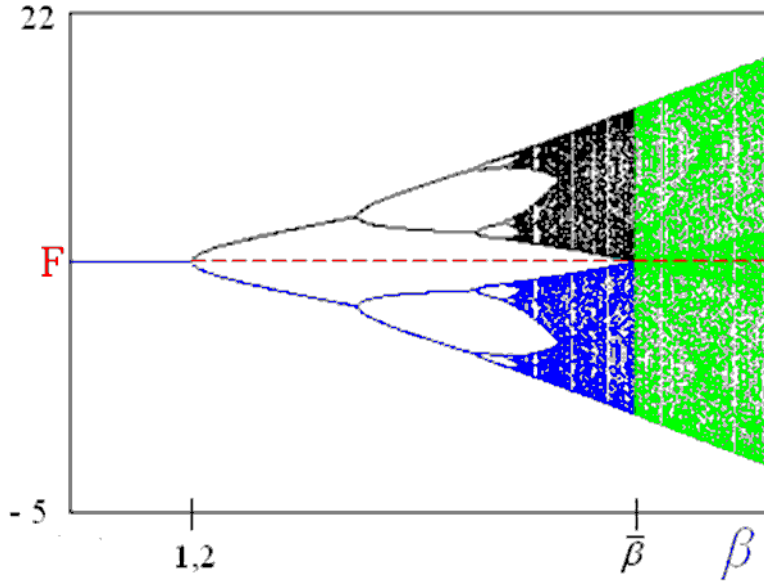


Figure 94: Bifurcauion diagram with coexisting attractors after the pitchfork bifurcation.

After replacing this trial solution into (74) we get

$$\begin{cases} \lambda^{t+1}v_1 = a_{11}\lambda^t v_1 + a_{12}\lambda^t v_2 \\ \lambda^{t+1}v_2 = a_{21}\lambda^t v_1 + a_{22}\lambda^t v_2 \end{cases}$$

and dividing for  $\lambda^t$  we get the usual eigenvalue problem

$$\begin{cases} (a_{11} - \lambda)v_1 + a_{12}v_2 = 0 \\ a_{21}v_1 + (a_{22} - \lambda)v_2 = 0 \end{cases}$$

that has non-trivial solutions if  $\lambda$  is a solution of the "characteristic equation"

$$P(\lambda) = \lambda^2 - Tr(A)\lambda + Det(A) = 0$$

where  $Tr(A) = a_{11} + a_{22}$  and  $Det(A) = a_{11}a_{22} - a_{12}a_{21}$

So again, like in the case of linear dynamical systems in continuous time, the problem of finding the solutions is reduced to a problem of linear algebra, the only difference being that the solutions are now in the form (76) instead of (23). In particular, if we denote by  $\Delta = Tr(A)^2 - 4det(A)$  we have that

- (i) If  $\Delta > 0$  then we have two real and distinct eigenvalues and the general solution has the form

$$\mathbf{x}(t) = c_1\mathbf{v}_1\lambda_1^t + c_2\mathbf{v}_2\lambda_2^t$$

where  $\mathbf{v}_1$  and  $\mathbf{v}_2$  are the corresponding eigenvectors and  $c_1, c_2$  are real constants that are uniquely determined by imposing the initial conditions  $x_i(0) = x_{i0}, i = 1, 2$

- (ii) If  $\Delta = 0$  then we have real and coincident eigenvalues  $\lambda_1 = \lambda_2 = \lambda$  and the general solution has the form

$$\mathbf{x}(t) = c_1\mathbf{v}\lambda^t + c_2\mathbf{v}t\lambda^t$$

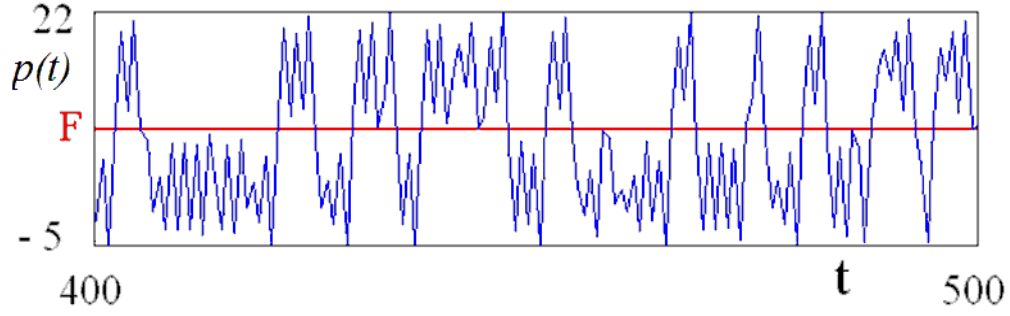


Figure 95: Chaotic patterns with a unique chaotic attractor obtained from the merging of the two attractors.

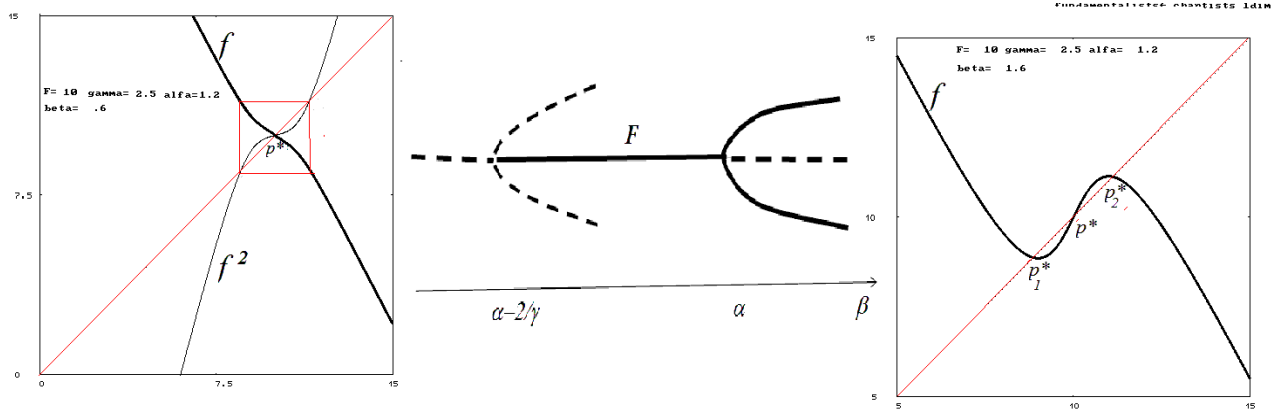


Figure 96: Subcritical flip and supercritical pitchfork in the nonlinear fundamentalists-chartists model.

- (iii) If  $\Delta < 0$  then we have two complex conjugate eigenvalues  $\lambda_{1,2} = -\frac{Tr(A)}{2} \pm i\frac{\sqrt{-\Delta}}{2} = |\lambda| (\cos \theta \pm i \sin \theta)$  where  $|\lambda| = \sqrt{\text{Re}(\lambda)^2 + \text{Im}(\lambda)^2} = \sqrt{\text{Det}(A)}$  and  $\theta = \arctan\left(\frac{\text{Im}(\lambda)}{\text{Re}(\lambda)}\right)$  or equivalently  $\cos \theta = -\frac{Tr(A)}{2\sqrt{\text{Det}(A)}}$ . The general real solution is obtained as

$$\mathbf{x}(t) = |\lambda|^t [(c_1 \mathbf{v}_1 - c_2 \mathbf{v}_2) \sin(\theta t) + (c_1 \mathbf{v}_1 + c_2 \mathbf{v}_2) \cos(\theta t)]$$

where  $\mathbf{v} = \mathbf{v}_1 + i\mathbf{v}_2$  is a complex eigenvector associated with  $\lambda_1 \in \mathbb{C}$ .

In any case, we can see that the general solution converges asymptotically to the equilibrium  $\mathbf{x} = \mathbf{0}$  if and only if  $|\lambda_i| < 1$ ,  $i = 1, 2$ , i.e. both the eigenvalues are inside the unit circle of the complex plane defined by  $\text{Re}(\lambda)^2 + \text{Im}(\lambda)^2 < 1$  (see fig.97).

The phase portraits associated to the different positions of the eigenvalues in the complex plane with respect to the unit circle are shown in the fig.98. The phase line represented in this qualitative picture looks quite similar to those shown for the phase portraits of linear dynamical systems in continuous time. Of course, the phase point along trajectories moves at discrete time pulses, i.e. it

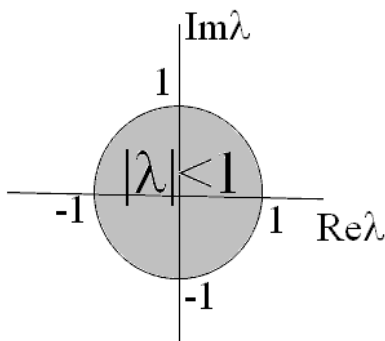


Figure 97: Stability region in the complex plane.

jumps from one point to another. However such discrete motion occurs along phase curves quite similar to those of continuous time dynamical systems, see fig.99).

The stability criterion, i.e. the necessary and sufficient conditions to have all the eigenvalues less than 1 in modulus, are given by

$$\begin{aligned}
 P(1) &= 1 - Tr(A) + Det(A) > 0 \\
 P(-1) &= 1 + Tr(A) + Det(A) > 0 \\
 Det(A) &< 1
 \end{aligned}
 \tag{77}$$

In the plane  $(Tr(A), Det(A))$  these three conditions define the interior of a triangle (known as *stability triangle*, see fig.100 bounded by the three straight lines whose equations are given by  $P(1) = 0$ ,  $P(-1) = 0$  and  $Det(A) = 1$ . When the point  $(Tr(A), Det(A))$  is inside the triangle then the fixed point  $\mathbf{x} = \mathbf{0}$  is globally asymptotically stable, whereas when the point  $(Tr(A), Det(A))$  is outside the triangle, the equilibrium  $\mathbf{x} = \mathbf{0}$  is unstable and the trajectories diverge. Along the triangle we have non generic (structurally unstable) situations of marginal stability. If the point  $(Tr(A), Det(A))$  exits the stability triangle along the side of equation  $P(1) = 1 - Tr(A) + Det(A) = 0$  then an eigenvalue exits the unit circle along the real axis in the point  $\lambda = 1$ ; if the point  $(Tr(A), Det(A))$  exits the stability triangle along the side of equation  $P(-1) = 1 + Tr(A) + Det(A) = 0$  then an eigenvalue exits the unit circle along the real axis in the point  $\lambda = -1$ ; if the point  $(Tr(A), Det(A))$  exits the stability triangle along the side of equation  $Det = 1$  then a pair of complex conjugate eigenvalues exit the unit circle of the complex plane. In the case of linear approximation of a nonlinear system in a neighborhood of a fixed point, such situations will represent bifurcations leading to the contact of fixed points and the creation of new kind of attractors, as we will see in the next section

## 7.2 Nonlinear discrete dynamical systems in 2 dimensions

Let us consider a nonlinear discrete dynamical system in two dimensions (72) and let  $\mathbf{x}^* = (x_1^*, x_2^*)$  be a fixed point, solution of (73). The linear approximation around the fixed point is given by

$$\mathbf{x}(t+1) - \mathbf{x}^* = \mathbf{J}_T(\mathbf{x}^*)(\mathbf{x}(t) - \mathbf{x}^*)$$

where  $\mathbf{J}_T$  is the jacobian matrix

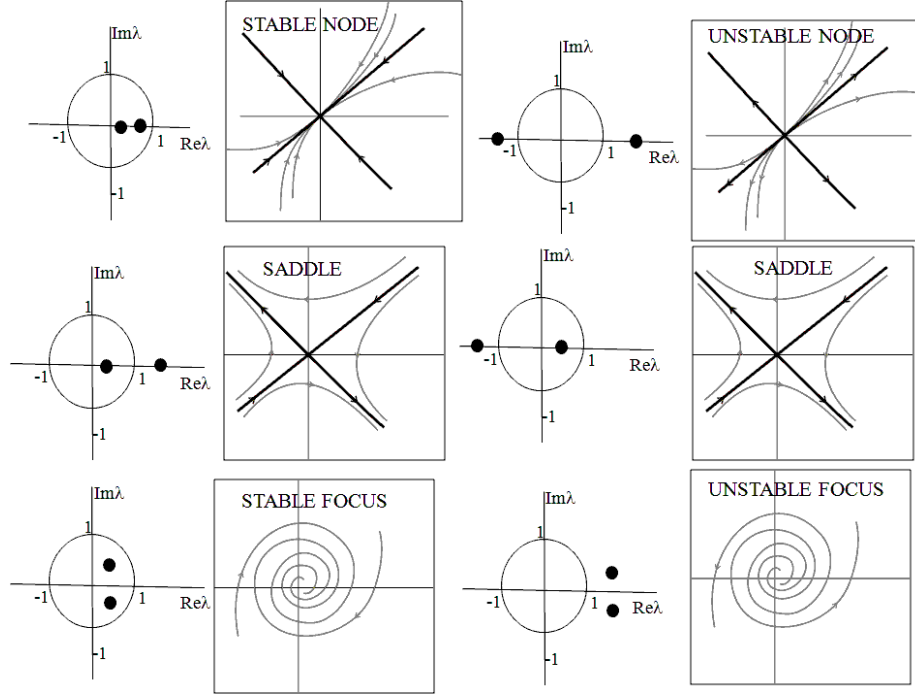


Figure 98: Eigenvalues in the complex plane and corresponding phase portrait in a neighborhood of the equilibrium.

$$\mathbf{J}_T(\mathbf{x}) = [J_{ij}] = \begin{bmatrix} \partial T_1 / \partial x_1 & \partial T_1 / \partial x_2 \\ \partial T_2 / \partial x_1 & \partial T_2 / \partial x_2 \end{bmatrix}$$

The necessary and sufficient conditions for asymptotic stability of 2-dimensional linear systems in (77) can be used as sufficient conditions for *local* asymptotic stability of an equilibrium point  $\mathbf{x}^*$  of a 2-dimensional *nonlinear* discrete dynamical system by using the Jacobian matrix evaluated at the fixed point  $\mathbf{J}_T(\mathbf{x}^*)$  as coefficient matrix.

When all the eigenvalues are less than one in absolute values (i.e. inside the unit circle of the complex plane) then the fixed point is locally attracting. When at least one eigenvalue is greater than one in absolute value then the fixed point is unstable.

If the structure of the discrete dynamical system (72) depends on a parameter, say  $\mu \in \mathbb{R}$ , and consequently any fixed point  $\mathbf{x}^* = \mathbf{x}^*(\mu)$  as well as  $\mathbf{J}_T(\mathbf{x}^*)$  depend on  $\mu$ , then as  $\mu$  varies a real eigenvalue, say  $\lambda_1(\mu)$  may exit the unit circle, or a pair of complex conjugate eigenvalues, say  $\lambda_{1,2}(\mu)$ , with  $\lambda_2(\mu) = \bar{\lambda}_1(\mu)$ , may exit the unit circle (see fig. 101). In the former case, i.e. for real eigenvalues, we have properties similar to those already described in the one-dimensional case. That is, when one eigenvalue crosses through  $\lambda = -1$  then a flip bifurcation may occur, while when one eigenvalue  $\lambda$  crosses through  $\lambda = +1$  then we may have a saddle-node or a transcritical or a pitchfork bifurcation.

However, as in the analogue situation for continuous-time dynamical systems of dimension greater than one, in the case of complex conjugate eigenvalues that exit the stability region of the complex plane (in this case the unit circle, whereas in the case of continuous time was the half plane characterized by negative real part) a new kind of bifurcation occurs which is the discrete-time analogue of the Hopf bifurcation for dynamical systems in continuous time. In the case of discrete time it



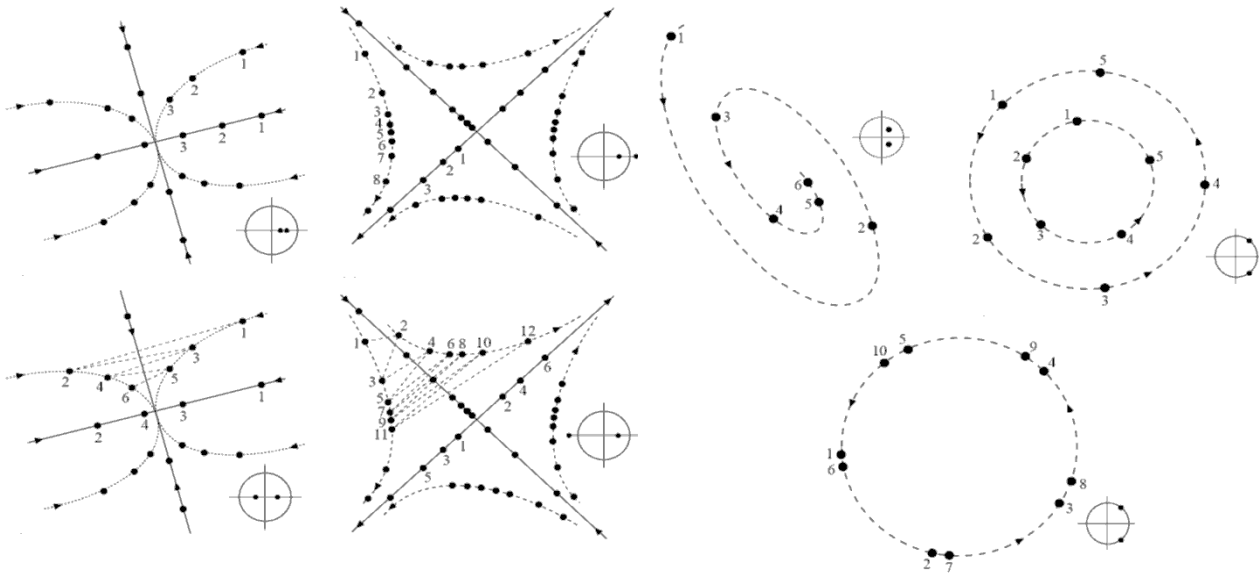


Figure 99: Phase portraits and trajectories in discrete time.

is called *Neimark-Sacker bifurcation*. Also in this case the presence of complex eigenvalues implies oscillatory dynamics along spiralling phase curves, hence oscillations around the equilibrium, and at the Neimark-Sacker bifurcation a closed invariant curve around the fixed point is created (or around the periodic point of a cycle, because as usual any  $k$ -periodic point of a map  $T$  corresponds to a fixed point of the map  $T^k$ ). Here we give a simplified description of the *Neimark-Sacker bifurcation theorem*, see more specialized books for a more rigorous statement.

**Neimark-Sacker bifurcation Theorem.** *Let  $T(x, \mu) : \mathbb{R}^2 \rightarrow \mathbb{R}^2$  be a one-parameter family of 2-dimensional maps which has a family of fixed points  $x^*(\mu)$  at which the eigenvalues are complex conjugate, say  $\lambda(\mu), \bar{\lambda}(\mu)$ . Assume that for  $\mu = \mu_0$  :*

- (1)  $|\lambda(\mu_0)| = 1$ , but  $\lambda^j(\mu_0) \neq 1$  for  $j = 1, 2, 3, 4$ ;
- (2)  $\frac{d|\lambda(\mu)|}{d\mu}(\mu_0) = d \neq 0$ . (transversality condition).

*Then in a neighborhood of  $x^*(\mu_0)$  the map  $T$  is topologically conjugate to the map given by (in polar coordinates)  $T_e(r, \theta) = (r(1 + d(\mu - \mu_0) + ar^2), \theta + c + br^2) + \text{higher-order terms}$ . If, in addition,*

- (3)  $a \neq 0$ ,

*then there is a simple closed invariant curve in a neighborhood of  $x^*(\mu_0)$ .*

The signs of the coefficients  $d$  and  $a$  determine the direction and stability of the bifurcating orbits. The Neimark-Sacker bifurcation is called supercritical (when  $a < 0$ ) or subcritical (when  $a > 0$ ) (fig. 102). We remark that numerically one can deduce the type of the bifurcation just from the stability of the fixed point at the bifurcation value: If the fixed point is locally attracting (resp. repelling), then the Neimark-Sacker bifurcation is supercritical (resp. subcritical). Let us notice that for *linear maps* the condition  $a \neq 0$  is never satisfied, not only at the fixed point, but in the whole region of definition of the map. And, indeed, considering a linear map, say with complex conjugate eigenvalues  $\lambda(\mu), \bar{\lambda}(\mu)$ , if  $|\lambda(\mu_0)| = 1$  then the fixed point is a center, so that the trajectory of any point different from the fixed point belongs to a different invariant ellipse and the motion is either periodic or quasi-periodic, depending on the parameters. For  $\mu \neq \mu_0$  the fixed point is either a globally attracting focus

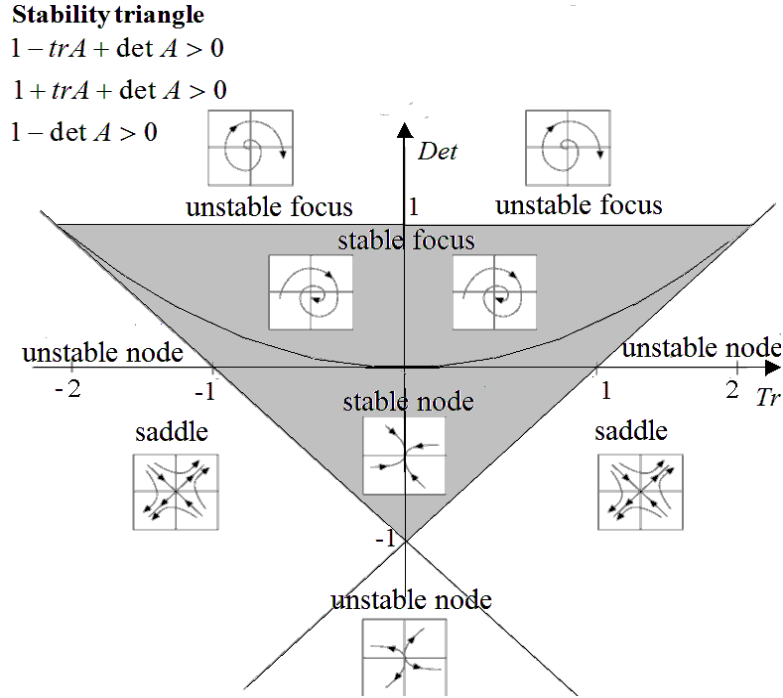


Figure 100: Stability region in the Trace-Determinant plane.

or a repelling focus (in which case the trajectories go to infinity). Thus the bifurcation which occurs in a linear map, when its complex-conjugate eigenvalues cross the unit circle, is also called *center bifurcation*. A similar bifurcation can be observed in nonlinear maps with  $a = 0$  as well.

The coefficients  $c$  and  $b$  give information on the rotation of the jumping phase point along the bifurcating closed invariant curve. In fact, the discrete time motion of the phase point along the closed invariant curve may be such that the jumping point completely fills the closed curve by a non-periodic trajectory (which is denoted as quasi-periodic trajectory because it oscillates with a given period and amplitude but never hits an already visited point) or after  $n$  iterations (and  $m$  revolutions along the closed curve) it may hit an already visited point and consequently it enters a  $n$ -cycle (a phenomenon called *frequency locking*).

As an example, let us consider the map

$$\begin{aligned} x(t+1) &= y(t) \\ y(t+1) &= y(t) - \alpha x(t) + x(t)^2 \end{aligned} \tag{78}$$

It has two fixed points:  $O = (0, 0)$  and  $P = (\alpha, \alpha)$ . The Jacobian matrix

$$J(x, y) = \begin{bmatrix} 0 & 1 \\ 2x - \alpha & 1 \end{bmatrix}$$

computed at the fixed point  $O$  is such that  $\text{Tr}(J(O)) = 1$  and  $\text{Det}(J(O)) = \alpha$ . According to the stability conditions in (77),  $O$  is a stable fixed point for  $0 < \alpha < 1$ : at  $\alpha = 0$  a transcritical bifurcation occurs at which  $O$  takes the stability of  $P$ ; at  $\alpha = \frac{1}{4}$  the eigenvalues become complex conjugate, so that  $O$  is transformed from a stable node to a stable focus (but this is not a bifurcation as the phase portrait

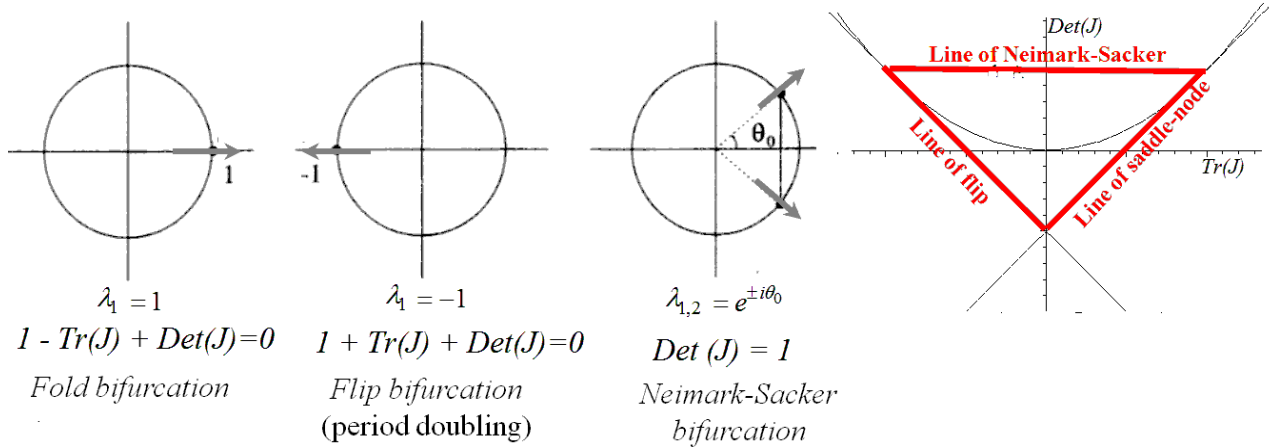


Figure 101: Bifurcations in the complex plane and in the Trace-Determinant plane.

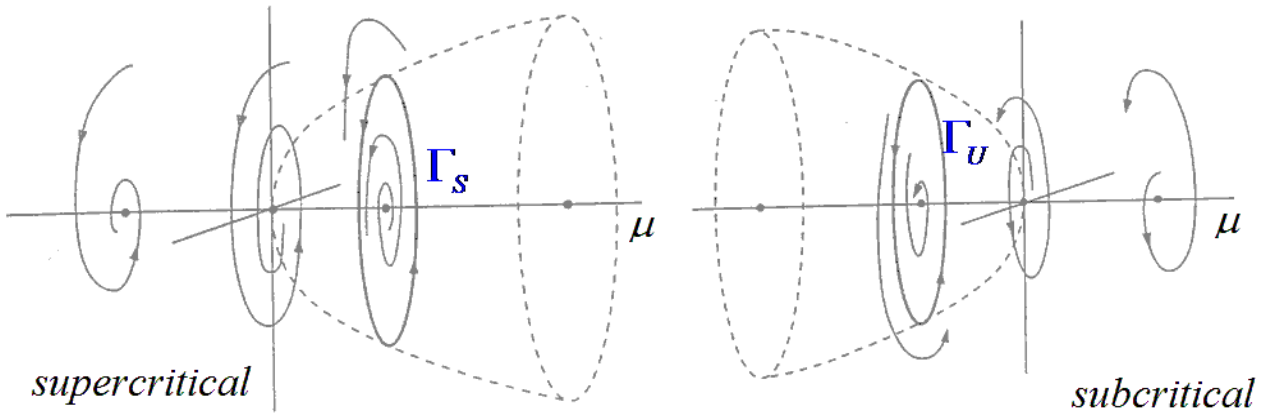


Figure 102: Neimark-Sacker bifurcation,

of a stable node is topologically conjugate to that of a stable focus). Then at  $\alpha = 1$ ,  $O$  loses stability and for  $\alpha > 1$  it becomes an unstable focus, with a stable invariant curve around it (supercritical Neimark-Sacker bifurcation). As  $\alpha$  is further increased the stable closed orbit enlarges and the motion is quasi-periodic on it (see fig. 103, where the development of the asymptotic trajectories is shown for increasing values of  $\alpha$ ). Just after the bifurcation the stable invariant curve is completely filled by the trajectories, and the amplitude increases as  $\alpha$  is increased. The for  $\alpha = 1.4$  a frequency locking occurs and the trajectories converge at a periodic cycle of period 7 with periodic points located along the invariant curve. Then for higher values of  $\alpha$  the closed invariant curve is broken and a more complex attracting set can be observed (see in fig. 103 the enlarged portion of the attractor obtained for  $\alpha = 1.505$ ) whose shape depends on the nonlinearities of the map prevailing far from the fixed point.

This is even more evident in fig. 104, obtained for  $\alpha = 1.54$ , where the points of the trajectories starting from initial conditions in the white region around the fixed point  $O$  asymptotically form the chaotic attractor clearly visible in the left panel. The trajectories starting from the grey region diverge,

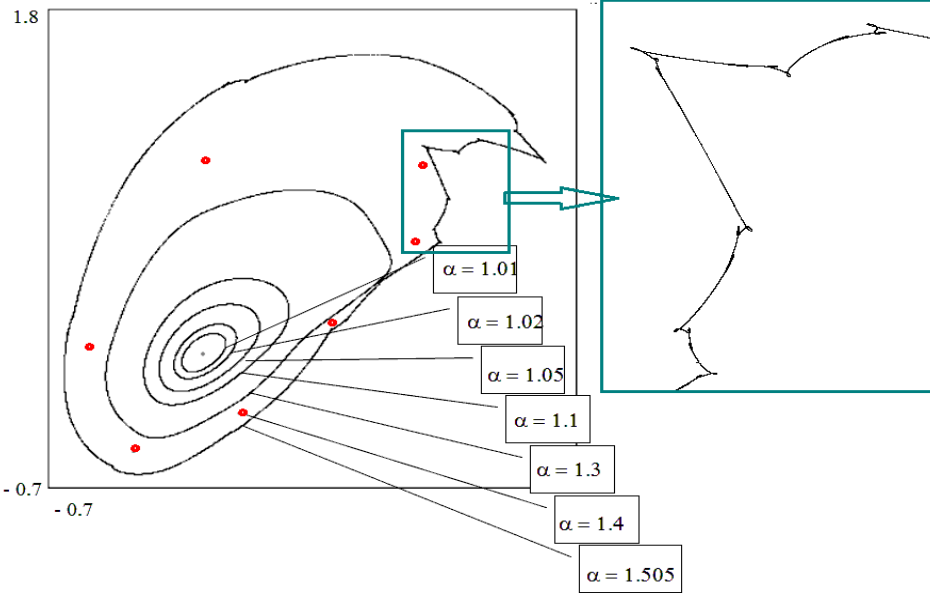


Figure 103: The attractors of the map (78) for increasing values of the parameter  $\alpha$ .

and the boundary that separates the two basins of attraction is the stable set of the saddle point  $P$ . The right panel of the picture shows the points  $x(t)$  and  $y(t)$  versus time, joined by segments (just a visual trick to give more emphasis to the chaotic oscillatory pattern).

### 7.3 Some economic examples

#### 7.3.1 A model of financial markets with heterogeneous traders

Let us consider again the dynamics of price of a risky asset (70) with fundamentalists and chartists, and let us assume that the fundamental price  $F$  is only in the information set of fundamentalists, i.e. the chartists ignore  $F$  and they compute the price expected at time  $t + 1$  by extrapolating the trend observed in the last two observed prices  $p(t - 1)$  and  $p(t)$ :

$$\Delta D^C(t) = \beta(p(t) - p(t - 1)) \quad \beta > 0$$

where  $\beta$  gives a measure of the weight of the chartists in the market. Plugging this expression of chartists' excess demand and the usual one of fundamentalists  $\Delta D^F(t) = \alpha(F - p(t))$  into (70), we get

$$p(t + 1) = [1 + \gamma(\beta - \alpha)]p(t) - \gamma\beta p(t - 1) + \gamma\alpha F. \quad (79)$$

This is a second order difference equation, as it involves the values of the dynamic variable  $p$  at three successive time periods (and, consequently, it needs two prices to get a trajectory, say  $p(-1) = p_{-1}$  and  $p(0) = p_0$ ). By introducing the auxiliary dynamic variable  $z(t) = p(t - 1)$  the second order difference equation (79) can be written in the equivalent system of two difference equation of order one, i.e. the standard form of a two-dimensional dynamical system

$$\begin{cases} z(t + 1) = p(t) \\ p(t + 1) = -\gamma\beta z(t) + [1 + \gamma(\beta - \alpha)]p(t) + \gamma\alpha F \end{cases}$$

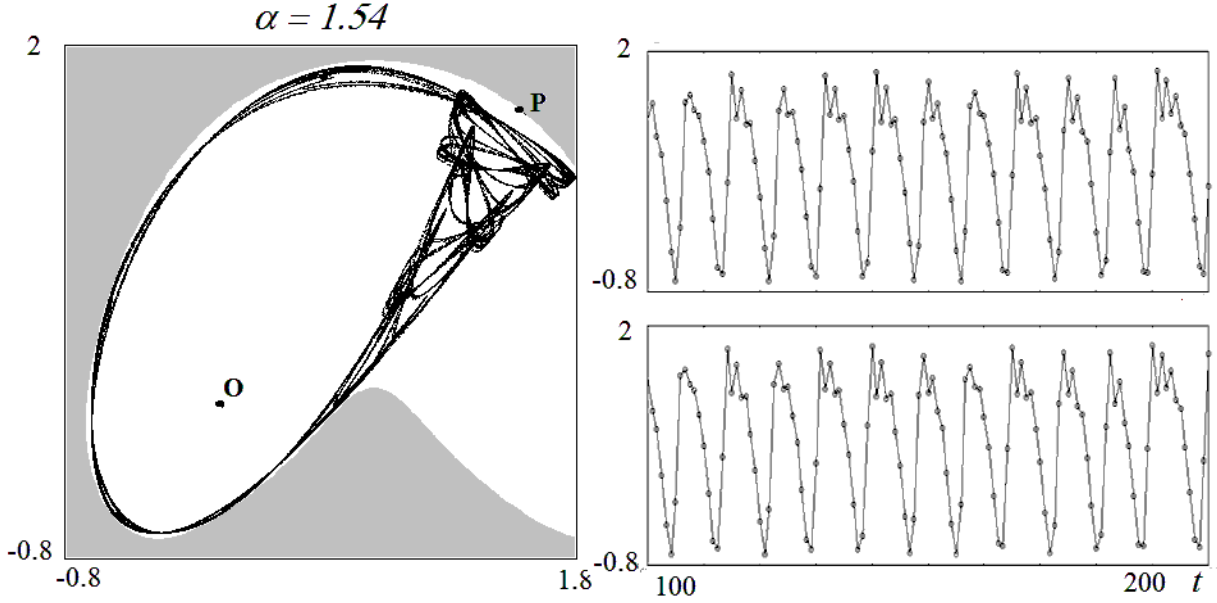


Figure 104: Chaotic attractor of the map (78) for  $\alpha = 1.54$ , its basin of attraction (white region) and a typical trajectory represented versus time.

with initial conditions  $z(0) = p_{-1}$  and  $p(0) = p_0$ . This is an affine (i.e. linear non homogeneous) model with the unique equilibrium  $(F, F)$  and jacobian matrix

$$\mathbf{J} = \begin{bmatrix} 0 & 1 \\ -\gamma\beta & 1 + \gamma(\beta - \alpha) \end{bmatrix}$$

hence  $Tr(J) = 1 + \gamma(\beta - \alpha)$  and  $Det(J) = \gamma\beta$ . The conditions for the asymptotic stability are

$$\begin{aligned} 1 - Tr(J) + Det(J) &= \gamma\alpha > 0 \\ 1 + Tr(J) + Det(J) &= 2 + 2\gamma\beta - \gamma\alpha > 0 \\ \gamma\beta &< 1 \end{aligned}$$

The first condition is always satisfied the second condition is equivalent to  $\beta > \frac{\alpha}{2} - \frac{1}{\gamma}$ , hence the stability range can be written as

$$\frac{\alpha}{2} - \frac{1}{\gamma} < \beta < \frac{1}{\gamma}$$

In fig. 105 the stability region is represented in the plane of parameters  $(\alpha, \beta)$ . Increasing  $\beta$ , i.e. an increased weight of chartists, leads to diverging sinusoidal oscillations, whereas increasing  $\alpha$  values, i.e. increasing fundamentalists reaction, instability with flip-type oscillations (or improper oscillations) is reached, due to overshooting.

The same model with prudent chartists, i.e.

$$\Delta D^C(t) = \beta \arctan(p(t) - p(t-1))$$

leads to a nonlinear model

$$\begin{cases} z(t+1) = p(t) \\ p(t+1) = (1 - \gamma\alpha)p(t) + \gamma\beta \arctan(p(t) - z(t)) + \gamma\alpha F \end{cases}$$

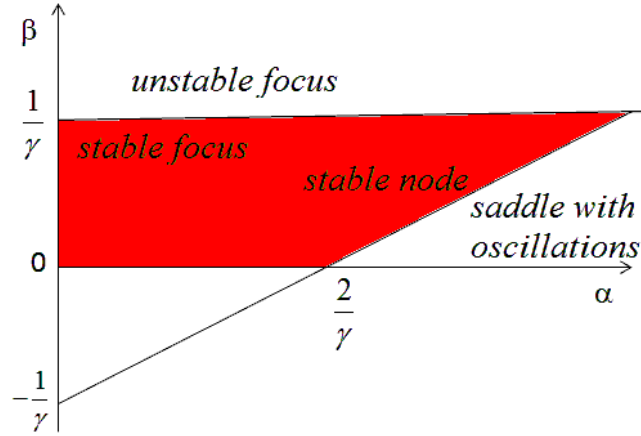


Figure 105: Stability region in the plane of parameters  $\alpha, \beta$  for the linear model.

with the same unique fixed point  $(F, F)$  and the same Jacobian matrix computed in it. So the same stability conditions are obtained, and consequently the same stability region in the space of the parameters. However, when the parameters vary so that the boundaries of the stability region are crossed, flip and Neimark-Sacker bifurcations occur, as shown in fig. 106.

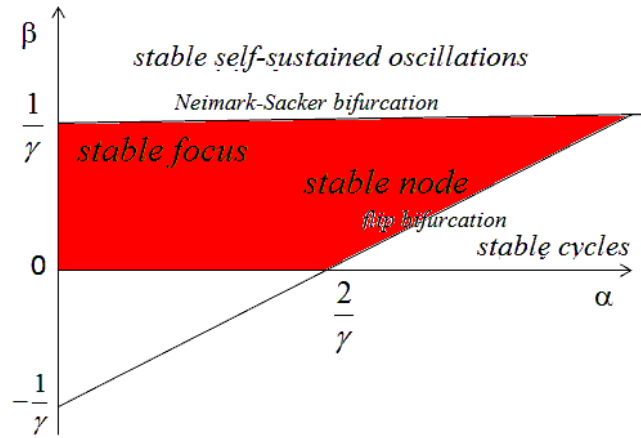


Figure 106: Stability region and bifurcation curves in the plane of parameters  $\alpha, \beta$  for the nonlinear model.

Another possible modification of the model consists in the assumption that also fundamentalists are prudent, i.e.

$$\Delta D^F(t) = \alpha \arctan(F - p(t))$$

leading to the following model

$$\begin{cases} z(t+1) = p(t) \\ p(t+1) = p(t) + \gamma D(t) = p(t) + \gamma [\alpha \arctan(F - p(t)) + \beta \arctan(p(t) - z(t))] \end{cases}$$

Even in this case, the unique fixed point  $(F, F)$  is obtained, with same Jacobian matrix computed in it, hence the same stability conditions as well as the same stability region in the space of the parameters. However, when the parameters vary so that the boundaries of the stability region are crossed some different dynamic scenarios arise, especially along the flip bifurcation side.

A good exercise consists in the numerical investigation of the dynamic scenarios prevailing in the regions of the parameters' space  $(\alpha, \beta)$  outside the stability region, starting from the bifurcation lines.

### 7.3.2 A duopoly game with linear demand and gradient dynamics

We consider a Cournot duopoly, i.e. an industry consisting of two quantity-setting firms, labelled by  $i = 1, 2$ , producing the same good for sale on the market. Production decisions of both firms occur at discrete time periods  $t = 0, 1, 2, \dots$ . Let  $q_i(t)$  represent the output of the  $i$ th firm during period  $t$ , at a production cost  $C_i(q_i)$ . The price prevailing in period  $t$  is determined by the total supply  $Q(t) = q_1(t) + q_2(t)$  through a demand function

$$p = f(Q) \quad (80)$$

from which the single-period profit of the  $i$ th firm is given by

$$\Pi_i(q_1, q_2) = q_i f(Q) - C_i(q_i) . \quad (81)$$

We assume that each duopolist does not have a complete knowledge of the demand function, and tries to infer how the market will respond to its production changes by an empirical estimate of the marginal profit. This estimate may be obtained by a market research or by brief experiments of small (or local) production or price variations performed at the beginning of period  $t$ , and we assume that even if the firms are quite ignorant about the market demand, they are able to obtain a correct empirical estimate of the marginal profits  $\left(\frac{\partial \Pi_i}{\partial q_i}\right)^{(e)} = \frac{\partial \Pi_i}{\partial q_i}(q_1, q_2)$   $i = 1, 2$ . This local estimate of expected marginal profits is much easier to obtain than a global knowledge of the demand function (involving values of  $Q$  that may be very different from the current ones). With this kind of information the producers behave as local profit maximizers, the local adjustment process being one where a firm increases its output if it perceives a positive marginal profit and decreases its production if it is negative:

$$q_i(t+1) = q_i(t) + \alpha_i(q_i) \frac{\partial \Pi_i}{\partial q_i}(q_1, q_2) ; \quad i = 1, 2 \quad (82)$$

where  $\alpha_i(q_i)$  is a positive function which gives the extent of production variation of firm  $i$  following a given profit signal. An adjustment mechanism similar to (82) has been proposed by some authors with constant  $\alpha_i$ . Instead we assume  $\alpha_i$  proportional to  $q_i$ ,  $\alpha_i(q_i) = v_i q_i$  ;  $i = 1, 2$ , where  $v_i$  is a positive constant which will be called *speed of adjustment*, equivalent to the assumption that the "relative production change" is proportional to the estimated marginal profit:

$$\frac{q_i(t+1) - q_i(t)}{q_i(t)} = v_i \frac{\partial \Pi_i}{\partial q_i}(q_1, q_2).$$

We also assume a linear demand function

$$f(Q) = a - bQ \quad (83)$$

with  $a, b$  positive constants, and linear cost functions

$$C_i(q_i) = c_i q_i ; \quad i = 1, 2, \quad (84)$$

where the positive constants  $c_i$  are the marginal costs. With these assumptions

$$\Pi_i(q_1, q_2) = q_i [a - b(q_1 + q_2) - c_i] \quad , \quad i = 1, 2 \quad , \quad (85)$$

and the marginal profit for firm  $i$  is

$$\frac{\partial \Pi_i}{\partial q_i} = a - c_i - 2bq_i - bq_j \quad , \quad i, j = 1, 2, \quad j \neq i. \quad (86)$$

With the above assumptions, the dynamic model is expressed by the iteration of the following two-dimensional nonlinear map  $T(q_1, q_2) \rightarrow (q'_1, q'_2)$  defined as

$$T : \begin{cases} q'_1 = (1 + v_1(a - c_1))q_1 - 2bv_1q_1^2 - bv_1q_1q_2 \\ q'_2 = (1 + v_2(a - c_2))q_2 - 2bv_2q_2^2 - bv_2q_1q_2 \end{cases} \quad (87)$$

where  $'$  denotes the unit-time advancement operator, that is, if the right-hand side variables are productions of period  $t$  then the left-hand ones represent productions of period  $(t + 1)$ .

The fixed points of the map (87) are the solutions of the algebraic system

$$\begin{cases} q_1(a - c_1 - 2bq_1 - bq_2) = 0 \\ q_2(a - c_2 - bq_1 - 2bq_2) = 0 \end{cases}$$

obtained by setting  $q'_i = q_i$ ,  $i = 1, 2$ , in (87). We can have at most four fixed points:  $E_0 = (0, 0)$ ,  $E_1 = (\frac{a-c_1}{2b}, 0)$  if  $c_1 < a$ ,  $E_2 = (0, \frac{a-c_2}{2b})$  if  $c_2 < a$ , which will be called *boundary equilibria*, and the fixed point  $E_* = (q_1^*, q_2^*)$ , with

$$q_1^* = \frac{a + c_2 - 2c_1}{3b} \quad , \quad q_2^* = \frac{a + c_1 - 2c_2}{3b} \quad , \quad (88)$$

which is positive (i.e. it belongs to the strategy space of the duopoly model) provided that

$$\begin{cases} 2c_1 - c_2 < a \\ 2c_2 - c_1 < a. \end{cases} \quad (89)$$

The equilibrium point  $E_*$ , when it exists, is the unique Nash equilibrium, located at the intersection of the two reaction curves given by the two straight lines which represent the locus of points of vanishing marginal profits (86).

The study of the local stability of the fixed points is based on the localization, on the complex plane, of the eigenvalues of the Jacobian matrix of (87)

$$\mathbf{J}(q_1, q_2) = \begin{bmatrix} 1 + v_1(a - c_1 - 4bq_1 - bq_2) & -v_1bq_1 \\ -v_2bq_2 & 1 + v_2(a - c_2 - bq_1 - 4bq_2) \end{bmatrix} \quad (90)$$

It is easy to prove that whenever the equilibrium  $E_*$  exists (i.e. (89) are satisfied), the boundary fixed points  $E_i$ ,  $i = 0, 1, 2$ , are unstable. In fact at  $E_0$  the Jacobian matrix becomes a diagonal matrix

$$\mathbf{J}(0, 0) = \begin{bmatrix} 1 + v_1(a - c_1) & 0 \\ 0 & 1 + v_2(a - c_2) \end{bmatrix} \quad (91)$$



whose eigenvalues, given by the diagonal entries, are greater than 1 if  $c_1 < a$  and  $c_2 < a$ . Thus  $E_0$  is a repelling node with eigendirections along the coordinate axes. At  $E_1$  the Jacobian matrix becomes a triangular matrix

$$\mathbf{J}\left(\frac{a-c_1}{2b}, 0\right) = \begin{bmatrix} 1 - v_1(a-c_1) & -\frac{v_1}{2}(a-c_1) \\ 0 & 1 + \frac{v_2}{2}(a-2c_2+c_1) \end{bmatrix} \quad (92)$$

whose eigenvalues, given by the diagonal entries, are  $\lambda_1 = 1 - v_1(a-c_1)$ , with eigenvector  $\mathbf{r}_1^{(1)} = (1, 0)$  along the  $q_1$  axis, and  $\lambda_2 = 1 + \frac{v_2}{2}(a-2c_2+c_1)$ , with eigenvector  $\mathbf{r}_1^{(2)} = (1, 2\frac{1-v_1(a-c_1)}{v_1(a-c_1)})$ . When (89) are satisfied  $E_1$  is a saddle point, with local stable manifold along  $q_1$  axis and the unstable one tangent to  $\mathbf{r}_1^{(2)}$ , if

$$v_1 < \frac{2}{a-c_1}, \quad (93)$$

otherwise  $E_1$  is an unstable node. The bifurcation occurring at  $v_1 = \frac{2}{a-c_1}$  is a flip bifurcation at which  $E_1$  from attracting becomes repelling along the  $q_1$  axis, on which a saddle cycle of period 2 appears.

The same arguments hold for the other boundary fixed point  $E_2$ . It is a saddle, with local stable manifold along the  $q_2$  axis and the unstable one tangent to  $\mathbf{r}_2^{(2)} = (1, 2\frac{1-v_2(a-c_2)}{v_2(a-c_2)})$ , if

$$v_2 < \frac{2}{a-c_2}, \quad (94)$$

otherwise it is an unstable node. Also in this case the bifurcation that transforms the saddle into the repelling node is a flip bifurcation creating a 2-cycle saddle on the  $q_2$  axis.

To study the local stability of the Nash equilibrium we consider the Jacobian matrix at  $E_*$

$$\mathbf{J}(q_1^*, q_2^*) = \begin{bmatrix} 1 - 2v_1bq_1^* & -v_1bq_1^* \\ -v_2bq_2^* & 1 - 2v_2bq_2^* \end{bmatrix}. \quad (95)$$

Its eigenvalues are real because the characteristic equation  $\lambda^2 - Tr\lambda + Det = 0$ , where  $Tr$  represents the trace and  $Det$  the determinant of (95), has positive discriminant

$$Tr^2 - 4Det = 4b^2 \left[ (v_1q_1^* - v_2q_2^*)^2 + v_1v_2q_1^*q_2^* \right] > 0.$$

It is easy to realize that  $\lambda_i < 1$ ,  $i = 1, 2$ , since  $1 - Tr + Det > 0$  when (89) hold, thus a sufficient condition for the local asymptotic stability of  $E_*$  is  $1 + Tr + Det > 0$ , which ensures  $\lambda_i > -1$ ,  $i = 1, 2$ . This condition, which becomes

$$3b^2q_1^*q_2^*v_1v_2 - 4bq_1^*v_1 - 4bq_2^*v_2 + 4 < 0, \quad (96)$$

defines a region of stability in the plane of the speeds of adjustment  $(v_1, v_2)$  whose shape is like the shaded area of fig. 107. This stability region is bounded by the portion of hyperbola, with positive  $v_1$  and  $v_2$ , whose equation is given by the vanishing of the left hand side of (96). For values of  $(v_1, v_2)$  inside the stability region the Nash equilibrium  $E_*$  is a stable node, and the hyperbola represents a bifurcation curve at which  $E_*$  loses its stability through a period doubling (or *flip*) bifurcation. This bifurcation curve intersects the axes  $v_1$  and  $v_2$  in the points  $A_1$  and  $A_2$  respectively, whose coordinates are given by

$$A_1 = \left( \frac{3}{a+c_2-2c_1}, 0 \right) \quad \text{and} \quad A_2 = \left( 0, \frac{3}{a+c_1-2c_2} \right). \quad (97)$$

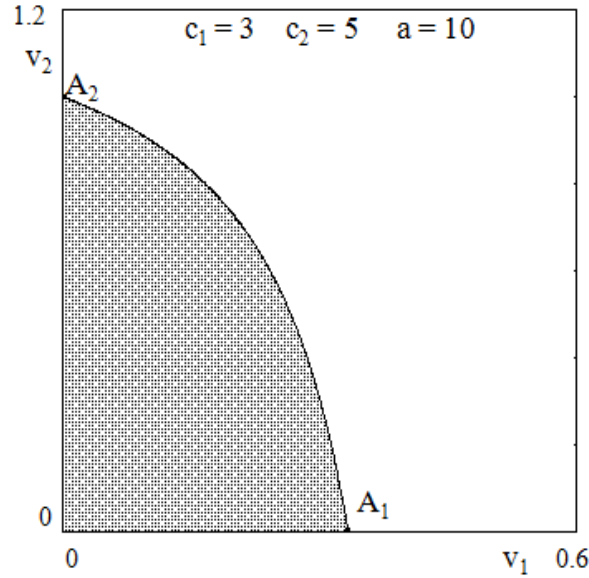


Figure 107: The shaded area represents, in the plane of speeds of adjustment  $(v_1, v_2)$ , the region of local asymptotic stability of the Nash equilibrium. The values of the other parameters are  $c_1 = 3$ ,  $c_2 = 5$ ,  $a = 10$ .

From these results we can obtain information on the effects of the model's parameters on the local stability of  $E_*$ . For example, an increase of the speeds of adjustment, with the other parameters held fixed, has a destabilizing effect. In fact, an increase of  $v_1$  and/or  $v_2$ , starting from a set of parameters which ensures the local stability of the Nash equilibrium, can bring the point  $(v_1, v_2)$  out of the stability region, crossing the flip bifurcation curve.

Similar arguments apply if the parameters  $v_1, v_2, c_1, c_2$  are fixed and the parameter  $a$ , which represents the maximum price of the good produced, is increased. In this case the stability region becomes smaller, as can be easily deduced from (97), and this can cause a loss of stability of  $E_*$  when the moving boundary is crossed by the point  $(v_1, v_2)$ . An increase of the marginal cost  $c_1$ , with  $c_2$  held fixed, causes a displacement of the point  $A_1$  to the right and of  $A_2$  downwards. Instead, an increase of  $c_2$ , with  $c_1$  held fixed, causes a displacement of  $A_1$  to the left and of  $A_2$  upwards. In both cases the effect on the local stability of  $E_*$  depends on the position of the point  $(v_1, v_2)$ . In fact, if  $v_1 < v_2$ , i.e. the point  $(v_1, v_2)$  is above the diagonal  $v_1 = v_2$ , an increase of  $c_1$  can destabilize  $E_*$ , whereas an increase of  $c_2$  reinforces its stability. The situation is reversed if  $v_1 > v_2$ .

From these arguments the combined effects due to simultaneous changes of more parameters can be deduced. For example if  $E_*$  becomes unstable because of a price increase (due to a shift of the demand curve), its stability can be regained by a reduction of the speeds of reaction, whereas an increase of a marginal cost  $c_i$  can be compensated by a decrease of the corresponding  $v_i$ : in the presence of a high marginal cost, stability is favored by a more prudent behavior (i.e. lower reactivity to profit signals).

### 7.3.3 A duopoly game with isoelastic demand and gradient dynamics

We consider now the same duopoly model (82) but with a different demand function (often used in economics as an alternative of linear demand) called isoelastic

$$p = \frac{1}{Q} \quad (98)$$

In this case the one-period profit of firm  $i$  is given by

$$\Pi_i(q_1, q_2) = \frac{q_i}{q_1 + q_2} - c_i q_i \quad ; i = 1, 2. \quad (99)$$

hence the estimated marginal profits are

$$\frac{\partial \Pi_1}{\partial q_1} = \frac{q_2}{(q_1 + q_2)^2} - c_1 \quad \text{and} \quad \frac{\partial \Pi_2}{\partial q_2} = \frac{q_1}{(q_1 + q_2)^2} - c_2.$$

With these assumptions, model (82) becomes

$$T : \begin{cases} q_1' = q_1 \left( 1 - c_1 v_1 + v_1 \frac{q_2}{(q_1 + q_2)^2} \right) \\ q_2' = q_2 \left( 1 - c_2 v_2 + v_2 \frac{q_1}{(q_1 + q_2)^2} \right) \end{cases} \quad (100)$$

The fixed points of (100) are defined as the nonnegative solutions of the algebraic system

$$\begin{cases} q_1 \left( \frac{q_2}{(q_1 + q_2)^2} - c_1 \right) = 0 \\ q_2 \left( \frac{q_1}{(q_1 + q_2)^2} - c_2 \right) = 0 \end{cases}$$

obtained by setting  $q_i' = q_i$ ,  $i = 1, 2$ , in (100). As the map (100) is not defined in  $(0, 0)$ , the unique equilibrium point is

$$E^* = (q_1^*, q_2^*) = \left( \frac{c_2}{(c_1 + c_2)^2}, \frac{c_1}{(c_1 + c_2)^2} \right) \quad (101)$$

which is also the unique Nash equilibrium of the classical Cournot duopoly game, as  $E^*$  is located at the intersection of the two reaction curves  $\frac{\partial \Pi_i}{\partial q_i} = 0$ ,  $i = 1, 2$ , (first order conditions) and also the second order sufficient conditions are satisfied at  $E^*$ , since  $\frac{\partial^2 \Pi_i}{\partial q_i^2}(E^*) = -2(c_1 + c_2)c_i < 0$ ,  $i = 1, 2$ . At  $E^*$  the optimal profits of the two firms are

$$\Pi_1^* = c_2 \quad \text{and} \quad \Pi_2^* = c_1. \quad (102)$$

The study of the local stability of the Nash equilibrium is based on the localization, on the complex plane, of the eigenvalues of the Jacobian matrix of (100)

$$J(q_1, q_2) = \begin{bmatrix} 1 - v_1 c_1 + v_1 \frac{q_2(q_2 - q_1)}{(q_1 + q_2)^3} & v_1 \frac{q_1(q_1 - q_2)}{(q_1 + q_2)^3} \\ v_2 \frac{q_2(q_2 - q_1)}{(q_1 + q_2)^3} & 1 - v_2 c_2 + v_2 \frac{q_1(q_1 - q_2)}{(q_1 + q_2)^3} \end{bmatrix}$$

computed at  $E^*$

$$J^* = \begin{bmatrix} 1 + v_1 c_1 \left( \frac{c_1 - c_2}{c_1 + c_2} - 1 \right) & v_1 c_2 \frac{c_2 - c_1}{c_1 + c_2} \\ v_2 c_1 \frac{c_1 - c_2}{c_1 + c_2} & 1 + v_2 c_2 \left( \frac{c_2 - c_1}{c_1 + c_2} - 1 \right) \end{bmatrix}$$

The characteristic equation  $\lambda^2 - Tr(J^*)\lambda + Det(J^*) = 0$ , where

$$Tr(J^*) = 2 \left( 1 - (v_1 + v_2) \frac{c_1 c_2}{c_1 + c_2} \right) \quad \text{and} \quad Det(J^*) = 1 + v_1 v_2 c_1 c_2 - 2(v_1 + v_2) \frac{c_1 c_2}{c_1 + c_2}$$

has complex conjugate roots if

$$(c_2 v_2 - c_1 v_1)(c_1 v_2 - c_2 v_1) < 0. \quad (103)$$

This condition can be easily visualized in the space  $\mathcal{V} = \{v_1, v_2 \mid v_1 \geq 0, v_2 \geq 0\}$  of the speeds of adjustment shown in fig. 108, where (103) is satisfied in the region, which we call region  $\mathcal{F}$ , between the two lines of equation

$$v_2 = \frac{c_1}{c_2} v_1 \quad \text{and} \quad v_2 = \frac{c_2}{c_1} v_1. \quad (104)$$

The Nash equilibrium  $E^*$  is locally asymptotically stable if the usual stability conditions hold

$$\begin{cases} 1 - Tr(J^*) + Det(J^*) = v_1 v_2 c_1 c_2 > 0 \\ 1 + Tr(J^*) + Det(J^*) = c_1 c_2 v_1 v_2 - 4 \frac{c_1 c_2}{c_1 + c_2} (v_1 + v_2) + 4 > 0 \\ Det(J^*) - 1 = c_1 c_2 v_1 v_2 - 2 \frac{c_1 c_2}{c_1 + c_2} (v_1 + v_2) < 0 \end{cases} \quad (105)$$

The first of (105) is always satisfied (which means that loss of stability through the critical value  $\lambda = 1$  cannot occur (in fact a unique equilibrium always exists, and no fold, nor transcritical nor pitchfork bifurcation can be obtained with a unique equilibrium)). The other two conditions define a bounded region of stability in the parameters' space, that can be represented in the plane  $\mathcal{V}$  of the speeds of adjustment by the region  $\mathcal{S} = OB_1 A_1 A_2 B_2$ , shaded in fig. 108. This region, which is symmetric with respect to the diagonal  $v_1 = v_2$ , is bounded by the positive branches of two equilateral hyperbolae whose equations are obtained from the second and the third of (105) taken as equalities. From these equations the coordinates of the points  $A_i$  and  $B_i$ ,  $i = 1, 2$ , can be easily obtained

$$A_1 = \left( \frac{2}{c_1}, \frac{2}{c_2} \right) \quad A_2 = \left( \frac{2}{c_2}, \frac{2}{c_1} \right) \quad B_1 = \left( \frac{c_1 + c_2}{c_1 c_2}, 0 \right) \quad B_2 = \left( 0, \frac{c_1 + c_2}{c_1 c_2} \right). \quad (106)$$

If the marginal costs  $c_1$  and  $c_2$  are fixed the shape of the stability region  $\mathcal{S}$  remains the same, and by increasing  $v_1$  and/or  $v_2$  the point  $P = (v_1, v_2)$  can move out of it. If  $P$  crosses the boundary of  $\mathcal{S}$  along the arc  $A_1 A_2$  (belonging to the hyperbola of equation  $Det(J^*) = 1$ ) then the fixed point  $E^*$  changes from a stable focus to an unstable focus via a Neimark-Sacker bifurcation. If  $P$  exits the region  $\mathcal{S}$  by crossing one of the arcs  $B_1 A_1$  or  $B_2 A_2$  (both belonging to the other hyperbola, of equation  $1 + Tr(J^*) + Det(J^*) = 0$ ) the fixed point  $E^*$  is changed from an attracting node to a saddle point through a period doubling (or flip) bifurcation.

Similar arguments apply if the marginal costs  $(c_1, c_2)$  are varied. For example, if  $c_1$  and  $c_2$  are increased the stability region  $\mathcal{S}$  becomes smaller, as can be easily deduced from (106), and this can cause the exit of  $P$  from  $\mathcal{S}$  even if the speeds of adjustment  $v_1$  and  $v_2$  are held constant. Also in this case the loss of stability can occur via a Neimark-Sacker or a flip bifurcation depending on the boundary arc which is crossed by the point  $P$ .

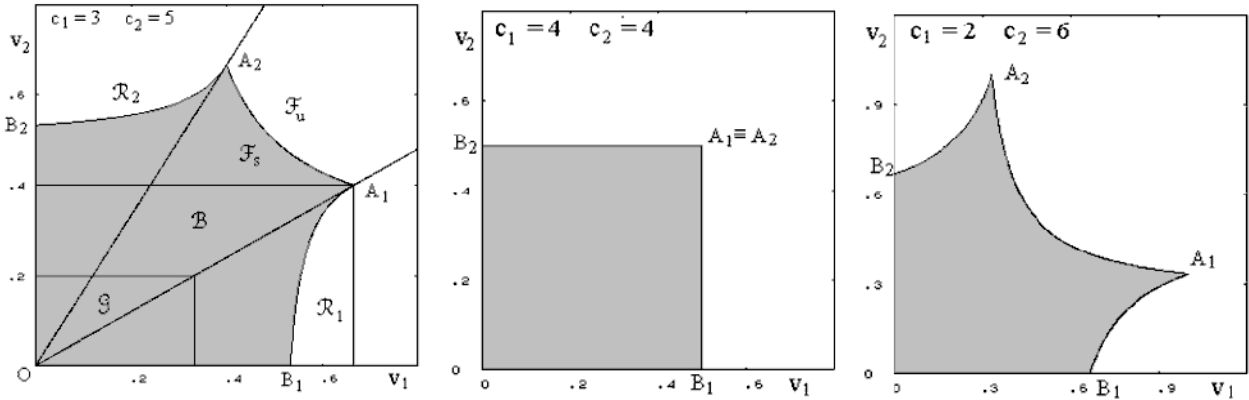


Figure 108: Stability region for the model (100) in the plane of speeds of reaction  $v_1$  and  $v_2$ .

We observe that if  $c_1 > c_2$  the positions of the vertices  $A_1$  and  $A_2$  are swapped, and if  $c_1 = c_2$  these vertices merge, and the region  $\mathcal{S}$  becomes a square, like in the central panel of fig. 108, bounded by the branches of a degenerate hyperbola. In this particular case the region  $\mathcal{F}$  disappears, and the possibility of Neimark-Sacker bifurcations is lost. On the contrary, if the difference between the marginal costs of the two firms is increased, the region  $\mathcal{F}$  enlarges and the arc  $A_1A_2$ , representing the curve where Neimark-Sacker bifurcations occur, becomes larger (see right panel of fig. 108).

The fact that an increase of the speeds of adjustment has a destabilizing role in a oligopoly dynamic model is a typical result, well known in the literature. However our stability analysis reveals a new phenomenon: starting from a set of parameters for which the Nash equilibrium  $E^*$  is unstable, stability of  $E^*$  can be obtained by increasing one (or both)  $v_i$ . This happens when the point  $P = (v_1, v_2)$  belongs to one of the regions denoted by  $\mathcal{R}_1$  or  $\mathcal{R}_2$  in the left panel of fig. 108. Furthermore, if the parameters of the model are varied in such a way that the point  $P$  moves from region  $\mathcal{R}_1$ (or  $\mathcal{R}_2$ ) to the region  $\mathcal{F}_u$  by increasing  $v_1$  (or  $v_2$ ) we obtain two bifurcations, which cause a transition from two instability situations separated by a “window” of stability.

This particular bifurcation sequence is characterized by two different local bifurcations: a period halving (or backward flip) bifurcation followed by a supercritical Neimark-Sacker bifurcation, as shown in fig. 109, where the left panel, obtained with parameters  $v_1 = 0.61$ ,  $v_2 = 0.1$ ,  $c_1 = 3$ ,  $c_2 = 5$ , numerically shows a dynamic scenario where the fixed point  $E^*$  is unstable and the initial conditions in the white region generate trajectories converging to a periodic cycle of period 4, represented by the 4 black dots in the picture, whereas the initial conditions in the grey region generate diverging trajectories. In the central panel, obtained with the same set of parameters except an increased value of  $v_2 = 0.4$ , the fixed point  $E^*$  is stable. In the right panel, obtained with  $v_2 = 0.5$ ,  $E^*$  is unstable again, due to a supercritical Neimark-Sacker bifurcation at which a stable closed invariant curve is created on which quasi-periodic motion takes place.

A rich variety of other dynamic scenarios can be numerically shown, see e.g. the sequences of pictures in the figures 110, 111, 112. In the first sequence a phenomenon of frequency locking is observed for a set of parameters very close to the one used in fig. 109, namely  $v_1 = 0.61$ ,  $v_2 = 0.443$ ,  $c_1 = 3$ ,  $c_2 = 5$ . At this stage the motion along the stable closed invariant curve is locked at the periodic cycle of period 7 whose periodic points are shown in the upper-left panel. Then, starting

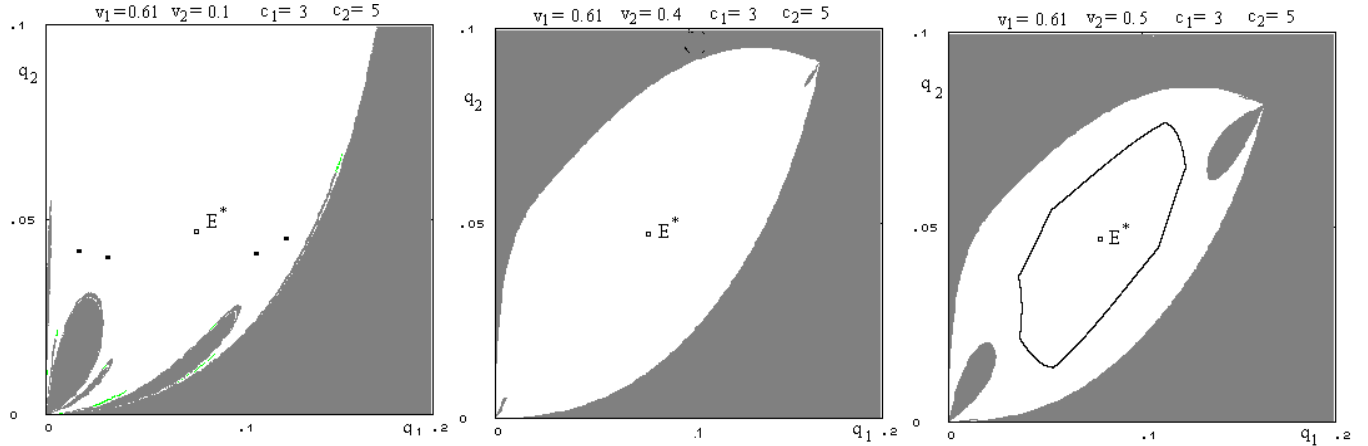


Figure 109: Some dynamic scenarios with attractors and basins for the map (100)

from this situation, the speed of adjustment  $v_1$  is increased and the 7-cycle undergoes a period-doubling bifurcation leading to an attracting 14-cycle, then a 7-pieces (or 7-cyclic) chaotic attractor and finally a unique large annular chaotic attractor.

The next sequence, starting from  $v_1 = 0.501$ ,  $v_2 = 0.501$ ,  $c_1 = 3$ ,  $c_2 = 5$ , shows what happens just after the Neimark-Sacker bifurcation of the fixed point  $E^*$  occurred. An increase of the speeds of adjustment cause an enlargement of the stable closed orbit and then it is transformed into an annular chaotic attractor.

The final sequence is obtained starting from the set of parameters  $v_1 = 0.2$ ,  $v_2 = 0.405$ ,  $c_1 = 3$ ,  $c_2 = 5$ , at which  $E^*$  is stable. An increase of  $v_2$  causes the occurrence of a flip bifurcation at which the equilibrium  $E^*$  becomes a saddle point and a stable cycle of period 2 is created (see the upper-right panel of fig. 112). As  $v_2$  is further increased a period-doubling cascade is observed leading to chaotic motion along a two-pieces chaotic attractor (lower-left panel) and then a unique big attractor.

It is worth to notice that in the sequences of dynamic scenarios shown above, leading to the creation of chaotic attractors starting from sequences of local bifurcations, an attractor is eventually obtained whose points are very close to the boundary of its own basin, see last picture in fig. 112. Indeed, when a chaotic attractor has a contact with its basin's boundary it is destroyed, at a global (or contact) bifurcation denoted as "final bifurcation" or "boundary crisis". After this contact the generic initial condition in the basin of the "died attractor" belong to the basin that was "on the other side" of the basin boundary where the contact occurred. However, the skeleton of the former attractor, formed by the dense set on infinitely many repelling periodic points that where nested inside it, still exists. It is called the "ghost" of the "just died" chaotic attractor, and it implies that many trajectories spend a long number of steps (i.e. a long transients) in the region occupied by the former attractor before converging to the other attractor (that may be an attractor at finite distance or at infinity, i.e. with trajectories that diverge).

## 7.4 Discrete dynamical system represented by noninvertible maps

As we have seen through the examples of nonlinear dynamical systems discussed in the previous sections, an analysis of their global properties is necessary to understand the structure of the attractors

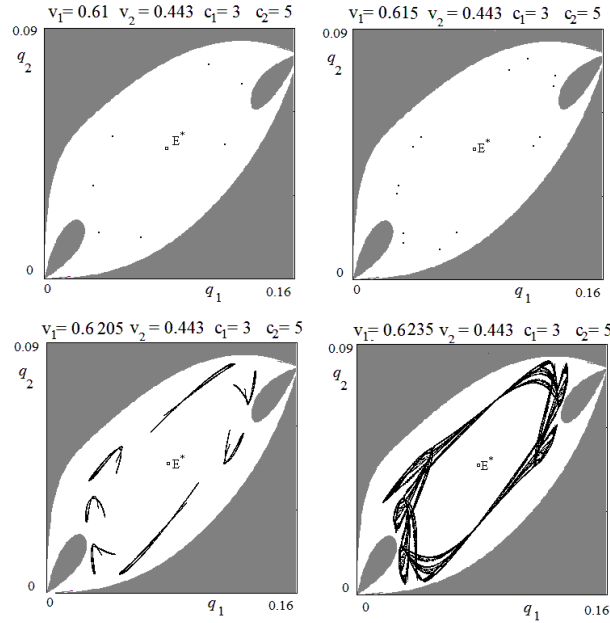


Figure 110: Attractors and basins of attraction.

and their basins of attraction, as well as their qualitative changes. Global properties and bifurcations are such that they cannot be deduced from the linearization procedure, based on the study of eigenvalues and eigenvectors of the Jacobian matrix.

In the case of discrete-time dynamical systems, the two kinds of complexities observed in the previous sections, given by the complex structures of the attracting sets and the complex structures of the basins of attraction, can be often characterized by the global folding properties of maps whose iteration inductively define the trajectories. In particular, as we have already discussed in the sections 6.4 and 6.5, a delimitation of the trapping sets (including chaotic sets) as well as a study of the complex topological structure of basins of attraction (including the case of non-connected basins), can be characterized through the analysis of noninvertible maps and their properties. The definition of critical sets, that are generalizations of local maximum and minimum values of one-dimensional maps to maps defined in higher dimensional spaces, will give us a very useful tool to detect the global (or contact) bifurcations giving rise to qualitative changes of the invariant sets and their basins.

#### 7.4.1 Critical sets. Definitions and simple examples

A map  $T : S \rightarrow S$ ,  $S \subseteq \mathbb{R}^n$ , defined by  $\mathbf{x}' = T(\mathbf{x})$ , transforms a point  $\mathbf{x} \in S$  into a unique point  $\mathbf{x}' \in S$ . The point  $\mathbf{x}'$  is called the *rank-1 image* of  $\mathbf{x}$ , and a point  $\mathbf{x}$  such that  $T(\mathbf{x}) = \mathbf{x}'$  is a *rank-1 preimage* of  $\mathbf{x}'$ .

If  $\mathbf{x} \neq \mathbf{y}$  implies  $T(\mathbf{x}) \neq T(\mathbf{y})$  for each  $\mathbf{x}, \mathbf{y}$  in  $S$ , then  $T$  is an *invertible map* in  $S$ , because the inverse mapping  $\mathbf{x} = T^{-1}(\mathbf{x}')$  is uniquely defined; otherwise  $T$  is said to be a *noninvertible map*, because points  $\mathbf{x}$  exist that have several rank-1 preimages, i.e. the inverse relation  $\mathbf{x} = T^{-1}(\mathbf{x}')$  is multivalued. So, noninvertible means “many-to-one”, that is, distinct points  $\mathbf{x} \neq \mathbf{y}$  may have the same image,  $T(\mathbf{x}) = T(\mathbf{y}) = \mathbf{x}'$ .

A one-dimensional example has been given by the logistic map (60) where points symmetric with

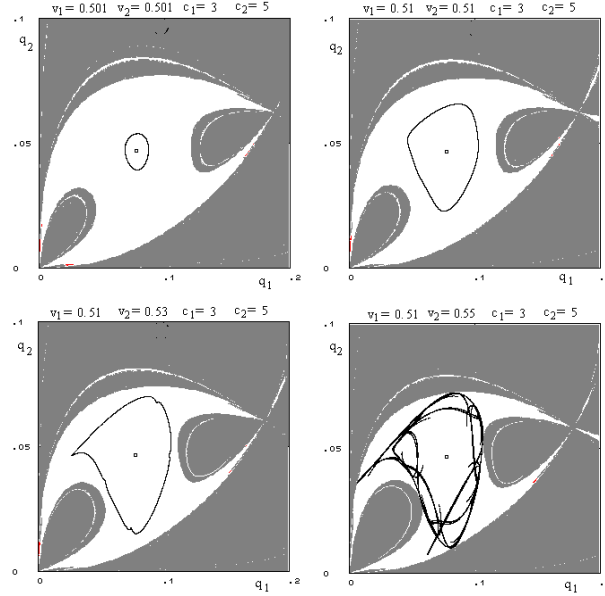


Figure 111: Attractors and basins of attraction.

respect to its symmetry axis  $x = \frac{1}{2}$  have the same image (see fig. 82). The corresponding two inverses have been computed in (64).

To give an example in two dimensions, let us again consider a quadratic map  $T : (x, y) \rightarrow (x', y')$  defined by

$$T : \begin{cases} x' = ax + y \\ y' = x^2 + b \end{cases} \quad (107)$$

It can map distinct points into the same point. For example if we consider the map with parameters  $a = \frac{1}{2}$  and  $b = -2$ , then the two points  $P_1 = (-2, 2)$  and  $P_2 = (2, 0)$  are mapped into the same point  $P = (1, 2)$ . This means that at least two inverses must be defined in  $P$ , one mapping it into the rank- $q$  preimage  $P_1$  and the other one into the other preimage  $P_2$  (see fig. 113). Indeed, like in the case of the logistic map, also for this two-dimensional map we can explicitly compute the two inverses: given  $x'$  and  $y'$ , if we solve the algebraic system (107) with respect to the unknowns  $x$  and  $y$  we get two solutions, given by

$$T_1^{-1} : \begin{cases} x = -\sqrt{y' - b} \\ y = x' + a\sqrt{y' - b} \end{cases} ; \quad T_2^{-1} : \begin{cases} x = \sqrt{y' - b} \\ y = x' - a\sqrt{y' - b} \end{cases} \quad (108)$$

Geometrically, the action of a noninvertible map can be expressed by saying that it “folds and pleats” the space  $S$ , so that distinct points are mapped into the same point. This is equivalently stated by saying that several inverses are defined in some points of  $S$ , and these inverses “unfold”  $S$ .

For a noninvertible map,  $S$  can be subdivided into regions  $Z_k$ ,  $k \geq 0$ , whose points have  $k$  distinct rank-1 preimages. Generally, for a continuous map, as the point  $\mathbf{x}'$  varies in  $\mathbb{R}^n$ , pairs of preimages appear or disappear as it crosses the boundaries separating different regions. Hence, such boundaries are characterized by the presence of at least two coincident (merging) preimages. This leads us to the definition of the *critical sets*, one of the distinguishing features of noninvertible maps



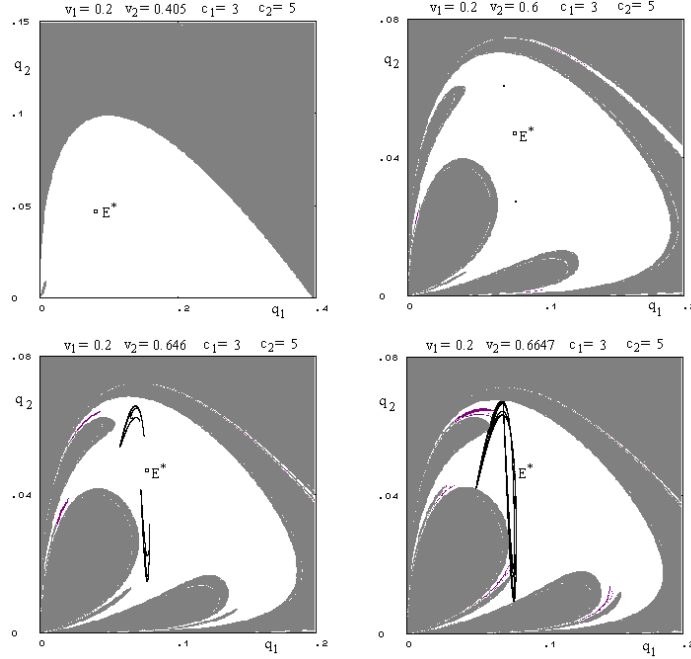


Figure 112: Attractors and basins of attraction.

**Definition (Gumowski and Mira, 1980).** The *critical set*  $CS$  of a continuous map  $T$  is defined as the locus of points having at least two coincident *rank*  $- 1$  preimages, located on a set  $CS_{-1}$ , called *set of merging preimages*.

The critical set  $CS$  is generally formed by  $(n - 1)$ -dimensional hypersurfaces of  $\mathbb{R}^n$ , and portions of  $CS$  separate regions  $Z_k$  of the phase space characterized by a different number of *rank*  $- 1$  preimages, for example  $Z_k$  and  $Z_{k+2}$  (this is the standard occurrence for continuous maps). The critical set  $CS$  is the  $n$ -dimensional generalization of the notion of local minimum or local maximum value of a one-dimensional map, and of the notion of *critical curve*  $LC$  of a noninvertible two-dimensional map<sup>19</sup>. The set  $CS_{-1}$  is the generalization of local extremum point of a one-dimensional map, and of the *fold curve*  $LC_{-1}$  of a two-dimensional noninvertible map. In a differentiable one-dimensional map the critical points  $c_{-1}$  can be searched among the points where the derivative vanishes, as we have seen for the logistic map (see also fig. 114).

However, we remark that in general the condition of vanishing derivative is not sufficient to define the critical points of rank-0 since such condition may be also satisfied by points which are not local extrema (e.g. the inflection points with horizontal tangent). Moreover, for continuous and piecewise differentiable maps, as well as for discontinuous maps, the condition of vanishing derivative is not necessary as well, because such maps may have the property that the images of points where the map is not differentiable are critical points, according to the definition given above. This occurs whenever such points are local maxima or minima, like in the cases shown in fig.115.

In the case of piecewise continuous maps, a point of discontinuity may behave as a critical point

<sup>19</sup>The terminology and notation originate from the notion of critical point as it is used in the classical works of Julia and Fatou.

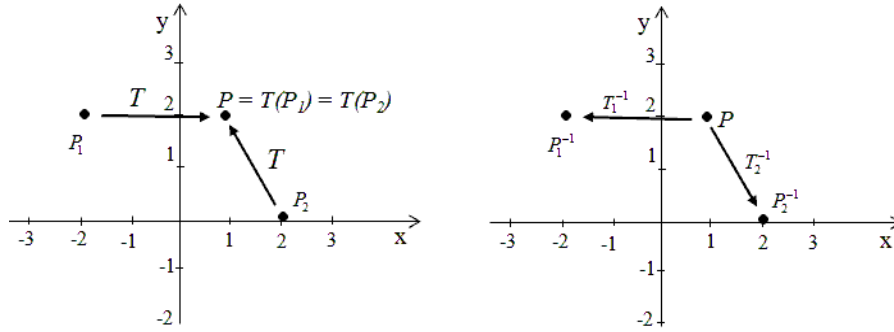


Figure 113:

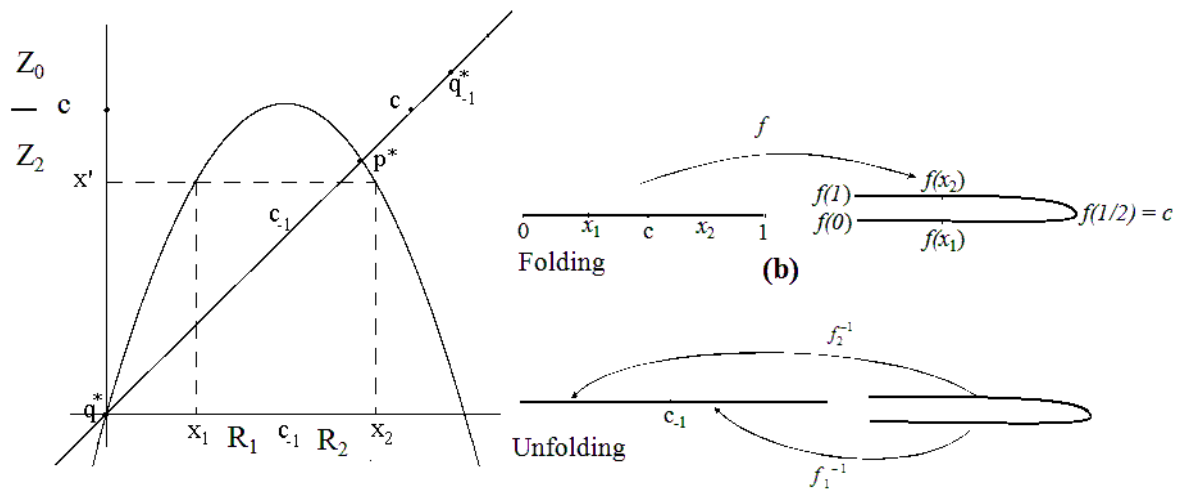


Figure 114: Folding and unfolding action of the logistic map

of  $T$ , even if the definition in terms of merging preimages cannot be applied. This happens when the ranges of the map on the two sides of the discontinuity have an overlapping zone, so that at least one of the two limiting values of the function at the discontinuity separates regions having a different number of rank-1 preimages (see e.g. the right panel of fig. 115). The difference with respect to the case of a continuous map is that now the number of distinct rank-1 preimages through a critical point differs generally by one (instead of two), that is, a critical value  $c$  (in general the critical set  $CS$ ) separates regions  $Z_k$  and  $Z_{k+1}$ .

In order to explain the geometric action of a critical point in a continuous map, let us consider, again, the logistic map in fig. 114, and as already stressed in section 6.4 let us notice that as  $x$  moves from 0 to 1 the corresponding image  $f(x)$  spans the interval  $[0, c]$  twice, the critical point  $c$  being the turning point. In other words, if we consider how the segment  $\gamma = [0, 1]$  is transformed by the map  $f$ , we can say that it is *folded and pleated* to obtain the image  $\gamma' = [0, c]$ . Such folding gives a geometric reason why two distinct points of  $\gamma$ , say  $x_1$  and  $x_2$ , located symmetrically with respect to the point  $c_{-1} = 1/2$ , are mapped into the same point  $x' \in \gamma'$  due to the folding action of  $f$  (see fig.114b). The same arguments can be explained by looking at the two inverse mappings  $f_1^{-1}$  and  $f_2^{-1}$  defined in

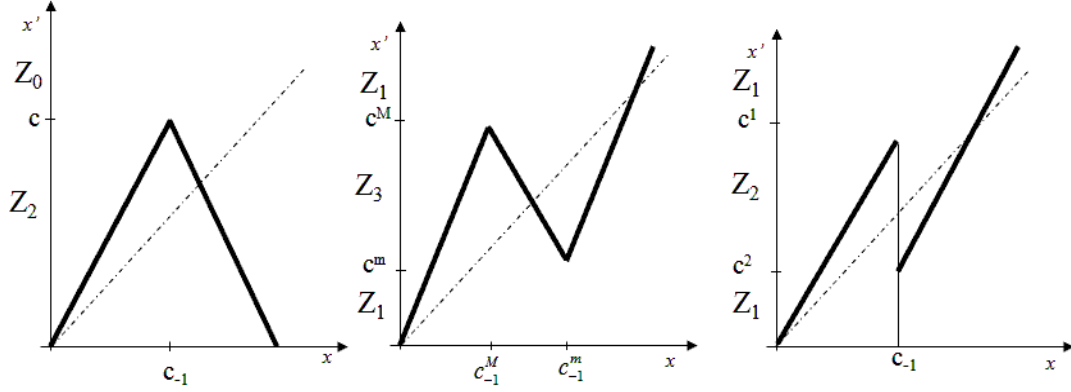


Figure 115: Folding of piecewise differentiable and piecewise continuous maps.

$(-\infty, \mu/4]$  according to (64). We can consider the range of the map  $f$  formed by the superposition of two half-lines  $(-\infty, \mu/4]$ , joined at the critical point  $c = \mu/4$ , and on each of these half-lines a different inverse is defined. In other words, instead of saying that two distinct maps are defined on the same half-line we say that the range is formed by two distinct half lines on each of which a unique inverse map is defined. This point of view gives a geometric visualization of the critical point  $c$  as the point in which two distinct inverses merge. The action of the inverses, say  $f^{-1} = f_1^{-1} \cup f_2^{-1}$ , causes an unfolding of the range by mapping  $c$  into  $c_{-1}$  and by opening the two half-lines one on the right and one on the left of  $c_{-1}$ , so that the whole real line  $\mathbb{R}$  is covered. So, the map  $f$  folds the real line, the two inverses unfold it.

Another interpretation of the folding action of a critical point is the following. Since  $f(x)$  is increasing for  $x \in [0, 1/2)$  and decreasing for  $x \in (1/2, 1]$ , its application to a segment  $\gamma_1 \subset [0, 1/2)$  is orientation preserving, whereas its application to a segment  $\gamma_2 \subset (1/2, 1]$  is orientation reversing. This suggests that an application of  $f$  to a segment  $\gamma_3 = [a, b]$  including the point  $c_{-1} = 1/2$  preserves the orientation of the portion  $[a, c_{-1}]$ , i.e.  $f([a, c_{-1}]) = [f(a), c]$ , whereas it reverses the portion  $[c_{-1}, b]$ , i.e.  $f([c_{-1}, b]) = [f(b), c]$ , so that  $\gamma'_3 = f(\gamma_3)$  is folded, the folding point being the critical point  $c$ .

Let us now consider the case of a continuous two-dimensional map  $T : S \rightarrow S$ ,  $S \subseteq \mathbb{R}^2$ , defined by

$$T : \begin{cases} x'_1 = T_1(x_1, x_2) \\ x'_2 = T_2(x_1, x_2) \end{cases}, \quad (109)$$

If we solve the system of the two equations (109) with respect to the unknowns  $x_1$  and  $x_2$ , then, for a given  $(x'_1, x'_2)$ , we may have several solutions, representing rank-1 preimages (or backward iterates) of  $(x'_1, x'_2)$ , say  $(x_1, x_2) = T^{-1}(x'_1, x'_2)$ , where  $T^{-1}$  is in general a multivalued relation. In this case we say that  $T$  is noninvertible, and the critical set (formed by critical curves, denoted by  $LC$  from the French “Ligne Critique”) constitutes the set of boundaries that separate regions of the plane characterized by a different number of rank-1 preimages. According to the definition, along  $LC$  at least two inverses give merging preimages, located on  $LC_{-1}$ .

For a continuous and (at least piecewise) differentiable noninvertible map of the plane, the set  $LC_{-1}$  is included in the set where  $\det \mathbf{J}(x_1, x_2)$  changes sign, since  $T$  is locally an orientation preserving map near points  $(x_1, x_2)$  such that  $\det \mathbf{J}(x_1, x_2) > 0$  and orientation reversing if  $\det \mathbf{J}(x_1, x_2) < 0$ . In order to explain this point, let us recall that when an affine transformation  $\mathbf{x}' = \mathbf{A}\mathbf{x} + \mathbf{b}$ , where

$A = \{a_{ij}\}$  is a  $2 \times 2$  matrix and  $\mathbf{b} \in \mathbb{R}^2$ , is applied to a plane figure, then the area of the transformed figure grows, or shrinks, by a factor  $\rho = |\det A|$ , and if  $\det A > 0$  then the orientation of the figure is preserved, whereas if  $\det A < 0$  then the orientation is reversed. This property also holds for the linear approximation of (109) in a neighborhood of a point  $\mathbf{p} = (x_1, x_2)$ , given by an affine map with  $A = \mathbf{J}$ ,  $\mathbf{J}$  being the Jacobian matrix evaluated at the point  $\mathbf{p}$

$$\mathbf{J}(\mathbf{p}) = \begin{bmatrix} \partial T_1/\partial x_1 & \partial T_1/\partial x_2 \\ \partial T_2/\partial x_1 & \partial T_2/\partial x_2 \end{bmatrix} \quad (110)$$

A qualitative visualization is given in fig. 116. Of course, if the map is continuously differentiable then the change of the sign of  $\mathbf{J}$  occurs along points where  $\mathbf{J}$  vanishes, thus giving the characterization of the fold line  $LC_{-1}$  as the locus where the jacobian vanishes.

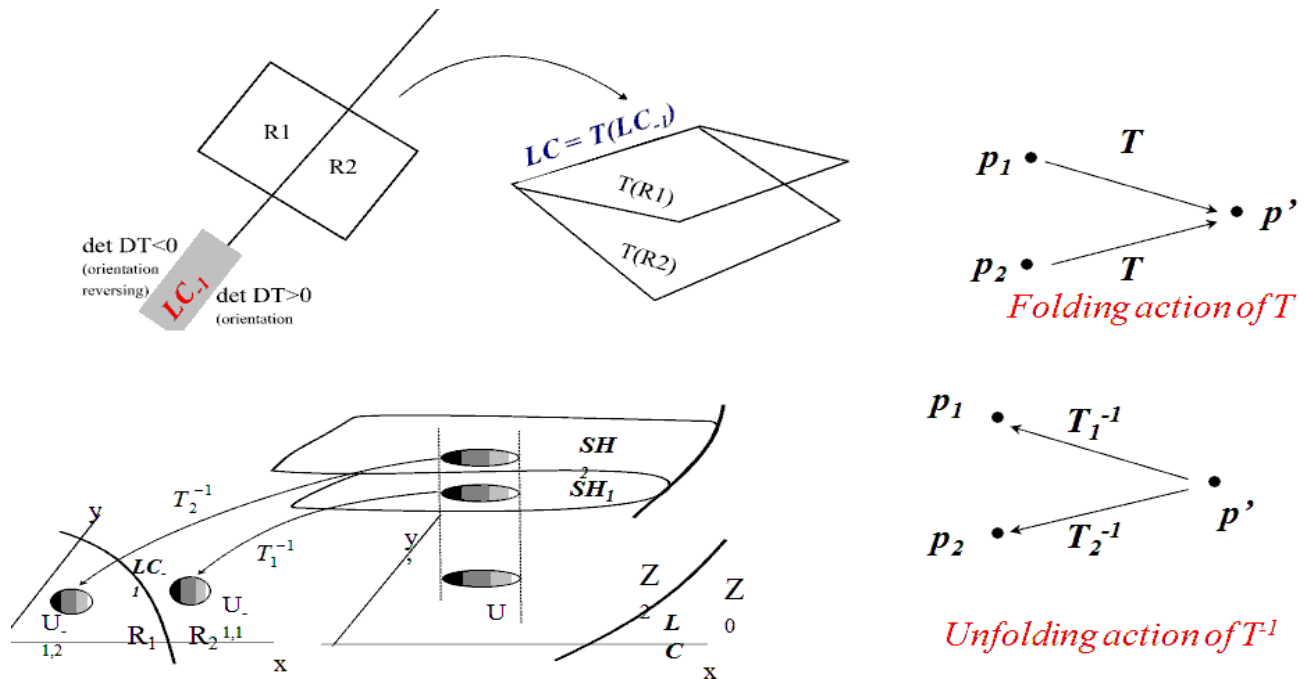


Figure 116: Folding and unfolding for a two-dimensional map.

In order to give a geometrical interpretation of the action of a multi-valued inverse relation  $T^{-1}$ , it is useful to consider a region  $Z_k$  as the superposition of  $k$  sheets, each associated with a different inverse. Such a representation is known as *Riemann foliation* of the plane. Different sheets are connected by folds joining two sheets, and the projections of such folds on the phase plane are arcs of  $LC$ . This is shown in the qualitative sketch of fig.116, where the case of a  $Z_0 - Z_2$  noninvertible map is considered. This graphical representation of the unfolding action of the inverses also gives an intuitive idea of the mechanism which causes the creation of non-connected basins for noninvertible maps of the plane.

Let us consider again the map (107) as a canonical example of a two-dimensional noninvertible map. Given a point  $(x', y')$ , according to (108) it has two rank-one preimages if  $y' \geq b$ , and no preimages if  $y' < b$ . So, (107) is a  $Z_0 - Z_2$  noninvertible map, where  $Z_0$  (region whose points have no preimages) is the half plane  $Z_0 = \{(x, y) | y < b\}$  and  $Z_2$  (region whose points have two distinct rank-1 preimages) is the half plane  $Z_2 = \{(x, y) | y > b\}$ . The line  $y = b$ , which separates these two

regions, is  $LC$ , i.e. the locus of points having two merging rank-1 preimages, located on the line  $x = 0$ , that represents  $LC_{-1}$ . Being (107) a continuously differentiable map, the points of  $LC_{-1}$  necessarily belong to the set of points at which the Jacobian determinant vanishes, i.e.  $LC_{-1} \subseteq J_0$ , where  $J_0 = \{(x, y) \mid \det J(x, y) = -2x = 0\}$ . In this case  $LC_{-1}$  coincides with  $J_0$  (the vertical axis  $x = 0$ ) and the critical curve  $LC$  is the image by  $T$  of  $LC_{-1}$ , i.e.  $LC = T(LC_{-1}) = T(\{x = 0\}) = \{(x, y) \mid y = b\}$ .

In order to show the folding action related to the presence of the critical lines fact, we consider a planar shape  $U$  separated by  $LC_{-1}$  into two portions, say  $U_1 \in R_1$  and  $U_2 \in R_2$  and we apply the map (107) to the points of  $U$  (fig.117, left panel). The image  $T(U_1) \cap T(U_2)$  is a nonempty set included in the region  $Z_{k+2}$ , which is the region whose points  $p'$  have rank-1 preimages  $p_1 = T_1^{-1}(p') \in U_1$  and  $p_2 = T_2^{-1}(p') \in U_2$ . This means that two points  $p_1 \in U_1$  and  $p_2 \in U_2$ , located at opposite sides with respect to  $LC_{-1}$ , are mapped in the same side with respect to  $LC$ , in the region  $Z_{k+2}$ . This is also expressed by saying that the ball  $U$  is “folded” by  $T$  along  $LC$  on the side with more preimages (see fig.117, left panel). The same concept can be equivalently expressed by stressing the “unfolding” action of  $T^{-1}$ , obtained by the application of the two distinct inverses in  $Z_{k+2}$  which merge along  $LC$ . Indeed, if we consider a ball  $V \subset Z_{k+2}$ , then the set of its *rank* - 1 preimages  $T_1^{-1}(V)$  and  $T_2^{-1}(V)$  is made up of two balls  $T_1^{-1}(V) \in R_1$  and  $T_2^{-1}(V) \in R_2$ . These balls are disjoint if  $V \cap LC = \emptyset$  (fig. 117, right panel)

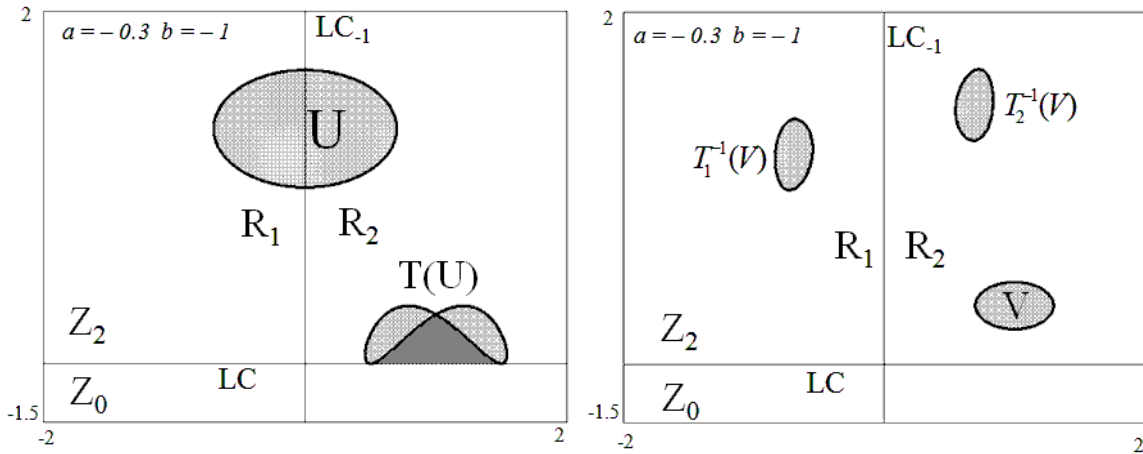


Figure 117: Folding (left) and unfolding (right).

Many of the considerations made above, for 1-dimensional and 2-dimensional noninvertible maps, can be generalized to  $n$ -dimensional ones, even if their visualization becomes more difficult. First of all, from the definition of critical set it is clear that the relation  $CS = T(CS_{-1})$  holds in any case. Moreover, the points of  $CS_{-1}$  where the map is continuously differentiable are necessarily points where the Jacobian determinant vanishes:

$$CS_{-1} \subseteq J_0 = \{p \in \mathbb{R}^n \mid \det \mathbf{J}(p) = 0\} \quad (111)$$

In fact, in any neighborhood of a point of  $CS_{-1}$  there are at least two distinct points which are mapped by  $T$  in the same point. Accordingly, the map is not locally invertible in points of  $CS_{-1}$ , and (111) follows from the implicit function theorem. This property provides an easy method to compute the critical set for continuously differentiable maps: from the expression of the jacobian determinant one

computes the locus of points at which it vanishes, then the set obtained after an application of the map to these points is the critical set  $CS$ .

### 7.4.2 Trajectories, attractors and basins

A *discrete-time dynamical system*, defined by the difference equation

$$\mathbf{x}(t+1) = T(\mathbf{x}(t)) \quad (112)$$

can be seen as the result of the repeated application (or *iteration*) of a map  $T$ . Indeed, the point  $\mathbf{x}$  represents the state of a system, and  $T$  represents the “unit time advancement operator”  $T : \mathbf{x}(t) \rightarrow \mathbf{x}(t+1)$ . Starting from an *initial condition*  $\mathbf{x}_0 \in S$ , the iteration of  $T$  inductively defines a unique *trajectory*

$$\tau(\mathbf{x}_0) = \{\mathbf{x}(t) = T^t(\mathbf{x}_0), t = 0, 1, 2, \dots\},$$

where  $T^0$  is the identity map and  $T^t = T(T^{t-1})$ . As  $t \rightarrow +\infty$ , a trajectory may diverge, or it may converge to a fixed point of the map  $T$ , i.e. a point  $\bar{\mathbf{x}}$  such that  $T(\bar{\mathbf{x}}) = \bar{\mathbf{x}}$ , or it may asymptotically approach another kind of invariant set, such as a periodic cycle, or a closed invariant curve or a more complex attractor, for example a so called chaotic attractor. We recall that a set  $A \subset \mathbb{R}^n$  is *invariant* for the map  $T$  if it is mapped onto itself,  $T(A) = A$ . This means that if  $x \in A$  then  $T(x) \in A$ , i.e.  $A$  is *trapping*, and every point of  $A$  is image of some point of  $A$ . A closed invariant set  $A$  is an *attractor* if (i) it is *Lyapunov stable*, i.e. for every neighborhood  $W$  of  $A$  there exists a neighborhood  $V$  of  $A$  such that  $T^t(V) \subset W \forall t \geq 0$ ; (ii) a neighborhood  $U$  of  $A$  exists such that  $T^t(\mathbf{x}) \rightarrow A$  as  $t \rightarrow +\infty$  for each  $\mathbf{x} \in U$ . The *basin* of an attractor  $A$  is the set of all points that generate trajectories converging to  $A$

$$\mathcal{B}(A) = \{\mathbf{x} | T^t(\mathbf{x}) \rightarrow A \text{ as } t \rightarrow +\infty\}$$

Let  $U(A)$  be a neighborhood of an attractor  $A$  whose points converge to  $A$ . Of course  $U(A) \subseteq \mathcal{B}(A)$ , and also the points that are mapped into  $U$  after a finite number of iterations belong to  $\mathcal{B}(A)$ . Hence, the basin of  $A$  is given by

$$\mathcal{B}(A) = \bigcup_{n=0}^{\infty} T^{-n}(U(A)) \quad (113)$$

where  $T^{-1}(\mathbf{x})$  represents the set of the rank-1 preimages of  $\mathbf{x}$  (i.e. the points mapped into  $x$  by  $T$ ), and  $T^{-n}(x)$  represents the set of the rank- $n$  preimages of  $x$  (i.e. the points mapped into  $x$  after  $n$  applications of  $T$ ).

Let  $\mathcal{B}$  be a basin of attraction and  $\partial\mathcal{B}$  its boundary. From the definition it follows that  $\mathcal{B}$  is trapping with respect to the forward iteration of the map  $T$  and invariant with respect to the backward iteration of all the inverses  $T^{-1}$ . Points belonging to  $\partial\mathcal{B}$  are mapped into  $\partial\mathcal{B}$  both under forward and backward iteration of  $T$ . This implies that if an unstable fixed point or cycle belongs to  $\partial\mathcal{B}$  then  $\partial\mathcal{B}$  must also contain all of its preimages of any rank. Moreover, if a saddle-point, or a saddle-cycle, belongs to  $\partial\mathcal{B}$ , then  $\partial\mathcal{B}$  must also contain the whole stable set.

A problem that often arises in the study of nonlinear dynamical systems concerns the existence of several attracting sets, each with its own basin of attraction. In this case the dynamic process becomes path-dependent, i.e. which kind of long run dynamics characterizes the system depends on the starting condition. Another important problems in the study of applied dynamical systems is the delimitation of a bounded region of the state space where the system dynamics are ultimately trapped, despite of the complexity of the long-run time patterns. This is an useful information, even more useful than a detailed description of step by step time evolution.

Both these questions require an analysis of the global dynamical properties of the dynamical system, that is, an analysis which is not based on the linear approximation of the map. When the map  $T$  is noninvertible, its global dynamical properties can be usefully characterized by using the formalism of critical sets, by which the folding action associated with the application of the map, as well as the “unfolding” associated with the action of the inverses, can be described. Loosely speaking, the repeated application of a noninvertible map repeatedly folds the state space along the critical sets and their images, and often this allows one to define a bounded region where asymptotic dynamics are trapped. As some parameter is varied, global bifurcations that cause sudden qualitative changes in the properties of the attracting sets can be detected by observing contacts of critical curves with invariant sets. Instead, the repeated application of the inverses “repeatedly unfold” the state space, so that a neighborhood of an attractor may have preimages far from it, thus giving rise to complicated topological structures of the basins, that may be formed by the union of several (even infinitely many) non connected portions. In fact, from (113) it follows that in order to study the extension of a basin and the structure of its boundaries one has to consider the properties of the inverse relation  $T^{-1}$ . The route to more and more complex basin boundaries, as some parameter is varied, is characterized by global bifurcations, also called contact bifurcations, due to contacts between the critical set and the invariant sets that form the basins’ boundaries.

### 7.4.3 Critical sets and the delimitation of trapping regions.

Portions of the critical set  $CS$  and its images  $CS_k = T^k(CS)$  can be used to obtain the boundaries of trapping regions where the asymptotic dynamics of the iterated points of a noninvertible map are confined. This has already been explained for the logistic map in section 6.4, where we have shown that, for  $3 < \mu < 4$ , starting from an initial condition inside the interval  $[c_1, c]$ , with  $c_1 = f(c)$ , no images can be obtained out of this interval, i.e. the interval formed by the critical point  $c$  and its rank-1 image  $c_1$  is trapping. Moreover, any trajectory generated from an initial condition in  $(0, 1)$ , enters  $[c_1, c]$  after a finite number of iterations. This is expressed by saying that the interval  $[c_1, c]$  is *absorbing*. Examples have been shown in figures 75 and 77.

In general, for an  $n$ -dimensional map, an *absorbing region*  $\mathcal{A}$  (intervals in  $R$ , areas in  $R^2$ , volumes in  $R^3, \dots$ ) is defined as a bounded set whose boundary is given by portions of the critical set  $CS$  and its images of increasing order  $CS_k = T^k(CS)$ , such that a neighborhood  $U \supset \mathcal{A}$  exists whose point enter  $\mathcal{A}$  after a finite number of iterations and then never escape it, since  $T(\mathcal{A}) \subseteq \mathcal{A}$ , i.e.  $\mathcal{A}$  is trapping. Loosely speaking, we can say that the iterated application of a noninvertible map, folding and folding again the space, defines trapping regions bounded by critical sets of increasing order.

Sometimes, smaller absorbing regions are nested inside a bigger one, as it was illustrated for the logistic map (138), as shown in fig. 77, where inside the absorbing interval  $[c_1, c]$  a trapping subset is obtained by higher rank images of the critical point, given by  $\mathcal{A} = [c_1, c_3] \cup [c_2, c]$ .

Inside an absorbing region one or more attractors may exist. However, if a chaotic attractor exists which fills up a whole absorbing region then the boundary of the chaotic attractor is formed by portions of critical sets. To better illustrate this point, we also give a two-dimensional example, obtained by using the map (107). In Fig. 118a, a chaotic trajectory is shown, and in fig. 118b its outer boundary is obtained by the union of a segment of  $LC$  and three iterates  $LC_i = T^i(LC)$ ,  $i = 1, 2, 3$ .

A practical procedure can be outlined in order to obtain the boundary of an absorbing area (although it is difficult to give a general method). Starting from a portion of  $LC_{-1}$ , approximately taken in the region occupied by the area of interest, its images by  $T$  of increasing rank are computed until a closed region is obtained. When such a region is mapped into itself, then it is an absorbing area

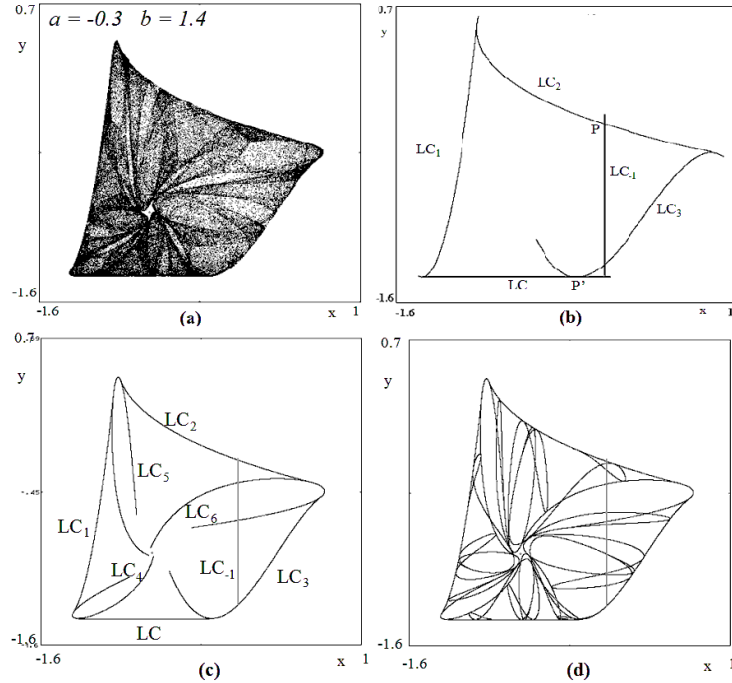


Figure 118: Boundary of chaotic attractor obtained by segments of critical curves.

$\mathcal{A}$ . The length of the initial segment is to be taken, in general, by a trial and error method, although several suggestions are given in the books in the bibliography. Once an absorbing area  $\mathcal{A}$  is found, in order to see if it is invariant or not the same procedure must be repeated by taking only the portion

$$\gamma = \mathcal{A} \cap LC_{-1} \quad (114)$$

as the starting segment. Then one of the following two cases occurs:

(**case I**) the union of  $m$  iterates of  $\gamma$  (for a suitable  $m$ ) covers the whole boundary of  $\mathcal{A}$ ; in which case  $\mathcal{A}$  is an invariant absorbing area, and

$$\partial\mathcal{A} \subset \bigcup_{k=1}^m T^k(\gamma) \quad (115)$$

(**case II**) no natural  $m$  exists such that  $\bigcup_{i=1}^m T^i(\gamma)$  covers the whole boundary of  $\mathcal{A}$ ; in which case  $\mathcal{A}$  is not invariant but strictly mapped into itself. An invariant absorbing area is obtained by  $\bigcap_{n>0} T^n(\mathcal{A})$  (and may be obtained by a finite number of images of  $\mathcal{A}$ ).

The application of this procedure to the problem of the delimitation of the chaotic area of fig. 118a by portions of critical curves suggests us, on the basis of Fig.118b, to take a smaller segment  $\gamma$  and to take an higher number of iterates in order to obtain also the inner boundary. The result is shown in fig.118c, where by four iterates we get the outer boundary. By a few more iterates also the inner boundary of the chaotic area is get, as shown in Fig.118d. As it can be clearly seen, and as clearly expressed by the strict inclusion in (115), the union of the images also include several arcs internal to the invariant area  $\mathcal{A}$ . Indeed, the images of the critical arcs which are mapped inside the area play a



particular role, because these curves represent the "foldings" of the plane under forward iterations of the map, and this is the reason why these inner curves often denote the portions of the region which are more frequently visited by a generic trajectory inside it (compare fig. 118a and fig. 118d). This is due to the fact that points close to a critical arc  $LC_i$ ,  $i \geq 0$ , are more frequently visited, because there are several distinct parts of the invariant area which are mapped in the same region (close to  $LC_i$ ).

#### 7.4.4 Critical sets and the creation of non connected basins

From (113) it is clear that the properties of the inverses are important in order to understand the structure of the basins and the main bifurcations which change their qualitative properties. In the case of noninvertible maps, the multiplicity of preimages may lead to basins with complex structures, such as multiply connected or non connected sets, sometimes formed by infinitely many non connected portions. As already stressed in section 6.5, in the context of noninvertible maps it is useful to define the *immediate basin*  $\mathcal{B}_0(A)$ , of an attracting set  $A$ , as the widest connected component of the basin which contains  $A$ . Then the total basin can be expressed as

$$\mathcal{B}(A) = \bigcup_{n=0}^{\infty} T^{-n}(\mathcal{B}_0(A))$$

where  $T^{-n}(x)$  represents the set of all the rank- $n$  preimages of  $x$ , i.e. the set of points which are mapped in  $x$  after  $n$  iterations of the map  $T$ . The backward iteration of a noninvertible map *repeatedly unfolds* the phase space, and this implies that the basins may be non-connected, i.e. formed by several disjoint portions.

Also in this case, we have already given an example of this property for by using a one-dimensional map, where in fig.88 the graph of a  $Z_1 - Z_3 - Z_1$  noninvertible map is shown,  $Z_3$  being the portion of the codomain bounded by the relative minimum value  $c_{\min}$  and relative maximum value  $c_{\max}$ . In the situation shown in fig. 88 there are three attractors, and after the global bifurcation where  $c_{\min} = q$ , the portion  $(c_{\min}, q)$  enters  $Z_3$ , so new preimages  $f^{-k}(c_{\min}, q)$  appear with  $k \geq 1$ . These preimages constitute an infinite (countable) set of non-connected portions of  $\mathcal{B}(r)$  nested inside  $\mathcal{B}(A)$ , represented by the thick portions of the diagonal in fig. 88, bounded by the infinitely many preimages of any rank, say  $q_{-k}$ ,  $k \in \mathbb{N}$ , of  $q$ , that accumulate in a left neighborhood of the fixed point  $z$ . In fact, as  $z$  is a repelling fixed point for the forward iteration of  $f$ , it is an attracting fixed point for the backward iteration of the same map. So, the contact between the critical point  $c_{\min}$  and the basin boundary  $q$  marks the transition from simple connected to non connected basins. Similar global bifurcations, due to contacts between critical sets and basin boundaries, also occur in higher dimensional maps. In fact, if a parameter variation causes a crossing between a basin boundary and a critical set which separates different regions  $Z_k$  so that a portion of a basin enters a region where an higher number of inverses is defined, then new components of the basin may suddenly appear at the contact. However, for maps of dimension greater than 1, such kinds of bifurcations can be very rarely studied by analytical methods, since the analytical equations of such singularities are not known in general. Hence such studies are mainly performed by geometric and numerical methods.

### 7.5 Some economic examples

In this section we show how the global properties of noninvertible two-dimensional maps can be used in the study of discrete dynamic models in economics. In particular we will see the practical usage of critical curves to detect global bifurcations that change the qualitative structure of the basins of

attraction and how critical curves and their images are employed to bound trapping regions where asymptotic dynamics are confined.

### 7.5.1 Global properties of the Cournot duopoly model with linear demand and gradient dynamics

We re-consider the duopoly model described in section 7.3.2. The map (87) is a noninvertible map of the plane, that is, starting from some nonnegative initial production strategy  $(q_{10}, q_{20})$  the iteration of (87) uniquely defines the trajectory  $(q_1(t), q_2(t)) = T^t(q_{10}, q_{20})$ ,  $t = 1, 2, \dots$ , whereas the backward iteration of (87) is not uniquely defined. In fact a point  $(q'_1, q'_2)$  of the plane may have several preimages, obtained by solving the fourth degree algebraic system (87) with respect to  $q_1$  and  $q_2$ . In order to understand the structure of the critical curves  $LC$  and consequently the subdivision of the phase plane into zones  $Z_k$  with  $k$  preimages, we start from  $LC_{-1}$ , that for a differentiable map like (87), according to (111), is given by the locus of points where the Jacobian determinant vanishes. From the expression of  $J$  given in (90), the condition  $\det J = 0$  becomes

$$q_1^2 + q_2^2 + 4q_1q_2 - \alpha_1q_1 - \alpha_2q_2 + \beta = 0$$

where

$$\alpha_i = \frac{4(1 + v_j(a - c_j)bv_i) + 1 + v_i(a - c_i)bv_j}{4b^2v_1v_2} ; \quad i = 1, 2 ; \quad j \neq i$$

and

$$\beta = \frac{(1 + v_1(a - c_1)bv_1)(1 + v_2(a - c_2)bv_2)}{4b^2v_1v_2} .$$

This is an hyperbola in the plane  $(q_1, q_2)$  with symmetry centre in the point  $(\frac{2\alpha_2 - \alpha_1}{3}, \frac{2\alpha_1 - \alpha_2}{3})$  and asymptotes of angular coefficients  $(-2 \pm \sqrt{3})$ . Thus  $LC_{-1}$  is formed by two branches, denoted by  $LC_{-1}^{(a)}$  and  $LC_{-1}^{(b)}$  in fig. 119. This implies that also  $LC$  is the union of two branches, denoted by  $LC^{(a)} = T(LC_{-1}^{(a)})$  and  $LC^{(b)} = T(LC_{-1}^{(b)})$ . Each branch of the critical curve  $LC$  separates the phase plane of  $T$  into regions whose points possess the same number of distinct rank-1 preimages. In the case of the map (87)  $LC^{(b)}$  separates the region  $Z_0$ , whose points have no preimages, from the region  $Z_2$ , whose points have two distinct rank-1 preimages, and  $LC^{(a)}$  separates the region  $Z_2$  from  $Z_4$ , whose points have four distinct preimages. In fact, it is possible to show (see below) that the point  $(q'_1, q'_2) = (0, 0)$  has four preimages obtained by solving the algebraic system (87) with respect to the unknowns  $(q_1, q_2)$ , hence  $(0, 0) \in Z_4$ . The other zones are classified by remembering that any branch of  $LC$  is characterized by the merging (and disappearance) of two preimages.

In order to study the action of the multivalued inverse relation  $T^{-1}$  it is useful to consider a region  $Z_k$  of the phase plane as the superposition of  $k$  sheets, each associated with a different inverse. Such a representation is known as *foliation* of the plane. Different sheets are connected by folds joining two sheets, and the projections of such folds on the phase plane are arcs of  $LC$ . The foliation associated with the map (87) is qualitatively represented in fig. 119. It can be noticed that the cusp point of  $LC$  is characterized by three merging preimages at the junction of two folds.

An important property of the map (87) is that each coordinate axis  $q_i = 0$ ,  $i = 1, 2$ , is trapping, that is, mapped into itself, since  $q_i = 0$  gives  $q'_i = 0$  in (87). This means that starting from an initial condition on a coordinate axis (*monopoly case*) the dynamics is confined in the same axis for each  $t$ , governed by the restriction of the map  $T$  to that axis. Such a restriction is given by the following one-dimensional map, obtained from (87) with  $q_i = 0$

$$q_j = (1 + v_j(a - c_j))q_j - 2bv_jq_j^2 \quad j \neq i . \quad (116)$$

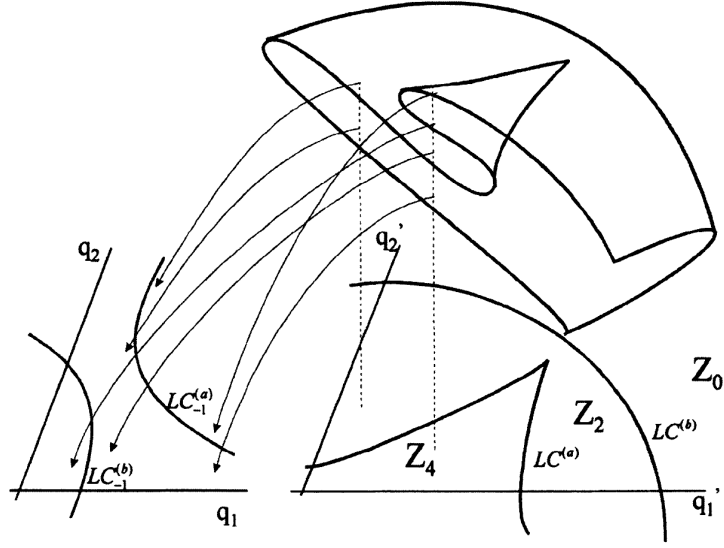


Figure 119: Riemann foliation.

This map is conjugate to the standard logistic map  $x' = \mu x(1 - x)$  through the linear transformation

$$q_j = \frac{1 + v_j(a - c_j)}{2bv_j}x \quad (117)$$

from which we obtain the relation

$$\mu = 1 + v_j(a - c_j) . \quad (118)$$

This means that the dynamics of (116) can be obtained from the well known dynamics of (138).

Another important feature of the map (87) is that it can generate unbounded (i.e. divergent) trajectories (this can be also expressed by saying that (87) has an attracting set at infinite distance). In fact, unbounded (and negative) trajectories are obtained if the initial condition is taken sufficiently far from the origin, i.e. in a suitable neighborhood of infinity, since if  $q_{i0} > \frac{1+a-c_i}{bv_i}$ ,  $i = 1, 2$ , then the first iterate of (87) gives negative values  $q'_i < 0$ ,  $i = 1, 2$ , so that the successive iterates give negative and decreasing values because  $q'_i = q_i + v_i q_i(a - c_i - 2bq_i - bq_j) < q_i$  being  $(a - c_i) > 0$  if (89) hold. This implies that any attractor at finite distance cannot be globally attracting in  $\mathbb{R}_+^2$ , since its basin of attraction cannot extend out of the rectangle  $\left[0, \frac{1+a-c_1}{bv_1}\right] \times \left[0, \frac{1+a-c_2}{bv_2}\right]$ .

In the following we call *attractor at finite distance*, denoted by  $\mathcal{A}$ , a bounded attracting sets (which may be the Nash equilibrium  $E_*$ , a periodic cycle or some more complex attractor around  $E_*$ ) in order to distinguish it from the limit sets at infinite distance, i.e. the unbounded trajectories, which represent exploding (or collapsing) evolutions of the duopoly system. We denote by  $\mathcal{B}(\mathcal{A})$  the basin of attraction of an attractor  $\mathcal{A}$ , defined as the open set of points  $(q_1, q_2)$  of the phase plane whose trajectories  $T^t(q_1, q_2)$  have limit sets belonging to  $\mathcal{A}$  as  $t \rightarrow +\infty$ . We also denote by  $\mathcal{B}(\infty)$  the *basin of infinity*, defined as the set of points which generate unbounded trajectories. Let  $\mathcal{F}$  be the boundary (or frontier) separating  $\mathcal{B}(\mathcal{A})$  from  $\mathcal{B}(\infty)$ . An exact determination of  $\mathcal{F}$  is the main goal of this section. Indeed, this boundary may be rather complex, as evidenced by the numerical results shown in fig.120

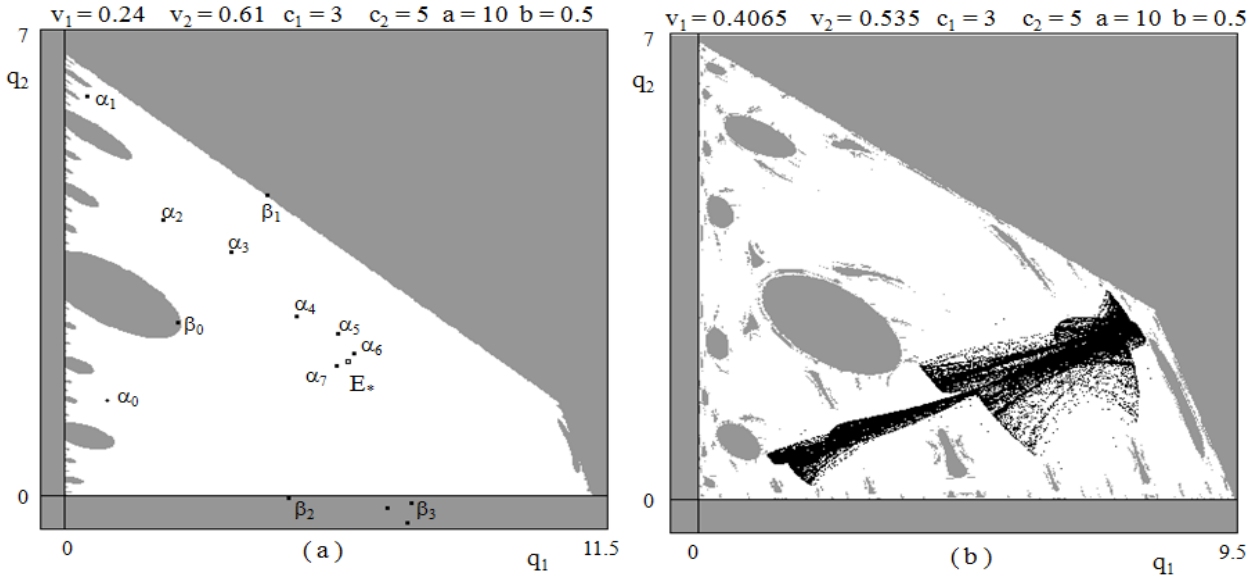


Figure 120: Numerical representation of the basins of attraction for the duopoly map. The two figures are obtained by taking a grid of initial conditions  $(q_{10}, q_{20})$  and generating, for each of them a numerically computed trajectory of the duopoly map. If the trajectory is diverging (i.e. if it reaches large negative values) then a grey dot is painted in the point corresponding to the initial condition, otherwise a white dot is painted. **(a)** the white region represents the basin of attraction of the Nash equilibrium, which is the only attractor at finite distance for that set of parameters; **(b)** the attractor at finite distance is given by a chaotic attractor surrounding the unstable Nash equilibrium.

In fig. 120a the attractor at finite distance is the Nash equilibrium  $E_*$ , and its basin of attraction is represented by the white area, whereas the grey-shaded area represents the basin of infinity. In the situation shown in fig. 120a the boundary separating  $\mathcal{B}(\mathcal{A})$  from  $\mathcal{B}(\infty)$  has a fractal structure, as will be explained below. In fig. 120b the bounded attractor  $\mathcal{A}$  is a chaotic set, with a multiply connected (or connected with holes) basin of attraction. The same property can be expressed by saying that  $\mathcal{B}(\infty)$  is a non connected set, with non connected regions given by the holes inside  $\mathcal{B}(\mathcal{A})$ . In this situation there is a great uncertainty about the long-run behavior of a given adjustment process, since a small change in the initial strategy of the game may cause a crossing of  $\mathcal{F}$ .

The frontier  $\mathcal{F} = \partial \mathcal{B}(\mathcal{A}) = \partial \mathcal{B}(\infty)$  behaves as a repelling line for the points near it, since it acts as a watershed for the trajectories of the map  $T$ . Points belonging to  $\mathcal{F}$  are mapped into  $\mathcal{F}$  both under forward and backward iteration of  $T$ , that is, the frontier is invariant for application of  $T$  and  $T^{-1}$ . More exactly  $T(\mathcal{F}) \subseteq \mathcal{F}, T^{-1}(\mathcal{F}) = \mathcal{F}$ . This implies that if a saddle-point, or a saddle-cycle, belongs to  $\mathcal{F}$ , then  $\mathcal{F}$  must also contain all the preimages of such singularities, and it must also contain the whole stable manifold  $W^s$ . In order to understand how complex basin boundaries, like those shown in fig. 120, are obtained, we start from a situation in which  $\mathcal{F}$  has a simple shape, and then we study the sequence of bifurcations that cause the main qualitative changes in the structure of the basin boundaries as some parameter is varied. Such bifurcations, typical of noninvertible maps, can be characterized by contacts of the basin boundaries with the critical curves.

Indeed, for the parameters' values used to obtain fig. 121, an exact determination of the boundaries

separating the basin of  $E_*$  from that of infinity can be obtained. In fact the saddle fixed points (or the saddle-cycles, if (93) or (94) no longer hold) located on the coordinate axes belong to  $\mathcal{F}$ , and also the invariant coordinate axes  $\omega_1$  and  $\omega_2$ , which form the local stable manifold (or inset) of the saddles, are part of  $\mathcal{F}$ . These axes behave as repelling lines because the unstable manifolds (or outsets) of the saddles are transverse to the axes, each of them having a branch pointing toward  $E_*$  and the opposite branch going to infinity (see fig. 121). The other parts of  $\mathcal{F}$  can be obtained by taking all the preimages of these invariant axes, in order to obtain the whole stable sets of the saddles

$$\mathcal{F} = (\cup_{n=0}^{\infty} T^{-n}(\omega_1)) \cup (\cup_{n=0}^{\infty} T^{-n}(\omega_2)) \quad (119)$$

The map  $T$ , defined in (87), is a noninvertible map. In fact, if we consider a generic point  $P = (0, p)$  of the  $q_2$  axis, its preimages are the real solutions of the algebraic system obtained from (87) with  $(q'_1, q'_2) = (0, p)$ :

$$\begin{cases} q_1 [1 + v_1(a - c_1) - 2bv_1q_1 - bv_1q_2] = 0 \\ (1 + v_2(a - c_2))q_2 - 2bv_2q_2^2 - bv_2q_1q_2 = p \end{cases} \quad (120)$$

From the first of (120) we obtain  $q_1 = 0$  or

$$1 + v_1(a - c_1) - 2bv_1q_1 - bv_1q_2 = 0 \quad (121)$$

which means that if the point  $P$  has preimages, then they must be located either on the same invariant axis or on the line of equation (121). With  $q_1 = 0$  the second equation becomes a second degree algebraic equation which has two distinct, coincident or no real solutions if the discriminant

$$(1 + v_2(a - c_2))^2 - 8bv_2p \quad (122)$$

is positive, zero or negative respectively. A similar conclusion holds if (121) is used to eliminate a state variable in the first equation of (120). From this we can deduce that the generic point  $P$  of the  $q_2$  axis can have no preimages or two preimages on the same axis (which are the same obtained by the restriction (116) of  $T$  to the axis  $q_2$ ) or four preimages, two on the same axis and two on the line of equation (121). This implies that the set of the rank-one preimages of the  $q_2$  axis belongs to the same axis and to the line (121). Following the same arguments we can state that the other invariant axis,  $q_1$ , has preimages on itself and on the line of equation

$$1 + v_2(a - c_2) - bv_2q_1 - 2bv_2q_2 = 0 . \quad (123)$$

It is straightforward to see that the origin  $O = (0, 0)$  has always 4 preimages:  $O_{-1}^{(0)} = (0, 0)$ ,  $O_{-1}^{(1)} = (q_1^{o-1}, 0)$ ,  $O_{-1}^{(2)} = (0, q_2^{o-1})$ , where  $q_j^{o-1}$ ,  $j = 1, 2$ , are given by  $q_j^{o-1} = \frac{1+v_j(a-c_j)}{2bv_j}$  (conjugate to the point  $x = 1$  of the standard logistic) and  $O_{-1}^{(3)} = (q_1^* + \frac{2v_2-v_1}{3bv_1v_2}, q_2^* + \frac{2v_1-v_2}{3bv_1v_2})$ , located at the intersection of the lines (121) and (123) (see fig. 121). In the situation, shown in fig. 121, the lines (121) and (123), labelled by  $\omega_2^{-1}$  and  $\omega_1^{-1}$  respectively, together with the coordinate axes, labelled by  $\omega_2$  and  $\omega_1$ , delimitate a bounded region of the strategy space  $(q_1, q_2)$  which is exactly the basin of attraction of  $E_*$ .

These four sides, given by the segments  $OO_{-1}^{(1)}$  and  $OO_{-1}^{(2)}$  of the coordinate axes and their rank-one preimages, constitute the whole boundary  $\mathcal{F}$  because no preimages of higher rank exist, since  $\omega_{-1}^1$  and  $\omega_{-1}^2$  belong to the region  $Z_0$  of the plane whose points  $(q'_1, q'_2)$  have no preimages, i.e. the fourth degree

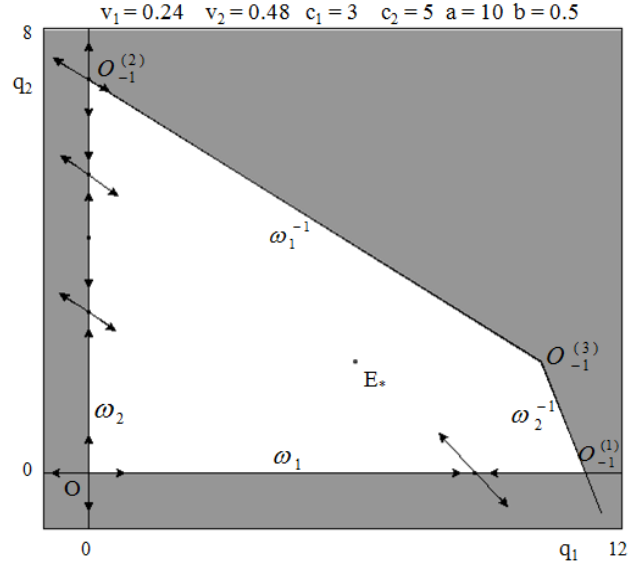


Figure 121: With  $c_1 = 3$   $c_2 = 5$   $a = 10$ ,  $b = 0.5$ ,  $v_1 = 0.24$ ,  $v_2 = 0.48$ , the boundary of the basin of attraction of the Nash equilibrium  $E_*$  is formed by the invariant axes, denoted by  $\omega_1$  and  $\omega_2$ , and their rank-1 preimages  $\omega_1^{-1}$  and  $\omega_2^{-1}$ . For this set of parameters the boundary fixed point  $E_1$  is a saddle point with local stable manifold along the  $q_1$  axis,  $E_2$  is a repelling node with a saddle cycle of period two around it, since  $v_2 > \frac{2}{a-c_2}$

algebraic system has no real solutions. This fact can be characterized through the study of the critical curves of the noninvertible map (87). As we have seen, since the map  $T$  is continuously differentiable, the critical curve  $LC_{-1}$  is the locus of points in which the determinant of  $J(q_1, q_2)$ , given in (90), vanishes, and the critical curve  $LC$ , locus of points having two coincident rank-one preimages, can be obtained as the image, under  $T$ , of  $LC_{-1}$ . For the map (87)  $LC_{-1}$  is formed by the two branches of an hyperbola, denoted by  $LC_{-1}^{(a)}$  and  $LC_{-1}^{(b)}$  in fig.122, thus also  $LC = T(LC_{-1})$  consists of two branches,  $LC^{(a)} = T(LC_{-1}^{(a)})$  and  $LC^{(b)} = T(LC_{-1}^{(b)})$ , represented by the thicker curves of fig.122a. These two branches of  $LC$  separate the phase plane into 3 regions, denoted by  $Z_0$ ,  $Z_2$  and  $Z_4$ , whose points have 0, 2 and 4 distinct rank-1 preimages respectively. It can be noticed that, as already stressed above, the origin always belongs to the region  $Z_4$ . It can also be noticed that the line  $LC_{-1}$  intersects the axis  $q_j$ ,  $j = 1, 2$ , in correspondence of the critical point  $c_{-1}$  of the restriction (116) of  $T$  to that axis.

The simple shape that the frontier  $\mathcal{F}$  assumes for values of the parameters like those used in fig.122a, where the basin of attraction of  $E_*$  is a simply connected set, is due to the fact that the preimages of the invariant axes, denoted in fig.122a by  $\omega_i^{-1}$ ,  $i = 1, 2$ , are entirely included inside the region  $Z_0$ , so that no preimages of higher rank exist. The situation is different when the values of the parameters are such that some portions of these lines belong to the regions  $Z_2$  or  $Z_4$ . In this case preimages of higher order of the invariant coordinate axes are obtained, which form new arcs of the frontier  $\mathcal{F}$ , so that its shape becomes more complex. The switch between these two qualitatively different situations can be obtained by a continuous variation of some parameters of the model, and determines a global (or contact) bifurcation. The occurrence of these global bifurcations can be revealed by the study of critical curves. In order to illustrate this, in the following of this section we fix the marginal costs and

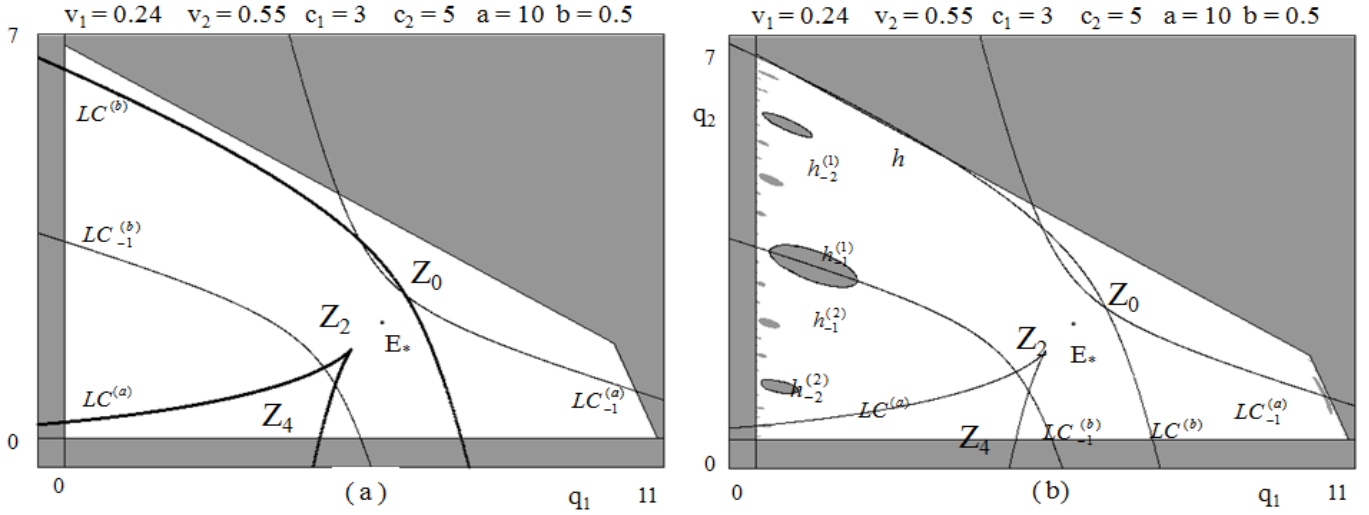


Figure 122: Graphical representation of the basin of attraction of the Nash equilibrium (white region) and the basin  $\mathcal{B}(\infty)$  of unbounded trajectories (grey region) together with the basic critical curve  $LC_{-1}$ , formed by the two branches of an equilateral hyperbola, and of critical curve  $LC$  (represented by heavy lines). The values of parameters  $c_1, c_2, a, b$  are the same as in fig.120, with (a)  $v_1 = 0.24$  and  $v_2 = 0.55$  ; (b)  $v_1 = 0.24$  and  $v_2 = 0.596$  (just after the contact of  $LC$  with  $\omega_1^{-1}$ ).

the parameters of the demand function at the parameters' values  $c_1 = 3$ ,  $c_2 = 5$ ,  $a = 10$ ,  $b = \frac{1}{2}$ , and we vary the values of the speeds of adjustment  $v_1$  and  $v_2$ . If, starting from the parameters' values used to obtain the simple basin structure of fig. 122a, the parameter  $v_2$  is increased, the two branches of the critical curve  $LC$  move upwards. The first global bifurcation of the basin occurs when the branch of  $LC$  which separates the regions  $Z_0$  and  $Z_2$  becomes tangent to  $\mathcal{F}$ , that is, to one of the lines (123) or (121). In fig.122b it can be seen that just after the bifurcation value of  $v_2$ , at which  $LC^{(b)}$  is tangent to the line  $\omega_1^{-1}$  of equation (123), a portion of  $\mathcal{B}(\infty)$ , say  $H_0$  (bounded by the segment  $h$  of  $\omega_1^{-1}$  and  $LC$ ) that before the bifurcation was in region  $Z_0$ , enters inside  $Z_2$ . The points belonging to  $H_0$  have two distinct preimages, located at opposite sides with respect to the line  $LC_{-1}$ , with the exception of the points of the curve  $LC^{(b)}$  inside  $\mathcal{B}(\infty)$  whose preimages, according to the definition of  $LC$ , merge on  $LC_{-1}^{(b)}$ . Since  $H_0$  is part of  $\mathcal{B}(\infty)$  also its preimages belong to  $\mathcal{B}(\infty)$ . The locus of the rank-1 preimages of  $H_0$ , bounded by the two preimages of  $h$ , is composed by two areas joining along  $LC_{-1}$  and forms a *hole* (or *lake*) of  $\mathcal{B}(\infty)$  nested inside  $\mathcal{B}(E_*)$ . This is the largest hole appearing in fig.122b, and is called the *main hole*. It lies entirely inside region  $Z_2$ , hence it has 2 preimages, which are smaller holes bounded by preimages of rank 3 of the  $q_1$  axis. Even these are both inside  $Z_2$ . So each of them has two further preimages inside  $Z_2$ , and so on. Now the boundary  $\mathcal{F}$  is given by the union of an external part, formed by the coordinate axes and their rank-1 preimages (123) and (121), and the boundaries of the holes, which are sets of preimages of higher rank of the  $q_1$  axis. Thus the global bifurcation just described transforms a *simply connected* basin into a *multiply connected* one, with a countable infinity of holes, called *arborescent sequence of holes*, inside it.

As  $v_2$  is further increased  $LC$  continues to move upwards and the holes become larger. This fact causes a sort of predictability loss, since a greater uncertainty is obtained with respect to the destiny

of games starting from an initial strategy falling in zone of the holes. If  $v_2$  is further increased a second global bifurcation occurs when  $LC$  crosses the  $q_2$  axis at  $O_{-1}^{(2)}$ . This happens when the condition (??) holds, that is  $v_2 = \frac{3}{a-c_2}$ , as in fig.123a. After this bifurcation all the holes reach the coordinate axis  $q_2$ , and the infinite contact zones are the intervals of divergence of the restriction (116), which are located around the critical point and all its preimages under (116) (compare fig. 123a with fig.87). After this bifurcation the basin  $\mathcal{B}(E_*)$  becomes simply connected again, but its boundary  $\mathcal{F}$  has now a fractal structure, since its shape, formed by infinitely many peninsulas, has the self-similarity property.

The sequence of pictures shown in fig.123 is obtained with  $v_1 = 0.24$  (as in fig.122) and increasing values of  $v_2$ . Along this sequence the point  $(v_1, v_2)$  reaches, in the plane of adjustment speeds, the line of flip bifurcations. When this line is crossed the Nash equilibrium  $E_*$  becomes a repelling saddle point, and an attracting cycle of period 2, say  $\mathcal{C}_2$ , is created near it (as in fig.123b). The flip bifurcation opens a cascade of period doublings, which creates a sequence of attracting cycles of period  $2^n$  followed by the creation of chaotic attractors, which may be cyclic chaotic areas, like the 2-cyclic one shown in fig.123c, or a unique chaotic area like that of fig.123d.

If  $v_2$  is further increased, new holes appear, like the one denoted by  $K$  in fig.123c. These are formed by the rank-1 preimages of portions of  $\mathcal{B}(\infty)$  which cross  $LC^{(a)}$  passing from  $Z_2$  to  $Z_4$ , like those evidenced in figures 123c,d. Even in this case the holes are created after a contact between  $LC$  and  $\mathcal{F}$ , but, differently from the hole  $H_{-1}$ , the hole  $K$  does not generate an arborescent sequence of holes since it has no preimages, belonging entirely to the region  $Z_0$ .

In fig.123d the chaotic area collides with the boundary of  $\mathcal{B}(\infty)$  causing the *final bifurcation*, leading to the destruction of the attractor. After this contact bifurcation the generic initial strategy generates an unbounded trajectory, that is, the adjustment process is not able to approach the Nash equilibrium, independently of the initial strategy of the duopoly game

It is worth to note that in general there are no relations between the bifurcations which change the qualitative properties of the basins and those which change the qualitative properties of the attractor at finite distance. In other words, we may have a simple attractor, like a fixed point or a cycle, with a very complex basin structure, or a complex attractor with a simple basin. Both these sequences of bifurcations, obtained by increasing the speeds of adjustment  $v_i$ , cause a loss of predictability. After the local bifurcations the myopic duopoly game no longer converges to the global optimal strategy, represented by the Nash equilibrium  $E_*$ , and even if the game starts from an initial strategy very close to  $E_*$  the duopoly system goes towards a different attractor, which may be periodic or aperiodic. These bifurcations cause in general a loss of predictability about the asymptotic behavior of the duopoly system: for example, in the sequence shown in fig.123 the situation of convergence to the unique Nash equilibrium, like in the static Cournot game, is replaced by asymptotic convergence to a periodic cycle, with predictable output levels, and then by a cyclic behavior with output levels which are not well predictable since fall inside cyclic chaotic areas, and, finally, a situation of erratic behavior, inside a large area of the strategy space, with no apparent periodicity. Instead, the global bifurcations of the basin boundaries cause an increasing uncertainty with respect to the destiny of a duopoly game starting from a given initial strategy, since a small change in the initial condition of the duopoly, or a small exogenous shock during the adjustment process, may cause a great modification about the long-run behavior of the system. Similar bifurcation sequences can also be obtained by increasing the parameter  $v_1$  with a fixed value of  $v_2$ . In this case a contact between  $LC$  and  $\omega_2^{-1}$ , rank-one preimage of the  $q_2$  axis, gives the first bifurcation that transforms the basin  $\mathcal{B}(\mathcal{A})$  from a simply connected into a multiply connected set, with holes near the  $q_1$  axis. Situations with values of  $v_1$  and  $v_2$  both near the critical values  $v_i = \frac{3}{a-c_i}$ ,  $i = 1, 2$ , can give complex basin boundaries near both the coordinate axes, with two arborescent sequences of holes, generated by contacts of  $LC$  with the lines (121) and (123).



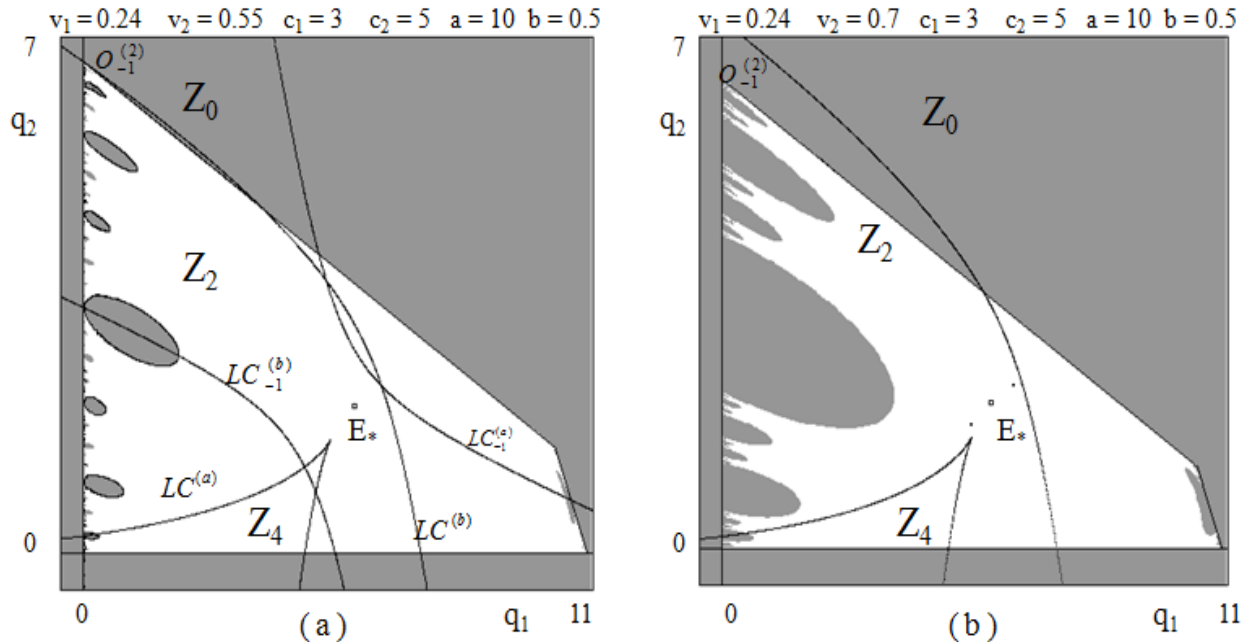


Figure 123: Sequence of numerical simulations of the duopoly map, obtained with fixed parameters  $c_1 = 3$ ,  $c_2 = 5$ ,  $a = 10$ ,  $b = 0.5$ ,  $v_1 = 0.24$ , and increasing values of  $v_2$

In any case, the computation of the preimages of the coordinate axes allows us to obtain, according to (119), the exact delimitation of the basin boundary also in these complex situations. For example, in fig. 124 the preimages of the  $q_1$  axis, up to rank-six, are represented for the same set of parameters as that used in fig. 120b. It can be noticed that some preimages of rank five and six bound holes that enter the region  $Z_4$ , thus giving a faster exponential growth of the number of higher order preimages. This is the cause for the greater complexity of the basin boundary which is clearly visible in fig. 120b.

### 7.5.2 Global analysis of a marketing Model

Let us consider  $n$  firms that sell homogeneous goods in a market with sales potential  $B$  in terms of customers' market expenditures, and let  $A_i(t)$ ,  $i = 1, \dots, n$ , denote the attraction of customers to firm  $i$  at time period  $t$ , where  $t \in \mathbb{N}$  represents an event-driven discrete time variable. The key assumption in marketing literature is that the market share for firm  $i$  at time  $t$  is given by

$$s_i(t) = \frac{A_i(t)}{\sum_{j=1}^n A_j(t)} \quad (124)$$

If  $x_i$  denotes *marketing spending* of firm  $i$ , we assume that attraction is given by

$$A_i = a_i x_i^{\beta_i}$$

where the positive constants  $a_i$  denote the relative effectiveness of effort expended by firm  $i$  and the parameters  $\beta_i$  denote the elasticity of the attraction of firm (or brand)  $i$  with regard to the marketing

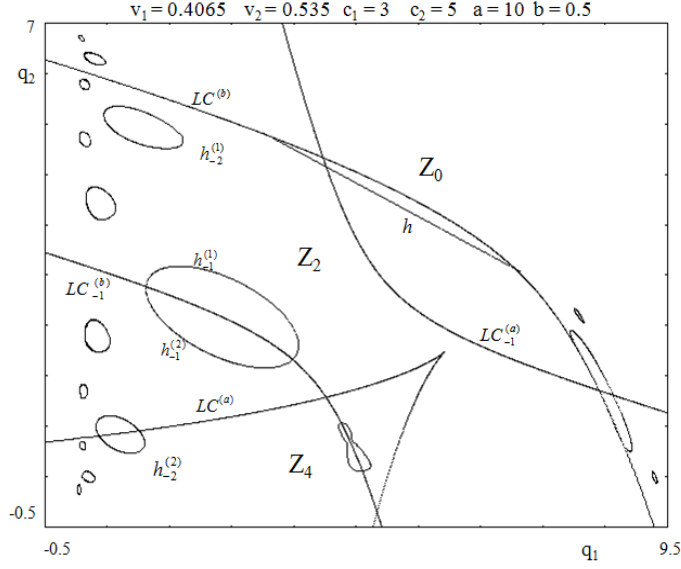


Figure 124: Preimages of the  $q_1$  axis, up to rank 6, obtained with the same set of parameters as those used in fig. 120b

effort, as  $\frac{dA_i}{dx_i} \frac{x_i}{A_i} = \beta_i$ . On the basis of these assumptions, the one-period net profit of firm  $i$  is given by

$$\Pi_i(t) = Bs_i(t) - x_i(t) = B \frac{a_i x_i^{\beta_i}(t)}{a_i x_i^{\beta_i}(t) + \sum_{j \neq i} a_j x_j^{\beta_j}(t)} - x_i(t) \quad (125)$$

The dynamic marketing model is based on the assumption that the two competitors change their marketing efforts adaptively in response to the profits achieved in the previous period. In particular, the marketing efforts in period  $t + 1$  are determined by

$$x_i(t+1) = x_i(t) + \lambda_i x_i(t) \Pi_i(t) = x_i(t) + \lambda_i x_i(t) \left( B \frac{a_i x_i^{\beta_i}(t)}{\sum_{j=i}^n a_j x_j^{\beta_j}(t)} - x_i(t) \right) \quad (126)$$

where (125) has been used. In this model the decision of the firms is driven by profits obtained in the previous period with a type of anchoring and adjustment heuristic widely used in decision theory. The parameters  $\lambda_i > 0$  measure the speed of adjustment. Also in this case a wide spectrum of rich dynamic scenarios is obtained, even in the case with  $n = 2$ .

Two exemplary cases are shown in Figure 125.

So, let us consider the model with two firms, i.e. for  $n = 2$ , given by

$$T : \begin{cases} x'_1 = x_1 + \lambda_1 x_1 \left( B \frac{a_1 x_1^{\beta_1}}{a_1 x_1^{\beta_1} + a_2 x_2^{\beta_2}} - x_1 \right) \\ x'_2 = x_2 + \lambda_2 x_2 \left( B \frac{a_2 x_2^{\beta_2}}{a_1 x_1^{\beta_1} + a_2 x_2^{\beta_2}} - x_2 \right) \end{cases} \quad (127)$$

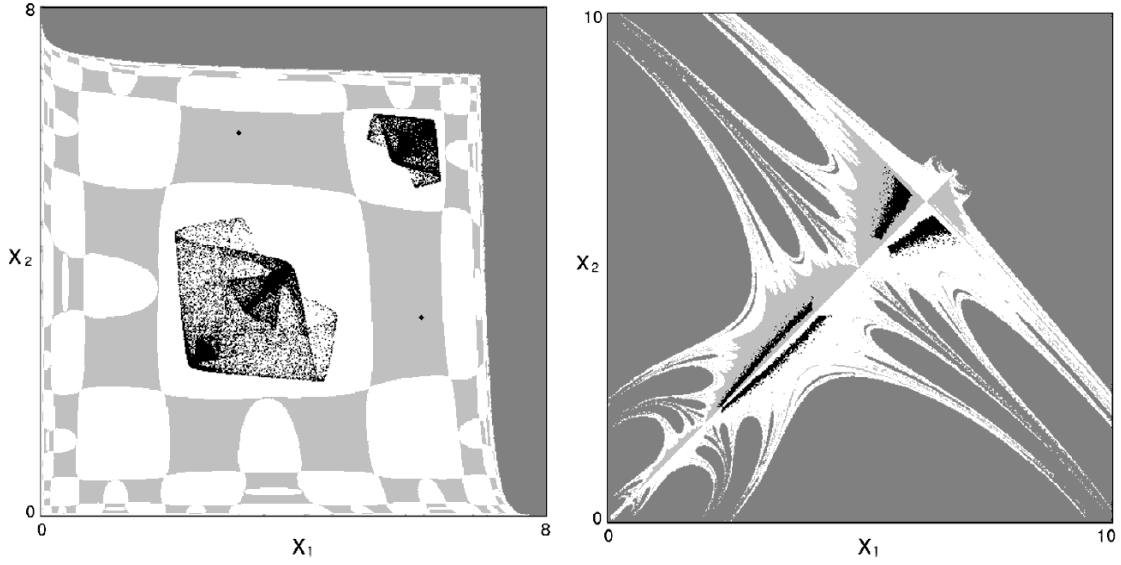


Figure 125: Two dynamic scenarios for the model (126) with  $n = 2$  identical firms with different initial conditions. The parameter values are  $B = 10$ ,  $\lambda_1 = \lambda_2 = 0.514961$ ,  $a_1 = a_2 = 1$ . Left:  $\beta_1 = \beta_2 = 0.05$ , a two-cyclic chaotic attractor coexists with a stable cycle of period 2. Right:  $\beta_1 = \beta_2 = 1.136$  two chaotic attractors coexist in symmetric positions. The different colors represent the basins of attraction of the coexisting attractors, represented by black dots, and the dark grey region represents the set of initial conditions that generate diverging trajectories.

Its fixed points are the solutions of the system

$$\begin{cases} x_1 \left( B \frac{a_1 x_1^{\beta_1}}{a_1 x_1^{\beta_1} + a_2 x_2^{\beta_2}} - x_1 \right) = 0 \\ x_2 \left( B \frac{a_2 x_2^{\beta_2}}{a_1 x_1^{\beta_1} + a_2 x_2^{\beta_2}} - x_2 \right) = 0 \end{cases} \quad (128)$$

There are three evident “boundary solutions”:

$$O = (0, 0); E_1 = (B, 0); E_2 = (0, B)$$

but  $O$  is not a fixed point because the map is not defined in it. There is also a positive fixed point, given by the solution of the system

$$\begin{cases} B \frac{a_1 x_1^{\beta_1}}{a_1 x_1^{\beta_1} + a_2 x_2^{\beta_2}} - x_1 = 0 \\ B \frac{a_2 x_2^{\beta_2}}{a_1 x_1^{\beta_1} + a_2 x_2^{\beta_2}} - x_2 = 0 \end{cases} \quad (130)$$

It is possible to see that one and only one solution exists given by

$$E^* = (x^*, B - x^*) \quad (131)$$

with  $x^* \in (0, B)$  unique solution of the equation

$$F(x) = \left(\frac{a_2}{a_1}\right)^{1/(1-\beta_2)} x^{(1-\beta_1)/(1-\beta_2)} + x - B = 0$$

obtained from (130) after some algebraic manipulations. In fact,  $F$  is a continuous function with  $F(0) < 0$ ,  $F(B) > 0$  and  $F'(x) > 0$  for each  $x > 0$ . An analytic expression of the solution is obtained in the case  $\beta_1 = \beta_2 = \beta$ , given by

$$x^* = \frac{B}{1 + \left(\frac{a_2}{a_1}\right)^{\frac{1}{(1-\beta)}}}$$

Moreover, under the further assumption  $a_2/a_1 = 1$ , i.e. in the case of identical firms, we get

$$E^* = \left(\frac{B}{2}, \frac{B}{2}\right) \quad (133)$$

With a given set of parameters  $B$ ,  $\beta_1$  and  $\beta_2$  the positive fixed point  $E^*$  is locally asymptotically stable for sufficiently small values of the adjustment speeds  $\lambda_1$  and  $\lambda_2$  and, as usual in dynamic models with adaptive adjustment, the fixed point  $E^*$  loses stability as one or both of the adjustment speeds are increased, after which more complex attractors are created around the unstable fixed point.

In the symmetric case of identical firms,  $\beta_1 = \beta_2$  and  $a_1 = a_2$ , the Jacobian matrix of (127) computed at  $E^*$  becomes

$$\mathbf{J}(E^*) = \begin{pmatrix} 1 - \frac{\lambda B}{2}(1 - \beta/2) & -\frac{\lambda B \beta}{4} \\ -\frac{\lambda B \beta}{4} & 1 - \frac{\lambda B}{2}(1 - \beta/2) \end{pmatrix} \quad (134)$$

hence the eigenvalues at the positive fixed point are  $\lambda_{\parallel} = 1 - \frac{1}{2}\lambda B$ , with eigendirection along  $\Delta$  and  $\lambda_{\perp} = 1 - \frac{1}{2}\lambda B(1 - \beta)$  with eigendirection orthogonal to  $\Delta$ . It is easy to see that the steady state  $E^*$  is locally asymptotically stable for  $\lambda B < 4$  and  $0 < \lambda B(1 - \beta) < 4$ , however only the first condition is important as only values of  $\beta_i \in (0, 1]$  are meaningful in applications

The map (127) is noninvertible, because computing the points  $(x, y)$  in terms of a given  $(x', y')$  in (127) by solving the system

$$\begin{cases} x \left(1 + \lambda_1 B \frac{x^{\beta_1}}{x^{\beta_1} + ky^{\beta_2}} - \lambda_1 x\right) = x' \\ y \left(1 + \lambda_2 B \frac{ky^{\beta_2}}{x^{\beta_1} + ky^{\beta_2}} - \lambda_2 y\right) = y' \end{cases} \quad (135)$$

we can have more than one solution. In fact, if we compute the preimages of the origin, by solving the system (135) with  $x' = 0$  and  $y' = 0$ , we obtain:  $0_{-1}^{(1)} = (\frac{1+\lambda_1 B}{\lambda_1}, 0)$ ;  $0_{-1}^{(2)} = (0, \frac{1+\lambda_2 B}{\lambda_2})$  and  $0_{-1}^{(3)}$  located at the intersection of the two curves  $\omega_1^{-1}$  and  $\omega_2^{-1}$ , which we will introduce later (see fig. 4b).

On the other hand, there are no preimages for points that are sufficiently far from the origin. In fact, if  $x' > \frac{(1+\lambda_1 B)^2}{4\lambda_1}$  or  $y' > \frac{(1+\lambda_2 B)^2}{4\lambda_2}$  then the system (135) has no real solutions, because from the inequality  $\frac{x^{\beta_1}}{x^{\beta_1} + ky^{\beta_2}} < 1$  it follows that  $x \left(1 + \lambda_1 B \frac{x^{\beta_1}}{x^{\beta_1} + ky^{\beta_2}} - \lambda_1 x\right) < x(1 + \lambda_1(B - x))$ . This is

a concave quadratic function with maximum value  $\frac{(1+\lambda_1 B)^2}{4\lambda_1}$ . Hence the left hand side of the first of (135) is always less than or equal to  $\frac{(1+\lambda_1 B)^2}{4\lambda_1}$ . Analogously from  $\frac{ky^{\beta_2}}{x^{\beta_1+ky^{\beta_2}}} < 1$  it follows that  $y \left( 1 + \lambda_2 B \frac{ky^{\beta_2}}{x^{\beta_1+ky^{\beta_2}}} - \lambda_2 y \right) < y (1 + \lambda_2 (B - y)) \leq \frac{(1+\lambda_2 B)^2}{4\lambda_2}$ .

The critical curves, given by the locus of points for which  $\det J(x, y) = 0$  according to (111), is given by the union of two branches, denoted by  $LC_{-1}^{(a)}$  and  $LC_{-1}^{(b)}$  in fig. 126a. Also  $LC$  is the union of two branches, denoted by  $LC^{(a)} = T(LC_{-1}^{(a)})$  and  $LC^{(b)} = T(LC_{-1}^{(b)})$  (fig.126b):  $LC^{(b)}$  separates the region  $Z_0$ , whose points have no preimages, from the region  $Z_2$ , whose points have two distinct rank-1 preimages;  $LC^{(a)}$  separates the region  $Z_2$  from  $Z_4$ , whose points have four distinct preimages.

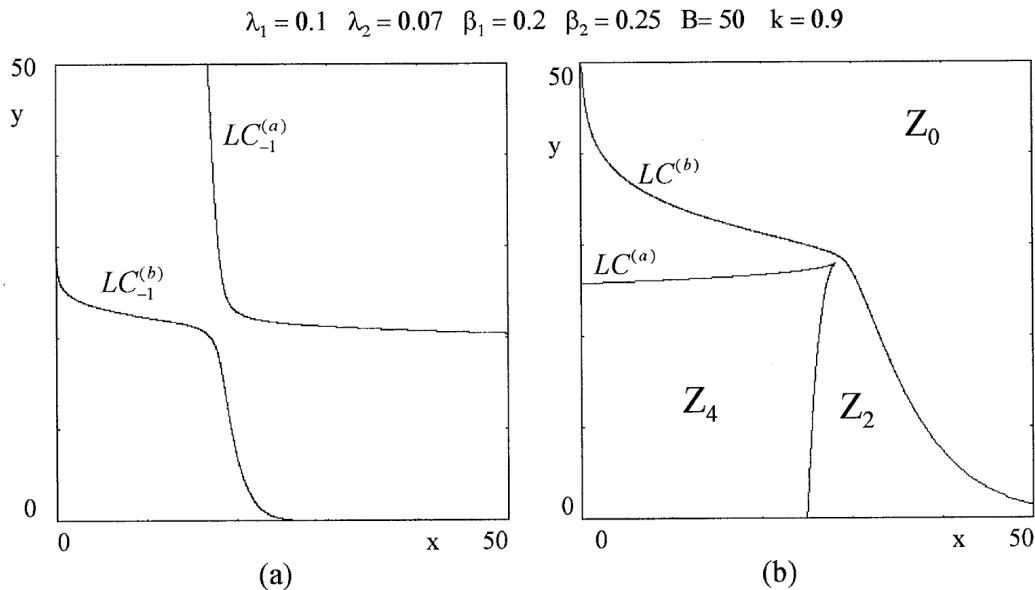


Figure 126: **(a)**  $LC_{-1}$ , obtained as the locus of points such that  $\det \mathbf{J}(x, y) = 0$ . **(b)** Critical curves  $LC = T(LC_{-1})$ . These curves separate the plane into three regions, denoted by  $Z_4$ ,  $Z_2$  and  $Z_0$  whose points have four, two or no rank-1 preimages respectively.

An important feature of the map (127) is that the two coordinate axes are invariant lines, since  $T(x, 0) = (x', 0)$  and  $T(0, y) = (0, y')$ . The dynamics of (127) along the  $x$  axis are governed by the one-dimensional map  $x' = f_1(x)$ , where  $f_1$  is the restriction of  $T$  to the  $x$  axis, given by

$$f_1(x) = (1 + \lambda_1 B)x - \lambda_1 x^2. \quad (136)$$

Since the situation is symmetric, the dynamics along the  $y$  axis are governed by the one-dimensional map  $y' = f_2(y)$ , where  $f_2$  is obtained from (136) simply by replacing  $x$  with  $y$  and swapping index 1 with index 2. The maps  $f_i$ ,  $i = 1, 2$ , are conjugated to the standard logistic maps  $z' = \mu_i z(1 - z)$ ,  $i = 1, 2$ , where the parameters  $\mu_i$  are given by

$$\mu_i = 1 + \lambda_i B \quad i = 1, 2 \quad (137)$$

the homeomorphisms being given by  $x = \frac{1+\lambda_1 B}{\lambda_1} z$  and  $y = \frac{1+\lambda_2 B}{\lambda_2} z$  respectively. Thus, the properties of the trajectories embedded in the invariant axes can be easily deduced from the well-known properties

of the standard logistic map

$$z' = f(z) = \mu z(1 - z), \quad (138)$$

In the following we denote by  $\mathcal{B}$  the *feasible set*, defined as the set of points which generate feasible trajectories. A feasible trajectory may converge to the positive steady state  $E_*$ , to other more complex attractors inside  $\mathcal{B}$  or to a one-dimensional invariant set embedded inside a coordinate axis (the last occurrence means that one of the two brands disappears). Trajectories starting outside of the set  $\mathcal{B}$  represent exploding (or collapsing) evolutions of the economic system. This can be interpreted by saying that the adjustment mechanism is not suitable to model the time evolution of a system starting outside of the set  $\mathcal{B}$ .

The invariant coordinate axes are transversely repelling, i.e. they act as repelling sets with respect to trajectories approaching them from the interior of the nonnegative orthant. Moreover, for the parameters used in our simulations, we have observed only one attractor inside  $\mathcal{B}$ , although more than one coexisting attractors may exist, each with its own basin of attraction. On the basis of such numerical evidence, in what follows we will often speak of a unique bounded and positive attracting set, denoted by  $\mathcal{A}$ , which attracts the generic feasible trajectory, even if its existence and uniqueness are not rigorously proved.

Let  $\partial\mathcal{B}$  be the boundary of  $\mathcal{B}$ . Such a boundary can have a simple shape, as in the situation shown in fig. 127a, where the attractor  $\mathcal{A}$  is the fixed point  $E_*$  and  $\mathcal{B}$  is represented by the white region, or a more complex structure, as in fig. 127d.

To understand the global bifurcations leading to more and more complex boundaries of the basins, let us first consider the dynamics of  $T$  restricted to the invariant axes. From the one-dimensional restriction  $f_1$  defined in (136), conjugated to the logistic map (138), we can deduce that bounded trajectories along the invariant  $x$  axis are obtained when  $\lambda_1 B \leq 3$  (corresponding to  $\mu_1 \leq 4$  in (137)), provided that the initial conditions are taken inside the segment  $\omega_1 = OO_{-1}^{(1)}$ , where  $O_{-1}^{(1)}$  is the rank-1 preimage of the origin  $O$  computed according to the restriction  $f_1$  (see fig.127b), i.e.

$$O_{-1}^{(1)} = \left( \frac{1 + \lambda_1 B}{\lambda_1}, 0 \right). \quad (139)$$

Divergent trajectories along the  $x$  axis are obtained starting from an initial condition out of the segment  $\omega_1$ . Analogously, when  $\lambda_2 B \leq 3$ , bounded trajectories along the invariant  $y$  axis are obtained provided that the initial conditions are taken inside the segment  $\omega_2 = OO_{-1}^{(2)}$ , where  $O_{-1}^{(2)}$  is the rank-1 preimage of the origin computed according to the restriction  $f_2$ , i.e.

$$O_{-1}^{(2)} = \left( 0, \frac{1 + \lambda_2 B}{\lambda_2} \right). \quad (140)$$

Also in this case, divergent trajectories along the  $y$  axis are obtained starting from an initial condition out of the segment  $\omega_2$ .

Consider now the region bounded by the segments  $\omega_1$  and  $\omega_2$  and their rank-1 preimages  $\omega_1^{-1} = T^{-1}(\omega_1)$  and  $\omega_2^{-1} = T^{-1}(\omega_2)$ . Such preimages can be analytically computed as follows. Let  $X = (p, 0)$  be a point of  $\omega_1$ , i.e.  $0 < p < \frac{1 + \lambda_1 B}{\lambda_1}$ . Its preimages are the real solutions of the algebraic system obtained from (135) with  $(x', y') = (p, 0)$ :

$$\begin{cases} x \left( 1 + \lambda_1 B \frac{x^{\beta_1}}{x^{\beta_1} + ky^{\beta_2}} - \lambda_1 x \right) = p \\ y \left( 1 + \lambda_2 B \frac{ky^{\beta_2}}{x^{\beta_1} + ky^{\beta_2}} - \lambda_2 y \right) = 0 \end{cases} \quad (141)$$

It is easy to see that the preimages of the point  $X$  are either located on the same invariant axis  $y = 0$  (in the points whose coordinates are the solutions of the equation  $f_1(x) = p$ ) or on the curve of equation

$$x = \left[ ky^{\beta_2} \left( \frac{\lambda_2 B - \lambda_2 y + 1}{\lambda_2 y - 1} \right) \right]^{\frac{1}{\beta_1}}. \quad (142)$$

Analogously, the preimages of a point  $Y = (0, q)$  of  $\omega_2$ , i.e.  $0 < q < \frac{1+\lambda_2 B}{\lambda_2}$ , belong to the same invariant axis  $x = 0$ , in the points whose coordinates are the solutions of the equation  $f_2(y) = q$ , or lie on the curve of equation

$$y = \left[ \frac{x^{\beta_1}}{k} \left( \frac{\lambda_1 B - \lambda_1 x + 1}{\lambda_1 x - 1} \right) \right]^{\frac{1}{\beta_2}}. \quad (143)$$

It is straightforward to see that the curve (142) intersects the  $y$  axis in the point  $O_{-1}^{(2)}$  given in (140), the curve (143) intersects the  $x$  axis in the point  $O_{-1}^{(1)}$  given in (139), and the two curves (142) and (143) intersect at a point  $O_{-1}^{(3)}$  interior to the positive orthant (see fig. 4b). As noted before,  $O_{-1}^{(3)}$  is another rank-1 preimage of the origin. These four preimages of the origin are the vertexes of a “quadrilateral”  $OO_{-1}^{(1)}O_{-1}^{(3)}O_{-1}^{(2)}$ , whose sides are  $\omega_1$ ,  $\omega_2$  and their rank-1 preimages located on the curves of equation (142) and (143), denoted by  $\omega_1^{-1}$  and  $\omega_2^{-1}$  in fig.127b. All the points outside this quadrilateral cannot generate feasible trajectories. In fact the points located on the right of  $\omega_2^{-1}$  are mapped into points with negative  $x$  coordinate after one iteration, as can be easily deduced from the first line of (112), and the points located above  $\omega_1^{-1}$  are mapped into points with negative  $y$  coordinate after one iteration, as can be deduced from the second line of (135).

The boundary of  $\mathcal{B}$  is given, in general, by the union of all the preimages, of any rank, of the segments  $\omega_1$  and  $\omega_2$ :

$$\partial\mathcal{B}(\infty) = \left( \bigcup_{n=0}^{\infty} T^{-n}(\omega_1) \right) \cup \left( \bigcup_{n=0}^{\infty} T^{-n}(\omega_2) \right). \quad (144)$$

As long as  $\lambda_1 B \leq 3$  and  $\lambda_2 B \leq 3$  the boundary of  $\mathcal{B}$  has the simple shape shown in fig. 127b. In this situation (obtained with the same parameter values as in fig.127a) the quadrilateral  $OO_{-1}^{(1)}O_{-1}^{(3)}O_{-1}^{(2)}$  constitutes the whole boundary  $\partial\mathcal{B}$ , because no preimages of higher rank of  $\omega_1$  and  $\omega_2$  exist. This is due to the fact that  $\omega_1^{-1}$  and  $\omega_2^{-1}$  are entirely included inside the region  $Z_0$  of the plane whose points have no preimages.

The situation is different when the values of the parameters are such that some portions of these curves belong to the regions  $Z_2$  or  $Z_4$  whose points have two or four preimages respectively. In this case preimages of higher order of  $\omega_1$  and  $\omega_2$  exist, say  $\omega_1^{-k}$  and  $\omega_2^{-k}$ , which form new portions of  $\partial\mathcal{B}$ . Such preimages of  $\omega_1$  and  $\omega_2$  of rank  $k > 1$  bound regions whose points are mapped out of the region  $\mathcal{B}$  after  $k$  iterations, just as we have shown for the standard logistic map (138) with parameter  $\mu > 4$ , i.e. after the contact between the critical point  $c = \mu/4$  and the boundary of the basin of infinity at  $O_{-1} = 1$ . This implies that the shape of the boundary of  $\mathcal{B}$  becomes more complex.

In analogy with the one-dimensional case, also in the two-dimensional case the bifurcations of the basins are characterized by contacts between the basins boundaries and the critical curve  $LC$ . If  $\lambda_1$  or  $\lambda_2$  are increased so that the bifurcation value  $\lambda_b = 3/B$  (which coincides with  $\mu = 4$  in (138)) is crossed by at least one of them, then  $\partial\mathcal{B}$  is changed from smooth to fractal. This transition between qualitatively different structures of the boundaries of the region  $\mathcal{B}$ , as some parameters are varied, constitutes a *global bifurcation*, occurring at  $\lambda_i = \lambda_b$ ,  $i = 1, 2$ , that can be characterized by a contact between  $\partial\mathcal{B}$  and arcs of the critical curves, as described below.

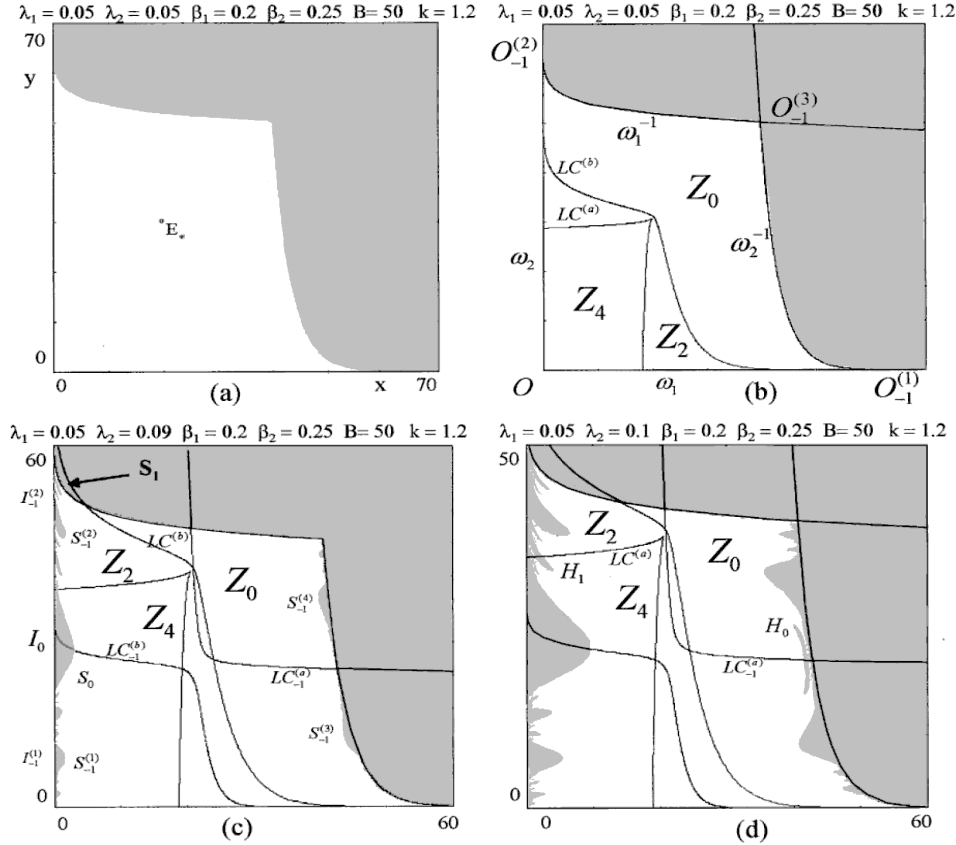


Figure 127: Contact bifurcations leading to the creation of fractal basins' boundaries.

We fix the parameters  $B$ ,  $k$ ,  $\beta_1$ ,  $\beta_2$  and  $\lambda_1$  and vary the speed of adjustment  $\lambda_2$ . As  $\lambda_2$  is increased, the branch  $LC^{(b)}$  of the critical curve that separates  $Z_0$  from  $Z_2$  moves upwards, and at  $\lambda_2 = 3/B$  it has a contact with  $\omega_1^{-1}$  at the point  $O_{-1}^{(2)}$ . After this contact the sides  $\omega_2$  and  $\omega_2^{-1}$  of  $\partial\mathcal{B}$  are transformed from smooth to fractal. In fact, for  $\lambda_2 > 3/B$ , just after the bifurcation, a segment of  $\omega_1^{-1}$  enters the region  $Z_2$ , so that a portion  $S_1$  of the complement of  $\mathcal{B}$ , bounded by  $LC^{(b)}$  and  $\omega_1^{-1}$  (see fig.127c), now has two preimages. These two preimages, say  $S_0^{(1)}$  and  $S_0^{(2)}$ , merge in points of  $LC_{-1}^{(b)}$  (as the points of  $LC^{(b)}$  have two merging preimages belonging to  $LC_{-1}^{(b)}$ ) and form a “grey tongue” issuing from the  $y$  axis (denoted by  $S_0$  in fig. 6b, being  $S_0 = S_0^{(1)} \cup S_0^{(2)}$ ).  $S_0$  belongs to the “grey set” of points that generate non feasible trajectories because the points of  $S_0$  are mapped into  $S_1$ , so that negative values are obtained after two iterations. The intersection of this “main tongue”  $S_0$  with the  $y$  axis is given by the neighborhood  $I_0$  of the critical point of the restriction  $f_2$ , i.e. the “main hole” of the logistic with  $\mu > 4$  (see fig.87).

This is only the first of infinitely many preimages of  $S_1$ . Preimages of  $S_1$  of higher rank form a sequence of smaller and smaller grey tongues issuing from the  $y$  axis, whose intersection with the  $y$  axis correspond to the infinitely many preimages  $I_{-k}$  of the main hole  $I_0$  (see again fig.87). Only some of them are visible in fig.127c, but smaller tongues become numerically visible by enlargements, as it usually happens with fractal curves.



In the situation shown in fig.127c the main tongue  $S_0$  has a wide portion in the region  $Z_4$ , hence, besides the two preimages along the  $y$  axis (denoted by  $S_{-1}^{(1)}$  and  $S_{-1}^{(2)}$  in fig.127c) issuing from the intervals  $I_{-1}^{(1)}$  and  $I_{-1}^{(2)}$ , two more preimages exist (denoted by  $S_{-1}^{(3)}$  and  $S_{-1}^{(4)}$  in fig.127c) issuing from  $\omega_2^{-1}$  and located at opposite sides with respect to  $LC_{-1}^{(a)}$ . The tongues  $S_{-1}^{(3)}$  and  $S_{-1}^{(4)}$  belong to  $Z_0$ , hence they do not give rise to new sequences of tongues, whereas  $S_{-1}^{(1)}$  and  $S_{-1}^{(2)}$  have further preimages, being located inside  $Z_4$  and  $Z_2$  respectively. If the preimages are two, as in the case of  $S_{-1}^{(2)}$ , they form two tongues issuing from the  $y$  axis, whereas in the case of four preimages, as in the case of  $S_{-1}^{(1)}$ , two of them are tongues issuing from the  $y$  axis and two are tongues issuing from the opposite side, i.e.  $\omega_2^{-1}$ .

As  $\lambda_2$  is further increased,  $LC^{(b)}$  moves upwards, the portion  $S_1$  enlarges and, consequently, all its preimages (i.e. the infinitely many tongues) enlarge and become more pronounced. This causes the occurrence of another global bifurcation, that changes the set  $\mathcal{B}$  from simply connected to multiply connected (or connected with holes). This bifurcation occurs whenever a tongue, belonging to  $Z_2$ , has a contact with  $LC^{(a)}$  and enters the region  $Z_4$ . If the contact occurs out of the  $y$  axis, it causes the creation of a pair of new preimages, merging along  $LC_{-1}^{(a)}$ , whose union is a *hole* (or *lake*) inside  $\mathcal{B}$ , i.e. a set of points that generate non feasible trajectories surrounded by points of  $\mathcal{B}$ . This can be seen in fig.127d, where the hole  $H_0$  is the preimage of the portion  $H_1$ , inside  $Z_4$ , of a tongue that crossed  $LC^{(a)}$ .

To sum up, the transformation of the set  $\mathcal{B}$  from a simply connected region with smooth boundaries into a multiply connected set with fractal boundaries occurs through two types of global bifurcations, both due to contacts between  $\partial\mathcal{B}$  and branches of the critical set  $LC$ .

As it can be noticed from the sequence of figures127, obtained with increasing values of the parameter  $\lambda_2$ , also the attractor  $\mathcal{A}$  existing inside  $\mathcal{B}$  changes its structure. For low values of  $\lambda_2$ , as in fig.127a, the attractor is the fixed point  $E_*$ , to which all the trajectories starting inside the set  $\mathcal{B}$  converge. As  $\lambda_2$  increases,  $E_*$  loses stability through a flip (or period doubling) bifurcation at which  $E_*$  becomes a saddle point, and an attracting cycle of period 2 is created near it. As  $\lambda_2$  is further increased, also the cycle of period two undergoes a flip bifurcation at which an attracting cycle of period 4 is created, which becomes the unique attractor inside  $\mathcal{B}$ , as in fig. 4c. In this case the generic<sup>20</sup> trajectory starting inside  $\mathcal{B}$  converges to the 4-cycle, so that  $\mathcal{B}$  can be identified with its basin of attraction for any practical purpose. These flip bifurcations are followed by a sequence of period doublings which creates a sequence of attracting cycles of period  $2^n$  followed by the creation of chaotic attractors, which may be cyclic chaotic sets or a connected chaotic set.

Of course, the same sequence of local and global bifurcations occurs if the other speed of adjustment,  $\lambda_1$ , is increased. The only difference is that at the bifurcation value  $\lambda_1 = \lambda_b = 3/B$  the contact between  $\partial\mathcal{B}$  and  $LC$  occurs at the point  $O_{-1}^{(1)}$  and consequently the infinitely many tongues with fractal structure are created along the segment  $\omega_1$  of the  $x$  axis. Preimages of some of these tongues, those belonging to  $Z_4$ , appear along the opposite side  $\omega_1^{-1}$  of the quadrilateral.

If both the speeds of adjustment  $\lambda_1$  and  $\lambda_2$  are greater than the bifurcation value  $\lambda_b = 3/B$ , tongues appear along all the four sides of the quadrilateral  $OO_{-1}^{(1)}O_{-1}^{(3)}O_{-1}^{(2)}$ , as it can be seen in the numerical simulation shown in fig.128.

---

<sup>20</sup>Not all the points of  $\mathcal{B}$  generate trajectories converging to the 4-cycle because we must exclude the invariant sets, like the repelling fixed point  $E_*$  as well as the points of the repelling 2-cycle whose flip bifurcation generated the attracting 4-cycle, and their stable sets. However, the subset of points in  $\mathcal{B}$  which do not converge to the 4-cycle is a set of measure zero, and this justifies the term “generic”.

In fig.128 the attractor  $\mathcal{A}$  inside the set  $\mathcal{B}$  is a 2-cyclic chaotic attractor. In this situation the long run behavior of the system is characterized by cyclical behavior of order two, but at each time period the exact state cannot be predicted.

As we have described in section 7.4.3, even in the analysis of the boundaries of the chaotic attractors the critical curves are quite helpful. In fact, in analogy to the critical points of the one-dimensional maps, that together with their images determine the boundaries of the chaotic intervals (as recalled in section 6.4 for the logistic map) the critical curve  $LC$  and its images can be used to bound invariant absorbing areas, which include the two-dimensional chaotic attractors of noninvertible maps. In two-dimensional maps the notion of chaotic area generalizes that of chaotic intervals, and the critical curves, that constitute the generalization of the concept of critical points (local minimum and maximum points), are expected to play a similar role in determining the boundaries of the chaotic areas. We recall that a chaotic area  $\mathcal{A}$  of the map  $T$  is an invariant set of  $T$ , i.e.  $T(\mathcal{A}) \equiv \mathcal{A}$ , which includes a chaotic set (a set that includes infinitely many and dense repelling periodic points and an aperiodic trajectory that densely covers the set). Numerically computed trajectories seem to cover the area, as shown in fig.128. Often the boundaries of  $\mathcal{A}$  can be obtained by following the procedure, described in 7.4.3, that starts from the portion  $\gamma = \mathcal{A} \cap LC_{-1}$  and then for a suitable integer  $m$

$$\partial\mathcal{A} \subseteq \bigcup_{k=1}^m T^k(\gamma) \quad (145)$$

An example is shown in the right panel of fig.128, where the boundary of the 2-cyclic chaotic area shown in the left panel is obtained by the images, up to rank 7, of the portion  $\gamma$  of  $LC_{-1}$ . In other words, the exact boundary of the chaotic attractor can be obtained by (145) with  $m = 7$ . It is worth noticing that the critical curves of increasing rank not only give the boundary of a chaotic attractor, but also the regions of greater density of points, i.e. the regions that are more frequently visited by the points of the generic trajectory in the invariant area  $\mathcal{A}$ .

## 8 Repeated and evolutionary games as dynamical systems

Games played by rational players with complete information sets are typically one-shot games: each player knows the complete payoffs' structure of the game and that other players are rational as well so that, having complete information, each player is able to forecast the choices of other players. Thus, the game is studied identifying the so-called "solution concepts", such as Nash equilibria. In fact, if each player is assumed to have all such information and computational skills to solve the optimization problem obtained by means of the rationality assumption (expressed as maximization of individual utility) then everybody will choose a Nash equilibrium. However, agents are sometimes not so astute nor informed, and they behave following adaptive methods, such as learning-by-doing or trial-and-error practices. Sometimes agents do not optimize at all, just following rough rules of thumb. This leads players to replace one-shot optimal decisions with repeated myopic or adaptive decisions, in other words to a dynamic process that may or may not converge to a Nash equilibrium, provided it is an equilibrium point of the dynamical system as well. Moreover, when a game has several Nash equilibrium points represented by equilibrium points of the dynamical system, then the step-by-step dynamic process may act as a selection device, i.e. the stability of the equilibria suggests which of them will prevail in the long-run. And if several equilibrium points are stable, then the study of their basins of attraction will give information about the path dependence, i.e. how the convergence will depend on historical accidents (represented by exogenous shifts of initial conditions).

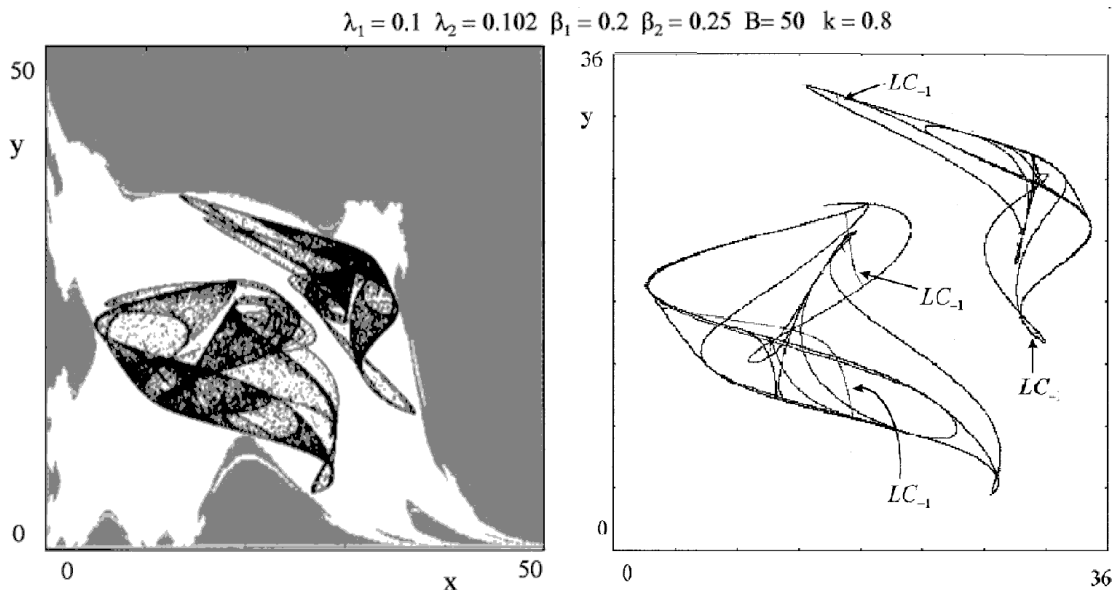


Figure 128: Left: A 2-cyclic chaotic attractor to which the generic feasible trajectory converges. Right: Boundary of the attractor obtained by arcs of critical curves  $LC, LC_1, \dots, LC_6$ , according to (145) with  $m = 7$ .

However, a very remarkable result regards whether a repeated boundedly rational (or trial-and-error) decision leads to an adaptive (or myopic) process that converges, in the long run, to the same 'optimal' equilibrium chosen in one shot by rational and informed players, who know the methods of game theory and possess high computational abilities. In fact, such boundedly rational players, whose behaviour is much more similar to real (imperfect) people, play the game repeatedly over time until they reach a situation where there is no further room for improvement. Their final behaviour will be as though they perfectly know any game theory book. An external observer may conclude that some invisible hand led them to the 'optimal' outcome. But nobody suggested them how reach it. It just emerged spontaneously, as a result emerged by itself from repeated trial-and-error steps. Sometimes economists call myopic or short sighted these agents, as they decide according to what is under their noses. To sum up, this may be seen as an evolutionary explanation of the outcome of a Nash equilibrium.

However, sometimes such repeated adaptive processes never converge, and continue to move around an equilibrium point following some periodic or chaotic time patterns. Or they may even irreversibly depart from it and even diverge. Such evolutions can be expressed by saying that players are not able to learn how to play a Nash equilibrium, and some global analysis may be required to understand the kind of time evolutions that characterize the long run behaviour of the repeated game.

Two examples have been considered in sections 7.3.2 and 7.3.3, where the two players (firms in a duopoly) are not aware of the global demand function that characterizes the market where they operate, and repeatedly play the game following a profit increasing myopic "rule of thumb" based on the local knowledge of profit gradient. Any Nash equilibrium of the game is a fixed point of the dynamical system, so that the repeated game becomes a dynamic process that may converge or not to a Nash equilibrium (see sections 7.3.2 and 7.3.3).

Some other examples are shown in the following, starting from the Cournot duopoly game introduced in section 6.

### 8.1 Cournot games with rational players

Let us consider again the classical Cournot oligopoly model (47). A market with  $N$  firms, producing homogeneous goods with outputs  $q_i$ ,  $i = 1 \dots N$ , is characterized by an inverse demand  $p = D^{-1}(Q) = f(Q)$ , where  $Q = \sum_{i=1}^N q_i$ . Let  $C_i(q_i)$ ,  $i = 1, \dots, N$ , be the cost functions. At time  $t$  each firm  $i$  chooses its next period production  $q_i(t+1)$  according to the optimization problem

$$q_i(t+1) = \arg \max_{q_i(t+1)} \pi_i(t+1) = \arg \max_{q_i} [f(q_i + q_{-i}^e(t+1)) q_i - C_i(q_i)].$$

where by  $q_{-i} = \sum_{j \neq i} q_j$  we indicate the aggregate production of firms other than  $i$ , so that  $Q = q_i + q_{-i}$ . Accordingly, by the notation  $q_{-i}^e(t+1)$  we denote the aggregate production of other players that player  $i$  expects at time  $t+1$  according to the information that she has at time  $t$ . So, the computation of an optimal production choice in one-shot requires that each firm has:

- (i) Knowledge of the demand function  $p = f(Q)$ ;
- (ii) Knowledge of its own cost function  $C_i(q_i)$ ;
- (iii) Perfect foresight about competitors' production choices  $q_{-i}^e(t+1) = q_{-i}(t+1)$ ;
- (iv) Computational skill to solve the optimization problem.

With this information set, each firm will compute its *Best Reply*, implicitly defined by the first order (necessary) conditions  $\frac{\partial \pi_i}{\partial q_i} = 0$ , that give

$$\frac{\partial \pi_i}{\partial q_i} = q_i f'(q_i + Q_i(t+1)) + f(q_i + Q_i(t+1)) + \frac{\partial C_i(q_i, q_{-i}(t+1))}{\partial q_i} = 0 \quad i = 1, \dots, n \quad (146)$$

together with (sufficient) second order conditions  $\frac{\partial^2 \pi_i}{\partial q_i^2} > 0$ . In some cases, a unique and explicit solution of (146) can be obtained, expressed by the *reaction functions*

$$q_i(t+1) = R_i(q_{-i}(t+1)) \quad i = 1, \dots, n \quad (147)$$

The solutions of the  $n$  equations with  $n$  unknowns  $q_i = R_i(q_{-i})$ ,  $i = 1, \dots, n$ , give the Nash Equilibrium points, located (according to the usual definition) at the intersections of the reaction functions (where each firm plays its best response to the other players' best response strategies).

Some examples of reaction curves and Nash equilibria at their intersections have been given in section 6, see (48) and (49). The corresponding graphs are shown in fig. 129.

If linear demand  $f(Q) = a - bQ$  and quadratic costs  $C_i(q_i) = c_i q_i + e_i q_i^2$  are considered, the profit function of firm  $i$  becomes  $\pi_i(t) = (a - b(q_1 + q_2))q_i(t) - (c_i q_i + e_i q_i^2)$  and the first order conditions  $\frac{\partial \pi_i}{\partial q_i} = 0$  become  $a - 2(b + e_1)q_i - bq_j - c_i = 0$ , from which the reaction functions:

$$\begin{aligned} q_1 &= R_1(q_2) = \max \left\{ -\frac{b}{2(b+e_1)} q_2 + \frac{a-c_1}{2(b+e_1)}, 0 \right\} \\ q_2 &= R_2(q_1) = \max \left\{ -\frac{b}{2(b+e_2)} q_1 + \frac{a-c_2}{2(b+e_2)}, 0 \right\} \end{aligned} \quad (148)$$

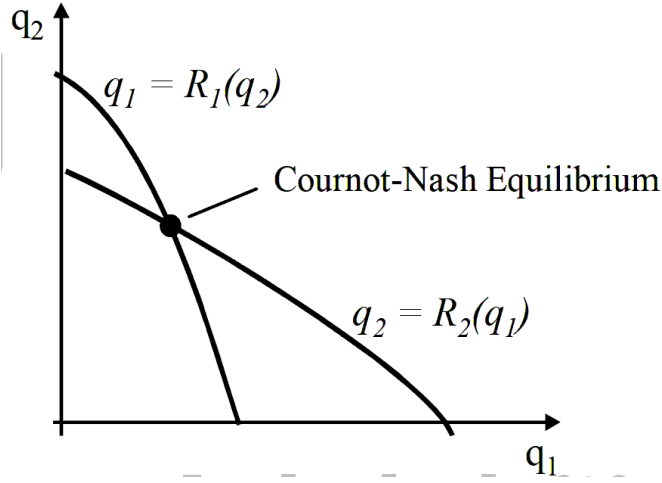


Figure 129: Schematic representation of *Best Reply* (or *Reaction*) curves

where the max operator is inserted to avoid meaningless negative output decisions (negative optimal values are interpreted as no-production decision). As it can be seen in fig.131, where the two reaction functions are represented, besides the positive Nash equilibrium

$$E = \left( \frac{2(b+e_2)(a-c_1) - b(a-c_2)}{4(b+e_1)(b+e_2) - b^2}, \frac{2(b+e_1)(a-c_2) - b(a-c_1)}{4(b+e_1)(b+e_2) - b^2} \right) \quad (149)$$

in the case  $b^2 > 4(b+e_1)(b+e_2)$ , i.e. slope of  $R_2$  more negative than slope of  $R_1$ , two further Nash equilibria exist at the three intersections of the reaction curves located along the coordinate axes, that can be denoted as "monopoly" Nash equilibria

$$E_1 = \left( \frac{a-c_1}{2(b+e_1)}, 0 \right), \quad E_2 = \left( 0, \frac{a-c_2}{2(b+e_2)} \right) \quad (150)$$

## 8.2 Bounded rationality and incomplete information

In this section we weaken the degree of rationality (or, better, the information degree) of players in the Cournot game. Let us first relax the assumption of perfect foresight about the expected aggregate production choice of other players, and replace it by assuming naive expectations

$$q_{-i}^e(t+1) = q_{-i}(t) \quad (151)$$

that is, in the absence of information about competitors' production decisions, each player assumes that competitors will produce in the next time period the same output as in the current period. Best Reply dynamics with naive expectations becomes a discrete dynamical system

$$q_i(t+1) = R_i(q_{-i}(t)) \quad (152)$$

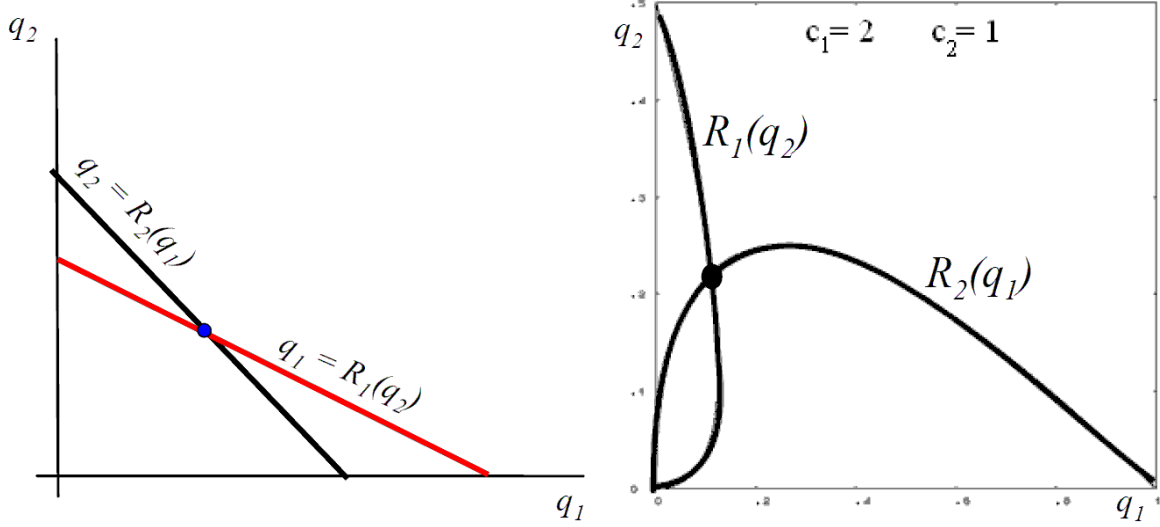


Figure 130: Left: Reaction curves (48). Right: Reaction curves (49)

In the case of linear demand and linear cost functions the dynamical system assumes the form of the linear dynamical system (48)

$$\begin{cases} q_1(t+1) = -\frac{1}{2}q_2(t) + \frac{a-c_1}{2b} \\ q_2(t+1) = -\frac{1}{2}q_1(t) + \frac{a-c_2}{2b} \end{cases}$$

where the unique equilibrium

$$E = \left( \frac{a+c_2-2c_1}{3b}, \frac{a+c_1-2c_2}{3b} \right)$$

is positive provided that  $a+c_2-2c_1 > 0$  and  $a+c_1-2c_2 > 0$ , two inequalities that define a nonempty set in the space of marginal costs  $(c_1, c_2)$  provided that  $c_1 < a$  and  $c_2 < a$ , the usual condition of unitary production costs less than unitary price.

The equilibrium  $E$  is always globally asymptotically stable, as the eigenvalues of the linear model are  $\lambda_{1,2} = \pm \frac{1}{2}$ . The eigenvector associated to  $\lambda_1 = \frac{1}{2}$  is  $\mathbf{v}_1 = (-1, 1)$  and with  $\lambda_2 = -\frac{1}{2}$  is  $\mathbf{v}_2 = (1, 1)$ , hence we have an oscillatory convergence with oscillations along  $(1, 1)$  direction (see fig.132).

Let us now consider the Cournot duopoly with isoelastic demand and naive expectations (49)

$$\begin{cases} q_1(t+1) = -q_2(t) + \sqrt{\frac{q_2(t)}{c_1}} \\ q_2(t+1) = -q_1(t) + \sqrt{\frac{q_1(t)}{c_2}} \end{cases} \quad (153)$$

A unique Nash equilibrium exists, given by

$$\mathbf{E} = \left( \frac{c_2}{(c_1+c_2)^2}; \frac{c_1}{(c_1+c_2)^2} \right), \quad (154)$$

whose local stability properties are given in terms of the ratio between the marginal costs  $c_1/c_2$ . First of all, feasible (i.e. bounded and non negative) trajectories of the best reply dynamics are obtained

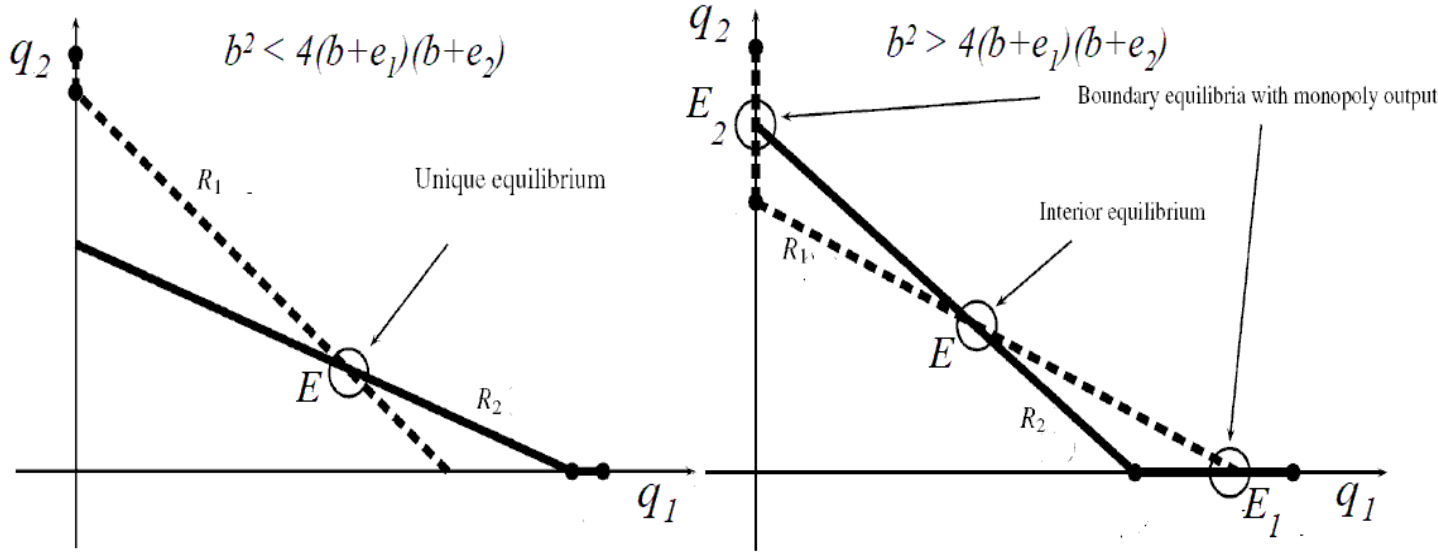


Figure 131: Linear reaction functions for the Cournot duopoly model with linear demand and quadratic cost.

provided that  $c_1/c_2 \in [4/25, 25/4] = [0.16, 6.25]$ . Moreover, the Nash equilibrium (154) is stable if and only if  $c_1/c_2 \in (3 - 2\sqrt{2}, 3 + 2\sqrt{2}) \simeq (0.17, 5.83)$ . See the left panel of fig. 133, where the white region represents the basin of attraction of the stable Nash equilibrium and the grey region the set of points that generate unfeasible trajectories. If  $c_1/c_2$  exits this interval then the Nash equilibrium loses stability via a period doubling bifurcation. Indeed, if  $c_1/c_2$  falls outside the interval  $(3 - 2\sqrt{2}, 3 + 2\sqrt{2})$  then the asymptotic dynamics may converge at periodic cycles or even exhibit chaotic motion around the Nash equilibrium, as shown in the right panel of fig. 133, where a chaotic trajectory is shown, together with the reaction curves, obtained with  $c_1 = 1$  and  $c_2 = 0.161$ .

In the former case we can say that Nash equilibrium is reached as a long run outcome of the repeated game. This may be seen as an *evolutionary explanation* of the outcome of a NE. Instead, in the latter case (characterized by a greater difference between production costs) Nash equilibrium is not reached in the long run, and players will never "learn to play" the Nash equilibrium.

In the case of several coexisting Nash equilibria, the *repeated game may act as an equilibrium selection device*. For example, in the case of a Cournot duopoly game with linear demand, quadratic costs and best reply dynamics with naive expectations, where the reaction functions (148) have been obtained, the corresponding dynamical system is again linear

$$\begin{aligned} q_1(t+1) &= R_1(q_2(t)) = -\frac{b}{2(b+e_1)}q_2(t) + \frac{a-c_1}{2(b+e_1)} \\ q_2(t+1) &= R_2(q_1(t)) = -\frac{b}{2(b+e_2)}q_1(t) + \frac{a-c_2}{2(b+e_2)} \end{aligned}$$

and the positive equilibrium (149) is stable if  $b^2 < 4(b+e_1)(b+e_2)$ . Instead, if the opposite inequality holds the positive equilibrium  $E$  is transformed from a stable to an unstable node, and the locally diverging dynamics can converge to one of the monopoly equilibria (150) or to a stable cycle of period 2, characterized by alternating periods where both firms produce monopoly quantities and both firms

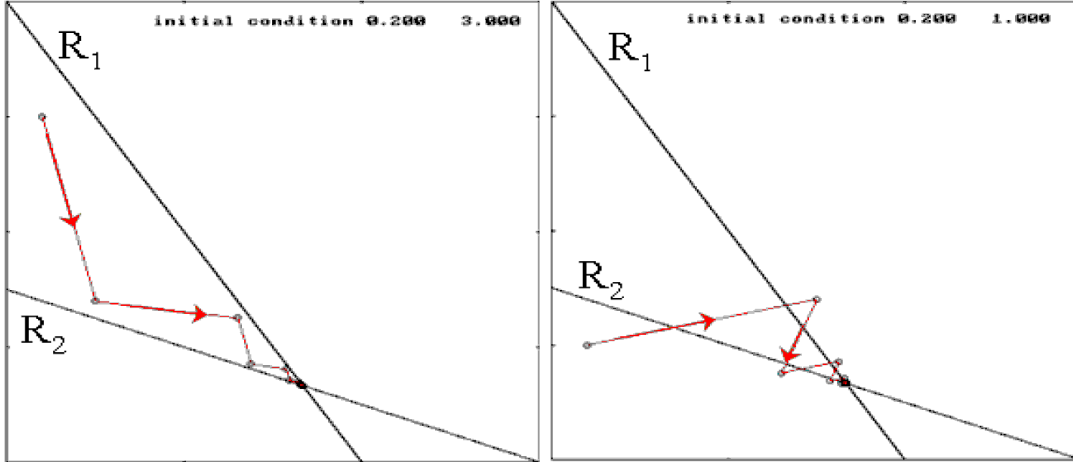


Figure 132: Trajectories for the Cournot model with linear demand and linear cost.

stop producing. So, we get a situation of multistability, with three attractors each with its own basin of attraction, as represented in fig.134 by different colors. In this case we have path dependence, as the repeated adjustment process converges to different asymptotic behaviours according to the initial conditions or, equivalently, according to possible 'historical accidents'.

**Naive expectation and adaptive adjustment towards Best Reply** An interesting kind of dynamic adjustment process, known as adaptive adjustment towards best reply, is obtained if an anchoring attitude, or inertia, is added to the oligopoly model with best reply and naive expectations (152)

$$q_i(t+1) = (1 - \lambda_i) q_i(t) + \lambda_i R_i(q_{-i}(t)), \quad 0 \leq \lambda \leq 1 \quad (155)$$

where  $i = 1, \dots, n$  and the constants  $\lambda_i \in [0, 1]$  represent the attitude of firm  $i$  to adopt the best reply, whereas  $(1 - \lambda_i)$  is the anchoring attitude to maintain previous production decisions, i.e. a measure of inertia. The model (155) is a generalization of (152) because it reduces to it for  $\lambda_i = 1, i = 1, \dots, n$ , whereas complete inertia of firm  $i$  occurs if  $\lambda_i = 0$ , i.e.  $x_i(t+1) = x_i(t)$ . Moreover, the model (155) has the same equilibria as the best reply model (153): in fact, from the condition  $q_i(t+1) = q_i(t) = q^*$  the equilibrium equation  $\lambda_i (q_i^* - R_i(q_{-i}^*)) = 0$  is obtained.

For example, in the case of isoelastic demand and linear cost the dynamical system becomes

$$\begin{aligned} q_1' &= (1 - \lambda_1) q_1 + \lambda_1 \left[ \sqrt{\frac{q_2}{c_1}} - q_2 \right] \\ q_2' &= (1 - \lambda_2) q_2 + \lambda_2 \left[ \sqrt{\frac{q_1}{c_2}} - q_1 \right] \end{aligned}$$

and from the study of the Jacobian matrix it can be seen that even if the inertia parameters  $\lambda_i$  do not have any influence on the localization of Nash equilibria, they have an important role in the stability properties of the equilibrium points. In particular, it is easy to check that stability is always obtained if both  $\lambda_i$  are sufficiently small.



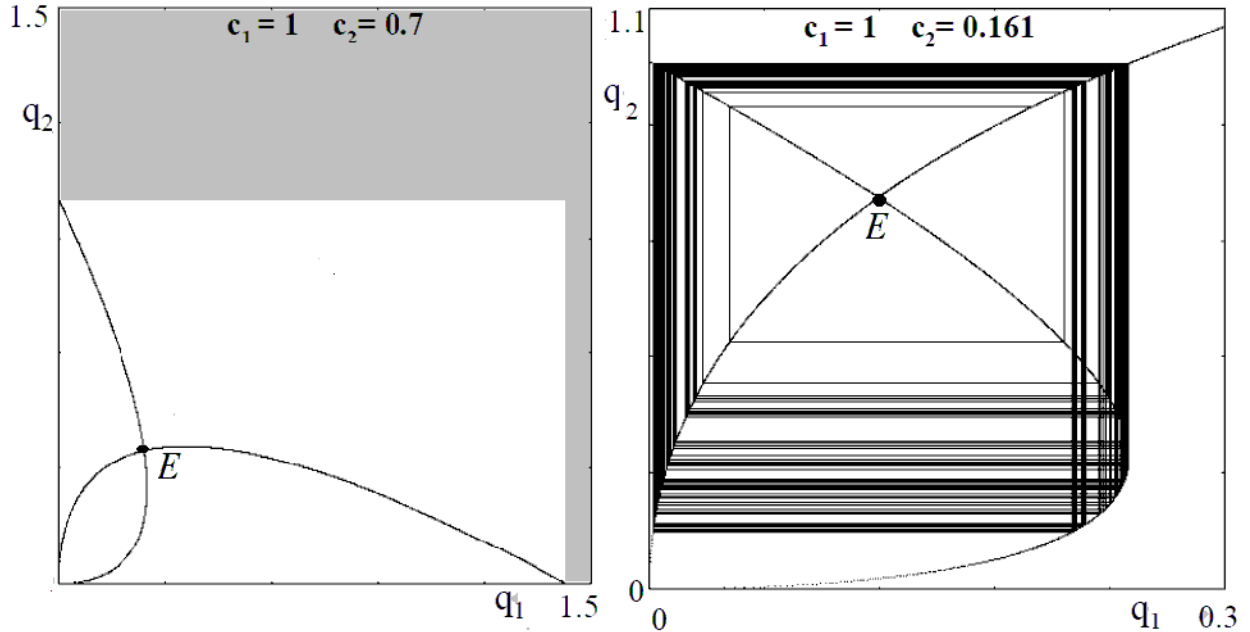


Figure 133: Reaction curves and Nash equilibrium for the Cournot duopoly model with isoelastic demand.

As a further Cournot duopoly model let us consider a case where the reaction curves are second degree functions, in the form of standard logistic maps  $R_i(q_j) = \mu_i q_j (1 - q_j)$ . They can be obtained by assuming a linear demand  $p = a - b(q_1 + q_2)$  and cost functions with externalities:  $C_i = C_i(q_i, q_j) = d + aq_i - b(1 + 2\mu)q_i q_j + 2b\mu q_i q_j^2$ .<sup>21</sup>

The adaptive adjustment with inertia becomes:

$$\begin{aligned} q_1(t+1) &= (1 - \lambda_1) q_1(t) + \lambda_1 \mu_1 q_2(t) (1 - q_2(t)) \\ q_2(t+1) &= (1 - \lambda_2) q_2(t) + \lambda_2 \mu_2 q_1(t) (1 - q_1(t)) \end{aligned} \quad (156)$$

As noticed above, this model reduces to the repeated game with best reply and naive expectations if  $\lambda_1 = \lambda_2 = 1$

$$\begin{aligned} q_1(t+1) &= \mu_1 q_2(t) (1 - q_2(t)) \\ q_2(t+1) &= \mu_2 q_1(t) (1 - q_1(t)) \end{aligned}$$

and, due to the unimodal shape of the "logistic reaction curves", several coexisting stable Nash equilibria can be obtained for certain sets of parameters, as well as other more complicated coexisting attractors, such as stable cycles or chaotic attractors. An exemplary case is shown in fig. 135, where

<sup>21</sup>see: Kopel, M., Simple and complex adjustment dynamics in Cournot duopoly models, *Chaos, Solitons & Fractals* 7 (12), 2031-2048.

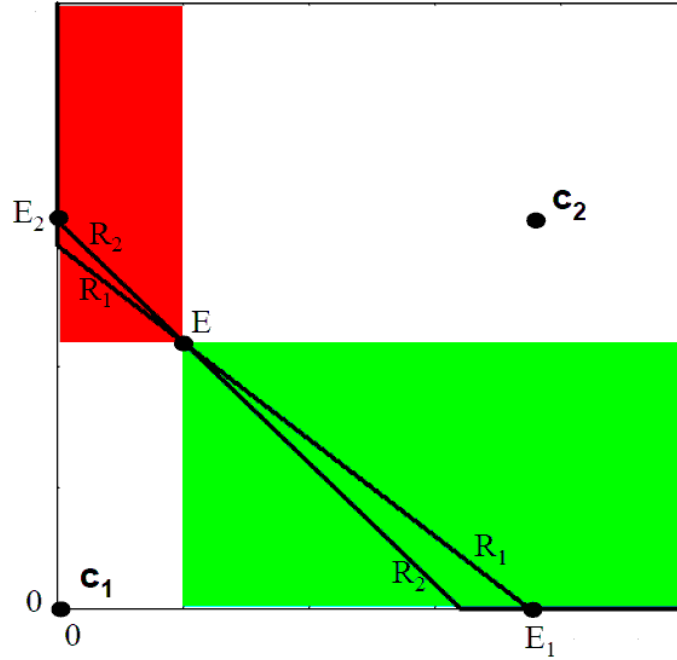


Figure 134: Nash equilibrium points and basins of attraction for the Cournot duopoly model with linear demand and quadratic cost.

two stable Nash equilibria coexist with a stable cycle of period 2, each with its own basin of attraction. The basins are multiply connected, i.e. besides the immediate basin several (really infinitely many) non connected portions exist that accumulate along the outer boundary of the phase space. As stressed in section 7.4, such a situation can only occur in the case of noninvertible maps.

In order to reduce the number of parameters in our model, we will assume that  $\mu_1 = \mu_2 = \mu$ . Under this assumption the fixed points can be analytically computed as follows. Two fixed points always exist, given by  $O = (0, 0)$  and  $S = \left(1 - \frac{1}{\mu}, 1 - \frac{1}{\mu}\right)$ . For  $\mu > 1$ ,  $S$  represents a Nash equilibrium of the duopoly game, at which the two firms produce the same quantities. Moreover, two further Nash equilibria, given by

$$E_1 = \left( \frac{\mu + 1 + \sqrt{(\mu + 1)(\mu - 3)}}{2\mu}, \frac{\mu + 1 - \sqrt{(\mu + 1)(\mu - 3)}}{2\mu} \right) \quad (157)$$

and

$$E_2 = \left( \frac{\mu + 1 - \sqrt{(\mu + 1)(\mu - 3)}}{2\mu}, \frac{\mu + 1 + \sqrt{(\mu + 1)(\mu - 3)}}{2\mu} \right), \quad (158)$$

are created at  $\mu = 3$ , and for  $\mu > 3$  they are located in symmetric positions with respect to the diagonal  $\Delta$  of equation  $q_1 = q_2$ . Each of them represents a Nash equilibrium, characterized by different quantities produced by two firms. In the presence of multiple Nash equilibria the problem of equilibrium selection arises. The following result holds (see also fig.136)

**Proposition (Local stability and bifurcations with homogeneous players).** *Let  $\mu_1 = \mu_2 = \mu$  and  $\lambda_1 = \lambda_2 = \lambda$ . Then*

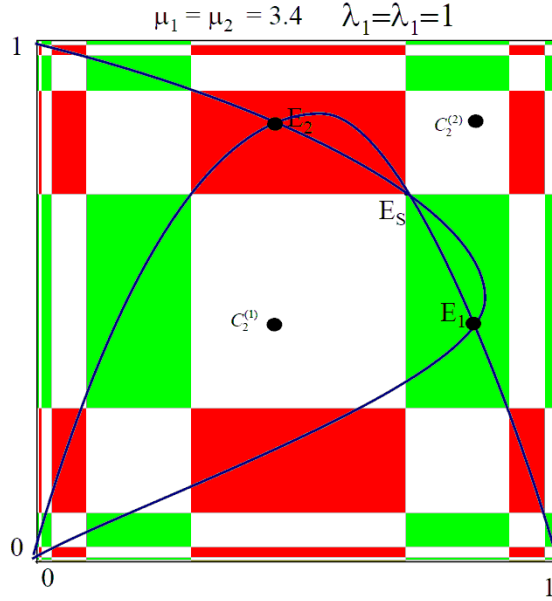


Figure 135: Nash equilibrium points and basins of attraction for the Cournot duopoly model with unimodal reaction functions.

(i) for  $0 < \mu < 1$  the fixed point  $O = (0, 0)$  is a stable node, for  $1 < \mu < 2/\lambda - 1$  it is a saddle point, with unstable set along  $\Delta$  and local stable set which crosses through  $O$  perpendicular to  $\Delta$ , and for  $\mu > 2/\lambda - 1$  it is an unstable node;

(ii) for  $1 < \mu < 3$  the fixed point  $S = (1 - 1/\mu, 1 - 1/\mu)$  is a stable node, for  $3 < \mu < 1 + 2/\lambda$  it is a saddle point, with local stable set along  $\Delta$  and unstable set which crosses through  $S$  perpendicular to  $\Delta$ , and for  $\mu > 1 + 2/\lambda$  it is an unstable node;

(iii) The fixed points  $E_i$ ,  $i = 1, 2$ , given in (157) and (158), are created at  $\mu = 3$  through a pitchfork bifurcation of  $S$ , and are stable nodes for  $3 < \mu < 1 + \sqrt{5}$ , stable foci for  $1 + \sqrt{5} < \mu < 1 + \sqrt{4 + \frac{2}{\lambda}}$  and at  $\mu = 1 + \sqrt{4 + \frac{2}{\lambda}}$  they become unstable foci through a Neimark-Sacker bifurcation.

Proof. The Jacobian matrix of (156) is

$$J(q_1, q_2; \mu, \lambda) = \begin{bmatrix} 1 - \lambda & \lambda\mu(1 - 2q_2) \\ \lambda\mu(1 - 2q_1) & 1 - \lambda \end{bmatrix} \quad (159)$$

In the points of the diagonal  $\Delta$  of equation  $q_1 = q_2$  on which both  $O$  and  $S$  are located, the matrix (159) assumes the structure

$$DT(x, x; \lambda, \mu) = \begin{bmatrix} 1 - \lambda & \lambda\mu(1 - 2x) \\ \lambda\mu(1 - 2x) & 1 - \lambda \end{bmatrix} \quad (160)$$

Such a matrix has real eigenvalues. In particular, in  $O$  the eigenvalues are:

$$z_{\parallel}(O) = 1 + \lambda(\mu - 1) \quad \text{with eigenvector } \mathbf{r}_{\parallel} = (1, 1) \text{ along } \Delta \quad (161)$$

and

$$z_{\perp}(O) = 1 - \lambda(\mu + 1) \quad \text{with eigenvector } \mathbf{r}_{\perp} = (1, -1) \text{ perpendicular to } \Delta \quad (162)$$

In the fixed point  $S$  we have

$$z_{\parallel}(S) = 1 + \lambda(1 - \mu) \quad \text{and} \quad z_{\perp}(S) = 1 + \lambda(\mu - 3)$$

So, the fixed point  $O$  is locally asymptotically stable (a stable node) in the region

$$\Omega_2(O) = \{(\mu, \lambda) \in \Omega_2 | \mu < 1\} \quad (163)$$

Analogously, since  $z_{\parallel}(S) \in (-1, 1)$  for  $0 < \lambda(\mu - 1) < 2$  and  $z_{\perp}(S) \in (-1, 1)$  for  $-2 < \lambda(\mu - 3) < 0$ , the fixed point  $S$  is locally asymptotically stable (a stable node) in the region

$$\Omega_2(S) = \{(\mu, \lambda) \in \Omega_2 | 1 < \mu < 3\} \quad (164)$$

At  $\mu = 1$ ,  $O \equiv S$  and a *transcritical* (or stability exchange) bifurcation occurs at which the two fixed points exchange their stability property along  $\Delta$ : for  $\mu < 1$ , just before the bifurcation,  $O$  is a stable node and  $S$  is a saddle, with local stable set along  $\Delta$ , and for  $\mu > 1$ , just after the bifurcation,  $O$  is a saddle, with unstable set along  $\Delta$ , and  $S$  is a stable node.

At  $\lambda(\mu + 1) = 2$  a *period doubling* (or flip) bifurcation of  $O$  occurs which creates a cycle of period 2 along the invariant manifold associated with  $z_{\perp}(O)$ . For  $\lambda \in (0, 1)$  this bifurcation occurs for  $\mu > 1$ , i.e. when  $O$  is a saddle, hence at the flip bifurcation  $O$  becomes an unstable node and a saddle cycle of period two is created, with stable set along the direction associated with  $z_{\perp}(O)$ .

At  $\mu = 3$  a *pitchfork bifurcation* occurs at which the fixed point  $S$  becomes a saddle point with unstable set in the direction transverse to  $\Delta$ , and the fixed points  $E_1$  and  $E_2$  are created. At  $\lambda(\mu - 1) = 2$  a flip bifurcation along  $\Delta$  occurs at which  $S$  becomes a repelling node and a saddle cycle of period 2 is created along  $\Delta$ , with stable set along  $\Delta$  and unstable set transverse to it.

The Jacobian matrix (159) computed at the two fixed points  $E_1$  and  $E_2$  which exist for  $\mu > 3$ , respectively assume the forms,

$$J(E_1; \lambda, \mu) = \begin{bmatrix} 1 - \lambda & -\lambda(1 - \sqrt{(\mu + 1)(\mu - 3)}) \\ -\lambda(1 + \sqrt{(\mu + 1)(\mu - 3)}) & 1 - \lambda \end{bmatrix}$$

$$J(E_2; \lambda, \mu) = \begin{bmatrix} 1 - \lambda & -\lambda(1 + \sqrt{(\mu + 1)(\mu - 3)}) \\ -\lambda(1 - \sqrt{(\mu + 1)(\mu - 3)}) & 1 - \lambda \end{bmatrix}$$

Hence  $E_1$  and  $E_2$  have the same characteristic equation with  $Tr = 2(1 - \lambda)$  and  $Det = (1 - \lambda)^2 - \lambda^2(4 + 2\mu - \mu^2)$ . Being  $Tr^2 - 4Det = 4\lambda^2(4 + 2\mu - \mu^2)$  the eigenvalues are real for  $\mu \leq 1 + \sqrt{5}$ , and are given by

$$z_1 = 1 - \lambda - \lambda\sqrt{4 + 2\mu - \mu^2} \quad \text{and} \quad z_2 = 1 - \lambda + \lambda\sqrt{4 + 2\mu - \mu^2}$$

For  $\mu > 1 + \sqrt{5}$  the eigenvalues are complex, and are given by

$$z_1 = 1 - \lambda - i\lambda\sqrt{\mu^2 - 2\mu - 4} \quad \text{and} \quad z_2 = 1 - \lambda + i\lambda\sqrt{\mu^2 - 2\mu - 4}$$

In the parameters space  $\Omega_2$  the region of stability of  $E_i$  is

$$\Omega_2(E_i) = \{(\mu, \lambda) \in \Omega_2 | \mu > 3 \text{ and } \lambda(\mu^2 - 2\mu - 3) < 2\} \quad (165)$$

At  $\lambda(\mu^2 - 2\mu - 3) = 2$  the eigenvalues exit the unit circle, so that the fixed points are transformed from stable to unstable foci through a supercritical Neimark-Sacker bifurcation at which two stable closed

orbits are created around the two Nash equilibria  $E_1$  and  $E_2$ . The rigorous proof of the occurrence of a supercritical Hopf bifurcation requires the evaluation of some long expressions involving derivatives of the map up to order three. We claim numerical evidence for the existence of a stable closed orbit around the unstable focus after the bifurcation (see fig.137).□

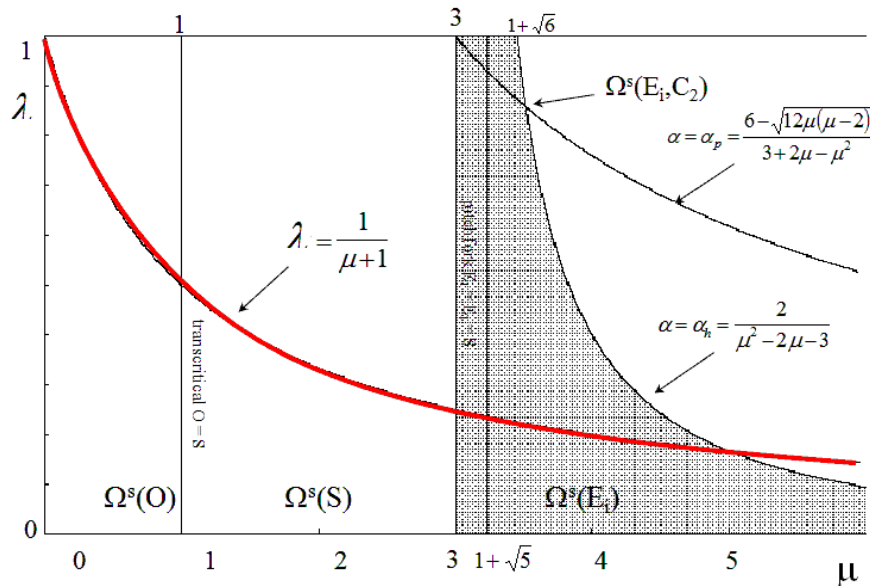


Figure 136: Stability region (grey shaded) and bifurcation curves in the parameters' plane  $(\mu, \lambda)$

In fig. 136, the red line of equation  $\lambda = \frac{1}{\mu+1}$  represents a global bifurcation curve at which the basins change their topological structure from simply to multiply connected, i.e. connected with holes, according to the following proposition (that we give without a proof)

**Proposition (Global bifurcation of the basing with homogeneous players).** *If  $\mu_1 = \mu_2 = \mu$ ,  $\lambda_1 = \lambda_2 = \lambda$  and  $(\mu, \lambda) \in \tilde{\Omega}_2(E_i)$ , the bounded trajectories of (156) converge to one of the stable Nash equilibria  $E_1$  or  $E_2$ , given by (157) and (158) respectively, and the common boundary which separates the basin  $\mathcal{B}(E_1)$  from the basin  $\mathcal{B}(E_2)$  is given by the stable set  $W^s(S)$  of the saddle point  $S$ . If  $\lambda(\mu+1) < 1$  then the two basins are simply connected sets; if  $\lambda(\mu+1) > 1$  then the two basins are non connected sets, formed by infinitely many simply connected components.*

We would like to emphasize that the bifurcation occurring at  $\lambda(\mu+1) = 1$  is a global bifurcation, i.e. it cannot be revealed by a study of the linear approximation of the dynamical system. The occurrence of such a bifurcation has been characterized by a contact between the stable set of  $S$  and a critical curve  $LC$ . i.e. a *contact* (or *global*) bifurcation.

The occurrence of the bifurcation, which transforms the basins from simply connected to non-connected, causes a loss of predictability about the long-run evolution of this Cournot game starting from given initial quantities of the two players. In fact, in contrast to what happens in the case of simply connected basins, when the basins are no longer simply connected, the adjustment dynamic

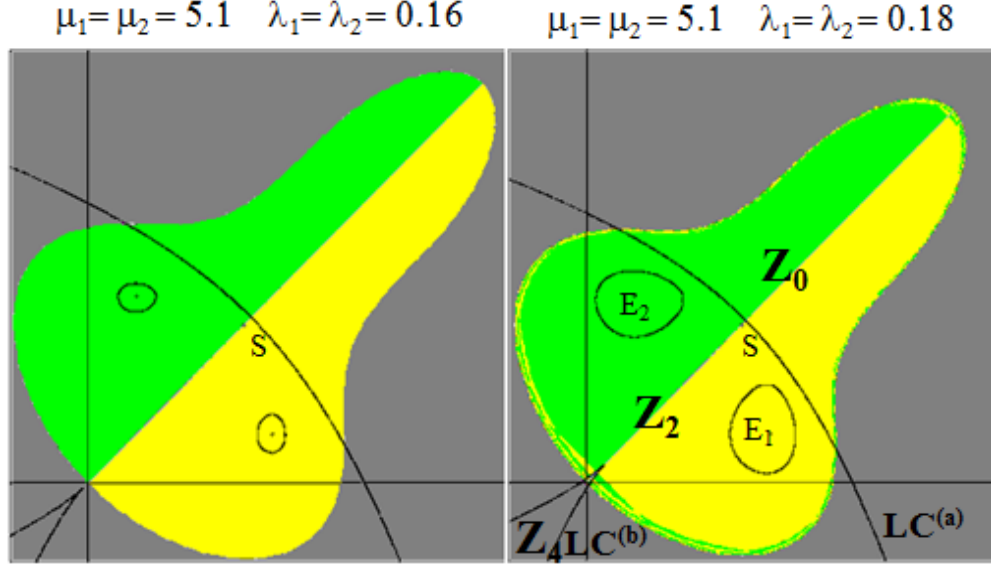


Figure 137: After Neimark-Sacker bifurcation (left) and after global basin bifurcation (right).

starting with  $q_1(0) > q_2(0)$  may lead to convergence to either of the Nash equilibria. Furthermore, if the initial quantities are sufficiently far away from a Nash equilibrium, for example near the boundary  $\partial\mathcal{B}$  of  $\mathcal{B}$ , then the presence of the infinitely many components of both basins causes a sort of sensitivity with respect to these initial conditions. Even a very small perturbation of the starting point of the Cournot game may lead to a crossing of the boundary that separates the two basins, with consequent convergence to a different Nash equilibrium.

We now turn to the case of heterogeneous behavior, and assume that  $\lambda_1 \neq \lambda_2$  holds. Although we get the same Nash equilibria since the fixed points do not depend on the speeds of adjustment, the eigenvalues of the Jacobian matrix of the map (156) depend on both of the parameters  $\lambda_1$  and  $\lambda_2$ . Furthermore, note that the diagonal  $\Delta$  is no longer trapping. The following proposition defines the stability regions for each Nash equilibrium in the three-dimensional parameters space  $\Omega_3 = \{(\mu, \lambda_1, \lambda_2) \in \mathbb{R}^3 | \mu > 0, 0 \leq \lambda_1 \leq 1, 0 \leq \lambda_2 \leq 1\}$ .

**Proposition (Local stability for heterogeneous behaviour).** *Let  $\mu_1 = \mu_2$ . Then*

- (i) *for  $0 < \mu < 1$  the fixed point  $O = (0, 0)$  is a stable node, for  $1 < \mu < \sqrt{1 + \frac{4-2(\lambda_1+\lambda_2)}{\lambda_1\lambda_2}}$  it is a saddle point, for  $\mu > \sqrt{1 + \frac{4-2(\lambda_1+\lambda_2)}{\lambda_1\lambda_2}}$  it is an unstable node;*
- (ii) *for  $1 < \mu < 3$  the fixed point  $S = (1 - 1/\mu, 1 - 1/\mu)$  is a stable node, for  $3 < \mu < 2 + \sqrt{1 + \frac{4-2(\lambda_1+\lambda_2)}{\lambda_1\lambda_2}}$  it is a saddle point, for  $\mu > 2 + \sqrt{1 + \frac{4-2(\lambda_1+\lambda_2)}{\lambda_1\lambda_2}}$  it is an unstable node;*
- (iii) *The fixed points  $E_i, i = 1, 2$ , given in (157) and (158) are created at  $\mu = 3$  through a pitchfork bifurcation of  $S$ , are stable nodes for  $3 < \mu < 1 + \sqrt{\frac{9}{2} + \frac{\lambda_1}{4\lambda_2} + \frac{\lambda_2}{4\lambda_1}}$ , stable foci for  $1 + \sqrt{\frac{9}{2} + \frac{\lambda_1}{4\lambda_2} + \frac{\lambda_2}{4\lambda_1}} < \mu < 1 + \sqrt{4 + \frac{1}{\lambda_2} + \frac{1}{\lambda_1}}$  and at  $\mu = 1 + \sqrt{4 + \frac{1}{\lambda_2} + \frac{1}{\lambda_1}}$  they become unstable foci through a Neimark-Sacker bifurcation.*

**Proof.** The analysis of the local stability of a fixed point is obtained through the localization of

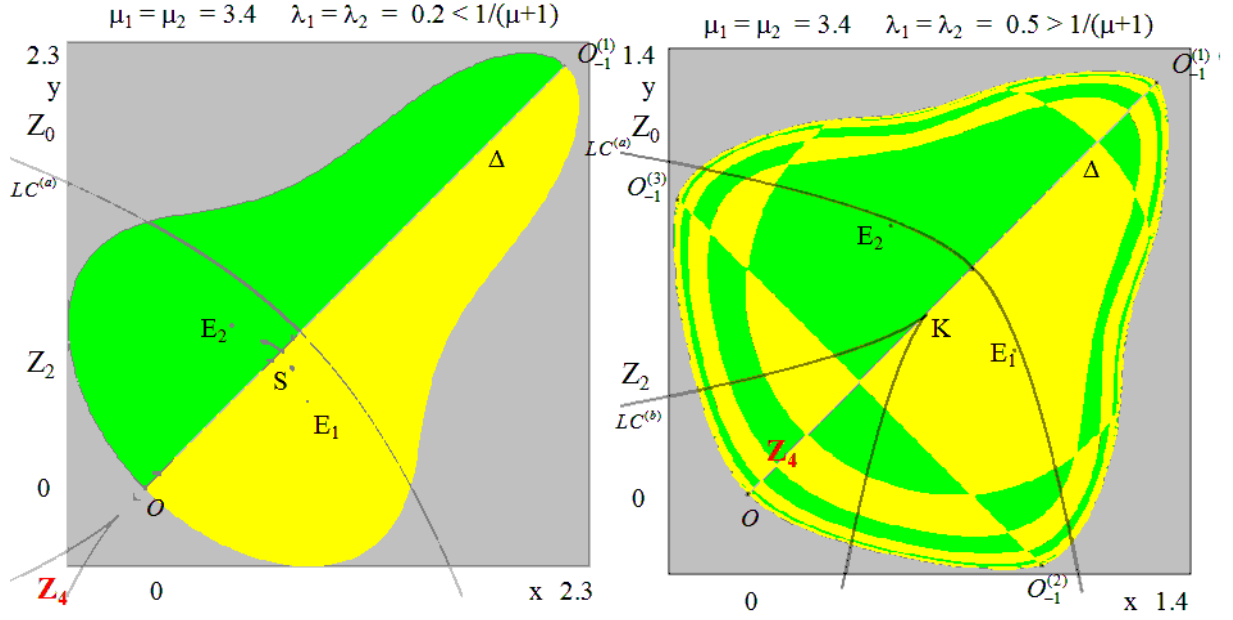


Figure 138: Coexisting Nash equilibria and corresponding basins.

the eigenvalues of the Jacobian matrix in the complex plane, where the Jacobian

$$(q_1, q_2) = \begin{bmatrix} 1 - \lambda_1 & \lambda_1 \mu (1 - 2q_2) \\ \lambda_2 \mu (1 - 2q_1) & 1 - \lambda_2 \end{bmatrix}$$

computed at the corresponding fixed point has to be considered. The stability conditions

$$P(1) = 1 - Tr + Det > 0; \quad P(-1) = 1 + Tr + Det > 0; \quad 1 - Det > 0$$

at the fixed point  $O = (0, 0)$  become

$$Tr^2 - 4Det = (\lambda_1 - \lambda_2)^2 + 4\lambda_1\lambda_2\mu^2 > 0 \quad \forall (\mu, \lambda) \in \Omega_3$$

$$P(1) = \lambda_1\lambda_2(1 + \mu)(1 - \mu) > 0 \quad \text{for } \mu < 1$$

$$P(-1) = 4 - 2(\lambda_1 + \lambda_2) + \lambda_1\lambda_2(1 - \mu^2) > 0 \quad \text{for } \mu < \sqrt{1 + 2\frac{2 - (\lambda_1 + \lambda_2)}{\lambda_1\lambda_2}}$$

At the fixed point  $S = (1 - 1/\mu, 1 - 1/\mu)$  we have

$$Tr^2 - 4Det = \lambda_1^2 + \lambda_2^2 + 14\lambda_1\lambda_2 + 4\lambda_1\lambda_2\mu(\mu - 4) \geq (\lambda_1 - \lambda_2)^2 \geq 0,$$

being  $\mu(\mu - 4) \geq -4$ . So the eigenvalues are always real at the fixed point  $S$ , and the stability conditions reduce to

$$P(1) = \lambda_1\lambda_2(-\mu^2 + 4\mu - 3) > 0 \quad \text{for } 1 < \mu < 3$$

$$P(-1) = \lambda_1\lambda_2\mu^2 - 4\lambda_1\lambda_2\mu + 3\lambda_1\lambda_2 + 2(\lambda_1 + \lambda_2) - 4 > 0 \quad \text{for } \mu < 2 + \sqrt{1 + 2\frac{2 - (\lambda_1 + \lambda_2)}{\lambda_1\lambda_2}}$$

Hence  $O$  is locally asymptotically stable (a stable node) in the region

$$\Omega_3(O) = \{(\mu, \lambda_1, \lambda_2) \in \Omega_3 | \mu < 1\}$$

and  $S$  is locally asymptotically stable (a stable node) in the region

$$\Omega_3(S) = \{(\mu, \lambda_1, \lambda_2) \in \Omega_3 | 1 < \mu < 3\}$$

At  $\mu = 1$  a transcritical bifurcation occurs at which  $O$  and  $S$  exchange stability, at  $\mu = 3$  a pitchfork bifurcation of  $S$  occurs at which the fixed points  $E_1$  and  $E_2$  are created. The main difference with respect to the homogeneous case lies in the fact that the eigendirections associated with the fixed points are no longer parallel and perpendicular to  $\Delta$ , and  $\Delta$  is no longer invariant.

At  $\mu = \sqrt{1 + 2\frac{2-(\lambda_1+\lambda_2)}{\lambda_1\lambda_2}} > 1$  a flip bifurcation of  $O$  occurs at which  $O$  is transformed from saddle to unstable node, and a saddle cycle of period 2 is created with stable set through  $O$ .

At  $\mu = 2 + \sqrt{1 + 2\frac{2-(\lambda_1+\lambda_2)}{\lambda_1\lambda_2}} > 3$  a flip bifurcation of  $S$  occurs at which  $S$  is transformed from saddle to unstable node, and a saddle cycle of period 2 is created with stable set through  $S$ .

The Jacobian matrix computed at the two fixed points  $E_1$  and  $E_2$  assumes, respectively, the forms,

$$J(E_1; \mu, \lambda_1, \lambda_2) = \begin{bmatrix} 1 - \lambda_1 & -\lambda_1 \left(1 - \sqrt{(\mu+1)(\mu-3)}\right) \\ -\lambda_2 \left(1 + \sqrt{(\mu+1)(\mu-3)}\right) & 1 - \lambda_2 \end{bmatrix}$$

and

$$J(E_2; \mu, \lambda_1, \lambda_2) = \begin{bmatrix} 1 - \lambda_1 & -\lambda_1 \left(1 + \sqrt{(\mu+1)(\mu-3)}\right) \\ -\lambda_2 \left(1 - \sqrt{(\mu+1)(\mu-3)}\right) & 1 - \lambda_2 \end{bmatrix}$$

It is easy to see that, like in the homogeneous case,  $E_1$  and  $E_2$  have the same characteristic equation, with  $Tr = 2 - \lambda_1 - \lambda_2$  and  $Det = 1 - \lambda_1 - \lambda_2 + \lambda_1\lambda_2(\mu+1)(\mu-3)$ .

The fixed points  $E_i$  are transformed from stable nodes into stable foci when

$$Tr^2 - 4Det = -4\lambda_1\lambda_2\mu^2 + 8\lambda_1\lambda_2\mu + 14\lambda_1\lambda_2 + \lambda_1^2 + \lambda_2^2 = 0$$

i.e. at  $\mu = 1 + \sqrt{\frac{9}{2} + \frac{\lambda_1}{4\lambda_2} + \frac{\lambda_2}{4\lambda_1}}$ .

Since

$$P(1) = \lambda_1\lambda_2(\mu+1)(\mu-3) > 0 \quad \text{for } \mu > 3$$

$$P(-1) = 4 - 2(\lambda_1 + \lambda_2) + \lambda_1\lambda_2(\mu+1)(\mu-3) > 0 \quad \text{for } \mu > 3$$

the stability conditions for  $E_i$ ,  $i = 1, 2$ , reduce to

$$Det - 1 = \lambda_1\lambda_2\mu^2 - 2\lambda_1\lambda_2\mu - 3\lambda_1\lambda_2 - \lambda_1 - \lambda_2 < 0.$$

Hence in the parameters space  $\Omega_3$  the region of stability of  $E_i$  is

$$\Omega_3(E_i) = \left\{ (\mu, \lambda_1, \lambda_2) \in \Omega_3 | \mu > 3 \text{ and } \mu < 1 + \sqrt{4 + \frac{\lambda_1 + \lambda_2}{\lambda_1\lambda_2}} \right\}$$



The equation  $\mu = 1 + \sqrt{4 + \frac{\lambda_1 + \lambda_2}{\lambda_1 \lambda_2}}$  defines a bifurcation surface in  $\Omega_3$  through which a supercritical Neimark-Sacker bifurcation occurs at which the fixed points  $E_1$  and  $E_2$  are transformed from stable to unstable foci and a stable closed invariant curve is created around them.  $\square$

From a comparison of the two propositions on local stability given above, it appears that the influence of heterogeneous behavior on the stability of the Nash equilibria is not too strong. However, in the case of coexisting stable Nash equilibria, an important question concerns the delimitation of their basins of attraction and the global bifurcations that cause qualitative modifications of their boundaries. In fact, due to the heterogeneous behavior of the two competing firms, the symmetry properties of the dynamical system which allowed us to obtain a simple analytical expression of the global bifurcation given in the proposition stated above no longer hold. Hence, the occurrence of contact bifurcations can only be revealed numerically. This is illustrated in fig.139, where in the left panel a contact between the boundary of the basin of  $E_1$  (formed by the stable set of the saddle point  $S$ ) and the critical curve  $LC$  that separates  $Z_2$  from  $Z_4$ . The portion of the basin of  $E_1$  that enters  $Z_4$  after the contact generates new preimages that give rise to a sequence of non-connected portion of the basin, as shown in the central panel of fig.139. However, as the equation of the boundary is not known in this case, an analytic computation of the values of the parameters at which the contact occurs is not possible. This is an usual occurrence, as the analytical expressions of the stable sets (that bound the basins) as well as the analytical expressions of the critical curves, are very rarely known. So, in order to study global bifurcations which are typical of two-dimensional noninvertible maps, numerical methods have to be employed. The delimitation of the basins of attraction of coexisting Nash equilibria requires a study of the global dynamical properties of the dynamical system, i.e. a study which is not based on the linear approximation of the map. Hence, the occurrence of contact bifurcations can only be revealed numerically. This happens frequently, since nonlinear dynamical systems are quite difficult to be analyzed mathematically. In order to study global bifurcations that are typical of two-dimensional noninvertible maps, numerical methods must be usually employed.

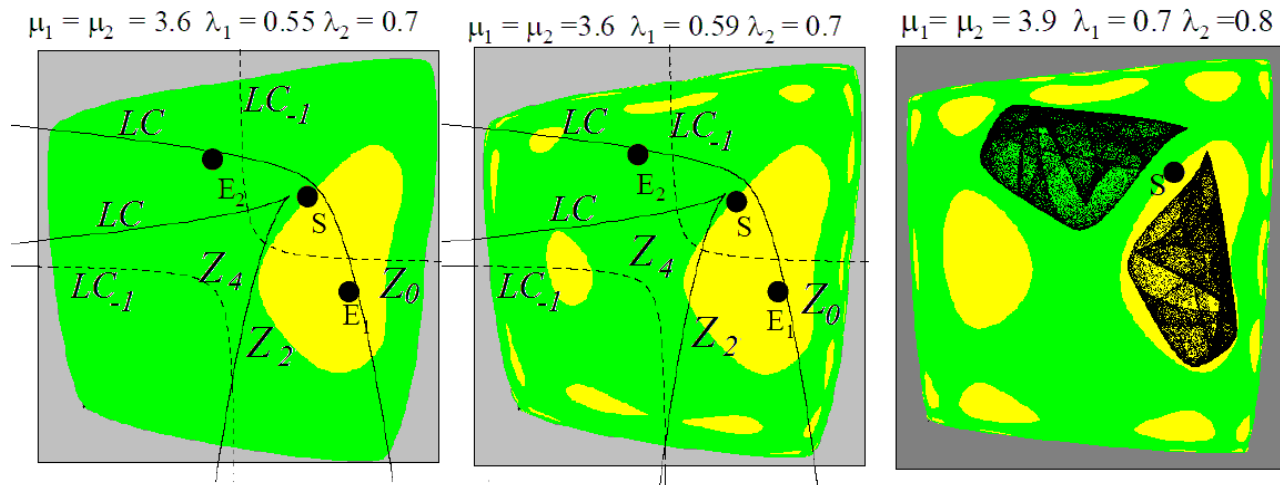


Figure 139: Basins, equilibrium points and attractors for the adaptive Cournot duopoly model with logistic reaction functions.

### 8.2.1 Adaptive expectations

Let us assume that, instead of using naive expectations, firms revise their beliefs according to the adaptive expectations rules

$$\begin{aligned} q_1^e(t+1) &= q_1^e(t) + \alpha_1 (q_1(t) - q_1^e(t)) = (1 - \alpha_1)q_1^e(t) + \alpha_1 R_1(q_2^e(t)) \\ q_2^e(t+1) &= q_2^e(t) + \alpha_2 (q_2(t) - q_2^e(t)) = (1 - \alpha_2)q_2^e(t) + \alpha_2 R_2(q_1^e(t)) \end{aligned} \quad (166)$$

where  $\alpha_i \in [0, 1]$  are referred to as the *adjustment coefficients*. This is a more enhanced way to form expectations, which takes into account the observed outputs and use them to correct the previous forecasting (a form of learning process). The rule of revision of adaptive expectations (166) defines a mapping in the beliefs space, and the real outputs at each step are obtained by the following mapping from beliefs to realizations

$$\begin{aligned} q_1(t) &= R_1(q_2^e(t)) \\ q_2(t) &= R_2(q_1^e(t)) \end{aligned}$$

Adaptive expectations have been proposed in many contexts as a more sophisticated kind of learning rule with respect to naive expectations.

If we insert this assumption in the duopoly models considered above we can easily see that the map in the belief space has the same form as in the case of adaptive adjustment with best reply and naive expectations. For example let us consider the case of logistic reaction functions. To simplify the notations let  $x(t) = q_1^e(t)$  and  $y(t) = q_2^e(t)$ . Inserting the reaction functions specified in (166), the time evolution of the competitors' beliefs is obtained by the iteration of the two-dimensional map

$$\begin{aligned} x(t+1) &= (1 - \alpha_1)x(t) + \alpha_1 \mu_1 y(t) (1 - y(t)) \\ y(t+1) &= (1 - \alpha_2)y(t) + \alpha_2 \mu_2 x(t) (1 - x(t)) \end{aligned}$$

that has the same form as the map (156).

### 8.3 Evolutionary games

Evolutionary game theory studies the behaviour of large populations of agents who repeatedly engage in strategic interactions. The individuals of each population  $i$  can choose among  $n_i$  alternative actions (or behaviors) whose payoffs (or utility) depends on the choices of others. At each time  $t$  the individuals of any population of players are classified according to the action they play. Thus, each population is subdivided into  $n_i$  classes of individuals playing the same strategy. The basic idea is that actions (or behaviors) which are more "fit" (i.e. give higher payoff or higher utility) given the current distribution of behaviors, tend over time to displace less fit behaviors. In other words, the distribution of behaviors in a population evolves, and fitter strategies (i.e. strategies that give higher payoffs) become more prevalent, that is, the classes of individuals playing more successful strategies grow up. The change over time of the numerosity of these classes, driven by payoffs' differences, generally influence payoffs, so that also growth rates of classes characterized by given behaviours will change. In this models, dynamics can indeed become quite complex. One can ask which behaviors will go extinct and which one will survive over time, whether the system approaches some stable steady-state, and so forth.

The birth of evolutionary game theory is marked by the publication of a series of papers by the mathematical biologist John Maynard Smith, in particular his book "Evolution and the Theory of Games" published in 1982. Maynard Smith adapted the methods of traditional game theory, which were created to model the behavior of rational economic agents, to the context of biological natural

selection. He also introduced some adaptive rules that govern the time evolution of strategies' distributions over a given population of players, so that the usual concepts of dynamical systems can be introduced, first of all the concepts of equilibrium points and their stability. After the book by Richard Dawkins "The selfish gene" in 1976 and the paper by Peter D. Taylor and Leo Jonker "Evolutionarily stable strategies and game dynamics" in 1978, the mainly adopted dynamic foundation of evolutionary dynamics is the one known as "replicator dynamics", explicitly expressed through differential or difference equations, thus recognizing the close links between this game-theoretic approach and the theory of dynamical systems. Replicator dynamics basically states that the number of individuals adopting a given strategy grows up if their expected payoff is greater than the average payoff of the whole population, whereas their number decreases if the payoff of their strategy is below the average.

In the biological interpretation, a population consists of animals each of which are genetically programmed to use some strategy that is inherited by its offspring. Initially, the population may consist of animals using different strategies (e.g. more or less aggressive, using different methods to get food etc.). In this context the payoff to an individual adopting a given strategy is called *fitness*, and this is generally compared with the average fitness in the population. Animals with higher fitness leave more offspring (by definition) so in the next generation the composition of the population will change. In the economic interpretation, the population changes because people play the game many times and consciously switch strategies. People are likely to switch to those strategies that give better payoffs and away from those that give poor payoffs. So, economists realized the value of the evolutionary approach to game theory in social science contexts, both as a method of providing foundations for the equilibrium concepts of traditional game theory, and as a tool for selecting among equilibria in games that admit more than one. Indeed, the two approaches sometimes lead to identical models: the replicator dynamic itself can be understood not only as a model of natural selection, but also as one of imitation of successful opponents.

While the majority of works in evolutionary game theory has been first undertaken by biologists to describe animal conflicts and genetic natural selection, and then by economists (competition among different marketing strategies, externalities and macroeconomic spillovers, heterogeneous agents in centralized markets), closely related models have been applied to questions in a variety of fields, including transportation science (trade-off between private and public transportation, network congestion), computer science (selfish routing of internet traffic), sociology. Some paradigms from evolutionary game theory are close relatives of certain models from physics, and so evolutionary game theory provides a common ground for scholars and practitioners from a wide range of disciplines.

### 8.3.1 Replicator dynamics with one population of players

At any time  $t$ , let us consider a large but finite population of  $N(t)$  agents, and assume that each agent chooses (each player plays) one and only one pure strategy taken from a finite set of  $k$  available strategies (or actions)  $S = \{s_1, \dots, s_k\}$ . Let  $N_i(t)$  be the number of agents that play strategy  $s_i$  at time  $t$ , and let  $x_i(t) = \frac{N_i(t)}{N(t)}$  be the corresponding fraction. The vector  $\mathbf{x} = (x_1(t), \dots, x_k(t))$  represents the state of the system at time  $t$ . As any agent is assumed to choose one and only one strategy at each time, then  $\sum_{i=1}^k N_i(t) = N$  and consequently

$$\sum_{i=1}^k x_i(t) = 1$$

holds. Hence the dimension (degrees of freedom) of the system described is  $k - 1$ .

In general an evolutionary process provides a selection mechanism that favors some population fraction  $x_i$  over others. This selection mechanism is expressed in terms of differential or difference equations (according to the continuous or discrete time scale considered) so that the usual methods for the study of stability, bifurcations and different kinds of attractors can be applied. A second important element is a mutation mechanism, i.e. how an invariant set is robust against perturbations of the state  $\mathbf{x}$ . This is indirectly taken into account through dynamic stability arguments. In a social or economic system, stability of an equilibrium may be thought as a convention. In fact, if a small displacement from an equilibrium is recovered so that the same equilibrium will prevail again in the long run despite the mutation, then this can be expressed by saying that the mutants will agree about the same convention.

A well known (and quite standard) dynamic evolutionary selection process is given by the so called "replicator dynamics". It is based on the assumption that individuals of a large population, that are programmed to play pure strategies, randomly pairwise match to play a two-person game with given payoffs. Of course the probability of matching with an agent playing a given strategy  $s_i$  is proportional to the fraction  $x_i$ . This implies that in the computation of the expected payoff associated to a given strategy, as well as in the computation of the average payoff in the whole population, one can interpret the fractions  $x_i(t)$  as probabilities, like in a game with mixed strategies. So, if  $A = \{a_{ij}\}$  is the symmetric payoffs matrix whose  $a_{ij}$  entry represents the payoff obtained by an agent playing pure strategy  $s_i$  in two-person match with an agent of the same population and playing pure strategy  $s_j$ , then the expected payoff by an agent programmed to play strategy  $s_i$  is

$$\pi_i = \sum_{j=1}^k a_{ij}x_j \quad (167)$$

and the average payoff in the whole population is

$$\bar{\pi} = \sum_{i=1}^k \pi_i x_i = \sum_{i=1}^k \sum_{j=1}^k a_{ij} x_i x_j . \quad (168)$$

The replicator dynamics state that the rate of change of a given population share associated to strategy  $s_i$  is proportional to its relative fitness, measured as the difference between the expected fitness for strategy  $s_i$  and the average fitness of the population

$$\dot{x}_i = (\pi_i(\mathbf{x}) - \bar{\pi}(\mathbf{x})) x_i . \quad (169)$$

The derivation of this dynamic equation can be outlined as follows.

Suppose that payoffs represent the incremental effects from playing the game measured as the number of offspring per unit time, and suppose that each offspring inherits its single parent's strategy (a true breeding of strategy, i.e. an agent always passes down a certain attitude in playing the game to its offsprings) If reproduction takes place continuously over time, then birthrate at any time  $t$  of individuals programmed to play pure strategy  $s_i$  is  $r + \pi_i(\mathbf{x})$ , where  $r = \beta - \delta$  is the background growth rate of individuals in the population (birth rate  $\beta$  minus death rate  $\delta$  independent of the outcomes in the game). Then the population dynamics becomes

$$\dot{N}_i = (r + \pi_i(\mathbf{x})) N_i .$$

As  $N_i(t) = N(t)x_i(t)$  it follows that  $\dot{N}_i = \dot{N}x_i + N\dot{x}_i$ , hence  $N\dot{x}_i = \dot{N}_i - \dot{N}x_i$ . Now, from  $N(t) = \sum_{i=1}^k N_i(t)$  follows that  $\dot{N} = \sum_{i=1}^k \dot{N}_i = \sum_{i=1}^k (r + \pi_i(\mathbf{x})) N_i = r \sum_{i=1}^k N_i(t) + \sum_{i=1}^k \pi_i(\mathbf{x})x_i(t)N(t) = rN(t) + \bar{\pi}(\mathbf{x})N(t) = (r + \bar{\pi}(\mathbf{x}))N(t)$ , so

$$N\dot{x}_i = \dot{N}_i - \dot{N}x_i = (r + \pi_i(\mathbf{x}))N_i - (r + \bar{\pi}(\mathbf{x}))N(t)x_i$$

and dividing both sides by  $N(t)$  (169) is get.

Notice that the growth rate is independent of the background birthrate and deathrate. Moreover if the payoff matrix is replaced by a positive affine transformation

$$\tilde{\mathbf{A}} = \lambda \mathbf{A} + \mu$$

with  $\lambda > 0$ , i.e. all the entries of the payoff matrix are multiplied by the same positive factor and/or all increased or decreased by the same quantity, then the effect of such a payoff transformation is equivalent to a change of time scale by the factor  $\lambda > 0$ . In this case, the invariance and stability properties are not changed, the only difference being that the population state moves along the phase curves with a different velocity.

As an example, let us consider a binary evolutionary game, i.e. a game played by the individuals of a population where each agent can choose between two different actions (or strategies): at time  $t$  a fraction  $x(t) \in [0, 1]$  of individuals play strategy  $s_1$  and the complementary fraction  $(1 - x(t))$  plays  $s_2$ . Let  $a_{ij}$  be the payoff obtained by an individual playing  $s_i$  against an individual playing  $s_j$ . Of course the game is *symmetric*, hence only one entry is sufficient to describe it (a simple matrix instead of a bimatrix)

$$\mathbf{A} = \begin{bmatrix} a_{11} & a_{12} \\ a_{21} & a_{22} \end{bmatrix} \quad (170)$$

or in the following (more informative) strategic form where the strategies are explicitly represented together with the respective population shares

$$\begin{array}{cc|cc} & & x & (1-x) \\ & & s_1 & s_2 \\ x & s_1 & a_{11} & a_{12} \\ (1-x) & s_2 & a_{21} & a_{22} \end{array}$$

The expected payoffs associated to strategies  $s_1$  and  $s_2$  are  $\pi_1 = a_{11}x + a_{12}(1-x) = (a_{11} - a_{12})x + a_{12}$  and  $\pi_2 = a_{21}x + a_{22}(1-x) = (a_{21} - a_{22})x + a_{22}$  respectively, or in matrix form:

$$\begin{bmatrix} \pi_1 \\ \pi_2 \end{bmatrix} = \mathbf{A}\mathbf{x} = \begin{bmatrix} a_{11} & a_{12} \\ a_{21} & a_{22} \end{bmatrix} \begin{bmatrix} x_1 \\ x_2 \end{bmatrix} = \begin{bmatrix} a_{11} & a_{12} \\ a_{21} & a_{22} \end{bmatrix} \begin{bmatrix} x \\ 1-x \end{bmatrix}$$

and the average population payoff  $\bar{\pi} = \pi_1x + \pi_2(1-x) = [(a_{11} - a_{12})x + a_{12}]x + [(a_{21} - a_{22})x + a_{22}](1-x)$ , or in matrix form

$$\mathbf{x}^T \mathbf{A} \mathbf{x} = (x_1, x_2) \begin{bmatrix} a_{11} & a_{12} \\ a_{21} & a_{22} \end{bmatrix} \begin{bmatrix} x_1 \\ x_2 \end{bmatrix}$$

with  $x_1 = x$  and  $x_2 = 1 - x$ .

All in all, the replicator dynamics (169) of  $x_1(t) = x(t)$  becomes

$$\dot{x} = [\pi_1(x) - \bar{\pi}(x)]x = [\pi_1(x) - (\pi_1(x)x + \pi_2(x)(1-x))]x = x(1-x)[\pi_1(x) - \pi_2(x)] \quad (171)$$

hence

$$\dot{x} = x(1-x)[(a_{11} - a_{21})x - (a_{22} - a_{12})(1-x)] \quad (172)$$

from which it is evident that equilibrium points are  $x^* = 0$  (all agents play strategy  $s_2$ ),  $x^* = 1$  (all agents play strategy  $s_1$ ) and, if any, points  $x^* \in (0, 1)$  such that the fitness associated to the two strategies is the same, i.e. expected payoffs satisfy the equation  $\pi_1(x^*) = \pi_2(x^*)$ . This equilibrium fraction  $x^*$  is equal to the Nash equilibrium in mixed strategies of the game (where  $x$  is interpreted as a probability to play  $s_1$ ), with  $x^* = \frac{a_{22}-a_{12}}{a_{11}+a_{22}-a_{12}-a_{21}}$ . However under the evolutionary interpretation we can also study the stability of these equilibrium points, on the basis of the 1-dimensional nonlinear dynamic equation (172). Indeed, a complete classification of existence and stability of equilibrium points in a one-population evolutionary game with two strategies is possible.

Let us consider the 2x2 payoff matrix (170). In order to reduce the number of parameters we can obtain an equivalent game by subtracting  $a_{21}$  from column 1 and  $a_{12}$  from column 2, to obtain the equivalent matrix

$$A = \begin{bmatrix} a_1 & 0 \\ 0 & a_2 \end{bmatrix}$$

where  $a_1 = a_{11} - a_{21}$  and  $a_2 = a_{22} - a_{12}$ . The following classification holds:

1. If  $a_1 < 0$  and  $a_2 < 0$  then  $x^* = \frac{a_2}{a_1 - a_2}$  is a stable Nash equilibrium, where  $x^* = 0$  and  $x^* = 1$  are unstable equilibrium points (and are not Nash equilibria). An example is the chicken game.
2. If  $a_1 > 0$  and  $a_2 > 0$  then  $x^* = \frac{a_2}{a_1 - a_2}$  is an unstable Nash equilibrium and the boundary equilibria (where all the population plays the same strategy) are asymptotically stable Nash equilibria. These are coordination games, like the battle of sexes. In this case the intermediate equilibrium  $x^* \in (0, 1)$  separates the two basins of attraction.
3. If  $a_1 a_2 \leq 0$ , a dominant strategy exists and one of the boundary equilibria is the global asymptotic attractor. If  $a_1 > 0$  (hence  $a_2 \leq 0$ ), this equilibrium is  $x = 1$ , and if  $a_1 < 0$  it is  $x = 0$ . This is the case of prisoner dilemma with, for instance,

$$A = \begin{bmatrix} 1 & -1 \\ 2 & 0 \end{bmatrix}$$

for which  $a_1 = -a_2 = -1$ .

These cases are summarized in fig. 140, where the 1-dimensional phase diagrams are shown.

Another famous example is the Hawk-Dove game, represented by the following payoff matrix.

$$\begin{array}{cc} & \begin{array}{cc} x & (1-x) \\ s_1(Hawk) & s_2(Dove) \end{array} \\ \begin{array}{cc} x & (1-x) \\ s_1(Hawk) & s_2(Dove) \end{array} & \begin{array}{cc} \frac{v}{2} - c; \frac{v}{2} - c & v; 0 \\ 0; v & \frac{v}{2}; \frac{v}{2} \end{array} \end{array} \quad (173)$$

Individuals of a large population have two strategies: behave aggressively ( $s_1$ ) or remissively ( $s_2$ ). A given resource  $v$  is available (for example food in an ecologic model, or customers in a marketing model). At any random match between two individuals of the population, if both behave remissively, a cooperation agreement is reached and the resource is shared (50-50),  $\frac{v}{2}$  each; if one is aggressive and the other one remissive, then the aggressive takes all the resource and the remissive one takes nothing;

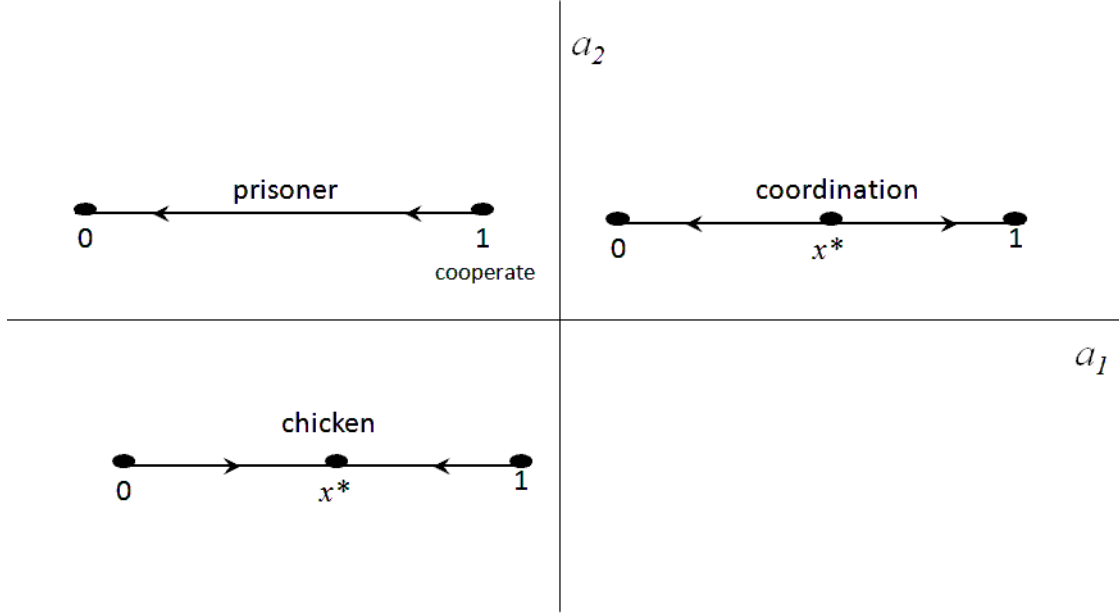


Figure 140: One-dimensional phase portraits of different cases of 2x2 population game endowed with replicator dynamics.

if both are aggressive then they fight to conquest the resource, and this fight has a cost  $c$ , and at the end of the fight they get  $\frac{v}{2}$  each, so the payoff is  $\frac{v}{2} - c$  each.

The classical Hawk-Dove game is obtained when injuries due to fighting are higher than the resource gained,  $c > \frac{v}{2}$ . Instead, when  $c < \frac{v}{2}$  a prisoner dilemma is obtained.

As an example of Hawk-Dove Game we consider the following bimatrix of payoffs (notice that due to the symmetry of the game double entries may be omitted as the payoff matrix of Doves is the transpose of the payoff matrix of Hawks) obtained for  $v = c = 2$ .

$$\begin{array}{cc}
 & \begin{array}{cc} x & (1-x) \\ s_1(Hawk) & s_2(Dove) \end{array} \\
 \begin{array}{cc} x & s_1(Hawk) \\ (1-x) & s_2(Dove) \end{array} & \begin{array}{cc} -1; -1 & 2; 0 \\ 0; 2 & 1; 1 \end{array}
 \end{array}$$

The payoffs of strategies  $s_1$  and  $s_2$  are given by

$$\begin{bmatrix} \pi_{s_1} \\ \pi_{s_2} \end{bmatrix} = \begin{bmatrix} -x + 2(1-x) \\ (1-x) \end{bmatrix}$$

and the average payoff of the population is:

$$\bar{\pi} = \mathbf{x}^T \mathbf{A} \mathbf{p} = [x \quad (1-x)] \begin{bmatrix} -1 & 2 \\ 0 & 1 \end{bmatrix} \begin{bmatrix} x \\ (1-x) \end{bmatrix} = -x^2 + 2(1-x)x + (1-x)^2$$

and the replicator dynamics are given by

$$\dot{x} = x(1-x)(\pi_{s_1}(x) - \pi_{s_2}(x)) = x(1-x)(1-2x)$$

It is straightforward to see that three equilibrium points exist in  $[0, 1]$ :  $x_1 = 0$ ,  $x_2 = 1$  and  $x_3 = \frac{1}{2}$ . Moreover,  $\dot{x} > 0$  for  $x < x_3$  and  $\dot{x} < 0$  per  $x > x_3$ . Hence  $x_3$  is the only evolutionary stable equilibrium. In other words, this evolutionary game states that populations formed by all aggressive individuals and all remissive individuals are unstable, so any mutation in the composition of the population (i.e. the entrance of some remissive individuals in a population of all aggressive ones, or the entrance of some aggressive individuals in a population of all remissive ones) spreads out destroying the pure composition, and a mix of aggressive and remissive individuals is reached in the long run, which is stable with respect to population mutations.

Let us consider now the case of prisoner dilemma obtained from (173) with  $c < \frac{v}{2}$ , for example  $v = 2; c = \frac{1}{2}$

$$\begin{array}{cc} & \begin{array}{cc} x & (1-x) \end{array} \\ \begin{array}{cc} x & (1-x) \end{array} & \begin{array}{cc} \begin{array}{cc} s_1 & s_2 \end{array} \\ \begin{array}{cc} \frac{1}{2}; \frac{1}{2} & 2; 0 \\ 0; 2 & 1; 1 \end{array} \end{array} \end{array}$$

In this case  $s_1$  is the dominant strategy, and the replicator equation is given by

$$\dot{x} = x(1-x)(\pi_{s_1}(x) - \pi_{s_2}(x)) = x(1-x)\left(1 - \frac{1}{2}x\right)$$

with the only feasible equilibria  $x_1 = 0$  and  $x_2 = 1$  (of course the further equilibrium point  $x_3 = \frac{1}{2}$  is not feasible).

As expected, in the long run the only possible evolution is towards the globally stable equilibrium  $x = 1$ , i.e. the whole population playing the dominant strategy  $s_1$ .

Up to now, we only considered examples where the individuals of a population have two available strategies, and the replicator dynamics is a one-dimensional continuous time dynamical system in the interval  $[0, 1]$ . Of course, an arbitrary finite number of strategies can be considered, say  $k > 1$  strategies, and the replicator dynamics becomes a  $k - 1$  dimensional system in the space defined by  $\sum_{i=1}^k x_i$ .

As an example, let us consider the following game with three strategies characterized by the payoff matrix

$$A = \begin{bmatrix} & s_1 & s_2 & s_3 \\ s_1 & 1 & 2+a & 0 \\ s_2 & 0 & 1 & 2+a \\ s_3 & 2+a & 0 & 1 \end{bmatrix}$$

that, for  $a = 0$ , gives the famous Rock-Scissors-Paper game (Rock loses against Paper, Scissors loses against Rock, Paper loses against Scissors) equivalent to the game represented by the following payoff matrix (subtract 1 from any entry to get the classical representation)

$$A = \begin{bmatrix} & R & S & P \\ R & 1 & 2 & 0 \\ S & 0 & 1 & 2 \\ P & 2 & 0 & 1 \end{bmatrix}$$

The equations of replicator dynamics are

$$\begin{aligned} \dot{x}_1 &= [x_1 + (2+a)x_2 - \mathbf{x}^T \mathbf{A} \mathbf{x}] x_1 \\ \dot{x}_2 &= [x_2 + (2+a)x_3 - \mathbf{x}^T \mathbf{A} \mathbf{x}] x_2 \\ \dot{x}_3 &= [x_3 + (2+a)x_1 - \mathbf{x}^T \mathbf{A} \mathbf{x}] x_3 \end{aligned}$$



which is a two-dimensional dynamical system as from  $x_1 + x_2 + x_3 = 1$  one can consider, for example, only the dynamics of  $x_1$  and  $x_2$  as  $x_3 = 1 - x_1 - x_2$ . Without entering the details, we state that besides the usual three corner equilibria where all players play the same strategy, i.e.  $(1, 0, 0)$ ,  $(0, 1, 0)$  and  $(0, 0, 1)$ , a unique interior equilibrium exists, given by  $x^* = (\frac{1}{3}, \frac{1}{3}, \frac{1}{3})$ . This interior equilibrium is stable (a stable focus) under the replicator dynamics if  $a > 0$ , unstable (unstable focus) if  $a < 0$  and it is a center in the case of classical R-S-P game  $a = 0$ . A graphical depiction is shown in fig. 141, where the triangular representation of the simplex is used, see also fig. 142.

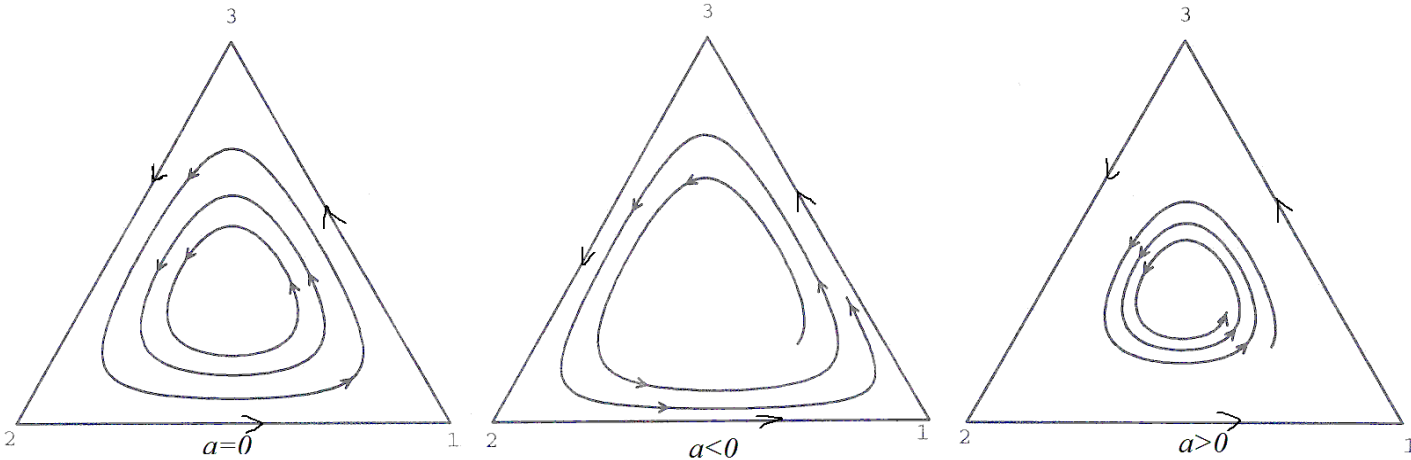


Figure 141: Phase portraits on the simplex for the modified R-S-P game with parameter  $a$ .

In this graphical representation the three vertexes correspond to the cases where all players use the same strategy (the corner equilibria). Notice that all the sides of the triangle, where the players play two of the three strategies, are invariant lines.

### 8.3.2 Replicator dynamics with two populations of players

So far the studied interactions have all been modelled as symmetric and pairwise random matches between individuals of the same population. We now consider two different populations, each with its own possible strategies and related payoff matrix, that describes the gains when an individual of a population only interacts with individuals of the other population. Let us consider the case of two populations, say  $P_a$  and  $P_b$ , each with two possible strategies, say  $\{a_1, a_2\}$  for  $P_a$  and  $\{b_1, b_2\}$  for  $P_b$ . Let  $x_1(t)$ ,  $x_2(t)$  be the fractions of the population  $P_a$  playing strategies  $a_1$  and  $a_2$  respectively, with  $x_1(t) + x_2(t) = 1$  for each  $t$ ,  $y_1(t)$ ,  $y_2(t)$  the fractions of the population  $P_b$  playing strategies  $b_1$  and  $b_2$ , with  $y_1(t) + y_2(t) = 1$  for each  $t$ , with the following payoff bimatrix giving the respective payoffs gained in pairwise matchings between individuals of different populations

$$\begin{array}{cc}
 & P_b \\
 & y_1 = y & y_2 = (1 - y) \\
 P_a & & \\
 x_1 = x & a_1 & a_{11}; b_{11} & a_{12}; b_{12} \\
 x_2 = (1 - x) & a_2 & a_{21}; b_{21} & a_{22}; b_{22}
 \end{array}$$

where  $\mathbf{A} = \{a_{ij}\}$  and  $\mathbf{B} = \{b_{ij}\}$  are the payoff matrix of population  $P_a$  and  $P_b$  respectively.

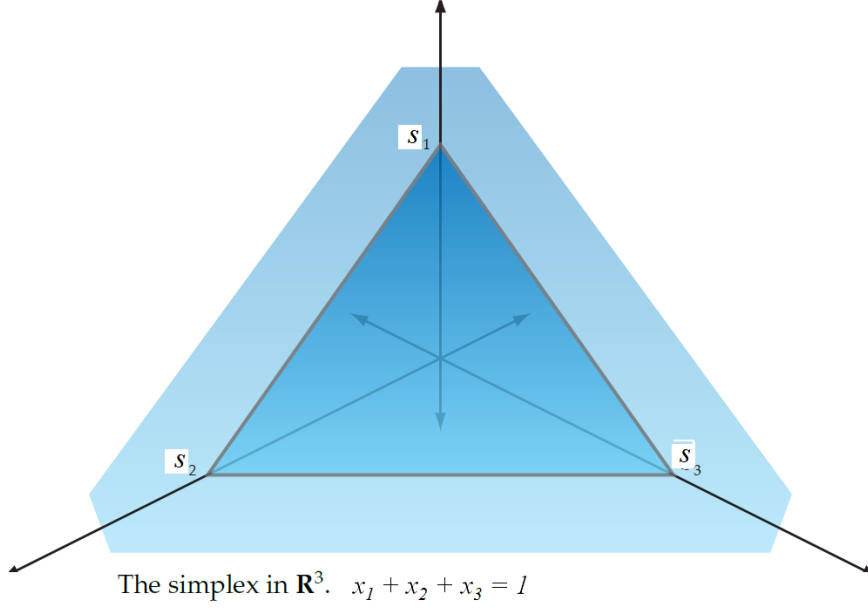


Figure 142: Simplex  $x_1 + x_2 + x_3 = 1$  in the 3-dim space  $\mathbb{R}^3$

The expected payoffs of a player of population  $P_a$  associated to its strategies are

$$\begin{aligned}\pi_{a_1}(y) &= a_{11}y_1 + a_{12}y_2 = a_{11}y + a_{12}(1-y) \\ \pi_{a_2}(y) &= a_{21}y_1 + a_{22}y_2 = a_{21}y + a_{22}(1-y)\end{aligned}$$

Average payoff of population  $P_a$  is

$$\bar{\pi}_a(x, y) = x_1\pi_{a_1} + x_2\pi_{a_2} = x\pi_{a_1}(y) + (1-x)\pi_{a_2}(y) = \mathbf{x}^T \mathbf{A} \mathbf{y}$$

where  $\mathbf{y} = \begin{bmatrix} y \\ 1-y \end{bmatrix}$  and  $\mathbf{x} = \begin{bmatrix} x \\ 1-x \end{bmatrix}$ .

Analogously for the other population  $P_b$  we get:

$$\begin{aligned}\pi_{b_1}(x) &= b_{11}x_1 + b_{21}x_2 = b_{11}x + b_{21}(1-x) \\ \pi_{b_2}(x) &= b_{12}x_1 + b_{22}x_2 = b_{12}x + b_{22}(1-x)\end{aligned}$$

and the average payoff of population  $P_b$  is

$$\bar{\pi}_b(x, y) = y_1\pi_{b_1} + y_2\pi_{b_2} = y\pi_{b_1}(x) + (1-y)\pi_{b_2}(x) = \mathbf{y} \mathbf{B}^T \mathbf{x}$$

Following the same arguments as in the previous section, the equations of replicator dynamics assume the form

$$\begin{cases} \dot{x} = [\pi_{a_1}(y) - \bar{\pi}_a(x, y)] x & \Rightarrow \begin{cases} \dot{x} = x(1-x)(\pi_{a_1}(y) - \pi_{a_2}(y)) \\ \dot{y} = y(1-y)(\pi_{b_1}(x) - \pi_{b_2}(x)) \end{cases} \end{cases} \quad (174)$$

$$\Rightarrow \begin{cases} \dot{x} = (\mathbf{e}_1^T \mathbf{A} \mathbf{y} - \mathbf{x}^T \mathbf{A} \mathbf{y}) x \\ \dot{y} = (\mathbf{e}_1^T \mathbf{B}^T \mathbf{x} - \mathbf{y}^T \mathbf{B}^T \mathbf{x}) y \end{cases} \quad (175)$$

where  $\mathbf{e}_1^T = [1 \ 0]$ .

Also in this case a complete classification of replicator dynamics for 2-population games with 2 strategies for each population can be given. First of all, notice that these are nonlinear 2-dimensional dynamical systems in continuous time with phase space given by the unit square  $[0, 1] \times [0, 1]$ . It is also important to notice that the edges of this square, located along the lines  $x = 0$ ,  $y = 0$ ,  $x = 1$ ,  $y = 1$  are invariant segments. Moreover the four vertexes  $(0, 0)$ ,  $(1, 0)$ ,  $(0, 1)$ ,  $(1, 1)$  of the unit square are always equilibrium points under the replicator dynamics.

After replacing the expressions of expected payoffs into the dynamic model (174) we get

$$\begin{aligned}\dot{x} &= x(1-x)[(a_{11} - a_{21})y + (a_{12} - a_{22})(1-y)] \\ \dot{y} &= y(1-y)[(b_{11} - b_{12})x + (b_{21} - b_{22})(1-x)]\end{aligned}$$

Like in the symmetric case with one population, an equivalent game can be obtained with the bimatrix

$$\begin{array}{cc} & P_b \quad \begin{array}{l} y_1 = y \\ y_2 = (1-y) \end{array} \\ \begin{array}{l} P_a \\ x_1 = x \\ x_2 = (1-x) \end{array} & \begin{array}{cc} & \begin{array}{l} b_1 \\ b_2 \end{array} \\ \begin{array}{l} a_1 \\ a_2 \end{array} & \begin{array}{l} \alpha_1; \beta_1 \\ 0; 0 \\ \alpha_2; \beta_2 \end{array} \end{array}\end{array}$$

where

$$\begin{aligned}\alpha_1 &= a_{11} - a_{21} \\ \alpha_2 &= a_{22} - a_{12} \\ \beta_1 &= b_{11} - b_{12} \\ \beta_2 &= b_{22} - b_{21}\end{aligned}$$

The dynamical system obtained through the replicator equations becomes

$$\begin{cases} \dot{x} = x(1-x)(\alpha_1 y - \alpha_2(1-y)) \\ \dot{y} = y(1-y)(\beta_1 x - \beta_2(1-x)) \end{cases}$$

The following cases are obtained:

1. (Corner case) If  $\alpha_1 \alpha_2 < 0$ , i.e. they have opposite signs, then a dominant strategy exists. If  $\alpha_1 < 0 < \alpha_2$  players of the population  $P_a$  have a dominant strategy,  $x = 0$ , and the players of population  $P_b$  play best reply to this strategy and the unique stable equilibrium is  $(0, 0)$ . If  $\alpha_1 > 0 > \alpha_2$ , then  $(1, 1)$  is the unique global attractor.
2. (Saddle) If  $\alpha_1, \alpha_2, \beta_1, \beta_2 > 0$ , then an interior Nash equilibrium exists given by  $S = (x^*, y^*)$  with  $x^* = \frac{\alpha_2}{\alpha_1 + \alpha_2}$  and  $y^* = \frac{\beta_2}{\beta_1 + \beta_2}$ , which is a saddle point. Two stable Nash equilibria exist in the corners  $E_1 = (1, 1)$  and  $E_0 = (0, 0)$ , whose basins are bounded by the stable set of the saddle  $S$ . If  $\alpha_1, \alpha_2, \beta_1, \beta_2 < 0$ , the stable Nash equilibria are  $(1, 0)$  and  $(0, 1)$ .
3. (Center) If  $\alpha_1, \alpha_2 < 0$  and  $\beta_1, \beta_2 > 0$ , then  $S = (x^*, y^*)$  with  $x^* = \frac{\alpha_2}{\alpha_1 + \alpha_2}$  and  $y^* = \frac{\beta_2}{\beta_1 + \beta_2}$  is the unique interior Nash equilibrium and its stability depends of the specification of the game. We can also get closed orbits on which periodic motion occurs, see the example of matching pennies given below.

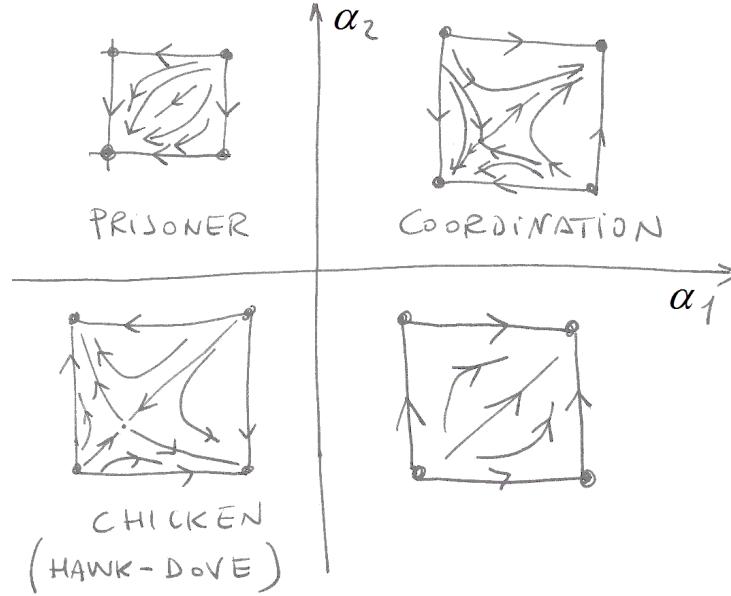


Figure 143: The different phase portraits for 2x2 population games with two-populations endowed with replicator dynamics.

In the case of symmetric payoffs, i.e.  $b_{ij} = a_{ji}$ , so that  $\beta_1 = \alpha_1$  and  $\beta_2 = \alpha_2$ , the classification is summarized in fig.

A famous example is the Matching Penny game. It is a zero-sum game between two players, say Player A and Player B, such that each player has a penny and must secretly turn the penny to heads or tails. The two players then reveal their choices simultaneously. If the pennies match (both heads or both tails) Player B keeps both pennies, so wins one from Player A (+1 for B, -1 for A). If the pennies do not match (one heads and one tails) Player A keeps both pennies, so receives one from Player B (-1 for B, +1 for A). It is the two strategy equivalent of Rock, Scissors, Paper game, and the payoff matrix is given by

	<i>B</i>	<i>y</i>	$(1 - y)$
<i>A</i>			
<i>x</i>		-1; 1	1; -1
$(1 - x)$		1; -1	-1; 1

The replicator dynamic equation becomes

$$\begin{aligned} \dot{x} &= x(1-x)(\pi_{A,1}(y) - \pi_{A,2}(y)) = x(1-x)(-4y+2) \\ \dot{y} &= y(1-y)(\pi_{B,1}(x) - \pi_{B,2}(x)) = y(1-y)(4x-2) \end{aligned}$$

The equilibrium points are  $(0, 0), (1, 1), (0, 1), (1, 0), (\frac{1}{2}, \frac{1}{2})$

To study their stability we consider the Jacobian matrix

$$J(x, y) = \begin{bmatrix} (1-2x)(-4y+2) & -4x(1-x) \\ 4y(1-y) & (1-2y)(4x-2) \end{bmatrix}$$

from which

$$J(0,0) = \begin{bmatrix} 2 & 0 \\ 0 & -2 \end{bmatrix}$$

has eigenvalues  $\lambda_1 = 2, \lambda_2 = -2$  hence the equilibrium  $(0,0)$  is a saddle.

$$J(1,1) = \begin{bmatrix} 2 & 0 \\ 0 & -2 \end{bmatrix}$$

has eigenvalues  $\lambda_1 = 2, \lambda_2 = -2$  hence the equilibrium  $(1,1)$  is a saddle.

$$J(0,1) = \begin{bmatrix} -2 & 0 \\ 0 & 2 \end{bmatrix}$$

has eigenvalues  $\lambda_1 = -2$  and  $\lambda_2 = 2$  hence  $(0,1)$  is a saddle too.

$$J(1,0) = \begin{bmatrix} -2 & 0 \\ 0 & 2 \end{bmatrix}$$

has eigenvalues  $\lambda_1 = -2$  and  $\lambda_2 = 2$  hence  $(1,0)$  is a saddle as well. Finally,

$$J\left(\frac{1}{2}, \frac{1}{2}\right) = \begin{bmatrix} 0 & -1 \\ 1 & 0 \end{bmatrix}$$

and the characteristic equation is

$$\rho(\lambda) = \lambda^2 + 1 = 0$$

from which  $\lambda_1 = +i, \lambda_2 = -i$ . So, the inner equilibrium is a centre (see fig.144).

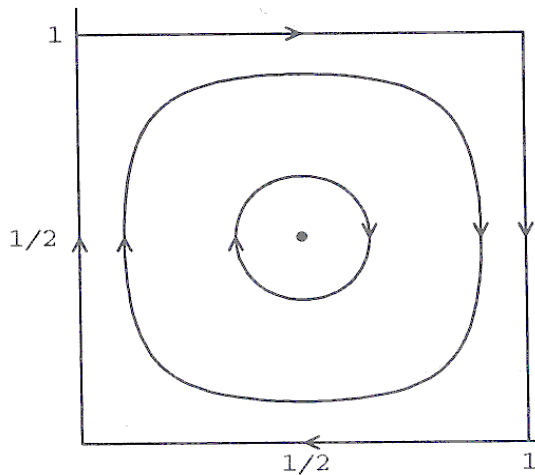


Figure 144: Phase portrait for the matching penny population game endowed with replicator dynamics.

As a final exercise let us consider the following Buyer-Seller game, characterized by the payoffs matrix

	$B$	$y$	$(1-y)$
$A$	$H$	$D$	
$x$	$I$	$3;2$	$2;1$
$(1-x)$	$T$	$4;3$	$1;4$

that describes a population  $A$  of buyers and a population  $B$  of sellers. Sellers have two possible strategies:  $H$  (be honest) and  $D$  (be dishonest). Buyers have two strategies:  $I$  (inspect the good they buy) and  $T$  (trust in honesty of sellers, hence do not inspect).

Let  $x(t)$  be the fraction of buyers that inspect in time period  $t$  and  $y(t)$  the fraction of honest sellers in the same period.

The replicator dynamics is

$$\begin{aligned}\dot{x} &= x(1-x)(1-2y) \\ \dot{y} &= y(1-y)(2x-1)\end{aligned}$$

The study of equilibria and their stability properties is an easy exercise.

Of course, the example becomes more interesting if payoffs are expressed with parameters that give a measure of how much is the damage a buyer incurs by purchasing a product from a dishonest seller without inspecting, or how much a honest seller is irritated by the inspection of the buyer, or how much is the cost for inspecting and so on.

### 8.3.3 Replicator dynamics in discrete time

A discrete time version of the replicator equation is often used, both in biological applications where populations with non overlapping generations are considered and in economic applications where strategy switching decisions are taken at discrete time periods. As usual, discrete time dynamics imply an attitude to oscillatory time paths due to overshooting in the dynamic adjustment.

The derivation of the discrete time replicator is quite similar, and even simpler, than the one described in continuous time. Let  $r$  be the background growth rate of the population, independent of the game played inside the population, and let  $N_i(t)$  be the number of individuals playing strategy  $s_i$ ,  $i = 1, \dots, k$ , at time  $t$ . The total number of individuals is  $N(t) = \sum_{i=1}^k N_i(t)$ . The state of the system is identified by the fractions  $x_i(t) = \frac{N_i(t)}{N(t)}$ ,  $i = 1, \dots, k$ , such that  $\sum_{i=1}^k x_i(t) = 1$ .

The growth rate of the portion of population playing strategy  $s_i$  is proportional to the average (or expected) payoff obtained by a player of that population class in random pairwise matches with other individuals of the same population

$$N_i(t+1) = [r + \pi_i(\mathbf{x}(t))] N_i(t)$$

where  $\pi_i(\mathbf{x})$  is given by (167). Summing up over classes  $i = 1, \dots, k$  we have

$$N(t+1) = [r + \bar{\pi}(\mathbf{x})] N(t)$$

as  $N_i(t) = N(t)x_i(t)$  and  $\sum x_i(t)\pi_i(\mathbf{x}(t)) = \bar{\pi}(\mathbf{x})$ . Dividing both sides of these two expressions we get

$$x_i(t+1) = \frac{r + \pi_i(\mathbf{x}(t))}{r + \bar{\pi}(\mathbf{x})} x_i(t) \tag{176}$$

provided that  $r + \pi_i(\mathbf{x}(t)) \geq 0$  for each  $i = 1, \dots, k$  and for each  $t$ . This is the discrete-time replicator dynamics with one population of players.

However another version can be proposed, which is more convenient in many cases because it avoids the positivity condition that may become problematic in economic applications. For example, in economic models where payoffs are given by profits,  $r + \pi_i(\mathbf{x}(t))$  may be negative for some periods even if it is positive in the long run. Nevertheless, values of  $x_i(t)$  outside the interval  $[0, 1]$  are

meaningless and even if such unfeasible values are obtained just at one time period then all the successive states are meaningless.

So, an interesting and useful alternative to (176) is obtained by considering a monotone transformation of payoffs given by  $u(\pi_i) = \exp(\alpha\pi_i)$ , with  $\alpha > 0$ , and consequently  $\bar{u} = \sum_{i=1}^k x_i \exp(\alpha\pi_i)$ .

The growth equation of the portion of population playing strategy  $s_i$  becomes

$$N_i(t+1) = \exp[r + \alpha\pi_i(\mathbf{x}(t))] N_i(t) = e^r e^{\alpha\pi_i(\mathbf{x}(t))} N_i(t) .$$

Summing up over classes  $i = 1, \dots, k$  we have

$$N(t+1) = \sum_{i=1}^k N_i(t) = e^r \sum_{i=1}^k e^{\alpha\pi_i(\mathbf{x}(t))} N_i(t) = e^r N(t) \sum_{i=1}^k e^{\alpha\pi_i(\mathbf{x}(t))} x_i(t) .$$

Dividing both sides of these two expressions we get

$$x_i(t+1) = \frac{e^{\alpha\pi_i(\mathbf{x}(t))}}{\sum_{i=1}^k x_i e^{\alpha\pi_i(\mathbf{x}(t))}} x_i(t) \quad (177)$$

which guarantees that  $x_i(t) \in [0, 1]$  for each  $t$  without further conditions.

As an example we propose a minority game, i.e. a population game characterized by the property that the players who select the option chosen by the minority are more rewarded. It is well known in the literature, and quite intuitive as well, that in a population of agents that repeatedly play a minority game in discrete time periods, oscillations between the two strategies are common. In fact, players that choose the majority strategy are oriented to revise their decision towards the option that has been chosen by the minority, so that oscillatory behaviours are typically observed. Such oscillations may be dumped and lead to convergence in the long run to an equilibrium, generally a Nash equilibrium characterized by identical payoffs associated to the two choices; in other cases, oscillations may continue indefinitely, through endogenous and self-sustained overshooting, so that the generic trajectory does not settle to any stationary equilibrium in the long run.

Let us consider a population of  $N$  players, each facing a binary choice between strategies  $R$  and  $L$ . At time  $t$  let  $x(t) \in [0, 1]$  be the fraction of agents playing  $R$  and, consequently, the share  $1 - x(t)$  plays  $L$  at the same time. Assume that the individual payoff of an agent employing a given strategy at time  $t$  depends only on the numbers of agents making the same choice or the other, say  $R(t) = R(x(t))$  and  $L(t) = L(x(t))$ . We now introduce a discrete-time evolutionary process to describe the number of agents that at each time period  $t = 0, 1, 2, \dots$  update their choice, under the assumption that payoff obtained by both fractions of players at time  $t$ , i.e.  $R(x(t))$  and  $L(x(t))$ , are common knowledge. The time evolution of the fraction  $x(t)$  of players choosing  $R$  is assumed to be monotonically influenced by the "gain" function

$$g(x) = R(x) - L(x) : [0, 1] \rightarrow \mathbb{R} \quad (178)$$

in the sense that higher gains cause an increase of the fraction of agents choosing  $R$ . The evolutionary selection dynamics in discrete time is expressed in the form of Exponential Replicator dynamics

$$\begin{aligned} x(t+1) = f(x(t)) &= \frac{x(t) \exp(\alpha R(x(t)))}{x(t) \exp(\alpha R(x(t))) + (1-x(t)) \exp(\alpha L(x(t)))} = \\ &= \frac{x(t)}{x(t) + (1-x(t)) \exp(-\alpha g(x))} \end{aligned} \quad (179)$$

where  $\alpha \geq 0$  is the speed of reaction, a parameter that expresses the propensity to switch to the opposite choice as a consequence of a payoff gain observed in the current time period. It is worth to remark that if  $x(0) \in [0, 1]$  then  $x(t) \in [0, 1]$  for each  $t \geq 0$ , as it follows from the evident inequality  $0 \leq \frac{x}{x+(1-x)\exp(-\alpha g(x))} \leq 1$ . Moreover, it is straightforward to see that  $x^* = 0$  and  $x^* = 1$ , which correspond to "pure strategies" where "all players play  $L$ " and "all players play  $R$ " respectively, are boundary equilibrium points. Interior equilibria exist at any  $x^*$  such that  $g(x^*) = 0$ , i.e. are characterized by identical payoffs.

Minority games are characterized by the property that players gain higher payoff when they choose the strategy which is chosen by the minority, i.e.  $R(x)$  is higher than  $L(x)$  when  $x$  is small, whereas  $R(x)$  is less than  $L(x)$  for values of  $x$  close to 1. A typical example is shown in fig. 145, where the payoff functions are linear, expressed by

$$R(x) = ax + b \ ; \ L(x) = cx + d \quad \text{with } b > d \text{ and } c > a \quad (180)$$

A first consequence of these assumption is that  $g'(x^*) < 0$ . When the evolutionary mechanism (179) is applied under these assumptions, a dynamic behaviour characterized by oscillations around the unique Nash equilibrium  $x^*$  is obtained, with oscillations that may converge or not to the Nash equilibrium in the long run according to its stability properties, as stated by the following proposition

**Proposition.** *If  $R : [0, 1] \rightarrow \mathbb{R}$  and  $L : [0, 1] \rightarrow \mathbb{R}$  are differentiable functions such  $R(0) > L(0)$ ,  $R(1) < L(1)$  and they intersect in only one interior point  $x^* \in (0, 1)$ , then the Nash equilibrium  $x^*$  is locally asymptotically stable, with oscillatory converge, provided that*

$$\alpha < \alpha_f = -\frac{2}{x^*(1-x^*)g'(x^*)} \quad (181)$$

where the derivative  $g'(x^*) = R'(x) - L'(x) < 0$  is the relative slope of the two payoff curves at their unique intersection  $x^*$ . As the parameter  $\alpha$  increases across the threshold value  $\alpha_f$  then a flip (or period doubling) bifurcation occurs.

**Proof.** The local stability condition immediately follows from the condition for local asymptotic stability  $-1 < f'(x^*) < 1$  that, from (179) becomes

$$-1 < 1 + \alpha x^* (1 - x^*) g'(x^*) < 1.$$

Being  $g'(x^*) < 0$  the right inequality is always satisfied, whereas the left one gives (181).□

A typical graph of the one-dimensional map (179) with payoff functions (180) is shown in fig. 145, obtained with parameters  $a = -0.5$ ,  $b = 0.5$ ,  $c = 0.8$ ,  $d = 0$  and  $\alpha = 7$ . In this case the Nash equilibrium  $x^* = \frac{d-b}{a-c} = \frac{5}{13}$  is unstable (being  $\alpha > \alpha_f = 6.5$ ) and the long run dynamics of the minority game settles on a stable cycle of period 2 (shown in the figure) starting from any initial condition  $x(0) \in (0, 1)$ .

As the speed of reaction  $\alpha$  is further increased the well known period-doubling route to chaos is observed, as shown in the bifurcation diagram of fig. 145. This is a quite expected and well known dynamic behavior in repeated minority games, characterized by contrarians' switches of choices associated with overshooting effects (represented by high values of the speed of reaction  $\alpha$ ).



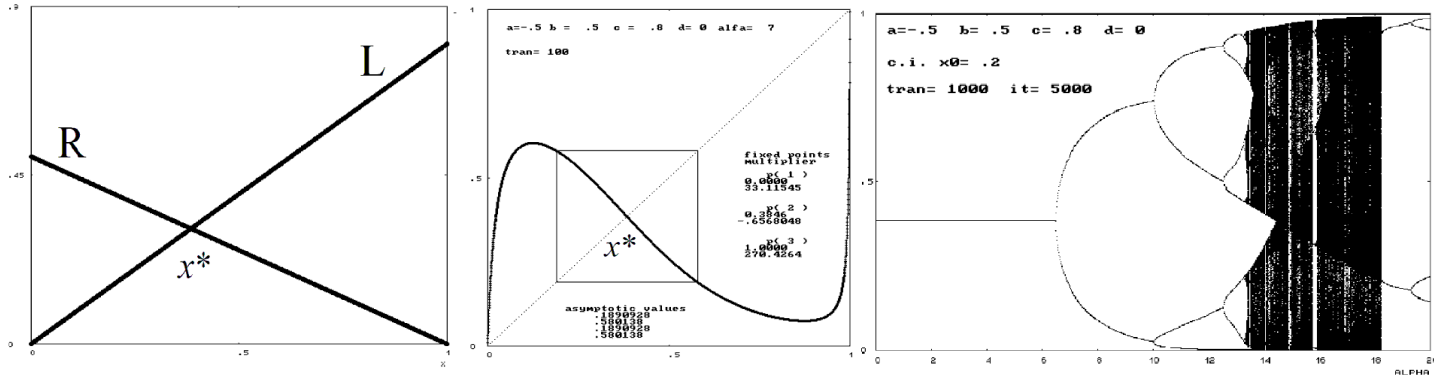


Figure 145: Left: Payoff curves for R choice and L choice as functions of fraction  $x$  of players choosing  $R$ . Center: iterated map with exponential replicator. Right: bifurcation diagram with bifurcation parameter  $\alpha$  (speed of reaction).

## 9 An introduction to optimal control in continuous time

Here we provide a very brief introduction to optimal control problems in continuous time. The following part does not aim at giving a complete nor mathematically detailed analysis of the topic, but just a non rigorous discussion on the theory of optimal control, some connections to the qualitative theory of dynamical systems and an overview on some applications in economics. We refer the reader to a more complete treatment in the bibliography.

In many economic application, it is necessary to solve a so-called optimal control problem, which assumes, in the easiest case, the form:

$$\max_{u(t) \in A(t)} \int_0^T f(x(t), u(t), t) dt + F(x(T), T) \quad (182)$$

such that:

$$\begin{cases} \dot{x} = g(x(t), u(t), t) \\ x(0) = x_0 \end{cases}$$

and with one of the following terminal conditions: (183)

$$(a) x(T) \text{ free} \quad (b) x(T) = x_T \quad (c) x(T) \geq x_T \quad (184)$$

where:

- $0$  is the *initial time*;
- $T \in (0, +\infty]$  is the *terminal time*;
- $x(t)$  is the *state variable* of the system, whose dynamics is determined by the following differential equation:
- $\dot{x} = g(x(t), u(t), t)$  (is) called the *state equation* or the *dynamics*;

- $u(t)$  is the *control*, to be determined to maximize the previous integral;
- $f(x(t), u(t), t)$  is the *instantaneous payoff*;
- $A(t)$  is the *constraint set* on the control, specifying that at each time  $t$  the control  $u(t)$  must belong to the set  $A(t)$ ;
- $F(x(T), T)$  is the *terminal payoff* (or scrap value or salvage value).

When  $T = +\infty$ , no condition is usually imposed on the state  $x(t)$ . In some cases, however, it is required that

$$\lim_{t \rightarrow +\infty} x(t) \geq \bar{x} .$$

Functions  $f(., ., .)$ ,  $g(., ., .)$  and  $F(., .)$  are assumed continuously differentiable.

Often in economic applications, in the problem (182) it is  $f(x(t), u(t), t) = f(x(t), u(t))$  and  $g(x(t), u(t))$ , i.e. the performance criterion and the differential equations do not depend directly on time.<sup>22</sup> In this case, the optimal control problem (182) is called *autonomous*. In many economic application it is also  $T = +\infty$  so that no scrap value is included in the problem, i.e.  $F(x(T), T) = 0$ . We will briefly review some other formulations of the basic problem, such as the formulation of the problem with discount, which is of primary importance in economics.

The control  $u(t)$  represents a choice variable that the agent can set continuously as long it is in the constraint set  $A(t)$ . Often this constraint on the control is imposed for reasons of feasibility. For instance, if the control  $u(t)$  represents the consumption of a good, this can not be negative, so that  $u(t) \geq 0$  for all  $t$ . In addition, some upper bound of consumption can be given, for instance through a budget constraint at time  $t$ ; denoting by  $B(t)$  the total budget of the agent, the constraint set  $A(t)$  becomes  $0 \leq u(t) \leq B(t)$ ,  $\forall t \in [0, T]$ .

Any function  $u(t)$ , with  $u(t) \in A(t)$  for all  $t \in [0, T]$ , such that  $u(t)$  is (piecewise) continuous represents an *admissible* control. Consider that we fix a particular admissible control, for instance  $u(t) = \bar{u}(t)$ . Then, for this choice of the control,  $\dot{x} = g(x(t), \bar{u}(t), t)$  is a (first order) differential equation that, together with the initial condition  $x(0) = x_0$ , determines entirely the trajectory of the state, i.e. the value of  $x(t)$  for all  $t \in [0, T]$ , which is called an *admissible* path provided that the constraints on the final state are met (e.g.  $x(T) = x_T$  or  $x(T) \geq x_T$ ). Thus, with this choice of  $\bar{u}(t)$ , the state and, consequently, the value of the performance criterion  $f(x(t), \bar{u}(t), t)$  is univocally determined. Since we are interested in maximizing the definite integral of the performance criterion over the interval  $[0, T]$ , the optimal control problem (182) consists in selecting, among all admissible controls  $u(t) \in A(t)$ , the control  $u^*(t)$  that maximizes the value of this definite integral plus, if present, the terminal payoff. Such an admissible control is called an '*optimal control*'. The corresponding state  $x^*(t)$  obtained as the solution of the *Cauchy problem* (differential equation with an initial condition)

$$\begin{cases} \dot{x} = g(x(t), u^*(t), t) \\ x(0) = x_0 \end{cases}$$

is called an *optimal trajectory* or *optimal path*.

Here we state the main results to find a candidate solution to the optimal control problem (182), i.e. an optimal control and the corresponding optimal path. The most important necessary conditions

<sup>22</sup>More precisely, in economic applications usually the performance criterion is given in the form  $f(x(t), u(t), t) = e^{-\delta t} h(x(t), u(t))$ , i.e. it depends directly on time but only through a discount term. This point is more extensively discussed below.

are *Bellman's Optimality principle* (or *Dynamic Programming principle*) and *Pontryagin's maximum principle*. In the following Section we provide a simplified derivation of these results.

For defining Bellman's optimality principle, define the following function  $V(x, t) : \mathbb{R} \times \mathbb{R} \rightarrow \mathbb{R}$

$$V(x, t) = \max_{u(t) \in A(t)} \int_t^T f(x(s), u(s), s) ds + F(x(T), T) \quad (185)$$

called the *value function*.  $V(x, t)$  represents the maximum (more precisely the sup) possible value attainable starting at time  $t$  with initial state  $x$ , as also explained below.

**Proposition (Bellman's Optimality Principle).** *If  $V(x, t)$  is differentiable in  $t$  and  $x$  then it solves the following (Partial) Differential Equation*

$$-\frac{\partial V}{\partial t} = \max_{u(t) \in A(t)} \left[ f(x(t), u(t), t) + \frac{\partial V}{\partial x} g(x(t), u(t), t) \right]$$

with terminal condition  $V(x(T), T) = F(x(T), T)$ .

For stating Pontryagin's maximum principle, define the Hamiltonian function

$$H := H(x, u, \lambda, t) = f(x, u, t) + \lambda g(x, u, t) \quad (186)$$

where  $\lambda = \lambda(t)$  is called the costate variable.

**Proposition (Pontryagin's Maximum Principle).** *If  $u^*(t) = u^*$  is an optimal control and  $x^*(t) = x^*$  is the corresponding optimal path for the problem (182), then there exists a costate variable  $\lambda^*(t) = \lambda^*$  such that  $x^*, \lambda^*, u^*$  are the solution in  $[0, T]$  of the following problem:*

$$\left\{ \begin{array}{l} \dot{x} = g(x^*, u^*, t) = H_\lambda \text{ (state equation)} \\ \dot{\lambda} = -[f_x(x^*, u^*, t) + \lambda g_x(x^*, u^*, t)] = -H_x \text{ (costate equation)} \\ u^* = \arg \max H(x^*, u, \lambda^*, t) \text{ (maximum principle)} \\ x^*(0) = x_0 \text{ (initial condition)} \\ \text{(a) } \lambda^*(T) = \frac{\partial}{\partial x} F(x_T, T) \text{ (transversality condition when } x(T) \text{ free)} \\ \text{or} \\ \text{(b) } \lambda^*(T) \geq \frac{\partial}{\partial x} F(x_T, T) \text{ (transversality condition when } x(T) \geq x_T) \end{array} \right.$$

Notice that when  $x(T) = x_T$  no transversality condition is imposed. Moreover, when  $F(x_T, T) = 0$ , i.e. without scrap value, the transversality condition when  $x(T)$  is free reduces to  $\lambda^*(T) = 0$ . Analogously, when  $F(x_T, T) = 0$  and  $x(T) \geq x_T$ , the transversality condition is  $\lambda^*(T) \geq 0$ . Before closing this Section, we would like to provide some important remarks.

The first remark concerns admissible controls. In particular, notice that continuity of the control  $u(t)$  is not assumed, as we defined an admissible control as a piecewise continuous function that belongs to the constraint set  $A(t)$  for all  $t$ . In some cases, such as when the Hamiltonian is linear in the control, it turns out that the optimal control can be (jump) discontinuous. The times at which a jump in the control occurs are called *switching points*. Whenever this happens, the state equation  $\dot{x}$  may have a different RHS (right hand side), and, consequently, the state can have a kink point. Nevertheless, the Maximum Principle continues to hold for all the points where the control  $u(t)$  is continuous and the costate equation holds whenever the control is continuous. It can be shown that the Hamiltonian is continuous even at the switching points. Also in dynamic programming, an admissible control is a function with a finite number of jump discontinuities. We provide some examples below.

The second remark is related to the formulation of the problem we presented. In some cases, the terminal time  $T$  is unspecified, but it is a variable of the problem. A typical example is the so-called *time-optimal* control, for which one wants to find the smallest time such that the state of the system reaches a given point starting from a given initial condition. This problem can be written in standard form and analyzed with the principles that we described above.

Another remark concerns the possible constraints that can be part of the problem. The most common kinds are the *mixed inequality constraints*, where it is required that for each  $t \in [0, T]$  inequalities of the form  $q(x(t), u(t), t) \geq 0$  or the more involved "pure-state" constraints of the form  $s(x(t), t) \geq 0$  hold. The maximum principle can be reformulated to deal with these cases. Given the introductory aim of this section, we do not enter the details here but we refer to [22] for a comprehensive overview.

In the next two Sections, which can be skipped for the first reading, we provide a justification for these results.

## 9.1 Bellman's optimality principle: the Hamilton-Jacobi-Bellman equation

The main tools at hand for solving an optimal control problem are Bellman's optimality principle and Pontryagin's maximum principle.

Let us first try to find a necessary condition for an optimal control. In other words, we try to answer the following questions: How does an optimal control look like? What are the main properties that an optimal control should possess?

A very clear answer is given in the famous optimality principle, which Bellman himself describes with these words in his book:<sup>23</sup>

*"An optimal policy has the property that whatever the initial state and initial decision are, the remaining decisions must constitute an optimal policy with regard to the state resulting from the first decision".*<sup>24</sup>

For an everyday life example, suppose that a marathon runner has to run 42km. If the marathon runner divided into two (not necessarily equals) parts the run and used her energies to take the first part of the race at full speed, then she would no longer have necessary energy for the second part of the run. Clearly it does not make sense to divide the entire path into two parts and maximize over the first part: the final outcome would not be the optimal one and she probably would not finish the race. However, if the runner divided the way into two parts, then she would run the second part of the journey at best, given the energy left over from the first part of the route. In other words, *the second part of an optimal path must be optimal.*

Now let us try to describe the optimality principle in mathematical terms, without providing rigorous proofs. Suppose that an optimal control exists and it is used in solving (182). Then the objective in (182) becomes a number, since it is the sum of the definite integral (an area) in (182) and the terminal payoff. Let us denote this number by  $V(x_0, 0)$ , emphasizing that the value of the definite integral in (182) plus the scrap value depends only on the initial state of the system  $x(0) = x_0$ , and not on the control if it has been chosen to be an optimal one. Assume that the value function (185) is well definite (e.g. the integral converges). The value function (185) returns the value of the integral plus the terminal payoff, for a generic initial time  $t$  and initial state  $x$  in the optimal path, i.e.  $x = x^*(t)$ . The optimality principle implies that the value function must satisfy the following condition: if at time  $t$  the state is  $x^*(t)$  (a point of the optimal path) and the interval  $[t, T]$  is split

<sup>23</sup>Bellman, R.E. 1957. Dynamic Programming. Princeton University Press, Princeton, NJ. Republished 2003: Dover.

<sup>24</sup>The word "policy" is nowadays substituted with the most common "control".

in two parts, say  $[t, t + \Delta t]$  and  $[t + \Delta t, T]$ , then the optimal control must maximize the integral of the instantaneous payoff in the period  $[t, t + \Delta t]$  and then, from  $t + \Delta t$  onwards to  $T$ , it must hold that the value function gives the maximum attainable starting at time  $t + \Delta t$  with the updated state  $x + \Delta x$ , reached through the optimal control during the interval  $[t, t + \Delta t]$ . In practice, the value function solves a *functional* equation of the form:

$$V(x, t) = \max_{u(s) \in A(s)} \left[ \int_t^{t+\Delta t} f(x(s), u(s), s) ds + V(x + \Delta x, t + \Delta t) \right] \quad (187)$$

where  $V(x + \Delta x, t + \Delta t)$  is the value of the "second part" of the optimal path that must be optimal. The functional equation (187) can be written as a differential equation, as follows.

By the fundamental theorem of the integral calculus, for a 'small'  $\Delta t$  increment it is

$$\int_t^{t+\Delta t} f(x(s), u(s), s) ds \approx f(x(t), u(t), t) \Delta t \quad (188)$$

If the value function  $V(x, t)$  is continuously differentiable, we can approximate it through a Taylor expansion about the point  $(x, t)$

$$V(x + \Delta x, t + \Delta t) \approx V(x, t) + \frac{\partial V}{\partial x} \Delta x + \frac{\partial V}{\partial t} \Delta t \quad (189)$$

By substituting (188) and (189) into (187), we get

$$V(x, t) \approx \max_{u(t) \in A(t)} \left[ f(x(t), u(t), t) \Delta t + V(x, t) + \frac{\partial V}{\partial x} \Delta x + \frac{\partial V}{\partial t} \Delta t \right]$$

which can be written as

$$0 \approx \max_{u(t) \in A(t)} \left[ f(x(t), u(t), t) \Delta t + \frac{\partial V}{\partial x} \Delta x + \frac{\partial V}{\partial t} \Delta t \right]$$

since  $V(x, t)$  does not depend on  $u(t)$  and the  $V(x, t)$  terms on the LHS and on the RHS cancel out.

Now if we divide both terms of the last expression by  $\Delta t$  we get

$$0 \approx \max_{u(t) \in A(t)} \left[ f(x(t), u(t), t) + \frac{\partial V}{\partial x} \frac{\Delta x}{\Delta t} + \frac{\partial V}{\partial t} \right]$$

which, taking the limit as  $\Delta t \rightarrow 0$ , becomes

$$0 = \max_{u(t) \in A(t)} \left[ f(x(t), u(t), t) + \frac{\partial V}{\partial x} g(x(t), u(t), t) + \frac{\partial V}{\partial t} \right] \quad (190)$$

where we use the fact that  $\lim_{\Delta t \rightarrow 0} \frac{\Delta x}{\Delta t} = \dot{x}$ , which is the state equation. Moreover, for (190) it must hold the boundary condition that

$$V(x(T), T) = F(x(T), T) \quad (191)$$

In words, if the problem starts at the terminal time, then the integral in (185) is zero and the value function coincides with the scrap value.

Since in (190)  $\frac{\partial V}{\partial t} = \frac{\partial V(x,t)}{\partial t}$  does not depend on  $u(t)$ , we can rewrite (190) as

$$-\frac{\partial V}{\partial t} = \max_{u(t) \in A(t)} \left[ f(x(t), u(t), t) + \frac{\partial V}{\partial x} g(x(t), u(t), t) \right] \quad (192)$$

Technically, (190) known as the Hamilton-Jacobi-Bellman (HJB) equation, is a (first order) Partial Differential Equation for the value function. This problem, in general, is very difficult to tackle. In the following, we will provide some examples for which the HJB equation can be written as an ODE or for which the value function can be found starting from some trial functions.

## 9.2 From HJB to Pontryagin's Maximum Principle

Consider the derivative  $\frac{\partial V}{\partial x}$  in (190), where  $x = x^*(t)$ . Define the *costate* variable  $\lambda(t)$  as follows

$$\lambda(t) := \frac{\partial V}{\partial x} = \frac{\partial V(x^*, t)}{\partial x} = \frac{\partial V(x^*(t), t)}{\partial x} \quad (193)$$

Notice that  $\lambda(t)$  represents the derivative of the value function with respect to the state variable at each time.

From (192) and the definition of costate variable, it follows that an optimal control maximizes the Hamiltonian function  $H$  in (186) with respect to  $u$ . This important fact is referred to as the "Maximum principle". Observe that (190) can be written in terms of the Hamiltonian function (186) as follows

$$0 = \max_{u(t) \in A} \left[ H(x, u, \lambda, t) + \frac{\partial V}{\partial t} \right] = H(x^*, u^*, \frac{\partial V(x^*, t)}{\partial x}, t) + \frac{\partial V(x^*, t)}{\partial t} \quad (194)$$

Note that in the RHS of (194) the max disappears since we are considering optimal control and optimal state.

Now imagine that the control remains  $u^*$  but the state is "perturbed": instead of the optimal state  $x^*$  consider the "perturbed" state

$$x = x^* + hv$$

where  $v = v(t)$  is an arbitrary function, which we assume continuous and  $h \in \mathbb{R}$ . Obviously, for  $h = 0$ , the perturbed state coincides with the optimal state. For any fixed  $t \in [0, T]$  and a fixed  $v(t)$ , define the function  $R(h)$

$$R(h) = H(x, u^*, \frac{\partial V(x, t)}{\partial x}, t) + \frac{\partial V(x, t)}{\partial t}$$

Notice that  $R(h)$  is a differentiable function of one variable ( $v$  is fixed as well as  $u^*$ ) and it has a maximum point at  $h = 0$ , being from (194)

$$R(0) = H(x^*, u^*, \frac{\partial V(x^*, t)}{\partial x}, t) + \frac{\partial V(x^*, t)}{\partial t} \geq H(x, u^*, \frac{\partial V(x, t)}{\partial x}, t) + \frac{\partial V(x, t)}{\partial t} = R(h)$$

Since  $R(h)$  is differentiable, it must be that  $R'(0) = 0$ . By the chain rule:

$$\begin{aligned} R'(h) &= \frac{d}{dh} \left[ H(x, u^*, \frac{\partial V(x, t)}{\partial x}, t) + \frac{\partial V(x, t)}{\partial t} \right] = \frac{d}{dh} \left[ f(x, u^*, t) + V_x(x, t)g(x, u^*, t) + \frac{\partial V(x, t)}{\partial t} \right] \\ &= f_x(x, u^*, t)v + V_x(x, t)g_x(x, u^*, t)v + V_{xx}(x, t)g(x, u^*, t)v + V_{tx}(x, t)v = \\ &= [f_x(x, u^*, t) + V_x(x, t)g_x(x, u^*, t) + V_{xx}(x, t)g(x, u^*, t) + V_{tx}(x, t)]v \end{aligned} \quad (195)$$

from which

$$R'(0) = [f_x(x^*, u^*, t) + V_x(x^*, t)g_x(x^*, u^*, t) + V_{xx}(x^*, t)g(x^*, u^*, t) + V_{tx}(x^*, t)]v = 0 \quad (196)$$

Since  $v$  is an arbitrary function, in (196) the term in square brackets must be zero.

Now derive  $\frac{\partial V(x^*(t), t)}{\partial x}$  in (193) with respect to  $t$ . Using again the chain rule one obtains

$$\frac{dV_x}{dt} = V_{xx}(x^*(t), t)\dot{x} + V_{xt}(x^*(t), t) = V_{xx}(x^*, t)g(x^*, u^*, t) + V_{tx}(x^*, t) \quad (197)$$

Substitute (197) in the square bracket term in (196) to obtain

$$f_x(x^*, u^*, t) + V_x(x^*, t)g_x(x^*, u^*, t) + \frac{dV_x}{dt} = 0$$

which, recalling the definitions of costate in (193) and Hamiltonian in (186), can be rewritten as

$$\dot{\lambda} = -\frac{\partial H}{\partial x} \quad (198)$$

Now consider the terminal condition on the costate, which is referred to as the *transversality* condition. In the simplest case, there is no constraint on the value that the optimal state must assume in  $T$ , i.e.  $x(T)$  is free. In this case, the scrap value  $F(x(T), T)$  in (182) is independent on  $x(T)$  so that  $\frac{\partial}{\partial x}F(x(T), T) = 0$ . From (191) and from the definition of (193) it is

$$0 = \frac{\partial}{\partial x}F(x(T), T) = \frac{\partial}{\partial x}V(x(T), T) = \lambda(T)$$

More generally, if  $x(T) = x_T$  is given, then from the same reasoning we obtain the transversality condition

$$\lambda(T) = \frac{\partial}{\partial x}F(x_T, T)$$

Summing up, we obtain the Maximum principle already recalled.

The differential equations for the state and costate variables, together with the boundary conditions  $x^*(0)$  and  $\lambda^*(T)$ , constitute a two-point boundary value problem, where it is specified the initial value of the state and the final value of the costate.

Necessary conditions are important to select possible candidates for the optimal control. In addition, the following sufficient conditions are useful to confirm that a solution candidate is indeed an optimum. We recall below the most important sufficient conditions.

**Proposition (Mangasarian sufficient condition).** *Consider a candidate solution of the optimal control problem (182), i.e. an admissible control  $u^*$ , the corresponding admissible path  $x^*$  and the costate variable  $\lambda^*$ , obtained through Pontryagin's maximum principle.*

- *If the Hamiltonian  $H$  in (186) is concave in  $x$  and  $u$  for all  $t \in [0, T]$  then  $u^*$  is an optimal control and  $x^*$  is an optimal path;*
- *If the Hamiltonian  $H$  in (186) is strictly concave in  $x$  and  $u$  for all  $t \in [0, T]$  then  $u^*$  is the unique optimal control and  $x^*$  is the unique optimal path.*

An immediate corollary of the previous proposition is the following.

**Corollary (Mangasarian sufficient condition).** *Consider a candidate solution of the optimal control problem (182), i.e. an admissible control  $u^*$ , the corresponding admissible path  $x^*$  and the costate variable  $\lambda^*$ , obtained through Pontryagin's maximum principle. Assume that the instantaneous payoff  $f(x, u, t)$  is concave in  $x$  and  $u$  for all  $t \in [0, T]$  and that one of the following conditions holds:*

- for all  $t \in [0, T]$ ,  $g(x, u, t)$  is concave in  $x$  and  $u$  and  $\lambda^* \geq 0$ ;
- for all  $t \in [0, T]$ ,  $g(x, u, t)$  is convex in  $x$  and  $u$  and  $\lambda^* \leq 0$ ;
- $g(x, u, t)$  is linear in  $x$  and  $u$ .

Then  $u^*$  is an optimal control and  $x^*$  is an optimal path.

Another useful sufficient condition is based on the concavity of the maximized Hamiltonian  $H_M$ , defined as

$$H_M(x, \lambda, t) = \max_u H(x, u, \lambda, t) = \max_u [f(x, u, t) + \lambda g(x, u, t)] \quad (199)$$

**Proposition (Arrow sufficient condition).** *Consider a candidate solution of the optimal control problem (182), i.e. an admissible control  $u^*$ , the corresponding admissible path  $x^*$  and the costate variable  $\lambda^*$ , obtained through Pontryagin's maximum principle. If the maximized Hamiltonian  $H_M$  in (199) is concave in  $x$  for all  $t \in [0, T]$  then  $u^*$  is an optimal control and  $x^*$  is an optimal path.*

These sufficient conditions are employed in the examples below.

### 9.3 Some basic examples

#### Example (Basic)

Consider the problem

$$\begin{aligned} & \max_u \int_0^2 (x - 2u^2) dt \\ & \text{such that:} \\ & \begin{cases} \dot{x} = 3 + u \\ x(0) = 5 \end{cases} \end{aligned} \quad (200)$$

The Hamiltonian function is

$$H = x - 2u^2 + \lambda(3 + u)$$

Notice that the Hamiltonian is concave in state  $x$  and control  $u$ , so the necessary conditions are also sufficient. We apply the maximum principle to find the optimal control. In this particular case, being the Hamiltonian strictly concave in  $u$  and since no constraints on  $u$  are imposed, the maximizer can be found through the first order condition:

$$\frac{\partial H}{\partial u} = -4u + \lambda = 0 \rightarrow u^* = \frac{\lambda}{4} \quad (201)$$

The costate equation is

$$\dot{\lambda} = -\frac{\partial H}{\partial x} = -1 \rightarrow \lambda(t) = -t + c \quad (202)$$



where  $c$  is a constant to be determined through the transversality condition, i.e. the value of the costate at terminal time  $T = 2$ .

Since the final state  $x(2)$  is free, the transversality condition becomes  $\lambda(2) = 0$ . Therefore, the costate is  $\lambda(t) = -t + 2$ , and the optimal control is  $u^*(t) = \frac{\lambda(t)}{4} = -\frac{t}{4} + \frac{1}{2}$ . Now, the optimal state path can be obtained by integrating the state equation with the obtained optimal control:

$$\dot{x} = 3 + u^* = -\frac{t}{4} + \frac{7}{2} \rightarrow x(t) = -\frac{t^2}{8} + \frac{7}{2}t + 5$$

The constant (5) in the optimal path has been obtained by the initial condition on the state, see (200).

Let us slightly modify problem (200) by including a scrap value, for instance consider the objective

$$\max_u \int_0^2 (x - 2u^2) dt + 4x(2) \quad (203)$$

such that

$$\begin{cases} \dot{x} = 3 + u \\ x(0) = 5 \end{cases}$$

Clearly, the Hamiltonian is unchanged as well as conditions (201) and (202). Now the right transversality condition is  $\lambda(T) = \lambda(2) = \frac{d(4x)}{dx} = 4$ . Through analogous calculations as before we obtain,  $\lambda^*(t) = -t + 6$ ,  $u^*(t) = -\frac{t}{4} + \frac{3}{2}$  and  $x^*(t) = -\frac{t^2}{8} + \frac{9}{2}t + 5$ .

Let us now try to solve problem (200) by dynamic programming. HJB equation for problem (200) implies that  $V(x, t)$  must solve

$$\begin{aligned} V_t + \max_u [x - 2u^2 + V_x(3 + u)] &= 0 \rightarrow \\ V_t + x + 3V_x + \max_u [-2u^2 + uV_x] &= 0 \end{aligned}$$

maximizing  $-2u^2 + uV_x$  with respect to  $u$  by setting  $\frac{\partial(-2u^2 + uV_x)}{\partial u} = 0$ , we get that the optimal control satisfies  $u = \frac{V_x}{4}$ . The HJB equation then becomes

$$V_t + x + 3V_x + \frac{1}{8}(V_x)^2 = 0 \quad (204)$$

Usually, it is extremely hard if not impossible to solve in closed form the HJB equation. In this case, we try to obtain a solution starting by a trial function. Consider a function of the form

$$V(x, t) = ax + bxt + ct^3 + dt^2 + et + f$$

where  $a, b, c, d, e, f$  are constant to be determined. Inserting the trial solution in (204) it is

$$V(x, t) = (b + 1)x + t^2 \left( \frac{b^2}{8} + 3c \right) + t \left( \frac{ab}{4} + 3b + 2d \right) + \frac{a^2}{8} + 3a + e$$

Moreover, the transversality condition  $V(x, 2) = 0$  implies that  $(a + 2b)x + 8c + 4d + 2e + f = 0$ . At this point, the HJB equation is satisfied for all  $x$  and  $t$  if and only if the following system of equations

is satisfied

$$\begin{cases} b + 1 = 0 \\ \frac{b^2}{8} + 3c = 0 \\ \frac{ab}{4} + 3b + 2d = 0 \\ \frac{a^2}{8} + 3a + e = 0 \\ 8c + 4d + 2e + f = 0 \\ a + 2b = 0 \end{cases} \quad (205)$$

which gives the solution

$$a = 2; b = -1; c = -\frac{1}{24}; d = \frac{7}{4}; e = -\frac{13}{2}; f = \frac{19}{3}$$

that determines the value function

$$V(x, t) = 2x - xt - \frac{1}{24}t^3 + \frac{7}{4}t^2 - \frac{13}{2}t + \frac{19}{3}$$

Notice that  $u^*(t) = \frac{V_x}{4} = \frac{2-t}{4}$  coincides with the solution previously obtained through the maximum principle.

In the case of scrap value, the transversality condition requires that  $V(x, 2) = 4x$ . In that case, the last equation of system (205) is replaced by  $a + 2b - 4 = 0$ . We left to the reader to verify that the value function in this case has coefficients

$$a = 6; b = -1; c = -\frac{1}{24}; d = \frac{9}{4}; e = -\frac{45}{2}; f = \frac{109}{3}.$$

### Example (Bang-bang control)

Consider the problem

$$\begin{aligned} & \min_{u \in [-1, 1]} \int_0^2 x^2 dt & (206) \\ & \text{such that:} \\ & \begin{cases} \dot{x} = u \\ x(0) = -2 \end{cases} \end{aligned}$$

Since the integrand  $x^2$  is the quadrate of the distance between a point  $x$  and the origin, the problem can be interpreted as follows: start from  $x(0) = -2$  and try to steer  $x$  as near to zero as possible. To write the problem as a maximization one, we rewrite the objective as

$$\max_{u \in [-1, 1]} \int_0^2 -x^2 dt$$

The Hamiltonian function is

$$H = -x^2 + \lambda u$$

so that, applying the Maximum Principle, we obtain

$$\begin{cases} \dot{x} = u \text{ (state equation)} \\ \dot{\lambda} = -H_x = 2x \text{ (costate equation)} \\ u^* = \arg \max_{u \in [-1,1]} H \text{ (maximum principle)} \\ x^*(0) = -2 \text{ (initial condition)} \\ \lambda^*(2) = 0 \text{ (transversality condition when } x(T) \text{ is free)} \end{cases}$$

Notice that Mangasarian's sufficient condition holds, as the instantaneous payoff is strictly concave and the state equation is linear.

$H$  is linear in  $u$ , so we must adopt a control of the type

$$u^* = \begin{cases} 1 & \text{if } \lambda > 0 \\ ? & \text{if } \lambda = 0 \\ -1 & \text{if } \lambda < 0 \end{cases} \quad (207)$$

In our example, since  $x^*(0) = -2 < 0$ , it is clear that, in order to steer the system towards zero, we must select  $u = 1$ . The state-costate system becomes

$$\begin{cases} \dot{x} = 1 \\ \dot{\lambda} = 2x \end{cases}$$

with the previously reminded initial conditions. Integrating the first equation with the initial condition  $x^*(0) = -2$  we get  $x(t) = t - 2$ , which then gives the following equation for the costate

$$\begin{aligned} \dot{\lambda} &= 2x = 2t - 4 \rightarrow \\ \lambda(t) &= t^2 - 4t + 4 = (t - 2)^2 \end{aligned}$$

Notice that  $\lambda(t) > 0$  for all  $t \in [0, 2)$ , confirming that the initial choice of  $u = 1$  was correct. This control is called *bang-bang*, since, of all the possible values of  $u$  in the interval  $[-1, 1]$ , we were only interested in the terminal points, see (207), at least for  $\lambda \neq 0$ . Next example clarifies the presence of the "?" in (207).

#### Example (Singular control)

Consider the problem

$$\max_{u \in [-1,1]} \int_0^3 -x^2 dt \quad (208)$$

such that:

$$\begin{cases} \dot{x} = u \\ x(0) = -2 \end{cases}$$

The problem is formally identical to the previous one, with the exception that the terminal time is now  $T = 3$ . Employing the same principle as before, it is clear that it is optimal to steer the system towards the origin. Thus we get that in the interval  $[0, 2]$  the optimal trajectory is  $x(t) = t - 2$  and  $\lambda(t) = (t - 2)^2$ . At  $T = 2$ , it is  $x(2) = 0$  and also  $\lambda(2) = 0$ . In (207) we observed that when  $\lambda = 0$  the control is undefined. In this example, it is obvious that in the interval  $(2, 3]$  the control must be

$u = 0$ : at  $t = 2$  the system has reached the value  $x = 0$  and any other control  $u \neq 0$  would bring the state away from the origin (remember that the interpretation of the problem is that of minimizing an area). Since in the interval  $(2, 3]$  it is  $\dot{x} = 0$  it is also  $\dot{\lambda} = 2x = 0$ , so that  $\lambda(t)$  is constant in  $(2, 3]$ . In order to guarantee that  $\lambda(3) = 0$  it must be  $\lambda(t) = 0$ , for all  $(2, 3]$ , with also  $x(t) = 0$ , for all  $(2, 3]$ . We have thus established that the "?" in (207) is indeed  $u = 0$ . This is a typical example of a *singular* control, since there exists an interval where the Hamiltonian is independent on the control  $u$ .

#### 9.4 Current value formulations

In economics, the typical problem of optimal control assumes the following form

$$\max_{u(t) \in A} \int_0^T e^{-\delta t} f(x(t), u(t)) dt + F(x(T), T) \quad (209)$$

such that:

$$\left\{ \begin{array}{l} \dot{x} = g(x(t), u(t)) \\ x(0) = x_0 \\ \text{and with one of the following terminal conditions:} \\ \text{(a) } x(T) \text{ free (b) } x(T) = x_T \text{ (c) } x(T) \geq x_T \end{array} \right.$$

where  $\delta > 0$  is the discount factor. Remember that in most economic applications it is  $T = +\infty$  and, clearly  $F(x(t), t) = 0$ . In the following, we reformulate the HJB equation and the maximum principle for this specific problem.

First consider the HJB equation in (192) for problem (209)

$$-\frac{\partial V}{\partial t} = \max_{u(t) \in A(t)} \left[ e^{-\delta t} f(x(t), u(t)) + \frac{\partial V}{\partial x} g(x(t), u(t)) \right]$$

and assume that the value function can be written as the product of a function in  $x$  times  $e^{-\delta t}$ :

$$V(x, t) = J(x)e^{-\delta t}$$

from which it is  $\frac{\partial V}{\partial t} = -\delta J(x)e^{-\delta t}$  and  $\frac{\partial V}{\partial x} = J'(x)e^{-\delta t}$ . Thus, the HJB equation becomes

$$\delta J(x)e^{-\delta t} = \max_{u(t) \in A(t)} \left[ e^{-\delta t} f(x(t), u(t)) + J'(x)e^{-\delta t} g(x(t), u(t)) \right].$$

Multiplying both sides by  $e^{\delta t}$ , we obtain the following ODE in the unknown function  $J(x)$ :

$$\delta J(x) = \max_{u(t) \in A(t)} [f(x(t), u(t)) + J'(x)g(x(t), u(t))] \quad (210)$$

It is easily verifiable that the transversality condition  $F(x(T), T) = V(x(T), T)$  now becomes

$$J(x(T)) = e^{\delta T} F(x(T), T)$$

Now we restate the maximum principle for problem (209). Consider the corresponding Hamiltonian in (186)

$$H(x, u, \lambda, t) = e^{-\delta t} f(x, u) + \lambda g(x, u)$$

and multiply it by  $e^{\delta t}$  to obtain the so-called Current-value Hamiltonian  $H^c$ :

$$H^c(x, u, \mu, t) = f(x, u) + \mu g(x, u) \quad (211)$$

where  $\mu = \mu(t) = \lambda(t)e^{\delta t}$ . From  $\lambda(t) = \mu(t)e^{-\delta t}$  we obtain that

$$\dot{\lambda} = \dot{\mu}e^{-\delta t} - \delta\mu e^{-\delta t}$$

and thus

$$\dot{\lambda}e^{\delta t} = \dot{\mu} - \delta\mu \quad (212)$$

Since the current value Hamiltonian is given by the Hamiltonian times a constant, the optimal control  $u^*$  maximizes the current-value Hamiltonian as well as the Hamiltonian; moreover  $H_\mu^c = H_\lambda$  so that the state equation can be written as  $\dot{x} = H_\mu^c$ . Now consider the costate equation

$$\dot{\lambda} = -H_x = -[f_x(x^*, u^*) + \lambda g_x(x^*, u^*)] = \quad (213)$$

$$\begin{aligned} &= -\left[e^{-\delta t} f_x(x^*, u^*) + \lambda g_x(x^*, u^*)\right] = \\ &= -\left[e^{-\delta t} f_x(x^*, u^*) + \mu e^{-\delta t} g_x(x^*, u^*)\right] \end{aligned} \quad (214)$$

Multiply (213) by  $e^{\delta t}$  and, considering (212), we can write

$$\dot{\mu} - \delta\mu = -[f_x(x^*, u^*) + \mu g_x(x^*, u^*)] = -H_x^c$$

It is now possible to restate Pontryagin's maximum principle for problem (209)

**Proposition (Maximum Principle with current-value formulation).** *If  $u^*$  is an optimal control and  $x^*$  is the corresponding optimal path for the problem (209), then there exists a costate variable  $\mu^*$  such that  $x^*, \mu^*, u^*$  are the solution in  $[0, T]$  of the following problem:*

$$\left\{ \begin{array}{l} \dot{x} = g(x^*, u^*) = H_\mu^c \text{ (state equation)} \\ \dot{\mu} = -[f_x(x^*, u^*) + \mu^* g_x(x^*, u^*)] + \delta\mu = -H_x^c + \delta\mu \text{ (costate equation)} \\ u^* = \arg \max H^c(x^*, u, \mu^*) \text{ (maximum principle)} \\ x^*(0) = x_0 \text{ (initial condition)} \\ \text{(a) } \mu^*(T) = \frac{\partial}{\partial x} F(x_T, T) \text{ (transversality condition when } x(T) \text{ free)} \\ \text{or} \\ \text{(b) } \mu^*(T) \geq \frac{\partial}{\partial x} F(x_T, T) \text{ (transversality condition when } x(T) \geq x_T) \end{array} \right.$$

Obviously, when the scrap value is zero, in the transversality conditions it is  $\frac{\partial}{\partial x} F(x_T, T) = 0$ . When  $T = +\infty$ , the following transversality condition is necessary

$$\begin{aligned} &\lim_{t \rightarrow +\infty} e^{-\delta t} H^c(x^*, u^*, \mu^*) \\ &= \lim_{t \rightarrow +\infty} e^{-\delta t} f(x^*, u^*) + e^{-\delta t} \mu^* g(x^*, u^*) = 0. \end{aligned} \quad (215)$$

In economic applications, the following "simplified" transversality condition is often employed:

$$\lim_{t \rightarrow +\infty} \mu^* e^{-\delta t} = 0. \quad (216)$$

Notice that condition (216) is not necessary, as it can be shown by counterexamples, see [24]. Clearly, if in the considered optimal control problem with infinite time horizon the optimal state converges to an equilibrium value  $(x^*, u^*)$ , then  $\lim_{t \rightarrow +\infty} e^{-\delta t} f(x^*, u^*) = 0$  and  $\lim_{t \rightarrow +\infty} g(x^*, u^*) = 0$  so that (216) implies (215). We refer to [2] for details on this point.

We conclude by recalling that Mangasarian as well as Arrow sufficient conditions hold. These conditions can be applied, respectively, to the current-value Hamiltonian and to the current-value maximized Hamiltonian  $H_M^c$ . In the following example, these two theorems are useful to provide sufficient conditions for optimality.

### 9.4.1 Economic Examples

**Example (Optimal use of a machine).** Suppose that you possess a machine whose value at time  $t$  is denoted by  $x(t)$ . For each unit of capital invested in the machine, you obtain a unit of a good, which is then sold in the market at constant price  $p$ . The machine depreciates over time at the rate  $\eta$ , but it is possible to reduce depreciation by investing in maintenance. Denote by  $u = u(t)$  the instantaneous maintenance activity (or repair effort), which is our control variable. The cost of maintenance is  $c(u) = \gamma u^2$ . Instantaneous profit is then  $px - \gamma u^2$  (revenues less costs). Assume that the total life of the machine is  $T > 0$ . Indicating by  $\delta$  the discount factor, the objective is

$$\max_{u \geq 0} \int_0^T e^{-\delta t} [px - \gamma u^2] dt \quad (217)$$

such that:

$$\begin{cases} \dot{x} = -\eta x + u \\ x(0) = x_0 \\ x(T) \text{ free} \end{cases}$$

The current-value Hamiltonian is

$$H^c = px - \gamma u^2 + \mu(-\eta x + u)$$

$H^c$  is concave in  $x$  and  $u$ , so by the Mangasarian theorem the necessary conditions are also sufficient for an optimal control. Moreover, since  $H^c$  is strictly concave in  $u$ , we can deduce that, under the assumption that the optimal control is strictly positive, i.e.  $u^* > 0$  (see below), the optimal control must satisfy the usual necessary condition for a max:  $\frac{\partial H^c}{\partial u} = -2\gamma u^* + \mu = 0$ . Thus,  $H^c$  is maximized at

$$u^* = \frac{\mu}{2\gamma} \quad (218)$$

The costate equation is

$$\dot{\mu} = -\frac{\partial H^c}{\partial x} + \mu\delta = -p + \mu(\eta + \delta) \quad (219)$$

with terminal condition (transversality)  $\mu(T) = 0$ . Equation (219) is a linear ODE with constant coefficients, whose general solution can be easily calculated (see Appendix):

$$\mu(t) = Ke^{(\eta+\delta)t} + \frac{p}{\eta + \delta}$$

Imposing the boundary condition  $\mu(T) = 0$ , we specify the value of the constant  $K$ . The required solution is  $\mu(t) = -p \frac{e^{(\eta+\delta)(t-T)}}{\eta+\delta} + \frac{p}{\eta+\delta}$ .

By (218), the optimal control is therefore

$$u^*(t) = \frac{1}{2\gamma} \left[ -p \frac{e^{(\eta+\delta)(t-T)}}{\eta + \delta} + \frac{p}{\eta + \delta} \right] \quad (220)$$

Observe from (220) that, being  $t < T$  it is  $u^*(t) > 0$  as conjectured above. Finally, the ODE  $\dot{x} = -\eta x + u^*$  is linear (but with nonconstant coefficients) and can be solved through the technique explained in the appendix. Fig.146(a) shows the time evolution of the optimal path  $x^*(t)$  (blue), optimal control  $u^*(t)$  (black) and costate  $\mu(t)$  (red) with parameters  $\delta = 0.8$ ;  $\eta = 0.8$ ;  $p = 1$ ;  $\gamma = 0.9$ ;  $T = 5$ ;  $x_0 = 1$ .

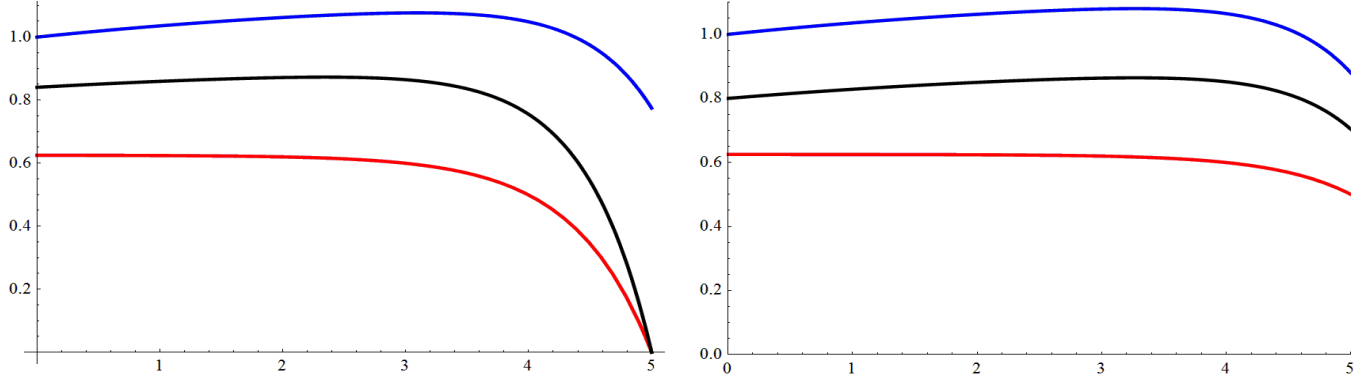


Figure 146: Time evolution of the optimal path  $x^*(t)$  (blue), optimal control  $u^*(t)$  (black) and costate  $\mu(t)$  (red) with parameters  $\delta = 0.8$ ;  $\eta = 0.8$ ;  $p = 1$ ;  $\gamma = 0.9$ ;  $T = 5$ ;  $x_0 = 1$ .

In fig.147, typical solutions of the state-costate ODE system are depicted, in the  $(x, \mu)$  plane.

$$\begin{cases} \dot{x} = -\eta x + \frac{\mu}{2\gamma} \\ \dot{\mu} = -p + \mu(\eta + \delta) \end{cases} \quad (221)$$

The nullclines are the red lines (obviously  $\dot{\mu} = 0$  is the horizontal line). Observe that the equilibrium of the system, obtained by solving the system  $\dot{x} = \dot{\mu} = 0$ .

$$(x^*, \mu^*) = \left( \frac{p}{2\gamma\eta(\delta + \eta)}, \frac{p}{\delta + \eta} \right)$$

is a saddle point, as the Jacobian  $J = \begin{bmatrix} -\eta & \frac{1}{2\gamma} \\ 0 & \eta + \delta \end{bmatrix}$  has  $Tr(J) = \delta > 0$  and  $Det(J) = -\eta(\eta + \delta) < 0$ .

Below the nullcline  $\dot{\mu} = 0$ , the optimal combination of state and control is a blue trajectory with the property that it ends exactly in the  $x$ -axis at time  $T$ . Above the nullcline  $\dot{\mu} = 0$ , the generic trajectory diverges and can not satisfy the transversality condition  $\mu(T) = 0$ .

Before ending the example, let us modify it slightly and suppose that at time  $T$  the machine has a scrap value, i.e. it can be sold in a second-hand market at price  $S(x) = ax$ . The problem can be stated as

$$\max_{u \geq 0} \left[ \int_0^T e^{-\delta t} [px - \gamma u^2] dt + e^{-\delta T} ax(T) \right]$$

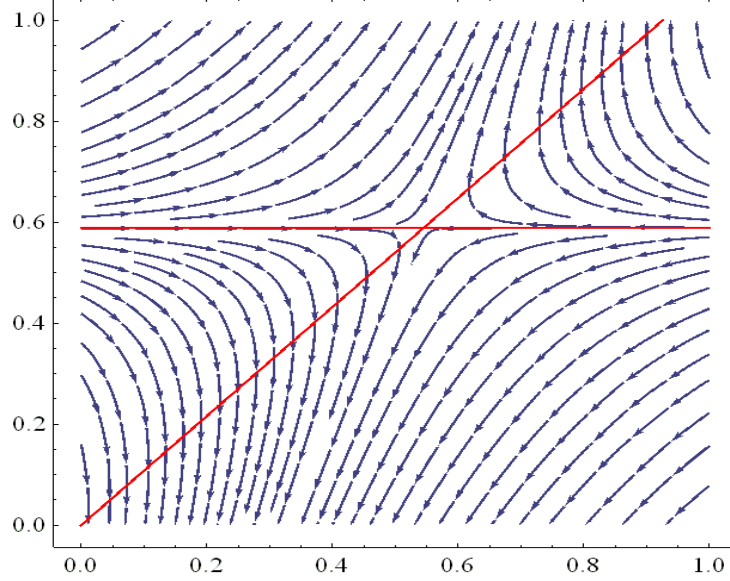


Figure 147: Typical solutions of the state-costate ODE system.

In this case, the ODE (221) remains unchanged, whereas only the transversality condition changes and becomes  $\mu(T) = \frac{\partial S(x)}{\partial x} = a$ . Fig. 146(b) shows the relevant quantities with the parameters as in Fig. 146(a) and with scrap value  $S(x) = \frac{x}{2}$ .

**Example (Linear-Quadratic optimal control).** Suppose that we want to solve the following problem

$$\min_{u=u(t)} \int_0^{+\infty} e^{-\delta t} [ax^2 + bu^2] dt \quad (222)$$

such that:

$$\begin{cases} \dot{x} = u \\ x(0) = x_0 \end{cases}$$

where  $a, b > 0$ . No constraints on the control are imposed. Being the integrand a quadratic function of state and control and the state equation linear in control, such a problem is often referred to as a *linear-quadratic* (LQ) optimal control problem.

Notice that, since we want to minimize the integral, we can restate the problem in equivalent form by considering the following objective:

$$\max_u \int_0^{+\infty} -e^{-\delta t} [ax^2 + bu^2] dt$$

Let us start the analysis by characterizing the solution through the maximum principle. The current-value Hamiltonian is given by

$$H^c(x, u, \mu) = -ax^2 - bu^2 + \mu u$$



Clearly Mangasarian's sufficient conditions are verified. Moreover, being  $H^c$  strictly concave in  $u$ , we can find the optimal control  $u^* = u$  by solving the equation of the first order condition

$$\frac{\partial H^c}{\partial u} = -2bu + \mu = 0 \rightarrow u^* = \frac{\mu}{2b}$$

Now consider the costate equation

$$\dot{\mu} = -H_x^c + \delta\mu = 2ax + \delta\mu$$

Summing up, a solution of the problem is given by  $x^*, u^*, \mu^*$  that solve the following system of linear differential equations

$$\begin{cases} \dot{x} = \frac{\mu}{2b} \\ \dot{\mu} = 2ax + \delta\mu \end{cases} \quad (223)$$

with initial condition on the state  $x(0) = x_0$  and such that the following transversality condition holds:

$$\lim_{t \rightarrow +\infty} e^{-\delta t} H^c(x^*, u^*, \mu^*) = \lim_{t \rightarrow +\infty} -e^{-\delta t} \left[ a(x^*)^2 + b \left( \frac{\mu^*}{2b} \right)^2 \right] + e^{-\delta t} \frac{(\mu^*)^2}{2b} = 0. \quad (224)$$

One particular solution of (223) is the fixed point, obtained by solving the system  $\dot{x} = \dot{\mu} = 0$ . Being a  $2 \times 2$  system of linear equations with nonzero determinant, this solution is unique and it is the equilibrium  $(x, \mu) = (0, 0)$ . The Jacobian matrix is given by

$$J = \begin{bmatrix} 0 & \frac{1}{2b} \\ 2a & \delta \end{bmatrix}$$

whose eigenvalues are

$$z_{1,2} = \frac{\delta \pm \sqrt{\delta^2 + 4ab}}{2}$$

Since it is  $z_1 = \frac{\delta - \sqrt{\delta^2 + 4ab}}{2} < 0 < \frac{\delta + \sqrt{\delta^2 + 4ab}}{2} = z_2$ , the origin  $(0, 0)$  is a saddle point. The equilibrium solution satisfies the transversality condition (224) because there  $\mu^*$  is constant. Thus, when  $x(0) = 0$  it is optimal to set  $u = 0$  for all  $t$ . This is elementary considering again the meaning of problem (222).

The interesting question is then the following: what happens when  $x(0) \neq 0$ ? To answer the question, one has to find out how the optimal path looks like in general. Deriving the maximum principle condition with respect to  $t$ , we obtain that the following relationship must hold:  $\dot{u} = \frac{\dot{\mu}}{2b}$ . Deriving  $\dot{x}$  with respect to  $t$ , and using the state equation  $\dot{x} = u$ , we obtain the following second-order differential equation in  $x$ :

$$\begin{aligned} \ddot{x} &= \dot{u} = \frac{\dot{\mu}}{2b} = \frac{2ax + \delta\mu}{2b} = \frac{2ax + 2b\delta u}{2b} = \\ &= \frac{a}{b}x + \delta\dot{x} \end{aligned}$$

The general solution of this equation is

$$x(t) = c_1 e^{r_1 t} + c_2 e^{r_2 t} \quad (225)$$

where  $r_1 = \frac{\delta - \sqrt{\delta^2 + 4a/b}}{2}$  and  $r_2 = \frac{\delta + \sqrt{\delta^2 + 4a/b}}{2}$ . The constants  $c_1$  and  $c_2$  can be determined through the boundary conditions, i.e. the initial condition on the state  $x(0) = x_0$  and the transversality condition on the costate. From the latter we get that condition (224) can be satisfied only if  $\lim_{t \rightarrow +\infty} \mu(t)e^{-\delta t} = 0$ . Thus, the transversality condition requires that

$$0 = \lim_{t \rightarrow +\infty} \mu(t)e^{-\delta t} = \lim_{t \rightarrow +\infty} 2bu(t)e^{-\delta t} = \lim_{t \rightarrow +\infty} 2b\dot{x}(t)e^{-\delta t} = c_2\infty$$

which tells us that the transversality condition can be satisfied only for  $c_2 = 0$ . Thus, from (225) the optimal path is

$$x^*(t) = x_0 e^{t \frac{\delta - \sqrt{\delta^2 + 4a/b}}{2}} \quad (226)$$

with corresponding optimal control

$$u^* = \dot{x}^* = x_0 \frac{\delta - \sqrt{\delta^2 + 4a/b}}{2} e^{t \frac{\delta - \sqrt{\delta^2 + 4a/b}}{2}} \quad (227)$$

Consider now the same problem with Dynamic Programming. Maximizing the right hand side of the HJB in (210), the optimal control must satisfy the condition

$$u^* = \arg \max [-ax^2 - bu^2 + J'(x)u]$$

from which it is  $u^* = \frac{J'(x)}{2b}$ , which coincides, if one recall the definition of the costate variable, with the optimal control obtained through Pontryagin's principle. The HJB equation (210) thus becomes

$$\begin{aligned} \delta J(x) &= -ax^2 - b \left( \frac{J'(x)}{2b} \right)^2 + \frac{[J'(x)]^2}{2b} = \\ &= -ax^2 + \frac{[J'(x)]^2}{4b} \end{aligned} \quad (228)$$

which is a nonlinear ODE in the unknown function  $J(x)$ . In this case, a way to tackle the problem is to "guess" a possible value function. For instance, consider a quadratic "trial" function of the form

$$J(x) = Ax^2$$

where  $A$  is a constant to be determined. With this choice of  $J(x)$ , the HJB equation (228) becomes

$$\delta Ax^2 = -ax^2 + \frac{A^2 x^2}{b}$$

which is equivalent to

$$\left( \frac{A^2}{b} - \delta A - a \right) x^2 = 0$$

Thus, the trial solution works if the quantity in parenthesis is zero, i.e. if  $A$  solves the quadratic equation  $\frac{A^2}{b} - \delta A - a = 0$ . The required values of  $A$  are

$$A = \frac{b\delta \pm \sqrt{b(4a + b\delta^2)}}{2}$$

At this point we have two possible values of  $A$  that do the trick. However, notice that the integrand function is negative, as it is the sum of two quadratic terms multiplied by  $-1$ . Thus, the value function, which gives the maximum value of this integral, can only assume nonpositive values. Thus, only the negative solution ( $A < 0$ ) is meaningful for our problem. In this way, the following value function has been found:

$$J(x) = \frac{b\delta - \sqrt{b(4a + b\delta^2)}}{2} x^2$$

Now consider the optimal control, which is, as shown before,

$$u^* = \frac{J'(x)}{2b} = \frac{1}{2} \left( \delta - \sqrt{\frac{4a}{b} + \delta^2} \right) x \quad (229)$$

Now from condition  $\dot{x} = u$  we have that  $x$  solves the ODE

$$\dot{x} = \frac{1}{2} \left( \delta - \sqrt{\frac{4a}{b} + \delta^2} \right) x$$

whose solution coincides with (226). The optimal control as a function of time is obviously (227). Notice that, although both (227) and (229) represent the optimal control, this control is given in (227) as a function of time of the form  $u^* = u(t, x_0)$  (*open-loop* control), whereas in (229) the optimal control is a function of the current state  $u^* = u(t, x(t))$  (*closed-loop* or *feedback* control).

Following similar steps, one can study a more general linear-quadratic problem of the form:

$$\max_{u(t)} \int_0^{+\infty} -e^{-\delta t} [ax^2 + bu^2] dt \quad (230)$$

such that:

$$\begin{cases} \dot{x} = cx + du \\ x(0) = x_0 \end{cases}$$

**Example (A simplified Capital Accumulation Model).** Consider now the optimal control problem

$$\max_{0 < u(t) \leq x^\alpha} \int_0^{+\infty} e^{-\delta t} \log u(t) dt \quad (231)$$

such that:

$$\begin{cases} \dot{x} = x^\alpha - \gamma x - u \\ x(0) = x_0 \end{cases}$$

where  $x = x(t) \geq 0$  can be interpreted as a physical capital that naturally grows through the technological coefficient  $\alpha \in (0, 1]$ , depreciates itself by an obsolescence factor  $\gamma > 0$  and is reduced by current consumption  $u$ . Capital  $x$  is the state variable and consumption  $u$  is the control variable. The objective of the problem is to maximize the discounted stream of utility of consumption, assumed logarithmic. The constraint on the consumption is introduced on the one hand to impose some consumption ( $u > 0$ ) and on the other hand to avoid that the capital is consumed ( $u(t) \leq x^\alpha$ ).

The current value Hamiltonian is

$$H^c = \log u + \mu [x^\alpha - \gamma x - u]$$

which is maximized, from condition  $\frac{\partial H^c}{\partial u} = 0$ , at  $u = \frac{1}{\mu}$ . The current-value Hamiltonian (211) is  $H_x^c = \mu [\alpha x^{\alpha-1} - \gamma]$ . Through these quantities, the state-costate system of ODE that a candidate to be an optimal solution solves becomes

$$\begin{cases} \dot{x} = x^\alpha - \gamma x - \frac{1}{\mu} \\ \dot{\mu} = \mu [(\gamma + \delta) - \alpha x^{\alpha-1}] \\ x(0) = x_0 \\ \lim_{t \rightarrow +\infty} e^{-\delta t} [\log u + \mu (x^\alpha - \gamma x - u)] = 0 \end{cases}$$

Notice that Mangasarian's sufficient conditions are satisfied, so the necessary conditions are also sufficient.<sup>25</sup>

Instead of considering the previous system of ODE, it is instructive to translate it in a ODE system in the state-control variables. First, derive the maximum condition  $u = \frac{1}{\mu}$  with respect to time:

$$\dot{u} = -\frac{\dot{\mu}}{\mu^2} = \frac{\alpha x^{\alpha-1} - (\gamma + \delta)}{\mu} = u [\alpha x^{\alpha-1} - (\gamma + \delta)]$$

so that the previous system in the state-control space is translated as

$$\begin{cases} \dot{x} = x^\alpha - \gamma x - u \\ \dot{u} = u [\alpha x^{\alpha-1} - (\gamma + \delta)] \\ x(0) = x_0 \\ \lim_{t \rightarrow +\infty} e^{-\delta t} [\log u + \mu (x^\alpha - \gamma x - u)] = 0 \end{cases} \quad (232)$$

Let us study the nullclines of system (232). Obviously,  $\dot{x} = 0 \Leftrightarrow u = f(x) = x^\alpha - \gamma x$ . In the plane  $(x, u)$ ,  $f(x)$  is a strictly concave function. Observe that below this curve, it is  $\dot{x} > 0$ . Now consider  $\dot{u} = 0 \Leftrightarrow u [\alpha x^{\alpha-1} - (\gamma + \delta)] = 0$  i.e. when  $u = 0$  or  $x = \bar{x} = \left(\frac{\gamma + \delta}{\alpha}\right)^{\frac{1}{\alpha-1}}$ : in the plane  $(x, u)$  the set of points such that  $\dot{u} = 0$  are the  $x$ -axis and the vertical line  $x = \bar{x}$ . Moreover, on the left of  $x = \bar{x}$  it is  $\dot{u} > 0$ . The positive orthant of the plane  $(x, u)$  can thus be subdivided into four regions according to the signs of the regions between nullclines, as represented in fig.148, where we depicted the locus of points such that  $\dot{x} > 0$  and  $\dot{u} > 0$  (light yellow region),  $\dot{x} > 0$  and  $\dot{u} < 0$  (white region),  $\dot{x} < 0$  and  $\dot{u} > 0$  (gray region),  $\dot{x} < 0$  and  $\dot{u} < 0$  (light gray region).

System (232) admits three equilibrium points  $(x, u)$ , obtained as points where  $\dot{x} = \dot{u} = 0$ :  $(0, 0)$ ,  $(\gamma^{\frac{1}{\alpha-1}}, 0)$  and  $(\bar{x}, \bar{u}) = (\bar{x}, \bar{x}^\alpha - \gamma \bar{x})$ . By the constraint on the control ( $u > 0$ ), we disregard the first two equilibrium points, as they involve zero consumption. The analysis with the nullclines suggests that  $(\bar{x}, \bar{x}^\alpha - \gamma \bar{x})$  is a saddle point. The same conclusions can be drawn by studying the linearization of the system about this fixed point. We perform this stability analysis in the next example in a more general setting.

---

<sup>25</sup>This can be verified by Sylvester's criterion, being  $H_{xx}^c < 0$  and  $\begin{vmatrix} H_{xx}^c & H_{xu}^c \\ H_{ux}^c & H_{uu}^c \end{vmatrix} > 0$ .

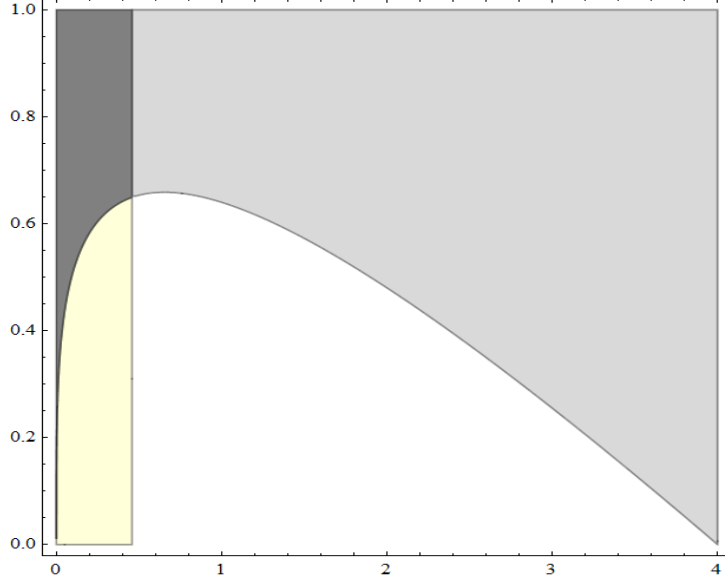


Figure 148: The positive orthant of the plane  $(x, u)$  subdivided into four regions bounded by nullclines.

The point  $(\bar{x}, \bar{u})$  is the optimal equilibrium. In fact, it is a solution of (232), being the simplified transversality condition  $\lim_{t \rightarrow +\infty} \frac{e^{-\delta t}}{u} = 0$  trivially satisfied, as  $\bar{u}$  is constant. When  $x(0) = \bar{x}$ , it is optimal to use the control  $\bar{u}$  for all  $t$  to stay at  $\bar{x}$ .

What happens when the initial condition on the capital is out-of-equilibrium, i.e. if  $x(0) \neq \bar{x}$ ? As  $(\bar{x}, \bar{u})$  is a saddle, every trajectory starting in the gray or in the white regions departs from  $(\bar{x}, \bar{u})$ . For a given initial state, it can not be optimal to take a control such that the trajectory belongs to these regions, as the trajectory would not satisfy the transversality condition in (232).

Thus, given an initial condition  $x(0) < \bar{x}$  [ $x(0) > \bar{x}$ ], the control should be chosen in the light yellow region [light gray region] such that the path belongs to the stable manifold of the saddle point, in order to guarantee the convergence to the optimal equilibrium  $(\bar{x}, \bar{u})$ . If we express the optimal control as a function of the state,  $u = u(x)$  such that the trajectory of the system belongs to the stable manifold of the saddle point  $(\bar{x}, \bar{u})$ , then  $u(x)$  is the feedback optimal control for problem (231).

We briefly study this model with the dynamic programming approach. To simplify the problem, consider the case  $\alpha = 1$ , so that the state equation becomes

$$\dot{x} = \theta x - u$$

where  $\theta = (1 - \gamma)$ . The HJB equation assumes the form

$$\delta J(x) = \max_u [\log u + J'(x)(\theta x - u)] \quad (233)$$

where  $J(x)$  is an unknown function. The RHS of (233) is maximized for  $u = \frac{1}{J'(x)} > 0$ , so that (233) can be written as

$$\delta J(x) = -\log J'(x) + \theta x J'(x) - 1$$

Given the logarithmic form of utility, we search for a solution candidate of the form  $J(x) = A[\log(x) + B]$ , where  $A$  and  $B$  are constant to be determined. Substituting this trial function in the HJB and sim-

plifying, we obtain the equation

$$1 - A\theta + AB\delta + \log A + \log x (A\delta - 1) = 0$$

which leads to the system

$$\begin{cases} A\delta - 1 = 0 \\ 1 - A\theta + AB\delta + \log A = 0 \end{cases}$$

so that  $A = \frac{1}{\delta}$  and  $B = \frac{\alpha}{\delta} - 1 + \log \delta$ . It is easy to check that function  $J(x) = \frac{1}{\delta} [\log(x + \delta) + \frac{\alpha}{\delta} - 1]$  satisfies (233). The optimal control is then  $u^* = \frac{1}{J'(x)} = \delta x$ , which gives the optimal quantity to consume as a function of the current stock of capital (feedback control).

**Example (A more general Capital Accumulation Model).** Consider a generalization of the previous example.<sup>26</sup> The production function  $Y$  depends on total capital  $X$  and on total labour force  $L$ , i.e.  $Y = Y(X, L)$ . Define per-capita production and capital as follows:  $y = \frac{Y}{L}$  and  $x = \frac{X}{L}$ . Assume that  $Y = Y(X, L)$  is linear homogeneous of degree 1, i.e.

$$Y = Y(X, L) = Y(Lx, L) = LY(x, 1)$$

from which the individual production function is  $y = f(x) = Y(x, 1)$ .  $f(x)$  is assumed twice differentiable with  $f'(x) > 0$  and  $f''(x) < 0$  and such that it satisfies the so-called *Inada* conditions:

$$\lim_{x \rightarrow 0^+} f'(x) = +\infty \text{ and } \lim_{x \rightarrow +\infty} f'(x) = 0^+ \quad (234)$$

Total production is split between total consumptions  $C$  and total investments  $I$ , i.e.  $Y = C + I$ . The variation of the capital stock in time is

$$\dot{X} = I - \rho X = Y - C - \rho X$$

where  $\rho > 0$  indicates capital depreciation over time. In per-capita terms the variation of capital stock is

$$\frac{\dot{X}}{L} = y - c - \rho x$$

where  $c = \frac{C}{L}$  denotes individual consumption, i.e. the consumption of a representative agent in the economy.

On the other hand, the derivative of capital  $X$  is

$$\dot{X} = \frac{d}{dt}(Lx) = \dot{L}x + L\dot{x}$$

that gives  $\frac{\dot{X}}{L} = \frac{\dot{L}}{L}x + \dot{x}$ . Denoting the growth rate of labour force  $\frac{\dot{L}}{L} = n$  (assumed constant) and recalling that  $y = f(x)$ , we obtain the equation of capital growth:

$$\dot{x} = f(x) - c - (n + \rho)x$$

The utility of a representative agent in the economy is denoted by  $u(c)$ , which is assumed three times differentiable with  $u'(c) > 0$  and  $u''(c) < 0$  and such that it satisfies the *Inada* conditions (234).

<sup>26</sup>Cass, David (1965). "Optimum Growth in an Aggregative Model of Capital Accumulation". *Review of Economic Studies* 32 (3): 233-240.

Assume that a social planner aims at maximizing the discounted value of the utility of consumers weighted by labour force over an infinite time horizon. Denoting by  $\beta > 0$ , the discount factor, the problem of the social planner is

$$\int_0^{+\infty} e^{-\beta t} u(c) L dt = L_0 \int_0^{+\infty} e^{(n-\beta)t} u(c) dt$$

where it is assumed that the population grows exponentially, with  $L = L(t) = L_0 e^{nt}$  and with initial population  $L(0) = L_0$ . Without loss of generality, one can normalize the initial population to 1, i.e.  $L_0 = 1$ . The objective of the social planner becomes

$$\max_{0 \leq u \leq f(x)} \int_0^{+\infty} e^{-\delta t} u(c) dt \quad (235)$$

such that:

$$\begin{cases} \dot{x} = f(x) - \gamma x - c \\ x(0) = x_0 \end{cases}$$

where  $\delta = \beta - n > 0$  (by assumption) and  $\gamma = n + \rho$ . Notice that the previous example in (231) is a particular case of the one considered here.

Let us study the model with the maximum principle. The current-value Hamiltonian is

$$H^c = u(c) + \mu [f(x) - c - \gamma x]$$

which is maximized at  $\frac{\partial H^c}{\partial u} = u'(c) - \mu = 0$ , i.e. for  $\mu = u'(c)$ . The state-costate system of ODE that a candidate optimal solution must satisfy is

$$\begin{cases} \dot{x} = f(x) - c - \gamma x \\ \dot{\mu} = -\mu [f'(x) - (\gamma + \delta)] \\ x(0) = x_0 \\ \lim_{t \rightarrow +\infty} e^{-\delta t} [u(c) + \mu(f(x) - c - \gamma x)] = 0 \end{cases} \quad (236)$$

where also the control  $c$  appear. Notice again that Mangasarian's sufficient conditions are satisfied, so that the necessary conditions are also sufficient.<sup>27</sup> To get rid of the costate variable, we transform system (236) in an ODE system in the state-control space. Deriving the maximization condition  $\mu = u'(c)$  with respect to  $t$  we get

$$\dot{\mu} = \frac{d}{dt} u'(c(t)) = u''(c) \dot{c}$$

so that from the second differential equation in (236) we get

$$\dot{c} = -\frac{u'(c)}{u''(c)} [f'(x) - (\gamma + \delta)] \quad (237)$$

---

<sup>27</sup>It can be verified by Sylvester's criterion, being  $H_{xx}^c = \mu f''(x) = u'(c) f''(x) < 0$  and  $\begin{vmatrix} H_{xx}^c & H_{xu}^c \\ H_{ux}^c & H_{uu}^c \end{vmatrix} = u'(c) u''(c) f''(x) > 0$ .

with the transversality condition

$$\lim_{t \rightarrow +\infty} e^{-\delta t} [u(c) + u'(c)(f(x) - c - \gamma x)] = 0. \quad (238)$$

Notice that by assumption it is  $u''(c) \neq 0$  and  $-\frac{u'(c)}{u''(c)} > 0$ . Thus, the nullcline  $\dot{c} = 0$  is the locus of points  $\bar{x}$  such that

$$f'(\bar{x}) = (\gamma + \delta) \quad (239)$$

From the Inada conditions, for any fixed  $(\gamma + \delta) > 0$  there exists a unique root  $\bar{x}$  to equation (239). Equation (239) is often referred to as the *Modified Golden rule* in capital accumulation models. This nullcline is a vertical line in the  $(x, c)$  plane.

By (237),  $\dot{c} > 0$  for  $f'(x) > (\gamma + \delta)$ , which occurs, being  $f'(x)$  decreasing, for  $x < \bar{x}$ .

Now consider the nullcline  $\dot{x} = 0$ , which represents the set of points such that  $c = f(x) - \gamma x$ . Consider the function

$$c(x) = f(x) - \gamma x$$

It is  $c(0) = 0$  for  $x = 0$  and for  $c(\tilde{x}) = 0$  such that  $f(\tilde{x}) - \gamma\tilde{x}$ . Moreover,  $c(x)$  has a maximum point at the point  $\hat{x}$  (*golden rule state*) such that  $c'(\hat{x}) = 0$ , i.e. such that  $f'(\hat{x}) = \gamma$ . In other words, the nullcline  $\dot{x} = 0$  is, in the plane  $(x, c)$  an unimodal function. It is interesting to observe that  $\hat{x} > \bar{x}$ , see discussion below.

Moreover,  $\dot{x} > 0$  for  $c < f(x) - \gamma x$  i.e. below the curve  $c(x)$ . Through the condition  $\dot{x} = \dot{c} = 0$  we identify the following equilibrium of the system of ODE:

$$E = (\bar{x}, \bar{c}) = (\bar{x}, c(\bar{x})) = (\bar{x}, f(\bar{x}) - \gamma\bar{x}) \quad (240)$$

By graphical analysis, this equilibrium is a saddle point. The qualitative graph of the nullclines is identical to the one presented in the previous example. Notice that at the equilibrium  $(\bar{x}, c(\bar{x}))$  the transversality condition is satisfied, since  $c(\bar{x})$  is constant and condition  $\lim_{t \rightarrow +\infty} u'(c(\bar{x}))e^{-\delta t} = 0$  implies (238).

The stability analysis of equilibrium (240) can be carried out as always considering the eigenvalues of the Jacobian matrix at equilibrium. It is

$$\begin{aligned} J(E) &= \begin{bmatrix} \frac{\partial \dot{x}}{\partial x} & \frac{\partial \dot{x}}{\partial c} \\ \frac{\partial \dot{c}}{\partial x} & \frac{\partial \dot{c}}{\partial c} \end{bmatrix} = \begin{bmatrix} f'(\bar{x}) - \gamma & -1 \\ -\frac{u'(\bar{c})}{u''(\bar{c})} f''(\bar{x}) & -\frac{[u''(\bar{c})]^2 - u'''(\bar{c})u'(\bar{c})}{[u''(\bar{c})]^2} [f'(\bar{x}) - (\gamma + \delta)] \end{bmatrix} = \\ &= \begin{bmatrix} \delta & -1 \\ -\frac{u'(\bar{c})}{u''(\bar{c})} f''(\bar{x}) & 0 \end{bmatrix} \end{aligned}$$

By (239), the element  $J_{11} = \delta$  and  $J_{22} = 0$ . Clearly,  $Tr(J) = \delta > 0$  and  $Det(J) = -\frac{u'(\bar{c})}{u''(\bar{c})} f''(\bar{x}) < 0$  so that  $E$  is indeed a saddle point. The eigenvalues are solutions of the characteristic equation in the unknown  $\lambda$ :

$$\lambda^2 - \delta\lambda - \frac{u'(\bar{c})}{u''(\bar{c})} f''(\bar{x}) = 0$$

i.e.

$$\lambda_{1,2} = \frac{\delta \pm \sqrt{\delta^2 + 4\frac{u'(\bar{c})}{u''(\bar{c})} f''(\bar{x})}}{2}$$



As for the previous example, any trajectory belonging to the stable manifold of  $E$  ensures the convergence to the *optimal long-run stationary equilibrium*  $E$  in (240).

In the economic literature, an equilibrium such as  $E$  is often called a *turnpike* and is obtained through the modified golden rule (239). Why modified? The reason is the following. In general the turnpike is different from the equilibrium that maximizes the integrand function (see (235)). In fact, from the state equation  $\dot{x} = f(x) - c - \gamma x$  we know that an equilibrium must satisfy condition  $\dot{x} = 0$ , i.e.  $c = f(x) - \gamma x$ . If we substitute this  $c$  in the integrand in (235) we get  $u(f(x) - \gamma x)$ , which is maximized at the  $\hat{x}$  such that  $u'(f(\hat{x}) - \gamma\hat{x})(f'(\hat{x}) - \gamma) = 0$ , i.e. for the  $\hat{x}$  such that  $f'(\hat{x}) = \gamma$ . State  $\hat{x}$  is called golden rule. Notice that the golden rule coincides with the modified golden rule in (239) only for  $\delta = 0$ .

**Example - Optimal fishery with constant price.** Another important optimal growth problem is the fishery model proposed by Clark and Munro,<sup>28</sup> which can be stated as follows

$$\max_{u(t) \geq 0} \int_0^{+\infty} e^{-\delta t} R(u, x) dt \quad (241)$$

such that:

$$\begin{cases} \dot{x} = f(x) - u \\ x(0) = x_0 \end{cases}$$

The interpretation of this problem is that a monopolist can harvest a renewable resource (fish) from a lake, whose time  $t$  stock is denoted by  $x = x(t)$ . The (instantaneous) profit from selling  $u$  units of fish in the market is given by the function  $R(u, x)$ . Clearly, this is a growth model and it is very similar to the one previously considered. However, two important differences are present in the optimal fishery model. First, the type of resource suggests a "production" function that is different from the one considered before, which was assumed to satisfy the Inada conditions (234). Second, the profit function depends, in general, not only on the harvesting  $u$ , but also on the level of the resource  $x$ .

With respect to the first point, if one considers the logistic "growth" function  $f(x) = \alpha x - \beta x^2$ , then the state ODE in (241) becomes

$$\begin{aligned} \dot{x} &= f(x) - u = \alpha x - \beta x^2 + \gamma x - \gamma x - u = \\ &= (\alpha + \gamma)x - \beta x^2 - \gamma x - u \end{aligned}$$

Thus, if  $R(u, x) = R(u)$ , that is profit does not depend on the level of biomass, model (241) has the same formulation of model (235). Notice, however, that the fishery "production" function  $g(x) = (\alpha + \gamma)x - \beta x^2$  does not satisfy the Inada conditions (234).

With respect to the second point, in the fishery model the "utility" (profit) does not depend only on consumption (harvesting) but also on the level of the stock. A simple motivation for this is related to the cost of harvesting: if fish is abundant, then harvesting should be cheaper and vice-versa when the fish stock is low. For instance, assume that the instantaneous profit is

$$R(u, x) = [p - c(x)]u \quad (242)$$

---

<sup>28</sup>Clark, C.W., Munro, G.R. (1975) The economics of fishing and modern capital theory: A simplified approach, *Journal of Environmental Economics and Management*, 2,92, 92-106.

where  $p$  is the (constant) selling price of fish,  $c(x)$  is the marginal cost of harvesting, which depends on the level of the resource, and  $u$  is the harvesting. Usually it is assumed that the harvesting  $u$  is given by

$$u = Ex$$

where  $E$  is the fishing effort (e.g. days fished). If the cost of an unit of effort is constant and equal to  $\theta$ , then the total cost of fishing is

$$\theta E = \theta \frac{u}{x}$$

i.e. in (242) it is  $c(x) = \frac{\theta}{x}$ . Since it is realistic to assume that fishing effort is nonnegative and below an upper bound (due to capacity constraints of the fleets), the control  $E$  must be taken such that  $0 \leq E \leq E_{\max}$ . Summing up, the optimal fishery model with constant price and stock-dependent marginal costs can be formulated as follows

$$\max_{0 \leq E \leq E_{\max}} \int_0^{+\infty} e^{-\delta t} Ex [p - c(x)] dt \quad (243)$$

such that:

$$\begin{cases} \dot{x} = f(x) - Ex \\ x(0) = x_0 \end{cases}$$

where  $Ex [p - c(x)]$  in the integral represents instantaneous profits.

The current-value Hamiltonian (211) for this problem is

$$H^c = Ex [p - c(x)] + \mu (f(x) - Ex) = \quad (244)$$

$$= Ex [p - c(x) - \mu] + \mu f(x) \quad (245)$$

Notice that (244) is linear in the control variable  $E$ : to maximize the current-value Hamiltonian (244) one requires to set  $E = 0$  whenever  $p - c(x) - \mu < 0$  and  $E = E_{\max}$  whenever  $p - c(x) - \mu > 0$ . Defining the *switching function*  $s(x) = p - c(x) - \mu$ , the optimal control then looks like this

$$E = \begin{cases} 0 & \text{if } s(x) < 0 \\ ? & \text{if } s(x) = 0 \\ E_{\max} & \text{if } s(x) > 0 \end{cases} \quad (246)$$

What happens when the switching function  $s(x)$  is zero? Assume that over an interval it is  $s(x) = 0$ , i.e.  $\mu = p - c(x)$ . Then, calculating from this relationship the derivative of the costate  $\mu$  with respect to time, one gets

$$\dot{\mu} = -c'(x) \dot{x} = -c'(x) (f(x) - Ex)$$

Since an optimal  $\mu$  must also satisfy the costate ODE, in this interval is:

$$\begin{aligned} \dot{\mu} &= -\frac{\partial H^c}{\partial x} + \mu\delta = -E \left[ \underbrace{p - c(x) - \mu}_{=0} \right] + Exc'(x) - \mu f'(x) + \mu\delta \\ &= Exc'(x) - \mu (f'(x) - \delta) = Exc'(x) - (p - c(x)) (f'(x) - \delta) \end{aligned}$$

where the last line follows from  $p - c(x) - \mu = 0$  in the interval. The two expressions for  $\dot{\mu}$  are equal when

$$-c'(x) (f(x) - Ex) = Exc'(x) - (p - c(x)) (f'(x) - \delta)$$

which is satisfied for a stock level  $x^*$  such that

$$f'(x^*) - \frac{c'(x^*)f(x^*)}{p - c(x^*)} = \delta \quad (247)$$

Equation (247) is called the *Modified Golden Rule* of fishery (with constant price). The particular level of resource  $x^*$  in (247) is called *singular solution* and is obtained when the switching function  $s(x)$  is zero over an interval. Being  $x^*$  constant, it is  $\dot{x} = f(x^*) - Ex^* = 0$ , from which we get that the optimal effort when  $s(x) = 0$  is exactly  $E^* = \frac{f(x^*)}{x^*}$ , which is the "?" in (246), called the *singular control*. Summing up, the optimal control (246) is obtained combining *bang-bang* controls, i.e. no fishing ( $E = 0$ ) when fishing is not remunerative or maximum harvesting ( $E = E_{\max}$ ) when fishing is high profitable, with the singular control when the state is singular. This optimal control constitutes the so-called *Most Rapid Approach* harvest strategy: when the resource is abundant, i.e.  $x(t) > x^*$ , then it is optimal to harvest as much as possible, i.e.  $E = E_{\max}$ , until the resource converges to  $x^*$  and then apply always the singular control. Analogously, when the resource is scarce, i.e.  $x(t) < x^*$ , then it is optimal not to harvest, i.e.  $E = 0$ , until the resource grows to the level  $x^*$ , to which it remains by employing the singular control. Thus, if we want to express the optimal control  $E^*$  as a function of the state of the system (stock of resource), we can write it in feedback form as follows

$$E^* = \begin{cases} 0 & \text{if } x(t) < x^* \\ \frac{f(x^*)}{x^*} & \text{if } x(t) = x^* \\ E_{\max} & \text{if } x(t) > x^* \end{cases}$$

**Example (Optimal fishery with nonconstant price).** We revisit the previous example and allow for nonconstant prices.<sup>29</sup> We state the problem as follows

$$\max_{h \geq 0} \int_0^{+\infty} e^{-\delta t} h [p(h) - c(x)] dt \quad (248)$$

such that:

$$\begin{cases} \dot{x} = f(x) - h \\ x(0) = x_0 \end{cases}$$

where the control variable is the harvesting rate  $h$ .<sup>30</sup> In this example, the instantaneous profit is  $\pi(h) = h [p(h) - c(x)]$ .

The current-value Hamiltonian (211) for this problem is

$$H^c = h [p(h) - c(x)] + \mu (f(x) - h) \quad (249)$$

With positive harvesting  $h > 0$ , the optimal control must satisfy the condition

$$\frac{\partial H^c}{\partial h} = p(h) + hp'(h) - c(x) - \mu = 0$$

from which it is

$$\mu = p(h) + hp'(h) - c(x) = \pi'(h) \quad (250)$$

<sup>29</sup>Clark, C.W. *Mathematical Bioeconomics: The Optimal Management of Renewable Resources*. 1990, John Wiley & Sons.

<sup>30</sup>In the previous example it was  $h = Ex$ . Here we reason directly in terms of harvesting  $h$  for the sake of simplicity.

The costate equation is

$$\dot{\mu} = -\frac{\partial H^c}{\partial x} + \mu\delta = hc'(x) + \mu(\delta - f'(x)) \quad (251)$$

Deriving (250) with respect to time, one gets  $\dot{\mu} = \pi''(h)\dot{h}$  that equated with (251) gives

$$hc'(x) + \mu(\delta - f'(x)) = \pi''(h)\dot{h}$$

so that, using again (250), the dynamics of optimal harvesting must satisfy the condition

$$\dot{h} = \frac{hc'(x) + \pi'(h)(\delta - f'(x))}{\pi''(h)} \quad (252)$$

This last ODE, the stock dynamics  $\dot{x} = f(x) - h$  and the proper transversality condition constitute the necessary conditions that the optimal solution couple (harvesting and resource dynamics) must satisfy. From conditions  $\dot{h} = \dot{x} = 0$ , it is possible to obtain an optimal steady state of the system  $x^*$ , which satisfy the "modified golden rule" condition

$$\frac{f(x^*)c'(x^*) + \pi'(f(x^*))(\delta - f'(x^*))}{\pi''(f(x^*))} = 0$$

that can be rewritten as

$$f'(x^*) - \frac{c'(x^*)f(x^*)}{\pi'(f(x^*))} = \delta \quad (253)$$

which is the analogous of (247) with nonlinear demand.

For instance assume that fish is sold with linear inverse demand

$$p(h) = a - bh$$

and that the cost of harvesting is independent on the stock,  $c(x) = c$ . As for  $f(x)$ , assume logistic growth

$$f(x) = x(\alpha - \beta x) \quad (254)$$

The optimal control problem (248) particularizes to

$$\max_{h \geq 0} \int_0^{+\infty} e^{-\delta t} [mh - bh^2] dt \quad (255)$$

such that:

$$\begin{cases} \dot{x} = x(\alpha - \beta x) - h \\ x(0) = x_0 \end{cases}$$

where we denoted  $m = a - c$ , which represents the unitary markup. Clearly,  $\pi(h) = mh - bh^2$  is the instantaneous profit. We already established that  $\mu = \pi'(h)$ . Through the previous reasoning, applied to the current-value Hamiltonian

$$H^c = mh - bh^2 + \mu(x(\alpha - \beta x) - h)$$

we obtain the following nonlinear system of ODE that the solution candidate must satisfy:

$$\begin{cases} \dot{x} = x(\alpha - \beta x) - h \\ \dot{h} = \frac{\pi'(h)(\delta - f'(x))}{\pi''(h)} = -\frac{(m-2bh)(\delta - \alpha + 2\beta x)}{2b} \end{cases} \quad (256)$$

Notice, in particular that,  $H^c$  is concave with respect to  $x$  and  $h$ . In the  $(x, h)$  plane, the nullcline  $\dot{x} = 0$  is represented by the parabola  $f(x)$  in (254); the nullcline  $\dot{h} = 0$  is represented by two lines: one horizontal line of equation  $h = \frac{m}{2b}$ , which maximizes instantaneous profits being there  $\pi'(h) = 0$ , and one vertical line of equation  $x = \frac{\alpha - \delta}{2\beta}$ , which corresponds to the modified golden rule stock, since in this case (253) reduces to  $f'(x^*) = \delta$  being  $c'(x) = 0$ .

Equilibria of the ODE system (256) solve the system of equations (256) with  $\dot{x} = \dot{h} = 0$ . To easy the algebra without loosing generality, assume, from now on, that the demand is normalized so that  $b = \frac{1}{2}$ .

When  $x = \frac{\alpha - \delta}{2\beta}$  (vertical nullcline  $\dot{h} = 0$ ), a unique equilibrium exists

$$E_1 = (x_1, h_1) = \left( \frac{\alpha - \delta}{2\beta}, \frac{(\alpha - \delta)(\alpha + \delta)}{4\beta} \right)$$

which is meaningful provided that  $\alpha \geq \delta$ . As already observed,  $x_1$  in  $E_1$  is exactly the (modified) golden rule level (253).

When  $h = \frac{m}{2b} = m$  (horizontal nullcline  $\dot{h} = 0$ ) from the first equation in (256) we get the following two equilibrium values  $(x, h)$ :

$$\begin{aligned} E_2 &= \left( \frac{\alpha - \sqrt{\alpha^2 - 4m\beta}}{2\beta}, m \right) \\ E_3 &= \left( \frac{\alpha + \sqrt{\alpha^2 - 4m\beta}}{2\beta}, m \right) \end{aligned}$$

The  $x$  components in  $E_2$  and  $E_3$  are real numbers provided that  $\alpha^2 - 4m\beta \geq 0$ . When  $\alpha^2 - 4m\beta < 0$ , i.e. when

$$m > \frac{\alpha^2}{4\beta} \quad (257)$$

$E_2$  and  $E_3$  are not meaningful equilibria. From an economic point of view, the harvesting that would maximize instantaneous profits ( $h = m$ ) is "out-of-reach", as it is greater than the vertex of the parabola (254),  $f\left(\frac{\alpha}{2\beta}\right) = \frac{\alpha^2}{4\beta}$ , which is called the maximum sustainable yield (*MSY*) in resource economics.<sup>31</sup> Thus, the model has different number of equilibria and different dynamic properties, as explained below.

---

<sup>31</sup>Notice that  $\frac{\alpha}{2\beta}$  is indeed the golden rule level of the stock. To be more precise, from  $\dot{x} = 0$ , we get that at equilibrium it is

$$\bar{h} = x(\alpha - \beta x)$$

so that instantaneous profit is

$$\begin{aligned} \bar{\pi} &= m\bar{h} - b\bar{h}^2 = \\ &= m[x(\alpha - \beta x)] - b[x(\alpha - \beta x)]^2 \end{aligned}$$

Consider first the case  $\alpha^2 - 4m\beta < 0$ , i.e. the case where condition (257) holds, where the unique equilibrium of the ODE (256) is  $E_1$ . The Jacobian of (256) is

$$J = \begin{bmatrix} \frac{\partial \dot{x}}{\partial x} & \frac{\partial \dot{x}}{\partial h} \\ \frac{\partial \dot{h}}{\partial x} & \frac{\partial \dot{h}}{\partial h} \end{bmatrix} = \begin{bmatrix} \alpha - 2\beta x & -1 \\ 2\beta(h - m) & -\alpha + 2\beta x + \delta \end{bmatrix}$$

from which we calculate

$$J(E_1) = \begin{bmatrix} \delta & -1 \\ \frac{\alpha^2 - 4m\beta - \delta^2}{2} & 0 \end{bmatrix}$$

Clearly  $Tr(J) = \delta > 0$  and  $Det(J) = \frac{\alpha^2 - 4m\beta - \delta^2}{2}$ . Notice that  $Det(J) < 0 \iff m > \frac{\alpha^2 - \delta^2}{4\beta}$ . Since we are assuming (257), we can conclude that when system (256) admits the unique equilibrium  $E_1$  then  $E_1$  is a saddle point. This equilibrium is a solution of system (256) and, being constant, satisfies a transversality condition of the form  $\lim_{t \rightarrow +\infty} \pi'(h_1)e^{-\delta t} = 0$ , which implies  $\lim_{t \rightarrow +\infty} H^c e^{-\delta t} = 0$ . This is exactly as in the capital accumulation model example. For any initial condition  $x(0) \neq \frac{\alpha - \delta}{2\beta}$ , the optimal trajectory belongs to the stable manifold of the saddle  $E_1$ , to which the solution converges in the long run. Notice also that in this case, the optimal path is analogous to the case of constant prices, although with constant prices the optimal control is a combination of bang-bang controls with the singular control to steer the system to the singular state as soon as possible, whereas with nonconstant prices the optimal control is along the stable manifold of the saddle.

Fig.149 shows this case, where the red curves are the nullclines. Different colors correspond to different signs of the vector field (256), namely  $\dot{x} > 0$  and  $\dot{h} > 0$  (red region),  $\dot{x} > 0$  and  $\dot{h} < 0$  (blue region),  $\dot{x} < 0$  and  $\dot{h} < 0$  (yellow region),  $\dot{x} < 0$  and  $\dot{h} > 0$  (white region). Clearly  $E_1$ , intersection between the parabola and the vertical line, is a saddle point.

Now consider what happens when  $\alpha^2 - 4m\beta > 0$ , i.e. when all three equilibria exist. After  $E_2$  and  $E_3$  are created, through a fold bifurcation for (256) at  $m = \frac{\alpha^2}{4\beta}$  (see Figure 150)(a),  $E_1$  remains a saddle point as long as  $m > \frac{\alpha^2 - \delta^2}{4\beta}$ .

At  $E_2$  the Jacobian is

$$J(E_2) = \begin{bmatrix} \sqrt{\alpha^2 - 4m\beta} & -1 \\ 0 & -\sqrt{\alpha^2 - 4m\beta} + \delta \end{bmatrix}$$

and the eigenvalues are the entries along the diagonal. So it is  $\sqrt{\alpha^2 - 4m\beta} > 0$  and  $-\sqrt{\alpha^2 - 4m\beta} + \delta > 0$  for  $m \in \left(\frac{\alpha^2 - \delta^2}{4\beta}, \frac{\alpha^2}{4\beta}\right)$ . Hence, for  $m \in \left(\frac{\alpha^2 - \delta^2}{4\beta}, \frac{\alpha^2}{4\beta}\right)$ ,  $E_2$  is an unstable node and  $E_1$  is a saddle (see Figure 150)(b)); when  $m \in \left(0, \frac{\alpha^2 - \delta^2}{4\beta}\right)$ ,  $E_2$  is a saddle and  $E_1$  is an unstable node (Figure 150)(c): at  $m = \frac{\alpha^2 - \delta^2}{4\beta}$  a transcritical bifurcation occurs at which  $E_2$  and  $E_1$  exchange their stability properties.

At  $E_3$  the Jacobian is

$$J(E_3) = \begin{bmatrix} -\sqrt{\alpha^2 - 4m\beta} & -1 \\ 0 & \sqrt{\alpha^2 - 4m\beta} + \delta \end{bmatrix}$$

---

Instantaneous profit  $\bar{\pi}(x)$  is maximized at  $x = \frac{\alpha}{2\beta}$  if  $m > \frac{\alpha^2}{4\beta}$  as  $\bar{\pi}'\left(\frac{\alpha}{2\beta}\right) = 0$  and  $\bar{\pi}''\left(\frac{\alpha}{2\beta}\right) < 0$  however, for  $m < \frac{\alpha^2}{4\beta}$ ,  $\bar{\pi}(x)$  has at  $x = \frac{\alpha}{2\beta}$  a minimum point, whereas  $\bar{\pi}(x)$  is maximized at the "golden rule" levels given by the state values in  $E_2$  and  $E_3$ , namely at  $x = \frac{\alpha \pm \sqrt{\alpha^2 - 4m\beta}}{2\beta}$ .

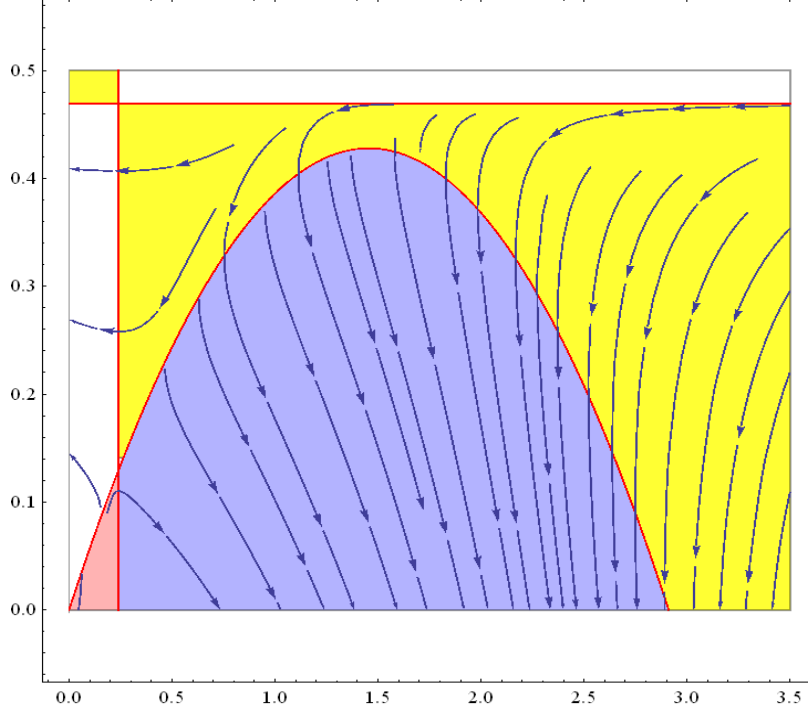


Figure 149: Phase portrait for the model of optimal fishery with nonconstant price. Red curves are the nullclines, different colors correspond to different signs of the vector field (256).

with eigenvalues, again, on the diagonal. Since  $\sqrt{\alpha^2 - 4m\beta} < 0$  and  $\sqrt{\alpha^2 - 4m\beta} + \delta > 0$  for all  $m \in \left(0, \frac{\alpha^2}{4\beta}\right)$ , we conclude that  $E_3$ , when exists, is a saddle.

Summing up, for  $m \in \left(\frac{\alpha^2}{4\beta}, +\infty\right)$ , with  $\alpha > \delta$ , the only equilibrium is the saddle  $E_1$ . This equilibrium constitutes the optimal equilibrium of the system and the stable manifold of the equilibrium is the optimal combination of state and control to maximize profits, i.e. it provides the feedback control (see fig. 149).

When  $m \in \left(\frac{\alpha^2 - \delta^2}{4\beta}, \frac{\alpha^2}{4\beta}\right)$  the saddle  $E_1$  coexists with the unstable node  $E_2$  and the saddle  $E_3$ . Depending on the initial condition of the system, the optimal trajectory is either along the stable manifold of the saddle  $E_1$  or along the stable manifold of the saddle  $E_3$  (see fig.150)(b))

When  $m \in \left(0, \frac{\alpha^2 - \delta^2}{4\beta}\right)$ , the saddle  $E_2$  coexists with the unstable node  $E_1$  and the saddle  $E_3$ : when  $x(0) > \frac{\alpha - \delta}{2\beta}$  it is optimal to harvest  $h = m$  in perpetuity to converge to  $E_3$ ; when  $x(0) < \frac{\alpha - \delta}{2\beta}$ , then it is convenient to stay along the stable manifold of the saddle  $E_2$  to let the resource grow until it is sustainable to harvest  $h = m$ . Then it is optimal to harvest  $m$  in perpetuity (see fig.150)(c)). Notice that in this scenario, the modified golden rule does not identify the optimal biomass level since it is optimal to harvest according to the golden rule.

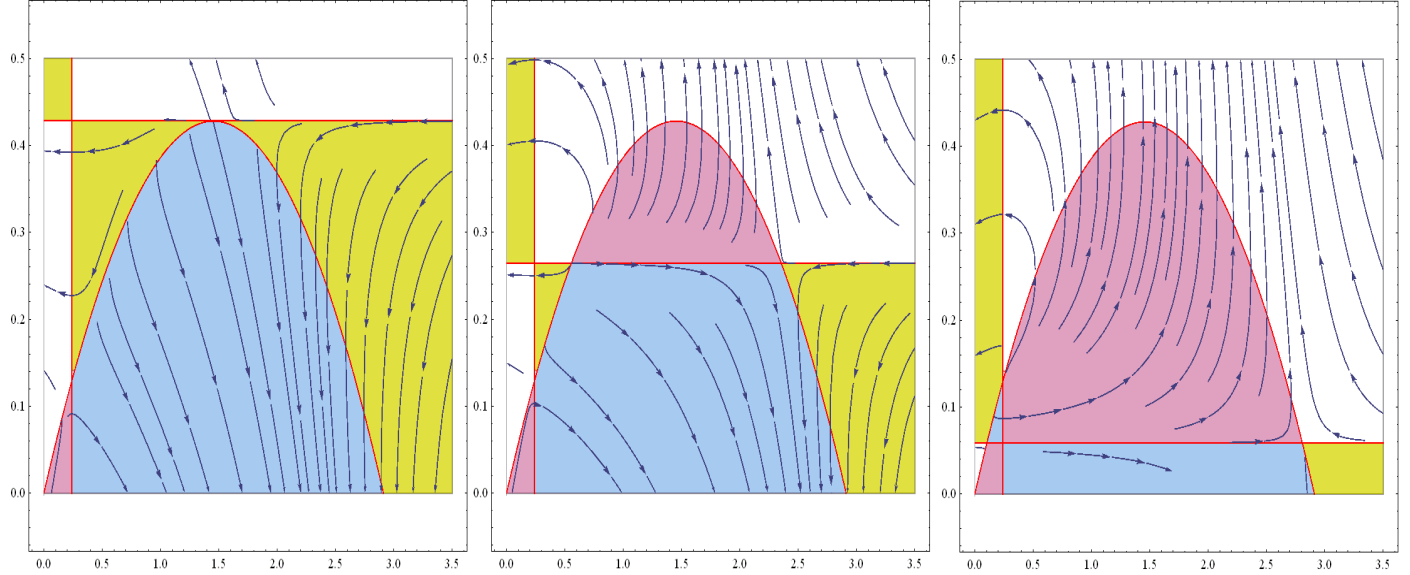


Figure 150: Different dynamic scenarios for the model of optimal fishery with nonconstant price. Red curves are the nullclines, different colors correspond to different signs of the vector field (256).

## 10 Appendix

### 10.1 Complex Numbers

It is well known from elementary algebra that a second degree equation of the form  $ax^2 + bx + c = 0$  has real solutions if and only if  $\Delta = b^2 - 4ac \geq 0$ . For instance, equation  $x^2 + 2x + 3 = 0$  has no real solution, since if we try to write them we get  $x = -1 \pm \frac{\sqrt{-8}}{2}$ .

Thus, second degree equations with  $\Delta < 0$  do not admit (real) solutions since the square root of a negative number can not be defined in the set of real numbers  $\mathbb{R}$  as a consequence of the sign rule: the square of any real number is nonnegative. To overcome this problem, let us define the quantity  $i$  which satisfies the condition  $i^2 = -1$ , from which it is  $\sqrt{-1} = i$ . reworking the previous example we get that the solutions of  $x^2 + 2x + 3 = 0$  are

$$-1 \pm \frac{\sqrt{-8}}{2} = -1 \pm \frac{\sqrt{-1 \cdot 8}}{2} = -1 \pm \frac{\sqrt{-1}\sqrt{8}}{2} = -1 \pm i\sqrt{2}$$

Motivated by this example, in this appendix we provide a concise treatment of complex numbers.

**Definition.** *The set of complex numbers  $\mathbb{C}$  is the set of the ordered couples  $(x,y)$  of real numbers for which the operations of sum and product are defined satisfying properties listed (P1) to (P9) below.*

The imaginary unity is  $i = (0,1)$ . Any complex number  $(x,y)$  can be expressed in the form  $x + iy = x(1,0) + y(0,1)$ , where  $x$  is called the real part of  $x + iy$  and  $y$  is the imaginary part of  $x + iy$ . From a geometric point of view, a complex number  $q = a + ib$  can be represented in a Cartesian plane, called Complex plane, through the vector  $[a, b]$ . Usually, in the horizontal axis a segment of length  $a$  is traced (the real part of  $q$ ) and, analogously, a segment of length  $b$  is considered in the vertical axis (the imaginary part of  $q$ ). A complex number with imaginary part equals to zero becomes a



real number, i.e.  $\mathbb{R} \subset \mathbb{C}$ . All the operations between complex numbers defined below are the usual arithmetic operations between real numbers whenever they are applied to complex numbers with zero imaginary part.

Let us define the operations of sum and product of complex numbers.

**Definition.** If  $q = a + ib$  and  $w = c + id$ , then the sum  $q + w$  is defined as follows:  $q + w = (a + ib) + (c + id) = (a + c) + i(b + d)$ .

**Definition.** If  $q = a + ib$  and  $w = c + id$ , then the product  $q \cdot w$  is defined as follows:  $q \cdot w = (a + ib) \cdot (c + id) = (ac - bd) + i(bc + ad)$ .

To remember how to perform the two operations, it is useful to notice the followings. For the sum one has to sum the real parts of the two numbers to obtain the real part of the complex number and, analogously, for the imaginary parts. For the product, one calculates the product in the usual way recalling that  $i^2 = -1$ .

Examples:

$$(2 + 3i) + (1 + 5i) = 3 + 8i;$$

$$(2 + 3i) - (1 + 5i) = (2 + 3i) + (-1 - 5i) = 1 - 2i$$

$$(3 + i6) \cdot (2 - i3) = 24 + i3 ; i^2 = (0, 1) \cdot (0, 1) = -1.$$

### 10.1.1 Properties of sum and product of complex numbers.

Let us consider  $a, b, c \in \mathbb{C}$

$$(P1) \ a + b = b + a$$

$$(P2) \ (a + b) + c = a + (b + c)$$

$$(P3) \ a + 0 = a + (0, 0) = a$$

$$(P4) \ a + (-a) = 0$$

$$(P5) \ a \cdot b = b \cdot a$$

$$(P6) \ (a \cdot b) \cdot c = a \cdot (b \cdot c)$$

$$(P7) \ 1 \cdot a = (1, 0) \cdot a = a$$

$$(P8) \ \text{if } a = x + iy \neq 0 \Rightarrow \exists a^{-1} \in \mathbb{C} \text{ such that } a^{-1} \cdot a = 1$$

$$(P9) \ (a + b) \cdot c = a \cdot c + b \cdot c$$

Another useful definition is the following:

**Definition.** The modulus of the complex number  $q = a + ib$  is

$$|q| = \sqrt{a^2 + b^2}$$

The modulus of a complex number has the following properties:

$$(M1) \ |q| = |a + ib| = 0 \Leftrightarrow q = 0 \text{ (that is } a = b = 0)$$

$$(M2) \ |q + w| \leq |q| + |w|$$

$$(M3) \ |qw| = |q| \cdot |w|$$

For instance  $|-2 + 3i| = \sqrt{4 + 9} = \sqrt{13}$ ;  $|-3| = 3$ . Notice that the modulus extends in  $\mathbb{C}$  the definition of absolute value of a real number. By Pythagorean's theorem, the modulus of the complex number  $q = a + ib$  represents the (Euclidean) distance between the point  $(a, b)$  and the origin  $(0, 0)$ .

**Definition.** Given the complex number  $q = a + ib$ , the complex conjugate of  $q$  is  $\bar{q} = a - ib$ .

Notice that a number  $q$  coincides with its complex conjugate if and only if  $q \in \mathbb{R}$ . Moreover, it is easy to verify that given any  $q \in \mathbb{C}$ ,  $q \cdot \bar{q} \in \mathbb{R}$ , since it is

$$(a + ib)(a - ib) = a^2 + iab - iab + b^2 = |a + ib|^2 = |a - ib|^2.$$

For instance  $(2 + i)(2 - i) = 5$  and it is  $|2 + i| = |2 - i| = \sqrt{5}$ .

The definitions of modulus and complex conjugate of a complex number are useful to define the inverse of a complex number.

Let us consider  $q = a + ib \neq 0$ . Then, by property (P8) an element  $q^{-1}$  exists such that  $q \cdot q^{-1} = q^{-1} \cdot q = 1$ . Through the relationship  $(a + ib)(a - ib) = |a + ib|^2 = |a - ib|^2$  it is easy to see that

$$q^{-1} = \frac{\bar{q}}{|q|^2}$$

in fact it is

$$q \cdot q^{-1} = q \cdot \frac{\bar{q}}{|q|^2} = \frac{|q|^2}{|q|^2} = 1$$

**Definition.** Given the complex numbers  $q, z \in \mathbb{C}$ , the division  $\frac{z}{q}$  is defined as:

$$\frac{z}{q} = z \cdot q^{-1}$$

For example, let us consider the division  $\frac{3-5i}{2-6i}$ . Being

$$(2 - 6i)^{-1} = \frac{1}{20} + \frac{3}{20}i$$

it is

$$\frac{3 - 5i}{2 - 6i} = (3 - 5i) \cdot \left( \frac{1}{20} + \frac{3}{20}i \right) = \left( \frac{9}{10} + \frac{1}{5}i \right)$$

### 10.1.2 Polar form of a complex number

From elementary geometry, we know that a point in the plane can be indicated in a unique way through its Cartesian coordinates  $(a, b)$ . An alternative way to identify the same point is to indicate the distance between the point  $(a, b)$  and the origin  $(0, 0)$ , which is the modulus, and the angle  $\theta$  that the vector  $[a, b]$  forms with the positive semiaxis. Consider the complex number  $q = a + ib$ , with  $\rho = |q|$ . Then it is  $\cos \theta = \frac{a}{\rho}$  and  $\sin \theta = \frac{b}{\rho}$ . Hence, we can write the complex number in *polar form* as follows

$$q = a + ib = \rho \cdot \cos \theta + \rho \cdot i \cdot \sin \theta = \rho \cdot (\cos \theta + i \cdot \sin \theta).$$

For instance, consider the complex number  $q = 1 + i$ , whose modulus is  $|q| = \sqrt{2}$ . We can write

$$q = \sqrt{2} \left( \frac{1}{\sqrt{2}} + i \frac{1}{\sqrt{2}} \right)$$

moreover, recalling that  $\cos \theta = 1/\sqrt{2}$  and  $\sin \theta = 1/\sqrt{2}$ , we get that it is  $\theta = \frac{\pi}{4}$ . Summing up, we can write  $q$  as follows:

$$q = 1 + i = \sqrt{2} \left( \cos \frac{\pi}{4} + i \sin \frac{\pi}{4} \right)$$

The polar form of a complex number is useful since it allows to apply trigonometric relationships in calculations with complex numbers. In particular, recall the rules of adding and subtracting:  $\forall \alpha, \beta \in \mathbb{R}$  it is:

$$\begin{aligned}\sin(\alpha + \beta) &= \sin \alpha \cos \beta + \sin \beta \cos \alpha \\ \cos(\alpha + \beta) &= \cos \alpha \cos \beta - \sin \beta \sin \alpha \\ \sin(\alpha - \beta) &= \sin \alpha \cos \beta - \sin \beta \cos \alpha \\ \cos(\alpha - \beta) &= \cos \alpha \cos \beta + \sin \beta \sin \alpha\end{aligned}$$

Thus, we can perform the product of complex numbers in polar form in the following way. Let us consider two complex numbers  $q = \rho(\cos \alpha + i \sin \alpha)$  and  $w = \sigma(\cos \beta + i \sin \beta)$ . Then it is

$$\begin{aligned}q \cdot w &= \rho(\cos \alpha + i \sin \alpha) \cdot \sigma(\cos \beta + i \sin \beta) = \\ &= \rho \cdot \sigma(\cos \alpha \cos \beta - \sin \alpha \sin \beta + i(\sin \alpha \cos \beta + \sin \beta \cos \alpha)) = \\ &= \rho \cdot \sigma[\cos(\alpha + \beta) + i \sin(\alpha + \beta)]\end{aligned}$$

For instance, consider  $q = \sqrt{2}(\cos \frac{\pi}{4} + i \sin \frac{\pi}{4})$  and  $w = 3(\cos \frac{3}{4}\pi + i \sin \frac{3}{4}\pi)$ , then it is

$$\begin{aligned}q \cdot w &= \left[ \sqrt{2} \left( \cos \frac{\pi}{4} + i \sin \frac{\pi}{4} \right) \right] \cdot \left[ 3 \left( \cos \frac{3}{4}\pi + i \sin \frac{3}{4}\pi \right) \right] = \\ &= 3\sqrt{2}(\cos(\frac{\pi}{4} + \frac{3}{4}\pi) + i \sin(\frac{\pi}{4} + \frac{3}{4}\pi)) = -3\sqrt{2}\end{aligned}$$

The previous rule is particularly useful when one wants to calculate the power of a complex number (De Moivre's formula). Consider the complex number  $q = \rho(\cos \alpha + i \sin \alpha)$ . Then, by the previous argument, the product of  $q$  with itself  $n$  times can be written as

$$q^n = \rho^n(\cos(n\alpha) + i \sin(n\alpha)).$$

### 10.1.3 Exponential form of a complex number

An alternative way to write a complex number is through the exponential function. We motivate this point by considering expansions in Taylor series of the exponential function

$$e^x = 1 + x + \frac{x^2}{2!} + \frac{x^3}{3!} + \frac{x^4}{4!} + \dots = \sum_{j=0}^{\infty} \frac{x^j}{j!}$$

and the Taylor series of trigonometric functions:

$$\begin{aligned}\cos x &= 1 - \frac{x^2}{2!} + \frac{x^4}{4!} - \frac{x^6}{6!} + \dots \\ \sin x &= x - \frac{x^3}{3!} + \frac{x^5}{5!} - \frac{x^7}{7!} + \dots\end{aligned}$$

Thus, we can write a complex number in the so called *exponential form* as follows:

$$\begin{aligned}q &= \rho(\cos \alpha + i \sin \alpha) = \rho \left[ \left( 1 - \frac{\alpha^2}{2!} + \frac{\alpha^4}{4!} - \frac{\alpha^6}{6!} + \dots \right) + i \left( \alpha - \frac{\alpha^3}{3!} + \frac{\alpha^5}{5!} - \frac{\alpha^7}{7!} + \dots \right) \right] = \\ &= \rho \left[ \left( 1 + \frac{i^2 \alpha^2}{2!} + \frac{i^4 \alpha^4}{4!} + \frac{i^6 \alpha^6}{6!} + \dots \right) + \left( i\alpha + \frac{i^3 \alpha^3}{3!} + \frac{i^5 \alpha^5}{5!} + \frac{i^7 \alpha^7}{7!} + \dots \right) \right] = \\ &= \rho \left[ 1 + i\alpha + \frac{i^2 \alpha^2}{2!} + \frac{i^3 \alpha^3}{3!} + \frac{i^4 \alpha^4}{4!} + \frac{i^5 \alpha^5}{5!} + \frac{i^6 \alpha^6}{6!} + \dots \right] = \\ &= \rho \left[ 1 + i\alpha + \frac{(i\alpha)^2}{2!} + \frac{(i\alpha)^3}{3!} + \frac{(i\alpha)^4}{4!} + \dots \right] = \rho e^{i\alpha}.\end{aligned}$$

Considering the product of complex numbers in trigonometric form, the following relationship holds:  $q^n = \rho^n e^{in\alpha}$ ,  $\forall n \in \mathbb{N}$ . Moreover, it is possible to show that the complex exponential maintains all the properties that the exponential has in  $\mathbb{R}$ . For instance, it is  $e^q e^w = e^{q+w}$ . Thus, it is  $e^{a+ib} = e^a e^{ib} = e^a (\cos b + i \sin b)$ .

#### 10.1.4 Complex numbers and polynomial equations

The most important application of complex numbers is the famous *Fundamental theorem of algebra*, which states that any polynomial with complex coefficients has roots in the set of complex numbers. Obviously, the theorem applies as a particular case to polynomial with real coefficients.

**Fundamental Theorem of Algebra.** *Every polynomial equation in the unknown  $z$  of the type*

$$a_n z^n + a_{n-1} z^{n-1} + \dots + a_1 z + a_0 = 0 \quad (258)$$

*with  $a_i \in \mathbb{C}$ ,  $i=0, \dots, n$ , has  $n$  roots in  $\mathbb{C}$ , each one counted with its multiplicity.*

We recall that  $z_0$  is a root of multiplicity  $m$  of the polynomial equation  $P(z) = a_n z^n + a_{n-1} z^{n-1} + \dots + a_1 z + a_0$  if  $P(z_0) = 0$  and  $P(z) = (z - z_0)^m Q(z)$ , with  $Q(z_0) \neq 0$ . In particular, if we consider a polynomial equation of degree  $n$  with real coefficients, i.e. (258) with  $a_i \in \mathbb{R}$ , and all its roots  $z_1, z_2, \dots, z_k$  of multiplicity  $m_1, m_2, \dots, m_k$ , respectively, it is  $m_1 + m_2 + \dots + m_k = n$ , and it is possible to write the polynomial as  $P(z) = a_n (z - z_1)^{m_1} (z - z_2)^{m_2} \dots (z - z_k)^{m_k}$ .

Moreover, it is useful to observe that for polynomial equations  $P(z) = 0$  with real coefficients, if  $a + ib \in \mathbb{C}$  is a root of the equation, i.e.  $P(a + ib) = 0$ , then also the complex conjugate  $a - ib$  is a root of the equation, i.e.  $P(a - ib) = 0$ .

## 10.2 Some examples of solutions of first order ODE

Recall that a solution of an ordinary differential equation (ODE)

$$\frac{dx}{dt} = f(x, t)$$

in an interval  $(a, b)$  is a function  $x = x(t)$  such that

$$\frac{dx}{dt} = f(x(t), t)$$

$\forall t \in (a, b)$ . If in addition to the ODE also an initial condition on  $x$  is specified, e.g.  $x(0) = x_0$ , then it is defined a *Cauchy problem*. We briefly review some techniques to solve an ODE for the most basic cases. In the following, we also use the notations  $\dot{x}$  and  $x'(t)$  interchangeably with  $\frac{dx}{dt}$ . The reader is referred to more specialized books for a broader treatment on the topic.

### 10.2.1 Integrals as ODE

The easiest examples of differential equations are those whose right hand side does not depend on  $x$ . In this case, to solve the equation it suffices to solve an indefinite integral.<sup>32</sup> For example, consider the differential equation

$$\frac{dx}{dt} = t^2 + e^{2t}$$

---

<sup>32</sup>Note that even in this case, it could be impossible to write the solution in terms of elementary functions!

Since it is  $\frac{dx}{dt} = f(t)$ , i.e.  $f$  does not depend on  $x$ , it suffices to calculate the integral

$$\int t^2 + e^{2t} dt = \frac{t^3}{3} + \frac{e^{2t}}{2} + c$$

thus obtaining infinite functions varying the constant  $c \in \mathbb{R}$ .

### 10.2.2 First order linear ODE

Consider the linear ODE

$$\frac{dx}{dt} = f(x, t) = p(t)x(t) + q(t) \quad (259)$$

If  $q(t) = 0$ , then the equation is called homogeneous. In the easiest case  $p(t)$  and  $q(t)$  are constant functions,  $p(t) = a$  and  $q(t) = b$ . Equation (259) then becomes

$$x'(t) = ax(t) + b. \quad (260)$$

One solution to this equation is the constant function  $\bar{x}(t) = -\frac{b}{a}$ , with  $\frac{dx}{dt} = 0$ . Let us consider a generic solution different to the constant one. If  $x(t) \neq -\frac{b}{a}$ , we can rewrite equation (260) as

$$\frac{x'(t)}{ax(t) + b} = 1$$

from which

$$\frac{x'(t)}{x(t) + \frac{b}{a}} = a \quad (261)$$

Observe that

$$\frac{d}{dt} \left( \log \left| x(t) + \frac{b}{a} \right| \right) = \frac{x'(t)}{x(t) + \frac{b}{a}}$$

so that (261) can be written as

$$\frac{d}{dt} \left( \log \left| x(t) + \frac{b}{a} \right| \right) = a.$$

Integrating both sides of this equality we get

$$\int \frac{d}{dt} \left( \log \left| x(t) + \frac{b}{a} \right| \right) dt = \int a dt$$

so that, by definition of indefinite integral, it is

$$\log \left| x(t) + \frac{b}{a} \right| = at + c$$

We have obtained so far an equation (not differential anymore!) in the unknown  $x(t)$ , which we can easily solve taking the exponential of both terms:

$$e^{\log \left| x(t) + \frac{b}{a} \right|} = e^{at+c}$$

from which

$$\left| x(t) + \frac{b}{a} \right| = e^{at} e^c$$

and, finally,

$$x(t) = K e^{at} - \frac{b}{a}$$

where  $K = \pm e^c$ . It is useful to observe that the solution to the original differential equation is the sum between a particular solution to the equation ( $\bar{x}(t) = -\frac{b}{a}$ ) and the general solution of the homogeneous equation:  $x'(t) = ax(t)$  has general solution  $x(t) = K e^{at}$ .

For instance, consider the equation  $\dot{x}(t) = -2x(t)$ , with  $x(0) = 2$  (a Cauchy problem). Being  $b = 0$  and  $a = -2$ , the solution is  $x(t) = K e^{-2t}$ . From the initial condition, we get  $K = 2$ .

Now consider  $\dot{x}(t) = 3x(t) - 6$ ,  $x(0) = 1$ . The solution is  $x(t) = K e^{3t} + 2$ . From  $x(0) = K + 2 = 1$  we get  $K = -1$ . Thus the solution is  $x(t) = -e^{3t} + 2$ .

Now we tackle the differential equation (259). In order to find a solution, we try to write the left hand side of this equation as the derivative of a function. For this reason, we multiply both sides of equation (259) for the function  $\mu(t)$  (to be determined), thus obtaining

$$\mu(t) \frac{dx}{dt} - \mu(t)p(t)x(t) = q(t)\mu(t) \quad (262)$$

If we impose that  $\frac{d\mu}{dt} = -\mu(t)p(t)$ , then (262) becomes the derivative of  $\mu(t)x(t)$ . In fact, from the product rule of derivatives it is

$$\frac{d}{dt}[\mu(t)y(t)] = \frac{dx}{dt}\mu(t) + \frac{d\mu}{dt}x(t) = \mu(t) \frac{dx}{dt} - \mu(t)p(t)x(t).$$

In order to choose the "right"  $\mu(t)$  we have to pick  $\mu(t)$  such that  $\frac{d\mu}{dt} = -\mu(t)p(t)$ . This means that  $\mu(t)$  itself must solve the differential equation

$$\frac{d\mu}{dt} = -\mu(t)p(t)$$

If  $\mu(t) \neq 0$ , we can write

$$\frac{d\mu}{dt} \cdot \frac{1}{\mu(t)} = -p(t)$$

and taking the integrals of both sides

$$\int \left( \frac{d\mu}{dt} \cdot \frac{1}{\mu(t)} \right) dt = - \int p(t) dt$$

from which

$$\int \left( \frac{d}{dt} \log \mu(t) \right) dt = - \int p(t) dt$$

Thus,  $\log \mu(t) = - \int p(t) dt$  and finally  $\mu(t) = e^{-\int p(t) dt}$ . Now consider that  $\mu(t) = e^{-\int p(t) dt}$  in the previous relationships. From

$$\frac{d}{dt}[\mu(t)x(t)] = q(t)\mu(t)$$

we get, taking the integrals of both terms:

$$\int \frac{d}{dt} [\mu(t)x(t)] dt = \int q(t)\mu(t)dt$$

so that

$$\mu(t)x(t) + c = \int q(t)\mu(t)dt$$

and, finally,

$$x(t) = \frac{\int q(t)\mu(t)dt + K}{\mu(t)} = e^{\int p(t)dt} \left[ \int (q(t)e^{-\int p(t)dt}) dt + K \right] \quad (263)$$

where  $K$  is a constant that can be determined through the initial condition.

As an example, consider the Cauchy problem  $\frac{dx}{dt} - 4t^3x(t) = t^3$  with initial condition  $x(0) = 2$ . Obviously,  $p(t) = -4t^3$  and  $q(t) = t^3$ . First calculate

$$\int p(t)dt = \int -4t^3 dt = -t^4 + c$$

then, by the previous formula, we obtain the solution of the differential equation

$$x(t) = e^{t^4} \left[ \int t^3 e^{-t^4} dt + K \right] = e^{t^4} \left[ -\frac{1}{4} e^{-t^4} + K \right] = -\frac{1}{4} + K e^{-t^4}$$

From the initial condition, it is  $x(0) = -\frac{1}{4} + K = 2$ , from which  $K = \frac{9}{4}$ . The solution of the Cauchy problem is thus

$$x(t) = \frac{1}{4} \left( -1 + 9e^{-t^4} \right)$$

Note that, although the formula in (263) has been easily obtained, it could be that the integrals in (263) can not be expressed in terms of elementary functions.

### 10.2.3 Separation of variables

This technique is useful when the ODE is in the form

$$\frac{dx}{dt} = f(x, t) = g(t)h(x)$$

with the initial condition  $x(0) = K$ . If  $h(K) = 0$ , then  $\frac{dx}{dt} = 0$  and a solution is  $x(t) = K$ . Otherwise, it can be shown that the equation can be written as

$$\frac{dx}{h(x)} = g(t)dt$$

from which

$$\int \frac{dx}{h(y)} - \int g(t)dt = c$$

where  $c$  is a constant.

For instance, consider the equation  $\frac{dx}{dt} = \sin(t) e^{2x}$ , with initial condition  $x(0) = 0$ .

$$\int \frac{dx}{e^{2x}} - \int \sin(t) dt = c \Rightarrow -\frac{1}{2}e^{-2x} + \cos t = c$$

from which

$$x(t) = -\frac{1}{2} \log [2(\cos t - c)]$$

From the initial condition it is  $c = 1/2$ .

As an additional example, consider the logistic growth equation, already encountered in various parts of the text:

$$\dot{x} = \alpha x - sx^2$$

where  $x = x(t)$ . If  $x(0) = 0$  (or  $x(0) = \frac{\alpha}{s}$ ), then a solution is  $x(t) = 0$  (or  $x(t) = \frac{\alpha}{s}$ ). Otherwise, if  $x \neq 0$  or  $x \neq \frac{\alpha}{s}$ , we can write the logistic equation as

$$\frac{dx}{\alpha x - sx^2} = dt$$

and the solution of the equation has the form

$$\int \frac{dx}{\alpha x - sx^2} - \int dt = c \tag{264}$$

With few algebraic manipulation it is possible to write down  $x(t)$  in explicit form. In fact, the first integral in (264) is

$$\int \frac{dx}{\alpha x - sx^2} = \int \frac{dx}{x(\alpha - sx)} = \frac{1}{\alpha} \log \left( \frac{x}{\alpha - sx} \right) + k$$

So from (264):

$$\begin{aligned} \frac{1}{\alpha} \log \left( \frac{x}{\alpha - sx} \right) &= t + c \Rightarrow \frac{x}{\alpha - sx} = e^{\alpha t + c} \\ \Rightarrow \frac{x}{\alpha - sx} &= e^{\alpha t} e^c \Rightarrow x = e^{\alpha t} e^c (\alpha - sx) \\ \Rightarrow x(1 + se^c e^{\alpha t}) &= \alpha e^{\alpha t} e^c \end{aligned}$$

from which we get

$$x(t) = \frac{\alpha e^{\alpha t} e^c}{1 + se^c e^{\alpha t}} = \frac{\alpha e^{\alpha t}}{e^{-c} + se^{\alpha t}}$$

Now remember that  $x(0) = x_0$ , i.e.  $x_0 = \frac{\alpha}{e^{-c} + s}$ . Hence,  $-c = \log \left( \frac{\alpha - sx_0}{x_0} \right)$  so that

$$x(t) = \frac{\alpha e^{\alpha t}}{\frac{\alpha - sx_0}{x_0} + se^{\alpha t}} = \frac{x_0 \alpha e^{\alpha t}}{\alpha + sx_0 (e^{\alpha t} - 1)}$$



## References

- [1] Abraham, R., L. Gardini and C. Mira, *Chaos in discrete dynamical systems (a visual introduction in two dimension)* Springer-Verlag, 1997.
- [2] Acemoglu, D., *Introduction to Modern Economic Growth*, Princeton University Press, 2008.
- [3] Bischi G.I., Carini R., Gardini L., Tenti P. "*Sulle orme del caos*", Bruno Mondadori 2004
- [4] Bischi, G.I. and M. Kopel «Equilibrium Selection in a Nonlinear Duopoly Game with Adaptive Expectations» *Journal of Economic Behavior and Organization*, vol. 46/1, pp. 73-100 (2001).
- [5] Bischi, G.I., Chiarella, C., Kopel, M., Szidarovszky, F. *Nonlinear Oligopolies: Stability and Bifurcations*, Springer, 2010.
- [6] Bischi, G.I., L. Gardini and M. Kopel «Analysis of Global Bifurcations in a Market Share Attraction Model», *Journal of Economic Dynamics and Control*, 24, pp. 855-879 (2000).
- [7] Clark, C.W. *Mathematical Bioeconomics: The Optimal Management of Renewable Resources*. John Wiley & Sons, 1990.
- [8] R. Clark Robinson, *An Introduction to Dynamical Systems*, American Mathematical Society, 2012.
- [9] Richard Dawkins. *The Selfish Gene*. Oxford University Press, Oxford, 1976.
- [10] R.L. Devaney, *An Introduction to Chaotic Dynamical Systems*, The Benjamin/Cummings Publishing Co., Menlo Park, California, 1987.
- [11] Daniel Friedman. "Evolutionary games in economics". *Econometrica*, 59:637–666 (1991)
- [12] G. Gandolfo "Economic Dynamics", Springer 2007
- [13] Guckenheimer, J., Holmes, P. *Nonlinear Oscillations, Dynamical Systems and Bifurcations of Vector Fields*. Springer, 1983.
- [14] Gumowski, I. and C. Mira, *Dynamique Chaotique*. Cepadues Editions, Toulouse, 1980.
- [15] Josef Hofbauer and Karl Sigmund. *Theory of Evolution and Dynamical Systems*. Cambridge University Press, Cambridge, 1988.
- [16] Hofbauer, J. and K. Sigmund *Evolutionary Games and Population Dynamics*, Cambridge University Press, 1998.
- [17] Lorenz, H.W., 1993 *Nonlinear dynamical economics and chaotic motion*, Springer-Verlag.
- [18] A. Medio and M. Lines *Nonlinear Dynamics*, Cambridge University Press, 2001
- [19] Mira, C., Gardini, L., Barugola, A., Cathala, J.C. (1996). *Chaotic Dynamics in Two-Dimensional Noninvertible Maps*. World Scientific, Singapore
- [20] F. Patrone "Decisori (razionali) interagenti", Edizioni Plus (2006)

- [21] Puu, T. (1991). "Chaos in duopoly pricing". *Chaos, Solitons & Fractals* 1, 573–581.
- [22] Sethi, S.P., Thompson, G.L., *Optimal Control Theory: Applications to Management Science and Economics*, Springer, 2000.
- [23] R. Shone, *Economic Dynamics: Phase Diagrams and their Economic Application*, Cambridge University Press, 2003.
- [24] Sydsaeter, K., Hammond, P., Seierstad A., Strom A., *Further Mathematics for Economic Analysis* (2nd Edition), Prentice Hall, 2008
- [25] John Maynard Smith. *Evolution and the Theory of Games*. Cambridge University Press, Cambridge, 1982
- [26] Taylor, P. and L. Jonker "Evolutionarily stable strategies and game dynamics" *Mathematical Biosciences*, 40, 145-156. (1978).
- [27] Weibull, J.W. *Evolutionary Game Theory*, The MIT Press, 1995.
- [28] Hommes C.H. *Behavioral Rationality and Heterogeneous Expectations in Complex Economic Systems*. Cambridge University Press, 2013.
- [29] Vega-Redondo F. *Evolution, Games and Economic Behaviour*, Oxford University Press, 1996.